E_n Ligand Complexes

Synthesis, Functionalization and Transfer of Polypnictogen Units

Dissertation

zur Erlangung des
DOKTORGRADES DER NATURWISSENSCHAFTEN
(Dr. rer. nat.)
der Naturwissenschaftlichen Fakultät für Chemie und
Pharmazie der Universität Regensburg

vorgelegt von

Veronika Heinl

aus Windischeschenbach

Regensburg 2021

Diese Arbeit wurde angeleitet von Prof. Dr. Manfred Scheer.

Promotionsgesuch eingereicht am: 20.10.2021

Tag der mündlichen Prüfung: 03.12.2021

Vorsitzender: Prof. Dr. Alkwin Slenczka

Prüfungsausschuss: Prof. Dr. Manfred Scheer

Prof. Dr. Henri Brunner

Prof. Dr. Frank-Michael Matysik

Eidesstattliche Erklärung

Ich erkläre hiermit an Eides statt, dass ich die vorliegende Arbeit „E_n Ligand Complexes – Synthesis, Functionalization and Transfer of Polypnictogen Units“ ohne unzulässige Hilfe Dritter und ohne Benutzung anderer als der angegebenen Hilfsmittel angefertigt habe; die aus anderen Quellen direkt oder indirekt übernommenen Daten und Konzepte sind unter Angabe der Literaturzitats gekennzeichnet.

Veronika Heinl

This thesis was elaborated within the period from January 2018 until October 2021 in the Institute of Inorganic Chemistry at the University of Regensburg, under the supervision of Prof. Dr. Manfred Scheer.

List of Publications:

- V. Heinl, G.r Balázs, S. Koschabek, M. Eckhardt, M. Piesch, M. Seidl, M. Scheer, *Molceucles* **2021**, *26*, 2966.

- V. Heinl, A. E. Seitz, G. Balázs, M. Seidl, M. Scheer, *Chem. Sci.* **2021**, *12*, 9726-9732.

- V. Heinl, M. Schmidt, M. Eckhardt, M. Eberl, A. E. Seitz, G. Balázs, M. Seidl, M. Scheer, *Chem. Eur. J.* **2021**, *27*, 11649-11655.

dedicated to my parents

„Was wirklich zählt, ist Intuition“

Albert Einstein

Preface

Some chapters have already been published (vide supra) and are reprinted with the permission of the respective scientific publisher. These chapters are only slightly modified to enable a uniform design of the work. Corresponding information are given at the beginning of the respective chapter.

At the beginning of this thesis, a short and general introduction is given and the research objectives are described. After the presentation of the different chapters, a comprehensive conclusion of this work is given followed by the appendix, which includes lists of the used abbreviations and numbered compounds.

The chapters have a uniform design and are subdivided equally. They start with a graphical abstract, an abstract followed by the author contribution. There the individual part of each author for this work is described in detail. Furthermore, the main part is divided into a short introduction, results and discussion, conclusion, supporting information and references. The numeration of the chapters (compounds, schemes, figures, etc.) begins anew as well as the numeration of the corresponding references.

Table of Contents

1 Introduction

> *„Die Natur und das Unerforschliche, das hinter ihr verborgen bleibt und Verehrung fordert, hat dem Chemiker eine Orgel mit nun schon über 100 verschiedenen Tönen zur Verfügung gestellt, auf der er komponieren und musizieren darf. Er kann aber auch dem immer noch unendlich schöneren Spiel ihrer selbst lauschend und forschend nachgehen“* [1]
>
> *Ernst Otto Fischer*
>
> Banquet Speech – Nobel Price (1973)

These words from *Ernst Otto Fischer* are an excerpt of his speech at the Nobel banquet in 1973.[1] Freely translated this citation means, that nature and the unfathomable provide the chemists an organ with more than 100 different sounds on which they can compose and play. Furthermore, they can listen to the endless beautiful play and pursues them scientifically. *Fischer* exemplifies with his metaphoric description the unlimited possibilities given in chemistry. It is ubiquitous and an aspect in every part of the universe, nature and life. The combination of elements, the reaction or interaction between them and the variation of external influences, enables expansion of the collection of compositions or replacement of some notes. Therefore, it can be said that the discovery of the elements brought the possibility to expand the chemical insights and focused research.

The discovery of the chemical elements occurred one by one over the last thousand years. Their history started already in antiquity and as evidenced by old records 12 elements were already known.[2] Alchemy, a part of the natural philosophy in the 13th till 17th century, leads to an extension of the spectrum. Even if alchemists never succeeded in the conversion of base metals to gold or its synthetic preparation, they revealed the preparation of arsenic, zinc and phosphorus, respectively. However, the peak of the discovery of the elements started in the 18th century[2] and is with a number of 118 still rising.[3] With the increasing number of elements, attempts were made to divide them into categories, based on their properties. This resulted in the periodic table of the elements, an essential tool for every chemist.

Not only the number of elements has increased over the centuries, but also the understanding of how compounds are formed, which properties can be expected or exploited and how the desired goals can be achieved. Step by step we learn how the world is built up and how we can benefit from that knowledge, even though we only know so little.

1.1 Phosphorus, Arsenic and Antimony – A Short Overview

The elements phosphorus, arsenic and antimony represent elements of the pnictogen group. Even if they are located in the same group in the periodic table and show some similarities, also huge differences in their properties are present. While phosphorus represents a non-metal, the metallic character increases within the group and arsenic and antimony are already metalloids with differences in their reactivity and properties. Therefore, the areas of applications are huge and their usage in industry and nature is widely varying.

Phosphorus constitutes an essential component in living organisms, mostly in the form of phosphoric acid esters and phosphates. Therefore, 700 g of phosphorus can be found in an average human adult and the daily requirement is about 1-1.2 g phosphorus. Mainly, it is stored in bones and teeth in form of hydroxyapatite ($Ca_5(PO_4)_3(OH)$), it can be found in phospholipids in cell membranes or as a building block for macromolecules like DNA or ATP.[3,4] Furthermore, phosphorus containing compounds are used in industry in large scale. The main application areas are the usage of sodium-, potassium- or ammonium-phosphates in fertilizers in agriculture or cleaning agents.[3–5] Phosphorus containing compounds are also used as auxiliary materials in flame retardants, corrosion inhibitors or plasticizers. For the industrial synthesis of elemental phosphorus, apatites ($Ca_5(PO_4)_3(OH,F,Cl)$) with a high level of fluoride are used.[3,4]

Phosphorus is present in the three allotropic modifications, white, black and red phosphorus. The latter represents a kind of intermediate modification between white and black phosphorus and can be divided into subgroups of crystalline phases (violet- or Hittorf's phosphorus and fibrous phosphorus) and amorphous phases (red phosphorus).[6,7,8] An overview of the structural framework of the allotropes is given in figure 1. The thermodynamically stable modification is black phosphorus. However, the conversion time of the other modifications is relatively small at r.t. and atmospheric pressure and therefore they are isolable. White phosphorus represents the most important modification, since it is used as starting material to form the other modifications.[3,8] The structure of white phosphorus consists of discrete P_4 tetrahedra (figure1)[9] and can be obtained by an electrothermal process using apatites as raw materials. It represents the only soluble modification in organic solvents, which enables an extensive application in chemistry.[3] Annealing of P_4 over 200 °C leads to conversion into the amorphous red phosphorus.[3] By increasing temperature it reorganizes and the crystalline fibrous modification is obtained above 500 °C.[8] Further annealing leads to the formation of the violet modification, which is also called the *Hittorf´s* phosphorus.[7] Both consist of parallel arranged pentagonal tubes with alternating phosphorus units $[P_2]$-$[P_8]$-$[P_2]$-$[P_9]$ (*cf*. figure 1) and the cubes are crosslinked via the $[P_9]$ unit.[10] A single layer in violet phosphorus is constructed of parallel orientated tubes, which are crosslinked with another layer in

perpendicular orientation. Fibrous phosphorus consists of the same pentagonal tubes connected parallel via the [P_9] unit to double strands.[8] Orthorhombic black phosphorus can be obtained by annealing white phosphorus up to 200 °C under a pressure of 12 kbar. This modification has the highest density and therefore its formation is favored at higher pressures. The structure is based on six membered rings forming a layer with a zigzag conformation.[11] Depending on the applied pressure and additives (Hg, As) also the rhombohedral black phosphorus and cubic, metallic phosphorus is formed. The rhombohedral modification also consists of six membered rings forming a layer, while in this case the rings are arranged diagonally among each other (exo conformation).[3,12]

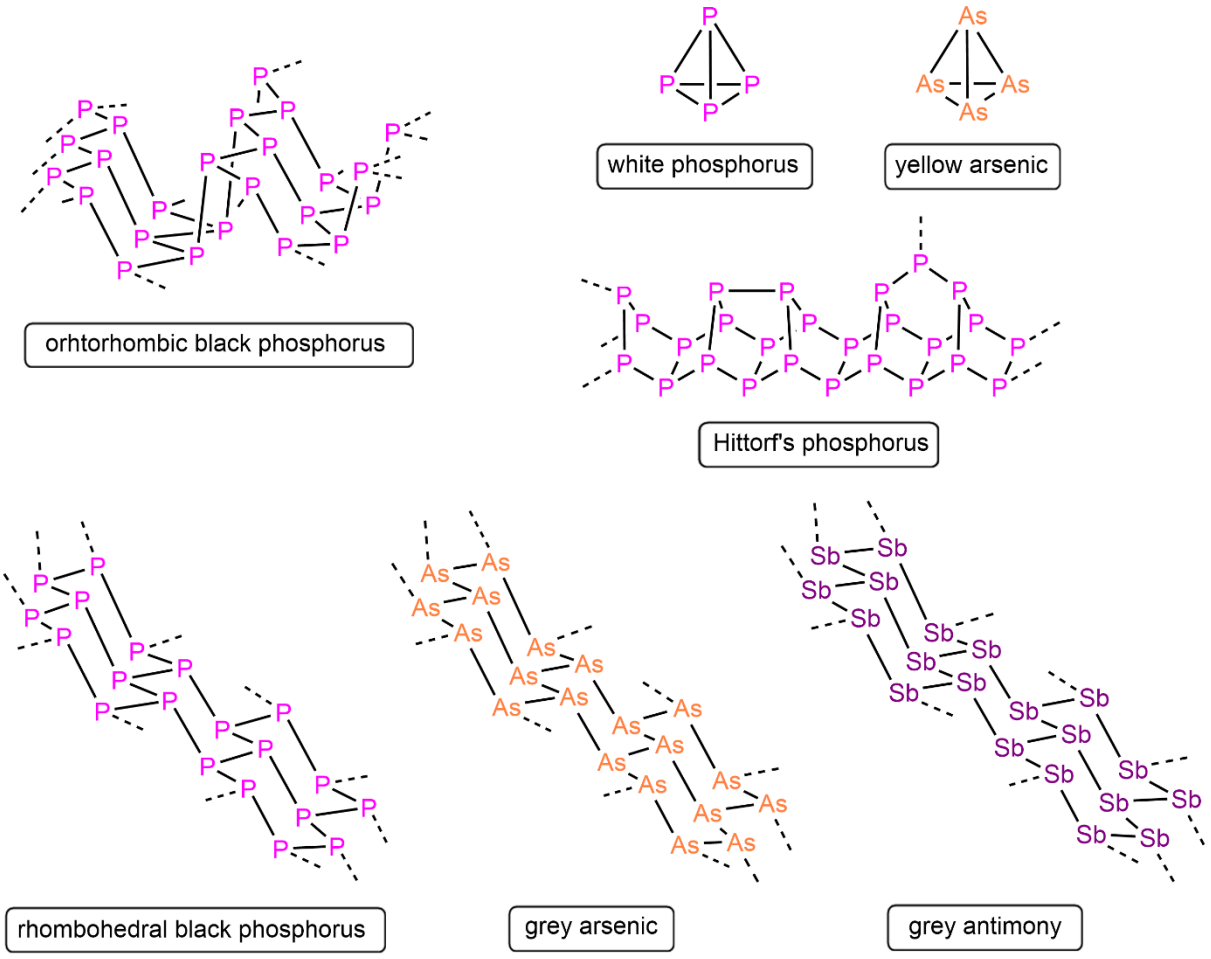

Figure 1: Overview of selected allotropic modifications of phosphorus, arsenic and antimony, respectively.

Arsenic, as the heavier homolog of phosphorus, is mostly known for its poisonous nature. Especially ‚white arsenic' (As_2O_3) was used for many murders in the last centuries.[13,14] However, arsenic is an important element in nature and industry. Arsenic is considered as a trace element for the human body and even for animals and plants. In an average human body, 3.5 mg can be found.[3] Nowadays many applications for arsenic and its compounds in pharmaceuticals, herbicides and insecticides exist. Furthermore, arsenic is used as an alloy additive or semiconductor component.[3,14]

The element antimony is known since antiquity. Over time antimony and its compounds were used as eye make-up or for skin medication.[3,15,16] A typical application in middle age was the usage of pellets of antimony as a laxative.[3,15,16] Even nowadays pharmaceuticals including antimony are used. However, the main application is the usage as an additive in semiconductors to harden soft metals like tin or lead.[3,15,16]

Comparable with the modifications of phosphorus and arsenic, antimony occurs in similar modifications. The thermodynamically most stable modifications represent grey arsenic and grey antimony, which have the same structure as rhombohedral black phosphorus (figure 1). Tempering of grey arsenic over 616 °C leads to the formation of the labile yellow arsenic. It consists of discrete As_4 tetrahedra, analog to white phosphorus.[3,17] Yellow arsenic is highly light- and air-sensitive and thus has to be treated with care. Comparable Sb_4 units are only known in gas phase or trapped in a solid neon matrix.[18]

1.2 E_n Ligand Complexes

E_n or polypnictogen ligand complexes are complexes containing at least one pnictogen atom directly bound to a metal center and not bearing any organic substituents. The first reported complex which covers this category was $[(CO)_3Co(\eta^3\text{-}As_3)]$ (**I**, figure 2), synthesized in 1969 from *Dahl et. al*.[19] Already one year later the same group succeeded in the preparation of the first Sb_n ligand complex $[\{(CO)_3Co\}_4(\mu_3\text{-}Sb)_4]$ (**II**) by the reaction of $Co(OAc)_2{\cdot}H_2O$ with $SbCl_3$.[20] In the same period, G*insberg* and *Lindsell* also reported on the synthesis of $[(PPh_3)_3RhCl(\eta^2\text{-}P_4)]$ (**III**), a polyphosphorus ligand complex of rhodium.[21]

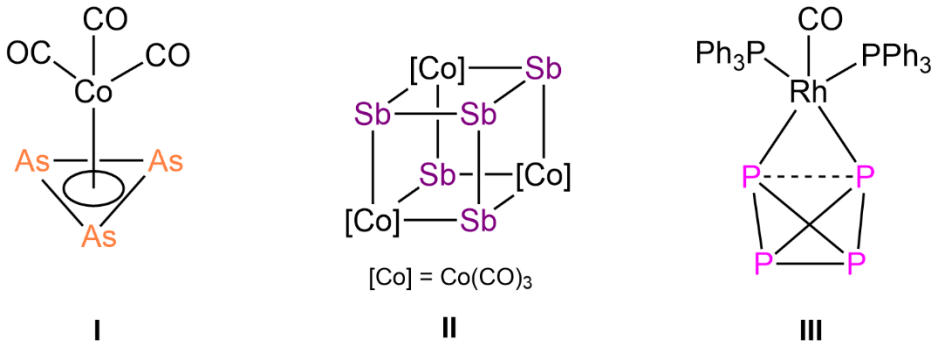

Figure 2: Overviewe of the first En ligand complexes (E = As (I), Sb (II), P (III)).

Even if the first discovery of such complexes was already 50 years ago, the synthesis and reactivity of E_n ligand complexes are still an active field of chemical research. Especially for phosphorus and arsenic, a variety of such complexes are known so far. For their synthesis, the conversion of white phosphorus and yellow arsenic on transition metal centers or main

group compounds led to success.[22–25] This resulted in numerous examples of which a small overview is given in figure 3. However, the number of polyantimony ligand complexes is rather limited. Responsible for this is the lack of suitable antimony sources for synthesis, such as Sb_4. Additionally, the high light- and air-sensitivity of antimony containing compounds and the weak Sb-Sb bond[26] complicates the working process. Nevertheless, meanwhile there are some representatives known (figure 3). Over time it was possible to synthesize complexes with different numbers of pnictogen atoms. While there are several representatives including E_n units with n = 1-6, higher numbers are rather limited.

There are many representatives with a single pnictogen atom bound to one or more metal centers. Remarkable examples are the complexes [(N_3N)WE] ($N_3N = N(CH_2CH_2NSiMe_3)_3$; E = P (**IVa**),[27] As (**IVb**),[28] Sb (**IVc**)[29]), bearing a tungsten pnictogen triple bond. For n = 2 also different coordination modes of the E_2 unit have been observed. For instance, the E_2 unit can be a part of a tetrahedron formed with two molybdenum fragments [$(CpMo(CO)_2)_2(\mu,\eta^{2:2}\text{-}E_2)$] (E = P (**Va**)[30], As (**Vb**),[31] Sb (**Vc**)[32]). Similar compounds for E = P and As are also known with chromium and tungsten.[31,33] In **VIa** and **VIb** the E_2 unit is a part of a triple decker complex, where two E_2 dumbbells are coordinated by two [Cp'''Co] fragments (Cp''' = $C_5H_2{}^tBu_3$, E = P, As), respectively.[34] Furthermore, threefold coordination of a tungsten center is possible in the antimony complex [{$(CO)_3W$}$_2(\mu_3,\eta^{2:2:2}\text{-}Sb_2)$] (**VII**), reported by *Franck et. al*. in 1982.[35] If the pnictogen unit is extended to n = 3 mostly *cyclo*-E_3 ligands are known, which coordinate to one or two metal fragments, as shown in figure 3 by the complexes [$Cp^RNi(\eta^3\text{-}E_3)$] (E = P (**VIIIa**),[36,37] As (**VIIIb**)[37]), [$(Cp'''Ni)_2(\mu,\eta^{3:3}\text{-}P_3)$] (**IX**)[38] or [$CpMo(CO)_2(\eta^3\text{-}Sb_3)$] (**X**).[32] A further extension of the polypnictogen unit leads to a variety of complexes with different coordination modes. Some of them are also depicted in figure 3. An E_4 chain can be formed and stabilized by two metal fragments as demonstrated by the prismane shaped complex [$(LNi)_2(\mu,\eta^{3:3}\text{-}E_4)$] (E = P (**XIa**, **XII**),[37,39] As (**XIb**);[37] L = ^{4iPr}Cp, L^1) or the triple decker complex [$(Cp^RFe)_2(\mu,\eta^{4:4}\text{-}E_4)$] (E = P (**XIIIa**),[40] As (**XIIIb**),[40–42] Cp^R = Cp''', Cp^{BIG}, Cp*). Furthermore, E_4 cycles or butadiene-like E_4 ligands can be formed and coordinated by one or two metal fragments. In the case of the synthesis of **XIIIb** also a bonding isomer with a *cyclo*-As_4 ligand is observed.[41] Another interesting example of such a representative is **XIV** reported in 2017, which contains an aromatic P_4 unit.[43] *Schulz et al.* demonstrated the formation of compounds containing an Sb_4 unit by the reduction of Cp*$_4Sb_4$. Therefore, the reaction with $[L^2Mg]_2$ and $[L^1Ga]$ leads to the polyantimony complexes [$(L^3Mg)_4(\mu_4,\eta^{2:1:1:1:1:1}\text{-}Sb_4)$] (**XV**) and [$(L^2Ga)_2(\mu,\eta^{1:1:1:1}\text{-}Sb_4)$] (**XVI**), respectively.[44] E_5 units usually have a cyclic form and possess an aromatic character. The best known representatives are pentaphosphaferrocene, pentaarsaferrocene and their derivatives (*cf.* **XVIIa**,[45] **XVIIb**,[46] **XVIIIa**[47] and **XVIIIb**[47,48] in figure 3). It is also possible to form triple decker complexes, where the E_5 cycle is coordinating two metal fragments as shown in [$(Cp^RCr)_2(\mu,\eta^{5:5}\text{-}E_5$] (E = P (**XIXa**),[49] As (**XIXb**)[48,50]). Similar compounds are also known for manganese and molybdenum.[51] Furthermore, the synthesis

of the triple decker complex [Cp'''Mo(μ,η$^{5:5}$-Sb$_5$)MoCp^R] (**XX**, Cp^R = η^5-C$_5$H$_2$^{t}Bu$_2$Me) was reported by *Rösler et. al.*, synthesized by the reaction of ^{t}Bu$_4$Sb$_4$ with [Cp'''Mo(CO)$_3$Me].[52]

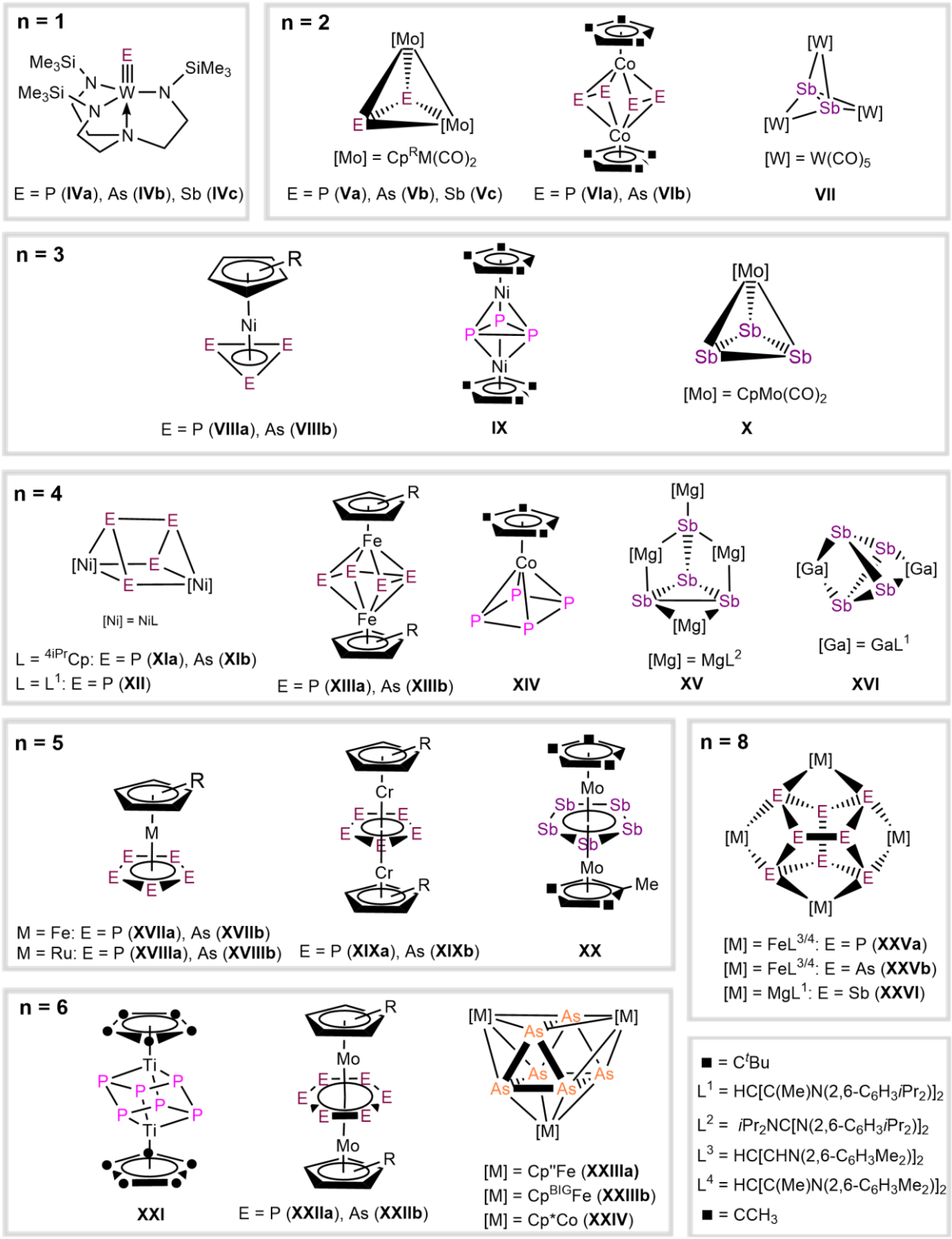

Figure 3: Selected E$_n$ ligand complexes, sorted by the number of the atoms in the E$_n$ unit.

If the number of the polypnictogen unit is higher than 5, the number of corresponding complexes decreases. E_6 units are stabilized as a chair type cycle, shown in the titanium complex $[(Cp^*Ti)_2(\mu,\eta^{1:1:1:1:1:1}\text{-}P_6)]$ (**XXI**),[53] or as planar benzene like ligands shown in the complexes $[(Cp^RMo)_2(\mu,\eta^{6:6}\text{-}E_6)]$ (E = P (**XXIIa**),[54] As (**XXIIb**)[55]). In the case of phosphorus, such complexes are also known with V, Nb, or W[56] Furthermore, some examples exist containing an As_6 prismane, where all rectangular faces are coordinated by a metal fragment (*cf.* **XXIIIa, XXIIIb** and **XXIV**, figure 3).[40,57] Remarkable examples of complexes with larger polypnictogen units are the iron and magnesium complexes **XXVa**, **XXVb** and **XXVI**.[58] They bear a realgar like E_8 cage, formed by the polypnictogen atoms. In 2010 it was even possible to extend the polypnictogen units in a neutral complex up to n = 12.[59]

In summary, the number of E_n ligand complexes is steadily increasing and therefore a variety of different structural motifs and coordination modes are already observed. However, compared to polyphosphorus compounds much less is known for polyarsenic compounds. The number decreases enormously for polyantimony ligand complexes. Even if not all known compounds are depicted in figure 3, they can almost be counted on two hands.

1.3 The Concept of Transfer Reactions

In general, conventional synthetic methods like thermolysis and photolysis are used for the synthesis of the desired E_n ligand complexes. Furthermore, complexes containing unsaturated fragments can provide the opportunity for the synthesis of new structural motifs. In the case of phosphorus and arsenic, the metastable and highly reactive E_4 modification white phosphorus and yellow arsenic are mostly used as starting materials, respectively.[22,24,25,60] Due to the missing antimony analogue, i.e. yellow antimony (Sb_4), organo-substituted compounds such as R_4Sb_4 (R = Cp*, ^{t}Bu) or compounds like $SbCl_3$ or $Sb(NMe_2)_3$ are used as molecular antimony source. However, some disadvantages arise from the mentioned reaction paths. In thermolysis, often harsh reaction conditions are needed and hence the thermodynamically most stable products are formed. In addition to this, usually more than one product is formed. Photolysis reactions are limited to compounds bearing labile ligands and bonds. Furthermore, the work with light-sensitive compounds is more complicated.

Therefore, the usage of transfer reactions could be of advantage. This concept is based on E_n ligand complexes of early transition metals and facilitates the synthesis of a variety of unprecedented compounds. Transfer reactions are normally based on metathesis reactions, which proceed under mild reaction conditions. In scheme 1, a schematic description of a general transfer reaction is given. A polypnictogen unit (E_n) bound to an early transition metal fragment (M) is transferred to later transition metal or main group fragments (M'). The formation of thermodynamically more stable compounds (MX) is the driving force. In doing so, higher

yields and selectivity, compared to conventional methods, could be achieved and the mild conditions enable the formation of metastable compounds that are not accessible by other means. Furthermore, it would be a promising tool in the case of the formation of As_n and Sb_n ligand complexes, respectively, which can not be, as stated above, synthesized via conventional routes.

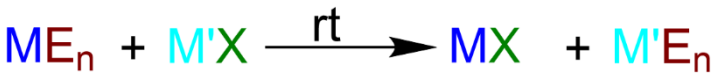

Scheme 1: Schematic description of a transfer reaction. (M = early transition metal, M' = later transition metal or main group compound, E_n = polypnictogen unit, X = any group)

First reports on the application of transfer reactions were already published in the late 1980s. Different groups described independently the synthesis of main group heterocycles by the reaction of organozirconium and organotitanium complexes with compounds of the form $RECl_2$ (E = P, As).[61] Later on, *Regitz et. al.* published the synthesis of some organophosphorus compounds starting from $[Cp_2Zr(\eta^{1:1}\text{-}C_2{}^tBu_2P_2)]$.[62]

One of the first transfers of an intact E_n unit, started by the corresponding ligand complex, was published by *Scherer et. al.* in 1995. They used derivatives of pentaphosphaferrocene **XVIIIa** and pentaarsaferrocene **XVIIIb** to transfer the E_5 unit to heavier homologs ruthenium and osmium, respectively (**A**, scheme 2).[47] Furthermore, *Cummins et. al.* took advantage of this concept. A remarkable example was published in 2009. The synthesis of the metastable tetrahedral compound P_3As was achieved by the transfer of a P_3^- unit of $[(ODipp)_3Nb(\eta^3\text{-}P_3)]$ to $AsCl_3$ (**B**).[63]

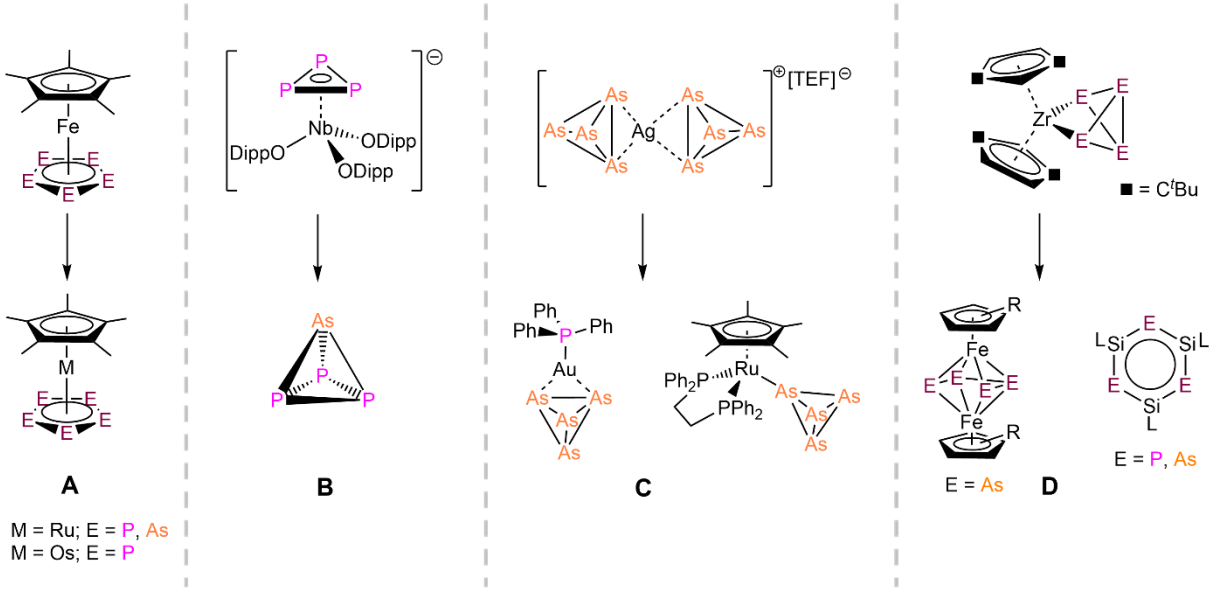

Scheme 2: Selected examples of transfer reactions.

With the advantages of transfer reactions in mind, our group used the ionic complex $[Ag(\eta^2\text{-}As_4)_2][TEF]$ (TEF = $Al\{OC(CF_3)_3\}_4$) to synthesize gold and ruthenium based complexes bearing an almost intact As_4 tetrahedron as ligand (**C**).[64] Furthermore, the complexes $[Cp''_2Zr(\eta^{1:1}\text{-}E_4)]$ (E = P, As) show a high potential to release the E_4 unit in presence of suitable halogenated reaction partners.[41,65] In doing so, the reaction with $[Cp'''FeBr]_2$ leads to the transfer of the As_4 unit in form of a chain and the formation of an iron triple decker complex (**D**, left).[41] We also succeeded in the synthesis of heteroaromatic sila-phospha and sila-arsa-derivatives of benzene using $[PhC(N^tBu)_2SiCl]$ as reagent (**D**, right).[65] This overview shows the possibilities given with the concept of transfer reactions. Therefore, this could be the way to go for the synthesis of Sb_n ligand complexes. As mentioned before, there are some challenges concerning their preparation, which can be remedied by the advantages of such metathesis reactions. However, a suitable starting material must be found, where an ideally big polyantimony unit is bound to an early transition metal.

1.4 References

[1] E. O. Fischer – Banquet speech. NobelPrize.org. Nobel Prize Outreach AB 2021. Wed. 11 Aug 2021. https://www.nobelprize.org/prizes/chemistry/1973/fischer/speech/.

[2] M. E. Weeks, *Discovery of the Elements*, Chem. Educ. Publ. Company, Easton, **1945**.

[3] A. F. Holleman, N. Wiberg, *Lehrbuch der Anorganischen Chemie*, Walter de Gruyter, Berlin - New York, **2007**.

[4] D. E. Corbridge, *Phosphorus 2000*, Elsevier, Amsterdam, **2000**.

[5] F. Rashchi, J. A. Finch, *Miner. Eng.* **2000**, *13*, 1019–1035.

[6] a) W. L. Roth, T. W. DeWitt, A. J. Smith, *J. Am. Chem. Soc.* **1947**, *69*, 2881–2885; b) A. Pfitzner, *Angew. Chem. Int. Ed.* **2006**, *45*, 699–700; c) F. S. R. Scholder, *Angew. Chem. Int. Ed.* **1966**, *5*, 1047–1048; d) A. Pfitzner, *Angew. Chem. Int. Ed.* **2006**, *45*, 699–700.

[7] W. Hittorf, *Ann. Phys. Chem.* **1865**, *126*, 193.

[8] M. Ruck, D. Hoppe, B. Wahl, P. Simon, Y. Wang, G. Seifert, *Angew. Chem. Int. Ed.* **2005**, *44*, 7616–7619.

[9] R. E. Dinnebier, A. Simon, *Z. Kristallogr.* **2005**, *220*, 259–264.

[10] H. K. H. Thurn, *Acta Crystallogr., Sect. B* **1969**, *25*, 125–135.

[11] P. W. Bridgman, *J. Am. Chem. Soc.* **1914**, *36*, 1344–1363.

[12] a) J. C. Jamieson, *Science* **1963**, *139*, 1291–1292; b) H. I. T. Kikegawa, *Acta Crystallogr., Sect. B* **1983**, *39*, 158–164.

[13] G. Süss-Fink, *Chemie in unserer Zeit* **2012**, *46*, 100–109.

[14] J. Parascandola, *Kings of Poisons - A History of Arsenic*, Potomac Books, Washington D. C., **2012**.

[15] C. Hansell, *Nat. Chem.* **2015**, *7*, 88.

[16] R. I. McCallum, *Proc. roy. Soc. Med.* **1977**, *70*, 756–763.

[17] A. Bettendorff, *Liebigs Ann. Chem.* **1867**, *144*, 110–114.

[18] a) V. E. Bondybey, G. P. Schwart, J. E. Griffiths, *J. Mol. Spectrosc.* **1981**, *89*, 328–332; b) J. Kordis, K. A. Gingerich, *J. Chem. Phys.* **1973**, *58*, 5141–5149; c) R. Prasad, V. Venugopal, Z. Sigh, D. D. Sood, *J. Chem. Thermodynamics* **1979**, *11*, 963–970.

[19] A. S. Foust, M. S. Foster, L. F. Dahl, *J. Am. Chem. Soc.* **1969**, *24*, 5632–5633.

[20] L. F. Dahl, A. S. Foust, *J. Am. Chem. Soc.* **1970**, *92*, 7337–7341.

[21] Alvin P. Ginsberg, W. E. Lindsell, *J. Am. Chem. Soc.* **1971**, *93*, 2082–2084.

[22] B. M. Cossairt, N. A. Piro, C. C. Cummins, *Chem. Rev.* **2010**, *110*, 4164–4177.

[23] M. Caporali, L. Gonsalvi, A. Rossin, M. Peruzzini, *Chem. Rev.* **2010**, *110*, 4178–4235.

[24] M. Seidl, G. Balázs, M. Scheer, *Chem. Rev.* **2019**, *119*, 8406–8434.

[25] M. Scheer, G. Balázs, A. Seitz, *Chem. Rev.* **2010**, *110*, 4236–4256.

[26] Y. R. Luo, *Comprehensive Handbook of Chemical Bond Energies*, CRC Press, Boca Raton, **2007**.

[27] N. C. Zanetti, R. R. Schrock, W. M Davis, *Angew. Chem. Int. Ed. Engl.* **1995**, *34*, 2044–2046.

[28] M. Scheer, J. Müller, M. Häser, *Angew. Chem. Int. Ed. Engl.* **1996**, *35*, 2492–2496.

[29] G. Balázs, M. Sierka, M. Scheer, *Angew. Chem. Int. Ed.* **2005**, *44*, 4920–4924.

[30] O. J. Scherer, H. Sitzmann, G. Wolmershäuser, *J. Organomet. Chem.* **1984**, *268*, C9-C12.

[31] P. J. Sullivan, A. L. Rheingold, *Organometallics* **1982**, *1*, 1547–1549.

[32] H. J. Breunig, R. Rösler, E. Lork, *Angew. Chem. Int. Ed. Engl.* **1997**, *36*, 2819–2821.

[33] a) L. Y. Goh, R. C. S. Wong, W. H. Yip, T. C. W. Mak, *Organometallics* **1991**, *10*, 875–879; b) L. Y. Goh, C. K. Chu, R. C. S. Wong, T. W. Hambley, *J. Chem. Soc., Dalton Trans.* **1989**, 1951–1956; c) J. E. Davies, M. C. Klunduk, M. J. Mays, P. R. Raithby, G. P. Shields, P. K. Tompkin, *J. Chem. Soc., Dalton Trans.* **1997**, 715–720.

[34] a) C. Graßl, M. Bodensteiner, M. Zabel, M. Scheer, *Chem. Sci.* **2015**, *6*, 1379–1382; b) O. J. Scherer, G. Berg, G. Wolmershäuser, *Chem. Ber.* **1995**, *128*, 635–639.

[35] B. Franck, W. Bock, U. Wolters, *Angew. Chem. Int. Ed. Engl.* **1982**, *21*, 215–216.

[36] a) O. J. Scherer, J. Braun, G. Wolmershäuser, *Chem. Ber.* **1990**, *173*, 417–475; b) O. J. Scherer, *J. Organomet. Chem.* **1988**, *350*, C20-C24.

[37] O. J. Scherer, G. Berg, P. Walther, G. Wolmershäuser, *Chem. Ber.* **1992**, *125*, 2661–2665.

[38] E. Mädl, G. Balázs, E. V. Peresypkina, M. Scheer, *Angew. Chem. Int. Ed. Engl.* **2016**, *55*, 7702–7707.

[39] S. Yao, Y. Xiong, C. Milsmann, E. Bill, S. Pfirrmann, C. Limberg, M. Driess, *Chem. Eur. J.* **2010**, *16*, 436–439.

[40] S. Heinl, A. Y. Timoshkin, J. Müller, M. Scheer, *Chem. Commun.* **2018**, *54*, 2244–2247.

[41] M. Schmidt, A. E. Seitz, M. Eckhardt, G. Balázs, E. V. Peresypkina, A. V. Virovets, F. Riedlberger, M. Bodensteiner, E. M. Zolnhofer, K. Meyer, M. Scheer, *J. Am. Chem. Soc.* **2017**, *139*, 13981–13984.

[42] M. Schmidt, D. Konieczny, E. V. Peresypkina, A. V. Virovets, G. Balázs, M. Bodensteiner, F. Riedlberger, H. Krauss, M. Scheer, *Angew. Chem. Int. Ed.* **2017**, *56*, 7307–7311.

[43] F. Dielmann, A. Timoshkin, M. Piesch, G. Balázs, M. Scheer, *Angew. Chem. Int. Ed.* **2017**, *56*, 1671–1675.

[44] C. Ganesamoorthy, J. Krüger, C. Wölper, A. S. Nizovtsev, S. Schulz, *Chem. Eur. J.* **2017**, *23*, 2461–2468.

[45] a) O. J. Scherer, T. Brück, *Angew. Chem. Int. Ed. Engl.* **1987**, *99*, 59; b) O. J. Scherer, T. Brück, G. Wolmershäuser, *Chem. Ber.* **1988**, *121*, 935–938.

[46] O. J. Scherer, C. Blath, G. Wolmershäuser, *J. Organomet. Chem.* **1990**, *387*, C21-C24.

[47] B. Rink, O. J. Scherer, G. Wolmershäuser, *Chem. Ber.* **1995**, *128*, 71–73.

[48] O. J. Scherer, C. Blath, G. Heckmann, G. Wolmershäuser, *J. Organomet. Chem.* **1991**, *409*, C15-C18.

[49] a) L. Y. Goh, R. C. S. Wong, C. K. Chu, T. W. Hambley, *J. Chem. Soc., Dalton Trans.* **1990**, 977–982; b) O. J. Scherer, J. Schwalb, G. Wolmershäuser, W. Kaim, R. Gross, *Angew. Chem. Int. Ed. Engl.* **1986**, *25*, 363–364.

[50] O. J. Scherer, W. Wiedemann, G. Wolmershäuser, *Chem. Ber.* **1990**, *123*, 3–6.

[51] a) A. L. Rheingold, M. J. Foley, P. J. Sullivan, *J. Am. Chem. Soc.* **1982**, *104*, 4727-4726; b) S. Heinl, G. Balázs, M. Bodensteiner, M. Scheer, *Dalton Trans.* **2016**, *45*, 1962–1966.

[52] H. J. Breunig, N. Burford, R. Rösler, *Angew. Chem. Int. Ed.* **2000**, *39*, 4148–4150.

[53] O. J. Scherer, H. Swarowsky, G. Wolmershäuser, W. Kaim, S. Kohlmann, *Angew. Chem. Int. Ed. Engl.* **1987**, *26*, 1153–1155.

[54] a) O. J. Scherer, H. Sitzmann, G. Wolmershäuser, *Angew. Chem. Int. Ed. Engl.* **1985**, *24*, 351–353; b) M. Fleischmann, C. Heindl, M. Seidl, G. Balázs, A. V. Virovets, E. V. Peresypkina, M. Tsunoda, F. P. Gabbaï, M. Scheer, *Angew. Chem. Int. Ed.* **2012**, *51*, 9918–9921.

[55] O. J. Scherer, H. Sitzmann, G. Wolmershäuser, *Angew. Chem. Int. Ed. Engl.* **1989**, *28*, 212–213.

[56] a) O. J. Scherer, J. Schwalb, H. Swarowsky, G. Wolmershäuser, W. Kaim, R. Gross, *Chem. Ber.* **1988**, *121*, 443–449; b) O. J. Scherer, J. Vondung, G. Wolmershäuser, *Angew. Chem. Int. Ed. Engl.* **1989**, *28*, 1355–1357.

[57] a) C. Hänisch, D. Fenske, F. Weigend, R. Ahlrichs, *Chem. Eur. J.* **1997**, *3*, 1494–1498; b) H. F. Krauss, *PhD Thesis*, University of Regensburg, **2011**.

[58] a) C. Ganesamoorthy, C. Wölper, A. S. Nizovtsev, S. Schulz, *Angew. Chem. Int. Ed.* **2016**, *55*, 4204–4209; b) F. Spitzer, C. Graßl, G. Balázs, E. M. Zolnhofer, K. Meyer, M. Scheer, *Angew. Chem. Int. Ed.* **2016**, *55*, 4340–4344; c) F. Spitzer, G. Balázs, C. Graßl, M. Scheer, *Chem. Commun.* **2020**, *56*, 13209–13212.

[59] F. Dielmann, M. Sierka, A. V. Virovets, M. Scheer, *Angew. Chem. Int. Ed.* **2010**, *49*, 6860–6864.

[60] C. M. Hoidn, D. J. Scott, Daniel, R. Wolf, *Chem. Eur. J.* **2020**.

[61] a) P. J. Fagan, W. A. Nugent, *J. Am. Chem. Soc.* **1988**, *110*, 2310–2312; b) W. Tumas, J. A. Suriano, R. L. Harlow, *Angew. Chem. Int. Ed. Engl.* **1990**, *29*, 75–76; c) K. M. Doxsee, G. S. Shen, C. B. Knobler, *J. Am. Chem. Soc.* **1989**, *111*, 9129–9130.

[62] a) T. Wettling, B. Geissler, R. Schneider, S. Barth, P. Binger, M. Regitz, *Angew. Chem. Int. Ed. Engl.* **1992**, *30*, 758–759; b) T. Wettling, J. Schneider, O. Wagner, C. G. Kreiter, M. Regitz, *Angew. Chem. Int. Ed. Engl.* **1989**, *28*, 1013–1014; c) P. Binger, T. Wettling,

R. Schneider, F. Zurmühlen, U. Bergsträsser, J. Hoffmann, G. Maas, M. Regitz, *Angew. Chem. Int. Ed. Engl.* **1991**, *30*, 207–210.

[63] B. M. Cossairt, M. C. Diawara, C. C. Cummins, *Science* **2009**, *323*, 602.

[64] a) C. Schwarzmaier, M. Sierka, M. Scheer, *Angew. Chem. Int. Ed.* **2013**, *52*, 858–861; b) C. Schwarzmaier, A. Y. Timoshkin, M. Scheer, *Angew. Chem. Int. Ed.* **2013**, *52*, 7600–7603.

[65] A. E. Seitz, M. Eckhardt, A. Erlebach, E. V. Peresypkina, M. Sierka, M. Scheer, *J. Am. Chem. Soc.* **2016**, *138*, 10433–10436.

2 Research Objectives

As presented in the introduction the concept of transfer reactions gives the possibility for the synthesis of so far not accessible polypnictogen ligand complexes. The first objective is the search for a suitable starting material for the transfer of a polypnictogen unit. Prior works showed the high potential of the zirconium complexes [Cp''$_2$Zr($\eta^{1:1}$-E_4)] (E = P, As) to release the pnictogen unit in presence of halogenated reaction partners. Furthermore, in 2017 *A. E. Seitz* made reports on the synthesis of the triple decker complex [(Cp''Zr)$_2$(μ,$\eta^{1:1:1:1:1:1}$ Sb_6)]. Compared to already known results, this antimony complex could be used to transfer the antimony unit to later transition metals and gain Sb_n ligand complexes with unprecedented structural motifs. Accordingly, the first research objective of this work focused on:

- Transfer of polypnictogen moieties from zirconium to nickel fragments starting from [Cp''$_2$Zr($\eta^{1:1}$ E_4)] (E = P, As)
- Determination of the influence of reaction condition and steric impacts on the reaction outcome during the transfer of the E_4 units from [Cp''$_2$Zr($\eta^{1:1}$-E_4)] (E = P, As) to nickel fragments
- Usage of the zirconium-based Sb_n ligand complex [(Cp''Zr)$_2$(μ,$\eta^{1:1:1:1:1:1}$-Sb_6)] to transfer the polyantimony unit to iron, cobalt and nickel for the preparation of Sb_n ligand complexes with unprecedented structural motifs

Besides the transfer of intact polypnictogen units of [Cp''$_2$Zr($\eta^{1:1}$-E_4)] (E = P, As), also the functionalization is of great interest to possibly modify the chemical properties and learn about their reactivity. Therefore, the second research objective deals with:

- Investigation of the coordination behavior of [Cp''$_2$Zr($\eta^{1:1}$-As_4)] towards lewis acidic transition metal complexes and main group compounds
- Reactivity of [Cp''$_2$Zr($\eta^{1:1}$-E_4)] (E = P, As) towards nucleophiles

Furthermore, only a few examples of Sb_n ligand complexes are known so far. One reason for this is the lack of suitable antimony sources, which can be used for the synthesis. It was of special interest to synthesize novel Sb_n ligand complexes to expand the spectrum. For this reason, the last research objective deals with:

- Synthesis of Sb_n ligand complexes using Cp*$_4$$Sb_4$ and $KSb(SiMe_3)_2$ as antimony sources.

3 E_4 Transfer (E = P, As) to Ni Complexes

V. Heinl, M. Schmidt, M. Eckhardt, M. Eberl, A. E. Seitz, G. Balázs, M. Seidl, M. Scheer, *Chem. Eur. J*. **2021**, *27*, 11647-11655. (DOI: 10.1002/chem.202101119)

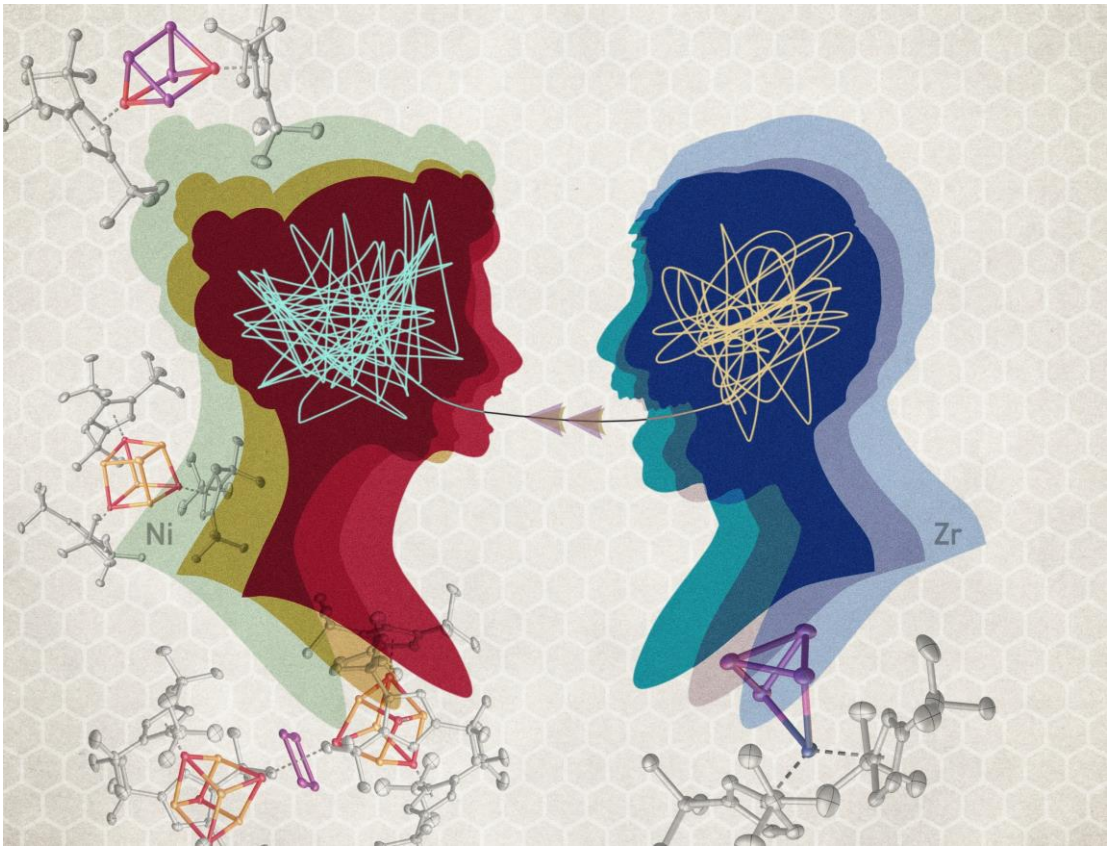

Abstract:

The utilization of $[Cp''_2Zr(\eta^{1:1}\text{-}E_4)]$ (E = P (**1a**), As (**1b**), Cp'' = 1,3-di-tertbutyl-cyclopentadienyl) as phosphorus or arsenic source, respectively, gives access to novel stable polypnictogen transition metal complexes at ambient temperatures. The reaction of **1a/1b** with $[Cp^RNiBr]_2$ (Cp^R = Cp^{Bn} (1,2,3,4,5-penta-benzyl-cyclopentadienyl), Cp''' (1,2,4-tri-tertbutylcyclopenta-dienyl)) was studied, to yield novel complexes depending on steric effects and stoichiometric ratios. Besides the transfer of the complete E_n unit, a degradation as well as aggregation can be observed. Thus, the prismane derivatives $[(Cp'''Ni)_2(\mu,\eta^{3:3}\text{-}E_4)]$ (**2a** (E = P); **2b** (E = As)) or the arsenic containing cubane $[\{(Cp'''Ni)_3(\mu_3\text{-}As)(As_4)]$ (**5**) are formed. Furthermore, the bromine bridged cubanes of the type $[(Cp^RNi)_3\{Ni(\mu\text{-}Br)\}(\mu_3\text{-}E)_4]_2$ (Cp^R = Cp''': **6a** (E = P), **6b** (E = As), Cp^R = Cp^{Bn}: **8a** (E = P), **8b** (E = As)) can be isolated. Here, a stepwise transfer of E_n units is possible, with a cyclo-E_4^{2-} ligand being introduced and unprecedented triple-decker compounds of the type $[\{(Cp^RNi)_3Ni(\mu_3\text{-}E)_4\}_2(\mu,\eta^{4:4}\text{-}E'_4)]$ (Cp^R = Cp^{Bn}, Cp'''; E/E' = P, As) are obtained.

3.1 Author Contribution

- Synthesis and complete characterization of the compounds **6b**, **10a**, and **11a**. Improved Synthesis of the compounds **4**, **5**, **6a** and **10b** as well as completed characterization of **2b**, **4**, **5**, **9a** and **10b** were performed by V. Heinl.
- Synthesis and complete characterization of the compounds **8a**, **8b**, **12a** and **12b** were performed by M. Schmidt during her Ph.D. thesis (University of Regensburg, **2016**).
- First Synthesis and parts of the characterization of the compounds **2b**, **4** and **5** were performed by M. Eckhardt during her Ph.D. thesis (University of Regensburg, **2014**).
- First synthesis and characterization of the compounds **2a** and **6a** were performed by M. Eberl during her Ph.D. thesis (University of Regensburg, **2011**).
- First synthesis and parts of the characterization of the compounds **9a** and **10b** were performed by A. E. Seitz
- Computational studies were performed by G. Balázs.
- M. Seidl recalculated the X-ray structures.
- The Manuscript was written by V. Heinl except parts of the computational details (G. Balázs).
- Supervision: M. Scheer.

3.2 Introduction

The synthesis and reactivity of polypnictogen transition metal complexes is an active field of research. Since their first discovery in the 1970s, a huge variety of such compounds has been synthesized so far.[1,2,3] In general, conventional synthetic methods such as the co-thermolysis or photolysis are used for their synthesis to convert white phosphorus and yellow arsenic, respectively, in the presence of corresponding transition metal complexes. These conversions often proceed under harsh conditions and, hence, the thermodynamically most stable compounds are obtained, which, however, usually results in an uncontrolled degradation and rearrangement of the E_4 tetrahedra. A mild activation would be of great interest since it allows the synthesis of metastable compounds. This is in line with recent activities of mild activation and fixation of small molecules such as H_2, N_2, NH_3 or CO_2,[4] triggering a selective bond cleavage. For instance, recent studies have shown the ability of complexes containing β-diiminato ligands (L) to activate small molecules such as N_2 or P_4.[5,6–9] Depending on the metal center and ligand design, white phosphorus is cleaved at r.t. in different ways by forming dinuclear complexes such as $[(LM)_2\{(P_2)_2\}]$, $[(LM)_2(P_4)]$ and $[(LM)_4(P_8)]$ (M = Ni, Fe, Co).[6–10] Further examples in which only one P-P bond is opened are the formation of the butterfly complexes $[\{Cp^RFe(CO)_2\}_2(\mu,\eta^{1:1}\text{-}E_4)]$ (Cp^R = Cp''' (1,2,4-tri-tertbutyl-cyclopentadienyl), Cp^{BIG}

(pentakis-(4-*n*-butyl-phenyl)cyclopentadienyl)) and [{Cp*Cr(CO)$_3$}$_2$(μ,η$^{1:1}$-E$_4$)] (Cp* = penta-methylcyclopentadienyl) by the reaction of E$_4$ (E = P, As) with metal carbonyl dimers.[11] By using the toluene complex [(Cp'''Co)$_2$(μ,η$^{4:4}$-C$_7$H$_8$)], it is possible to break two P-P bonds simultaneously in E$_4$ either into two E$_2$ dumbbells to give the triple-decker complexes [(Cp^{R}Co)$_2$(μ,η$^{2:2}$-E$_2$)$_2$] (E = P, As, Cp^R= Cp''', Cp*),[12] or compounds containing a *cyclo*-P$_4$ unit as end-deck as in [(Cp'''Co)(η^4-P$_4$)][13,14] or in [{CpRu(PPh$_3$)$_2$}{CoCp'''}-(μ,η$^{1:4}$-P$_4$)][CF$_3$SO$_3$] and [{Cp^{BIG}Mn(CO)$_2$}$_2${CoCp'''}(μ,η$^{1:1:4}$-P$_4$}], respectively.[14]

Beside a mild activation, the challenge is to avoid thermodynamic control to receive kinetic products of polypnictogen complexes. Therefore, the use of transfer reagents could be of advantage. These reactions proceed under very mild conditions and higher yields and selectivities can be achieved.[2,3,15] One interesting example was reported by *Russel et al.* by reacting [Cp$_2$Zr(η$^{1:1}$-(C^{t}Bu)$_2$P$_2$)] with ECl$_3$ (E = P, As, Sb) to obtain C$_2$^{t}Bu$_2$P$_2$ECl. Subsequent reactions lead to the formation of the cationic mixed-element compound [C$_2$^{t}Bu$_2$P$_2$E]$^+$.[16]

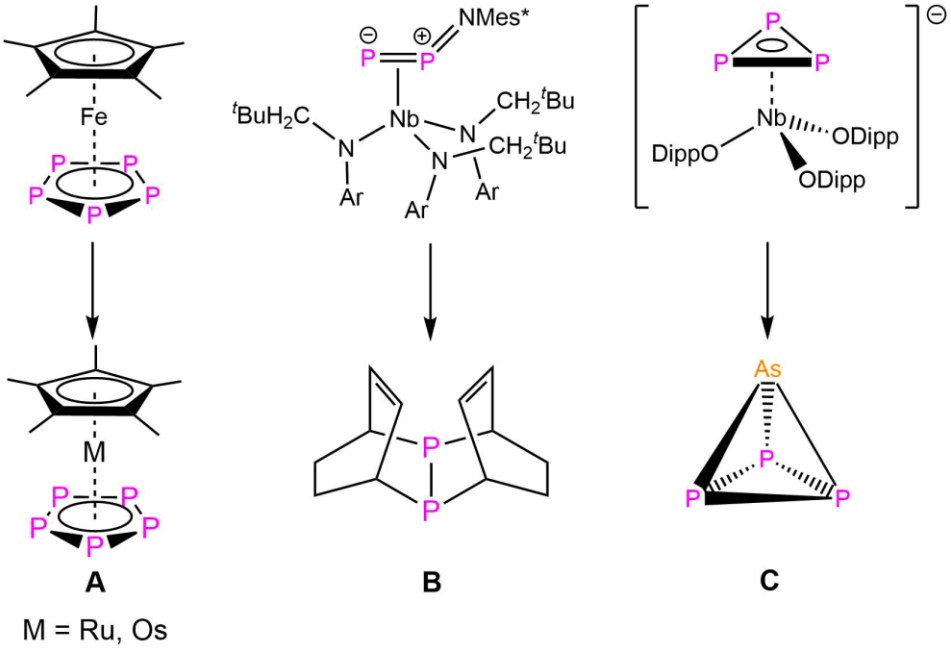

Scheme 1: Selected reactions using transfer reactions.

Pentaphosphaferrocene [Cp*Fe(η^5-P$_5$)] was also used to transfer a *cyclo*-P$_5$ unit from iron to its heavier homologues ruthenium and osmium, respectively (**A**, Scheme 1).[17] Moreover, *Cummins et al.* described the synthesis of the diphosphaazide complex [(η^2-Mes*NPP)Nb(N[CH$_2$^{t}Bu]Ar)$_3$] (Mes* = 2,4,6-tri-*tert*-butyl-phenyl, Ar = 3,5-Me$_2$C$_6$H$_3$), which upon heating liberates a P$_2$ unit that can be trapped with 1,3-cyclohexadiene to give **B** (Scheme 1).[18] In 2009, they reported the transfer of a P$_3$$^{3-}$ unit to AsCl$_3$ to form the neutral interpnictogen modification AsP$_3$ (**C**, Scheme 1).[19] Another remarkable example is the 2-phosphaethynolat anion [OCP$^-$] which can act as a P$^-$-transfer reagent.[20] For instance, using

Na[OCP] *Grützmacher et. al.* showed the transfer of a P_1 unit by the reaction with the imidazolium salt [^{Dipp}NHC-H][Cl] to form [^{Dipp}NHC=PH] (^{Dipp}NHC = 1,3-bis(2,6-di-isopropyl)imidazol-2-ylidene).[21]

In contrast, our group was interested in developing pnictogen- rich transfer reagents. For instance, we used the zirconium butterfly complexes [Cp''$_2$Zr(μ,η$^{1:1}$-E_4)] (E = P (**1a**),[22] As (**1b**),[23] Cp'' = 1,2-di-tertbutyl-cyclopentadienyl) as phosphorus and arsenic sources to transfer E_4^{2-} units to avoid e.g. the difficult handling of yellow As. Thus, it was possible to transfer the polypnictogen unit to LSi-moieties (L = PhC(N^{t}Bu)$_2$) to form heteroaromatic sila-phospha and -arsa derivatives of benzene.[24] Furthermore, iron triple-decker complexes were formed by the reaction of **1b** with [Cp'''FeBr]$_2$. In this case, arsenic bonds were broken to form bonding isomers of [(Cp'''Fe)$_2$(μ,η$^{4:4}$-As_4)] possessing either a *cyclo*-As_4 or tetraarsabutadiene ligand as middle deck.[23] Since, with Cp^{R}Fe-fragments only one type of products was obtained, the question arose if, with the 15 VE Cp^{R}Ni-moieties, also a selective transfer of a whole E_4 unit from **1a,b** can be achieved or whether fragmentation occurs, because such fragments only need a cyclo-E_3 unit to fulfil the 18 VE rule.[25] This intrigued us to study the reaction behavior of **1** towards [Cp^{R}NiBr]$_2$ (R = Cp^{Bn}, Cp'''), also in view of much better yields, if known products are formed for which a low yield synthesis is reported. Herein, we report on the selective transfer of an E_4 unit to Cp^{R}Ni fragments and the formation of unprecedented triple-decker-like complexes built up by Ni_4E_4 cubanes.

3.3 Results and Discussion

The reaction of **1a** with *in situ* generated [Cp'''NiBr]$_2$ in thf in a 1:1.3 stoichiometry leads to the formation of the prismane derivative [(Cp'''Ni)$_2$(μ,η$^{3:3}$-P_4)] (**2a**) and the *cyclo*-P_3 complex [Cp'''Ni(η^3-P_3)] (**3**) (Scheme 2). In comparison, the reaction of **1b** with [Cp'''NiBr]$_2$ yields the arsenic prismane [(Cp'''Ni)$_2$(μ,η$^{3:3}$-As_4)] (**2b**) and the dimeric cubane derivative [{(Cp'''Ni)$_3$Ni(μ$_3$-As)$_4$}$_2$(μ,η$^{4:4}$-As_4)] (**4**) (Scheme 2). Compounds **2** and **3** are reminiscent of the already reported compounds [Cp^{R}Ni(η^3-P_3)] (Cp^R = Cp*, Cp$^{4i\text{Pr}}$) and [(Cp$^{4i\text{Pr}}$Ni)$_2$(μ,η$^{3:3}$-E_4)] (E = P, As), respectively, obtained by cothermolysis methods, but here in much better yields.[26,27] Their full characterization is given in the supporting information. In the case of **2**, the whole E_4 unit of the starting material is transferred to two [Cp'''Ni] fragments to form an E_4-chain. In contrast, compound **4** consists of two [Ni_4As_4] subunits linked by a *cyclo*-As_4^{2-} unit and represents the first nickel complex coordinated by a *cyclo*-E_4 unit. All nickel atoms except one in the hetero cubane are coordinated by a Cp''' ligand. The origin of the nickel atom which does not bear a Cp''' substituent is not undoubtedly clear, but it might originate from the [$NiBr_2$·dme] used for the synthesis of [Cp'''NiBr]$_2$. To answer this question, the direct reaction of two equiv. of isolated [Cp'''NiBr]$_2$ with one equiv. of **1b** was performed, leading to the

formation of the entirely different reaction product [(Cp'''Ni)$_3$(μ$_3$-As)(As$_4$)] (**5**, Scheme 2), which is similar to the cubane [(Cp*Ni)$_3$(μ$_3$-As)(As$_4$)] reported by *Scherer* et al, but obtained in much better yields (74 vs 55%).[26] However, this result indicates that the nature of the [Cp'''NiBr]$_2$ source is crucial for the reaction progress.

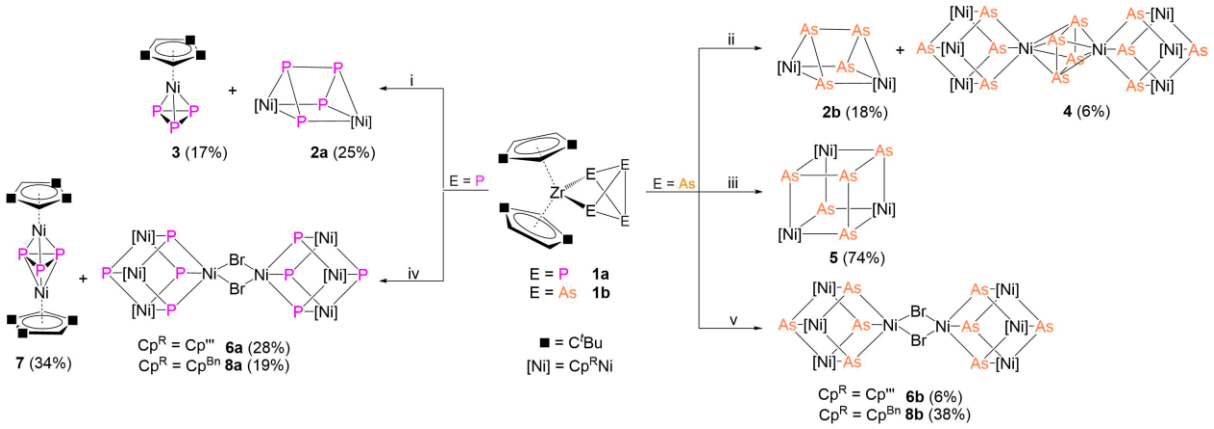

Scheme 2: Overview of the reactions of [Cp''$_2$Zr(η$^{1:1}$-E$_4$)] (**1a**: E = P; **1b**: E = As) with [Cp^{R}NiBr]$_2$ (R = Cp^{Bn}, Cp'''). i,ii: Reactions with 1.3 equiv. of *in situ* prepared [Cp'''NiBr]$_2$ in *n*-hexane; iii: Reaction with two equiv. of isolated [Cp'''NiBr]$_2$ in thf; iv: Reaction with 1.5 equiv. of [Cp'''NiBr]$_2$ and one equiv. of [NiBr$_2$·dme] in thf or with two equiv. of *in situ* prepared [Cp^{Bn}NiBr]$_2$ in toluene; v: Reaction with 1.5 equiv. of *in situ* prepared [Cp'''NiBr]$_2$ and one equiv. of [NiBr$_2$·dme] in thf or with two equiv. of *in situ* prepared [Cp^{Bn}NiBr]$_2$ in toluene. In all cases, [Cp''$_2$ZrBr$_2$] is eliminated, which is omitted for clarity.

To investigate this reaction behavior in more detail, the reaction of **1a** and **1b** with 1.5 equiv. [Cp'''NiBr]$_2$ and one equivalent of [NiBr$_2$·dme] was carried out, wherein the novel dimeric compounds [(Cp'''Ni)$_3${Ni(μ-Br)}(μ$_3$-E)$_4$]$_2$ (E = P (**6a**), E = As (**6b**)) are formed (Scheme 2).[28] In comparison to **4**, they also consist of two [Ni$_4$E$_4$] units which are bridged by two bromine atoms. Obviously, the [NiBr]-units in **6** originate from [NiBr$_2$·dme]. Interestingly, in the phosphorus case, also the triple-decker complex [(Cp'''Ni)$_2$(η$^{3:3}$-P$_3$)] (**7**) is formed.

To examine the influence of the Cp ligand on the reaction we, also investigated the reaction behavior of **1** towards [Cp^{Bn}NiBr]$_2$. The reaction of **1** with *in situ* generated [Cp^{Bn}NiBr]$_2$ in thf leads to the formation of [(Cp^{Bn}Ni)$_3${Ni(μ-Br)}(μ$_3$-E)$_4$]$_2$ (E = P: **8a**, E = As: **8b**).

After column chromatographic workup and layering a dichloromethane solution with acetonitrile (**4**) or *n*-hexane (**6a**, **6b**, **8a**, **8b**), crystals of the dimeric cubanes suitable for single crystal X-ray diffraction analysis are obtained. The molecular structures of **6a** and **6b** are exemplified in Figure 1 (**4**, **8a** and **8b** are depicted in the SI).

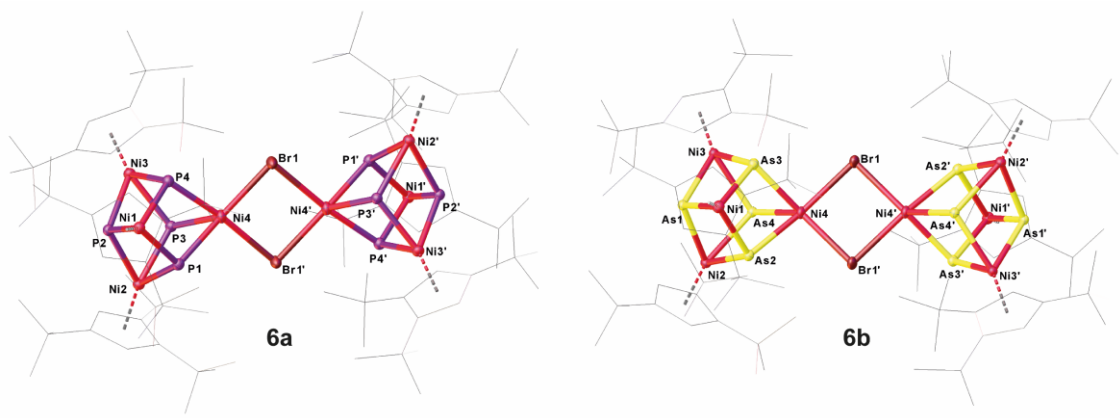

Figure 1: Molecular Structure of **6a** (left) and **6b** (right) in the solid state with thermal ellipsoids at 50% probability level. Hydrogen atoms are omitted and the Cp''' ligands are drawn in the wire frame model for clarity.

The molecular structures of **6a** and **6b** are exemplified in Figure 1 (**4**, **8a** and **8b** are depicted in the SI). They consist of two cubanes linked by two bromine ligands. The central [Ni_2Br_2] ring is slightly asymmetric (**6a**, **6b**, **8a**, **8b**), showing a kite-like distortion. In **6a**, two slightly different Ni-Br distances of 2.432(2) Å and 2.467(2) Å exist. This trend can also be observed for the compounds **6b**, **8a** and **8b**. Usual bromine-bridged nickel compounds show Ni-Br distances in the same range.[29] The square faces of the cubanes show a kite-like distortion, which can be ascribed to the steric demand of the bulky Cp''' and Cp^{Bn} ligands, respectively. Bond angles and bond lengths within the cubanes are similar to the reported values for known cubanes.[26,30] The short E···E distances within the cubanes (**6a**/**8a**: 2.5406(7) Å to 2.7048(6) Å; **6b**/**8b**: 2.7736(3) Å to 3.0186(3) Å) are remarkable. Even if they are longer than a usual single bond they are shorter than the sum of the van der Waals radii (P: 3.8 Å; As: 4.0 Å), indicating an E···E interaction.[31] The bonding interactions between the phosphorus atoms are also supported by the Mayer bond index (0.256 to 0.358) and localized orbitals (cf. SI, for more details exemplified for **9a** see vide infra).

The spectroscopic data of the compounds **2a**, **3** and **7** are in agreement with the reported data of related compounds (*cf.* SI).[26,27,32] The $^{31}P\{^{1}H\}$ NMR spectrum of **6a** at room temperature shows a broad singlet at δ = 169.3 ppm and a hardly resolved quartet at δ = 113.0 ppm. In order to detect a possible dynamic behavior in solution, ^{31}P NMR studies at different temperatures were carried out (Figure 2). By decreasing the temperature, both signals sharpen and, at -60 °C, they reveal a doublet and a quartet being in agreement with the solid-state structure of **6a** (Figure 1, left) and corresponding to an AX_3 spin system with a $^{2}J_{PP}$ coupling constant of 18.3 Hz. The VT-NMR investigations confirm the presumption of a dynamic behavior. In contrast, the $^{31}P\{1H\}$ NMR spectrum of the Cp^{Bn}-substituted compound **8a** shows two sharp singlets at δ = 130.8 ppm and δ = 194.1 ppm, which are shifted downfield compared to **6a**. Even at low temperatures, no further splitting can be observed. The divergent behavior

can be explained by the less steric bulk of the Cp^{Bn} ligands. Indeed, DFT calculations show that the dissociation of the model complex $[(CpNi)_3(NiBr)(\mu_3\text{-}P)_4]_2$ into the monomeric species $[(CpNi)_3(NiBr)(\mu_3\text{-}P)_4]$ is with 76.75 $kJ \cdot mol^{-1}$ disfavored. The steric bulk of the Cp''' substituents can, however, enforce the dissociation.

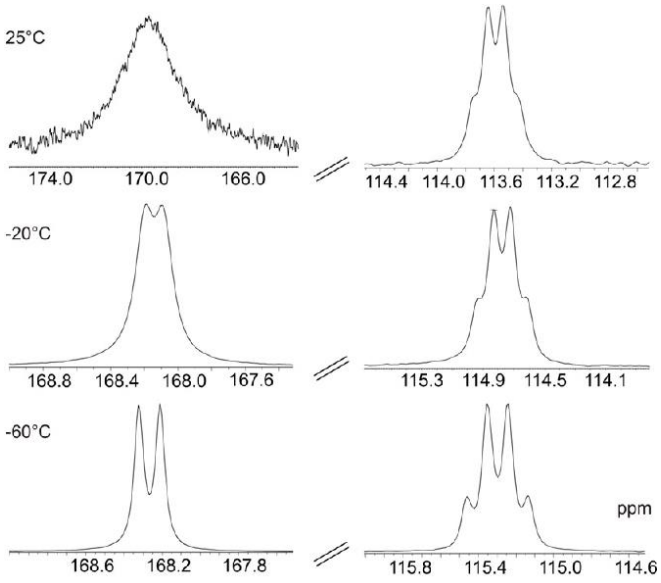

Figure 2: Sections of the $^{31}P\{^1H\}$ NMR spectrum of **6a** at different temperatures.

The presence of the bromide ligands in **6** and **8** enables the possibility of further functionalization. In view of the formed product **4**, a selective synthesis came into mind by a further transfer of a whole E_4 unit of **1** to the compounds **6** and **8**. Thus, the reaction of **6** and **8** with one equivalent of **1a** or **1b** results in the formation of the unprecedented triple-decker complexes $[\{(Cp^RNi)_3Ni(\mu_3\text{-}P)_4\}_2(\mu,\eta^{4:4}\text{-}E_4)]$ (Cp^R = Cp''', E = P: **9a**; Cp^R = Cp^{Bn}, E = P: **10a**, E = As: **10b**) and $[\{(Cp^RNi)_3Ni(\mu_3\text{-}As)_4\}_2(\mu,\eta^{4:4}\text{-}E_4)]$ ((Cp^R = Cp''': E = P: **11a**, E = As: **4**; Cp^R = Cp^{Bn}, E = P: **12a**, E = As: **12b**) (Scheme 3). In all these reactions, the E_4 unit in **1** is well transferred as a *cyclo*-E_4^{2-} unit, which bridges two $[Ni_4E_4]$ fragments. By this method, we successfully demonstrated that triple-decker complexes are accessible, even with different group 15 elements.

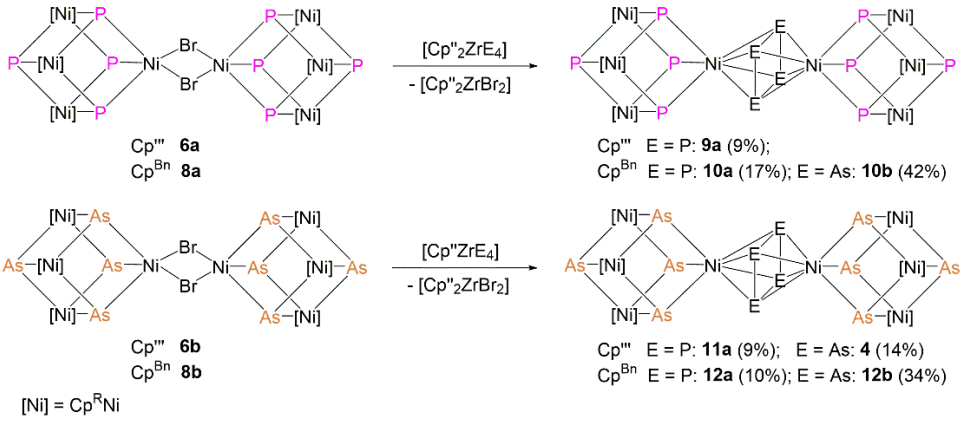

Scheme 3: Overview of the reactions of **6a**, **8a**, **6b** and **8b** with another equivalent of [Cp"$_2$Zr($\eta^{1:1}$-E$_4$)] (E = P (**1a**), As (**1b**)).

After column chromatographic workup and layering a dichloromethane solution with *n*-hexane or acetonitrile, crystals of the dimeric cubanes (**9a**, **10a**, **10b**, **11a**, **4**, **12a**, **12b**) suitable for single crystal X-ray diffraction analysis are obtained.[33] The molecular structures of the compounds **9a**, **11a** and **4** are depicted in Figure 3 (Figures of **10a**, **10b**, **12a** and **12b** are depicted in the SI).

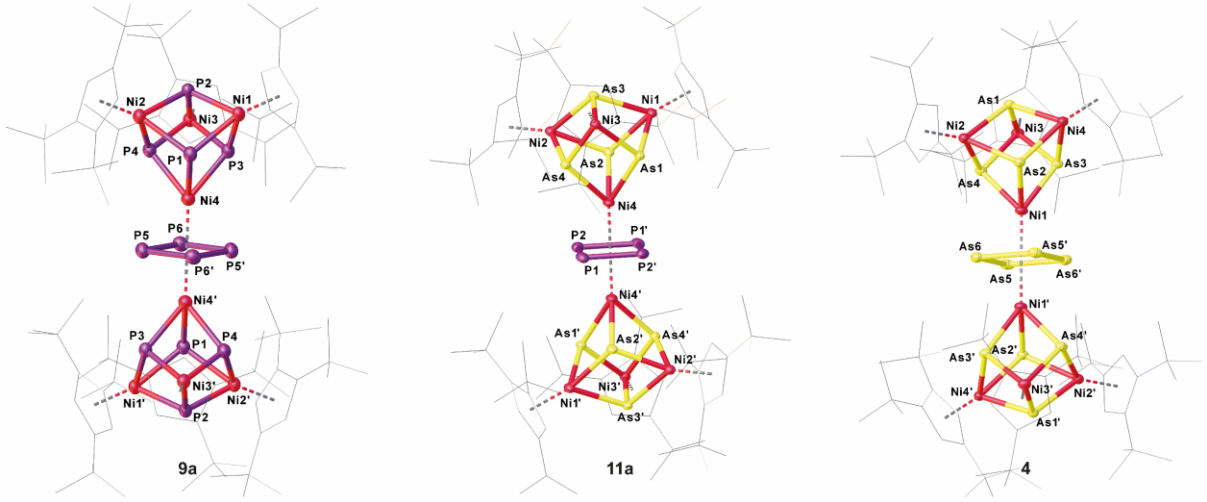

Figure 3: Molecular structure of **9a** (left), **11a** (middle) and **4** (right)in the solid state. Hydrogen atoms and solvent molecules are omitted and the Cp''' ligands are drawn in the wire frame model for clarity.

Their structural motif is exemplified based on the molecular structure of **9a**. They consist of two cubanes linked by a planar and almost rectangular *cyclo*-E$_4$ unit. Similar to the dimeric bromine-bridged cubanes they show also a kite-like distortion of the cage, due to the bulky Cp''' and Cp^{Bn} ligands. The bond angles and bond lengths within the cubanes are in the range of values reported for similar compounds[26,30] The Ni-P distances to the E$_4$ moiety of 2.3705(14) Å to 2.4193(15) Å are slightly elongated compared to the distances within the cubane. There are two slightly different P-P distances of 2.1982(18) Å and 2.2110(18) Å within

the E_4-ring, which are in the range of a single bond.[34] This, and the natural charge distribution (vide infra), indicates that a *cyclo*-E_4^{2-} moiety is present. The observed trend is also present in the other dimeric cubanes (**10a**, **10b**, **11a**, **4**, **12a**. **12b**). A comparison can also be drawn to the 'free' *cyclo*-E_4 moieties of the compounds $[K_2(18\text{-crown-}6)_2][P_4]\cdot 3NH_3$ and $[K_2(18\text{-crown-}6)_2][As_4]$ described by *Korber et al*., showing E-E distances in the same range (E = P: 2.160(2) Å to 2.172(2) Å; E = As: 2.3871(4) Å to 2.3898(4) Å).[35] Complexes containing a *cyclo*-E_4^{2-} unit are rare and usually the moiety is end-on coordinated, like in the complexes $[Cp''Ta(CO)_2(\eta^4\text{-}P_4)]$ or $[Cp^*Nb(CO)_2(\eta^4\text{-}As_4)]$.[36,37] The bond distances of such examples are in between a single and a double bond.[36,37,38] Also comparable triple-decker complexes with a *cyclo*-E_4 middle deck, for instance the ionic cobalt complexes $[(Cp'''Co)_2(\mu,\eta^{4:4}\text{-}E_4)][X]$ (E = P, As, X = BF_4, $[Al\{OC_6F_{10}(C_6F_5)\}_3]$)[39] or the cobalt β-diiminato compound $[(L^{Dipp}Co)_2(\mu,\eta^{4:4}\text{-}As_4)]$ (L = $CH[CHN(2,6\text{-}^iPr_2C_6H_3)]_2$), show distances in between a single and a double bond (E = P: 2.1837(8) Å to 2.3139(6) Å; E = As: 2.23299(5) Å to 2.5198(2) Å).[40] The slight elongation of the E-E bond distances of the *cyclo*-E_4 moiety of the compounds given here can be attributed to the bridging $\mu,\eta^{4:4}$-coordination to the more bulky $[Ni_4E_4]$ cubanes. The P-P and As-As distances within the cubanes (**9a**/**10a**: 2.6027(15) Å to 2.725(2) Å, **4**/**11a**/**12a**/**12b**: 2.78276(4) Å to 2.9707(4) Å) are still longer than a normal single bond but shorter than the sum of the van der Waals radii, indicating interactions between the pnictogen atoms (*cf.* SI).[31] This is also confirmed by DFT calculations (TPSSh/def2-TZVP level of theory, *cf.* SI). The Mayer bond index for the P···P interactions between P1, P3 and P4 vary from 0.31 to 0.38, for the P···P interactions involving P2 these are lower and vary from 0.28 to 0.31 (labeling according to Figure 3). The origin of the P2···P interactions is based on the P-Ni bonding orbitals to which contributions from the neighboring phosphorus atoms are mixed. The in-phase overlap of the P1, P3 and P4 orbitals with the nickel orbitals leads to a sigma-type Ni4-P bonding and to the relatively strong P···P bonding interaction. This can be nicely seen by the visualization of the localized molecular orbitals (Figure 4). The bonding interactions between the phosphorus atoms are also supported by the Electron Localization Function and Localized Orbital Locator analysis (*cf.* SI). Based on the natural charge distribution, for the model compound $[(CpNi)_3\{Ni(\mu_3\text{-}P)_4\}_2(\mu,\eta^{4:4}\text{-}P_4)]$, the *cyclo*-$P_4$ unit can be viewed as a *cyclo*-P_4^{2-} ligand (nat. charge: −0.57). The Ni-Ni distances in the $[Ni_4E_4]$ cubanes are too long to be indicative for considerable Ni-Ni interactions. This is also confirmed by the very low Mayer bond orders (*cf. SI*).

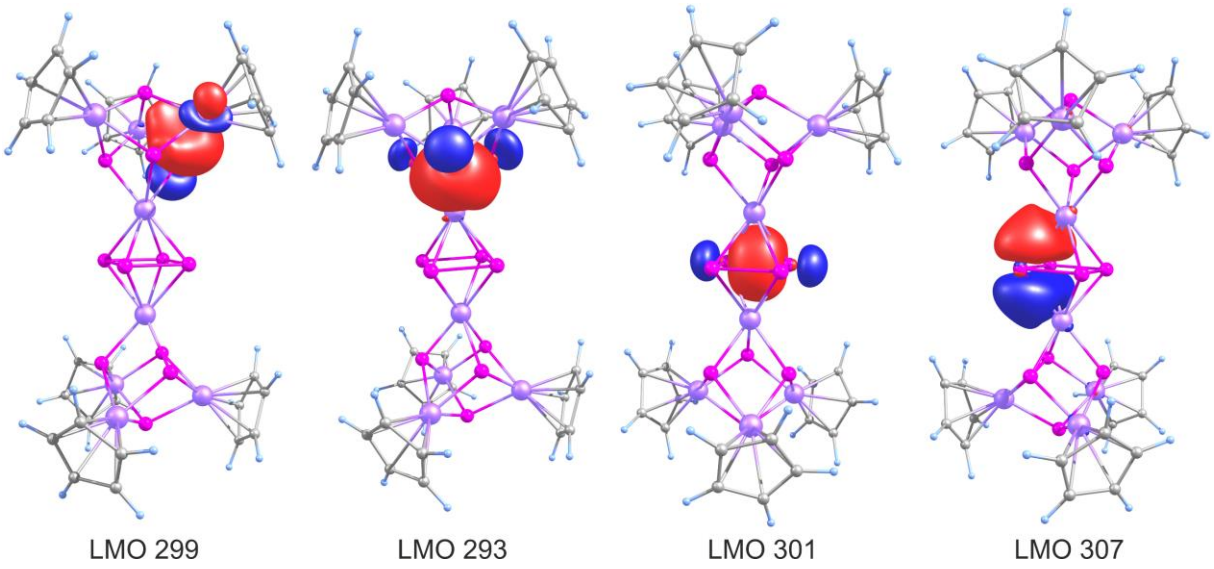

Figure 4: Selected localized molecular orbitals representing the Ni-P bonding (LMO 229 and 293) and the σ (LMO 301) and π (LMO 307) orbitals of the cyclo-P_4 unit in the model compound $[\{(CpNi)_3Ni(\mu_3\text{-}P)_4\}_2(\mu,\eta^{4:4}\text{-}P_4)]$ at the TPSSh/def2-TZVP level of theory.

Furthermore, for **9a**, **10a**, **10b**, **11a**, **4**, **12a** and **12b**, NMR investigations were carried out. The ^{1}H and $^{13}C\{^{1}H\}$ NMR spectra of these compounds show the corresponding sets of signals for the Cp''' or Cp^{Bn} ligands. Interestingly, compound **9a** shows three well-resolved signals in the $^{31}P\{^{1}H\}$ NMR spectrum already at room temperature (Figure 5). The observed signals at δ = 169.1 ppm, 122.8 ppm and 58.4 ppm can be assigned to an $A_4M_6X_2$ spin system. The phosphorus atoms P_X couple with three P_M atoms to give the quartet at δ = 58.4 ppm with a coupling constant of $^{2}J_{PP}$ = 16.8 Hz. Due to the coupling of the four P_A atoms of the *cyclo*-P_4^{2-} ligand with six equivalent P_M atoms, a septet at δ = 169.1 ppm with a coupling constant of $^{2}J_{PP}$ = 23.8 Hz arises. Furthermore, a coupling of the six P_M atoms in **9a** to the P_X as well as the P_A atoms results in a rather broad, unresolved multiplet at δ = 122.8 ppm. The ^{31}P NMR spectroscopic data clearly shows that the solid-state structure of **9a** is retained in solution.

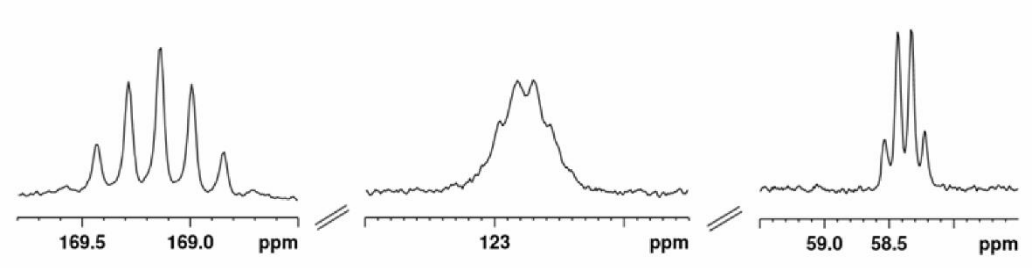

Figure 5: Sections of the $^{31}P\{^{1}H\}$ NMR spectrum of **9a** at r.t.

While the $^{31}P\{^{1}H\}$ NMR spectrum of **10b** shows two singlets (δ = 159.6 ppm, δ = 126.8 ppm), the $^{31}P\{^{1}H\}$ NMR spectrum for **10a** shows a further splitting due to the *cyclo*-P_4^{2-} middle deck. A singlet at δ = 118.7 ppm can be assigned to the atoms P2/P2', while the quintet at δ = 168.3

ppm and the septet at δ = 163.9 ppm can be assigned to an A_6X_4 spin system with a coupling constant of $^2J_{PP}$ = 27.4 Hz. For the compounds **11a** and **12a** containing a *cyclo*-P_4^{2-} middle deck, the $^{31}P\{^1H\}$ NMR spectra display one singlet (**11a**: δ = 149.5 ppm, **12a**: δ = 148.3 ppm).

3.4 Conclusion

In conclusion, we were able to show that the transfer of a complete E_4 unit by the reaction of $[Cp''_2Zr(\eta^{1:1}\text{-}E_4)]$ (E = P (**1a**), As (**1b**)) with $[Cp^RNiBr]_2$ (R = Cp^{Bn}, Cp''') leads to the formation of novel and unprecedented polypnictogen nickel complexes in high yields. Applying the concept of transfer reactions, the difficult handling and toxicity of white phosphorus and especially yellow arsenic can be eluded and metastable, otherwise not accessible, products can be prepared. By studying the reactivity of **1** towards $[Cp^RNiBr]_2$ (R = Cp^{Bn}, Cp'''), depending on the steric effects, reaction conditions and stoichiometry used, the polypnictogen units are transferred leading to products with different structural motifs. Thus, the reaction of **1** with *in situ* generated $[Cp^RNiBr]_2$ and, in the case of **6a**/**6b**, additional $[NiBr_2{\cdot}dme]$ leads to the formation of novel bromide-bridged cubanes $[(Cp^RNi)_3\{Ni(\mu\text{-}Br)\}(\mu_3\text{-}E)_4]_2$ (Cp^R = Cp''': **6a** (E = P), **6b** (E = As), Cp^R = Cp^{Bn}: **8a** (E = P), **8b** (E = As)). By further reactions with another equivalent of **1**, it was possible to transfer another E_4 unit as a *cyclo*-E_4^{2-} ligand, which is stabilized by two nickel-cage fragments to build up the unprecedented triple-decker-like complexes **4**, **9**, **10**, **11a** and **12**, containing also mixed polypnictogen ligands. Hence, we were able to transfer complete E_4 units to Cp^RNi fragments although they are known to need only 3VE to fulfill the nobel gas rule and prefer the formation of complexes with a *cyclo*-E_3 unit. Therefore, the use of $[Cp''_2Zr(\mu,\eta^{1:1}\text{-}E_4)]$ (**1a**: E = P, **1b**: E = As) as transfer reagents opens an improved and easily accessible way to create novel metastable polypnictogen ligand complexes.

3.5 Supporting Information

3.5.1 Experimental Detail

All experiments were performed under an atmosphere of dry nitrogen or argon using schlenk and glovebox techniques. Solvents were purified, dried and degassed prior use. ^{1}H, ^{13}C and ^{31}P NMR spectra were recorded at room temperature on a Bruker Avance 400 spectrometer (^{1}H: 400,130 MHz, ^{31}P: 161,976 MHz, ^{13}C: 100.613 MHz) and on a Bruker Advance 300 spectrometer (1H: 300,132 MHz, ^{31}P: 121,495 MHz, ^{13}C: 75.468 MHz). ^{1}H, ^{13}C and ^{31}P NMR chemical shifts are reported in parts per million (ppm) relative to external standards Me_4Si or H_3PO_4 (85%). Elemental analysis was determined with a Vario micro cube apparatus. For mass spectrometry a Finnigan MAT 95 (LIFDI MS, FD MS), Finnigan MAT SSQ 710 A (EI MS) or a ThermoQuest Finnigan MAT TSQ 7000 device were used. NaCp''',[41] $Cp^{Bn}H$,[42] [$NiBr_2$·dme],[43] [$Cp''_2Zr(\eta^{1:1}\text{-}P_4)$],[44] [$Cp''_2Zr(\eta^{1:1}\text{-}As_4)$],[45] were synthesized as reported in the literature.

Preparation of $[Cp'''NiBr]_2$:[46]

A solution of NaCp''' (1.20 g, 4.68 mmol) in dme is added to a suspension of [$NiBr_2$·dme] (1.50 g, 4.90 mmol) in dme at –30 °C. The solution is stirred for 2 h at –30 °C and additional 2 h at room temperature. After removing the solvent, the red residue is dissolved in *n*-hexane (20 mL) and filtered via canula. The solution is concentrated to approx. 10 mL and stored at –30 °C. Yield: 0.756 g (1.22 mmol, 52%)

Preparation of $[(Cp'''Ni)_2(\mu,\eta^{3:3}\text{-}P_4)]$ (2a) and $[Cp'''Ni(\eta^3\text{-}P_3)]$ (3):

A solution of NaCp''' (259 mg, 1.01 mmol) in thf is added to a suspension of [$NiBr_2$·dme] (312 mg, 1.01 mmol) in thf at –30 °C. The solution is stirred for 2 h at –30 °C and additional 2 h at room temperature. After removing the solvent, the red residue is dissolved in *n*-hexane (20 mL) and filtered via canula to yield a highly air sensitive red solution of $[Cp'''NiBr]_2$. Accordingly, a solution of $[Cp''_2Zr(\eta^{1:1}\text{-}P_4)]$ (**1a**) (430 mg, 0.755 mmol) is added and stirred for 12 h at room temperature. The solvent of the the dark brown reaction mixture is removed *in vacuo*. Subsequent column chromatographic workup (SiO_2, *n*-pentane, 1.5 x 30 cm) afforded $[Cp''_2ZrBr_2]$ as first fraction. Using *n*-pentane, an orange-red fraction of **3**, followed by a dark brown fraction of **2a** can be obtained. Crystals of **2a** and **3** suitable for single crystal X-ray diffraction analysis can be obtained by storing a concentration solution in *n*-pentane at –30 °C. Yield: **2a**: 135 mg (0.191 mmol, 25%); **3**: 49 mg (0.13 mmol, 17%)

2a: **^{1}H NMR** (C_6D_6, 298 K): *δ* [ppm] = 1.38 (s, 9 H, C(*CH*$_3$)$_3$), 1.48 (s, 18 H, C(*CH*$_3$)$_3$), 5.37 (s, 2 H, $C_5H_2^tBu_3$). **^{13}C{^{1}H} NMR** (C_6D_6, 298 K): *δ* [ppm] = 31.7 (s, *C*(CH$_3$)$_3$), 32.2 (s, *C*H$_3$), 33.5 (s, *C*(CH$_3$)$_3$), 34.1 (s, *C*H$_3$), 92.3 (s, *C*H), 117.7 (s, *C*C(CH$_3$)$_3$), 118.7 (s, *C*C(CH$_3$)$_3$); **^{31}P{^{1}H} NMR** (C_6D_6, 298 K): *δ* [ppm] = 68.2 (s). **FD MS** (toluene): *m*/*z* (%): 706.2 (M$^+$, 81) 644.3 (M$^+$-2P, 99); **Elemental analysis** (%): calculated for [$C_{34}H_{58}Ni_2P_4$] (708.06 g·mol^{-1}): C, 57.67; H, 8.26; found: C, 57.34; H, 8.37.

3: Analytical data are in agreement with the literature.[47]

Preparation of [(Cp'''Ni)$_2$(μ,η$^{3:3}$-As$_4$)] (2b) and [{(Cp'''Ni)$_3$Ni(μ$_3$-As)$_4$}$_2$(μ,η$^{4:4}$-As$_4$)] (4):

A solution of NaCp''' (259 mg, 1.01 mmol) in thf is added to a suspension of [NiBr$_2$·dme] (313 mg, 1.01 mmol) in thf at –30 °C. The solution is stirred for 2 h at –30 °C and additional 2 h at room temperature. After removing the solvent, the red residue is dissolved in *n*-hexane (20 mL) and filtered via canula to yield a highly air sensitive red solution of [Cp'''NiBr]$_2$. Accordingly, a solution of [Cp''$_2$Zr(η$^{1:1}$-As$_4$)] (**1b**) (566 mg, 0.761 mmol) is added and stirred for 12 h at room temperature. The solvent of the the dark brown reaction mixture is removed *in vacuo*. Subsequent column chromatographic workup (SiO_2, *n*-hexane, 1.5 x 30 cm) afforded [Cp''$_2$ZrBr$_2$] as first fraction. Changing the solvent to toluene a brown fraction of **2b,** changing the solvent to CH_2Cl_2 a third fraction containing **4** is eluted. Crystals of **2b** and **4** suitable for single crystal X-ray diffraction analysis can be obtained by storing a concentrated CH_2Cl_2 solution at –30 °C. Crystalline yield: **2b**: 122 mg (0.14 mmol, 18% reffered to **1b**); **4**: 40 mg (0.02 mmol, 6%)

2b: **^{1}H NMR** (C_6D_6, 298 K): *δ* [ppm] = 1.43 (s, 28 H, C(*CH*$_3$)$_3$), 5.38 (s, 2 H, $C_5H_2^tBu_3$); **^{13}C{^{1}H} NMR** (C_6D_6, 298 K): *δ* [ppm] = 32.0 (s, *C*(CH$_3$)$_3$), 32.6 (*C*H$_3$), 33.5 (s, *C*(CH$_3$)$_3$), 34.3 (s, *C*H$_3$), 91.4 (s, *C*H), 116.2 (*C*C(CH$_3$)$_3$), 118.6 (*C*C(CH$_3$)$_3$); **EI MS** (toluene, 70 eV): *m*/*z* (%): 881.9 (M$^+$, 1.2), 515.9 ([Cp'''NiAs$_3^+$], 8); **FD MS** (toluene): *m*/*z* (%): 881.9 (M$^+$); **Elemental analysis** (%): calculated for [$C_{34}H_{58}As_4Ni_2$] (883.90 g·mol^{-1}): C, 46.20; H, 6.61; found: C, 46.55; H, 6.48.

4: The analytical data for compound **4** is described below.

Preparation of [(Cp'''Ni)$_3$Ni(μ$_3$-As)(As$_4$)] (5):

A solution of [Cp'''NiBr]$_2$ (185 mg, 0.248 mmol) in thf is added to a solution of [Cp''$_2$Zr(η$^{1:1}$-As$_4$)] (**1b**) (100 mg, 0.134 mmol) in thf and stirred for 1 d at room temperature. After removing the solvent *in vacuo*, the red-brown residue is purified by column chromatographic workup (SiO_2, 15 x 2 cm). A dark brown fraction of **5** is eluted with *n*-hexane as solvent, followed by a light

red fraction of [Cp''$_2$ZrBr$_2$]. Crystals of **5** suitable for single crystal X-ray diffraction analysis can be obtained by storing a concentrated *n*-hexane solution at –30 °C. Crystalline yield: 124 mg (0.0993 mmol, 74%)

5: **^{1}H NMR** (thf-d$_8$, 298 K): *δ* [ppm] = 1.33 (s, 9 H, C(*CH*$_3$)$_3$), 1.46 (s, 9 H, C(*CH*$_3$)$_3$), 5.06 (s, 2 H, C$_5$*H*$_2$^{t}Bu$_3$), **^{1}H NMR** (C$_6$D$_6$, 298 K): *δ* [ppm] = 1.55 (s, 19 H, C*CH*$_3$), 1.56 (s, 18 H, C*CH*$_3$), 5.11 (s, 2 H, C$_5$*H*$_2$^{t}Bu$_3$), **^{13}C{^{1}H} NMR** (C$_6$D$_6$, 298 K): *δ* [ppm] = 31.8 (s, *C*(CH$_3$)$_3$), 32.5 (s, *C*H$_3$), 33.8 (s, *C*(CH$_3$)$_3$), 34.0 (s, *C*H$_3$), 89.5 (s, *C*H), 118.1 (s, *C*C(CH$_3$)$_3$), 118.9 (s, *C*C(CH$_3$)$_3$); **EI MS** (*n*-hexane, 70 eV): *m*/*z* (%): 1249.6 (M$^{+\cdot}$, 1.5), 881.9 ([Cp'''$_2$Ni$_2$As$_4$$^+$], 9.1), 516.1 ([Cp'''NiAs$_3$$^+$], 25.5); **LIFDI MS** (toluene): *m*/*z* (%): 1250.12 (M$^{+\cdot}$100); **Elemental analysis** (%):calculated for [C$_{51}$H$_{87}$As$_5$Ni$_3$] (1250.92 g·mol^{-1}): C, 48.97; H, 7.01; found: C, 48.72; H, 6.79.

Preparation of [(Cp'''Ni)$_3${Ni(μ-Br)}(μ$_3$-P)$_4$]$_2$ (6a) and [(Cp'''Ni)$_2$(μ,η$^{3:3}$-P$_3$)] (7):

A solution of [Cp''$_2$Zr(η$^{1:1}$-P$_4$)] (**1a**) (250 mg, 0.439 mmol) in thf is added to a suspension of [NiBr$_2$·dme] (135 mg, 0.441 mmol) and [Cp'''NiBr]$_2$ (500 mg, 0.676 mmol) in thf. The colour turns immediately to dark brown. After stirring for 2 h at room temperature, the solvent was removed *in vacuo* and the residue is purified by column chromatographic workup (SiO$_2$, *n*-hexane, 2.5 x 10 cm). With *n*-hexane as solvent a yellow fraction [Cp''$_2$ZrBr$_2$] is eluted followed by a green fraction of [(Cp'''Ni)$_2$(μ,η$^{3:3}$-P$_3$)] (**7**). Using toluene a brown fraction of [(Cp'''Ni)$_3${Ni(μ-Br)}(μ$_3$-P)$_4$]$_2$ (**6a**) is afforded. Crystals of **6a** suitable for single crystal X-ray diffraction analysis can be obtained by layering a CH$_2$Cl$_2$ solution with *n*-hexane. Yield: **6a**: 131 mg (0.0577 mmol, 33%), **7**: 101 mg (0.149 mmol, 34%)

6a:**^{1}H NMR** (CD$_2$Cl$_2$, 298 K): *δ* [ppm] = 1.18 (s, 54 H, C(*CH*$_3$)$_3$), 1.56 (s, 108 H, C(*CH*$_3$)$_3$), 5.30 (s, br, 12 H; C$_5$*H*$_2$^{t}Bu$_3$); **^{13}C{^{1}H} NMR** (CD$_2$Cl$_2$, 298 K): *δ* [ppm] = 31.5 (s, *C*(CH$_3$)$_3$), 31.6 (s, *C*H$_3$), 33.9 (s, *C*(CH$_3$)$_3$), 34.2 (s, *C*H$_3$), 90.8 (s, *C*H), 121.9 (s, *C*C(CH$_3$)$_3$); **^{31}P{^{1}H} NMR** (C$_6$D$_6$, 298 K): *δ* [ppm] = 168.9 (s, br), 113.0 (s, br); **^{31}P NMR** (CD$_2$Cl$_2$, 298 K): *δ* [ppm] = 169.3 (s, br (ω$_{1/2}$ = 423.0 Hz), 3 P), 113.6 (q, 1 P); **^{31}P{^{1}H} NMR** (CD$_2$Cl$_2$, 213 K): *δ* [ppm] = 168.3 (d, $^2J_{PP}$ = 18.3 Hz), 115.3 (q, $^2J_{PP}$ = 18.3 Hz); **FD MS** (CH$_2$Cl$_2$): *m*/*z* (%): 1138.1 (1/2 M$^+$, 25); 708.6 ([1/2 M$^+$-NiCp'''-Ni-Br], 99); **Elemental analysis** (%): calculated for [C$_{102}$H$_{174}$Br$_2$Ni$_8$P$_8$] (2277.50 g·mol^{-1}): C, 53.79; H, 7.70; found: C, 53.88; H, 8.04.

7: Analytical data are in agreement with the literature.[47]

Preparation of [(Cp'''Ni)$_3${Ni(μ-Br)}(μ$_3$-As)$_4$]$_2$ (6b):

A solution of NaCp''' (208 mg, 0.813 mmol) in thf is added to a suspension of [NiBr$_2$·dme] (248 mg, 0.810 mmol) in thf at –30 °C. The solution is stirred for 2 h at –30 °C and further 2 h

at room temperature. After removing the solvent, the red residue is dissolved in *n*-hexane and filtered via canula to yield a highly air sensitive red solution of $[Cp'''NiBr]_2$. The solvent is removed again and the residue is deluted in thf. After addition of a suspenstion of $[NiBr_2 \cdot dme]$ in thf (84.0 mg, 0.275 mmol) a solution of $[Cp''_2Zr(\eta^{1:1}\text{-}As_4)]$ (**1b**) (200 mg, 0.269 mmol) in thf is added.The colour turns immediately to dark brown. After stirring for 1 d at room temperature, the solvent is removed *in vacuo* and the residue is purified by column chromatographic workup (SiO_2, *n*-hexane, 2.5 x 10 cm). Using *n*-hexane as solvent a yellow fraction of $[Cp''_2ZrBr_2]$, with toluene as solvent a green fraction of **6b** is obtained. Crystals of **6b** suitable for single crystal X-ray diffraction analysis can be obtained by storing a concentrated Et_2O solution at -30 °C. Crystalline Yield: **6b**: 20 mg ($7.6 \cdot 10^{-3}$ mmol, 6%)

6b:^{1}**H NMR** (thf-d_8, 298 K): δ [ppm] = 1.23 (s, 54 H, C(CH_3)$_3$), 1.59 (s, 108 H, C(CH_3)$_3$), 5.27 (s, br, 12 H, $C_5H_2{}^tBu_3$); **ESI MS** (dme, 120 eV): *m*/*z* (%): 1175.17 ($[Cp'''Ni_3As_4]^+$, 1.2); **elemental analysis** (%): calculated for $[C_{102}H_{174}Br_2Ni_8As_8]$ (2620.05 g·mol^{-1}): C, 46.60; H, 6.67; found: C, 46.69; H, 6.77.

Preparation of $[(Cp^{Bn}Ni)_3\{Ni(\mu\text{-}Br)\}(\mu_3\text{-}E)_4]_2$ (E =P (8a); E = As (8b)):

A solution of *n*-BuLi in *n*-hexane (**8a**: 0.65 mL, c = 1.6 mol/L, 1.04 mmol, **8b**: 0.6 mL, c = 1.6 mol/L, 0.96 mmol) is added dropwise to a solution of $Cp^{Bn}H$ (**8a**: 516 mg, 0.999 mmol, **8b**: 502 mg, 0.97 mmol) in thf at –30 °C. The resulting purple solution is stirred for 1 h at -30 °C and additionally for 1 h at room temperature. Then, the reaction mixture is added dropwise to a suspension of $[NiBr_2 \cdot dme]$ (**8a**: 308 mg, 0.999 mmol; **8b**: 300 mg, 0.981 mmol) in thf at -30 °C. The orange brownish reaction mixture is stirred for 1 h at this temperature and additionally for 1 h at room temperature. The solvent is removed under reduced pressure, the brown oily residue is dissolved in toluene and filtered into a solution of $[Cp''_2Zr(\eta^{1:1}\text{-}E_4)]$ (**1**) (E = P: 142 mg, 0.249 mol, E = As: 181 mg, 0.243 mmol) in toluene. After stirring for 7 days at room temperature, the solvent is removed *in vacuo*. Subsequent column chromatographic workup (SiO_2, *n*-hexane, 15 x 2 cm) afforded $[Cp''_2ZrBr_2]$ as first fraction. A mixture of *n*-hexane/toluene (1:2) yielded a green fraction of **8a** and **8b**, respectively. Crystals of **8a** and **8b** suitable for single crystal X-ray diffraction analysis can be obtained by layering a toluene solution with *n*-hexane. Crystalline Yield: **8a**: 95 mg (0.024 mmol, 19%); **8b**: 196 mg (0.0455 mmol, 37%).

8a: ^{1}**H NMR** (CD_2Cl_2, 298 K): δ [ppm] = 4.14 (s, 60H, CH_2), 6.61 (d, 60H, C_6H_5), 6.81-6.92 (m, 90H, C_6H_5). ^{13}**C{^{1}H} NMR** (CD_2Cl_2, 298 K): δ [ppm] = 32.4 (CH_2), 108.5 (C_5), 125.5 (C_6H_5), 127.8 (C_6H_5), 128.7 (C_6H_5), 139.5 (C_6H_5). **31P{^{1}H} NMR** (CD_2Cl_2, 298 K): δ [ppm] = 194.08 (s), 130.79 (s). ^{31}**P NMR** (CD_2Cl_2, 298 K): δ [ppm] = 194.08 (s), 130.79 (s). **ESI MS** (CH_2Cl_2): m/z (%) = 655.3 (45) $[Cp^{Bn}Ni(CH_3CN)_2]^+$, 614.2 (100) $[Cp^{Bn}Ni(CH_3CN)]^+$, 573.1 (65) $[Cp^{Bn}Ni]^+$.

elemental analysis (%): calculated for [$C_{240}H_{210}Ni_8P_8Br_2$] (3971.38 g/mol): C, 72.58; H, 5.32; found C, 72.43; H, 5.47.

8b: **^{1}H NMR** (CD_2Cl_2, 298 K): δ [ppm] = 4.09 (s, 60H, CH_2), 6.56 (d, 60H, C_6H_5), 6.77-6.91 (m, 90H, C_6H_5). **EI MS** (toluene, 70 eV): m/z (%) = 514.2 (47) ([Cp^{Bn}-H_2]$^+$), 423.2 (17) ([Cp^{Bn}-H_2-C_7H_7]$^+$), 331.1 (10) ([Cp^{Bn}-H_2-2 C_7H_7]$^+$), 242.1 (4) ([Cp^{Bn}-H_2-3 C_7H_7]$^+$, 91.1 (100) ([C_7H_7]$^+$). **Elemental Analysis** (%): calculated for [$C_{240}H_{210}Ni_8As_8Br_2$ · 2 CH_2Cl_2] (4492.83 g/mol): C, 64.69; H, 4.80; found C, 64.82; H, 4.77.

Preparation of [(Cp‴Ni)$_3${Ni(μ$_3$-P)$_4$}$_2$(μ,η$^{4:4}$-E$_4$)] (E = P (9a)):

[(Cp‴Ni)$_3$(μ$_3$-P)$_4${Ni(μ-Br)}]$_2$ (**9a**: 50 mg, 0.022 mmol) and [Cp''$_2$Zr(η$^{1:1}$-E_4)] (**1**) (E = P: 13 mg, 0.022 mmol) are dissolved in toluene. After stirring the reaction mixture for approximately 1 day at room temperature, the solvent is removed *in vacuo*. Subsequent column chromatographic workup (SiO_2, *n*-hexane, 2 x 15 cm) afforded [Cp''$_2$ZrBr_2] as first fraction and with toluene a brown fraction of **9a**. Crystals suitable for single crystal X-ray diffraction analysis can be obtained by layering a CH_2Cl_2 solution with CH_3CN. Crystalline yield: **9a**: 4 mg (2 μmol, 9%).

9a:**^{1}H NMR** (C_6D_6, 298 K): *δ* [ppm] = 1.55 (s, 54 H, C(*C*H$_3$)$_3$), 1.64 (s, 108 H, C(*C*H$_3$)$_3$), 5.54 (12 H, s, br, C_5H_2^{t}Bu$_3$); **^{13}C{^{1}H} NMR** (C_6D_6, 298 K): *δ* [ppm] = 32.0 (s, *C*(CH$_3$)$_3$), 32.1 (s, *C*H$_3$), 33.7 (s, *C*(CH$_3$)$_3$), 34.7 (s, *C*H$_3$), 90.5 (s, *C*H), 120.8 (s, *C*C(CH$_3$)$_3$), 121.0 (s, *C*C(CH$_3$)$_3$); **^{31}P{^{1}H} NMR** (C_6D_6, 298 K): *δ* [ppm] = 58.38 (q, $^2J_{PP}$ = 16.7 Hz), 122.76 (m, ω$_{1/2}$ = 76 Hz) 169.14 (sept, $^2J_{PP}$ = 23.8 Hz); **^{31}P NMR** (C_6D_6, 298 K): *δ* [ppm] = 58.38 (q, $^2J_{PP}$ = 16.7 Hz), 122.76 (q, $^2J_{PP}$ = 19.8 Hz) 169.14 (quint, $^2J_{PP}$ = 23.8 Hz); **LIFDI MS** (toluene): *m*/*z* (%): 2240.5 (M^+, 100).

Preparation of [(Cp^{Bn}Ni)$_3${Ni(μ$_3$-P)$_4$}$_2$(μ,η$^{4:4}$-E$_4$)] (E = P (10a); E = As (10b)):

[(Cp^{Bn}Ni)$_3$(μ$_3$-P)$_4${Ni(μ-Br)}]$_2$ (30 mg, 7.6 μmol) and [Cp''$_2$Zr(η$^{1:1}$-E_4)] (**1**) (E = P: 20 mg, 0.035 mmol, E = As: 30 mg, 0.040 mmol) are dissolved in toluene. After stirring the reaction mixture for approximately 1 day at room temperature, the solvent is removed *in vacuo*. Subsequent column chromatographic workup (SiO_2, *n*-hexane, 15 x 2 cm) afforded [Cp''$_2$ZrBr_2] as first fraction and with toluene a brown fraction of **10a** and **10b**, respectively. Crystals of **10a** and **10b** suitable for single crystal X-ray diffraction analysis can be obtained by layering a CH_2Cl_2 solution with CH_3CN. Crystalline yield: **10a**: 5 mg (1 μmol, 17%); **10b**: 13 mg (3.2 μmol, 42%).

10a: **^{1}H NMR** (CD_2Cl_2, 298 K): δ [ppm] = 4.27 (s, 60H, CH_2), 6.60 (d, 60H, C_6H_5), 6.70-6.95 (m, 90H, C_6H_5). **^{13}C{^{1}H} NMR** (CD_2Cl_2, 298 K): δ [ppm] = 33.1 (*C*H$_2$), 108.7 (*C*$_5$), 126.1 (*C*$_6$H$_5$),

128.4 (C_6H_5), 129.4 (C_6H_5), 140.4 (C_6H_5). **$^{31}P\{^1H\}$ NMR** (CD_2Cl_2, 298 K): δ [ppm] = 118.7 (s), 163.9 (sept, $^2J_{PP}$ = 27.4 Hz), 168.3 (quint, $^2J_{PP}$ = 27.4 Hz). **^{31}P NMR** (CD_2Cl_2, 298 K): δ [ppm] = 118.7 (s), 163.9 (sept, $^2J_{PP}$ = 27.4 Hz), 168.3 (quint, $^2J_{PP}$ = 27.4 Hz). **Elemental analysis** (%): calculated for [$C_{240}H_{210}Ni_8P_{12}$ · 3 CH_2Cl_2] (4178.67 g/mol): C, 69.65, H; 5.20; found C, 69.89; H, 4.71.

10b: **^1H NMR** (CD_2Cl_2): δ [ppm] = 4.23 (s, 60H, CH_2), 6.57 (d, 60H, C_6H_5), 6.70- 6.90 (m, 90H, C_6H_5). **$^{13}C\{^1H\}$ NMR** (CD_2Cl_2): δ [ppm] = 33.09 (CH_2), 108.29 (C_5), 126.01 (C_6H_5), 128.31 (C_6H_5), 129.34 (C_6H_5), 140.35 (C_6H_5). **$^{31}P\{^1H\}$ NMR** (CD_2Cl_2): δ [ppm] = 126.83 (s), 159.59 (s) **^{31}P NMR** (CD_2Cl_2): δ [ppm] = 126.83 (s), 159.59 (s). **Elemental analysis** (%): calculated for [$C_{240}H_{210}Ni_8P_8As_4$] (4102.60 g/mol): C, 70.11; H, 5.15; found C, 70.09; H, 4.93.

Preparation of [(Cp‴Ni)$_3${Ni(μ$_3$-As)$_4$}$_2$(μ,η$^{4:4}$-E$_4$)] (E = P (11a); E = As (4)):

[(Cp‴Ni)$_3$(μ$_3$-As)$_4${Ni(μ-Br)}]$_2$ (**11a**: 57 mg, 0.022 mmol, **4**: 57 mg, 0.022 μmol) and [Cp''$_2$Zr(η$^{1:1}$-E$_4$)] (**1**) (E = P: 13 mg, 0.022 mmol; E = As: 16 mg, 0.022 mmol) are dissolved in toluene. After stirring the reaction mixture for approximately 1 day at room temperature, the solvent is removed *in vacuo*. Subsequent column chromatographic workup (SiO_2, *n*-hexane, 2.5 x 15 cm) afforded [Cp''$_2$ZrBr_2] as first fraction and with toluene a brown fraction of **11a** and **4**, respectively. Crystals suitable for single crystal X-ray diffraction analysis can be obtained by layering a CH_2Cl_2 solution with CH_3CN. Crystalline yield: **11a**: 4 mg (2 μmol, 9%); **4**: 8 mg (3·μmol, 14%).

11a:^{1}**H NMR** (CD_2Cl_2, 298 K): *δ* [ppm] = 1.36 (s, 54 H, C(CH_3)$_3$), 1.42 (s, 108 H, C(CH_3)$_3$), 5.18 (12 H, s, br, $C_5H_2{}^tBu_3$); **$^{31}P\{^1H\}$ NMR** (CD_2Cl_2, 298 K): *δ* [ppm] = 149.5 (s); **^{31}P NMR** (CD_2Cl_2, 298 K): *δ* [ppm] = 149.5 (s); **FD MS** (CH_2Cl_2): *m*/*z* (%): 2591.9 (M^+, 72), 1175.1 ([$C_{51}H_{87}Ni_3As_4$], 100).

4:^{1}**H NMR** (thf-d^8, 298 K): *δ* [ppm] = 1.23 (s, 54 H, CCH_3), 1.58 (s, 108 H, CCH_3), 5.25 (12 H, s, br, $C_5H_2{}^tBu_3$); **FD MS** (toluene): *m*/*z* (%): 2767.5 (M^+); **elemental analysis** (%): calculated for [$C_{102}H_{174}Ni_8As_{12}$ · 2.5 C_7H_8] (2749.81 g/mol): C, 47.86; H, 6.50; found C, 47.93; H, 6.44.

Preparation of [(Cp^{Bn}Ni)$_3${Ni(μ$_3$-As)$_4$}$_2$(μ,η$^{4:4}$-E$_4$)] (E = P (12a); E = As (12b)):

[(Cp^{Bn}Ni)$_3$(μ$_3$-As)$_4${Ni(μ-Br)}]$_2$ (**12a**: 20 mg, 4.6 μmol, **12b**: 25 mg, 5.8 μmol) and [Cp''$_2$Zr(η$^{1:1}$-E$_4$)] (**1**) (E = P: 10 mg, 0.02 mmol, E = As: 20 mg, 0.03 mmol) are dissolved in toluene. After stirring the reaction mixture for approximately 1 day at room temperature, the solvent is removed *in vacuo*. Subsequent column chromatographic workup (SiO_2, *n*-hexane, 10 x 2 cm) afforded [Cp''$_2$ZrBr_2] as first fraction and with toluene or CH_2Cl_2 a brown fraction of **12a** and **12b**, respectively. Crystals of **12a** suitable for single crystal X-ray diffraction analysis

can be obtained by layering a CH_2Cl_2 solution with CH_3CN. Crystals of **12b** are obtained by layering a CH_2Cl_2 solution with *n*-hexane. Crystalline yield: **12a**: 2 mg (0.5 µmol, 10%); **12b**: 8 mg (2 µmol, 34%).

12a: **^{1}H NMR** (CD_2Cl_2, 298 K): δ [ppm] = 4.24 (s, 60H, C*H*$_2$), 6.58 (d, 60H, C$_6$*H*$_5$), 6.75-6.90 (m, 90H, C$_6$*H*$_5$). **^{13}C{^{1}H} NMR** (CD_2Cl_2, 298 K): δ [ppm] = 33.5 (*C*H$_2$), 107.5 (C$_5$), 126.0 (*C*$_6$H$_5$), 128.3 (*C*$_6$H$_5$), 129.3 (*C*$_6$H$_5$), 140.4 (*C*$_6$H$_5$). **^{31}P{^{1}H} NMR** (CD_2Cl_2, 298 K): δ [ppm] = 148.29 (s). **^{31}P NMR** (CD_2Cl_2, 298 K): δ [ppm] = 148.29 (s). **EI MS** (70 eV, toluene): m/z (%) = 514.2 (45) ([Cp^{Bn}-H$_2$]$^+$), 423.2 (20) ([Cp^{Bn}-H$_2$-C$_7$H$_7$]$^+$), 331.1 (11) ([Cp^{Bn}-H$_2$-2 C$_7$H$_7$]$^+$), 241.1 (18) ([Cp^{Bn}-H$_2$ 3 C$_7$H$_7$]$^+$, 91.1 (100) ([C$_7$H$_7$]$^+$). **Elemental analysis** (%): calculated for [$C_{240}H_{210}Ni_8As_8P_4 \cdot CH_2Cl_2$] (4371.98 g/mol): C, 66.21, H; 5.32; found C, 66.29; H, 5.02.

12b: **^{1}H NMR** (CD_2Cl_2, 298 K): δ [ppm] = 4.24 (s, 60H, C*H*$_2$), 6.58 (d, 60H, C$_6$*H*$_5$), 6.75- 6.90 (m, 90H, C$_6$*H*$_5$). **^{13}C{^{1}H} NMR** (CD_2Cl_2, 298 K): δ [ppm] = 32.9 (*C*H$_2$), 106.5 (*C*$_5$), 125.4 (*C*$_6$H$_5$), 127.7 (*C*$_6$H$_5$), 128.7 (*C*$_6$H$_5$), 139.9 (*C*$_6$H$_5$). **EI MS** (toluene, 70 eV): m/z (%) = 514.2 (58) ([Cp^{Bn}-H$_2$]$^+$), 423.2 (17) ([Cp^{Bn}-H$_2$-C$_7$H$_7$]$^+$), 331.1 (10) ([Cp^{Bn}-H$_2$-2 C$_7$H$_7$]$^+$), 241.1 (16) ([Cp^{Bn}-H$_2$-3 C$_7$H$_7$]$^+$, 91.1 (100) ([C$_7$H$_7$]$^+$). **Elemental analysis** (%): calculated for [$C_{240}H_{210}Ni_8As_{12} \cdot 2\ CH_2Cl_2$] (4632.71 g/mol): C, 62.74; H, 4.66; found C, 62.69; H, 4.75.

3.5.3 Crystallographic Data

Crystals suitable for single crystal X-ray diffraction analysis were obtained as described above. The diffraction intensities were collected either on a Gemini Ultra diffractometer equipped with an Atlas^{S2} CCD detector and with a fine-focus sealed Cu-K_α X-ray tube (**2a**, **5**, **6a**, **6b**, **8a**, **10b**, **11a**, **12a**),on a XtaLAB Synergy R, DW system diffractometer equipped with a HyPix-Arc 150 detector and a rotating-anode Cu-K_α X-ray tube (**2b**), a GV50 diffractometer equipped with a Titan^{S2} CCD detector and a micro-focus Cu-K_α X-ray tube (**9a**, **10a, 12b**) or at a SuperNova diffractometer equipped with a Atlas CCD detector and a micro-focus Cu-K_α X-ray tube (**4**, **8b**). Data collection and reduction were performed with **CrysAlisPro** [Version 1.171.32.15 (**6a**), Version 1.171.32.30 (**2a**), Version 1.171.34.34a (**4**), Version 1.171.37.35e (**12b**), Version 1.171.38.42b (**8a**, **8b**, **12a**), Version 1.171.38.43 (**5**, **9a**), Version 1.171.40.14a (**6b**, **10b**, **11a**), Version 1.171.41.76a (**10a**), Version 1.171.41.83a (**2b**)] software package.[48] For the compounds **2b**, **8a**, **8b**, **9a** and **10a** a numerical absorption correction based on a gaussian integration over a multifaceted crystal model and an empirical absorption correction using spherical harmonics as implemented in SCALE3 ABSPACK was applied.[48] For the compounds **5**, **6b**, **11a** and **12a** an analytical numeric absorption correction using a multifaceted crystal model based on expressions derived by R.C. Clark & J.S. Reid. (Clark, R. C. & Reid, J. S. (1995). Acta Cryst. A51, 887-897) and an empirical absorption correction using spherical harmonics, as implemented in SCALE3 ABSPACK scaling algorithm, was applied.[48] For the compounds **2a, 4**, **6a**, **10b** and **12b** a multi-scan absorption correction using spherical harmonics as implemented in SCALE3 ABSPACK was applied.[48] The structures were solved with **Olex2**,[49] using **olex2.solve**[50] (**2a**, **4**, **6a**) or **ShelXT**[51] (**2b**, **5**, **6b**, **8a**, **8b**, **9a**, **10a**, **10b**, **11a**, **12a**, **12b**) and a least-square refinement on F^2 was carried out with **ShelXL**.[52] All non-hydrogen atoms were refined anisotropically. Hydrogen atoms at the carbon atoms were located in idealized positions and refined with isotropic displacement parameters according to the riding model.

Using **Olex2**,[49] all pictures of the respective molecular structures were made.

CCDC reference numbers 2071421 (**2a**), 2071422 (**2b**), 2071423 (**4** · 2 CH_2Cl_2), 2071424 (**5**), 2071425 (**6a**), 2071426 (**6b**), 2071396 (**8a**·· 7 C_7H_8), 2071427 (**8b**·· 6.5 C_7H_8), 2071428 (**9a** · 3 CH_2Cl_2), 2071429 (**10a** · 3 CH_2Cl_2), 2071430 (**11a** · 2 CH_2Cl_2), 2071431 (**12a** · 2.7 CH_2Cl_2) and 2071432 (**12b** · 3 CH_2Cl_2) contain the supplementary crystallographic data for this paper. These data can be obtained free of charge at www.ccdc.cam.ac.uk/conts/retreving.html (or from the Cambridge Crystallographic Data Center, 12 Union Road, Cambridge CB2 1EZ, UK; Fax: (internat.) + 44-1223-336-033; e-mail: deposit@ccdc.cam.ac.uk).

$[(Cp'''Ni)_2(\mu,\eta^{3:3}\text{-}P_4)]$ (2a)

Compound **2a** crystallizes from a concentrated *n*-pentane solution at -30 °C in form of violet plates in the monoclinic space group *P*2/*c*. The asymmetric unit contains one molecule of **2a**.

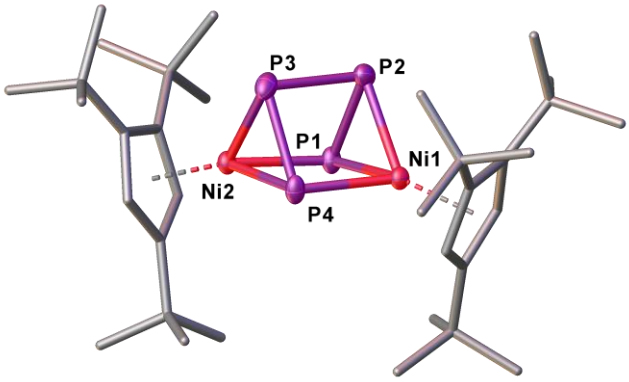

Figure S1: Molecular structure of **2a** in the solid state with thermal ellipsoids at 50% probability level. Hydrogen atoms are omitted and the Cp''' ligands are drawn in the tube model for clarity. Selected bond lengths [Å] and angles [°]: Ni1-P1 2.2388(6), Ni1-P2 2.2472(6), Ni1-P4 2.2281(6), Ni2-P1 2.2282(6), Ni2-P3 2.2416(6), Ni2-P4 2.2399(6), P1-P2 2.1650(7), P2-P3 2.2307(8), P3-P4 2.1678(8), P1-P4 2.6184(7); P2-Ni1-P4 82.95(2), P1-Ni1-P2 57.71(2), Ni1-P1-Ni2 108.05(3), P1-Ni2-P3 82.65(2), P1-Ni2-P4 71.75(2), P3-Ni2-P4 57.86(2), Ni1-P1-P2 61.34(2), P1-Ni1-P4 71.77(2), Ni2-P1-P2 97.00(3), Ni1-P2-P1 60.95(2), Ni1-P2-P3 94.39(3), Ni2-P3-P2 94.75(3), Ni2-P3-P4 61.03(2), Ni1-P4-Ni2 108.01(3), Ni1-P4-P3 96.71(3), Ni2-P4-P3 61.11(2), P1-P2-P3 84.35(3), P2-P3-P4 84.72(3).

$[(Cp'''Ni)_2(\mu,\eta^{3:3}\text{-}As_4)]$ (2b)

Compound **2b** crystallizes from a concentrated CH_2Cl_2 solution at -30 °C in form of red blocks in the monoclinic space group $P2_1/c$. The asymmetric unit contains one molecule of **2b**.

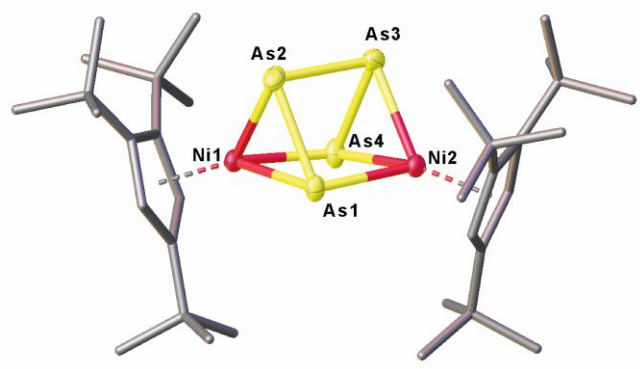

Figure S2: Molecular structure of **2b** in the solid state with thermal ellipsoids at 50% probability level. Hydrogen atoms are omitted and the Cp''' ligands are drawn in the tube model for clarity. Selected bond lengths [Å] and angles [°]: As3-As4 2.4068(3), As3-Ni2 2.3530(4), As3-Ni1 2.3426(4), As2-As1 2.4084(3), As2-Ni2 2.3406(4), As2-Ni1 2.3509(4), As4-As1 2.4589(3), As4-Ni2 2.3423(4), As1-Ni1 2.3410(4); Ni2-As3-As4 58.944(10), Ni1-As3-As4 94.151(12), Ni1-As3-Ni2 107.584(13), Ni2-As2-As1 94.284(12), Ni2-As2-Ni1 107.721(13), Ni1-As2-As1 58.914(11), As3-As4-As1 83.445(9), Ni2-As4-As3 59.383(11), Ni2-As4-As1 92.929(12), As2-As1-As4 83.297(10), Ni1-As1-As2 59.317(11), Ni1-As1-As4 92.839(12), As2-Ni2-As3 70.833(12), As2-Ni2-As4 87.383(13), As4-Ni2-As3 61.673(11), As3-Ni1-As2 70.835(12), As1-Ni1-As3 87.489(13), As1-Ni1-As2 61.768(11).

[{(Cp'''Ni)$_3$Ni(μ_3-As)$_4$}$_2$(μ,$\eta^{4:4}$-As$_4$)] (4)

Compound **4** crystallizes from a concentrated CH_2Cl_2 solution at -30 °C in form of brown blocks in the orthorhombic space group *Pbca*. The asymmetric unit contains half a molecule of **4** and one molecule of toluene, which is disordered over two positions (occupancy 0.56 and 0.44).

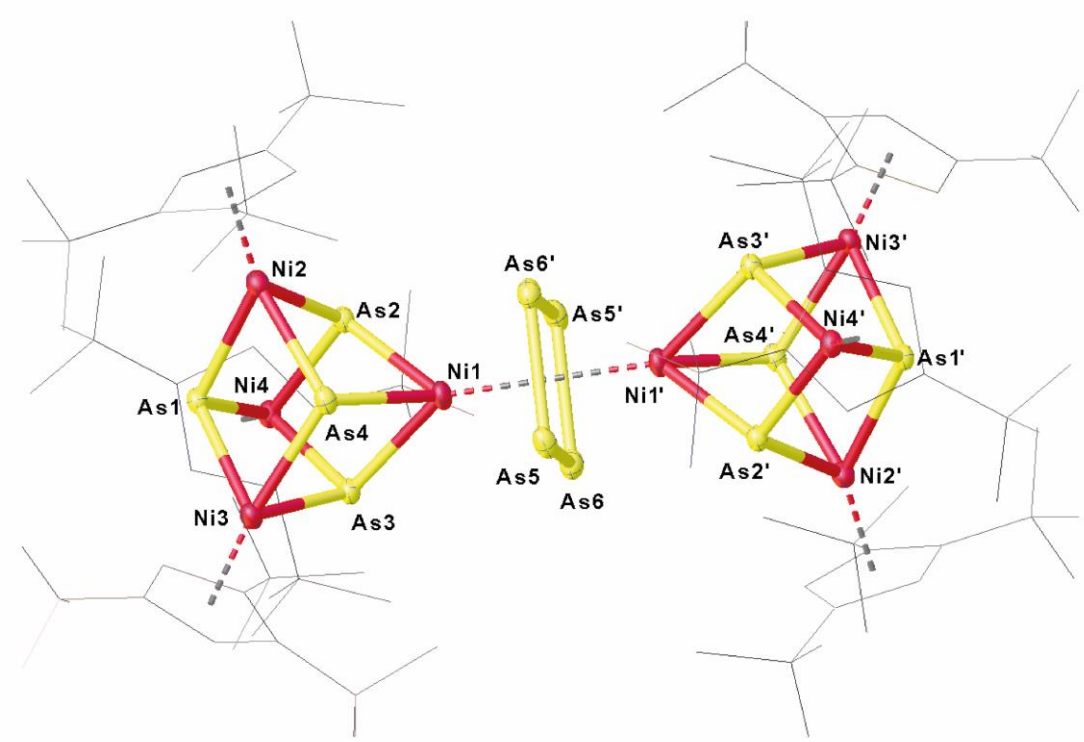

Figure S3: Molecular structure of **4** in the solid state with thermal ellipsoids at 50% probability level. Hydrogen atoms and solvent molecules are omitted and the Cp''' ligands are drawn in the wireframe model for clarity. Selected bond lengths [Å] and angles [°]: As5-As6 2.4282(3), As5-As6' 2.4420(3), Ni1-As5 2.4819(3), Ni1-As6 2.4675(4), Ni1'-As5' 2.4793(3)), Ni1'-As6' 2.5241(4), As1-Ni2 2.3664(3), As3-Ni1 2.3656(3), As1-Ni3 2.3511(3), As3-Ni3 2.3436(3), As1-Ni4 2.3523(3), As3-Ni4 2.3353(3), As2-Ni1 2.3390(3), As4-Ni1 2.3564(3), As2-Ni2 2.3323(3), As4-Ni2 2.3377(4), As2–Ni4 2.3189(3), As4-Ni3 2.3376(3); As6-As5-As6' 90.736(10), As5-As6-As5' 89.261(10), Ni1-As6-Ni1' 92.060(11), Ni1-As5-Ni1' 92.797(11), As2-Ni1-As3 72.587(10), As2-Ni1-As4 77.711(11), Ni2-As1-Ni3 105.576(12), Ni3-As1-Ni4 99.383(12), Ni1-As2-Ni4 106.706(12), As1--Ni2-As4 72.828(11), Ni1–As3–Ni4 105.306(12), As1-Ni3-As3 76.612(11), Ni2-As4-Ni3 106.949(12), As1-Ni3-As4 73.110(11), As1-Ni4-As3 76.748(11), As2-Ni4-As3 73.504(11).

Preparation of [(Cp'''Ni)$_3$Ni(μ$_3$-As)(As$_4$)] (5)

Compound **5** crystallizes from a concentrated *n*-hexane solution at -30 °C in form of brown blocks in the monoclinic space group $P2_1/c$. The asymmetric unit contains two molecules of **5**.

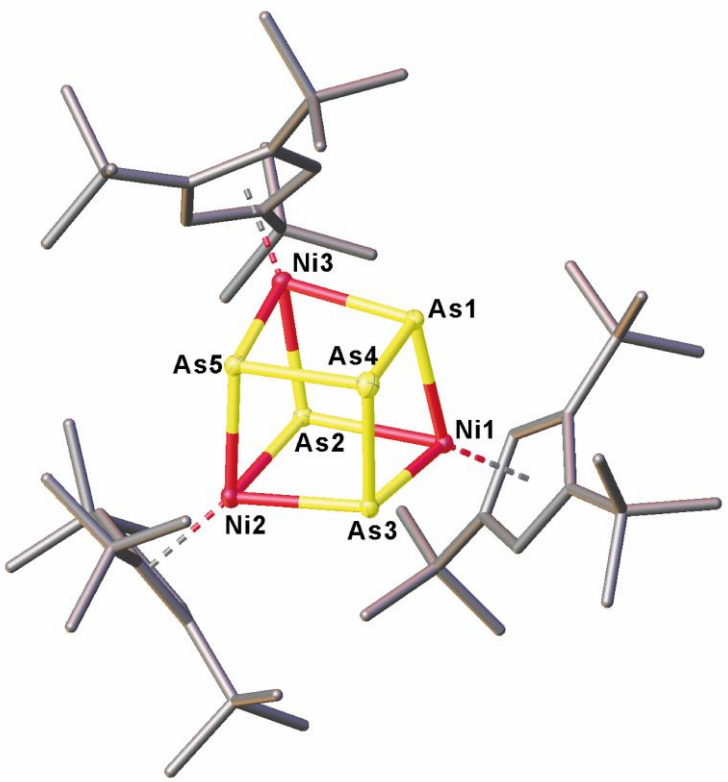

Figure S4: Molecular structure of **5** in the solid state with thermal ellipsoids at 50% probability level. Hydrogen atoms are omitted and the Cp''' ligands are drawn in the tube model for clarity. Selected bond lengths [Å] and angles [°]: As1-As4 2.4551(7), As3-As4 2.4544(8), As5-As4 2.4498(7), Ni3-As1 2.3490(9), Ni3-As5 2.3258(9), Ni2-As3 2.3399(9), Ni2-As5 2.3399(10), Ni1-As1 2.3311(9), Ni1-As3 2.3462(9); As5-As4-As3 80.86(2), As1-As4-As3 80.79(2), As1-As4-As5 79.85(2), As1-Ni3-As2 74.79(3), As1-Ni3-As5 84.66(3), As5-Ni2-As3 85.62(3), As4-As3-Ni1 95.04(3), As4-As3-Ni2 95.46(3), Ni3-As5-As4 97.13(3), Ni3-As2-Ni1 103.95(3), Ni3-As2-Ni2 102.14(3), Ni2-As2-Ni1 104.07(3), As5-Ni2-As2 75.94(3), As1-Ni1-As2 75.01(3), As3- Ni1-As2 74.88(3).

$[(Cp'''Ni)_3\{Ni(\mu\text{-}Br)\}(\mu_3\text{-}P)_4]_2$ (6a)

Compound **6a** crystallizes by layering a CH_2Cl_2 solution with *n*-hexane in form of black prisms in the orthorhombic space group *Pbca*. The asymmetric unit contains half a molecule of **6a**. The bromine atoms are disordered over two positions (occupancy 0.78 and 0.22).

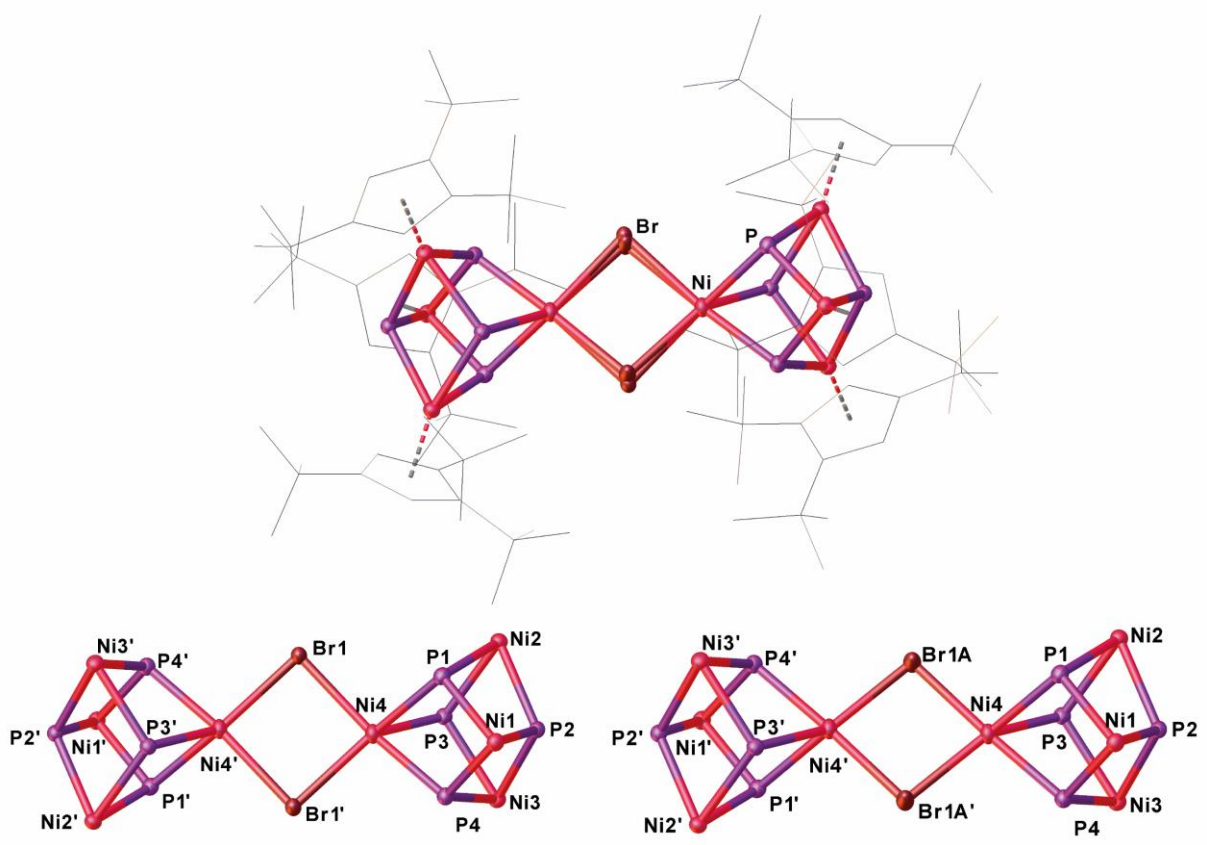

Figure S5: Molecular structure of **6a** in the solid state with thermal ellipsoids at 50% probability level. Hydrogen atoms are omitted and the Cp''' ligands are drawn in the wireframe model for clarity. Depicted are part 1 (left, occupancy of 78%) and part 2 (right, occupancy of 22%). Selected bond lengths [Å] and angles [°]: Br-Ni4 2.432(2), Br'-Ni4 2.467(2), Ni1-P1 2.2101(6), Ni1-P2 2.2421(6), Ni1-P4 2.2187(6), Ni2-P1 2.2149(6), Ni2-P2 2.2675(6), Ni2-P3 2.2043(6), Ni3-P2 2.5687(6), Ni3-P3 2.2014(6), Ni3-P4 2.2188(6), Ni4-P1 2.2065(6), Ni4-P3 2.1990(6), Ni4-P4 2.2083(6); Ni4-Br1-Ni4' 89.02(8), Br1-Ni4-r1' 90.98(8), P1-Ni1-P4 75.25(2), P2-Ni1-P4 70.83(2), P1-Ni2-P2 70.657(19), P1-Ni2-P3 70.19(2), P2-Ni2-P3 70.104(19), P2-Ni3-P3 70.472(19), P3-Ni3-P4 75.08(2), P1-Ni1-P2 71.214(19), Ni1-P1-Ni2 107.42(2), Ni1-P1-Ni4 101.64(2), Ni2-P1-Ni4 107.64(2), Ni1-P2-Ni2 104.54(2), Ni1-P2-Ni3 107.12(2), Ni2-P2-Ni3 104.74(2), Ni2-P3-Ni3 108.61(2), Ni2-P3-Ni4 108.28(2), Ni3-P3-Ni4 101.69(2), Ni1-P4-Ni3 109.07(2).

[(Cp'''Ni)$_3${Ni(μ-Br)}(μ$_3$-As)$_4$]$_2$ (6b)

Compound **6b** crystallizes by storing a concentration Et_2O solution at -30 °C in form of black cubes in the orthorombic space group *Pbca*. The asymmetric unit contains half a molecule of **6b**.

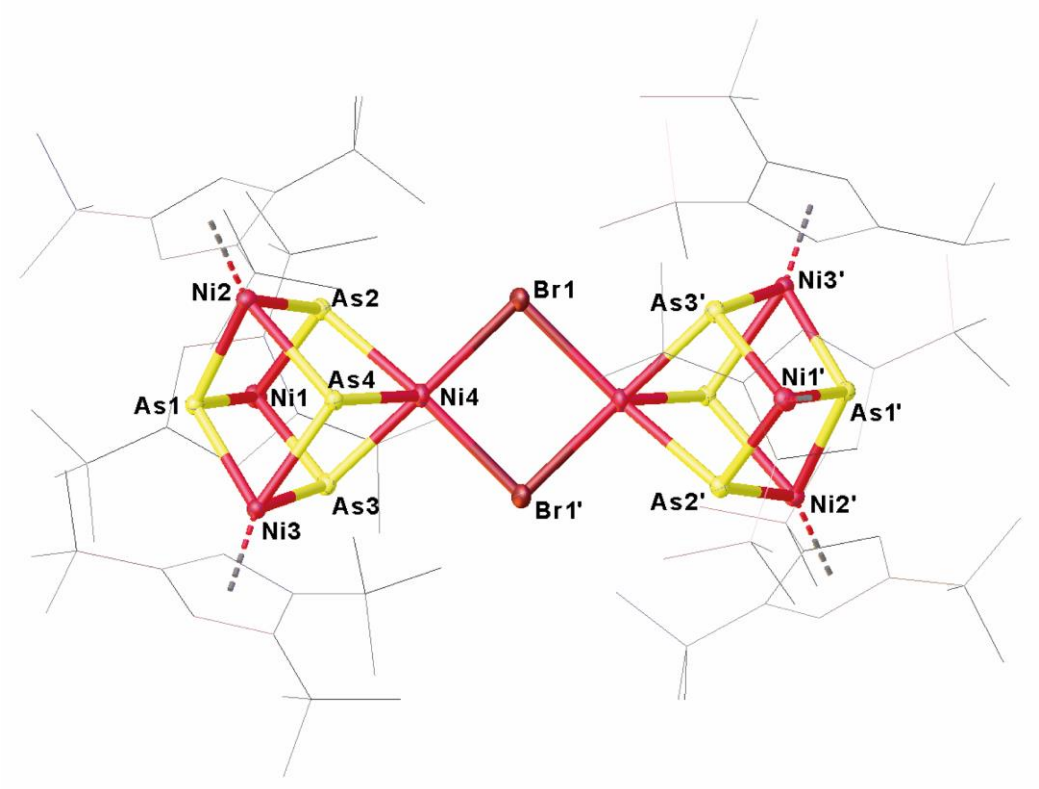

Figure S6: Molecular structure of **6b** in the solid state with thermal ellipsoids at 50% probability level. Hydrogen atoms are omitted and the Cp''' ligands are drawn in the wireframe model for clarity. Selected bond lengths [Å] and angles [°]: Br1–Ni4 2.4153(4), Br1–Ni4' 2.4476(4), As1- Ni3 2.3670(4), As1- Ni2 2.3523(4), As1-Ni1 2.3634(4), As4-Ni3 2.3443(4), As4-Ni2 2.3293(4), As4-Ni4 2.3388(4), As2-Ni2 2.3327(4), As2-Ni4 2.3296(4), As2-Ni1 2.3241(4), As3-Ni3 2.3124(4), As3-Ni4 2.3182(4), As3-Ni1 2.3271(4); Ni4-Br1-Ni4' 90.711(13), Br1-Ni4-Br1' 89.291(12), , Ni2-As1-Ni3 100.052(13), Ni2-As4-Ni3 101.399(13), Ni2-As4-Ni4 105.711(14), Ni4-As4-Ni3 104.217(13), Ni4-As2-Ni2 105.899(14), Ni1-As2-Ni2 105.752(13), Ni1-As2-Ni4 94.245(14), Ni3-As3-Ni4 105.903(14), Ni3-As3-Ni1 108.213(14), Ni4-As3-Ni1 94.470(13), As4-Ni3-As1 74.950(11), As3-Ni3-As1 72.691(12), As3-Ni3-As4 73.702(11), As4-Ni2-As1 75.507(12), As4-Ni2-As2 73.537(12), As2-Ni2-As1 74.246(12), As2-Ni4-As4 73.419(12), As3-Ni4-As4 73.698(11), As3-Ni4-As2 81.005(12), As2-Ni1-As1 74.197(12), As2-Ni1-As3 80.932(12), As3-Ni1-As1 72.498(12).

[(Cp^{Bn}Ni)$_3${Ni(μ-Br)}(μ$_3$-P)$_4$]$_2$ (8a)

Compound **8a** crystallizes by layering a toluene solution with *n*-hexane in form of brown blocks in the triclinic space group $P\bar{1}$. The asymmetric unit contains one molecule of **8a** and seven molecules of toluene. Two of these toluene molecules are disordered over two positions (occupancy: 0.70:0.30; 0.66:0.34). The restraints SADI and SIMU were used during the crystal structure refinement to restrict respective bond lengths and a.d.p. parameters of the atoms belonging to the disordered fragments.

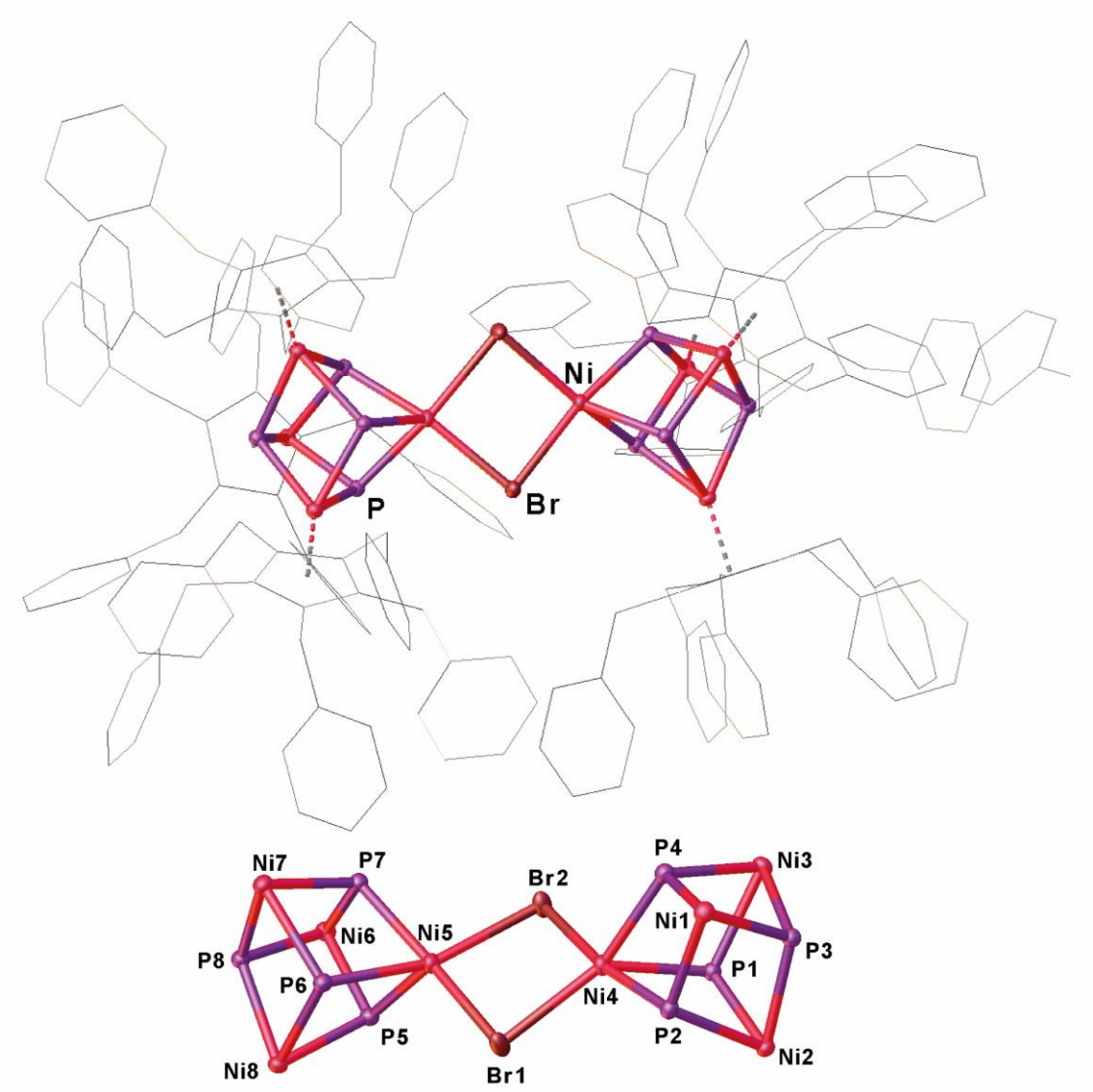

Figure S7: Molecular structure of **8a** in the solid state with thermal ellipsoids at 50% probability level (above). Hydrogen atoms and solvent molecules are omitted and the Cp^{Bn} ligands are drawn in the wireframe model for clarity. Central structural core motif of **8a** (below). Cp^{Bn} ligands are omitted for clarity. Selected bond lengths [Å] and angles [°]: Br2-Ni4 2.4552(3), Br2-Ni5 2.4288(4), Br1-Ni4 2.4204(3), Br1-Ni5 2.4586(3), Ni2-P1 2.1899(5), Ni2-P2 2.2176(5), Ni2-P3 2.2284(5), Ni7-P7 2.2045(5), Ni7-P8 2.2343(5), Ni7-P6 2.2009(5), Ni8-P5 2.1957(5), Ni8-P8 2.2350(5), Ni8-P6 2.2119(5), Ni3-P4 2.2129(5), Ni3-P1 2.1935(5), Ni3-P3 2.2468(5), Ni4-P4 2.2104(5), Ni4-P1 2.2005(5), Ni4-P2 2.2142(5), Ni1-P4 2.1931(5), Ni1-P2 2.2067(5), Ni1-P3 2.2330(5), Ni6-P7 2.2161(5), Ni6-P5

2.1903(5), Ni6-P8 2.2477(5), Ni5-P7 2.2246(5), Ni5-P5 2.1935(5), Ni5-P6 2.2171(5); Ni5-Br2-Ni4 87.958(12), Ni4-Br1-Ni5 88.070(12), Br1-Ni4-Br2 90.503(11), P4-Ni4-Br2 99.205(17), P4-Ni4-Br1 147.353(19), P1-Ni4-Br2 99.679(17), P2-Ni4-Br2 171.588(19), P2-Ni4-Br1 97.904(17) Br2-Ni5-Br1 90.225(11), P7-Ni5-Br2 95.492(17), P7-Ni5-Br1 168.06(2), P5-Ni5-Br2 116.437(18), P5-Ni5-Br1 115.074(17), P6-Ni5-Br2 162.223(19), P6-Ni5-Br1 98.123(17), P1-Ni2-P2 74.002(18), P1-Ni2-P3 72.854(18), P2-Ni2P373.281(19), P7-Ni7-P8 73.007(19), P6-Ni7-P7 74.340(19), P6-Ni7-P8 75.154(18), P5-Ni8-P8 72.943(18), P5-Ni8-P6 74.158(19), P6-Ni8-P8 74.925(18), P4-Ni4-P2 73.815(19), P1-Ni4-P4 71.569(19), P1-Ni4-P2 73.861(18), P4-Ni1-P2 74.300(19), P4-Ni1-P3 74.728(19), P2-Ni1-P3 73.399(18), P7-Ni6-P8 72.533(18), P5-Ni6P7 71.779(18), P5-Ni6-P8 72.796(18), P5-Ni5-P7 71.560(18), P5-Ni5-P6 74.096(19), Ni7-P7-Ni6 106.35(2), Ni7-P7-Ni5 103.62(2), Ni6-P7-Ni5 104.84(2), Ni4-P4-Ni3 105.90(2), Ni1-P4-Ni3 104.16(2), Ni1-P4-Ni4 103.98(2), Ni6-P5-Ni8 106.54(2), Ni6-P5-Ni5 106.79(2), Ni5-P5-Ni8 103.98(2), Ni2-P1-Ni3 106.68(2), Ni2-P1-Ni4 103.64(2), Ni3-P1-Ni4 106.92(2), Ni7-P8-Ni8 102.18(2), Ni7-P8-Ni6 104.28(2), Ni8-P8-Ni6 103.29(2), Ni7-P6-Ni8 104.02(2), Ni7-P6-Ni5 103.99(2), Ni8-P6-Ni5 102.67(2), Ni4-P2-Ni2 102.29(2), Ni1-P2-Ni2 105.96(2), Ni1-P2-Ni4 103.40(2), Ni2-P3-Ni3 103.58(2), Ni2-P3-Ni1 104.70(2), Ni1-P3-Ni3 101.77(2).

[(Cp^{Bn}Ni)$_3${Ni(μ-Br)}(μ$_3$-As)$_4$]$_2$ (8b)

Compound **8b** crystallizes by layering a toluene solution with *n*-hexane in form of brown blocks in the triclinic space group $P\bar{1}$. The asymmetric unit contains one molecule of **8b** and six and a half toluene molecules. Two of these toluene molecules were disordered over two positions (occupancy 0.65 and 0.35) and other toluene molecules were so heavily disordered that the content of solvent molecules per formula unit had to be estimated using a solvent mask. A total of 139 electrons were found in a volume of 968 Å^3 in 14 voids per unit cell. This is consistent with the presence of 1.5 toluene molecules per asymmetric unit, which account for 150 electrons per unit cell. Further, the bromine atoms are disordered over two positions (occupancy 0.98 and 0.02). Furthermore, a benzyl group is disordered over two positions (occupancy 0.6 and 0.4). The restraints SADI and SIMU were used during the crystal structure refinement to restrict respective bond lengths and a.d.p. parameters of the atoms belonging to the disordered fragments.

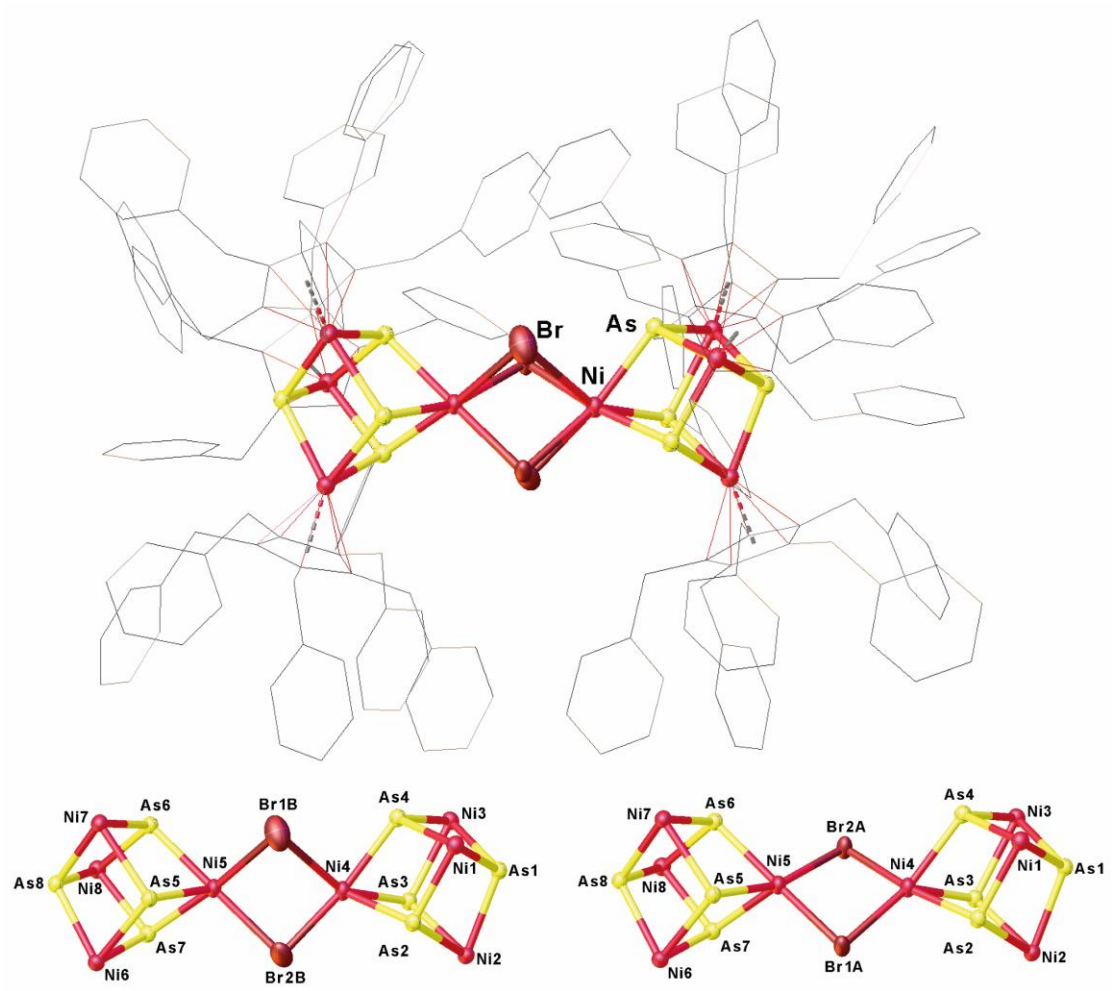

Figure S8: Molecular structure of **8b** in the solid state (above) with thermal ellipsoids at 50% probability level. Hydrogen atoms and solvent molecules are omitted and the Cp^{Bn} ligands are drawn in the wireframe model for clarity. Central structural core motif of **8b** (below). Cp^{Bn} ligands are omitted for clarity. Depicted are part 1 (left, occupancy of 97.5%) and part 2 (right, occupancy of 2.5%). Selected bond lengths [Å] and angles [°]: Br2A-Ni5

2.4177(4), Br2A-Ni4 2.4516(4), Br1A-Ni5 2.4512(5), Br1A-Ni4 2.4075(5), Ni5-Br1B 2.778(14), Ni5-Br2B 2.440(17), Ni4-Br1B 2.792(14), Ni4-Br2B 2.265(15);Ni5-Br2A-Ni4-84.542(13), Ni4-Br1A-Ni5-84.768(15), As7-Ni5-Br2A 114.057(16), As7-Ni5-Br1A 110.650(16), As5-Ni5-Br2A 162.941(18), As5-Ni5-Br1A 96.158(16), As6-Ni5-Br2A 93.425(14), As6-Ni5-Br1A 169.770(19), Br2A-Ni5-Br1A 92.375(14), As3-Ni4-Br2A 95.795(14), As3-Ni4-Br1A 133.500(18), As4-Ni4-Br2A 97.567(14), As4-Ni4-Br1A 149.128(19), As2-Ni4-Br2A 171.027(17), As2-Ni4-Br1A 96.141(16), Br1A-Ni4-Br2A 92.613(15), Ni4-Br2B-Ni5 88.2(5), Br2B-Ni4-As3 120.6(5), Br2B-Ni4-As2 101.8(4), Br2B-Ni4-As4 164.2(5), Ni5-Br1B-Ni4 72.0(3), Br2B-Ni4-Br1B 83.3(6), As2-Ni4-Br1B 107.5(3), As4-Ni4-Br1B 82.6(3), As3-Ni4-Br1B 154.9(3), Br2B-Ni5-Br1B 80.6(6), As6-Ni5-Br1B 102.0(3), As6-Ni5-Br2B 175.3(4), As5-Ni5-Br1B 90.9(3), As5-Ni5-Br2B 107.9(4), As7-Ni5-Br1B 167.4(3), As7-Ni5-Br2B 103.8(4).

$[(Cp'''Ni)_3\{Ni(\mu_3\text{-}P)_4\}_2(\mu,\eta^{4:4}\text{-}P_4)]$ (9a)

Compound **9a** crystallizes by layering a CH_2Cl_2 solution with CH_3CN in form of violet plates in the orthorhombic space group *Pbca*. The asymmetric unit contains half a molecule of **9a** and one and a half molecules of CH_2Cl_2 whereat one is disordered over two positions (0.87:0.13). The restrains SADI, SIMU, DFIX and RIGU were used during the crystal structure refinement to restrict respective bond lengths and a.d.p. parameters of the atoms belonging to the disordered fragments.

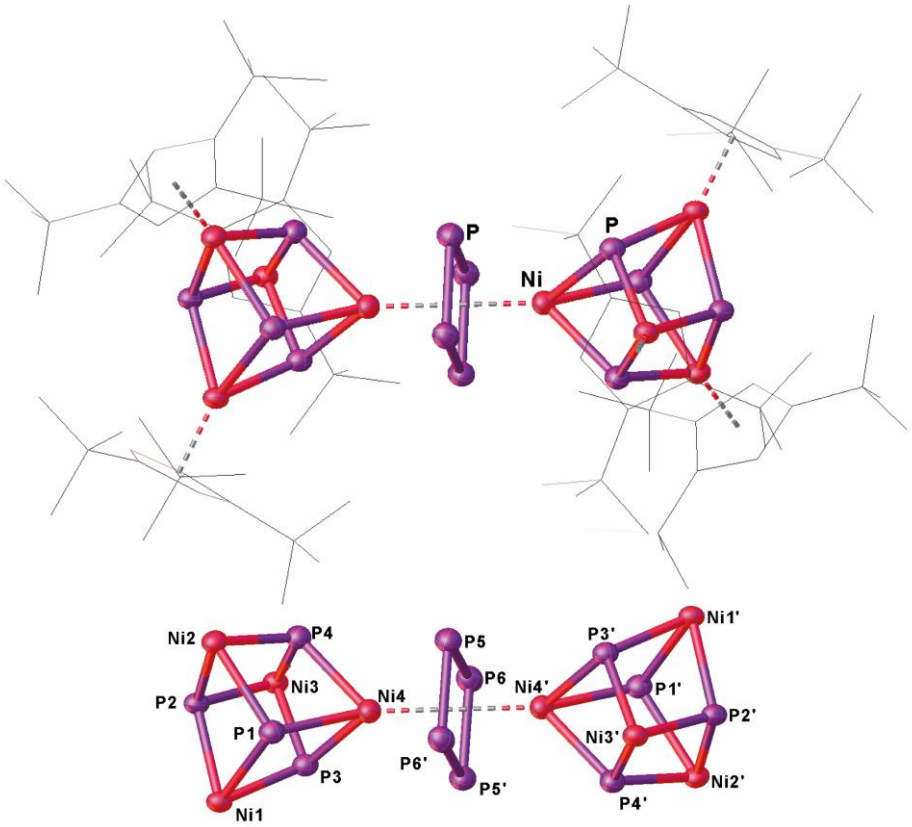

Figure S9: Molecular structure of **9a** in the solid state (above) with thermal ellipsoids at 50% probability level. Hydrogen atoms and solvent molecules are omitted and the Cp''' ligands are drawn in the wireframe model for clarity. Central structural core motif of **9a** (below). Cp''' ligands are omitted for clarity. Selected bond lengths [Å] and angles [°]: Ni1-P3 2.1951(14), Ni1-P2 2.2423(13), Ni1-P1 2.2246(13), Ni4-P3 2.2291(13), Ni4-P1 2.2513(15), Ni4-P4 2.2348(14), Ni2-P2 2.2512(13), Ni2-P1 2.2285(14), Ni2-P4 2.2061(15), Ni3-P3 2.2185(13), Ni3-P2 2.2562(14),

Ni3-P4 2.2211(13), P6-P5 2.1982(18), P6-P5' 2.2110(18), Ni4-P6' 2.4193(15), Ni4-P6 2.3705(14), Ni4-P5 2.3886(14), Ni4-P5' 2.3838(15); P3-Ni1-P2 71.20(5), P3-Ni1-P1 70.34(5), P1-Ni1-P2 74.52(5), P3-Ni4-P1 69.25(5), P3-Ni4-P4 75.16(5), P4-Ni4-P1 71.90(5), P1-Ni2-P2 74.27(5), P4-Ni2-P2 69.64(5), P4-Ni2-P1 72.87(5), Ni1-P3-Ni4 110.07(5), Ni1-P3-Ni3 108.63(6), Ni3-P3-Ni4 98.64(5), Ni1-P2-Ni2 100.25(5), Ni1-P2-Ni3 105.67(5), Ni2-P2-Ni3 108.21(5), Ni1-P1-Ni4 108.20(5), Ni1-P1-Ni2 101.50(5), Ni2-P1-Ni4 104.75(5), Ni2-P4-Ni4 106.06(6), Ni2-P4-Ni3 111.12(6), Ni3-P4-Ni4 98.40(5), Ni3-P4-P2 56.01(4), P6-Ni4-P 6' 81.64(5), P6-Ni4-P5' 55.43(5), P6-Ni4-P5 55.02(5), P5-Ni4-P6' 54.75(5), P5'-Ni4-P6' 54.46(5), P5'-Ni4-P5 81.15(5), P4-Ni4-P6' 102.88(5), P4-Ni4-P6 145.33(5), P4-Ni4-P5 99.22(5), P4-Ni4-P5' 152.06(6), P3-Ni4-P6' 111.20(5), P3-Ni4-P6 135.86(5), P3-Ni4-P5 163.95(5), P3-Ni4-P5' 96.76(5), P1-Ni4-P6' 174.59(5), P1-Ni4-P6 101.82(5), P1-Ni4-P5' 130.93(5), P1-Ni4-P5 123.90(5), Ni4-P6-Ni4' 98.36(5), P5-P6-Ni4 62.91(5), P5-P6-Ni4' 61.95(5), P5'-P6-Ni41 61.92(5), P51-P6-Ni4 62.59(5), Ni4'-P5-Ni4 98.85(5), P6-P5-Ni41 63.59(5), P6'-P5-Ni4' 61.98(5), P6'-P5-Ni4 63.33(5), P6-P5-Ni4 62.07(5), P6-P5-P6' 90.49(6), P5-P6-P5' 89.50.

[(Cp^{Bn}Ni)$_3${Ni(μ$_3$-P)$_4$}$_2$(μ,η$^{4:4}$-P$_4$)] (10a)

Compound **10a** crystallizes by layering a CH_2Cl_2 solution with CH_3CN in form of brown needles in the monoclinic space group *C*2/*c*. The asymmetric unit contains half a molecule of **10a** and one and a half molecules of CH_2Cl_2. The *cyclo*-P_4 unit is disordered over two positions and located on a center of symmetry (2-fold rotation axe) (occupancy 0.4 and 0.1). Furthermore, a CH_2Cl_2 molecule (0.5:0.5) and a benzyl group (0.7;0.3) are disordered over two positions. The restrains SADI and SIMU were used during the refinement of the disordered fragments.

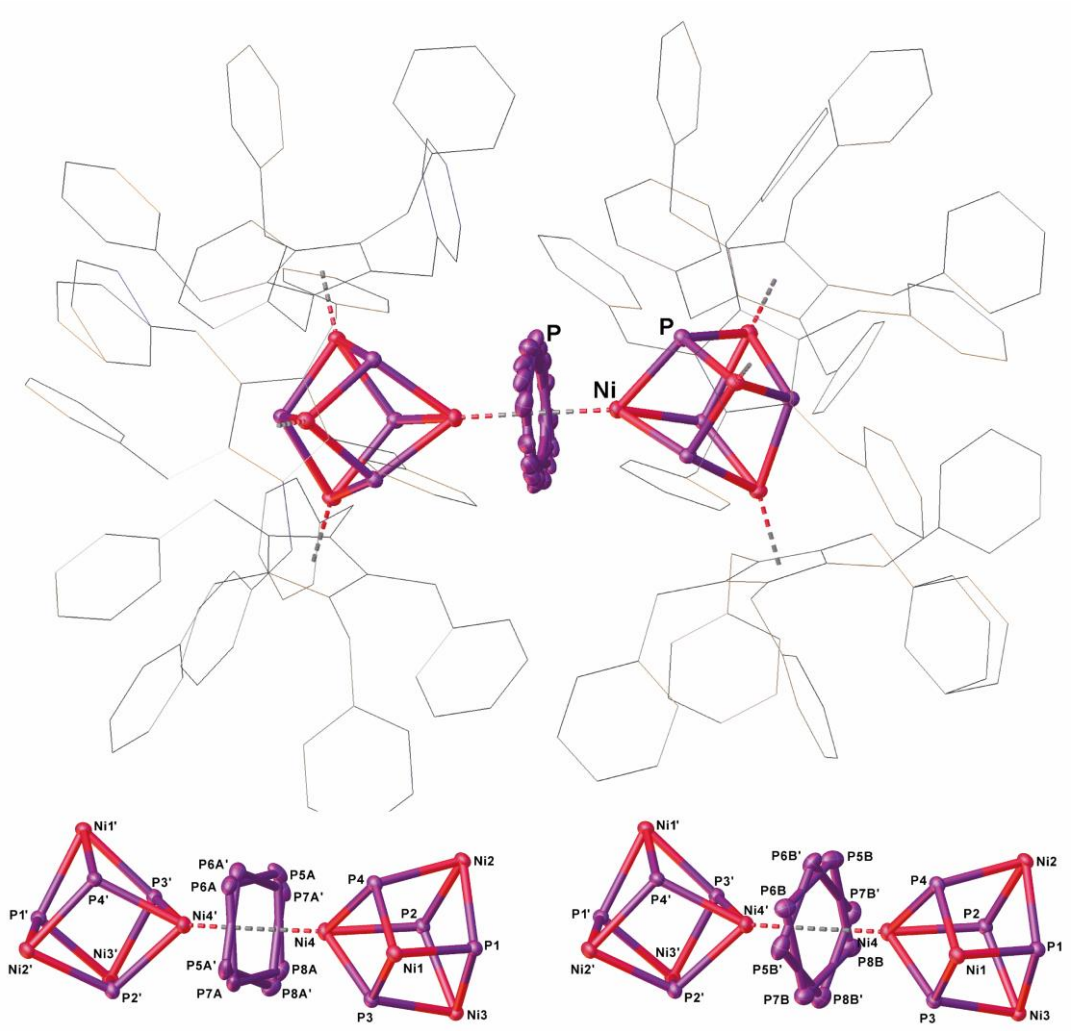

Figure S10: Molecular structure of **10a** in the solid state (above) with thermal ellipsoids at 50% probability level. Hydrogen atoms and solvent molecules are omitted and the Cp^{Bn} ligands are drawn in the wireframe model for clarity. Central structural core motif of **10a** (below). Cp^{Bn} ligands are omitted for clarity. Depicted are part 1 (left, occupancy of 80%) and part 2 (right, occupancy of 20%). Selected bond lengths [Å] and angles [°]: P6A-P7A 2.209(7), P6A-P5A 2.203(7), P7A-P8A 2.203(6), P8A-P5A 2.211(5), P7B-P8B 2.200(13), P7B-P6B 2.216(11), P8B-P5B 2.232(12), P5B P6B 2.213(13), Ni1-P3 2.1989(5), Ni1-P1 2.2287(5), Ni1-P4 2.2257(5), Ni3-P3 2.1944(5), Ni3-P1 2.2254(5), Ni3-P2 2.1987(5), Ni4-P3 2.2300(5), Ni4-P4 2.2379(5), Ni4-P2 2.2441(5), Ni4-P6A 2.382(11), Ni4-P7A 2.347(7), Ni4-P8A 2.394(7), Ni4-P5A 2.384(7), Ni4-P7B 2.403(13), Ni4-P8B 2.382(18), Ni4-P5B 2.361(14), Ni4-P6B 2.380(17), Ni2-P1 2.2269(5), Ni2-P4 2.1948(5), Ni2-P2 2.2047(5); P5B-P6B-P7B 90.7(6), P7B-P8B-P5B 90.6(6), P8B-P7B-P6B 89.7(7), P6B-P5B-P8B 89.0(6), P5A-P6A-P7A 89.69(18) , P5A-P8A-P7A 89.61(17), P8A-P7A-P6A 90.4(2), P6A-P5A-P8A 90.3(2), P3-Ni1-P1-72.646(18), P3-Ni1-P4-72.075(18), P4-Ni1-P1-73.176(18),

P3-Ni3-P1-72.795(18), P3-Ni3-P2-76.040(19), P2-Ni3-P1-75.332(19, PNi4-P4-71.273(18), P3-Ni4-P2-74.424(18), Ni1-P3-Ni4-106.38(2), Ni3-P3-Ni1-106.84(2), Ni3-P3-Ni4-101.90(2), Ni3-P1-Ni1-104.76(2), Ni3-P1-Ni2-102.08(2), Ni2-P1-Ni1-103.26(2), Ni1-P4-Ni4-105.20(2), Ni3-P2-Ni4-101.31(2), Ni3-P2-Ni2-103.66(2), Ni2-P2-Ni4-105.82(2) P3-Ni4-P6A-131.2(2), P3-Ni4-P7A-94.92(18), P3-Ni4-P8A-114.70(14), P3-Ni4-P5A-169.09(11), P3-Ni4-P7B-95.3(3), P3-Ni4-P8B-125.6(3), P3-Ni4-P5B-175.7(3), P3-Ni4-P6B-120.1(4), P4-Ni4-P2-71.466(18), P4-Ni4-P6A-99.9(2), P4-Ni4-P7A-133.28(14), P4-Ni4-P8A-170.33(10), P4-Ni4-P5A-118.22(12), P4-Ni4-P7B-146.4(3), P4-Ni4-P8B-156.8(2), P4-Ni4-P5B-108.3(3) P4-Ni4-P6B-104.2(4), P2-Ni4-P6A-150.05(16), P2-Ni4-P7A-149.12(11), P2-Ni4-P8A-102.21(11), P2-Ni4-P5A-102.73(16), P2-Ni4-P7B-135.9(3), P2-Ni4-P8B-96.3(3), P2-Ni4-P5B-109.7(3), P2-Ni4-P6B-163.4(3).

$[(Cp^{Bn}Ni)_3\{Ni(\mu_3\text{-}P)_4\}_2(\mu,\eta^{4:4}\text{-}As_4)]$ (10b)

Compound **10b** crystallizes by layering a CH_2Cl_2 solution with CH_3CN in form of brown plates in the monoclinic space group *C*2/*c*. The asymmetric unit contains half of a molecule of **10b** and one and a half molecule of CH_2Cl_2. Due to the bad quality of the crystals a satisfactory structure refinement could not be achieved. Nevertheless, the heavy atom framework of the central structural motif could be unambiguously determined.

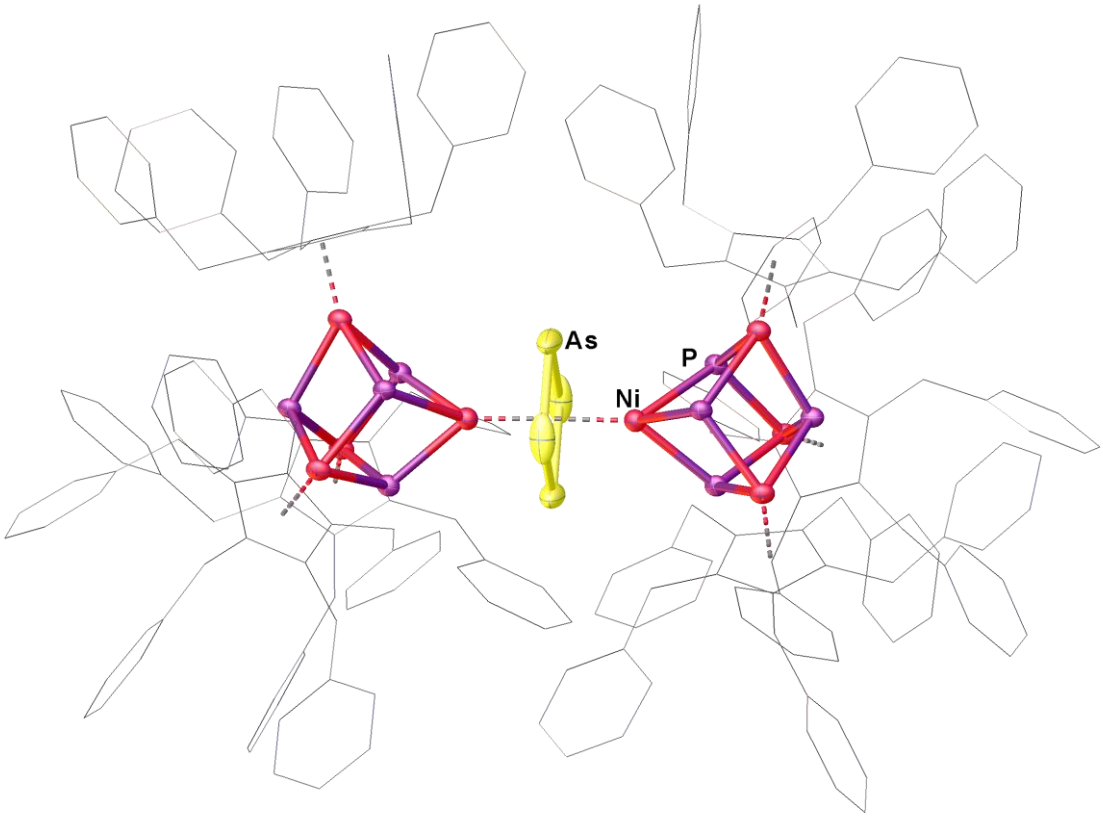

Figure S11: Molecular structure of **10b** in the solid state. Hydrogen atoms and solvent molecules are omitted and the Cp^{Bn} ligands are drawn in the wireframe model for clarity.

[(Cp‴Ni)$_3${Ni(μ$_3$-As)$_4$}$_2$(μ,η$^{4:4}$-As$_4$)] (11a)

Compound **11a** crystallizes by layering a CH_2Cl_2 with CH_3CN in form of violet cubes in the monoclinic space group $P2_1/c$. The asymmetric unit contains half a molecule of **11a** and one molecule of CH_2Cl_2.

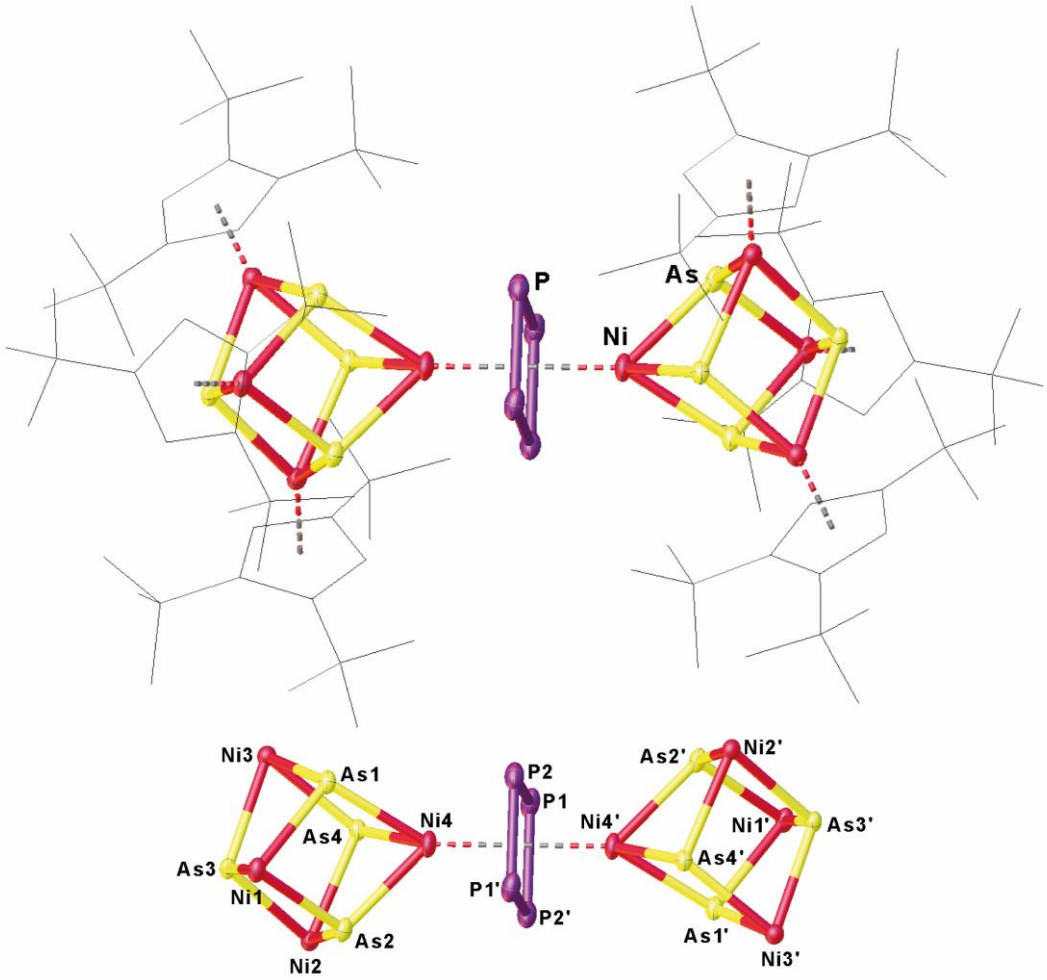

Figure S12: Molecular structure of **11a** in the solid state (above) with thermal ellipsoids at 50% probability level. Hydrogen atoms are omitted and the Cp‴ ligands are drawn in the wireframe model for clarity. Central structural core motif of **11a** (below). Cp‴ ligands are omitted for clarity. Selected bond lengths [Å] and angles [°]: Ni4-P2' 2.4062(8), Ni4-P2 2.3552(8), Ni4-P1' 2.3811(9), Ni4-P1 2.3652(9), P2-P1' 2.2182(11), P2-P1 2.2008(12), As3-Ni3 2.3568(5), As3-Ni2 2.3665(5), As3-Ni1 2.3601(5), As4-Ni3 2.3208(5), As4-Ni2 2.3228(5), As4-Ni4 2.3407(5), As1-As2 2.8744(4), As1-Ni3 2.3404(5), As1-Ni1 2.3405(6), As1-Ni4 2.3751(5), As2-Ni2 2.3324(5), As2-Ni1 2.3260(5), As2-Ni4 2.3551(6); P2-Ni4-As1 100.40(3), As4-Ni4-P2 134.57(3), As4-Ni4-P2' 109.22(3), As4-Ni4-P1 163.14(3), As4-Ni4-P1' 94.36(3), As1-Ni4-P2' 175.94(3), As1-Ni4-P1' 129.30(3), As2-Ni4-P2' 101.16(3), As2-Ni4-P1 96.86(3), As2-Ni4-P1' 151.40(3), Ni3-As3-Ni2 102.870(19), Ni3-As3-Ni1 99.129(19), Ni1-As3-Ni2 105.808(19), Ni3-As4-Ni2 105.371(19), Ni3-As4-Ni4 108.934(19), Ni2-As4-As3 53.625(14), Ni2-As4-As1 102.646(17), Ni2-As4-Ni4 96.75(2), Ni3-As1-Ni1 100.167(19), Ni3-As1-Ni4 107.11(2), Ni1-As1-Ni4 102.30(2), Ni2-As2-Ni4 96.09(2), Ni1-As2-Ni2 108.057(19), Ni1-As2-Ni4 103.35(2), As4-Ni3-As3 74.384(17), As4-Ni3-As1 71.920(16), As1-Ni3-As3 76.679(17), As4-Ni2-As3 74.164(16), As4-Ni2-As2 79.307(17), As2-Ni2-As3 72.591(16), As1-Ni1-As3 76.614(17), As2-Ni1-As3 72.822(17), As2-Ni1-As1 76.046(17), As4-Ni4-As1 70.958(16), As4-Ni4-As2 78.487(17), As2-Ni4-As1 74.841(17).

[(Cp^{Bn}Ni)$_3${Ni(μ$_3$-As)$_4$}$_2$(μ,η$^{4:4}$-P$_4$)] (12a)

Compound **12a** crystallizes by layering a CH_2Cl_2 solution with *n*-hexane in form of brown blocks in the monoclinic space group *Cc*.The crystal of compound **12a** proved to be an inversion twin and was therefore refined as a 2-component inversion twin with twin batches refined to 0.15(3)/0.85. The asymmetric unit contains one molecule of **12a** and several disordered CH_2Cl_2 molecules. The content of solvent molecules per formula unit was estimated using a solvent mask. A total of 488 electrons were found in a volume of 2372 Å^3 in 28 voids per unit cell. This is consistent with the presence of 2.7 CH_2Cl_2 molecules per formula unit, which account for 454 electrons per unit cell. The cyclo-P_4 middle deck is disordered over two positions (occupancy of 0.62 and 0.38). To describe this disorder the restrain SIMU was used. Additionally, the restrains SIMU and ISOR were used during the refinement of some of the Cp^{Bn} ligands.

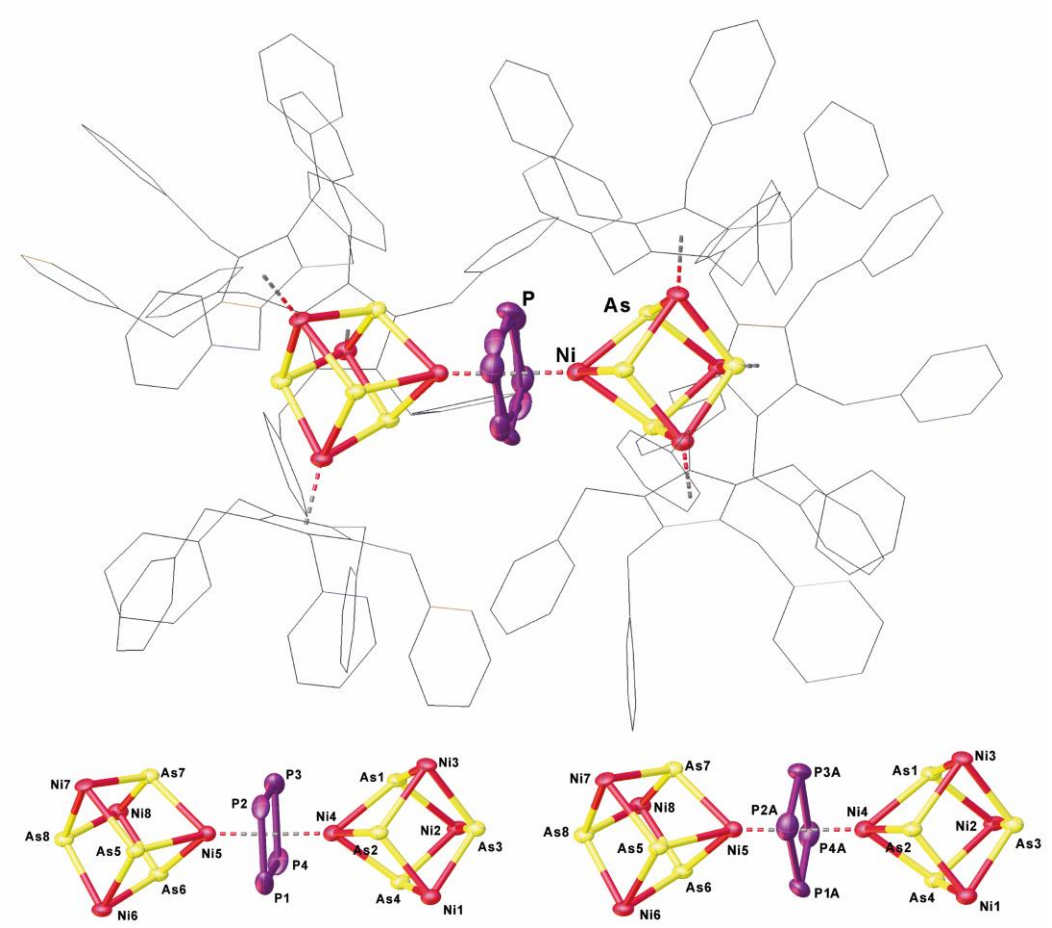

Figure S13: Molecular structure of **12a** in the solid state (above) with thermal ellipsoids at 50% probability level. Hydrogen atoms are omitted and the Cp^{Bn} ligands are drawn in the wireframe model for clarity. Central structural core motif of **12a** (below). Cp^{Bn} ligands are omitted for clarity. Depicted are part 1 (left, occupancy of 62%) and part 2 (right, occupancy of 38%). Selected bond lengths [Å] and angles [°]: P3-P2 2.208(12), P3-P4 2.222(14), P2-P1 2.181(13), P1-P4 2.195(13), P3A-P4A 2.14(2), P3A-P2A 2.23(2), P4A-P1A 2.15(2), P1A-P2A 2.16(2), Ni5-P3 2.340(11), Ni5-P2 2.362(8), Ni5-P1 2.360(9), Ni5-P4 2.334(9), Ni4-P3 2.351(11), Ni4-P2 2.341(8), Ni4-P1 2.372(9), Ni4-P4 2.377(9), Ni4-P3A 2.337(19), Ni4-P4A 2.342(16), Ni4-P1A 2.320(15), Ni4-P2A 2.341(17), Ni5-P3A

2.334(19), Ni5-P4A 2.330(16), Ni5-P1A 2.390(16),Ni5-P2A 2.331(17),As6-Ni5 2.337(2), As6-Ni6 2.313(2), As6-Ni8 2.302(3), As4-Ni2 2.325(2), As4-Ni4 2.361(2), As4-Ni1 2.315(2), As5-Ni5 2.363(2), As5-Ni7 2.327(2), As5-Ni6 2.311(2), As2-Ni4 2.337(2), As2-Ni1 2.316(3), As2-Ni3 2.309(2), As8-Ni7 2.334(2), As8-Ni6 2.349(3),As8-Ni8 2.340(2), As3-As1 2.912(2), As3-Ni2 2.339(2), As3-Ni1 2.352(2), As3-Ni3 2.333(2), As7-Ni5 2.343(3), As7-Ni7 2.311(2), As7-Ni8 2.316(2), As1-Ni2 2.307(2), As1-Ni4 2.346(2), As1-Ni3 2.319(2); P2-P3-P4 89.2(5), P1-P2-P3 90.5(5), P2-P1-P4 90.6(5), P1-P4-P3 89.8(5), P4A-P3A-P2A 88.7(9), P1A-P2A-P3A 89.3(9), P4A-P1A-P2A 90.2(9), P3A-P4A-P1A 91.7(9).

[(Cp^{Bn}Ni)$_3${Ni(μ$_3$-As)$_4$}$_2$(μ,η$^{4:4}$-As$_4$)] (12b)

Compound **12b** crystallizes by layering a CH_2Cl_2 wich *n*-hexane in form of brown blocks in the monoclinic space group *Cc*. The crystal of compound **12b** proved to be an inversion twin and was therefore refined as a 2-component inversion twin with twin batches refined to 0.15(3)/0.85. The asymmetric unit contains one molecule of **12b** and several disordered CH_2Cl_2 molecules. The content of solvent molecules per formula unit was estimated using a solvent mask. A total of 536 electrons were found in a volume of 2412 Å^3 in 28 voids per unit cell. This is consistent with the presence of 3 CH_2Cl_2 molecules per formula unit, which account for 504 electrons per unit cell. The cyclo-As$_4$ middle deck is disordered over two positions (occupancy of 0.9 and 0.1). To describe this disorder the restrains SADI and SIMU were used. Additionally, the restrains SADI, SIMU and ISOR were used during the refinement of some of the Cp^{Bn} ligands.

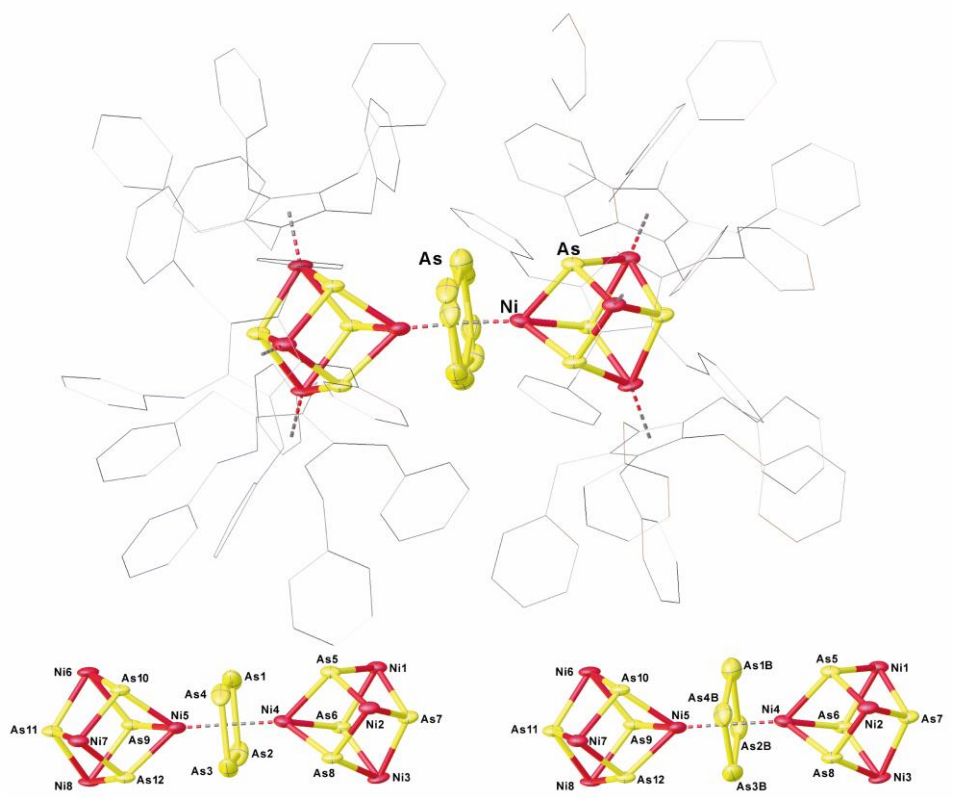

Figure S14: Molecular structure of **12b** in the solid state (above) with thermal ellipsoids at 50% probability level. Hydrogen atoms are omitted and the Cp^{Bn} ligands are drawn in the wireframe model for clarity. Central structural core motif of **12b** (below). Cp^{Bn} ligands are omitted for clarity. Depicted are part 1 (left, occupancy of 90%) and part 2 (right, occupancy of 10%). Selected bond lengths [Å] and angles [°]: As12-Ni8 2.3043(18), As12-Ni5 2.346(2), As12-Ni7 2.3209(19), As9-Ni8 2.3264(19), As9-Ni5 2.3613(19), As9-Ni6 2.313(2), As10-Ni5 2.341(2), As10-Ni6 2.3148(19), As10-Ni7 2.303(2), As11-Ni8 2.3355(19), As11-Ni6 2.355(2), As11-Ni7 2.3420(19), As5-Ni2 2.322(2), As5-Ni1 2.3188(19), As5-Ni4 2.3640(19), As6-Ni3 2.3004(19), As6-Ni1 2.307(2), As6-Ni4 2.346(2), As8-Ni2 2.302(2), As8-Ni3 2.3180(19), As8-Ni4 2.352(2), As7-Ni2 2.3422(18), As7-Ni3 2.335(2), As7-Ni1 2.351(2), Ni5-As3 2.457(3), Ni5-As2 2.478(2), Ni5-As1 2.488(2), Ni5-As4 2.439(2), Ni5-As2B 2.419(15), Ni5-As4B 2.414(19), Ni5-As3B 2.42(2), Ni5-As1B 2.58(2), Ni4-As3 2.454(3), Ni4-As2 2.449(2), Ni4-As1 2.473(2), Ni4-As4 2.483(3), Ni4-

As2B 2.461(17), Ni4-As4B 2.350(17), Ni4-As3B 2.36(2) Ni4-As1B 2.47(2), As2B-As3B 2.52(2), As2B-As1B 2.30(2), As4B-As3B 2.24(3), As4B-As1B 2.41(3), As3-As2 2.447(3), As3-As4 2.422(3), As2-As1 2.437(3), As1-As4 2.436(3); As3-As4-As1 90.59(10), As4-As1-As2 89.67(9), As1-As2-As3 89.95(10), As4-As3-As2 89.78(11), As3B-As4B-As1B 94.6(9), As1B-As2B-As3B 90.2(9), As4B-As3B-As2B 86.9(9), As2B-As1B-As4B 88.2(9).

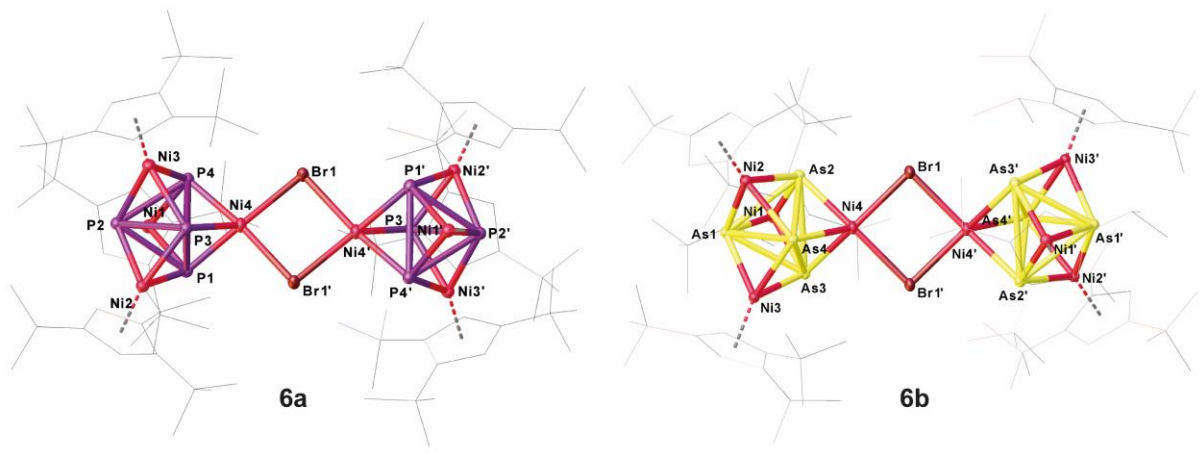

Figure S15: Molecular Structure of **6a** (left) and **6b** (right) in the solid state with thermal ellipsoids at 50% probability level. Hydrogen atoms are omitted and the Cp''' ligands are drawn in the wire frame model for clarity. Illustration of the short E-E distances within the cubanes. E-E distances [Å]: **6a**: P1-P2 2.5923(7), P1-P3 2.5406(7), P1-P4 2.7037(7), P2-P3 2.5687(6), P2-P4 2.5850(7), P3-P4 2.6932(7); **6b**: As1-As2 2.8276(3), As1- As3 2.7736(3), As1-As4 2.8664(3), As2-As3 3.0186(3), As2-As4 2.7906(3), As3-As4 2.7929(3).

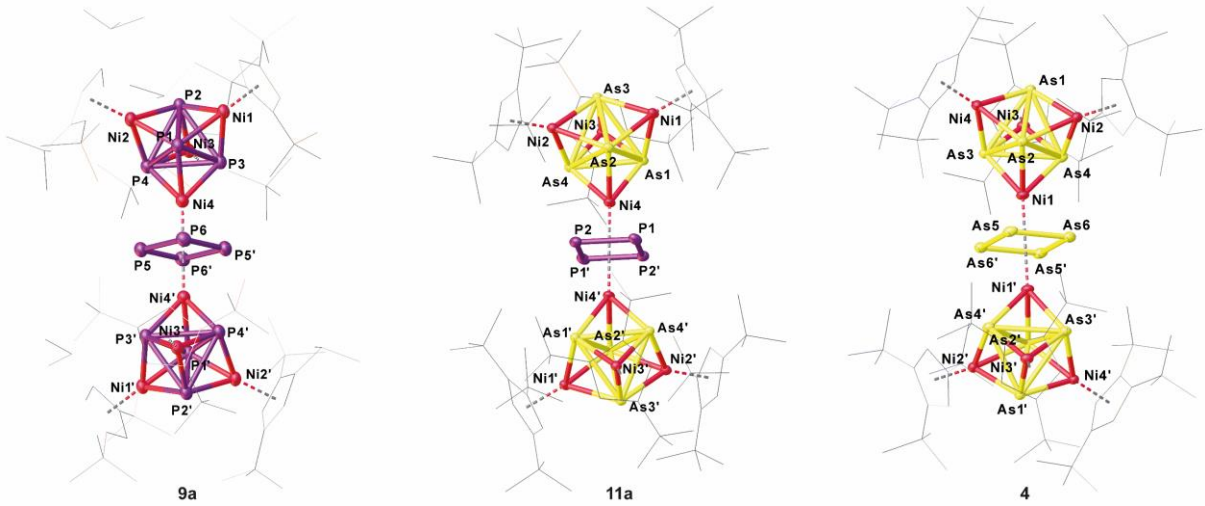

Figure S16: Molecular Structure of **9a** (left), **11a** (middle) and **4** (right) in the solid state with thermal ellipsoids at 50% probability level. Hydrogen atoms are omitted and the Cp''' ligands are drawn in the wire frame model for clarity. Illustration of the short E-E distances within the cubanes. Selected E-E distances [Å]: **9a**: P1-P2 2.7045(16), P1-P3 2.5459(16), P1-P4 2.6339(17), P2-P3 2.5834(17), P2-P4 2.5454(17), P3-P4 2.7225(16); **11a**: As1-As2 2.744(4), As1- As3 2.9138(4), As1-As4 2.7372(4), As2-As3 2.7816(4), As2-As4 2.9707(4), As3-As4 2.8276(4); **4**: As1-As2 2.80624(19), As1-As3 2.9101(2), As1-As4 2.79253(19), As2-As3 2.7854(2), As2-As4 2.9460(2), As3-As4 2.8420(2).

Table S1: Structure determination summary of the complexes **2a**, **2b**, **4** and **5**.

Compound	**2a**	**2b**	**4 · 2 C_7H_8**	**5**
Formula	$C_{34}H_{58}Ni_2P_4$	$C_{34}H_{58}Ni_2As_4$	$0.5\cdot(C_{116}H_{190}As_{12}Ni_8)$	$2\cdot(C_{51}H_{87}As_5Ni_3)$
CCDC number	2071421	2071422	2071423	2071424
$D_{calc.}$/ g cm^{-3}	1.301	1.584	1.583	1.495
m/mm^{-1}	3.114	5.372	5.172	4.705
Formula Weight	708.10	883.90	2953.25	2501.894
Colour	violet	red	brown	brown
Shape	plate	block	block	block
Size/mm^3	0.21×0.17×0.01	0.52×0.14×0.09	0.19×0.11×0.08	0.33×0.26×0.12
T/K	123.15	123.00(10)	123(1)	123(1)
Crystal System	monoclinic	monoclinic	orthorhombic	monoclinic
Space Group	*P*2/*c*	*P*2$_1$/*c*	*Pbca*	*P*2$_1$/*c*
a/Å	13.8516(4)	13.23460(10)	20.4966(1)	30.8415(6)
b/Å	15.1569(2)	17.99420(10)	19.0759(1)	14.1261(2)
c/Å	19.6161(7)	16.00540(10)	31.6699(2)	28.4033(5)
α/°	90	90	90	90
β/°	118.654(2)	103.4930(10)	90	116.075(2)
γ/°	90	90	90	90
V/Å^3	3613.98(18)	3706.42(4)	12382.65(12)	11115.0(4)
Z	4	4	4	4
Z'	1	1	0.5	1
Wavelength/Å	1.54178	1.54184	1.54178	1.54184
Radiation type	CuK$_\alpha$	Cu K$_\alpha$	Cu K$_\alpha$	Cu K$_\alpha$
θ_{min}/°	2.915	3.434	3.46	3.51
θ_{max}/°	66.634	75.697	76.58	73.06
Measured Refl's.	16022	39838	200342	62283
Ind't Refl's	6229	7528	12983	21396
Refl's with I≥σ(I)	4913	7194	12666	20879
R_{int}	0.0298	0.0283	0.0301	0.0211
Parameters	379	379	706	1117
Restraints	0	0	0	0
Largest Peak	0.321	0.930	0.3392	0.9168
Deepest Hole	-0.378	-0.930	-0.3158	-0.7936
GooF	1.002	1.079	1.0516	0.9915
wR_2 (all data)	0.0823	0.0788	0.0407	0.1101
wR_2	0.0781	0.0776	0.0404	0.1096
R_1 (all data)	0.0449	0.0296	0.0170	0.0448
R_1	0.0324	0.0281	0.0164	0.0438

Table S2: Structure determination summary of the complexes **6a**, **6b**, **8a** and **8b**.

Compound	**6a**	**6b**	**8a · 7 C_7H_8**	**8b · 6 C_7H_8**
Formula	½·($C_{102}H_{174}Br_2Ni_8P_8$)	½·($C_{102}H_{174}As_8Br_2Ni_8$)	$C_{289}H_{266}P_8Ni_8Br_2$	$C_{282}H_{258}As_8Ni_8Br_2$
CCDC number	2071425	2071426	2071396	2071427
$D_{calc.}$/ g cm^{-3}	1.357	1.530	1.328	1.373
m/mm^{-1}	3.661	5.093	2.060	2.781
Formula Weight	1138.83	2629.26	4616.26	4783.60
Colour	black	black	metallic dark brown	dark brown
Shape	prism	cube	block	block
Size/mm^3	0.15×0.12×0.07	0.14×0.13×0.09	0.76×0.39×0.34	0.19×0.16×0.06
T/K	123.15	123(1)	123.1(2)	123.02(10)
Crystal System	orthorhombic	orthorhombic	triclinic	triclinic
Space Group	*Pbca*	*Pbca*	*P*-1	*P*-1
a/Å	21.6733(2)	22.2049(2)	17.71184(9)	17.7192(2)
b/Å	18.0072(2)	18.46511(19)	22.61704(12)	22.6405(2)
c/Å	28.5600(2)	27.8301(2)	29.89807(18)	29.9422(3)
α/°	90	90	95.0607(5)	94.9583(8)
β/°	90	90	90.6755(4)	91.1153(8)
γ/°	90	90	104.5530(5)	104.6084(9)
V/Å^3	11146.27(18)	11410.82(18)	11540.23(11)	11569.5(2)
Z	8	4	2	2
Z'	1	0.5	1	1
Wavelength/Å	1.54184	1.54184	1.54184	1.54184
Radiation type	CuK_α	Cu K_α	Cu K_α	Cu K_α
θ_{min}/°	3.095	3.495	3.435	3.171
θ_{max}/°	66.714	67.073	67.080	67.080
Measured Refl's.	27966	33054	580698	142910
Ind't Refl's	9614	10146	41091	41024
Refl's with I≥σ(I)	8068	9459	40282	37473
R_{int}	0.0255	0.0272	0.0517	0.0285
Parameters	578	568	2877	2825
Restraints	0	0	399	278
Largest Peak	0.658	0.372	0.707	0.500
Deepest Hole	-0.336	-0.343	-0.705	-0.423
GooF	1.027	1.080	1.100	1.052
wR_2 (all data)	0.0717	0.0520	0.0866	0.0687
wR_2	0.0687	0.0509	0.0861	0.0668
R_1 (all data)	0.0361	0.0260	0.0349	0.0314
R_1	0.0279	0.0227	0.0342	0.0278

Table S3: Structure determination summary of the complexes **9a**, **9b**, **10a** and **10b**.

Compound	**9a · 3 CH_2Cl_2**	**10a · 3 CH_2Cl_2**	**10b · 3 CH_2Cl_2**
Formula	½·($C_{105}H_{180}P_{12}Ni_8Cl_6$)	½·($C_{243}H_{216}Cl_6Ni_8P_{12}$)	½·($C_{243}H_{216}Cl_6Ni_8P_8As_4$)
CCDC number	2071428	2071429	
$D_{calc.}$/ g cm^{-3}	1.387	1.379	
m/mm^{-1}	9.641	2.854	2.854
Formula Weight	2496.50	2095.08	4366.84
Colour	violet	dark brown	dark brown
Shape	plate	needle	plate
Size/mm^3	0.11×0.07×0.06	0.22×0.04×0.04	0.256×0.142×0.081
T/K	123.00(13)	122.96(11)	123
Crystal System	orthorhombic	monoclinic	monoclinic
Space Group	Pbca	$C2/c$	$C2/c$
a/Å	19.8872(5)	29.0657(3)	29.0539(6)
b/Å	19.3591(5)	16.5186(2)	16.5362(5)
c/Å	31.0589(8)	43.3792(5)	43.4946(11)
α/°	90	90	90
β/°	90	104.2320(10)	104.336(2)
γ/°	90	90	90
V/Å^3	11957.6(5)	20188.2(4)	20245.9(9)
Z	4	8	4
Z'	0.5	1	0.5
Wavelength/Å	1.39222	1.54184	1.54184
Radiation type	Cu K_α	Cu K_α	Cu K_α
θ_{min}/°	3.260	3.396	
θ_{max}/°	56.277	74.211	
Measured Refl's.	34480	58153	
Ind't Refl's	10664	19698	
Refl's with I≥σ(I)	8075	17152	
R_{int}	0.0761	0.0364	
Parameters	658	1334	
Restraints	58	230	
Largest Peak	0.732	0.624	
Deepest Hole	-0.912	-0.368	
GooF	1.025	1.041	
wR_2 (all data)	0.1690	0.0845	
wR_2	0.1502	0.0809	
R_1 (all data)	0.0796	0.0425	
R_1	0.0608	0.0348	

Table S4 Structure determination summary of the complexes **11a**, **12a** and **12b**.

Compound	**11a · 2 CH_2Cl_2**	**12a · 2.7 CH_2Cl_2**	**12b · 3 CH_2Cl_2**
Formula	½·($C_{104}H_{178}As_8Ni_8Cl_4P_4$)	$C_{242.7}H_{215.4}As_{12}Ni_8Cl_{5.4}$	$C_{243}H_{216}As_{12}Ni_8Cl_6$
CCDC number	2071430	2071431	2071432
$D_{calc.}$/ g cm^{-3}	1.535	1.450	1.512
m/mm^{-1}	5.430	3.550	4.033
Formula Weight	2763.17	4516.29	4718.57
Colour	dark violet	black	dark brown
Shape	cube	block	block
Size/mm^3	0.16×0.13×0.05	0.31×0.11×0.06	0.22×0.14×0.11
T/K	123(1)	122.9(5)	123.01(18)
Crystal System	monoclinic	monoclinic	monoclinic
Flack Parameter		0.15(3)	0.15(3)
Hooft Parameter		0.057(12)	0.055(10)
Space Group	$P2_1/c$	Cc	Cc
a/Å	16.9589(2)	28.9845(4)	29.0686(4)
b/Å	20.4796(2)	16.8386(3)	16.8745(2)
c/Å	18.2399(2)	43.0838(9)	43.0146(6)
α/°	90	90	90
β/°	109.2680(10)	100.396(2)	100.7428(13)
γ/°	90	90	90
V/Å^3	5980.08(12)	20682.2(6)	20729.7(5)
Z	2	4	4
Z'	0.5	1	1
Wavelength/Å	1.54184	1.54184	1.54184
Radiation type	Cu K_α	Cu K_α	Cu K_α
θ_{min}/°	3.504	3.311	3.042
θ_{max}/°	67.078	66.714	73.037
Measured Refl's.	32468	76170	56395
Ind't Refl's	10623	31447	27766
Refl's with I≥σ(I)	9090	28906	27276
R_{int}	0.0297	0.0554	0.0324
Parameters	604	2379	2342
Restraints	0	512	392
Largest Peak	0.614	1.659	1.386
Deepest Hole	-0.797	-1.033	-0.935
GooF	1.089	1.064	1.022
wR_2 (all data)	0.0685	0.1565	0.1640
wR_2	0.0657	0.1536	0.1633
R_1 (all data)	0.0412	0.0737	0.0641
R_1	0.0317	0.0681	0.0634

3.5.4 NMR Investigations

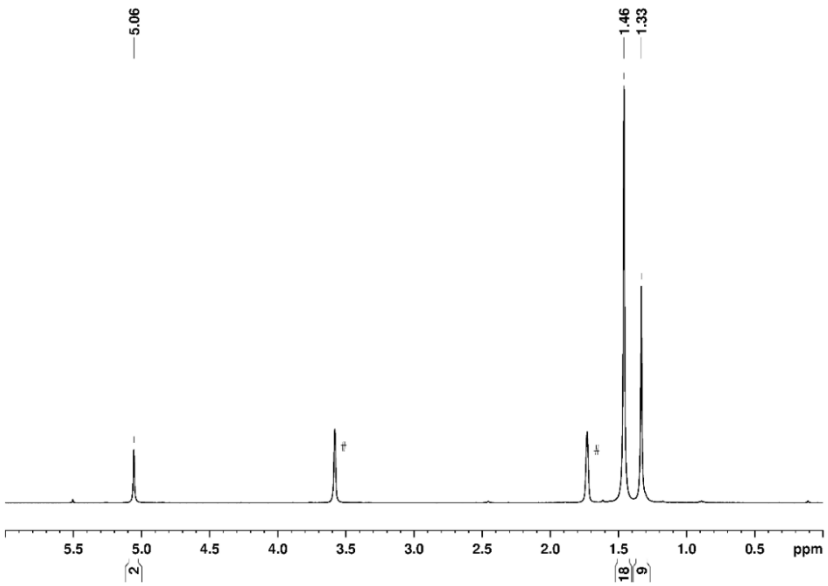

Figure S17: ^{1}H NMR spectrum of **5** at 293 K in thf-d_8 (#).

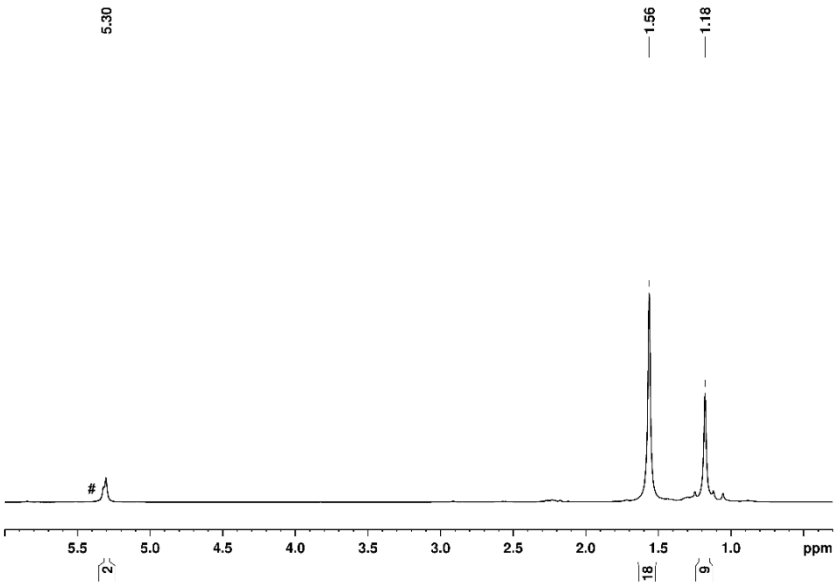

FigureS18: ^{1}H NMR spectrum of **6a** at 293 K in CD_2Cl_2 (#).

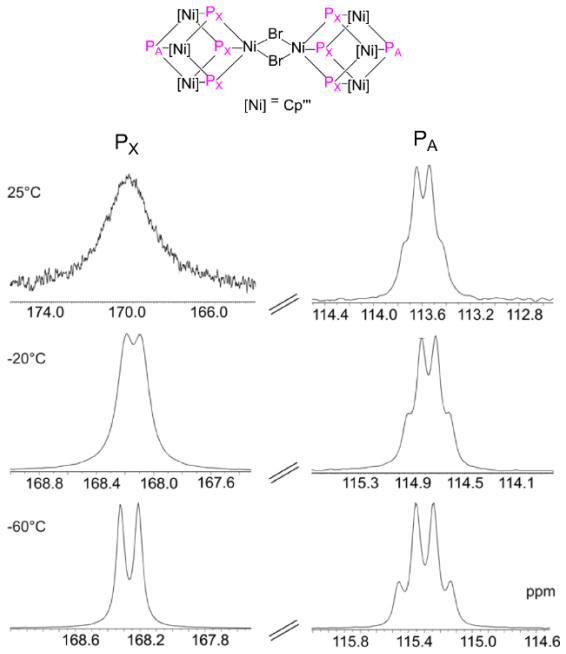

Figure S19: ^{31}P NMR spectrum of **6a** at 293 K in C_6D_6.

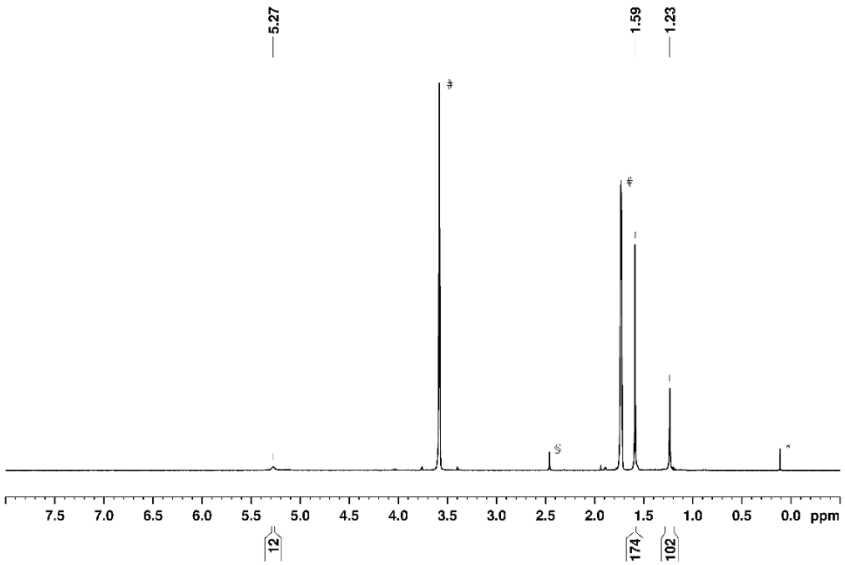

Figure S20: ^{1}H NMR spectrum of **6b** at 293 K in thf-d_8 (#). The signal marked with * is due to silicon grease, the signal marked with § is due to an unknown impurity.

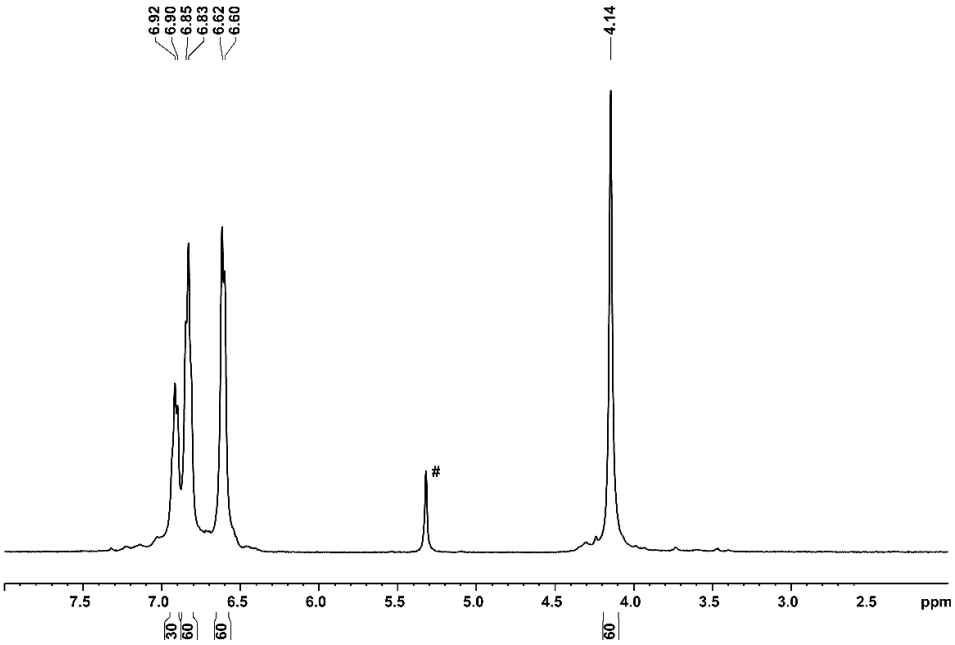

Figure S21: ^{1}H NMR spectrum of **8a** at 293 K in CD_2Cl_2 (#).

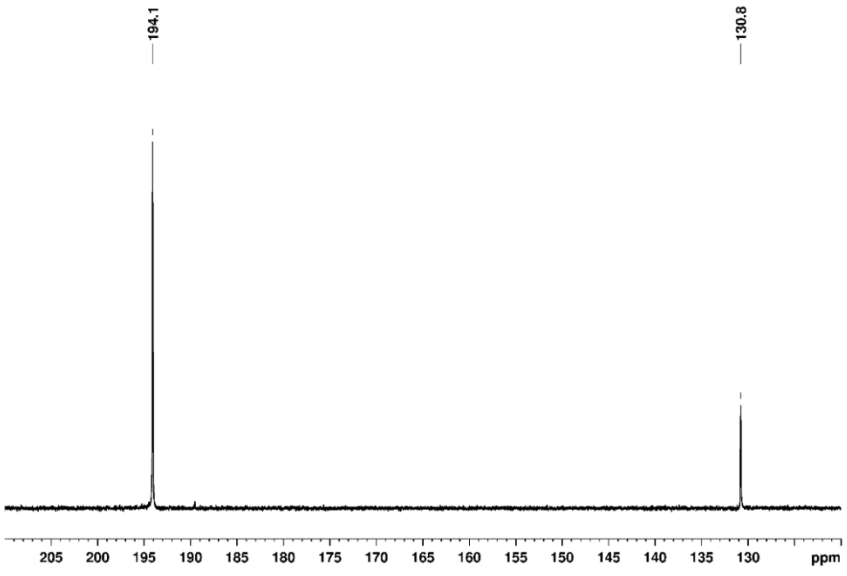

Figure S22: ^{31}P NMR spectrum of **8a** at 293 K in CD_2Cl_2.

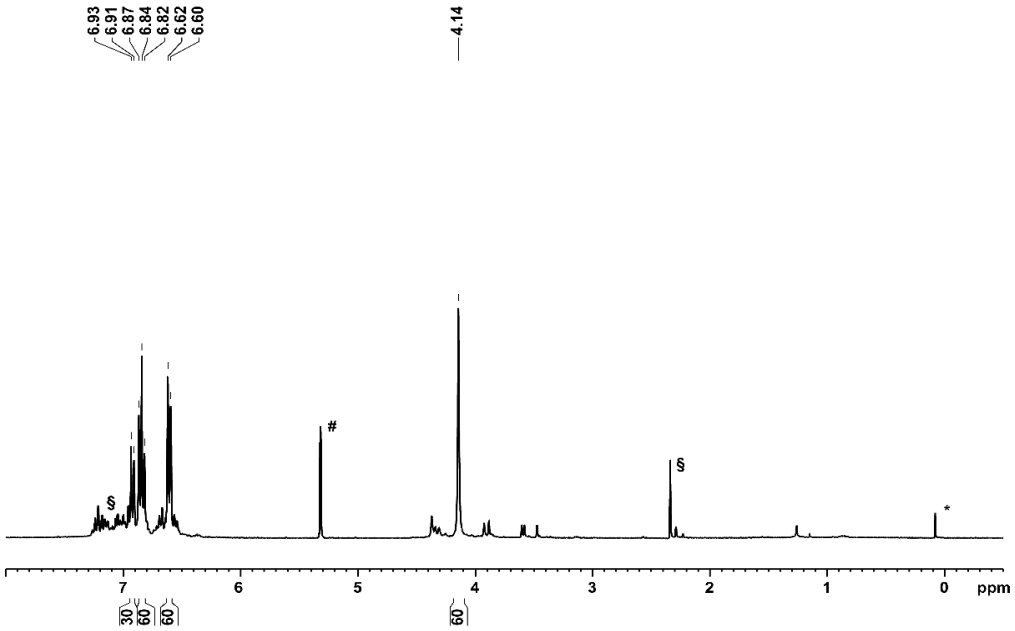

Figure S23: ^{1}H NMR spectrum of **8b** at 293 K in CD_2Cl_2 (#). The signal marked with * is due to silicon grease.

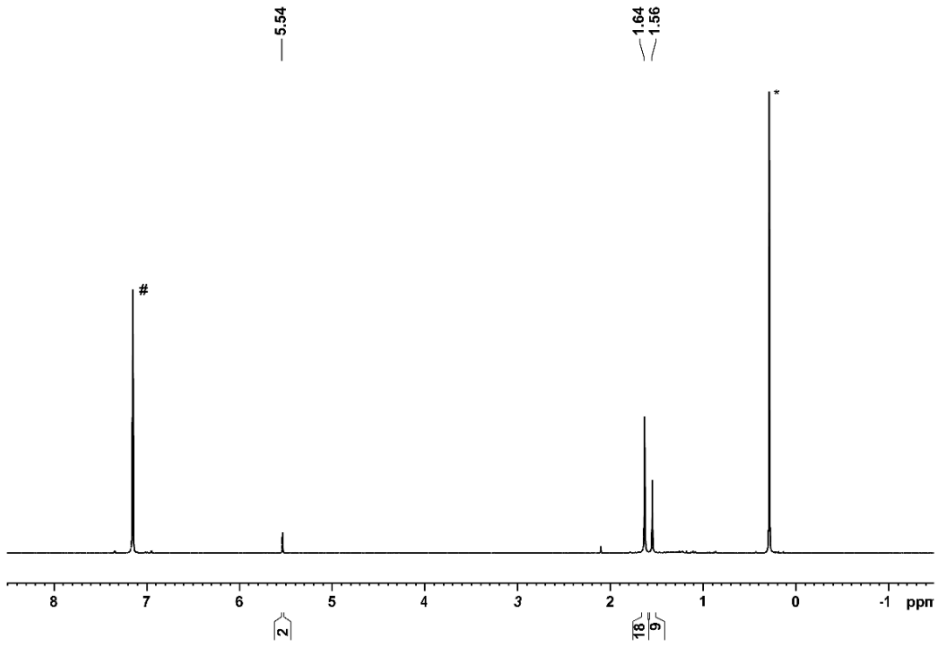

Figure S24: ^{1}H NMR spectrum of **9a** at 293 K in C_6D_6 (#). The signal marked with * is due to silicon grease.

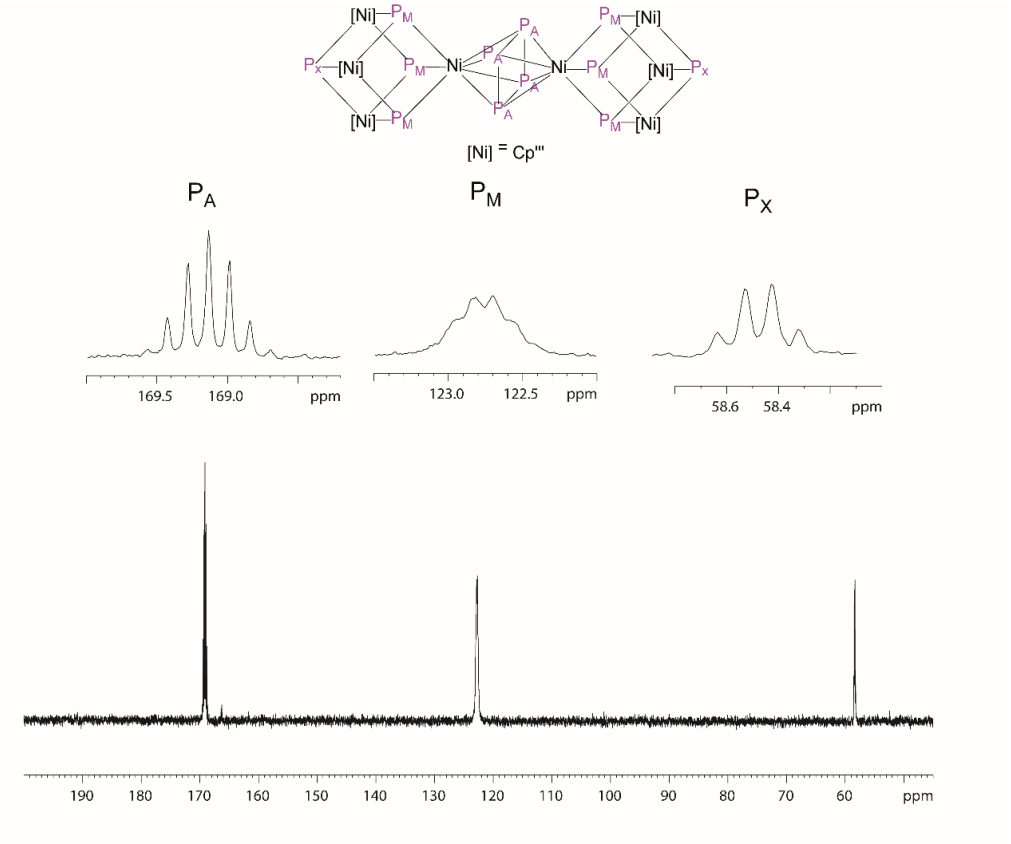

Figure S25: $^{31}P\{^{1}H\}$ NMR spectrum of **9a** at 293 K in C_6D_6.

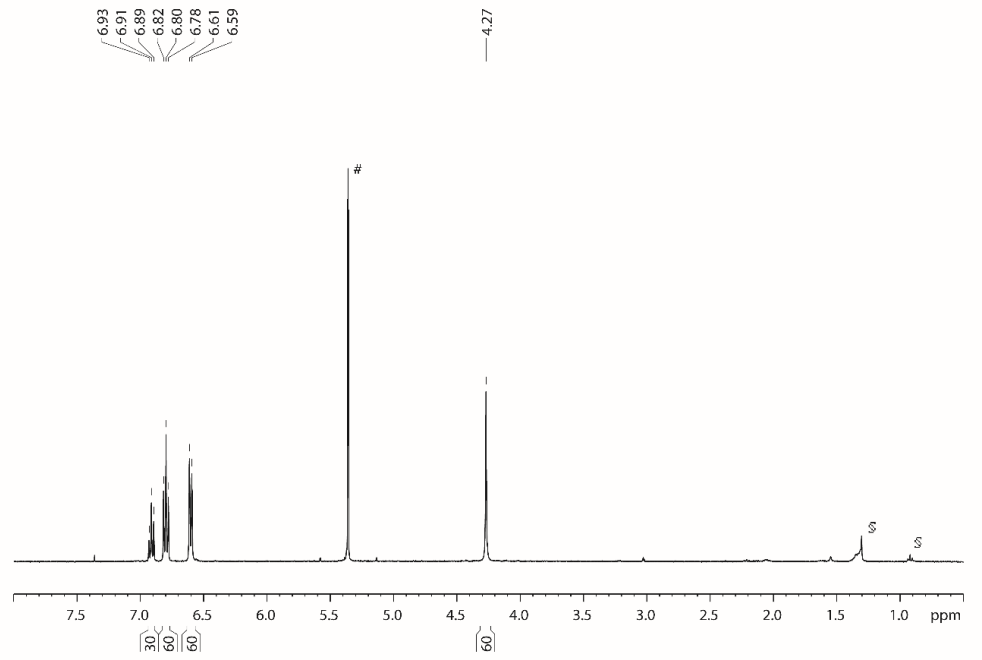

Figure S26: ^{1}H NMR spectrum of **10a** at 293 K in CD_2Cl_2 (#). The signal marked with § is due to *n*-hexane.

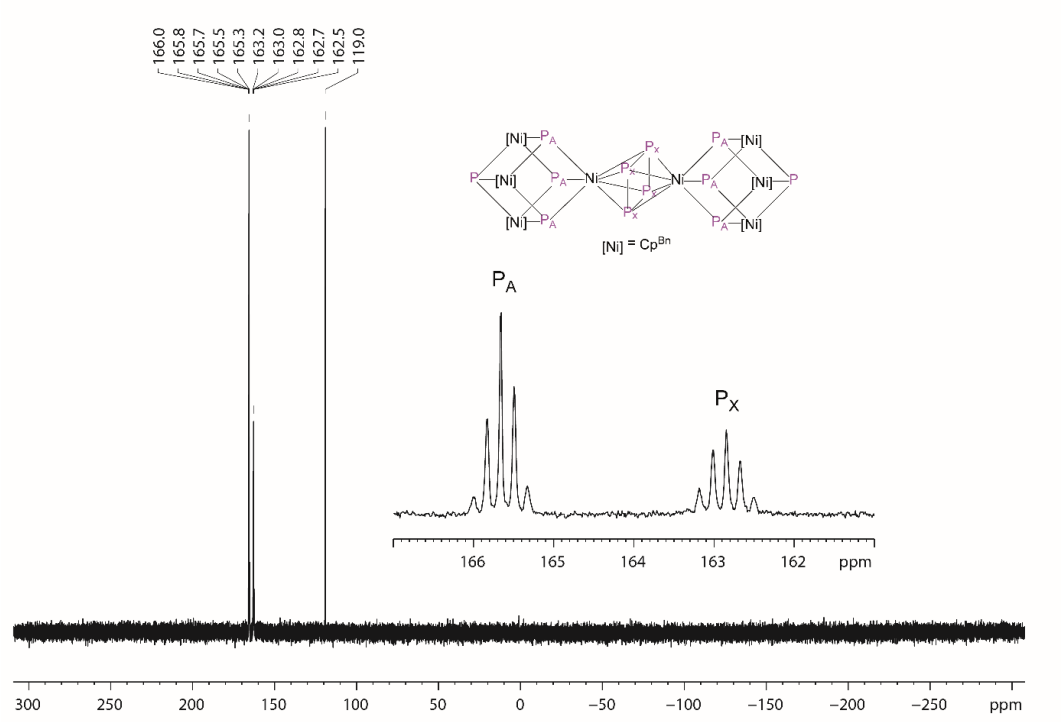

Figure S27: $^{31}P\{^{1}H\}$ NMR spectrum of **10a** at 273 K in CD_2Cl_2.

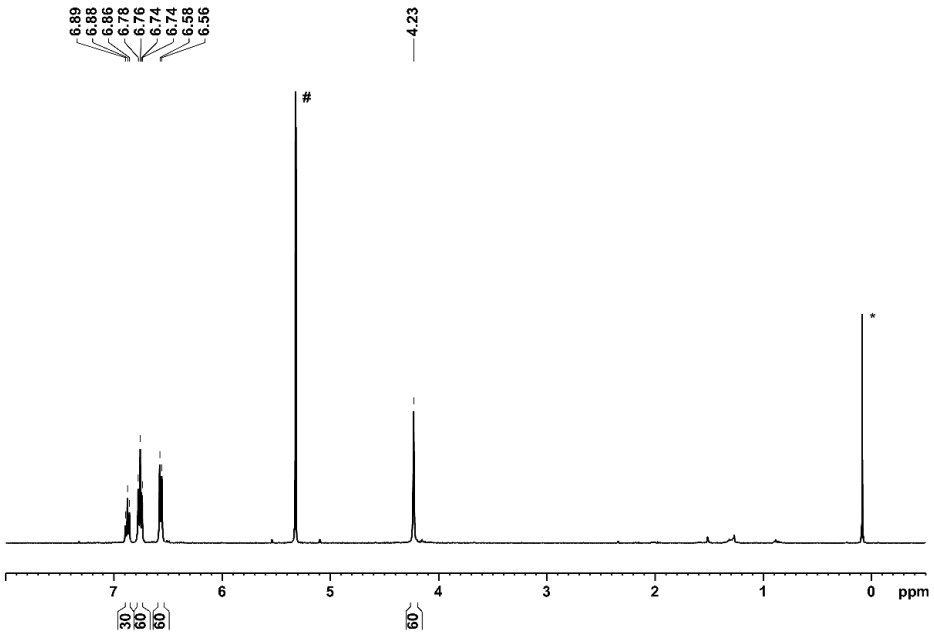

Figure S28: ^{1}H NMR spectrum of **10b** at 293 K in CD_2Cl_2 (#). The signal marked with * is due to silicon grease.

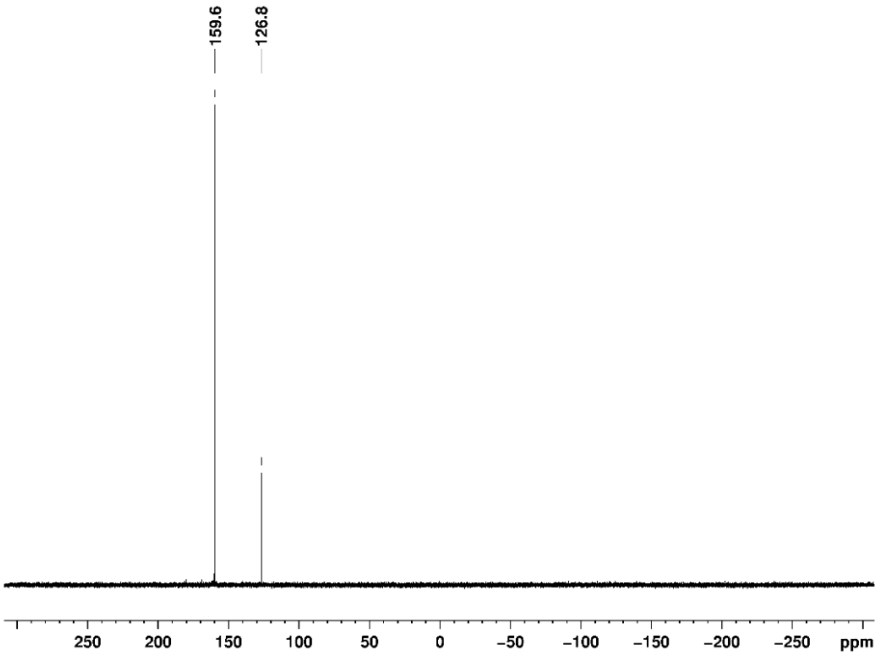

Figure S29: $^{31}P\{^{1}H\}$ NMR spectrum of **10b** at 293 K in CD_2Cl_2.

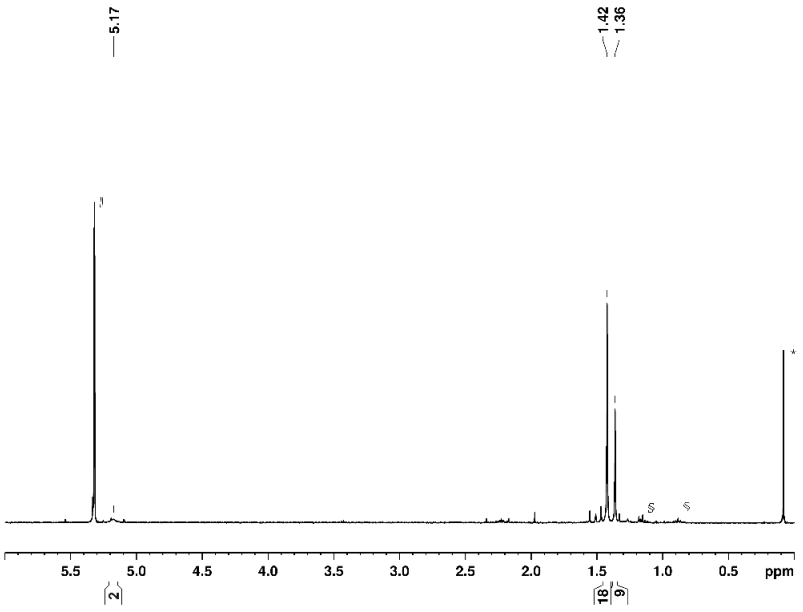

Figure S30: ^{1}H NMR spectrum of **11a** at 293 K in CD_2Cl_2 (#). The signal marked with * is due to silicon grease, the signals marked with § are due to *n*-pentane.

13

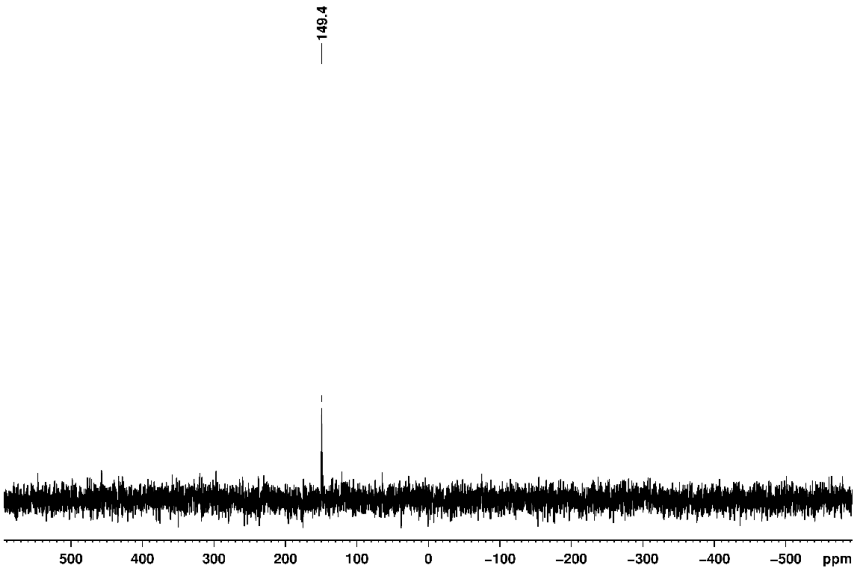

Figure S31: $^{31}P\{^{1}H\}$ NMR spectrum of **11a** at 293 K in CD_2Cl_2.

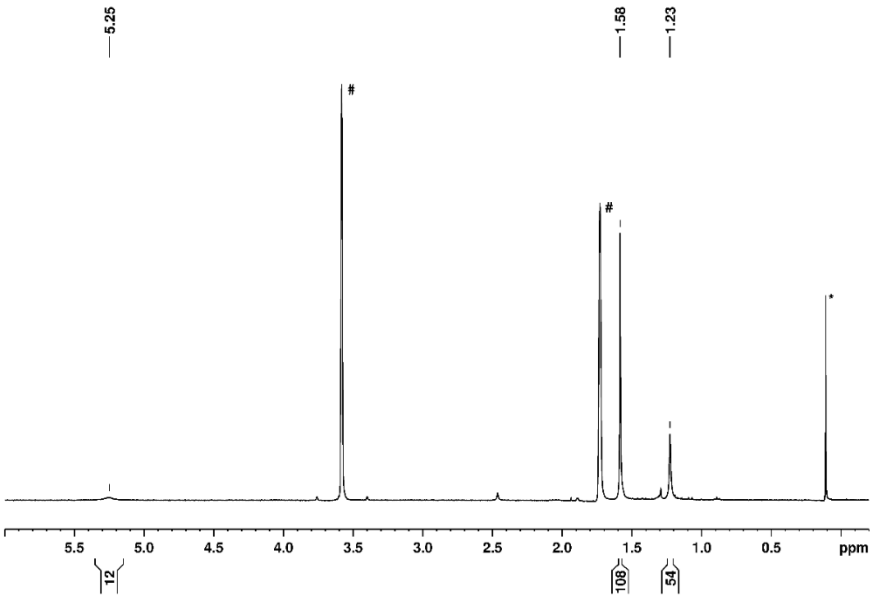

Figure S32: ^{1}H NMR spectrum of **4** at 293 K in thf-d^8 (#). The signal marked with * is due to silicon grease.

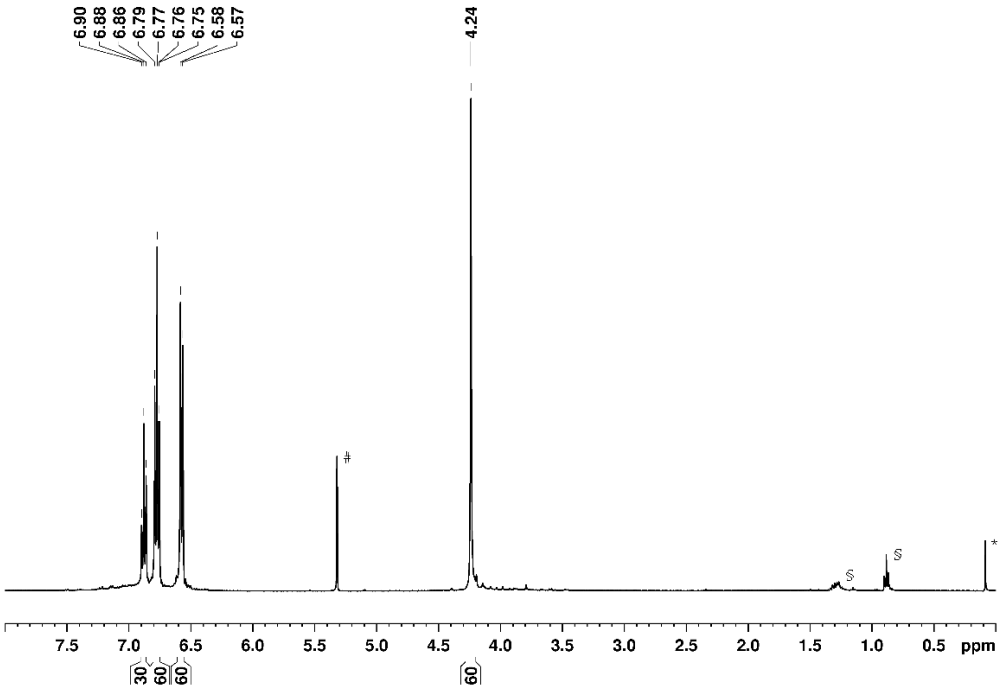

Figure S33: ^{1}H NMR spectrum of **12a** at 293 K in CD_2Cl_2 (#). The signal marked with * is due to silicon grease, the signals marked with § are due to *n*-pentane.

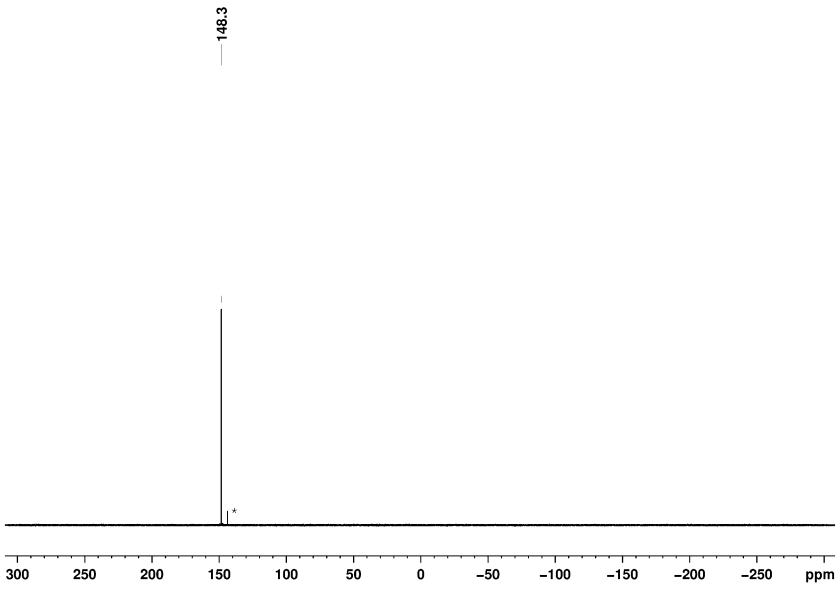

Figure S34: $^{31}P\{^{1}H\}$ NMR spectrum of **12a** at 293 K in CD_2Cl_2. The signal marked with * is due to an unidentified impurity.

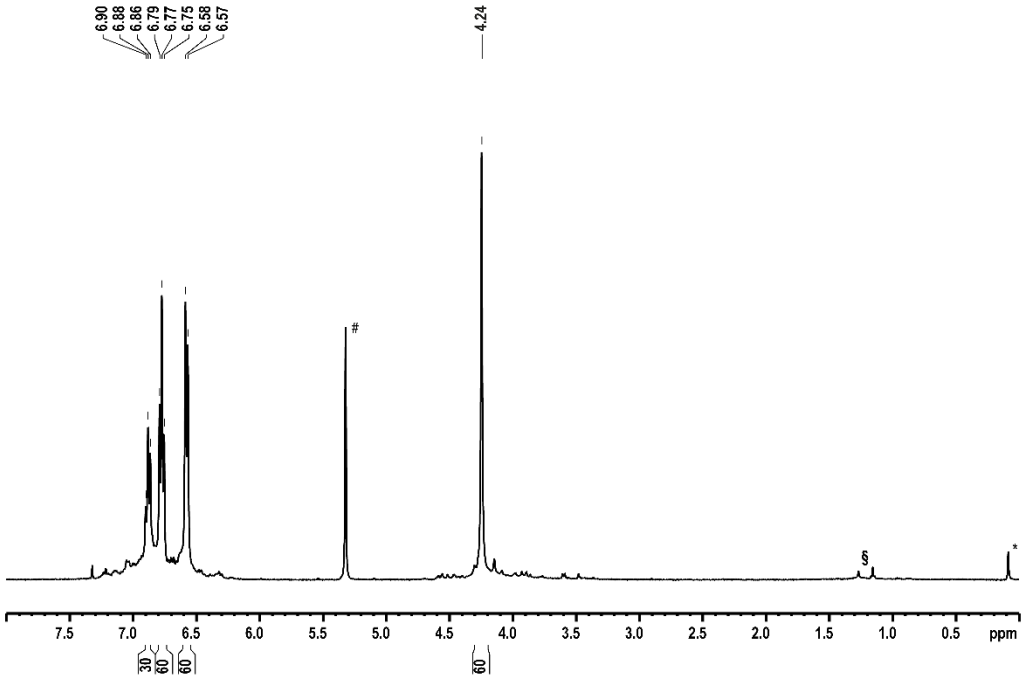

Figure S35: ^{1}H NMR spectrum of **12b** at 293 K in CD_2Cl_2 (#). The signal marked with * is due to silicon grease, the signals marked with § are due to solvent residues.

3.5.5 Computational Details

The geometry of the molecules has been optimized using the TURBOMLE program package[53] at the RI-[54,55] TPSSh[56] level together with the def2-TZVP basis set for all atoms.[55,57,58] To speed up the calculations, the Coulomb part was evaluated by using the Multipole Accelerated Resolution of Identity method (MARI-*J*)[54,59] along with optimized auxiliary basis sets on all atoms.[58] For the calculation of the reaction energies the SCF energies have been used without further corrections. The calculation of the Meyer bond indices as well as the Electron Localization Function (ELF)[60] and Localized Orbital Locator (LOL)[61] analysis have been performed using the Multiwfn program (version 3.6).[62]

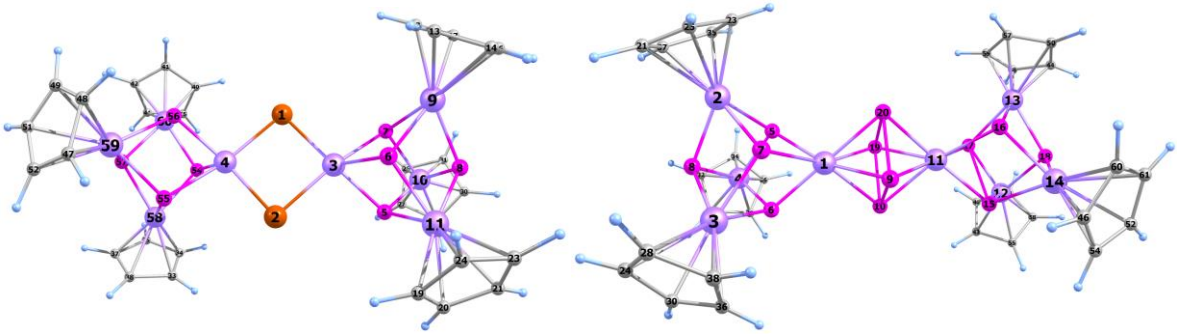

Figure S36: Atom labeling for the model complexes [{(CpNi)$_3$Ni(μ$_3$-P)$_4$}$_2$(μ-Br)$_2$] (left) and [{(CpNi)$_3$Ni(μ$_3$-P)$_4$}$_2$(μ,η$^{4:4}$-P$_4$)] (right).

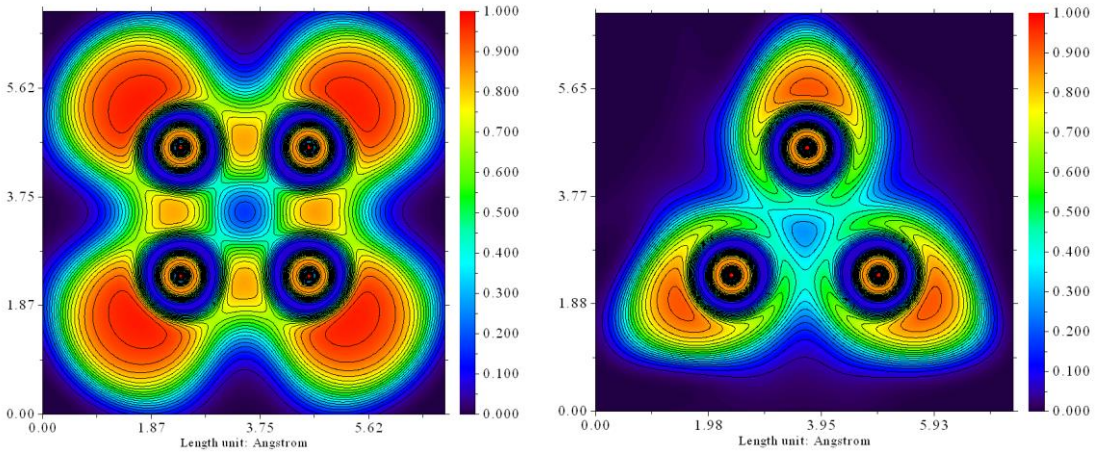

Figure S37: ELF function plot for the model complex [{(CpNi)$_3$Ni(μ$_3$-P)$_4$}$_2$(μ,η$^{4:4}$-P$_4$)], in the plane of the *cyclo*-P$_4$ unit (left) and in the plain defined by the atoms P5,P6 and P7 (right). Labeling of the atoms according to figure S36.

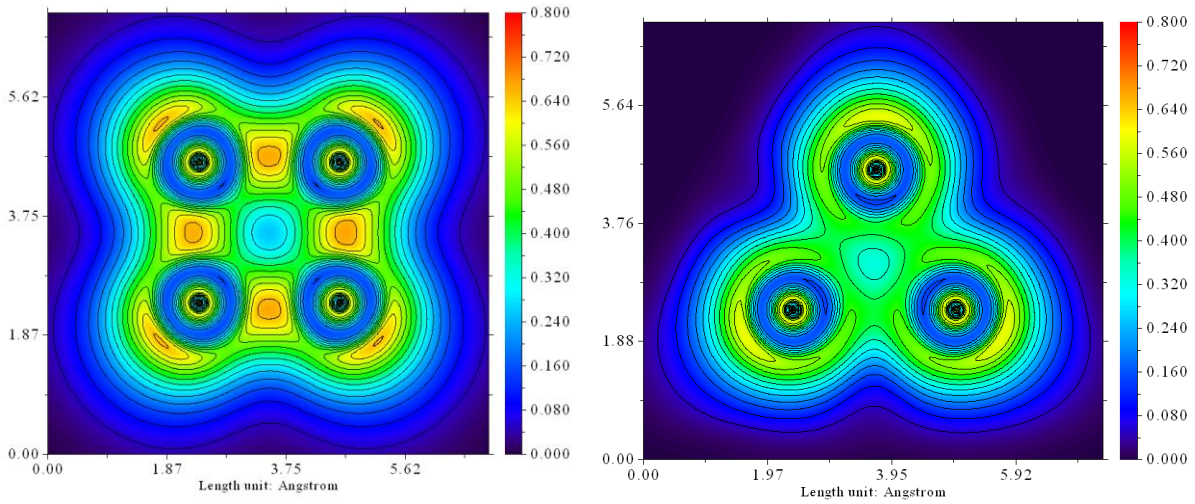

Figure S38: LOL function plot for the model complex [{(CpNi)$_3$Ni(μ$_3$-P)$_4$}$_2$(μ,η$^{4:4}$-P$_4$)], in the plane of the cyclo-P$_4$ unit (left) and in the plain defined by the atoms P5,P6 and P7 (right). Labeling of the atoms according to figure S36.

Table S5: Meyer bond order matrix for [{(CpNi)$_3$Ni(μ$_3$-P)$_4$}$_2$(μ,η$^{4:4}$-P$_4$)]. Atom number according to figure S36.

	1	2	3	4	5	6	7	8	9	10	11	12	13	14	15	16	17	18	19	20
1	3.976	0.066	0.058	0.057	0.658	0.635	0.652	0.029	0.390	0.407	0.056	0.006	0.006	0.007	0.009	0.009	0.011	0.003	0.401	0.420
2	0.066	4.048	0.058	0.058	0.716	0.043	0.718	0.743	0.011	0.006	0.007	0.003	0.003	0.001	0.002	0.003	0.005	0.000	0.009	0.007
3	0.058	0.058	4.054	0.062	0.043	0.723	0.716	0.749	0.007	0.009	0.006	0.001	0.002	0.003	0.003	0.004	0.002	0.000	0.007	0.011
4	0.057	0.058	0.062	4.064	0.719	0.723	0.042	0.755	0.008	0.009	0.006	0.003	0.001	0.003	0.004	0.002	0.002	0.000	0.008	0.011
5	0.658	0.716	0.043	0.719	3.407	0.334	0.358	0.256	0.021	0.017	0.009	0.004	0.003	0.002	0.005	0.001	0.005	0.000	0.046	0.021
6	0.635	0.043	0.723	0.723	0.334	3.419	0.314	0.298	0.017	0.071	0.011	0.002	0.002	0.005	0.005	0.006	0.001	0.000	0.017	0.025
7	0.652	0.718	0.716	0.042	0.358	0.314	3.397	0.278	0.042	0.017	0.009	0.002	0.004	0.003	0.001	0.005	0.006	0.000	0.019	0.023
8	0.029	0.743	0.749	0.755	0.256	0.298	0.278	3.398	0.004	0.004	0.003	0.000	0.000	0.000	0.000	0.000	0.000	0.000	0.004	0.004
9	0.390	0.011	0.007	0.008	0.021	0.017	0.042	0.004	3.132	0.993	0.420	0.011	0.010	0.007	0.022	0.022	0.025	0.004	0.094	0.980
10	0.407	0.006	0.009	0.009	0.017	0.071	0.017	0.004	0.993	3.162	0.402	0.008	0.007	0.009	0.045	0.019	0.017	0.004	0.988	0.094
11	0.056	0.007	0.006	0.006	0.009	0.011	0.009	0.003	0.420	0.402	3.972	0.058	0.057	0.066	0.657	0.649	0.637	0.030	0.403	0.390
12	0.006	0.003	0.001	0.003	0.004	0.002	0.002	0.000	0.011	0.008	0.058	4.057	0.061	0.058	0.717	0.043	0.723	0.750	0.010	0.008
13	0.006	0.003	0.002	0.001	0.003	0.002	0.004	0.000	0.010	0.007	0.057	0.061	4.055	0.059	0.043	0.711	0.732	0.747	0.009	0.007
14	0.007	0.001	0.003	0.003	0.002	0.005	0.003	0.000	0.007	0.009	0.066	0.058	0.059	4.056	0.717	0.719	0.043	0.743	0.006	0.011
15	0.009	0.002	0.003	0.004	0.005	0.005	0.001	0.000	0.022	0.045	0.657	0.717	0.043	0.717	3.404	0.354	0.336	0.258	0.016	0.021
16	0.009	0.003	0.004	0.002	0.001	0.006	0.005	0.000	0.022	0.019	0.649	0.043	0.711	0.719	0.354	3.398	0.311	0.289	0.017	0.046
17	0.011	0.005	0.002	0.002	0.005	0.001	0.006	0.000	0.025	0.017	0.637	0.723	0.732	0.043	0.336	0.311	3.422	0.289	0.070	0.017
18	0.003	0.000	0.000	0.000	0.000	0.000	0.000	0.000	0.004	0.004	0.030	0.750	0.747	0.743	0.258	0.289	0.289	3.395	0.004	0.004
19	0.401	0.009	0.007	0.008	0.046	0.017	0.019	0.004	0.094	0.988	0.403	0.010	0.009	0.006	0.016	0.017	0.070	0.004	3.157	0.994
20	0.420	0.007	0.011	0.011	0.021	0.025	0.023	0.004	0.980	0.094	0.390	0.008	0.007	0.011	0.021	0.046	0.017	0.004	0.994	3.135

Table S6: Meyer bond order matrix for[{(CpNi)$_3$Ni(μ$_3$-P)$_4$}$_2$(μ-Br)$_2$]. Atom number according to figure S37.

	1	2	3	4	5	6	7	8	9	10	11	54	55	56	57	58	59	60
1	1.179	0.017	0.504	0.469	0.029	0.017	0.006	0.008	0.009	0.009	0.007	0.010	0.038	0.009	0.009	0.007	0.009	0.009
2	0.017	1.179	0.467	0.504	0.010	0.010	0.038	0.009	0.007	0.009	0.009	0.016	0.005	0.029	0.008	0.009	0.009	0.008
3	0.504	0.467	3.741	0.008	0.813	0.751	0.816	0.047	0.067	0.058	0.081	0.004	0.000	0.001	0.002	0.001	0.001	0.001
4	0.469	0.504	0.008	3.745	0.001	0.003	0.001	0.002	0.001	0.001	0.001	0.749	0.819	0.814	0.048	0.067	0.058	0.081
5	0.029	0.010	0.813	0.001	3.400	0.354	0.233	0.307	0.036	0.722	0.694	0.000	0.001	0.001	0.000	0.000	0.000	0.000
6	0.017	0.010	0.751	0.003	0.354	3.450	0.292	0.335	0.709	0.048	0.714	0.000	0.000	0.000	0.000	0.000	0.000	0.000
7	0.006	0.038	0.816	0.001	0.233	0.292	3.353	0.305	0.716	0.721	0.031	0.000	0.001	0.002	0.000	0.000	0.001	0.000
8	0.008	0.009	0.047	0.002	0.307	0.335	0.305	3.384	0.703	0.728	0.693	0.000	0.000	0.000	0.000	0.000	0.000	0.000
9	0.009	0.007	0.067	0.001	0.036	0.709	0.716	0.703	4.009	0.066	0.072	0.000	0.000	0.000	0.000	0.000	0.000	0.000
10	0.009	0.009	0.058	0.001	0.722	0.048	0.721	0.728	0.066	3.999	0.065	0.000	0.001	0.000	0.000	0.000	0.001	0.000
11	0.007	0.009	0.081	0.001	0.694	0.714	0.031	0.693	0.072	0.065	4.023	0.000	0.000	0.000	0.000	0.000	0.000	0.000
54	0.010	0.016	0.004	0.749	0.000	0.000	0.000	0.000	0.000	0.000	0.000	3.451	0.291	0.354	0.339	0.708	0.048	0.715
55	0.038	0.005	0.000	0.819	0.001	0.000	0.001	0.000	0.000	0.001	0.000	0.291	3.357	0.234	0.306	0.714	0.721	0.032
56	0.009	0.029	0.001	0.814	0.001	0.000	0.002	0.000	0.000	0.000	0.000	0.354	0.234	3.398	0.302	0.036	0.721	0.695
57	0.009	0.008	0.002	0.048	0.000	0.000	0.000	0.000	0.000	0.000	0.000	0.339	0.306	0.302	3.384	0.703	0.728	0.693
58	0.007	0.009	0.001	0.067	0.000	0.000	0.000	0.000	0.000	0.000	0.000	0.708	0.714	0.036	0.703	4.008	0.066	0.073
59	0.009	0.009	0.001	0.058	0.000	0.000	0.001	0.000	0.000	0.001	0.000	0.048	0.721	0.721	0.728	0.066	3.998	0.064
60	0.009	0.008	0.001	0.081	0.000	0.000	0.000	0.000	0.000	0.000	0.000	0.715	0.032	0.695	0.693	0.073	0.064	4.024

Table S7: Wiberg Bond Indices for [{(CpNi)$_3$Ni(μ$_3$-P)$_4$}$_2$(μ,η$^{4:4}$-P$_4$)] and [{(CpNi)$_3$Ni(μ$_3$-P)$_4$}$_2$(μ-Br)$_2$], calculated at the TPSSh/def2-TZVP level. Atom number according to figure S37.

[{(CpNi)$_3$Ni(μ$_3$-P)$_4$}$_2$(μ,η$^{4:4}$-P$_4$)]		[{(CpNi)$_3$Ni(μ$_3$-P)$_4$}$_2$(μ-Br)$_2$]	
	WBI		WBI
p 5 - ni 1	0.658	ni 3 - br 1	0.504
p 5 - ni 2	0.716	ni 3 - br 2	0.467
p 5 - ni 4	0.719	ni 4 - br 1	0.469
p 6 - ni 1	0.635	ni 4 - br 2	0.504
p 6 - ni 3	0.723	p 5 - ni 3	0.813
p 6 - ni 4	0.723	p 6 - ni 3	0.751
p 6 - p 5	0.334	p 6 - p 5	0.354
p 7 - ni 1	0.652	p 7 - ni 3	0.816
p 7 - ni 2	0.718	p 7 - p 5	0.233
p 7 - ni 3	0.716	p 7 - p 6	0.292
p 7 - p 5	0.358	p 8 - p 5	0.307
p 7 - p 6	0.314	p 8 - p 6	0.335
p 8 - ni 2	0.743	p 8 - p 7	0.305
p 8 - ni 3	0.749	ni 9 - p 6	0.709
p 8 - ni 4	0.755	ni 9 - p 7	0.716
p 8 - p 5	0.256	ni 9 - p 8	0.703
p 8 - p 6	0.298	ni 10 - p 5	0.722
p 8 - p 7	0.278	ni 10 - p 7	0.721
p 9 - ni 1	0.390	ni 10 - p 8	0.728
p 10 - ni 1	0.407	ni 11 - p 5	0.694
p 10 - p 9	0.993	ni 11 - p 6	0.714
ni 11 - p 9	0.420	ni 11 - p 8	0.693
ni 11 - p 10	0.402	p 54 - ni 4	0.749
p 15 - ni 11	0.657	p 55 - ni 4	0.819
p 15 - ni 12	0.717	p 55 - p 54	0.291
p 15 - ni 14	0.717	p 56 - ni 4	0.814
p 16 - ni 11	0.649	p 56 - p 54	0.354
p 16 - ni 13	0.711	p 56 - p 55	0.234
p 16 - ni 14	0.719	p 57 - p 54	0.339
p 16 - p 15	0.354	p 57 - p 55	0.306
p 17 - ni 11	0.637	p 57 - p 56	0.302
p 17 - ni 12	0.723	ni 58 - p 54	0.708
p 17 - ni 13	0.732	ni 58 - p 55	0.714
p 17 - p 15	0.336	ni 58 - p 57	0.703
p 17 - p 16	0.311	ni 59 - p 55	0.721
p 18 - ni 12	0.750	ni 59 - p 56	0.721
p 18 - ni 13	0.747	ni 59 - p 57	0.729
p 18 - ni 14	0.743	ni 60 - p 54	0.715
p 18 - p 15	0.258	ni 60 - p 56	0.695
p 18 - p 16	0.289	ni 60 - p 57	0.693
p 18 - p 17	0.289		
p 19 - ni 1	0.401		
p 19 - p 10	0.988		
p 19 - ni 11	0.403		
p 20 - ni 1	0.420		
p 20 - p 9	0.980		
p 20 - ni 11	0.390		
p 20 - p 19	0.994		

Table S8: Total energies calculated at the TPSSh/def2-TZVP level.

Compound	Total energy (hartree)
$[\{(CpNi)_3Ni(\mu_3\text{-}P)_4\}_2(\mu,\eta^{4:4}\text{-}P_4)]$	-17325.93166596117
$[\{(CpNi)_3Ni(\mu_3\text{-}P)_4\}_2(\mu\text{-}Br)_2]$	-21108.547319478
$[(CpNi)_3Ni(\mu_3\text{-}P)_4(Br)]$	-10554.2590437451

Table S9: Natural charge of selected fragments in $[\{(CpNi)_3Ni(\mu_3\text{-}P)_4\}_2(\mu,\eta^{4:4}\text{-}P_4)]$ and $[\{(CpNi)_3Ni(\mu_3\text{-}P)_4\}_2(\mu\text{-}Br)_2]$ calculated at the TPSSh/def2-TZVP level.

Fragment	Natural charge	
	$[\{(CpNi)_3Ni(\mu_3\text{-}P)_4\}_2(\mu,\eta^{4:4}\text{-}P_4)]$	$[\{(CpNi)_3Ni(\mu_3\text{-}P)_4\}_2(\mu\text{-}Br)_2]$
$(CpNi)_3(\mu_3\text{-}P)_4$	0.125	0.150
cyco-P_4	-0.566	—
Ni1	0.157	0.368
Ni11	0.157	0.368
Br1	—	-0.517
Br2	—	-0.517

Table S10: Cartesian coordinates of the optimized geometry of $[\{(CpNi)_3Ni(\mu_3\text{-}P)_4\}_2(\mu,\eta^{4:4}\text{-}P_4)]$ at the TPSSh/def2-TZVP level.

Ni	-1.1469258	1.3695095	-0.1368216
Ni	-4.3316238	2.4061504	-1.4107990
Ni	-1.6382470	4.6226258	-1.4257945
Ni	-3.1867192	3.7080435	1.5908137
P	-3.2615166	1.8323042	0.4337013
P	-1.3038617	3.5203436	0.4551643
P	-2.1573951	2.5086986	-1.7801922
P	-3.6205268	4.2906951	-0.4988341
P	0.7223908	0.4659076	-1.3075000
P	0.9469360	0.9183625	0.8468529
Ni	1.1531616	-1.3587699	0.1847165
Ni	3.6388792	-2.8990045	2.2171080
Ni	1.4969424	-4.8696710	0.2692711
Ni	4.0214228	-2.9590174	-1.2278313
P	3.3606785	-1.6478201	0.4220625
P	1.8286197	-3.1166965	-1.0288284
P	1.5409406	-3.0806758	1.5570234
P	3.6201402	-4.2869603	0.4936775
P	-0.7153520	-0.4660355	1.3121046
P	-0.9489672	-0.9114462	-0.8425628
C	-5.8353869	2.9274251	-2.8582938
H	-5.8854729	3.8851580	-3.3532935
C	-5.3126454	0.7385959	-2.3698064
C	-1.8304344	6.5707682	-2.3251130
C	-5.1302556	1.7828239	-3.3187550
C	-3.2310053	3.2124844	3.6898260
H	-2.8278658	2.2979374	4.0969543
C	-1.4556219	5.6282130	-3.3212060
H	-2.0281419	5.3689318	-4.1985665
C	-0.8030810	6.6084720	-1.3415988
H	-0.7940053	7.2238186	-0.4550480
C	-4.6749905	4.7420980	2.7524244
H	-5.5568217	5.1932428	2.3239574
C	-4.5631176	3.4055265	3.2194489
C	-6.1424588	1.2373486	-1.3257344
C	0.2124608	5.6895295	-1.7355233
C	-6.4639019	2.5886787	-1.6233493
C	-0.1897556	5.0838435	-2.9544699
C	-2.5257117	4.4335533	3.5163282
C	-3.4130465	5.3796936	2.9321006
C	4.1487316	-3.8754444	4.0691230
H	3.8248614	-4.8691408	4.3379913
C	4.2232324	-1.5863104	3.8275565
C	1.5499264	-7.0196942	0.4131718
C	3.4630190	-2.6623835	4.3581509
C	4.6637087	-1.8767978	-2.9814349
H	4.1713068	-0.9906043	-3.3513295
C	0.6533691	-6.5057041	1.3891477
H	0.7469395	-6.6151888	2.4587267
C	1.0671447	-6.6462784	-0.8720787

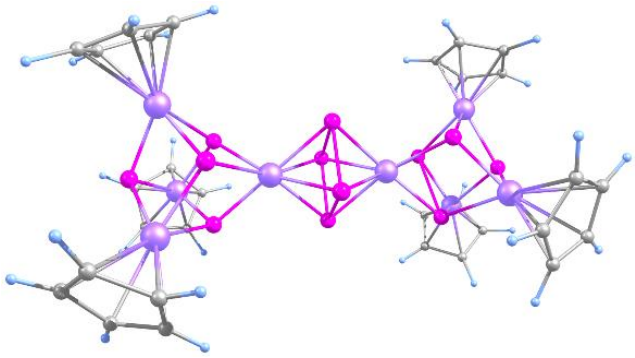

H	1.5284624	-6.8843654	-1.8182828
C	6.0702351	-3.2713533	-1.8043513
H	6.8347498	-3.6289950	-1.1318230
C	5.7249866	-1.9121429	-2.0326860
C	5.3886350	-2.1326140	3.2141152
H	6.1647768	-1.5719166	2.7161559
C	-0.1356523	-5.9042262	-0.6882804
C	5.3415233	-3.5444385	3.3635140
C	-0.3906330	-5.8161010	0.7051364
C	4.3593101	-3.2182159	-3.3447915
C	5.2223078	-4.0810752	-2.6163875
H	3.5905596	-3.5270434	-4.0365571
H	5.2327698	-5.1591524	-2.6655196
H	6.1755043	-1.0548995	-1.5561515
H	2.4511125	-7.5790538	0.6128976
H	-1.2203597	-5.3028843	1.1665228
H	-0.7368277	-5.4664926	-1.4704558
H	3.9599927	-0.5405778	3.8712954
H	6.0736468	-4.2462416	2.9943369
H	2.5166398	-2.5760835	4.8698219
H	-7.0719745	3.2454072	-1.0202998
H	-6.4558225	0.6888045	-0.4506432
H	-4.8899070	-0.2527233	-2.4269559
H	-4.5391759	1.7223535	-4.2197795
H	-2.7445182	7.1444343	-2.3077551
H	1.1197190	5.4757441	-1.1914669
H	0.3584703	4.3299097	-3.4983079
H	-1.4887578	4.6051888	3.7616386
H	-5.3452960	2.6619685	3.2100238
H	-3.1744339	6.3996460	2.6723980

Table S11: Cartesian coordinates of the optimized geometry of [{(CpNi)$_3$Ni(μ$_3$-P)$_4$}$_2$(μ-Br)$_2$] at the TPSSh/def2-TZVP level.

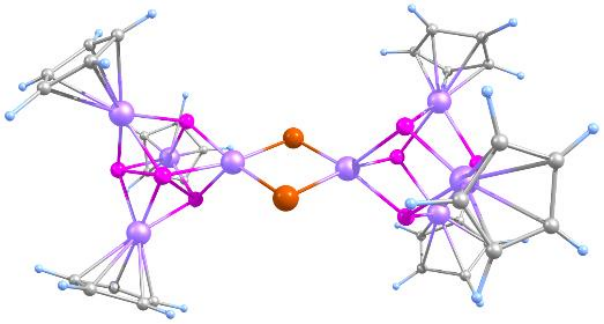

Br	-0.5069076	1.3156683	1.0433864
Br	0.3944153	-1.3246653	-1.0475112
Ni	0.1770041	-1.0011557	1.3878384
Ni	-0.2581341	1.0022014	-1.3897018
P	1.3942505	-2.7280901	2.0017810
P	-1.1394124	-2.5556349	2.1932225
P	0.2997642	-0.8849390	3.5844641
P	0.2008867	-3.4219768	4.2157877
Ni	-1.4892220	-1.9834434	4.2862816
Ni	2.0255703	-2.1874466	4.0411367
Ni	0.0067268	-4.4329069	2.2417752
C	-2.9488655	-0.5107688	4.8610041
C	-3.6065679	-1.6540600	4.3415877
C	-3.2740546	-2.7716173	5.1661889
H	-3.6197941	-3.7850431	5.0308488
C	-2.4179934	-2.3091345	6.2040526
C	-2.2053091	-0.9182636	6.0098277
H	-1.5877284	-0.2790569	6.6220371
C	-0.2546667	-5.6392097	0.4817827
C	0.9535690	-6.0062267	1.1370432
C	0.6306361	-6.4765089	2.4422926
H	1.3330628	-6.8240752	3.1840865
C	-0.7800453	-6.3902687	2.5997104
C	-1.3254493	-5.8695261	1.3897143
H	-2.3699022	-5.6764654	1.1978935
C	3.4952364	-0.8038638	4.8058382
C	4.1097945	-1.6650897	3.8609287
C	3.9963469	-3.0020096	4.3458072
H	4.3627268	-3.8887296	3.8514446
C	3.3188057	-2.9593155	5.5944838
C	3.0006472	-1.6030976	5.8780306
H	2.4794086	-1.2413290	6.7510559
C	2.8921466	0.4093616	-4.8030748
C	3.5768079	1.5382788	-4.2873701
C	3.2885852	2.6560348	-5.1284221
H	3.6629682	3.6600923	-4.9995000
C	2.4329293	2.2077966	-6.1727426
C	2.1759310	0.8262286	-5.9660179
H	1.5473038	0.1989115	-6.5792905
C	0.2758177	5.6294952	-0.4760075
C	-0.9090200	6.0285771	-1.1555065
C	-0.5476974	6.4882602	-2.4542461
H	-1.2255516	6.8538475	-3.2100903
C	0.8628741	6.3624204	-2.5838482
C	1.3699715	5.8291519	-1.3625565
H	2.4047549	5.6076460	-1.1501867
C	-3.5462091	0.9152486	-4.8506157
C	-4.1434926	1.7992968	-3.9157188
C	-3.9771847	3.1306000	-4.4009590
H	-4.3197262	4.0304468	-3.9132721
C	-3.2835445	3.0618345	-5.6394630

C	-3.0087074	1.6946645	-5.9165125
H	-2.4879506	1.3134214	-6.7815016
P	1.1091290	2.5210279	-2.1779359
P	-0.3636087	0.8919870	-3.5868944
P	-1.4216507	2.7619011	-2.0159507
P	-0.1742621	3.4230033	-4.2170537
Ni	1.4699717	1.9307061	-4.2641478
Ni	-2.0401106	2.2486071	-4.0667000
Ni	0.0151938	4.4281918	-2.2397574
H	-4.6246013	1.5163088	-2.9920736
H	-3.4898129	-0.1587712	-4.7602710
H	-2.9933864	3.9026779	-6.2506828
H	0.3298521	5.2201793	0.5208453
H	-1.9112901	5.9783842	-0.7581993
H	1.4461202	6.6164231	-3.4556040
H	2.8895537	-0.5817689	-4.3764388
H	4.1923944	1.5552062	-3.4010411
H	2.0256253	2.8176141	-6.9644871
H	4.5677642	-1.3642412	2.9312037
H	3.3999451	0.2676498	4.7183659
H	3.0666370	-3.8108035	6.2078057
H	-4.2332803	-1.6797201	3.4632995
H	-2.9817477	0.4845978	4.4456081
H	-1.9818910	-2.9150945	6.9833200
H	1.9461018	-5.9280438	0.7203297
H	-0.3396811	-5.2305363	-0.5131609
H	-1.3387710	-6.6610524	3.4824039

Table S12: Cartesian coordinates of the optimized geometry of $[(CpNi)_3Ni(\mu_3\text{-}P)_4(Br)]$ at the TPSSh/def2-TZVP level.

Br	-0.0845457	3.2235382	-4.0905063
Ni	-0.0887297	1.8513363	-2.3023484
P	1.1926614	0.2241886	-1.6390807
P	-1.4035194	0.3492783	-1.4360791
P	0.0574694	2.0333400	-0.1390935
P	0.0490937	-0.4772611	0.5583379
Ni	-1.6683303	0.9297305	0.6755093
Ni	1.8370205	0.8367488	0.3776952
Ni	-0.1802201	-1.4852888	-1.4128975
C	-3.1697837	2.3555707	1.2614809
C	-3.7952215	1.1503262	0.8548310
C	-3.3475807	0.1017811	1.7154625
H	-3.6461513	-0.9338698	1.6615655
C	-2.4476025	0.6665310	2.6593470
C	-2.3241263	2.0544094	2.3712177
H	-1.7053948	2.7600681	2.9042108
C	-0.8914100	-2.7052612	-3.0304878
C	0.5063593	-2.8808766	-2.8923303
C	0.7627325	-3.3990054	-1.5847784
H	1.7329595	-3.6396074	-1.1779501
C	-0.4852869	-3.5568467	-0.9235284
C	-1.5071610	-3.1107351	-1.8053952
H	-2.5654347	-3.0932471	-1.5941284
C	3.3494539	2.2755843	0.8783142
C	3.9406312	1.2115333	0.1568653
C	3.7384312	0.0065309	0.8993564
H	4.0734301	-0.9781273	0.6113371
C	3.0378458	0.3371937	2.0910873
C	2.7776897	1.7340480	2.0725936
H	2.2545399	2.2932356	2.8331862
H	4.4353993	1.2907709	-0.7988999
H	3.3149718	3.3096061	0.5716106
H	2.7265427	-0.3563195	2.8569733
H	-4.4787915	1.0401190	0.0269228
H	-3.2922048	3.3233214	0.8002733
H	-1.9276311	0.1320928	3.4393330
H	1.2515135	-2.6438196	-3.6361464
H	-1.4007018	-2.3127357	-3.8970205
H	-0.6289174	-3.9178816	0.0831597

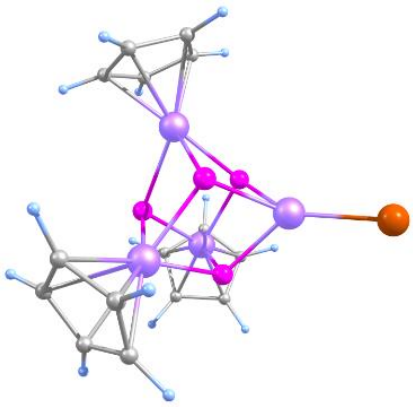

3.6 References

[1] a) O. J. Scherer, *Acc. Chem. Res.* **1999**, *32*, 751–762; b) N. A. Giffin, J. D. Masuda, *Coord. Chem. Rev.* **2011**, *255*, 1342–1359; c) M. Caporali, L. Gonsalvi, A. Rossin, M. Peruzzini, *Chem. Rev.* **2010**, *110*, 4178–4235; d) L. Qiao, C. Zhang, X. W. Zhang, Z. C. Wang, H. Yin, Z. M. Sun, *Chin. J. Chem.* **2020**, *38*, 295–304; e) F. Scalambra, M. Peruzzini, A. Romerosa, *Adv. Organomet. Chem.* **2019**, 173–222; f) M. Seidl, G. Balázs, M. Scheer, *Chem. Rev.* **2019**, *119*, 8406–8434.

[2] M. Scheer, G. Balázs, A. Seitz, *Chem. Rev.* **2010**, *110*, 4236–4256.

[3] B. M. Cossairt, N. A. Piro, C. C. Cummins, *Chem. Rev.* **2010**, *110*, 4164–4177.

[4] a) W. B. Tolman, *Activation of Small Molecules: Organometallic and Bioinorganic Perspectives*, Wiley, **2006**; b) S. Gambarotta, *J. Organomet. Chem.* **1995**, *500*, 117–126; c) H. K. Chae, D. Y. Siberio-Pérez, J. Kim, Y. Go, M. Eddaoudi, A. J. Matzger, M. O'Keeffe, O. M. Yaghi, *Nature* **2004**, *427*, 523–527; d) H.-Y. Chung, M. B. Weinberger, J. B. Levine, R. W. Cumberland, A. Kavner, J.-M. Yang, S. H. Tolbert, R. B. Kaner, *Science* **2007**, *316*, 436–439; e) C. W. Chang, D. Okawa, A. Majumdar, A. Zettl, *Science* **2006**, *314*, 1121–1124; f) D. W. Stephan, *Dalton Trans.* **2009**, 3129–3136; g) D. W. Stephan, G. Erker, *Angew. Chem. Int. Ed.* **2015**, *54*, 6400–6441.

[5] a) K. Ding, A. W. Pierpont, W. W. Brennessel, G. Lukat-Rodgers, K. R. Rodgers, T. R. Cundari, E. Bill, P. L. Holland, *J. Am. Chem. Soc.* **2009**, *131*, 9471–9472; b) J. M. Smith, R. J. Lachicotte, K. A. Pittard, Th. R. Cundari, G. Lukat-Rodgers, K. R. Rodgers, P. L. Holland, *J. Am. Chem. Soc.* **2001**, *123*, 9222–9223; c) D. J. E. Spencer, N. W. Aboelella, A. M. Reynolds, P. L. Holland, W. B. Tolman, *J. Am. Chem. Soc.* **2002**, *124*, 2108–2109; d) F. Spitzer, M. Sierka, M. Latronico, P. Mastrorilli, A. V. Virovets, M. Scheer, *Angew. Chem. Int. Ed.* **2015**, *54*, 4392–4396.

[6] F. Spitzer, C. Graßl, G. Balázs, E. M. Zolnhofer, K. Meyer, M. Scheer, *Angew. Chem. Int. Ed.* **2016**, *55*, 4340–4344.

[7] S. Yao, T. Szilvási, N. Lindenmaier, Y. Xiong, S. Inoue, M. Adelhardt, J. Sutter, K. Meyer, M. Driess, *Chem. Commun.* **2015**, *51*, 6153–6156.

[8] S. Yao, N. Lindenmaier, Y. Xiong, S. Inoue, T. Szilvási, M. Adelhardt, J. Sutter, K. Meyer, M. Driess, *Angew. Chem. Int. Ed.* **2015**, *127*, 1266–1270.

[9] S. Yao, Y. Xiong, C. Milsmann, E. Bill, S. Pfirrmann, C. Limberg, M. Driess, *Chem. Eur. J.* **2010**, *16*, 436–439.

[10] F. Spitzer, C. Graßl, G. Balázs, E. Mädl, M. Keilwerth, E. M. Zolnhofer, K. Meyer, M. Scheer, *Chem. Eur. J.* **2017**, *23*, 2716–2721.

[11] a) S. Heinl, M. Scheer, *Chem. Sci.* **2014**, *5*, 3221–3225; b) C. Schwarzmaier, A. Y. Timoshkin, G. Balázs, M. Scheer, *Angew. Chem. Int. Ed.* **2014**, *53*, 9077–9081.

[12] a) M. E. Barr, L. F. Dahl, *Organometallics* **1991**, *10*, 3991–3996; b) F. Dielmann, M. Sierka, A. V. Virovets, M. Scheer, *Angew. Chem. Int. Ed.* **2010**, *49*, 6860–6864; c) O. J. Scherer, K. Pfeiffer, G. Heckmann, G. Wolmershäuser, *J. Organomet. Chem.* **1992**, *425*, 141–149; d) C. Graßl, M. Bodensteiner, M. Zabel, M. Scheer, *Chem. Sci.* **2015**, *6*, 1379–1382.

[13] a) A. Cavaillé, N. Saffon-Merceron, N. Nebra, M. Fustier-Boutignon, N. Mézailles, *Angew. Chem.* **2018**, *57*, 1874–1878; b) F. Dielmann, A. Timoshkin, M. Piesch, G. Balázs, M. Scheer, *Angew. Chem. Int. Ed.* **2017**, *56*, 1671–1675.

[14] M. Modl, S. Heinl, G. Balázs, F. Delgado Calvo, M. Caporali, G. Manca, M. Keilwerth, K. Meyer, M. Peruzzini, M. Scheer, *Chem. Eur. J.* **2019**, *25*, 6300–6305.

[15] T. Wettling, B. Geissler, R. Schneider, S. Barth, P. Binger, M. Regitz, *Angew. Chem. Int. Ed.* **1992**, *31*, 758–759.

[16] C. Fish, M. Green, J. C. Jeffery, R. J. Kilby, J. M. Lynam, J. E. McGrady, D. A. Pantazis, C. A. Russell, C. E. Willans, *Chem. Commun.* **2006**, 1375–1377.

[17] B. Rink, O. J. Scherer, G. Wolmershäuser, *Chem. Ber.* **1995**, *128*, 71–73.

[18] N. A. Piro, J. S. Figueroa, J. T. McKellar, C. C. Cummins, *Science* **2006**, *313*, 1276-1279.

[19] B. M. Cossairt, M. C. Diawara, C. C. Cummins, *Science* **2009**, *323*, 602.

[20] J. M. Goicoechea, H. Grützmacher, *Angew. Chem. Int. Ed.* **2018**, *57*, 16968–16994.

[21] A. M. Tondreau, Z. Benkő, J. R. Harmer, H. Grützmacher, *Chem. Sci.* **2014**, *5*, 1545-1554.

[22] O. J. Scherer, M. Swarowsky, H. Swarowsky, G. Wolmershäuser, *Angew. Chem. Int. Ed.* **1988**, *27*, 694–695.

[23] M. Schmidt, A. E. Seitz, M. Eckhardt, G. Balázs, E. V. Peresypkina, A. V. Virovets, F. Riedlberger, M. Bodensteiner, E. M. Zolnhofer, K. Meyer, M. Scheer, *J. Am. Chem. Soc.* **2017**, *139*, 13981–13984.

[24] A. E. Seitz, M. Eckhardt, A. Erlebach, E. V. Peresypkina, M. Sierka, M. Scheer, *J. Am. Chem. Soc.* **2016**, *138*, 10433–10436.

[25] a) E. Mädl, E. Peresypkina, A. Y. Timoshkin, M. Scheer, *Chem. Commun.* **2016**, *52*, 12298–12301; b) C. Riesinger, L. Dütsch, G. Balázs, M. Bodensteiner, M. Scheer, *Chemistry* **2020**, *26*, 17165–17170.

[26] O. J. Scherer, J. Braun, G. Wolmershäuser, *Chem. Ber.* **1990**, *123*, 471–475.

[27] O. J. Scherer, J. Braun, P. Walther, G. Wolmershäuser, *Chem. Ber.* **1992**, *125*, 2661-2665.

[28] The crude NMR spectra of 6b show the formation of a complex mixture, which has to be separated by column chromatography. Therefore, the isolated yield is moderate.

[29] M. Schär, D. Saurenz, F. Zimmer, I. Schädlich, G. Wolmershäuser, S. Demeshko, F. Meyer, H. Sitzmann, O. M. Heigl, F. H. Köhler, *Organometallics* **2013**, *32*, 6298–6305.

[30] O. J. Scherer, T. Dave, J. Braun, G. Wolmershäuser, *J. Organomet. Chem.* **1988**, *350*, C20-C24.

[31] P. Pyykkö, M. Atsumi, *Chem. Eur. J.* **2009**, *15*, 186–197.

[32] E. Mädl, G. Balázs, E. V. Peresypkina, M. Scheer, *Angew. Chem. Int. Ed.* **2016**, *55*, 7702–7707.

[33] The crude NMR spectra of the triple-decker compounds show the formation of a complex mixture, which has to be separated by column chromatography. Therefore, the isolated yields are moderate.

[34] A. F. Holleman, N. Wiberg, *Lehrbuch der Anorganischen Chemie*, **2007**.

[35] F. Kraus, T. Hanauer, N. Korber, *Inorg. Chem.* **2006**, *45*, 1117–1123.

[36] O. J. Scherer, J. Vondung, G. Wolmershäuser, *J. Organomet. Chem.* **1989**, *376*, C35-C38.

[37] 0. J. Scherer, R. Winter, C. Wolmershäuser, *Z. Anorg. Allg. Chem.* **1993**, *619*, 827-883.

[38] a) M. Scheer, E. Herrmann, J. Sieler, M. Oehme, *Angew. Chem.* **1991**, *103*, 1023–1025; b) C. Schwarzmaier, A. Noor, G. Glatz, M. Zabel, A. Y. Timoshkin, B. M. Cossairt, C. C. Cummins, R. Kempe, M. Scheer, *Angew. Chem. Int. Ed.* **2011**, *50*, 7283–7286; c) M. Heberhold, G. Frohmader, W. Milius, *J. Organomet. Chem.* **1996**, *522*, 185–196.

[39] M. Piesch, C. Graßl, M. Scheer, *Angew. Chem. Int. Ed.* **2020**, *59*, 7154–7160.

[40] F. Spitzer, G. Balázs, C. Graßl, M. Keilwerth, K. Meyer, M. Scheer, *Angew. Chem. Int. Ed.* **2018**, *57*, 8760–8764.

[41] D. Shining, *diploma thesis*, University of Karlsruhe, **2020**.

[42] W. M. Tsai, M. D. Rausch, R. D. Rogers, *Organometallics* **1996**, *15*, 2591–2594.

[43] M. Scheer, J. Wachter, *Präparative Metallorganische Chemie für Fortgeschrittene*, Universität Regensburg, **2008**.

[44] a) O. J. Scherer, H. Swarowsky, G. Wolmhäuser, *Angew. Chem. Int. Ed. Engl.* **1988**, *27*, 694–695; b) A. E. Seitz, U. Vogel, M. Eberl, M. Eckhardt, G. Balázs, E. V. Peresypkina, M. Bodensteiner, M. Zabel, M. Scheer, *Chemistry* **2017**, *23*, 10319–10327.

[45] M. Schmidt, A. E. Seitz, M. Eckhardt, G. Balázs, E. V. Peresypkina, A. V. Virovets, F. Riedlberger, M. Bodensteiner, E. M. Zolnhofer, K. Meyer, M. Scheer, *J. Am. Chem. Soc.* **2017**, *139*, 13981–13984.

[46] M. Schär, D. Saurenz, F. Zimmer, I. Schädlich, G. Wolmershäuser, S. Demeshko, F. Meyer, H. Sitzmann, O. M. Heigl, F. H. Köhler, *Organometallics* **2013**, *32*, 6298–6305.

[47] E. Mädl, G. Balázs, E. V. Peresypkina, M. Scheer, *Angew. Chem. Int. Ed.* **2016**, *55*, 7702–7707.

[48] Rigaku Oxford Diffraction, *CrysAlisPro Software System Version 1.171.38.43*, (**2008--2020**).

[49] L. J. Bourhis, O. V. Dolomanov, R. J. Gildea, J. A. K. Howard, H. Puschmann, *J. Appl. Cryst.* **2009**, *42*, 339–341.

[50] L. J. Bourhis, O. V. Dolomanov, R. J. Gildea, J. A. K. Howard, H. Puschmann, *Acta Cryst.* **2015**, *A71*, 59–75.

[51] G. M. Sheldrick, *Acta Cryst.* **2015**, *A71*, 3–8.

[52] G. M. Sheldrick, *Acta Cryst.* **2015**, *C71*, 3–8.

[53] a) R. Ahlrichs, M. Bär, M. Häser, H. Horn, C. Kölmel, *Theor. Chem. Acc.* **1989**, *162*, 165–169; b) F. Furche, R. Ahlrichs, C. Hättig, W. Klopper, M. Sierka, F. Weigend, *WIREs Comput Mol Sci* **2014**, *4*, 91–100; c) O. Treutler, R. Ahlrichs, *J. Chem. Phys.* **1995**, *102*, 346–354; d) TURBOMOLE V6.4, a development of University of Karlsruhe and Forschungszentrum Karlsruhe GmbH, http://www.turbomole.com.

[54] K. Eichkorn, O. Treutler, H. Oehm, M. Häser, R. Ahlrichs, *Chem. Phys. Lett.* **1995**, *242*, 652–660.

[55] K. Eichkorn, F. Weigend, O. Treutler, R. Ahlrichs, *Theor. Chem. Acc.* **1997**, *97*, 119.

[56] a) J. Tao, J. P. Perdew, V. N. Staroverov, G. E. Scuseria, *Chem. Rev. Lett.* **2003**, *91*, 146401; b) V. N. Staroverov, G. E. Scuseria, J. Tao, J. P. Perdew, *J. Chem. Phys.* **2003**, *119*, 12129–12137.

[57] a) F. Weigend, R. Ahlrichs, *Phys. Chem. Chem. Phys.* **2005**, *7*, 3297–3305; b) A. Schäfer, H. Horn, R. Ahlrichs, *J. Chem. Phys.* **1992**, *97*, 2571–2577.

[58] F. Weigend, *Phys. Chem. Chem. Phys.* **2006**, *8*, 1057–1065.

[59] M. Sierka, A. Hogekamp, R. Ahlrichs, *J. Chem. Phys.* **2003**, *118*, 9136–9148.

[60] a) A. D. Becke, K. E. Edgecombe, *J. Chem. Phys.* **1990**, *92*, 5397–5403; b) A. Savin, O. Jepsen, J. Flad, O. K. Andersen, H. Preuss, H. G. von Schnering, *Angew. Chem. Int. Ed. Engl.* **1992**, *31*, 187–188.

[61] a) H. Jacobsen, *Can. J. Chem.* **2008**, *86*, 695–702; b) H. L. Schmider, A. D. Becke, *J. Molec. Struct.: THEOCHEM* **2000**, *527*, 51–61.

[62] T. Lu, F. Chen, *J. Comput. Chem.* **2012**, *33*, 580–592

4 Tranfer of Polyantimony Units

V. Heinl, A. E. Seitz, G.Balázs, M. Seidl, M.Scheer, *Chem. Sci.* **2021**, *12*, 9726-9732. (DOI: 10.1039/d1sc02498a)

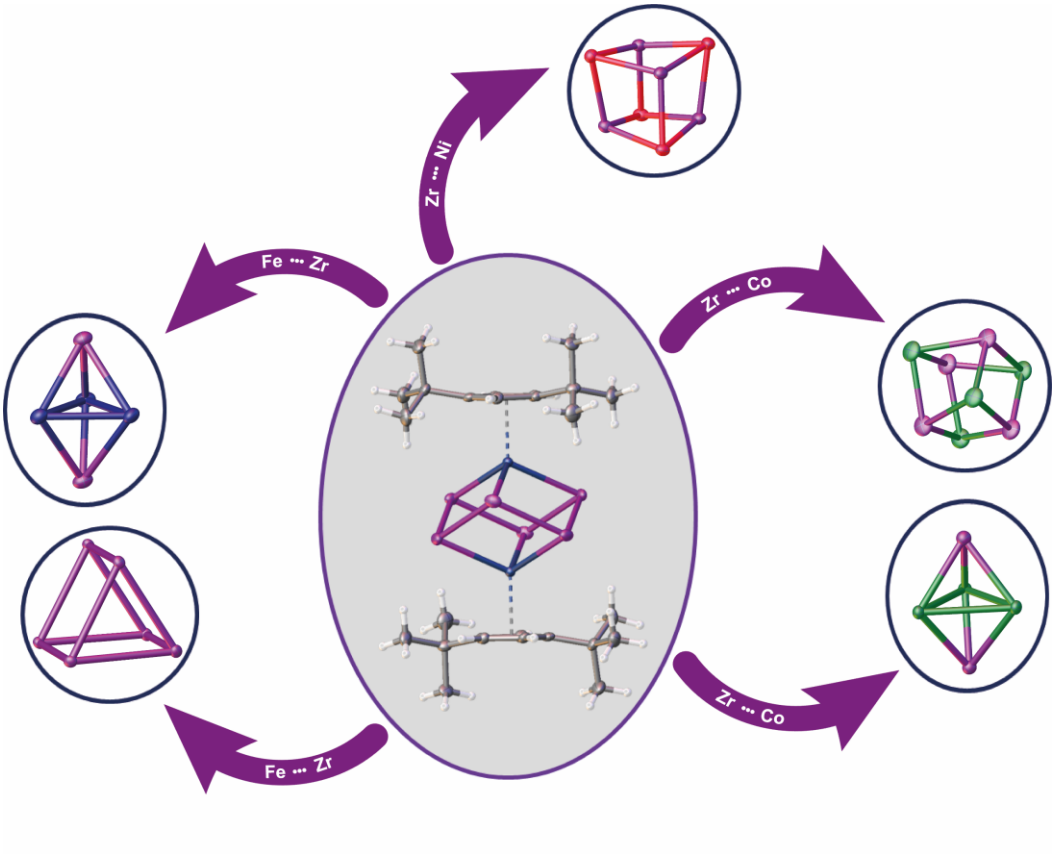

Abstract:

Transfer reagents are useful tools in chemistry to access metastable compounds. The reaction of $[Cp''_2ZrCl_2]$ with $KSb(SiMe_3)_2$ leads to the formation of the novel polyantimony triple decker complex $[(Cp''Zr)_2(\mu,\eta^{1:1:1:1:1:1}\text{-}Sb_6)]$ (**1**, Cp'' = 1,2-di-tertbutyl-cyclopentadienyl), containing a chair-like Sb_6^{6-} ligand. Compound **1** represents a valuable transfer reagent to form novel antimony ligand complexes. Thus, the reaction of **1** with Cp^R-substituted transition metal halides of nickel, cobalt and iron leads to the formation of a variety of novel Sb_n ligand complexes, such as the cubane-like compounds $[(Cp'''Ni)_4(\mu_3\text{-}Sb)_4]$ (**2**) and $[(Cp'''Co)_4(\mu_3\text{-}Sb_4)]$ (**3a**) or the complexes $[(Cp^{Bn}Co)_3(\mu_3\text{-}Sb)_2]$ (**4**) and $[(Cp'''Fe)_3(\mu_3\text{-}Sb)_2]$ (**5**), representing a trigonal bipyramidal structure. Moreover, beside the transfer of Sb_1 units, also the complete entity can be transferred as seen by the iron complex $[(Cp'''Fe)_3(\mu_3,\eta^{4:4:4}\text{-}Sb_6)]$ (**6**). DFT calculations shed light on the bonding situation of the products.

4.1 Author Contribution

- First Synthesis of the compounds **1**,**3b** and **4** were performed by A. E. Seitz during his Ph.D. thesis (University of Regensburg, **2017**).
- Synthesis and characterization of the compounds **2/2'**, **3a**, **5**, and **6** as well as completed characterization and optimized synthesis of **1** was performed by V. Heinl.
- Computational studies were performed by G. Balázs.
- M. Seidl recalculated the X-ray structures.
- The Manuscript was written by V. Heinl except parts of the computational details (G. Balázs).
- Supervision: M. Scheer.

4.2 Introduction

The reactivity of polypnictogen ligand complexes is an active field of chemical research, which resulted in numerous novel E_n complexes (E = P, As, Sb).[1,2] Especially for phosphorus and arsenic, a large variety of examples have been synthesized so far, usually by employing white phosphorus or yellow arsenic in the reaction with transition metal or main group compounds.[3,4-6] In contrast, the number of polyantimony ligand complexes is very limited and, therefore, their chemistry was far less investigated.[7] Reasons for this can be attributed to various challenges such as the sensitivity of antimony-containing compounds towards light, the weak Sb-Sb bonding[8] and especially the lack of suitable antimony sources. Since Sb_4 is only known in the gas phase or under special conditions, *e.g.* trapped in a solid neon matrix,[9] grey antimony, Zintl ions,[10] organo-substituted Sb precursors[11] and quite simply $SbCl_3$[12-14] and its derivatives were used as starting materials. In the 1970s, the first Sb_n ligand complex $[\{Co(CO)_3\}_4(\mu_3\text{-}Sb)_4]$ was published by *Dahl et al*. by the reaction of $Co(OAc)_2{\cdot}H_2O$ with $SbCl_3$ as antimony source (**I**, figure 1).[12] Even in the case of the complexes $[Sb_2\{W(CO)_5\}_3]$[13] (**II**) and $[\{(LGa(NMe_2)\}_2(\mu,\eta^{1:1}\text{-}Sb_4)]$[14] (**III**), $SbCl_3$ and $Sb(NMe_2)_3$ are used as precursors (Figure 1, L = $HC[C(Me)N(2,6\text{-}C_6H_3iPr_2)]_2$).

The most commonly applied antimony sources, to build polyantimony ligand complexes or main group compounds, are neutral organo-substituted antimony units such as R_4Sb_4 (R = Cp*, ^{t}Bu; Cp* = $\eta^5\text{-}C_5Me_5$)[15–17] and R'_4Sb_2 (R' = Me, Et).[18] *Rösler et al.* succeeded in the synthesis of the molybdenum complexes $[\{CpMo(CO)_2\}_2(\mu,\eta^2\text{-}Sb_2)]$ (**IV**) and $[Cp'''Mo(\mu,\eta^{5:5}\text{-}Sb_5)MoCp^R]$ (**V**, Figure 1; Cp''' = $\eta^5\text{-}C_5H_2{}^tBu_3$, Cp^R = $\eta^5\text{-}C_5H_2{}^tBu_2Me$) by thermolysis of $^tBu_4Sb_4$ with $[CpMo(CO)_3]_2$ and $[Cp'''Mo(CO)_3CH_3]$, respectively.[15,16] **V** represents the first triple-decker sandwich complex containing a *cyclo*-Sb_5 middle deck.

Interestingly, one *t*Bu group of the Cp''' ligand is degraded to a methyl group during the thermolytic reaction.[16]

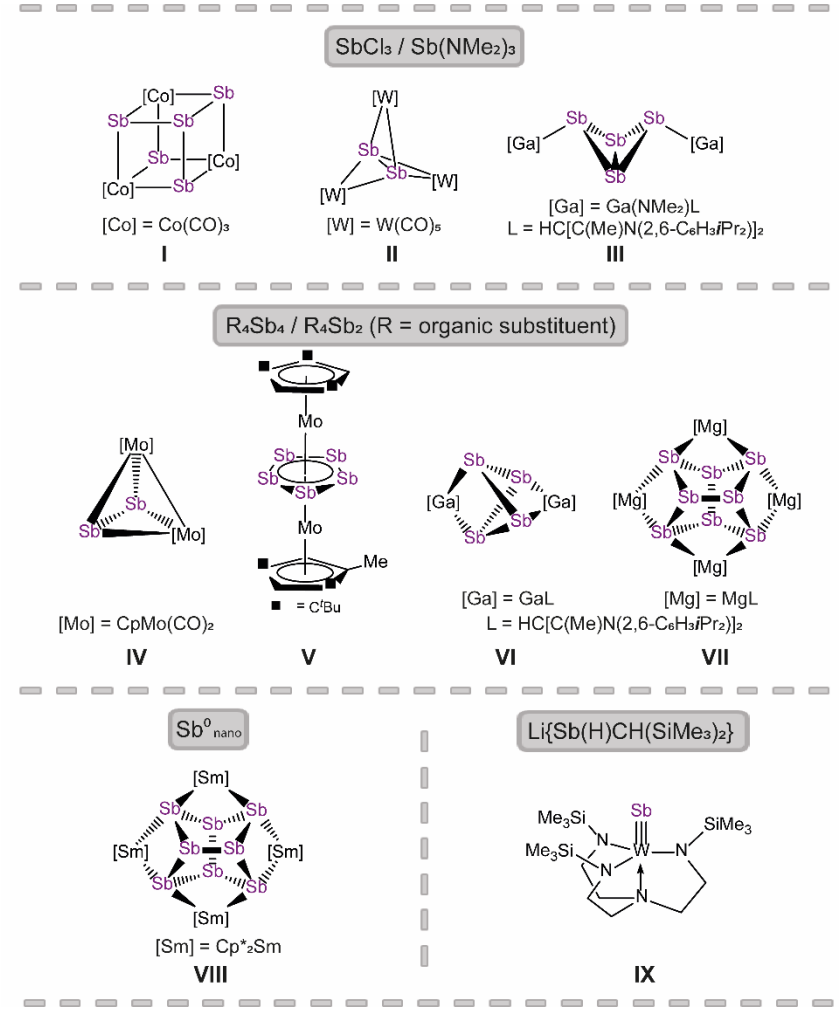

Figure 1: Selected examples of Sb_n ligand complexes.

Recently, the chemistry of the polyantimony main group compounds has experienced a revival[5,19] especially by the introduction of the nacnac ligand in combination with Mg and Ga (*i.e.* LMg and LGa) in this field. In addition to the aforementioned compound **III**, $[(LGa)_2(\mu,\eta^{2:2}\text{-}Sb_4)]$[17] (**VI**) and $[(LMg)_4(\mu_4,\eta^{2:2:2:2}\text{-}Sb_8)]$[18] (**VII**) are interesting representatives made of organo-substituted antimony precursors. **VI** is formed by the reaction of LGa with $Cp^*_4Sb_4$ via reductive elimination of decamethyl-dihydrofulvalene Cp^*_2 and oxidative addition of LGa to the Sb_4 subunit.[17] To form **VII**, the reducing agent $[(LMg)_2]$ was used to initiate the cleavage of the Sb-C bonds in R'_4Sb_2.[18] Another possibility to build polyantimony ligand complexes was shown by *Roesky et al.* by the usage of Sb^0 nanoparticles in the thermolysis reaction with $[Cp^*_2Sm]$, leading to the formation of the f-element polystibide $[(Cp^*_2Sm)(\mu_4,\eta^{2:2:2:2}\text{-}Sb_8)]$ (**VIII**), similar to **VII**.[20]

Also, our group is interested in the generation of Sb_n ligand complexes with unprecedented structural motifs. For instance, we succeeded in the synthesis of [$(N_3N)WSb$] (I**X**, N_3N = tren = $N(CH_2CH_2NSiMe_3)_3$) which possesses a first tungsten antimony triple bond compound.[21] Here, a lithium antimonide salt was used as Sb_1 source. Due to the lack of suitable antimony precursors, the access to polyantimony compounds is strongly limited (*vide supra*), in principle due to their instability. The classical synthetic procedures, *i.e.* thermolysis or photolysis, lead in most of the cases to gray antimony.

Besides the usual synthetic pathways such as thermolysis, photolysis or reactions with unsaturated fragments, the transfer of E_n units constitutes a promising procedure for the synthesis of metastable E_n ligand complexes, since such reactions proceed under mild conditions and enable the formation of compounds that are not accessible by other means.[4,6,22] A prominent product of such a transfer reaction is the synthesis of AsP_3, reported by *Cummins et al*, where a P_3^{3-} unit was transferred from a niobium complex to $AsCl_3$.[23] As_n units were also transferred from the zirconium complexes [$Cp''_2Zr(\mu,\eta^{1:1}\text{-}E_4)$] (E = P, As) to LSi, leading to the formation of the inorganic benzene derivatives $L_3Si_3E_3$ (E = P, As; L = $PhC(N^tBu)_2$.[24] Moreover, this approach was extended to transition metals.[25] Besides the transfer of the entire E_n unit, its degradation as well as aggregation were also observed. Therefore, the question arises whether it would be possible to synthesize a related zirconium complex containing a polyantimony unit. Such derivative could be used to transfer the antimony entity to transition metals or main group compounds to build metastable polyantimony compounds. Herein we report on the successful synthesis of [$(Cp''Zr)_2(\mu,\eta^{1:1:1:1:1:1}\text{-}Sb_6)$] (**1**) and its unprecedented use as transfer reagent for Sb_n species. Nevertheless, in comparison to P_n and As_n transfer reagents, one should keep in mind the lesser stability of Sb-Sb bonds during the transfer, due to the much lower E-E single bond energy.

4.3 Results and Discussion

To discover a suitable starting material for transfer reactions, we investigated the reaction of [$Cp''ZrCl_2$] with $KSb(SiMe_3)_2$, surprisingly leading to the formation of the polyantimony triple decker complex [$(Cp''Zr)_2(\mu,\eta^{1:1:1:1:1:1}\text{-}Sb_6)$] (**1**) as the only isolable and identified product (Scheme 1). Compound **1** is well soluble in solvents such as *n*-pentane, toluene or thf, and is highly air- and light-sensitive. It decomposes rapidly, especially in solution, even at low temperatures (- 80 °C) after few days. Therefore, the recorded ^1H NMR spectrum of **1** at r.t. reveals the expected signals for the Cp'' ligands,

but also unidentified decomposition products. Also, in the mass spectrum of **1**, the molecular ion peak with a correct isotopic pattern was detected at m/z = 1267.61, beside some other peaks, corresponding to decomposition products.

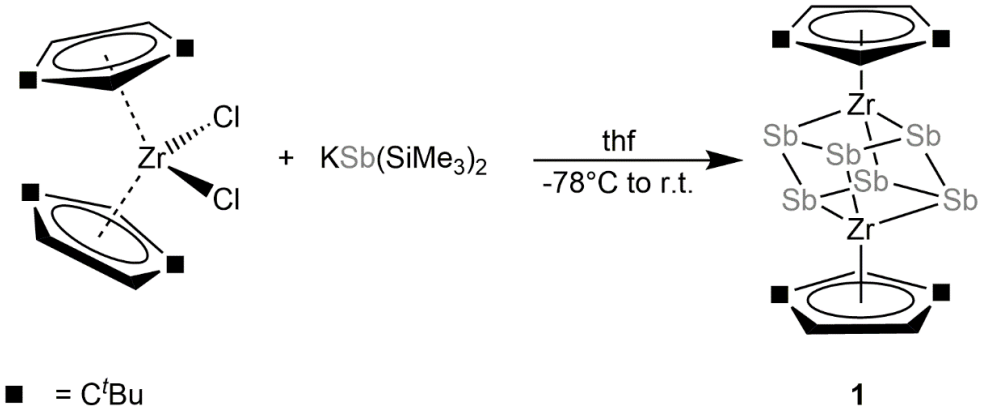

Scheme 1: Synthesis of **1**.

Crystals of **1** suitable for single crystal X-ray diffraction analysis were obtained by storing a concentrated solution in dichloromethane or *n*-pentane at −30°C. The molecular structure of **1** is depicted in Figure 2.

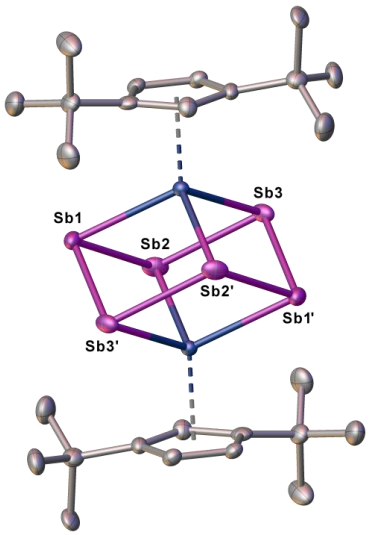

Figure 2: Molecular structure of **1** in the solid state with thermal ellipsoids at 50% probability level. H atoms are omitted for clarity.

The central structural core represents a chair-type Sb_6 unit attached to two [Cp''Zr] fragments in an $\eta^{1:1:1:1:1:1}$ fashion, leading to a cube-like Zr_2Sb_6 core. The Sb-Sb distances of 2.8381(7) Å to 2.8783(6) Å are in the range of a single bond and in good agreement with other polyantimony ligand complexes.[14,16–18,26] Complexes containing

chair-like Sb_6 ligands are not known. The most related compounds are the boat-like *cyclo*-Sb_6^{4-} species in the Zintl ion $[(Cp^*Ru)_2(\mu,\eta^{4:2:2}\text{-}Sb_6)]^{2-}$ reported by *B. Eichhorn et al*[10c] and the phosphine ligand stabilized compound $[(R_3P)_4Sb_6]^{4+}$ containing a bicyclic Sb_6 moiety.[10d] Otherwise, only organo-antimony compounds bearing organic substituents ($(RSb)_6$, R = C_6H_5, C_7H_7) were published.[26,27] Complexes containing chair-like or skew boat-like E_6 (E = P, Bi) moieties have also been reported.[28] The most related complex to **1**, $[(Cp^*Ti)_2(\mu,\eta^{1:1:1:1:1:1}\text{-}P_6)]$, was synthesized by the *co*-thermolysis of $[Cp^*Ti(CO)_2]$ with white phosphorus.[28a] This compound can be formally described as a lighter congener of **1**. Only a few examples of compounds containing antimony and zirconium are known so far, but organic substituents are attached to the antimony atoms.[29]

DFT calculations were performed at the B3LYP/def2-TZVP level of theory to elucidate the electronic structure and the nature of the Sb_6 ligand in **1**. The Wiberg Bond Indices (WBI) of the Zr-Sb bonds of 0.97 (in average) indicate a covalent nature of these bonds. This applies also to the Sb-Sb bonds with a slightly lower value of 0.84 (average), confirming the presence of single bonds within the Zr_2Sb_4 unit. The natural charge distribution shows a positive charge concentration on the *cyclo*-Sb_6 ligand (+0.48) and Zr (+0.11 each), while the negative charge is located on the Cp" ligand (−0.35 each).

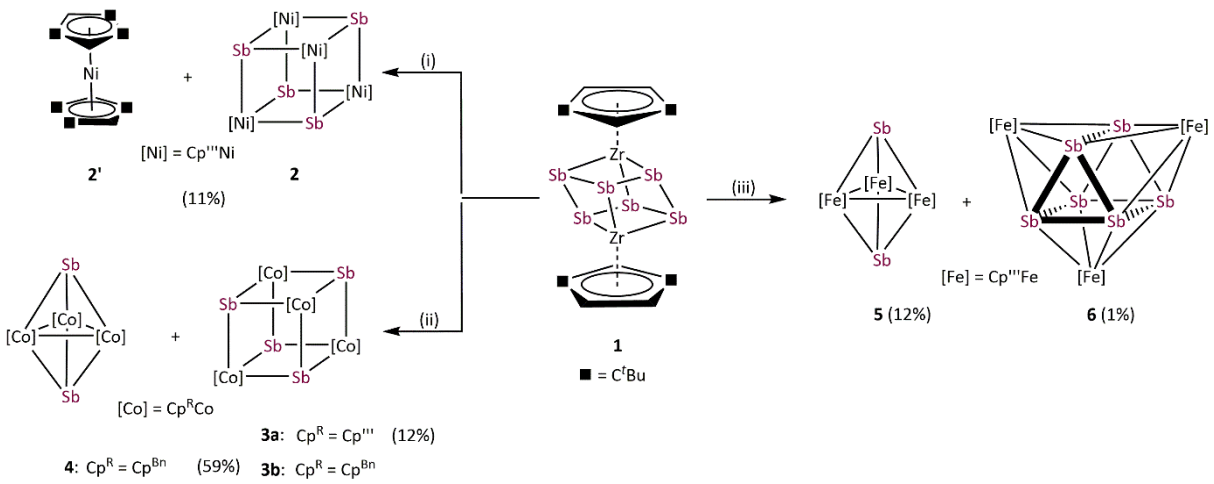

Scheme 2: Reaction of *in situ* prepared $[(Cp"Zr)_2(\mu,\eta^{1:1:1:1:1:1}\text{-}Sb_6)]$ (**1**) with transition metal halides at r.t. in THF. (i): **1** with $[Cp'''NiBr]_2$; (ii): **1** with $[Cp^RCoCl]_2$ (Cp^R = Cp^{Bn}, Cp'''); (iii): **1** with in situ prepared $[Cp'''FeBr]_2$: Isolated yields are given in parentheses.

With compound **1** in hand, we investigated its suitability to transfer Sb_n units under mild conditions to late transition metals. For this purpose, transition metal halides of the type $[Cp'''MX]_2$ of nickel, cobalt and iron were used. The formation of the thermodynamically favored zirconium halogen bond represents the driving force of these reactions. Due to

the very limited stability of **1**, *in situ* generated solutions were used under strict exclusion of light. All mentioned reactions were performed in THF at r.t. and a subsequent column chromatographic workup was needed for purifications, significantly reducing the yield of the formed products (*cf.* Scheme 2). The reaction of **1** with $[Cp'''NiBr]_2$ leads to $[(Cp'''Ni)_4(\mu_3\text{-}Sb)_4]$ (**2**), containing a cubane-like Ni_4Sb_4 core and the co-crystallization of nickelocene $[Cp'''_2Ni]$ (**2'**). Under similar reaction conditions, **1** reacts with $[Cp'''CoCl]_2$ exclusively to the heterocubane derivative $[(Cp'''Co)_4(\mu_3\text{-}Sb)_4]$ (**3a**). $[Cp^{Bn}CoCl]_2$, containing the sterically less encumbered Cp^{Bn} substituent, reacts with **1** to a mixture of $[(Cp^{Bn}Co)_4(\mu_3\text{-}Sb)_4]$ (**3b**) and $[(Cp^{Bn}Co)_3(\mu_3\text{-}Sb)_2]$ (**4**).[30] Despite numerous attempts, **3b** and **4** could not be separated to be obtained as analytically pure compounds. Furthermore, the reaction of **1** with $[Cp'''FeBr]_2$ leads to two products after chromatographic workup, $[(Cp'''Fe)_3(\mu_3\text{-}Sb)_2]$ (**5**) and $[(Cp'''Fe)_3(\mu_3,\eta^{4:4:4}\text{-}Sb_6)]$ (**6**). Whereas in the afore-reported products **2**, **3a**, **3b**, **4** and **5** only Sb_1 units are incorporated, in **6**, the complete Sb_6 entity was transferred. The ^1H and $^{13}C\{^1H\}$ NMR spectra of **2/2'** reveal the expected signals for **2**. Due to the paramagnetic nature of **2'**, no signals are detected in the diamagnetic region. ^1H NMR measurements of the mixture of **3b** and **4** show two sets of signals, which can be attributed to **3b** and **4**, respectively. Although **3b** is paramagnetic, the ^1H NMR signals occur in the diamagnetic region probably due to the strong localization of the spin density on the cobalt centers. Thus, the ratio between **3b** and **4** of 2:1 could be identified. In the ^1H NMR spectra of **3a**, **5** and **6**, only broad signals for the ^{t}Bu groups are observed, due to their paramagnetic character. The molecular ion peaks with the correct isotope pattern were detected for all mentioned compounds by mass spectrometry.[31]

Single crystals of **2/2'** and **3a** suitable for crystal X-ray diffraction analysis were obtained by layering a toluene solution with acetonitrile (**2/2'**) or by storing a concentrated *n*-hexane solution at −30°C (**3a**) (Figure 3). Surprisingly, **2** co-crystallizes with **2'** in a ratio of 2:1 (SI: figure S2). The central structural core of **2** and **3a** consists of a distorted hetero-cubane unit built up by four nickel or cobalt and four antimony atoms (Figure 3). The square faces of the cubanes show a kite-like distortion in which the Sb atoms approach each other. All nickel and cobalt atoms are coordinatively saturated by the coordination of a Cp''' ligand. The Ni-Sb bond lengths in **2** (2.5202(7) Å to 2.5602(7) Å)[32,33] and the Co-Sb bond lengths in **3a** (2.5023(19) Å to 2.6305(14) Å)[12,34-37] are in the range of corresponding single bonds. While, in **2**, the Ni-Ni distances are quite long (3.9352(9) Å to 3.962(1) Å) indicating no bonding interaction, in **3a,** there are two short Co⋯Co distances of 3.071(4) Å and two long Co⋯Co distances of 4.034(3) Å. Similarly, the Sb-Sb distances in **2** are reasonably similar (3.0767(4) Å to 3.1613(4) Å), while, in **3a**, there are two very short (2.9453(13) Å) and two longer (3.1763(13) Å) Sb-Sb distances. The former lies in the range of an elongated

single bond.[38] The distortion of the M_4Sb_4 core is more accentuated in **3a** than in **2**, probably due to the Co···Co and Sb···Sb interactions. The rhombic distortion of the cubanes $[(Cp^*M)_4E_4]$ (M = Cr, Mo, E = O, S) was attributed to ferromagnetic as well as antiferromagnetic couplings of the metal-based electrons.[39]

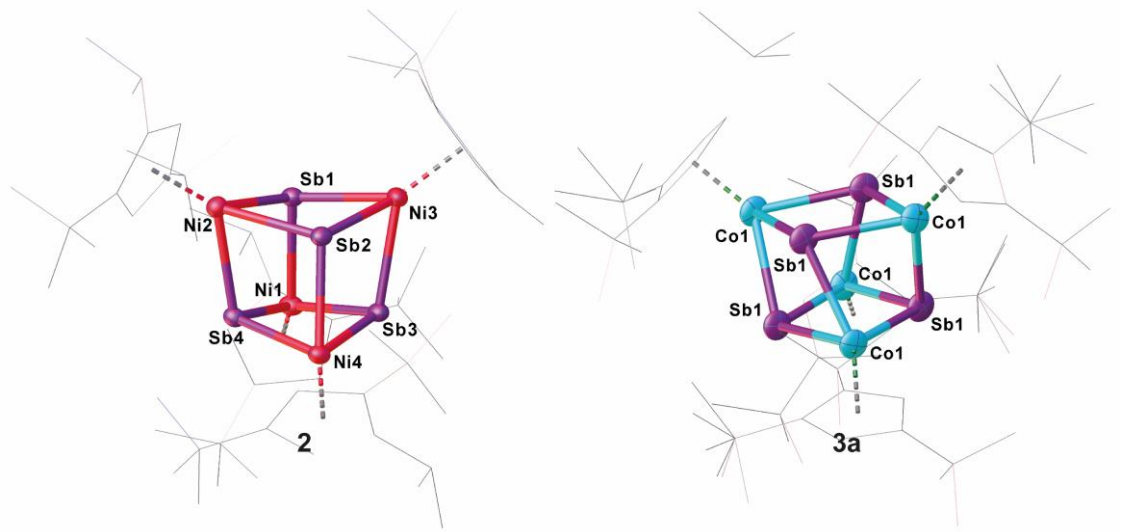

Figure 3: Molecular structures of **2** (left) and **3a** (right) in the solid state with thermal ellipsoids at 50% probability level. H atoms are omitted and the Cp''' ligands drawn in the *wire* frame model for clarity.

DFT calculations reproduce well the geometric parameters of the model compound $[(Cp^*Co)_3(\mu\text{-}Sb)_2]$ (**4m**; *vide infra*), while the short Co-Co distances in **3a** are slightly longer in the optimized geometry, irrespective of a singlet or a triplet spin state. The short Sb-Sb distances in **3a** are well reproduced. The presence of Sb···Sb interactions in **2** and **3a** are substantiated by the Mayer bond orders, which vary from 0.25 to 0.35 and from 0.27 to 0.52, respectively corelate with the corresponding distances. Based on the analysis of the Intrinsic Bonding Orbitals,[40] the Co···Co interaction in **3m** is realized via the Co-Sb σ-bond to which contributions of roughly 10% from the other two Co atoms are mixed. Additionally, on each Co center, there are three non-bonding d orbitals which do not overlap to give Co-Co bonds. The Mayer bond order for the Co-Co interactions in **4m** is roughly 0.48 while for the Co-Sb bonds vary from 0.92 to 0.98. To investigate the electronic structure of **3a** in more detail, EPR and Evans NMR investigations were performed. **3a** is EPR-silent and has an effective magnetic moment of μ_{eff} = 2.34 μ_B, corresponding roughly to two unpaired electrons as determined by the Evans method.[41]

Compounds **4** and **5** crystallize as brown and violet blocks, respectively, by layering a toluene solution with acetonitrile. Their central structural motif consists of an $[M_3Sb_2]$ trigonal bipyramide, built up by two antimony and three metal atoms (M = Co (**4**), Fe

(**5**), Figure 4). The cobalt and iron atoms are located in the equatorial plane and coordinated by a Cp^R ligand, the antimony atoms occupy the apical positions. While the Fe-Sb distances of 2.4895(6) Å to 2.55342(5) Å are in good agreement with reported single bonds,[1,42,43] the Co-Sb distances of **4** (2.4362(4) Å to 2.4547(4) Å) are shortened.[12,34–37] A remarkable difference between the geometry of **4** and **5** is represented by the M-M distances. While, in **4,** the Co-Co distances are all very similar (2.7284(6) Å to 2.7332(5) Å) and lie in the same range of elongated single bonds,[33,43] in **5**, there are one short (2.4489(6) Å and 2.4895(6) Å) and two longer Fe-Fe distances (2.8076(6) Å to 2.9230(6) Å).[44] Interestingly, the nitrogen congener of **5**, $[(Cp'''Fe)_3(\mu_3\text{-}N)_2]$, possesses uniform Fe-Fe distances varying from 2.4727(4) Å to 2.4734(4) Å,[45] while the phosphorus and arsenic derivatives $[(Cp^*Fe)_3(\mu_3\text{-}E)_2]$ (E = P, As)[46] show a distortion of the Fe_3 fragment that is similar to **5**, but less accentuated. The structure of **4** represents a new structural motif and can be regarded as a *closo*-type cluster with 12 skeletal electrons according to the Wade-Mingos rule. Similar complexes of iron and antimony are known only for antimony atoms coordinating to Lewis acidic metal fragments as in $([Fe_3(CO)_9(\mu_3\text{-}SbML_n)_2]$ (ML_n = $CpMn(CO)_2$, $Cr(CO)_5$, $W(CO)_5$, $Mo(CO)_5$).[1,42]

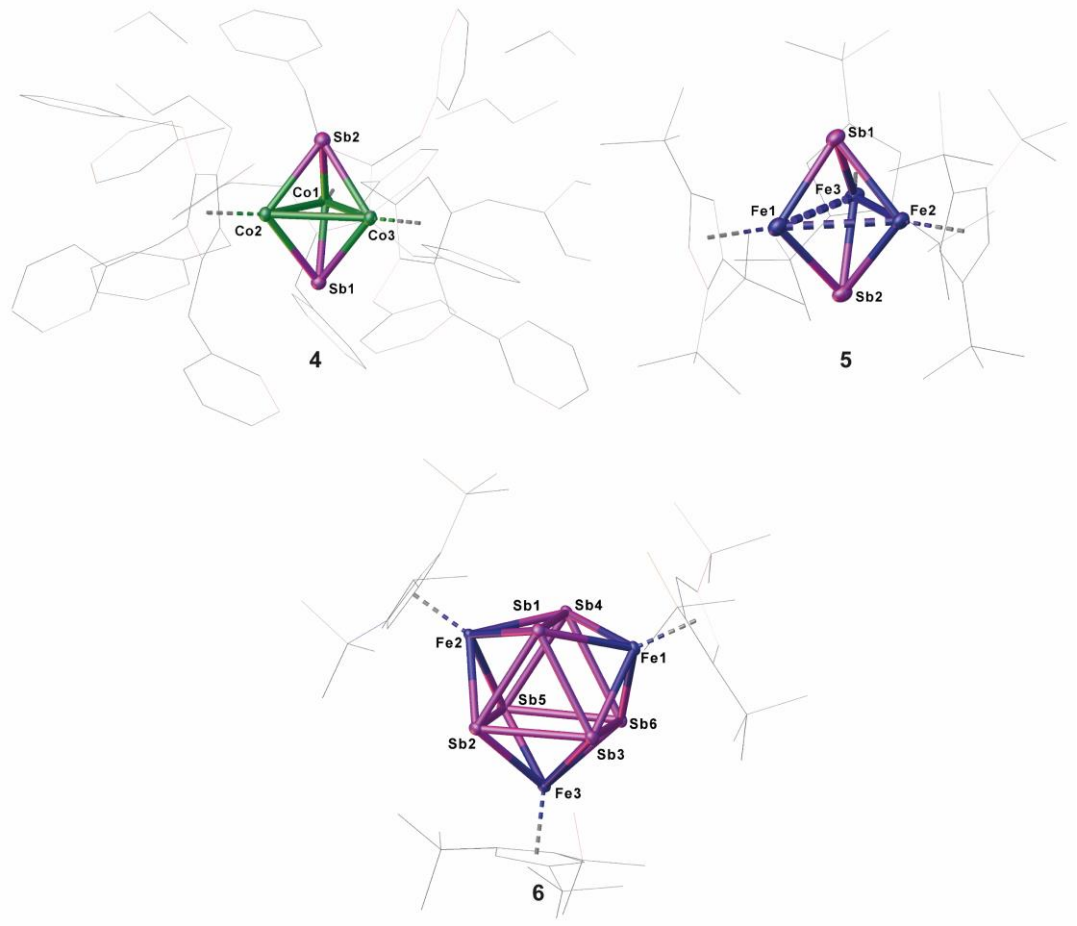

Figure 4: Molecular structures of **3b** (left), **5** (middle) and **6** (right) in the solid state with thermal ellipsoids at 50% probability level. H atoms are omitted and the Cp''' ligands drawn in the *wire* frame model for clarity.

To explore the electronic structure of **5**, EPR and Evans NMR investigations were performed. The X-band EPR spectrum of **5** at 77 K in frozen toluene shows an axial signal ($g_x = g_y = 2.177$ and $g_z = 2.443$ ($g_{iso} = 2.266$)) with no hyperfine splitting (Figure 5). The doublet spin state of **5** is further supported by Evans NMR measurements, resulting in $\mu_{eff} = 1.65\ \mu_B$, corresponding roughly to one unpaired electron.[41]

In order to elucidate the electronic structure of **5**, DFT calculations were performed. The geometry of **5** in different spin states (S = ½ to 4) was optimized by using different functionals. The results show that only the OPBE functional in a doublet spin state reproduces the experimental geometry of **5** found in the solid state. Hybrid functionals lead to optimized geometries with considerably longer Fe-Fe distances, while a similar trend is observed for the OPBE functional in higher spin states (*cf.* SI). Single point calculations with both functionals OPBE and B3LYP (OPBE, doublet spin state optimized geometry) predict the doublet spin state as the energetically lowest state, while the other spin states lie energetically higher (*cf.* SI). Therefore, the ground state of **5** can be viewed as being a doublet spin state, which is in accordance with the EPR and Evans NMR data (vide supra). For the nitrogen analog of **5**, $[(Cp'''Fe)_3(\mu_3\text{-}N)_2]$, the presence of three low-spin iron(III) (S = ½) centers and a total spin of S_{tot} = ½ was reported, due to complex antiferromagnetic coupling.[45]

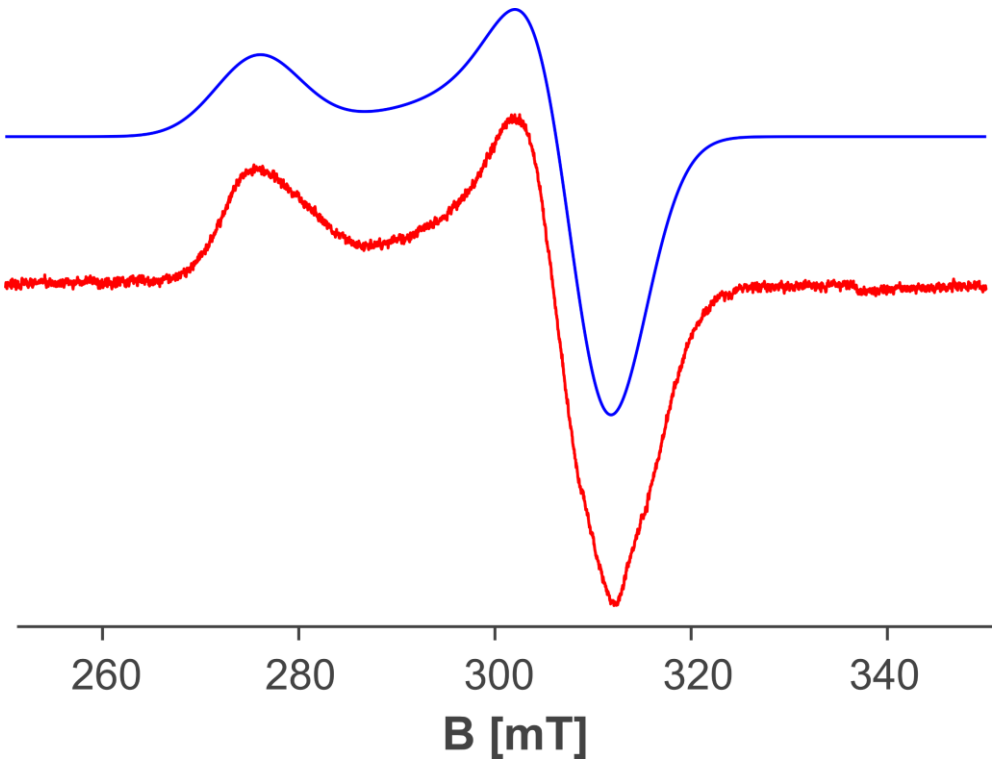

Figure 5: X-band EPR spectrum of **5** in toluene at 77 K: $g_x = g_y = 2.177$ and $g_z = 2.443$ ($g_{iso} = 2.266$). Red: experimental; blue: simulated.[47]

Single crystals of **6** suitable for X-ray diffractions were obtained after chromatographic workup by layering a toluene solution with acetonitrile. The central structural motif of **6** consists of a Sb_6 prism with its rectangular faces being capped by [Cp'''Fe] fragments (Figure 4, right). Within the triangular faces, the Sb-Sb distances (2.9029(4) Å to 2.9365(4) Å) are slightly shorter than the Sb-Sb distances between them (3.0283(4) Å to 3.0646(4) Å). This variation of the Sb-Sb distances nicely corelates with the corresponding Mayer bond orders (OPBE/def2-SVP, doublet spin state) of 0.53 and 0.33, respectively. The Mayer bond orders for the Fe-Sb bonds vary only slightly between 0.69 to 0.73. Although the Sb-Sb distances are slightly longer than usual Sb-Sb single bonds, they lie in the range of elongated single bonds.[14,16,18,48] DFT calculations at the OPBE/def2-SVP level predict the doublet spin state for **6** as ground state, with the spin density being evenly distributed over the three Fe centers, while the other spin states lie energetically higher (for example the quartet spin state is with 53 kJ mol^{-1} higher in energy; *cf.* SI). To the best of our knowledge, **6** is the first complex containing a Sb_6 prism. Comparable complexes are only known for other group 15 homologous.[49]

4.4 Conclusion

In summary, we herein report the synthesis of the first zirconium antimony ligand complex $[(Cp''Zr)_2(\mu,\eta^{1:1:1:1:1:1}\text{-}Sb_6)]$ (**1**), which contains an unprecedented chair-like Sb_6 ligand coordinated to two Cp''Zr fragments. Complex **1** can be used as an effective antimony transfer reagent towards transition metal halides of nickel, cobalt and iron. That way, a variety of novel Sb_n ligand complexes such as the cubane-like compounds $[(Cp'''Ni)_4(\mu_3\text{-}Sb)_4]$/$[Cp'''_2Ni]$ (**2/2'**) and $[(Cp'''Co)_4(\mu_3\text{-}Sb_4)]$ (**3a**) or the complexes $[(Cp^{Bn}Co)_3(\mu_3\text{-}Sb)_2]$ (**4**) and $[(Cp'''Fe)_3(\mu_3\text{-}Sb)_2]$ (**5**) containing a trigonal bipyramidal structure were obtained and fully characterized. Beside the partial transfer of the Sb_1 units, also the complete transfer of a Sb_6 unit was achieved. Here, the iron complex $[(Cp'''Fe)_3(\mu_3,\eta^{4:4:4}\text{-}Sb_6)]$ (**6**) is formed which shows the potential of **1** as transfer reagent for polyantimony units. In principle, an initial transfer of larger Sb_n units from **1** should have been possible, however, the low stability of such complexes (especially during column chromatographic work-up) might be the reason that mostly only Sb_1-unit-containing complexes were isolated. Future work in this area is dedicated to developing smoother reaction pathways.

4.5 Supporting Information

4.5.1 Experimental Detail

All experiments were performed under an atmosphere of dry nitrogen or argon using Schlenk and glovebox techniques. Solvents were purified, dried and degassed prior use. ^{1}H, $^{13}C\{1H\}$ NMR spectra were recorded at room temperature on a Bruker Avance 400 spectrometer (^{1}H: 400,130 MHz, ^{13}C: 100.613 MHz). ^{1}H, ^{13}C NMR chemical shifts are reported in parts per million (ppm) relative to the external standard Me_4Si. The X-band EPR measurements were carried out on a MiniScope MS400 devige (Magnettech GmbH) equipped with rectangular TE102 resonator at a frequency of 9.5 GHz. The compounds were dissolved in a glove box unter argon and placed in tip-sealed Pasteur pipetts. For each sample a spectrum at at room temperature and at 77 K were performed. Elemental analysis were determined with a Vario micro cube apparatus. For mass spectrometry a Finnigan MAT 95 (LIFDI MS, FD MS) or a Finnigan MAT SSQ 710 A (EI MS) device and a Joel AccuTOF GCX spectrometer were used. [$FeBr_2$·dme], [$NiBr_2$·dme],[50] $KSb(SiMe_3)_2$[51] and [Cp''_2ZrCl_2][52] were prepared according to literature procedures.

Preparation of NaCp''':[53]

A solution of Cp'''H (19.5 mL, 77.7 mmol) in 40 mL thf is added dropwise to a suspension of $NaNH_2$ (3.03 g, 77.7 mmol) in 100 mL thf. The mixture is refluxed for 20 h, resulting in a white suspension of NaCp'''. After decanting the supernatant thf solution, the white solid is washed with *n*-hexane and dried in vacuo. Yield: 18.7 g (72.9 mmol, 94%).

Preparation of $[Cp'''NiBr]_2$:[54]

A solution of NaCp''' (1.2 g, 4.7 mmol) in dme is added to a suspension of [$NiBr_2$·dme] (1.5 g, 4.9 mmol) in dme at -30°C. The solution is stirred for 2 h at -30 °C and further 2 h at room temperature. After removing the solvent, the red residue is dissolved in *n*-hexane (20 mL) and filtered via canula. The solution is concentrated to approx. 10 mL and stored at -30 °C for crystallization. More product can be obtained by concentrating the mother liquid and further storage at -30°C. Overall yield: 756 mg (1.02 mmol, 43%).

Preparation of $[Cp^{Bn}CoCl]_2$:[55]

A solution of ^{n}BuLi in *n*-hexane (12.1 mL, c = 1.6 mol/L, 19.4 mmol) is added dropwise to a solution of $Cp^{Bn}H$ (516 mg, 0.999 mmol) in thf at -30 °C. The resulting purple solution is stirred for 1 h at -30 °C and additionally for 1 h at room temperature. Then, the reaction mixture is

added dropwise to a blue suspension of $CoCl_2$ (2.51 g, 19.4 mmol) in thf at -30 °C. The reaction mixture is stirred for 2 h at -30 °C and further 6 h at room temperature. Meanwhile, a dark brown solution is formed. The solvent is removed in vacuo, the brown residue extracted with warm toluene and the acheaved solution filtered via canula. The solution is concentrated to approx. 10 mL and stored at -30 °C for crystallization. More product can be obtained by concentrating the mother liquid and further storage at -30 °C. Overall yield: 7.24 g (5.94 mmol, 61%).

Preparation of $[(Cp''Zr)_2(\mu,\eta^{1:1:1:1:1:1}\text{-}Sb_6)]$ (1):

All synthetic steps are carried out in the dark. A solution of $[Cp''_2ZrCl_2]$ (100 mg, 0.194 mmol) in thf is added to a solution of $KSb(SiMe_3)_2$ (122 mg, 0.399 mmol) in thf and stirred overnight. The colour changes to brown and a grey precipitate is formed. Subsequently, the solvent is removed *in vacuo*, the residue is dissolved in *n*-pentane and filtered over diatomaceous earth. Crystals suitable for single crystal X-ray structure analysis can be obtained by storing a concentrated solution in *n*-pentane or dichloromethane at -30 °C. **1** is highly air- and light-sensitive and decomposes rapidly. Crystalline yield: 19 mg (0.015 mmol, 21%).

1: **^{1}H NMR** (C_6D_6, 298 K): *δ* [ppm] = 1.41 (s, 36 H, C(*CH₃)₃*), 5.18 (d, 4 H, $C_5H_3{}^tBu_2$), 8.02 (t, 2 H, $C_5H_3{}^tBu_2$). **FD MS** (toluene): *m*/*z* (%): 1267.61 (M^+; 33); **Elemental analysis** (%): calculated for $[C_{26}H_{42}Zr_2Sb_6]$ (1259.56 g/mol): C, 24.64; H, 3.34; no satisfying elemental analysis could be obtained, even by using Sn capsules. This is caused by the air and light sensitivity of compound **1**.

Preparation of $[(Cp'''Ni)_4(\mu_3\text{-}Sb)_4]$/$[Cp'''_2Ni]$ (2/2'):

All synthetic steps are carried out in the dark. A solution of $KSb(SiMe_3)_2$ (525 mg, 1.71 mmol) in thf is added to a solution of $[Cp''_2ZrCl_2]$ (501 mg, 0.974 mmol) in thf and stirred overnight. A solution of $[Cp'''NiBr]_2$ (640 mg, 0.864 mmol) in thf is added to the red-brown solution of **1** and stirred for 3 d. Meanwhile, a grey suspension is formed. The solvent is removed *in vacuo* and subsequent column chromatographic workup (SiO_2, *n*-hexane, 18 x 3 cm) yield two fractions. With *n*-hexane a greenish brown fraction of **2/2'** can be obtained. The second fraction containing $[Cp''_2ZrCl_2]$ can be eluted with a mixture of *n*-hexane and toluene (3:1). Crystals of **2/2'** suitable for single crystal X-ray diffraction analysis can be obtained by layering a toluene solution with acetonitrile. Crystalline yield: **2/2'**: 59 mg (0.0309 mmol, 11%)

2/2': ^{1}H NMR (C_6D_6, 400 MHz, 300 K): δ [ppm] = 1.47 (s, 9 H, C(C*H₃)₃*), 1.60 (s, 18 H, C(C*H₃)₃*), 5.22 (s, 2 H, $C_5H_2tBu_3$); **^{13}C{^{1}H} NMR** (C_6D_6, 100 MHz, 300K): δ [ppm] = 32.5 (s, $C_5H_2(C(CH_3)_3)$), 32.5 (s, $C_5H_2(C(CH_3)_3)$), 33.5 (s, $C_5H_2(C(CH_3)_3)$), 34.9 (s, $C_5H_2(C(CH_3)_3)$), 87.1 (s, $C_5H_2(C(CH_3)_3)$), 117.9 (s, $C_5H_2(C(CH_3)_3)$), 119.3 (s, $C_5H_2(C(CH_3)_3)$); **LIFDI MS**

(toluene): m/z (%) = 1654.24 ($M^{+\cdot}$,100); **Elemental analysis** (%): calculated for [$C_{102}H_{174}Ni_{4,5}Sb_4$] (2143.69 g/mol): C, 53.22; H, 7.62; no satisfying elemental analysis could be obtained, even by using Sn capsules. This is caused by the air and light sensitivity of compound **2/2'**.

Preparation of [(Cp‴Co)$_4$(μ$_3$-Sb$_4$)] (3a):

All synthetic steps are carried out in the dark. A solution of $KSb(SiMe_3)_2$ (525 mg, 1.71 mmol) in thf is added to a solution of [Cp''$_2$ZrCl$_2$] (500 mg, 0.972 mmol) in thf and stirred overnight. A solution of [Cp'''CoCl]$_2$ (562 mg, 0.859 mmol) in thf is added to the red-brown solution of **1** and stirred for 6 d. The solvent of the grey suspension is removed *in vacuo*. Subsequent column chromatographic workup (SiO_2, *n*-hexane, 3 x 10 cm) afford two fractions. Using toluene as solvent **3a** is eluted as dark green fraction followed by a brown fraction of [$Sb_2(SiMe_3)_4$]. Crystals of **3a** suitable for single crystal X-ray diffraction analysis can be obtained by storing a concentrated *n*-hexane solution at –30 °C. Crystalline yield: **3a**: 54 mg (0.033 mmol, 12%).

3a: ^{1}H NMR (C_6D_6, 400 MHz, 300 K): δ [ppm] = 1.53 (s, 9 H, C(C*H$_3$)$_3$*), 1.61 (s, 18 H, C(C*H$_3$)$_3$*); **EVANS NMR** (C_6D_6, 400 MHz, 300K): μ_{eff}: 2.34 μ_B, corresponding to 1.54 unpaired electrons. **LIFDI MS** (toluene): m/z (%) = 1654.24 ($M^{+\cdot}$;100); **Elemental analysis** (%): calculated for [$C_{68}H_{116}Co_4Sb_4 \cdot C_6H_{14}$] (1738.37 g/mol): C, 51.00; H, 7.52; found: C, 51.15; H, 7,14 (*n*-hexane can also be detected in the ^{1}H NMR)

Preparation of [(Cp^{Bn}Co)$_4$(μ$_3$-Sb$_4$)] (3b) and [(Cp^{Bn}Co)$_3$(μ$_3$-Sb)$_2$] (4):

All synthetic steps are carried out in the dark. A solution of $KSb(SiMe_3)_2$ (675mg, 2.21 mmol) in thf is added to a solution of [Cp''$_2$ZrCl$_2$] (569 mg, 1.11 mmol) in thf and stirred overnight. After addition of a solution of [Cp^{Bn}CoCl]$_2$ (1.19 g, 0.975 mmol) in thf, the reaction mixture is stirred for 3 d. The solvent is removed *in vacuo* and subsequent column chromatographic workup (SiO_2, *n*-hexane, 18 x 3 cm) afforded [Cp''ZrCl$_2$] as first fraction. A brownish green fraction containing a mixture of **3b** and **4** can be obtained with dichloromethane. Crystals of **3** suitable for single crystal X-ray diffraction analysis can be obtained by layering a toluene solution with acetonitrile and isolate the crystals after a few hours. Overall yield (**3b**+**4**): 320 mg (59%).

NMR spectroscopic investigations revealed a ratio of 4:3b of approximately 2:1. This is in good agreement with the found values of the elemental analysis of the solid ([2 · 2 / 1 · 3] calc.: C, 71.49; H, 5.25; found: C, 71.83; H, 5.33).

3b: **^{1}H NMR** (CD_2Cl_2, 400 MHz, 300 K): δ [ppm] = 4.21 (s, 40 H, $CH_2\{C_6H_5\}$), 6.68 (d, ^{3}J(H,H) = 7.5 Hz, 40 H, $CH_2\{C_6H_5\}$), 6.81-6.91 (m, 60 H, $CH_2\{C_6H_5\}$); **^{13}C{^{1}H} NMR** (CD_2Cl_2,

100 MHz, 300 K): δ [ppm] = 36.4 (s, $C_5(\mathit{C}H_2\{C_6H_5\})_5$), 99.8 (s, $\mathit{C}_5(CH_2\{C_6H_5\})_5$), 126.0 (s, $C_5(CH_2\{\mathit{C}_6H_5\})_5$), 128.1 (s, $C_5(CH_2\{\mathit{C}_6H_5\})_5$), 129.6 (s, $C_5(CH_2\{\mathit{C}_6H_5\})_5$), 140.0 (s, $C_5(CH_2\{\mathit{C}_6H_5\})_5$); **FD MS** (toluene): m/z (%) = 2785.26 (M^+).

4: **^{1}H NMR** (CD_2Cl_2, 400 MHz, 300 K): δ [ppm] = 4.20 (s, 30 H, $C\mathit{H}_2\{C_6H_5\}$), 6.55 (d, ^{3}J(H,H) = 7.4 Hz, 30 H, $CH_2\{C_6\mathit{H}_5\}$), 6.82 (m, 30 H, $CH_2\{C_6\mathit{H}_5\}$), 6.90 (m, 15 H, $CH_2\{C_6\mathit{H}_5\}$); **^{13}C{^{1}H} NMR** (CD_2Cl_2, 100 MHz, 300 K): δ [ppm] = 37.1 (s, $C_5(\mathit{C}H_2\{C_6H_5\})_5$), 96.3 (s, $\mathit{C}_5(CH_2\{C_6H_5\})_5$), 126.0 (s, $C_5(CH_2\{\mathit{C}_6H_5\})_5$), 128.1 (s, $C_5(CH_2\{\mathit{C}_6H_5\})_5$), 129.3 (s, $C_5(CH_2\{\mathit{C}_6H_5\})_5$), 140.5 (s, $C_5(CH_2\{\mathit{C}_6H_5\})_5$); **FD MS** (toluene): m/z (%) = 1966.45 (M^+).

Preparation of $[(Cp'''Fe)_3(\mu_3\text{-}Sb)_2]$ (5) and $[(Cp'''Fe)_3(\mu_3,\eta^{4:4:4}\text{-}Sb_6)]$ (6):

A solution of NaCp''' (495 mg, 1.93 mmol) in dme is added to a suspension of $FeBr_2{\cdot}$dme (591 mg, 1.94 mmol) in dme at -30 °C. The colour changes immidiatly to green. After 2 h of stirring, the solvent is removed *in vacuo* and the green oily residue is extracted with *n*-hexane. The reaction mixture is filtered via canula, all volatiles are removed in vacuo and the orange solid is dissolved in thf.

All further synthetic steps are carried out in der dark. A solution of $KSb(SiMe_3)_2$ (520 mg, 1.69 mmol) in thf is added to a solution of $[Cp''_2ZrCl_2]$ (501 mg, 0.974 mmol) in thf and stirred overnight. The prepared solution of $[Cp'''FeBr]_2$ is added to the red-brown solution of **1**. Immediately, a grey suspension is formed. After stirring for 4 d the solvent is removed *in vacuo*. Subsequent column chromatographic workup (SiO_2, *n*-hexane, 18 x 3 cm) afforded three fractions. With *n*-hexane an unknown pinkish fraction followed by a dark brown fraction of **5** can be obtained. A mixture of *n*-hexane/toluene (1:1) yield a light brown fraction of **6**. Crystals of **5** and **6** suitable for single crystal X-ray diffraction analysis can be obtained by layering a toluene solution with acetonitrile. Crystalline yield: **5**: 38 mg (34.3 µmol, 12%); **6**: 4 mg (2.51 µmol, 1%).

5: **^{1}H NMR** (C_6D_6, 298 K): *δ* [ppm] = -0.17 (s, 18H, $\omega_{½}$ = 160 Hz, C(CH_3)$_3$), 3.31 (s, 9H, $\omega_{½}$ = 70 Hz, C(CH_3)$_3$); **EVANS NMR** (C_6D_6, 400 MHz, 300K): μ_{eff}: 1.65 μ_B, corresponding to 0.93 electrons. **LIFDI MS** (toluene): m/z (%) = 1111.37 ($M^{+\cdot}$,100); **EPR** (toluene, 77 K): $g_x = g_y = 2.1770$, $g_z = 2.4434$, $g_{iso} = 2.2658$. **elemental analysis** (%): calculated for $[C_{51}H_{87}Fe_3Sb_2]$ (1109.29 g/mol): C, 55.12; H, 7.89; no satisfying elemental analysis could be obtained, even by using Sn capsules. This is caused by the air and light sensitivity of compound **5**.

6: **^{1}H NMR** (C_6D_6, 298 K): *δ* [ppm] = 0.37 (s, 18H, $\omega_{½}$ = 17 Hz, C(CH_3)$_3$), 0.81 (s, 9H, $\omega_{½}$ = 14 Hz, C(CH_3)$_3$); **LIFDI MS** (toluene): m/z (%) =1596.91 (M^+; 100); Due to the small amount of **6** no elemental analysis could be performed.

4.5.2 Crystallographic Data

Crystals suitable for single crystal X-ray diffraction analyses were obtained as described above. Single crystal data were acquired using either a Gemini Ultra diffractometer (Rigaku Oxford Diffraction) equipped with an Atlas^{S2} CCD detector using Cu K_α radiation (**3a**, **6**), a GV50 diffractometer (Rigaku Oxford Diffraction) equipped with a Titan^{S2} CCD detector using Cu K_α radiation (**1**, **4**) or respectively Cu K_β radiation (**5**) or a SuperNova diffractometer (Rigaku Oxford Diffraction) equipped with an Atlas CCD detector using Cu K_α radiation (**2/2'**). Data collection and reduction were performed with the **CrysAlisPro** software package (version 1.171.38.43 (**1**, **2/2'**, **4**, **6**); 1.171.39.37b (**3a**); 1.171.40.14a (**5**)).[56] A numerical absorption correction based on gaussian integration over a multifaceted crystal model and an empirical absorption correction using spherical harmonics, implemented in SCALE3 ABSPACK scaling algorithm was performed for the compounds (**1**, **4**, **5**).[56] An analytical numeric absorption correction using a multifaceted crystal model based on expressions derived by R. C. Clark & J. S. Reid[57] and an empirical absorption correction using spherical harmonics, implemented in SCALE3 ABSPACK scaling algorithm was performed for the compounds (**2/2'**, **3a**, **6**). Using **Olex2**,[58] the structures were solved with **ShelXT**[59] and refined by full-matrix least-squares method against $|F|^2$ using **ShelXL**.[60] Hydrogen atoms were refined in calculated positions using the riding model. Using **Olex2**,[58] all pictures of the respective molecular structures were made.

CCDC reference number 2079755 (**1**), 2079756 (**2/2'**)), 2079757 (**3a**), 2079758 (**4**·C_7H_8), 2079759 (**5**) and 2079760 (**6**) contain the supplementary crystallographic data for **1**, **2/2'**, **3a**, **4**, **5** and **6**. These data can be obtained free of charge at www.ccdc.cam.ac.uk/conts/retrieving.html (or from the Cambridge Crystallographic Data Centre, 12 Union Road, Cambridge CB2 1EZ, UK; Fax: + 44-1223-336-033; e-mail: deposit@ccdc.cam.ac.uk).

[(Cp''Zr)$_2$(μ,η$^{1:1:1:1:1:1}$-Sb$_6$)] (1):

Compound **1** crystallizes by storing a concentrated *n*-pentane solution at -30 °C in form of orange plates in the triclinic space group $P\bar{1}$. The asymmetric unit contains half a molecule of **1**.

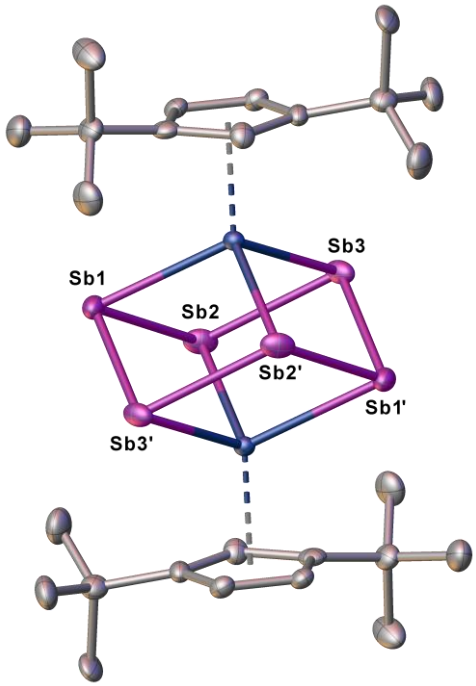

Figure S1: Molecular structure of **1** in the solid state (hydrogen atoms are omitted for clarity). Thermal ellipsoids are depicted at 50% probability level. Selected bond lengths [Å] and angles [°]: Sb1-Sb3$^{'}$ 2.8783(6), Sb1-Sb2 2.8381(7), Sb1-Zr1 2.8340(7), Sb3-Sb2 2.8414(7), Sb3-Zr1 2.8332(7), Sb2-Zr1$^{'}$ 2.8360(6), Zr1··Zr1$^{'}$ 3.6763(10); Sb2-Sb1-Sb3$^{'}$ 103.108(19), Zr1-Sb1-Sb3$^{'}$ 77.792(17), Zr1-Sb1-Sb2 77.841(19), Sb2-Sb3-Sb1$^{'}$ 101.303(17), Zr1-Sb3-Sb1$^{'}$ 75.986(18), Zr1-Sb3-Sb2 77.800(19), Sb1-Sb2-Sb3 102.015(19), Zr1$^{'}$-Sb2-Sb1 76.581(19), Zr1$^{'}$-Sb2-Sb3 78.364(17), Sb1-Zr1-Sb2$^{'}$ 102.54(2), Sb1-Zr1-Zr1$^{'}$ 63.846(17), Sb3-Zr1-Sb1 102.33(2), Sb3-Zr1-Sb2$^{'}$ 104.32(2), Sb3-Zr1-Zr1$^{'}$ 65.387(19), Sb2$^{'}$-Zr1-Zr1$^{'}$ 64.855(18).

[(Cp'''Ni)$_4$(μ$_3$-Sb)$_4$]/[Cp'''$_2$Ni] (2/2'):

Compound **2/2'** crystallizes by layering a toluene solution with CH_3CN in form of violet blocks in the monoclinic space group *C*2/*c*. Compound **2** co-crystallizes with **2'** in the composition **(2)$_2$2'**. The asymmetric unit contains one molecule of **2** and half a molecule of **2'**.

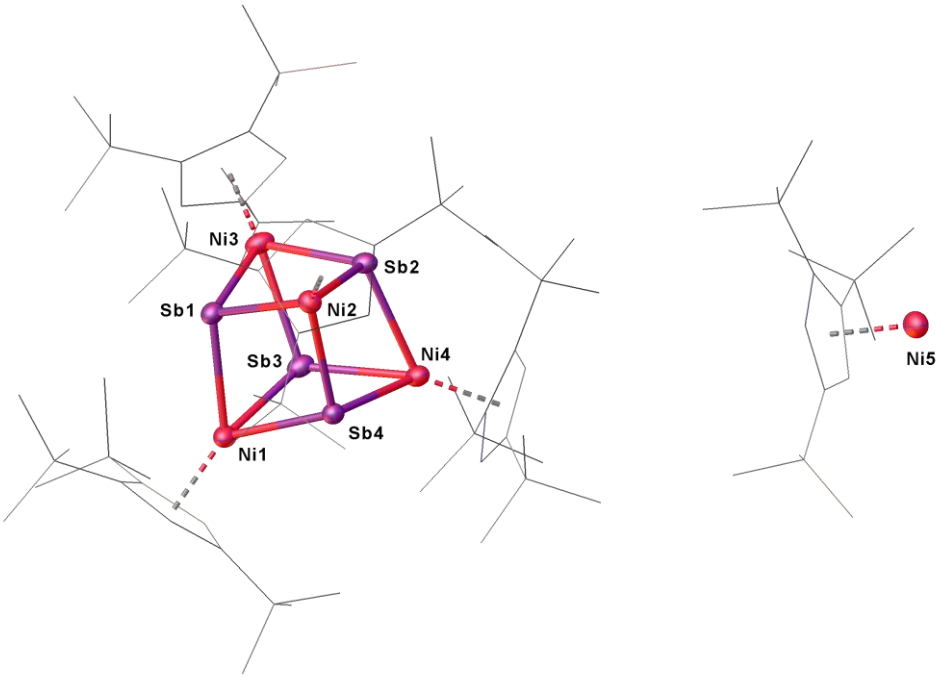

Figure S2: Molecular structure of **2/2'** in the solid state. Cp''' ligands are drawn in the wire frame model and hydrogen atoms are omitted for clarity. Thermal ellipsoids are depicted at 50% probability level. Selected bond lengths [Å] and angles [°]: Sb4-Ni2 2.5309(7) Sb4-Ni4 2.5201(7), Sb4-Ni1 2.5367(7), Sb1-Ni2 2.5565(7), Sb1-Ni1 2.5566(7), Sb1-Ni3 2.5565(7), Sb2-Ni2 2.5405(7), Sb2-Ni4 2.5548(7), Sb2-Ni3 2.5533(7), Sb3-Ni4 2.5541(7), Sb3-Ni1 2.5484(7), Sb3-Ni3 2.5602(7); Ni2-Sb4-Ni1 105.01(2), Ni4-Sb4-Sb1 101.537(17), Ni4-Sb4-Ni2 102.03(2), Ni4-Sb4-Ni1 102.19(2), Ni2-Sb1-Ni1 103.69(2), Ni2-Sb1-Ni3 101.59(2), Ni3-Sb1-Ni1 101.51(2), Ni2-Sb2-Sb1 52.071(15), Ni2-Sb2-Sb3 100.850(17), Ni2-Sb2-Ni4 100.81(2), Ni2-Sb2-Ni3 102.12(2), Ni3-Sb2-Ni4 105.17(2), Ni4-Sb3-Sb4 51.306(16), Ni4-Sb3-Ni3 104.99(2), Ni1-Sb3-Sb4 51.720(16), Ni1-Sb3-Ni4 100.93(2), Ni1-Sb3-Ni3 101.63(2), Sb4-Ni2-Sb1 74.726(18), Sb4-Ni2-Sb2 76.387(19), Sb2-Ni2-Sb1 76.313(19), Sb4-Ni1-Sb1 74.624(19), Sb4-Ni1-Sb3 76.225(19), Sb3-Ni1-Sb1 76.52(2), Sb1-Ni3-Sb3 76.32(2), Sb2-Ni3-Sb1 76.09(2), Sb2-Ni3-Sb3 73.980(19).

[(Cp'''Co)$_4$(μ_3-Sb)$_4$] (3a):

Compound **3a** crystallizes out of a *n*-hexane solution in form of dark violet blocks in the hexagonal space group *P*6$_2$22. The asymmetric unit contains a fourth of a molecule of **3a**. To describe the disorder of a tertbutyl-group of the Cp ligands the restrains SADI and SIMU were applied.

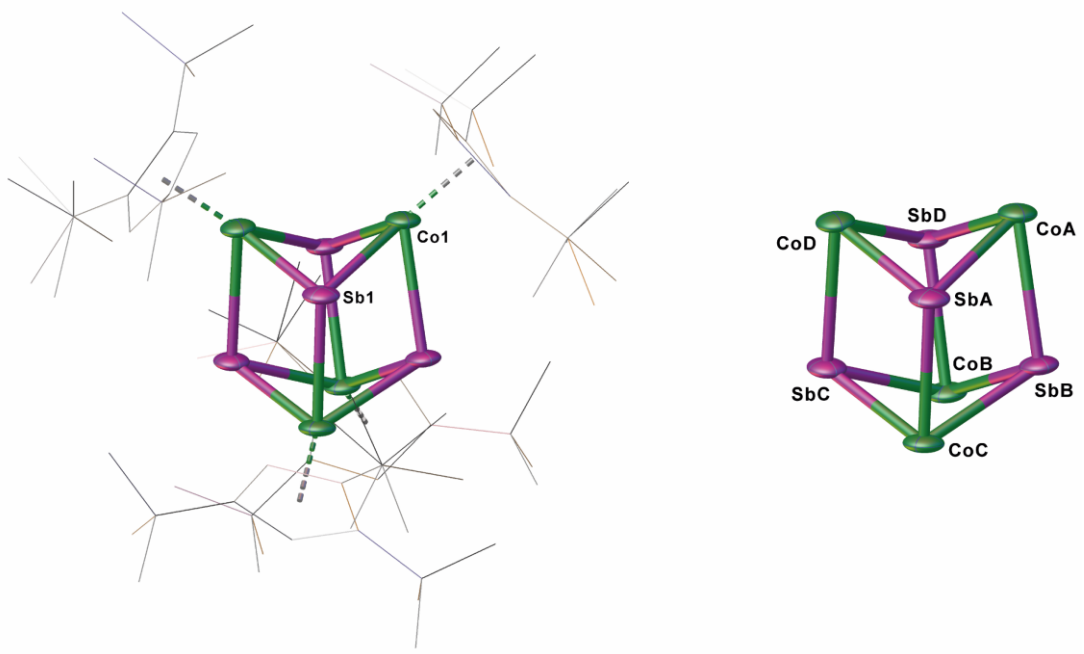

Figure S3: Molecular structure of **3a** in the solid state (left). Cp''' ligands are drawn in the wire frame model and hydrogen atoms are omitted for clarity. Thermal ellipsoids are depicted at 50% probability level. Closer few to the framework with a specific naming (right). Selected bond lengths [Å] and bond angles [°]: CoA-SbD 2.5023(19), CoA-SbA: 2.5528(19), CoA-SbB 2.6305(14); Selected anglesCoA-SbA-CoD 74.80(7), SbA-CoD-SbD 90.58(6), SbA-CoA-SbB 69.23(4), CoC-SbA-CoA 108.67(5), SbC-CoD-SbA 76.41(5), CoC-SbA-CoD 103.57(5).

[($Cp^{Bn}Co)_3(\mu_3$-Sb)$_2$] (4):

Compound **4** crystallizes by layering a toluene solution with CH_3CN in form of brown blocks in the monoclinic space group $P2_1/n$. The asymmetric unit contains one molecule of **4** and one toluene molecule.

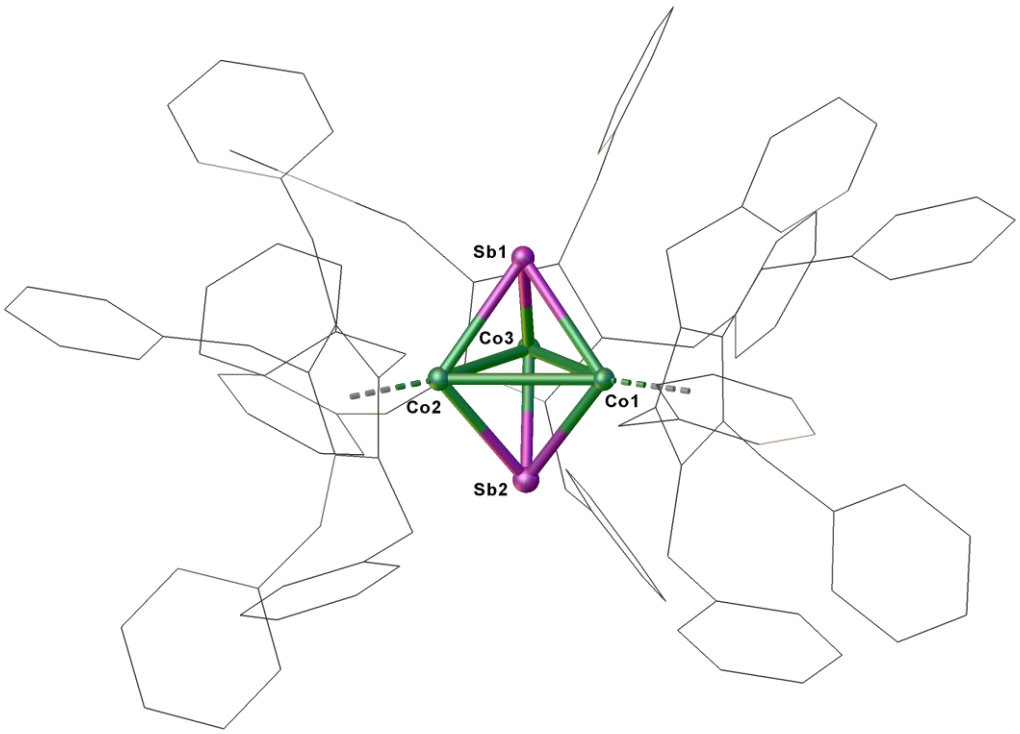

Figure S4 Molecular structure of **4** in the solid state. Cp^{Bn} ligands are drawn in the wire frame model and hydrogen atoms are omitted for clarity. Thermal ellipsoids are depicted at 50% probability level. Selected bond lengths [Å] and angles [°]: Sb1-Co2 2.4495(4), Sb1-Co3 2.4523(4), Sb1-Co1 2.4455(4), Sb2-Co2 2.4547(4), Sb2-Co3 2.4469(4), Sb2-Co1 2.4362(4), Co2-Co3 2.7304(5), Co2-Co1 2.7284(6), Co3-Co1 2.7331(5); Co1-Co2-Co3 60.090(14), Co2-Co1-Co3 59.992(14), Co2-Sb1-Co3 67.700(14), Co1-Sb1-Co2 67.748(14), Co1-Sb1-Co3 67.839(14), Co3-Sb2-Co2 67.704(14), Co1-Sb2-Co2 67.814(14), Co1-Sb2-Co3 68.072(14), Sb1-Co2-Sb2 99.543(15), Sb1-Co2-Co3 56.198(12), Sb1-Co2-Co1 56.057(12), Sb2-Co2-Co3 56.013(12), Sb2-Co2-Co1 55.771(13), Sb1-Co3-Co2 56.101(12), Sb1-Co3-Co1 55.963(12), Sb2-Co3-Sb1 99.680(14), Sb2-Co3-Co2 56.283(12), Sb2-Co3-Co1 55.777(12), Sb1-Co1-Co2 56.195(13), Sb1-Co1-Co3 56.198(12), Sb2-Co1-Sb1 100.168(15), Sb2-Co1-Co2 56.416(13), Sb2-Co1-Co3 56.151(12).

[(Cp'''Fe)$_3$(μ_3-Sb)$_2$] (5):

Compound **5** crystallizes by layering a toluene solution with CH_3CN in form of violet blocks in the triclinic space group $P\bar{1}$. The asymmetric unit contains two molecules of **5**.

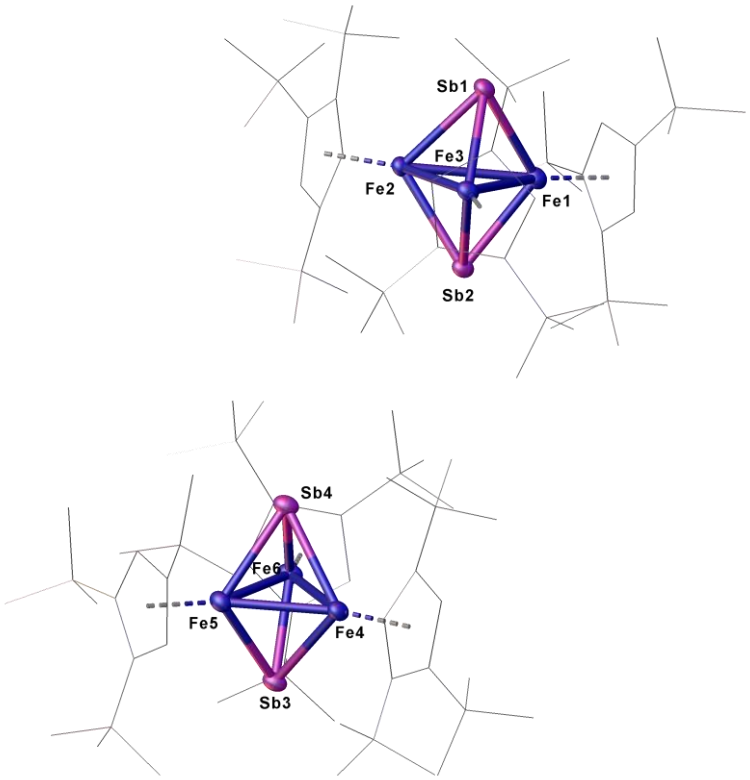

Figure S5: Molecular structure of **5** in the solid state. Cp''' ligands are drawn in the wire frame model and hydrogen atoms are omitted for clarity. Thermal ellipsoids are depicted at 50% probability level. Selected bond lengths [Å] and angles [°]: Sb1-Fe2 2.5007(5), Sb1-Fe3 2.5341(5), Sb1-Fe1 2.5211(5), Sb2-Fe2 2.5089(5), Sb2-Fe3 2.5169(5), Sb2-Fe1 2.5230(5), Sb3-Fe4 2.5144(5), Sb3-Fe6 2.5107(5), Sb3-Fe5 2.4920(5), Sb4-Fe4 2.5342(5), Sb4-Fe6 2.5037(5), Sb4-Fe5 2.4943(5), Fe2-Fe3 2.4489(6), Fe2-Fe1 2.9230(6), Fe3-Fe1 2.9161(7), Fe4-Fe6 2.8079(6), Fe4-Fe5 2.4895(6); Fe3-Fe1-Fe2 49.593(14), Fe3-Fe2-Fe1 65.057(17), Fe4-Fe6-Fe5 51.836(15), Fe5-Fe4-Fe6 65.690(18), Fe2-Sb1-Fe3 58.204(14), Fe2-Sb1-Fe1 71.191(15), Fe1-Sb1-Fe3 70.458(16), Fe2-Sb2-Fe3 58.323(15), Fe2-Sb2-Fe1 71.026(15), Fe3-Sb2-Fe1 70.705(16), Fe6-Sb3-Fe4 67.943(16), Fe5-Sb3-Fe4 59.637(16), Fe5-Sb3-Fe6 70.452(16), Fe6-Sb4-Fe4 67.743(16), Fe5-Sb4-Fe4 59.344(15), Fe5-Sb4-Fe6 70.528(16), Sb1-Fe2-Sb2 101.331(16), Sb1-Fe2-Fe1 54.730(13), Sb2-Fe2-Fe1 54.712(13), Fe3-Fe2-Sb1 61.583(15), Fe3-Fe2-Sb2 61.002(15), Sb1-Fe3-Fe1 54.562(13), Sb2-Fe3-Sb1 100.190(17), Sb2-Fe3-Fe1 54.746(14), Fe2-Fe3-Sb1 60.214(14), Fe2-Fe3-Sb2 60.675(15), Sb3-Fe4-Sb4 100.771(17), Sb3-Fe4-Fe6 55.967(14), Sb4-Fe4-Fe6 55.612(14), Fe5-Fe4-Sb3 59.735(15), Fe5-Fe4-Sb4 59.531(15), Sb3-Fe6-Fe4 56.090(13), Sb3-Fe6-Fe5 54.471(13), Sb4-Fe6-Sb3 101.718(17), Sb4-Fe6-Fe4 56.645(14), Sb4-Fe6-Fe5 54.584(14), Sb4-Fe5-Fe6 54.888(13), Fe4-Fe5-Sb3 60.628(16), Fe4-Fe5-Sb4 61.125(15), Sb1-Fe1-Sb2 100.379(17), Sb1-Fe1-Fe2 54.079(13), Sb1-Fe1-Fe3 54.981(14), Sb2-Fe1-Fe2 54.262(13), Sb2-Fe1-Fe3 54.550(13).

[(Cp'''Fe)$_3$(μ_3, $\eta^{4:4:4}$-Sb$_6$)] (6):

Compound **6** crystallizes by layering a toluene solution with CH_3CN in form of green needles in the triclinic space group $P\bar{1}$. The asymmetric unit contains one molecule of **6**.

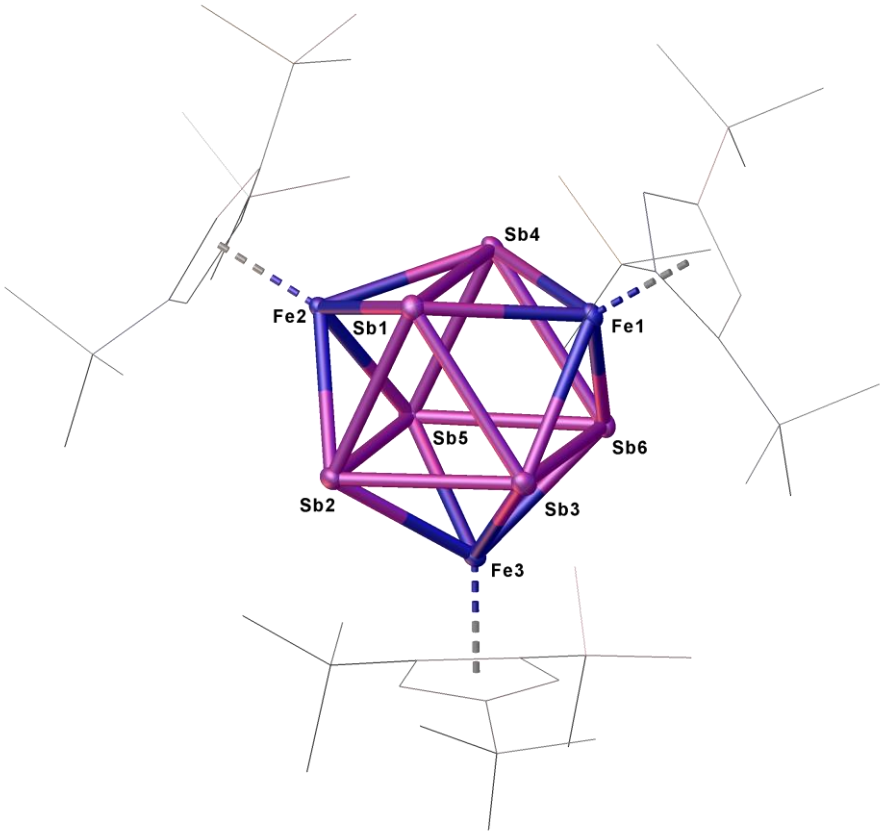

Figure S6: Molecular structure of **6** in the solid state. Cp''' ligands are drawn in the wire frame model and hydrogen atoms are omitted for clarity. Thermal ellipsoids are depicted at 50% probability level. Selected bond lengths [Å] and angles [°]: Sb6-Sb3 3.0286(3), Sb6-Sb4 2.9359(3), Sb6-Sb5 2.9367(3), Sb6-Fe3 2.6147(5), Sb6-Fe1 2.6287(5), Sb3-Sb2 2.9127(3), Sb3-Sb1 2.9236(3), Sb3-Fe3 2.6328(5), Sb3-Fe1 2.6055(5), Sb2-Sb1 2.9322(3), Sb2-Sb5 3.0648(3), Sb2-Fe2 2.6127(4), Sb2-Fe3 2.6030(5), Sb4-Sb1 3.0554(3), Sb4-Sb5 2.9033(3), Sb4-Fe2 2.6068(5), Sb4-Fe1 2.6099(5), Sb1-Fe2 2.6153(5), Sb1-Fe1 2.6231(5), Sb5-Fe2 2.6099(5), Sb5-Fe3 2.6146(5); Sb4-Sb6-Sb3 89.451(7), Sb4-Sb6-Sb5 59.257(6), Sb5-Sb6-Sb3 90.171(7), Sb2-Sb3-Sb6 90.530(7), Sb2-Sb3-Sb1 60.317(6), Sb1-Sb3-Sb6 91.076(7), Sb3-Sb2-Sb1 60.025(6), Sb3-Sb2-Sb5 89.913(7), Sb1-Sb2-Sb5 90.014(7), Sb6-Sb4-Sb1 90.312(7), Sb5-Sb4-Sb6 60.386(6), Sb5-Sb4-Sb1 90.744(7), Sb3-Sb1-Sb2 59.658(6), Sb3-Sb1-Sb4 89.161(7), Sb2-Sb1-Sb4 89.441(7), Sb6-Sb5-Sb2 89.372(7), Sb4-Sb5-Sb6 60.357(6), Sb4-Sb5-Sb2 89.796(7), Sb2-Fe2-Sb1 68.230(12), Sb4-Fe2-Sb2 107.681(16), Sb4-Fe2-Sb1 71.619(12), Sb4-Fe2-Sb5 67.634(12), Sb5-Fe2-Sb2 71.865(12), Sb5-Fe2-Sb1 108.552(16), Sb6-Fe3-Sb3 70.500(13), Sb6-Fe3-Sb5 68.332(12), Sb2-Fe3-Sb6 108.005(16), Sb2-Fe3-Sb3 67.599(13), Sb2-Fe3-Sb5 71.943(12), Sb5-Fe3-Sb3 107.246(16), Sb3-Fe1-Sb6 70.705(13), Sb3-Fe1-Sb4 107.198(16), Sb3-Fe1-Sb1 67.993(12), Sb4-Fe1-Sb6 68.171(12), Sb4-Fe1-Sb1 71.446(12), Sb1-Fe1-Sb6 108.000(16).

Table S1: Structure determination summary of complexes **1**, **2/2'** and **4**.

Compound	**1**	**2 · 0.5 (2')**	**4 · C_7H_8**
CCDC number	2079755	2079756	2079757
Formula	$C_{26}H_{42}Sb_6Zr_2$	$C_{85}H_{145}Ni_{4.5}Sb_4$	$C_{127}H_{113}Co_3Sb_2$
$D_{calc.}$/ g cm^{-3}	2.416	1.475	1.411
Formula Weight	1267.53	1918.20	2059.46
Colour	orange brown	violet	brown
Shape	plate	block	block
Size/mm^3	0.05×0.02×0.02	0.08×0.05×0.04	0.11×0.06×0.04
T/K	123.01(10)	122.97(13)	128.5(3)
Crystal System	triclinic	monoclinic	monoclinic
Space Group	$P\bar{1}$	*C*2/*c*	$P2_1/n$
a/Å	7.7940(6)	46.3369(13)	16.0588(2)
b/Å	10.9301(11)	19.0535(5)	19.7981(2)
c/Å	11.6145(7)	19.5836(6)	30.5084(4)
α/°	105.899(7)	90	90
β/°	96.387(6)	92.226(3)	91.1760(10)
γ/°	109.955(8)	90	90
V/Å^3	871.21(13)	17276.9(8)	9697.6(2)
Z	1	8	4
Z'	0.5	1	1
Wavelength/Å	1.54184	1.54184	1.54184
Radiation type	Cu K_α	Cu K_α	Cu K_α
μ/mm^{-1}	41.088	11.074	8.690
θ_{min}/°	4.063	3.350	2.661
θ_{max}/°	67.079	67.077	67.073
Measured Refl's.	6598	47158	34451
Ind't Refl's	3080	15359	17148
Refl's I≥2 *σ*(I)	2672	12426	15212
R_{int}	0.0465	0.0569	0.0252
Parameters	160	888	1190
Restraints	0	0	0
Largest Peak	1.624	0.754	0.443
Deepest Hole	-1.603	-0.795	-1.506
GooF	1.061	1.000	1.034
wR_2 (all data)	0.1036	0.0755	0.0771
wR_2	0.0981	0.0690	0.0742
R_1 (all data)	0.0422	0.0471	0.0370
R_1	0.0367	0.0326	0.0306

Table S2: Structure determination summary of complexes **3a**, **5** and **6**.

Compound	**3a**	**5**	**6**
CCDC number	2079758	2079759	2079760
Formula	$C_{68}H_{116}Co_4Sb_4$	$C_{51}H_{87}Fe_3Sb_2$	$C_{51}H_{87}Fe_3Sb_6$
$D_{calc.}$/ g cm^{-3}	1.543	1.422	1.862
Formula Weight	1656.32	1111.25	1598.25
Colour	dark violet	dark violet	dark green
Shape	block	block	needle
Size/mm^3	0.15×0.09×0.07	0.25×0.08×0.06	0.17×0.07×0.04
T/K	123(1)	123.0(2)	123(1)
Crystal System	hexagonal	triclinic	triclinic
Space Group	$P6_222$	$P\bar{1}$	$P\bar{1}$
Flack Parameter	-0.041(6)		
Hooft Parameter	-0.053(6)		
a/Å	13.0892(8)	12.3188(2)	10.4528(3)
b/Å	13.0892(8)	20.5303(4)	14.3499(4)
c/Å	36.0383(18)	20.5490(4)	20.1596(5)
α/°	90	87.329(2)	93.653(2)
β/°	90	89.4550(10)	101.854(2)
γ/°	120	88.3190(10)	104.007(2)
V/Å^3	5347.1(7)	5188.97(17)	2850.83(14)
Z	3	4	2
Z'	0.25	2	1
Wavelength/Å	1.54184	1.39222	1.54184
Radiation type	Cu K_α	Cu K_β	Cu K_α
μ/mm^{-1}	19.176	11.336	28.318
θ_{min}/°	3.679	3.733	3.687
θ_{max}/°	72.933	63.180	66.775
Measured Refl's.	19596	52581	29637
Ind't Refl's	3543	22736	10011
Refl's I≥2 *σ*(I)	3117	20653	9103
R_{int}	0.0545	0.0521	0.0277
Parameters	211	1063	568
Restraints	75	0	0
Largest Peak	0.722	1.114	0.955
Deepest Hole	-1.474	-1.346	-0.654
GooF	1.094	1.050	1.086
wR_2 (all data)	0.1153	0.1160	0.0495
wR_2	0.1063	0.1101	0.0482
R_1 (all data)	0.0572	0.0453	0.0263
R_1	0.0468	0.0411	0.0223

4.5.3 NMR Investigations

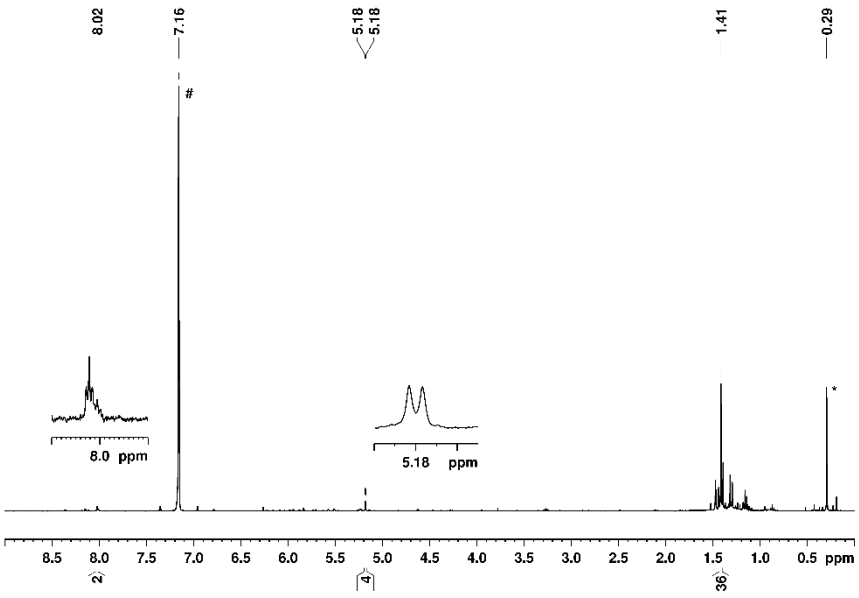

Figure S7: ^{1}H NMR spectrum of **1** at 293 K in C_6D_6 (#). The signal marked with * is due to silicon grease.

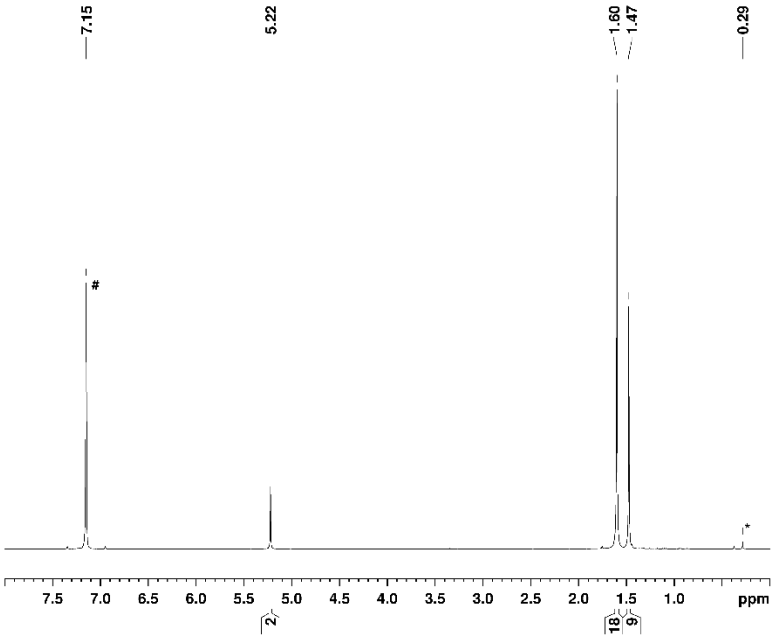

Figure S8: ^{1}H NMR spectrum of **2** at 293 K in C_6D_6 (#). The signal marked with * is due to silicon grease.

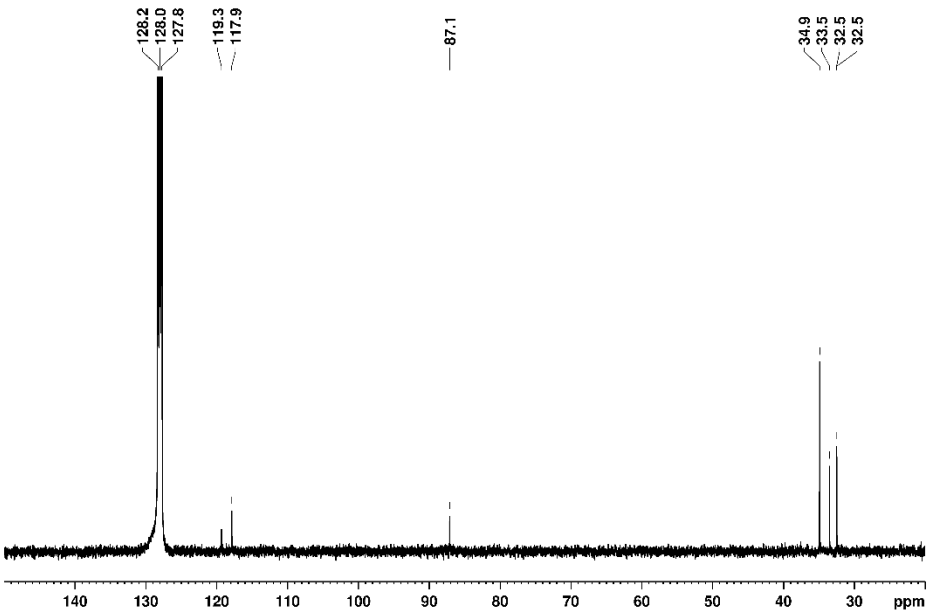

Figure S9: $^{13}C\{^{1}H\}$ NMR spectrum of **2** at 293 K in C_6D_6.

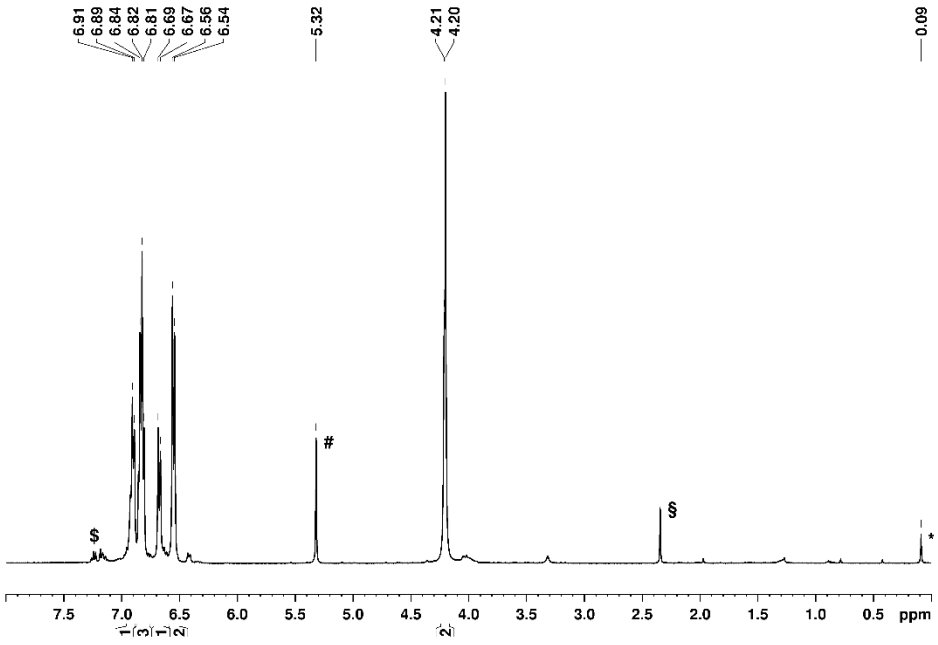

Figure S10: ^{1}H NMR spectrum of the mixture of **3b** and **4** at 273 K in CD_2Cl_2 (#). The signal marked with * is due to silicon grease, the signal marked with § is due to toluene.

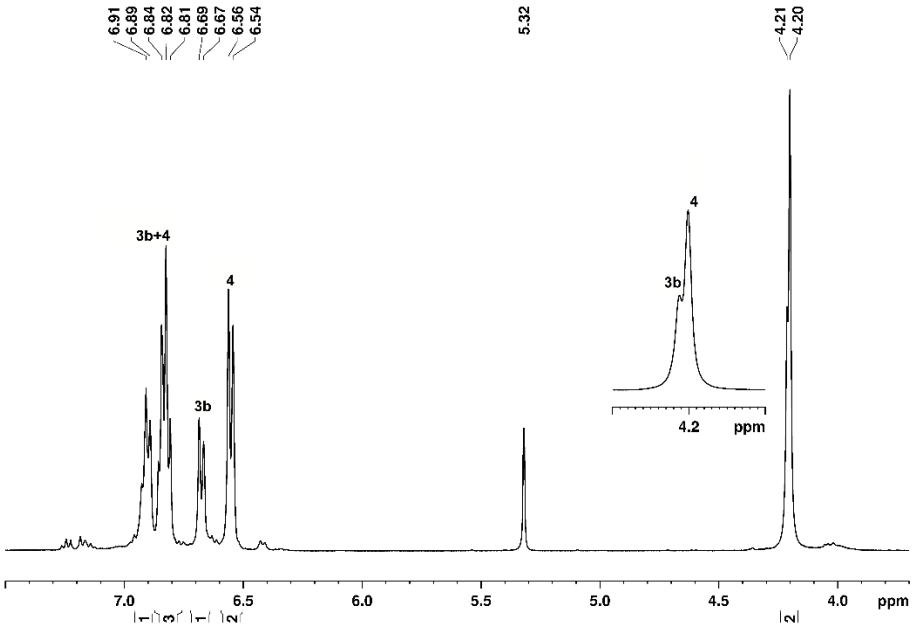

Figure S11: ^{1}H NMR spectrum of the mixture of **3b** and **4** at 273 K in CD_2Cl_2. The signals for the meta and para H atoms aof the phenyl rings of the Cp^{Bn} ligands are superimposed.

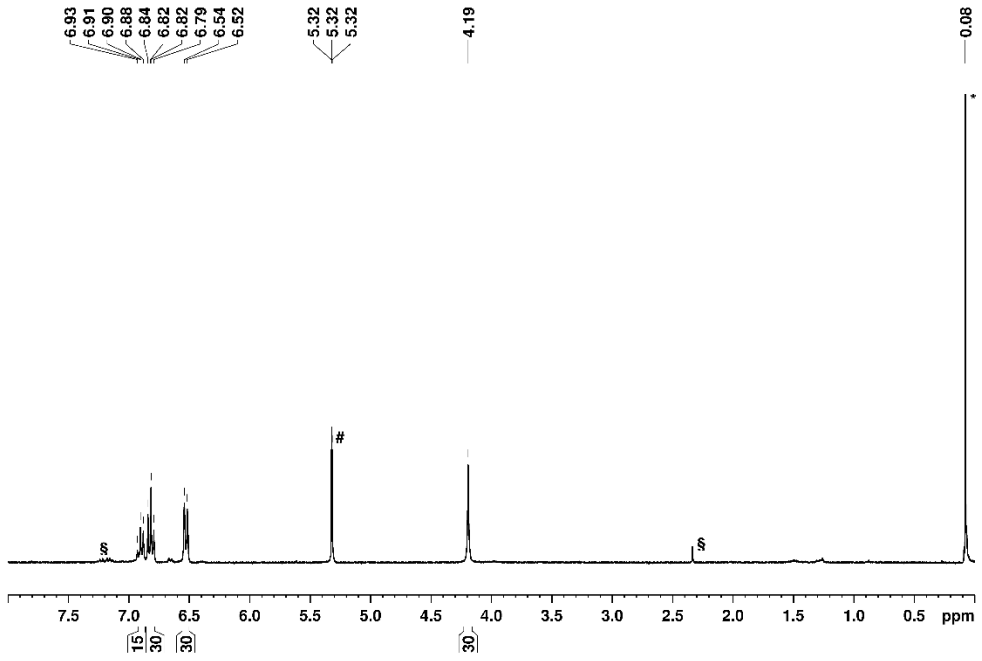

Figure S12: ^{1}H NMR spectrum of **4** at 273 K in CD_2Cl_2 (#). The signal marked with * is due to silicon grease, the signal marked with § is due to toluene.

4.5.4 EPR Measurements

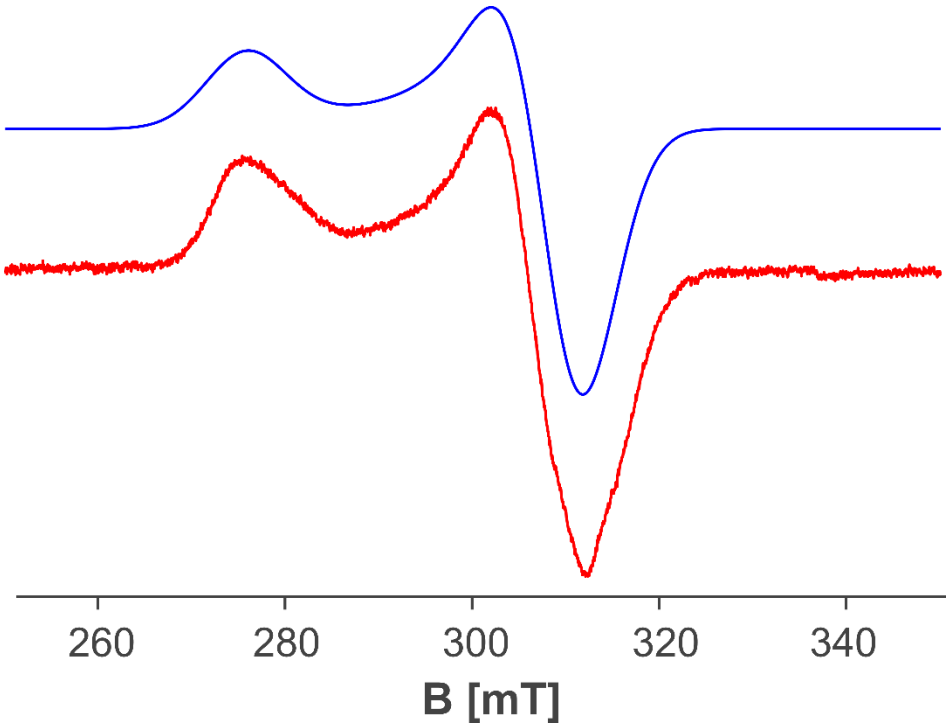

Figure S13: Red: X-band EPR spectrum of compound **5** in toluene at 77 K: $g_x = g_y = 2.1770$ and $g_z = 2.4434$ ($g_{iso} = 2.2658$). Blue: simulated spectrum using the EasySpin program.[61]

4.5.5 Computational Details

The DFT calculations for [{Cp"Zr}$_2$Sb$_6$] have been performed with the TURBOMOLE program package[62] at the RI[63]-B3LYP[64]/def2-TZVP[65] level of theory. To speed up the geometry optimization the Multipole Accelerated Resolution-of-Identity (MARI-*J*)[66] approximation has been used. The dispersion effects have been incorporated by using the dispersion correction scheme introduced by *Grimme et al.*[67] together with the BJ-damping[68] as implemented in TURBOMOLE. The final energy was determined by single point calculations without using the RI formalism. The DFT calculations for all other compounds have been performed with the ORCA program.[69] The OPBE[70] and/or B3LYP[64] functional together with the TZVP[65] basis set have been used. During the geometry optimisation cycles the RIJCOSX[71] approximation has been used. For the compounds **3a** and **6** the geometry has been optimised at the OPBE/def2-SVP level.

Table S3: Selected Wiberg Bond Indices for [{Cp"Zr}$_2$Sb$_6$] (**1**) calculated at the B3LYP/def2-TZVP level of theory.

Bond	Wiberg Bond Index
sb 2 - sb 1	0.84
sb 3 - sb 1	0.84
sb 3 - sb 2	0.04
zr 4 - sb 1	0.22
zr 4 - sb 2	0.97
zr 4 - sb 3	0.96
sb 39 - zr 4	0.93
sb 40 - sb 3	0.83
sb 40 - zr 4	0.18
sb 40 - sb 39	0.84
sb 41 - sb 1	0.04
sb 41 - sb 2	0.83
sb 41 - zr 4	0.18
sb 41 - sb 39	0.84
sb 41 - sb 40	0.04
zr 42 - sb 1	0.93
zr 42 - sb 2	0.18
zr 42 - sb 3	0.18
zr 42 - zr 4	0.13
zr 42 - sb 39	0.22
zr 42 - sb 40	0.97
zr 42 - sb 41	0.96

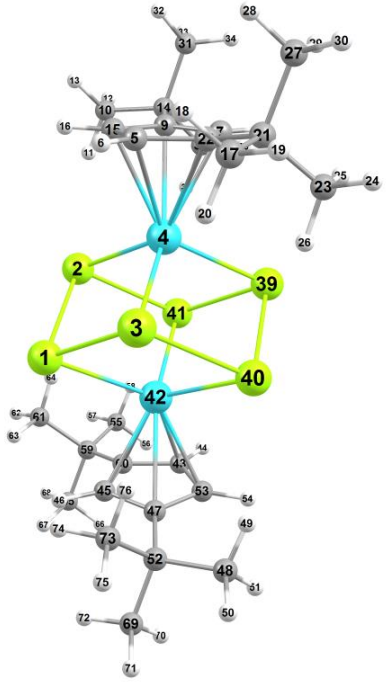

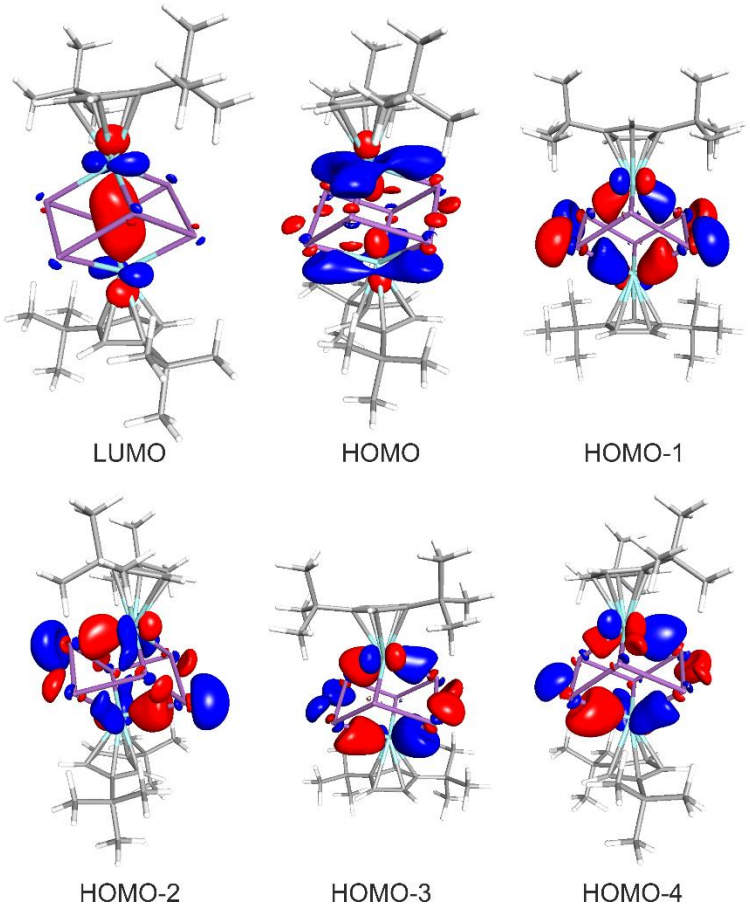

Figure S14: Selected frontier Molecular Orbitals of $[(Cp''Zr)_2(Sb_6)]$ (**1**) calculated at the B3LYP/def2-TZVP level of theory.

Table S4: Relative energies (single point calculations) of different spin multiplicities of $[(Cp'''Fe)_3(\mu_3\text{-}Sb)_2]$ (geometry optimised at the OPBE/def2-TZVP level with spin multiplicity 2), calculated at the OPBE/TZVP and B3LYP/TZVP levels of theory.

		Relative energy ($kJ \cdot mol^{-1}$)		Total energy (hartree)	
Total spin, *S*	Spin multiplicity	OPBE	B3LYP	OPBE	B3LYP
1/2	2	0.0	0.0	-6268.99040020	-6266.63853261
3/2	4	53.5	43.8	-6268.97000908	-6266.62186285
5/2	6	48.8	82.2	-6268.97182153	-6266.60723195
7/2	8	83.6	213.1	-6268.95857707	-6266.55738429
9/2	10	178.2	393.0	-6268.92253529	-6266.48883142

Table S5: Relative energies of the different spin multiplicities of $[(Cp'''Fe)_3(\mu_3\text{-}Sb)_2]$. The geometries have been optimised at the OPBE/TZVP level in different spin multiplicities. The B3LYP/TZVP energies have been calculated as single point calculations on the OPBE/TZVP optimised geometries in the corresponding spin states.

		Relative energy ($kJ \cdot mol^{-1}$)		Total energy (hartree)	
Total spin, *S*	Spin multiplicity	OPBE	B3LYP	OPBE	B3LYP
1/2	2	23.6	116.3	-6268.99040020	-6266.63853261
3/2	4	34.6	186.7	-6268.98620935	-6266.61171208
5/2	6	19.4	123.5	-6268.99199884	-6266.63577402
7/2	8	7.5	77.6	-6268.99653586	-6266.65325000
9/2	10	0.0	0.0	-6268.99938975	-6266.68281727

Table S6: Selected distances (Å) from X-ray diffractions as well as from the OPBE/def2-TZVP optimised geometries of $[(Cp'''Fe)_3(\mu_3\text{-}Sb)_2]$ in different spin states.

			Spin multiplicity				
Distance	Exp.	Exp.	2	4	6	8	10
Fe3-Fe5	2.490	2.4489	2.424	2.562	2.630	2.415	3.861
Fe3-Fe4	2.808	2.9161	2.991	2.545	3.536	4.157	3.957
Fe4-Fe5	2.886	2.923	3.022	2.989	2.724	4.203	4.031
Sb-Sb	3.889	3.875	3.806	3.824	3.597	2.800	2.777

Table S7: Total and relative energy of $[(Cp'''Fe)_3(\mu_3\text{-}Sb)_2]$ in different spin multiplicities calculated with the double hybrid functional B2PLYP[72]/TZVP, as single point calculations on the OPBE/TZVP optimised geometry in doublet spin sate.

Total spin, *S*	Spin multiplicity	Relative energy ($kJ \cdot mol^{-1}$)	total energy (Hartree)
1/2	2	89.7	-4850.99254455
3/2	4	97.4	-4850.98961574
5/2	6	64.1	-4851.00229258
7/2	8	0.0	-4851.02671511
9/2	10	71.3	-4850.99955754

Table S8: Cartesian coordinates of the optimized geometry of [{Cp''Zr}$_2$Sb$_6$] in the RI-B3LYP-D3/def2-TZVP level of theory. Total energy = -2551.97736891102 hartree.

Sb	-2.0614117	-0.1917940	-1.6966749
Sb	-0.5399553	2.2269774	-1.3138853
Sb	-2.1374956	-1.1784190	1.0100256
Zr	-0.5803419	1.1798409	1.3313900
C	-2.3941009	2.0948161	2.8064733
H	-3.3842502	1.6807714	2.7223520
C	-0.2534703	2.4880714	3.4653400
H	0.6707279	2.4439081	4.0160622
C	-0.5674837	3.4544910	2.4735669
C	-0.2857735	5.4412041	0.9447577
H	-0.3228256	4.8294162	0.0429050
H	0.3413191	6.3091213	0.7337667
H	-1.2939355	5.8025964	1.1540244
C	0.2884141	4.6612389	2.1311305
C	-1.8950289	3.1908559	2.0573476
H	-2.4461806	3.7407248	1.3137233
C	-2.8135585	-0.1370835	4.7440155
H	-3.6969272	0.5035128	4.7431571
H	-2.8942855	-0.8132699	5.5968681
H	-2.8291016	-0.7419127	3.8369493
C	-1.5245279	0.6830219	4.8518264
C	-1.3838396	1.6610805	3.6987176
C	-0.3250667	-0.2699355	4.9396080
H	-0.4013977	-0.8856218	5.8383130
H	0.6190602	0.2745790	4.9871265
H	-0.2837958	-0.9362333	4.0784595
C	-1.5874051	1.5252578	6.1439726
H	-2.4196727	2.2304078	6.1078719
H	-0.6680518	2.0950983	6.2858746
H	-1.7241104	0.8759852	7.0117330
C	0.2791398	5.5806559	3.3709670
H	-0.7405982	5.8677078	3.6336473
H	0.8519146	6.4892034	3.1718608
H	0.7217590	5.0808576	4.2337235
C	1.7370494	4.2609313	1.8215230
H	2.1749038	3.6770157	2.6323980
H	2.3510336	5.1532518	1.6825400
H	1.7980168	3.6656984	0.9108995
Sb	2.0614466	0.1917865	1.6966841
Sb	0.5399949	-2.2269949	1.3138747
Sb	2.1375329	1.1784045	-1.0100226
Zr	0.5803743	-1.1798514	-1.3313985
C	2.3941118	-2.0948196	-2.8065063
H	3.3842623	-1.6807742	-2.7224042
C	0.2534731	-2.4880802	-3.4653382
H	-0.6707352	-2.4439168	-4.0160430
C	0.5675027	-3.4544972	-2.4735693
C	0.2857764	-5.4411795	-0.9447166
H	0.3228191	-4.8293807	-0.0428713
H	-0.3413178	-6.3090939	-0.7337196
H	1.2939397	-5.8025749	-1.1539703
C	-0.2884037	-4.6612304	-2.1311037
C	1.8950543	-3.1908595	-2.0573715
H	2.4462193	-3.7407275	-1.3137563
C	2.8135032	0.1371323	-4.7440156
H	3.6968994	-0.5034260	-4.7431105
H	2.8942315	0.8133002	-5.5968832
H	2.8289875	0.7419844	-3.8369634
C	1.5245097	-0.6830304	-4.8518492
C	1.3838365	-1.6610869	-3.6987351
C	0.3250131	0.2698777	-4.9396708
H	0.4013469	0.8855614	-5.8383776
H	-0.6190908	-0.2746735	-4.9872158
H	0.2836914	0.9361785	-4.0785266
C	1.5874493	-1.5252759	-6.1439851
H	2.4197482	-2.2303877	-6.1078586
H	0.6681246	-2.0951602	-6.2858996
H	1.7241436	-0.8760062	-7.0117494
C	-0.2791483	-5.5806691	-3.3709254
H	0.7405846	-5.8677442	-3.6336005
H	-0.8519409	-6.4892022	-3.1718050
H	-0.7217568	-5.0808751	-4.2336896
C	-1.7370328	-4.2608962	-1.8214985
H	-2.1748879	-3.6770061	-2.6323915
H	-2.3510232	-5.1532059	-1.6824773
H	-1.7979862	-3.6656284	-0.9108964

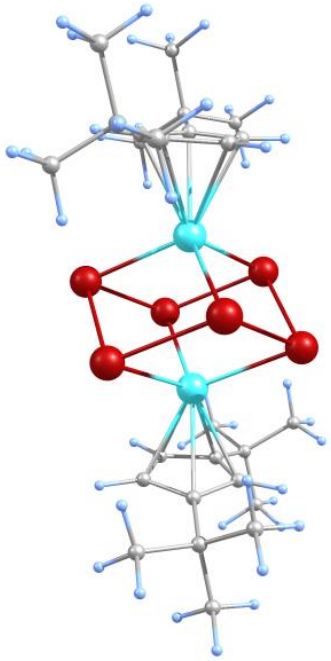

Table S9: Cartesian coordinates of the optimized geometry of [(Cp'''Ni)$_4$(μ_3-Sb)$_4$] (**2**) at the OPBE/TZVP level of theory, in the singlet spin state. Total energy: −9658.618384438727 hartree.

Sb	28.36612954452273	3.52737868439322	4.39895546683893
Sb	29.60967960299618	5.67302030865250	2.67298611473635
Sb	29.22993760496862	6.18240068148977	5.64900757841982
Sb	31.31567970738090	4.20314140295101	4.73470037815079
Ni	27.33617289745166	5.82202853080223	3.93331753809767
Ni	29.59506296476673	3.82237814021595	6.63061692978525
Ni	30.22844539539516	3.15539795160830	2.65678318804984
Ni	31.33113589161234	6.75971813491879	4.26409248657103
C	26.14534537630967	7.56548237687400	3.69202547858531
H	26.50419361497232	8.58250656088914	3.62563534672378
C	25.73986773177832	6.93743368395961	4.90205095453079
C	33.10473942393570	7.48698850955894	3.33829820566288
H	33.64021265997133	7.02315122139271	2.52290785848798
C	29.62942846321652	1.99438580445387	7.70548510524655
H	29.79553009955861	1.01068845593313	7.29090216761134
C	30.01206329239591	4.01503608832073	8.76911988916281
C	28.61051334994193	3.83794860923414	8.50352935922937
H	27.84872119079947	4.54609013272568	8.79154935307013
C	28.34725221805855	2.56981833570910	7.91902077422543
C	31.78151614826723	2.31646590449716	1.33489919863671
C	25.31667296853394	5.63613772501318	4.51466559458936
H	24.93815742544558	4.89211861103852	5.19890466923721
C	31.37046726166368	1.40687469098584	2.36905612563533
H	32.03664671207009	0.98194607667014	3.10598803822005
C	27.81938812620605	-0.12661011663479	2.77143322488801
H	27.44128667579086	0.71420650934307	3.35975478198424
H	27.38418621370393	-1.04691610847136	3.18043271702430
H	27.44128671209347	-0.01825621504143	1.74918700266618
C	32.11432265636783	8.51442021070168	3.16423453117276
C	30.67280769958636	2.81481658028555	8.25386841416063
C	25.87053787291621	6.73324617469164	2.55342464595019
C	30.58302924562350	2.59579676351447	0.54831175454367
C	29.52207389826961	1.83695462006016	1.15235791303265
H	28.51404555898958	1.79713635383820	0.76589268669447
C	31.70854404791178	8.91698419139401	4.50821695677875
C	25.33669609700785	5.48150387046709	3.08622411655108
C	30.00282982194783	1.04387806534297	2.22854471649904
C	32.48776367161141	8.11504434441125	5.41213201794522
H	32.44279368787007	8.19902715199627	6.48761420517307
C	33.41136670450484	7.29241243605357	4.71085894253015
C	25.39657363422102	7.63254963455652	6.21598195415567
C	32.04279757376723	2.13047864826456	8.47017774427519
C	27.01562714825473	1.82643385698138	7.95588925798593
C	25.81983959491241	2.77034138503074	7.80887487490711
H	25.77616123007215	3.50582432741286	8.61903962643835
H	24.88355451842926	2.19903797900930	7.83866197735686
H	25.85853516372267	3.31133325289666	6.86140579282001
C	29.81612245589570	-0.47502565232108	4.24151413020221
H	29.60352771856422	0.37633146324324	4.89141187111510
H	30.89290855421835	-0.67099984333712	4.28647542600400
H	29.30501616069489	-1.35733911227645	4.64614796396059
C	26.31196311816602	8.82047003569028	6.52049725422934
H	27.35108543327907	8.50489577403372	6.64512300751164
H	25.99348624986710	9.30701698531272	7.45120401484051
H	26.27952568775712	9.58039257616250	5.73294469935321
C	25.85157147957140	7.42794054616463	1.17251439624357
C	26.91330536347177	0.72598907593898	6.89746386863549
H	26.97820229250506	1.13514971423251	5.88512858333112
H	25.95013179158465	0.20799229697224	6.98643027528689
H	27.69625197479294	-0.03103267657832	7.00942323662033
C	29.34844047061641	-0.20241476720543	2.80865959151821
C	32.41700173628346	1.24063226145346	7.27064373418910
H	31.70834663717810	0.42676419856932	7.09919326997899
H	33.39343400357555	0.77601663304397	7.45687502859743
H	32.49509314290357	1.82421289896372	6.34867551670533
C	25.41914588940401	6.66891191158135	7.40404050592863
H	24.66409032502449	5.88287834582478	7.30576361784664
H	25.20243657901139	7.21064779094362	8.33317555939805
H	26.39506155341817	6.19079551912105	7.50830301483893
C	31.60957924791575	6.01857921256815	9.13148232976156
H	32.52553104619644	5.44800640240533	9.00201026181954
H	31.82934222730676	6.84653828331945	9.81734151920604
H	31.34000424693101	6.44553752373715	8.16218611658544
C	25.91757327894583	6.53386094465784	-0.06847173786911
H	26.81455731743089	5.91167392375710	-0.06873236877781
H	25.95977714684182	7.16925777003196	-0.96206441654692
H	25.04491526539121	5.88910155445428	-0.18599253716612
C	27.03093358547529	8.40458967772648	1.03968129700777
H	27.02130889511710	9.19491669283322	1.79459737283861
H	26.99027907712546	8.89836233311914	0.06104178896763
H	27.98455498622278	7.87445874702336	1.10978303562500
C	29.79041873096186	-1.38734650236785	1.92049965738775
H	29.35846313420362	-2.32479217806006	2.29528253351274
H	30.88102642989932	-1.49574972749517	1.91384029805419
H	29.46105710646194	-1.25560337044720	0.88375160912652

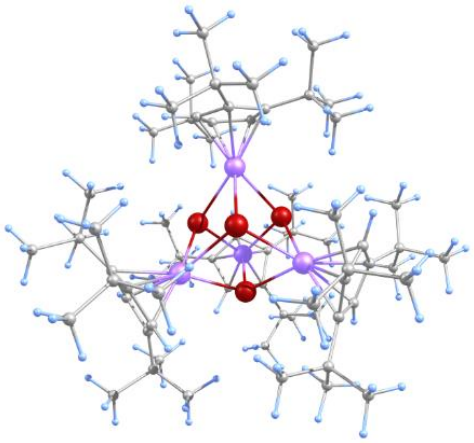

C	23.95397102730087	8.16605718516960	6.05605250354815
H	23.88487056281867	8.89426486870749	5.23938605389626
H	23.62651203839915	8.66290465092142	6.97917135568368
H	23.25043914425403	7.35357141164036	5.84250833968341
C	29.45090752509058	10.17580655520129	4.55137455806547
H	29.38989869578133	10.35904409354867	3.48091640481034
H	28.91654623751316	10.98899742057741	5.05809008299925
H	28.92304960528457	9.24243571699129	4.75673789696413
C	30.89124020596097	10.10017624130100	5.06852900102847
C	31.90241627673412	1.20394750963417	9.69961273653296
H	31.65358922166924	1.76017440612878	10.60800567201102
H	32.84617771532271	0.67255073439129	9.88136230978234
H	31.12088252476600	0.45215645958570	9.54575564631622
C	32.01947761255918	9.15023771425478	1.75828197751496
C	33.25050504319940	3.04141222998905	8.69945608476130
H	33.41068809608440	3.71529773058894	7.85566446980012
H	34.15080517818759	2.42164461619811	8.79700555289754
H	33.17375175417737	3.62988909380022	9.61486562374906
C	26.93483882138970	1.16217185893536	9.34966272864166
H	27.75401010223030	0.45025109200327	9.50303695420878
H	25.98858549694187	0.61448006178624	9.45524158116230
H	26.98510392816154	1.90955129488063	10.15018981953765
C	30.45481359221046	5.17822395407695	9.68403323575752
C	24.62172906221970	4.27115970378252	2.44735048565612
C	30.31263410807616	3.17732732712058	-0.85673295370087
C	33.25398947887899	10.06790460297406	1.59460986974201
H	33.26846839192014	10.87706927830177	2.32967086003725
H	33.25627687802815	10.52129597334120	0.59473598350081
H	34.18520513651178	9.50169533899468	1.70611127121417
C	25.46877469945591	3.50061680543960	1.42721121158558
H	25.77656359884996	4.10593109206572	0.57755290930713
H	24.89881149962646	2.64556280418458	1.04118563993270
H	26.37363500462919	3.11496306127890	1.90442238726548
C	33.64277338226320	4.08065606942804	1.06271213153058
H	33.21752012676599	4.58546240361704	0.19818793927225
H	34.73269693171617	4.20187047990244	1.01227089403791
H	33.28114983715419	4.59072626709390	1.95791546050192
C	24.55129090162645	8.26193125451156	1.10229889691164
H	23.65672270755143	7.63871145631086	1.19119887981003
H	24.49523289291377	8.79561016508370	0.14409314268121
H	24.51596183126885	9.00836414426854	1.90364632210020
C	31.22095719100141	4.31635146847350	-1.32692630402158
H	31.20412493242568	5.16129896247315	-0.63425898187897
H	30.86230493898809	4.68063712476414	-2.29766589010318
H	32.25547177099664	4.00499303219285	-1.47617714351953
C	30.42564385710431	2.01585357642243	-1.87001927530795
H	31.42987702282489	1.58426059124535	-1.89632993911757
H	30.18992940816786	2.37334151669577	-2.88128438721903
H	29.72463426040521	1.20908993463418	-1.62900514885141
C	33.28530325109760	2.59166784272737	1.12422818844325
C	30.76996248869125	9.97486064958621	1.44147963938610
H	29.85641255911171	9.39239399492311	1.57053502982508
H	30.80845336056662	10.29183075590937	0.39213384328692
H	30.69754183656332	10.88343876653138	2.03941059244120
C	32.10782176340535	8.07913416535452	0.65903964307011
H	33.06094620371748	7.54500637199606	0.65444412563705
H	32.01186401000221	8.55925755732422	-0.32318562455344
H	31.30351280996812	7.34381982361562	0.75130739254039
C	34.11165535710225	1.99583852613525	2.27913592402010
H	33.81868094024876	2.40101524668541	3.25222436214152
H	35.16908756505726	2.24138325907811	2.12671683654870
H	34.03813538675771	0.90338146038737	2.32370676293018
C	28.87860055976726	3.72233112261586	-0.95116118869503
H	28.11449274327198	2.95059409966435	-0.82716239679199
H	28.72252610282333	4.16684533668446	-1.94162496557567
H	28.70621989435737	4.49665821867953	-0.19958727328708
C	29.29655135937977	6.16620370512000	9.91815546887224
H	28.91899270895155	6.58739697546188	8.98058276066765
H	29.66208964648282	7.00073027593587	10.52805452515251
H	28.45836624929838	5.71538111063799	10.45996897762303
C	35.16904057141318	5.44625253606564	4.56707279317287
H	34.43787765439601	4.64416567137646	4.70516083757834
H	36.12539985209292	5.10753854037785	4.98497693134422
H	35.31692629200090	5.59034037819281	3.49298379996153
C	23.29939712002193	4.73221346838279	1.80060955668089
H	22.67244396716684	5.26220073125280	2.52751437674968
H	22.73530263347881	3.85943484354310	1.44700306352764
H	23.45056723865519	5.39147987547092	0.94466675342798
C	30.82471484560223	4.62611480554328	11.07635643013228
H	29.99841111886707	4.04199707599941	11.49913066717678
H	31.03288251970306	5.45604019675274	11.76411926797061
H	31.71165443741795	3.98898748812882	11.05775611293967
C	34.72087835042277	6.73462753455050	5.26253103632631
C	30.78656786563200	10.01122313015992	6.60247558569035
H	30.32682539330529	9.07453942207385	6.93119528535126
H	30.15562828354367	10.83055357929543	6.96654498040385
H	31.75884166466803	10.11208022515346	7.09706404646598
C	31.62353923669989	11.42689351485169	4.77774866654015
H	32.66107120262446	11.38892583247933	5.12844194979695

H	31.12303855910819	12.24930788998182	5.30529610224359
H	31.63446174840827	11.68425051443895	3.71701652347985
C	24.21711191835839	3.24042141890525	3.51830459195681
H	25.08037327741639	2.85391416586301	4.06727612741935
H	23.73350949406334	2.38757033273715	3.02668602013725
H	23.49643491133843	3.64180776333713	4.24034566722785
C	33.78250382738043	1.87511347762564	-0.14792237412168
H	33.53312935913112	0.80783717694579	-0.12162530325069
H	34.87527085307503	1.96058942567577	-0.21876801700547
H	33.36447631526099	2.29526251585374	-1.06435148639928
C	34.65299692547628	6.48865705236581	6.76995735096337
H	34.46794498805260	7.41109637586542	7.33029194260418
H	35.60620569354717	6.08059566173444	7.12770350219756
H	33.86577719408712	5.77684181924746	7.01856442298377
C	35.79156738700265	7.81998042525317	5.00829830391109
H	35.92194223254741	8.01516299148294	3.93819442669168
H	36.76025426293096	7.49915679308725	5.41388534874686
H	35.52146431105360	8.76592694878993	5.49221425366577

Tables10: Selected Meyer bond orders for [(Cp'''Ni)$_4$(μ_3-Sb)$_4$] (**2**) in the singlet spin state, calculated at the OPBE/TZVP level of theory.

B(0-Sb, 1-Sb) :	0.31	B(0-Sb, 2-Sb) :	0.25	B(0-Sb, 3-Sb) :	0.26
B(0-Sb, 4-Ni) :	0.71	B(0-Sb, 5-Ni) :	0.69	B(0-Sb, 6-Ni) :	0.69
B(0-Sb, 7-Ni) :	0.10	B(1-Sb, 2-Sb) :	0.31	B(1-Sb, 3-Sb) :	0.31
B(1-Sb, 4-Ni) :	0.62	B(1-Sb, 5-Ni) :	0.11	B(1-Sb, 6-Ni) :	0.65
B(1-Sb, 7-Ni) :	0.67	B(2-Sb, 3-Sb) :	0.35	B(2-Sb, 4-Ni) :	0.67
B(2-Sb, 5-Ni) :	0.65	B(2-Sb, 7-Ni) :	0.68	B(3-Sb, 5-Ni) :	0.59
B(3-Sb, 6-Ni) :	0.72	B(3-Sb, 7-Ni) :	0.65		

Table S11: Cartesian coordinates of the optimized geometry of [(Cp'''Co)$_4$(μ_3-Sb)$_4$] (**3a**) at the OPBE/SVP level of theory, in the unrestricted singlet spin state. Total energy: −9156.10473923027 hartree.

Sb	-0.92743399225559	1.11513047067921	-1.14014022001331
Sb	1.00276063420058	-1.09802823459449	-1.25173465844681
Sb	-0.98124075315992	-1.05919968240592	1.18417328095972
Sb	0.95783705420896	1.11390016918754	1.23698145574804
Co	-1.68250050350963	-1.44640190706671	-1.32059719968311
Co	1.68277738247495	-1.37871831106909	1.21638098614527
Co	-1.57207535851745	1.54783397353725	1.31026912683108
Co	1.65353100817180	1.44400220166090	-1.19820458975416
C	-2.74548248263480	3.25584196106953	0.89346701878036
C	-3.53270656065321	2.13024078023505	1.29759248798996
C	-1.82678296343743	3.46271240247823	1.96097078696737
H	-1.07562856646799	4.24752980973105	1.97052041434460
C	-2.09575796784503	2.57830689145515	3.07090437974506
C	-3.20466203270497	1.71456856280552	2.63833557125824
C	-3.11275832145668	4.30217197726327	-0.16082553186184
C	-4.21188348076717	0.79129301050166	3.36257788846807
C	-4.88414716943766	-0.15968851963701	2.35346613973255
H	-5.54754516731395	0.36706045086450	1.64889532213028
H	-5.51308821539160	-0.88828960023687	2.89116700223996
H	-4.13875415432218	-0.71362773955085	1.76605036416001
C	-5.33685252816715	1.67970907832270	3.94625324523849
H	-4.98123930994697	2.36590038593517	4.72731711972542
H	-6.12812424913193	1.05062423068608	4.39153579038906
H	-5.80375432093473	2.29314821959663	3.15809239636429
C	-3.62748941775590	-0.08964417568556	4.47334568280445
H	-2.79626533676846	-0.70619201261659	4.09897491529216
H	-4.40328240291215	-0.77409636358431	4.85577097837560
H	-3.27034213264283	0.48977941735369	5.33488056692111
C	-1.42248917834167	2.86615797006693	4.43730186006257
C	-2.48322807809489	3.36336440826621	5.44185761278441
H	-3.07053680963633	4.19886152646374	5.02568754000545
H	-1.99313672095259	3.72558535905319	6.36164377467054
H	-3.18107164458596	2.57066203109086	5.73968263028339
C	-0.66752864602068	1.67033219509075	5.02324699249630
H	-1.30391215700512	0.79307218314230	5.16778006561527
H	-0.23386763376152	1.93177144736832	6.00422524582093
H	0.15274570907594	1.37567332120660	4.35427123096220
C	-0.38701177630145	4.00279618071635	4.31257820103452
H	0.41299554274763	3.75647423298710	3.59806136972623
H	0.09281376271533	4.16763606175358	5.29214425559200
H	-0.84055316445409	4.96147596945967	4.01382437235930
C	-1.89615847916882	5.12194120796288	-0.60800030184964
H	-1.46049554409346	5.70438585990157	0.21768810483902
H	-2.18299047721207	5.83915137760370	-1.39521984601818

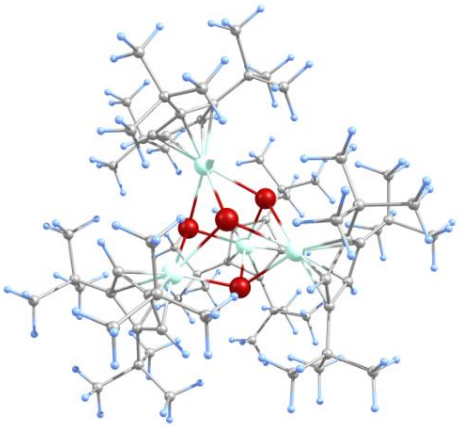

H	-1.10969030577363	4.46958458205075	-1.01093714261360
C	-4.11793825740337	5.24974980346677	0.53800510317226
H	-5.02716951408043	4.71187982454299	0.85319853500480
H	-4.42674994245282	6.05932591740506	-0.14692411295396
H	-3.67799578397823	5.71368409038236	1.43579168250508
C	-3.79972571711339	3.70900124767761	-1.39722360068135
H	-3.13902400954871	3.01337035962008	-1.93672207330903
H	-4.07861098759274	4.51494727098372	-2.09740184474983
H	-4.72348685898836	3.16926598488882	-1.14020238066005
C	2.78297595305340	-3.20214594920152	0.84933909372946
C	3.61821735588040	-2.12583191114088	1.27544893280113
C	1.81821639322413	-3.35110833631545	1.88615491397804
H	1.03052095607645	-4.09872994791793	1.87639522501702
C	2.09995183859466	-2.48412683325423	3.00054038102523
C	3.26501326157525	-1.67710912851077	2.59651534626107
C	3.13133666608257	-4.27402359689074	-0.18642596661876
C	4.29128033475556	-0.79009196067561	3.34094169379667
C	4.99412889975247	0.15444915573681	2.34608974471469
H	5.65024389488161	-0.38035356654154	1.64080057897547
H	5.63596278246605	0.86370522613139	2.89464300842379
H	4.26316701661741	0.72953134271337	1.76011421972918
C	5.38690316630615	-1.71275974951507	3.92703246396900
H	5.00373731322688	-2.39876845709416	4.69549106112592
H	6.18786968494422	-1.10939526483955	4.39027073603364
H	5.84859435727474	-2.32835045253215	3.13777907349838
C	3.72575977964307	0.09599523796964	4.45774226080572
H	2.91615650152439	0.74481381699465	4.08954145762085
H	4.52125533121896	0.75004021415617	4.85282992634550
H	3.34642588435634	-0.48244941037988	5.31049515458033
C	1.40556781403957	-2.75716037398783	4.35844048940936
C	2.43851904192043	-3.31531808080081	5.36062586003664
H	2.99346218184687	-4.16630615639361	4.93186172847638
H	1.92850130100388	-3.67326555075818	6.27134602411531
H	3.16722923150717	-2.55789373629136	5.67642747441011
C	0.70018268361655	-1.53692451017442	4.95570994924280
H	1.36809158785413	-0.68354533573839	5.10013903239505
H	0.26255588819555	-1.78656200198426	5.93802061091561
H	-0.11472697290987	-1.21037439906042	4.29505647433917
C	0.32012951055444	-3.84368867954760	4.21339338482129
H	-0.45773187108442	-3.55234635888581	3.49139135303017
H	-0.17771868897632	-3.99378647085937	5.18639529609171
H	0.73144229217474	-4.81935164433692	3.90962593626599
C	1.89345761260582	-5.05234157112275	-0.64970742396701
H	1.43245080487302	-5.62179562586314	0.17112261651981
H	2.16748234905922	-5.77825349538926	-1.43346614971201
H	1.13188449096124	-4.37584606206848	-1.06098940052311
C	4.08330099856483	-5.25358606447406	0.54270719888964
H	5.01145421220107	-4.75263940826254	0.86333112690123
H	4.36484135627224	-6.08632668757700	-0.12594544598850
H	3.61074354283265	-5.68424941091608	1.44063103197127
C	3.86751823174528	-3.72270302211235	-1.41367623271500
H	3.24230102071697	-3.01730798230054	-1.98162752761481
H	4.13841401222492	-4.54833868614971	-2.09394596137429
H	4.80229633128084	-3.20981130510011	-1.14145467517356
C	-2.80328280348704	-3.25997616746123	-0.91043396979679
C	-3.62553081627122	-2.17452018041854	-1.33030456675318
C	-1.86158259134891	-3.43986856421694	-1.96582262757130
H	-1.08463109850566	-4.19888293470972	-1.95967605248324
C	-2.14295230506438	-2.57926603447155	-3.07889920522337
C	-3.27934881336886	-1.73577861360460	-2.65852342442480
C	-3.14777556394926	-4.31621901395027	0.14184474030788
C	-4.28728424681906	-0.81889065954322	-3.39013476405297
C	-4.96981259901380	0.12809909505740	-2.38326053629732
H	-5.63636510965386	-0.40141682792449	-1.68363666855878
H	-5.59776783613756	0.85648230557650	-2.92291431203479
H	-4.22798181544763	0.68303891049582	-1.79129991724142
C	-5.40263201773989	-1.70828537035280	-3.98923545588538
H	-5.03428493879556	-2.39136023312853	-4.76739084193014
H	-6.19112178930887	-1.08175086259789	-4.44319848999274
H	-5.87641228573100	-2.32592978816839	-3.20847670773548
C	-3.69533424386440	0.06987214895623	-4.49115801671507
H	-2.87222721105614	0.69109281944782	-4.10610330065266
H	-4.47133956275573	0.75000160535258	-4.88123883947720
H	-3.32449599965805	-0.50518580582288	-5.34990161437522
C	-1.45608232035653	-2.85654080327325	-4.44008138721795
C	-2.50369715001794	-3.36044779080353	-5.45467190533698
H	-3.08497171609682	-4.20366986885737	-5.04570912050218
H	-2.00359145398832	-3.71318400726989	-6.37289092594416
H	-3.20846702450934	-2.57425433390676	-5.75368598410163
C	-0.70526160298866	-1.65262985104896	-5.01622486432393
H	-1.34580450335174	-0.77823420555788	-5.16148441299234
H	-0.26320908175571	-1.90646810120171	-5.99565420644242
H	0.10969526317293	-1.35784561326871	-4.34096390227744
C	-0.41104373910801	-3.98340376395263	-4.30768012656788
H	0.38194168232592	-3.72598492091684	-3.58938156452728
H	0.07522575715775	-4.14652343522335	-5.28448979509234
H	-0.85823276768915	-4.94456611571319	-4.00723959393952
C	-1.91105825715161	-5.10017975423515	0.59902233362186
H	-1.45810104892789	-5.67551200173224	-0.22238436301861

H	-2.18307916134885	-5.82095510920256	1.38823836024942
H	-1.14345717874821	-4.42585902503770	1.00217318158430
C	-4.11865472743163	-5.29604391375273	-0.56127592969697
H	-5.04651956777754	-4.78999112331528	-0.87473767616993
H	-4.39809197951426	-6.11844947692627	0.12103782736756
H	-3.66296440303410	-5.74138720700595	-1.46076619950977
C	-3.86003444667914	-3.74173815876372	1.37280789413662
H	-3.21809440387328	-3.03626726203145	1.92115582517193
H	-4.13017286882850	-4.55580774320566	2.06715346842631
H	-4.79248607587512	-3.22066174378478	1.10786449299678
C	2.77419273218278	3.22294109731838	-0.83612588591720
C	3.58799342266743	2.12411990724624	-1.25231824175029
C	1.81242539260790	3.37037405127545	-1.87381361608751
H	1.03365319518751	4.12770186313782	-1.87492163641234
C	2.09129448527762	2.48958053456397	-2.98872184989339
C	3.24276956122520	1.67804262833926	-2.58075728677723
C	3.13285647782102	4.29161884680158	0.19878476620419
C	4.27057146270305	0.78888188823874	-3.31962490652896
C	4.97103407307712	-0.15376173194540	-2.32179564039212
H	5.62511085037532	0.38243735568873	-1.61571164876706
H	5.61448758301539	-0.86298132142506	-2.86827348016963
H	4.24008295445531	-0.72910367148551	-1.73653413483768
C	5.36850020537618	1.71158373248537	-3.90173303885904
H	4.98925592586165	2.39569221796113	-4.67376264414023
H	6.17225696746633	1.10749700482987	-4.35900886132119
H	5.82598497653413	2.32897346091154	-3.11135214196853
C	3.70812613678844	-0.09793322177749	-4.43751309731918
H	2.89690134987515	-0.74592024242176	-4.07152206030665
H	4.50468190217542	-0.75292995579987	-4.82872106250870
H	3.33234816590510	0.47949940173955	-5.29254265359635
C	1.39637207012575	2.76059095571947	-4.34710363634764
C	2.43261656524069	3.31020364958230	-5.35079375359761
H	2.99049473802247	4.16109298698685	-4.92557653536630
H	1.92473138299723	3.66601562408773	-6.26345883340921
H	3.15857686398708	2.54846751542942	-5.66199715389592
C	0.68584632411428	1.54090970092947	-4.93890898832434
H	1.35058435077067	0.68466915594427	-5.08040493958680
H	0.24900536483470	1.78875938438720	-5.92195540703971
H	-0.13024033597088	1.21879685250260	-4.27727451846587
C	0.31702010750661	3.85404914410508	-4.20861700467800
H	-0.46390487190217	3.57209199445112	-3.48631432704631
H	-0.17947986656300	4.00086719653426	-5.18270857045895
H	0.73297968239185	4.82971428544970	-3.91116590077069
C	1.90462017600705	5.09514820918502	0.64422038766867
H	1.46150761721503	5.66806215124229	-0.18413225056940
H	2.18300263524539	5.82047670943593	1.42699132936281
H	1.12657508749534	4.43473878597909	1.05084410694429
C	4.11403108434899	5.24847281570553	-0.52060332790932
H	5.03401193041050	4.72622353780574	-0.83077109920228
H	4.40749345120780	6.07674227583468	0.14857186208540
H	3.66017034205066	5.68709722447347	-1.42430683523819
C	3.84040221603449	3.72846177969937	1.43768471639102
H	3.19573283842243	3.03186550958637	1.99502068840200
H	4.11359366536948	4.54911948170530	2.12294552681017
H	4.77031435543566	3.19950152697486	1.18053469023800
H	-4.33739522534300	1.70035876785161	0.70409621157552
H	-4.45565562854017	-1.77526180446159	-0.74992082043653
H	4.46651782517549	-1.74792155936349	0.70755887690279
H	4.42266550426918	1.73013612922093	-0.6747822992140

Table S12: Cartesian coordinates of the optimized geometry of [(Cp'''Co)$_4$(μ_3-Sb)$_4$] (**3a**) at the OPBE/SVP level of theory, in the triplet spin state. Total energy: −9156.10520769705 hartree.

Sb	-0.91428130448516	1.07853662861176	-1.15029788612519
Sb	1.01962621423413	-1.11097927407631	-1.27334469142508
Sb	-0.91408410308650	-1.07932724158541	1.14997380145124
Sb	1.01541543472010	1.11325644922133	1.27486923356345
Co	-1.65604294543192	-1.45877331131480	-1.29841708261901
Co	1.65464354250331	-1.43634666574489	1.18366186523384
Co	-1.66330263369410	1.46021441712267	1.29177053622707
Co	1.65202476096509	1.44057082435357	-1.18516607810352
C	-2.78067624589300	3.24125968214741	0.89505440669445
C	-3.60798283448098	2.15861663410308	1.31606984175493
C	-1.84033715945533	3.42032832047745	1.95390335789913
H	-1.06408314121079	4.18004057034648	1.94824440273773
C	-2.12939301335461	2.56255569588859	3.07064676542574
C	-3.26446718087868	1.72456325252400	2.64622721087632
C	-3.12238588180212	4.29434702005712	-0.16099804268537
C	-4.27163516619109	0.80545864385153	3.37515109654554
C	-4.95233914401073	-0.14090290085187	2.36633493905470
H	-5.62079705497268	0.38888074500808	1.66882209644079
H	-5.57758355575326	-0.87246099074000	2.90462762304413
H	-4.20937537536164	-0.69122424897723	1.77181619201338
C	-5.38878279766014	1.69447221786663	3.97203298200357

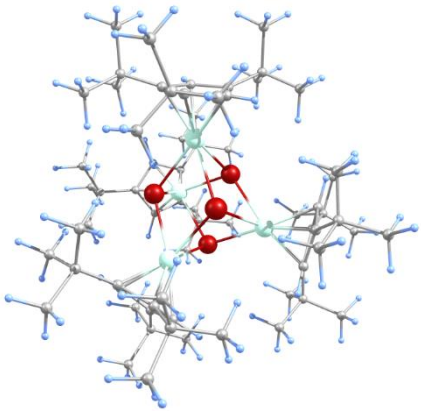

H	-5.02285775435735	2.37556265459677	4.75293839105109
H	-6.17852528752644	1.06659919737602	4.42179518346458
H	-5.86013646569349	2.31350701354047	3.19095550271625
C	-3.68114722549928	-0.08262489391418	4.47707423430959
H	-2.85480604573609	-0.70043994446497	4.09351769532982
H	-4.45660125335583	-0.76571359092147	4.86284612282048
H	-3.31482975044052	0.49206218685819	5.33794787936022
C	-1.45139774641714	2.84654138338491	4.43512366523559
C	-2.50481866877337	3.35402274614889	5.44214278121585
H	-3.08636057206328	4.19314514299513	5.02512056034372
H	-2.00945088347934	3.71405420748902	6.36008932724615
H	-3.20874519762864	2.56796681505731	5.74368878913204
C	-0.70136126365739	1.64725368227654	5.02186300223852
H	-1.34018009236851	0.77160156756780	5.16656965591403
H	-0.26661644002010	1.90708471994285	6.00296099889573
H	0.11870258945603	1.35229426440586	4.35312011004554
C	-0.40720063598670	3.97444129428303	4.30331093955551
H	0.38865247964068	3.71472186781086	3.58900367333545
H	0.07466678060003	4.14131189713094	5.28164772414481
H	-0.85390258946519	4.93425020547682	3.99784276344970
C	-1.88825140158594	5.09069367905514	-0.60251970783657
H	-1.45025385869785	5.66923879109809	0.22465847861770
H	-2.15776732316258	5.80935821960373	-1.39444011332696
H	-1.10898218399817	4.42438728745651	-0.99671617313264
C	-4.11091314342120	5.26430334997631	0.53112851966353
H	-5.03756132961687	4.74931809842463	0.83326508658644
H	-4.38976922261474	6.08514157267006	-0.15320935604872
H	-3.66947342411329	5.71237910469255	1.43633475296604
C	-3.81407664432246	3.71259924402506	-1.40020269452959
H	-3.16130510295542	3.00792546359540	-1.93728041133539
H	-4.07983090305168	4.52235816388002	-2.10115563751007
H	-4.74600831310820	3.18576402029361	-1.14590498385035
C	2.78637391721680	-3.22372431506071	0.82851516642591
C	3.59002648959352	-2.11798610508605	1.23680063639383
C	1.81989586993099	-3.36151335362315	1.86339557378908
H	1.03819903861210	-4.11607445896372	1.86235425150697
C	2.10108054794787	-2.48363217083915	2.98116705643121
C	3.24336464484173	-1.66903526033976	2.56809759475952
C	3.14648411911546	-4.30168413866018	-0.19594962055192
C	4.27100960336579	-0.77577605741504	3.30229878333104
C	4.96350420072882	0.17072715268841	2.30230501069032
H	5.61881872531190	-0.36258712579291	1.59512921957671
H	5.60458308694787	0.88343302695411	2.84691134107657
H	4.22802177607212	0.74206089041639	1.71846601481482
C	5.37523375917179	-1.69552138094380	3.87737024140277
H	5.00197656210481	-2.38071139154432	4.65137205601228
H	6.17970587101347	-1.08900252084094	4.33010255040493
H	5.83021673149625	-2.31142708952961	3.08440902703465
C	3.71119353332555	0.10666441550586	4.42474663290723
H	2.89669276272067	0.75350953179192	4.06407390593425
H	4.50762934982737	0.76270858707854	4.81443653915097
H	3.34039681543111	-0.47420571501857	5.27953814715086
C	1.40978697300258	-2.75927957187454	4.34063813077374
C	2.45031813706000	-3.30668283722571	5.34130968104825
H	3.00847728214430	-4.15657462142240	4.91448203212414
H	1.94592867561475	-3.66312641603474	6.25564314575645
H	3.17560410459453	-2.54321906469130	5.64988762287198
C	0.69618163558096	-1.54362433078829	4.93701885483133
H	1.35859598658676	-0.68598955770858	5.08062832200256
H	0.26062745463808	-1.79579906442361	5.91950405567924
H	-0.12114491804695	-1.22127468431624	4.27696319637793
C	0.33444980743722	-3.85668773693597	4.20226700839957
H	-0.45008396732961	-3.57629462909401	3.48328204784283
H	-0.15792617861630	-4.00819476472304	5.17770465400770
H	0.75343636719283	-4.82988066316489	3.90089190909109
C	1.91437758537851	-5.08781154993103	-0.66159636970069
H	1.45008171643431	-5.65317284970460	0.16033450454551
H	2.19530670010950	-5.81823821229512	-1.43865817667175
H	1.15340390732275	-4.41654232630526	-1.08230272459616
C	4.09836069586004	-5.27124324284065	0.54593487233716
H	5.02016420365994	-4.76227003632745	0.87254963946847
H	4.39217969763857	-6.10544811144068	-0.11567189996646
H	3.62124208470913	-5.70121435942013	1.44185304988469
C	3.88784724078388	-3.75406605554860	-1.42182175802436
H	3.26448160744198	-3.05189368837640	-1.99571932814989
H	4.16397100276718	-4.58199932082251	-2.09708391007948
H	4.82011973010174	-3.23833211365084	-1.14607190509955
C	-2.77608657043939	-3.23958567004522	-0.89393048620618
C	-3.60154709497791	-2.15525878452614	-1.31485077975596
C	-1.83684762961915	-3.42099268393870	-1.95313867798544
H	-1.06194437865612	-4.18208532179447	-1.94777729728619
C	-2.12551739494715	-2.56376094872654	-3.07040830370016
C	-3.25935027081311	-1.72384238122047	-2.64611091978885
C	-3.11982818433545	-4.29182812085362	0.16230709738007
C	-4.26722878214756	-0.80557034617998	-3.37540782707149
C	-4.94812663521877	0.14124694962457	-2.36724053323039
H	-5.61600102293838	-0.38820360242600	-1.66892868530881
H	-5.57392253472501	0.87195775406639	-2.90603032119421
H	-4.20524408533959	0.69247991883472	-1.77351114267571

C	-5.38407670326807	-1.69580745248639	-3.97107997644789
H	-5.01781077556589	-2.37724433959885	-4.75151426416525
H	-6.17440689385685	-1.06893032415959	-4.42118593177307
H	-5.85472173905586	-2.31450961291347	-3.18932305236509
C	-3.67800619201817	0.08194565732366	-4.47847862126447
H	-2.85261289659061	0.70165257063518	-4.09589375077353
H	-4.45463394285121	0.76333221146063	-4.86492236366644
H	-3.31096294824937	-0.49315520878857	-5.33874423631415
C	-1.44766352386275	2.84865814688916	-4.43482183287305
C	-2.50070295396353	-3.35710880991049	-5.44165275889367
H	-3.08200481673064	-4.19608187208703	-5.02397099661176
H	-2.00510333877719	-3.71774766624652	-6.35923430261748
H	-3.20495440931194	-2.57163091927962	-5.74389781979100
C	-0.69781011733217	-1.64926972165253	-5.02168089249737
H	-1.33675251802388	-0.77379439756027	-5.16687501296054
H	-0.26246642334655	-1.90917049268684	-6.00250121800956
H	0.12168668362142	-1.35398314158197	-4.35236179728114
C	-0.40311141839405	-3.97611380724308	-4.30221859862101
H	0.39344943239036	-3.71544133809808	-3.58906954154346
H	0.07798218970587	-4.14434828143376	-5.28071822028354
H	-0.84939164838305	-4.93560423810639	-3.99508126499437
C	-1.88670678712097	-5.08946718448283	0.60470633314355
H	-1.44859444092484	-5.66833903428675	-0.22215891738720
H	-2.15718702612230	-5.80776310752580	1.39662998951896
H	-1.10729128256954	-4.42360502647608	0.99933845959687
C	-4.10879501247742	-5.26068190903269	-0.53069205334704
H	-5.03453122509414	-4.74457559228378	-0.83370456197088
H	-4.38921241430130	-6.08111996355180	0.15349790939226
H	-3.66699337301873	-5.70931043127324	-1.43543118189626
C	-3.81189822107385	-3.70955475201711	1.40094813364017
H	-3.15906276850010	-3.00501004792204	1.93813998614212
H	-4.07811279699987	-4.51914437501015	2.10192359721871
H	-4.74361173042615	-3.18256066310718	1.14628900955439
C	2.78631781903001	3.22432622597283	-0.82946025585414
C	3.58889508787151	2.11740534187953	-1.23591145187143
C	1.82171476452154	3.36408615226985	-1.86596956752985
H	1.04118090886475	4.11986744194263	-1.86561177663839
C	2.10242049950182	2.48486750204691	-2.98280186726656
C	3.24311078195068	1.66859096676475	-2.56782618309403
C	3.14560926306206	4.30226191762272	0.19543206753730
C	4.27039100359687	0.77462977032679	-3.30132656214770
C	4.96300257646554	-0.17096602348160	-2.30060765621613
H	5.61711879212497	0.36307428505765	-1.59288134260627
H	5.60509504876988	-0.88323309824278	-2.84458918159867
H	4.22765487973105	-0.74308495744379	-1.71735060532332
C	5.37455336632228	1.69401776796565	-3.87701055294891
H	5.00117871508120	2.37850452100004	-4.65155017071843
H	6.17901380010073	1.08718646449738	-4.32937457019227
H	5.82958316663862	2.31057272150837	-3.08457721287221
C	3.71028056028041	-0.10864980064407	-4.42293315836632
H	2.89490590827320	-0.75397884392719	-4.06158714618419
H	4.50614369297595	-0.76607339015924	-4.81145506028013
H	3.34053526294578	0.47158930818307	-5.27860304720845
C	1.41090820166822	2.75951726575604	-4.34236556131993
C	2.45108266657563	3.30557127792420	-5.34422744858942
H	3.00979734749520	4.15582058881108	-4.91885354248441
H	1.94607555626295	3.66107204588361	-6.25860401349601
H	3.17581178764469	2.54151352569204	-5.65264868043758
C	0.69690432151969	1.54339330352496	-4.93744541232601
H	1.35945890231793	0.68590935137666	-5.08123362609440
H	0.26055602766398	1.79484106988554	-5.91976902115417
H	-0.11975534264267	1.22131939919196	-4.27641101754503
C	0.33586451348449	3.85718616438998	-4.20454658329251
H	-0.44863817701827	3.57722181714233	-3.48535871775553
H	-0.15644029267513	4.00818682461989	-5.18009736194707
H	0.75494927088146	4.83052381862969	-3.90377052824221
C	1.91336541108149	5.08827197835918	0.66068658533379
H	1.44947145914901	5.65393794698065	-0.16127780031389
H	2.19410794260302	5.81856128809259	1.43794779882932
H	1.15203375980904	4.41708739100878	1.08088865897300
C	4.09809525805688	5.27206918581933	-0.54532645340943
H	5.01994813886893	4.76307667806838	-0.87179470303697
H	4.39180527851087	6.10577174594150	0.11695728560817
H	3.62158146589050	5.70275165580891	-1.44122528293775
C	3.88619512539971	3.75389839956556	1.42153197306268
H	3.26249178165521	3.05141410142766	1.99468027404432
H	4.16217955461724	4.58132355966647	2.09746285178507
H	4.81843717213728	3.23813473667985	1.14569944105984
H	-4.43754622660121	1.75811684267442	0.73610139738839
H	-4.42985031885907	-1.75278719992030	-0.73447474545113
H	4.42482693281284	-1.72365708400999	0.65974264335479
H	4.42204672210992	1.72164411151575	-0.65751159433261

Table S13: Selected Meyer bond orders for [(Cp'''Co)$_4$(μ_3-Sb)$_4$] (**3a**) in the triplet spin state, calculated at the OPBE/TZVP level of theory.

B(0-Sb, 1-Sb) :	0.53	B(0-Sb, 2-Sb) :	0.27	B(0-Sb, 3-Sb) :	0.30
B(0-Sb, 4-Co) :	0.52	B(0-Sb, 6-Co) :	0.69	B(0-Sb, 7-Co) :	0.55
B(0-Sb,147-C) :	-0.13	B(1-Sb, 2-Sb) :	0.30	B(1-Sb, 4-Co) :	0.50
B(1-Sb, 5-Co) :	0.79	B(1-Sb, 7-Co) :	0.60	B(2-Sb, 3-Sb) :	0.53
B(2-Sb, 4-Co) :	0.69	B(2-Sb, 5-Co) :	0.55	B(2-Sb, 6-Co) :	0.51
B(2-Sb, 57-C) :	-0.13	B(3-Sb, 5-Co) :	0.60	B(3-Sb, 6-Co) :	0.50
B(3-Sb, 7-Co) :	0.79	B(4-Co, 6-Co) :	0.16	B(4-Co, 7-Co) :	0.12
B(4-Co, 98-C) :	0.39	B(4-Co, 99-C) :	0.60	B(4-Co,100-C) :	0.57
B(4-Co,102-C) :	0.41	B(4-Co,103-C) :	0.38	B(5-Co, 6-Co) :	0.12
B(5-Co, 7-Co) :	0.19	B(5-Co, 53-C) :	0.39	B(5-Co, 54-C) :	0.61

Table S14: Cartesian coordinates of the optimized geometry of [(Cp'''Co)$_3$(μ_3-Sb)$_2$] (**3m**) at the OPBE/TZVP level of theory, in the singlet spin state.

Sb	0.11389417875039	-0.02119927888256	1.78649239039132
Sb	-0.00539365778615	-0.04363123771272	-1.92328605399182
Co	0.88808682281100	-1.37640866287519	-0.08852098585645
Co	-1.52450215035696	-0.07650206583724	-0.01649880348559
Co	0.80655898586835	1.35753306369451	-0.09959415414357
C	-3.24382205788528	0.12057191689996	-1.15691007531088
C	2.65808702757706	-2.21749288149677	0.52323201130729
C	2.66751870732670	2.27739161455834	-0.16274569301666
C	1.55665186776325	-2.94807111002193	1.08745941684458
C	0.75962113235899	-3.44500300652500	0.00272985022651
C	0.71831218930339	3.27879049959302	0.60277933368779
C	-3.16407315703314	0.35391592738748	1.16065031882289
C	1.95083572151999	2.66743759717047	1.01951903227132
C	2.53885321165157	-2.26761412448404	-0.91300952218714
C	-3.15355094880531	-1.19218293688179	-0.57987250949705
C	-3.36917033765138	0.93995017993471	2.52097983738698
H	-2.96335115824036	1.95196166276067	2.60554847575281
H	-2.90207851684174	0.33562419974607	3.30377305510658
C	1.88522035459550	2.64284450999597	-1.31039495447435
C	-3.25179026842743	1.07054303328328	-0.08138189296164
C	-0.30175061605792	3.99142491853675	-1.69885274256992
H	-1.25901528430442	4.14123130018538	-1.19822493146516
H	-0.49513478175413	3.47013341751407	-2.64109458194857
C	-3.10588743538384	-1.04947616988487	0.85359105857826
C	0.67865145298199	3.26538953631856	-0.83831721516921
C	-3.33924609428804	-2.46649022427371	-1.33458673845169
H	-3.00806953100244	-3.33302923390041	-0.76137620681998
H	-2.80190419290621	-2.46780510229284	-2.28636640940296
C	3.84123600421772	-1.73212877499408	1.29349553185286
H	3.56077645881056	-1.31049698678733	2.26328218446960
H	4.40657978417529	-0.97378449362150	0.74906755001988
C	1.36235937960745	-3.02971318257808	-1.23351865739631
C	4.09481921148395	1.85013287175253	-0.20217633908149
H	4.31269669541678	1.18882324112690	-1.04363905727710
H	4.40640005589092	1.35239432900990	0.71840875730491
C	-3.22772598696244	-2.14979636025535	1.85638017431983
H	-2.63552177453610	-1.96067261694036	2.75639547655076
H	-2.91599273479925	-3.11360301256109	1.45031238451106
C	-0.21833307119553	4.01380164463443	1.50379015673392
H	-0.34090557210444	3.51538908761174	2.46962518886909
H	-1.20867208549903	4.13305552137925	1.06125003586729
C	-3.58718488099171	2.51648054646247	-0.21965265216595
H	-3.25678447602656	2.93142117000336	-1.17393304618454
H	-3.16361929830653	3.12323035767612	0.58291414019040
C	1.41103549019726	-3.34169567815560	2.52304790829883
H	1.93414245875690	-4.29338041173087	2.70948955628432
H	1.83645395326929	-2.59762649835432	3.20224221373250
C	3.57784605165303	-1.83900344743998	-1.89712543573597
H	4.20119761324314	-1.02730018003566	-1.51543269638702
H	3.14277068146521	-1.50704477184351	-2.84433912013908
C	2.36534590371561	2.62613283665229	-2.72675889220211
H	1.54122741095304	2.57073265894678	-3.44377899876752
H	3.03073460482519	1.78223783298205	-2.93047572563000
C	-3.55147484855405	0.42464165446877	-2.58889389815223
H	-3.13597047882689	-0.32376160343743	-3.26994235604488
H	-3.16101115231163	1.39741547356708	-2.90121015838753
C	-0.32682413025867	-4.45765701608652	0.13381510407433
H	-1.02563102495606	-4.43274898833699	-0.70494027733401
H	-0.89549046009987	-4.34263568151848	1.05904926996044

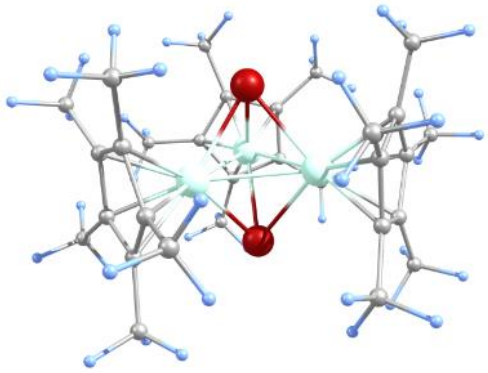

C	2.50651526941115	2.67740091696944	2.40824844971074
H	3.18096963088443	1.83584063827207	2.59275824066908
H	1.72145932440349	2.63500366383376	3.16888240061044
C	0.97950514515160	-3.51859457422886	-2.59434029261957
H	1.29293900703347	-2.82896128234471	-3.38307244292266
H	-0.10085250285261	-3.65890434607573	-2.69579576102211
H	0.36480857771401	-3.48307656173399	2.81005069467419
H	0.11478642352913	-5.46720721307779	0.15303467649206
H	4.52916016974276	-2.57004330086099	1.48975491795174
H	4.25149098978496	-2.68071799661491	-2.12365590568308
H	1.45787163743959	-4.48997444234632	-2.79692748523497
H	2.93160722042060	3.54628178187338	-2.94427830736136
H	4.73773805791017	2.73706259995230	-0.31799589398332
H	3.08390603951965	3.60047009284921	2.57835562442279
H	0.16864549173223	5.02510160371290	1.70416431296881
H	0.09014949080666	4.98883693712016	-1.95166659096283
H	-4.64171892996071	0.44374481378454	-2.74514997141318
H	-4.68074899079799	2.64342611956270	-0.17550516260844
H	-4.44506853399954	1.00082634649778	2.74839651994335
H	-4.27773956669307	-2.25741401069217	2.16930250657834
H	-4.40685789521602	-2.61614074055941	-1.55865258598794

Table S15: Selected Meyer bond orders for [(Cp'''Co)$_3$(μ_3-Sb)$_2$] (**3m**) in the singlet spin state, calculated at the OPBE/TZVP level of theory.

B(0-Sb, 2-Co)	0.94	B(0-Sb, 3-Co)	0.96	B(0-Sb, 4-Co)	0.96
B(1-Sb, 2-Co)	0.97	B(1-Sb, 3-Co)	0.92	B(1-Sb, 4-Co)	0.95
B(2-Co, 3-Co)	0.47	B(2-Co, 4-Co)	0.48	B(3-Co, 4-Co)	0.47

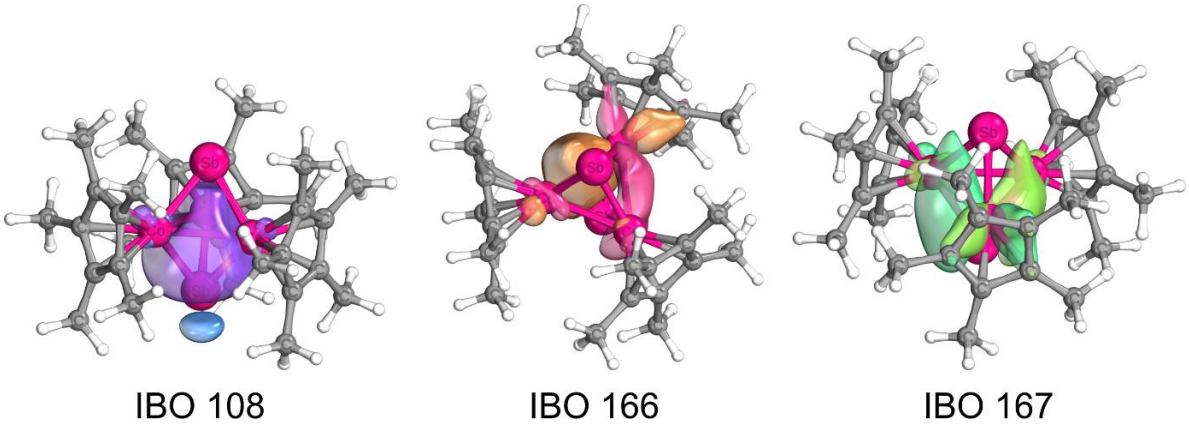

Figure S15: Selected Intrinsic Bonding Orbitals of [(Cp'''Co)$_3$(μ_3-Sb)$_2$] (**3m**) in the singlet spin state, calculated at the OPBE/TZVP level of theory. IBO 108: SB2 1.174 Co4 0.284 Co3 0.210 Sb1 0.147 Co5 0.137 (other: 0.047); IBO166 Co3 1.001 Sb2 0.380 Co5 0.331 Sb1 0.114 Co4 0.094 C10 0.021 (other: 0.059); IBO 167: Co4 1.031 Co5 0.316 Sb2 0.301 Sb1 0.141 Co3 0.119 (other: 0.091).

Table S16: Cartesian coordinates of the optimized geometry of [(Cp'''Fe)$_3$(μ_3-Sb)$_2$] at the OPBE/TZVP level of theory, in the doublet spin state.

Sb	3.13565562751790	19.92303483979375	5.42214204916052
Sb	2.72445041538463	16.23533020234116	4.57459754717904
Fe	3.38878228974659	17.69147760844119	6.52695623668602
Fe	3.85991216561666	18.26980563757314	3.63048326141166
Fe	1.35005801350535	18.18054532209338	5.31113500035496
C	5.02213725625285	18.21282204333016	8.00812357721525
C	-0.39724897585977	18.52687515155236	6.47951065400245
H	-0.38423854995653	18.74323546533278	7.53808641923326
C	-0.43309449068513	19.54045777407334	5.45622778781457
C	3.09313964838218	18.87560466430457	9.85906798512115
C	3.76375546790331	18.05859095139635	8.73287731479488
C	4.24601232908666	16.00028162903688	7.67768576901582
C	-0.52380611880783	17.22417746085858	5.92371203447455
C	5.48363321991858	17.49964750056737	2.34090197299322
C	3.30650674443877	16.72922640500196	8.45984894507343

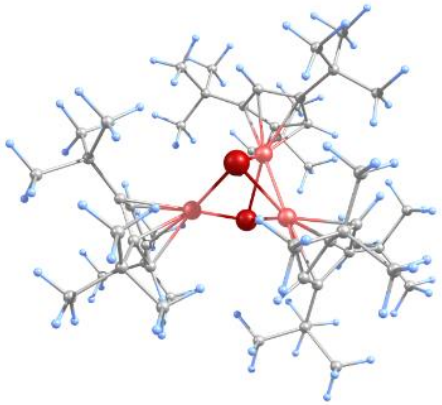

H	2.40627537565475	16.30878690070417	8.87781619776794
C	5.24255833876460	16.95797722935563	7.34891460370681
H	6.11810683128083	16.74181226742506	6.75576622690728
C	-0.49671128488117	17.42549755785723	4.51658876713294
H	-0.57681978531840	16.63052527322671	3.79130285726382
C	3.63225728368216	16.94109307140597	0.35634822260588
C	6.51179540985272	16.35253015040133	2.44259836173431
C	6.22071138202027	19.18504789280823	8.10011190247343
C	5.83793163572760	18.77479889031159	2.90340780723600
H	6.67950311689444	18.92983244177289	3.56365143183661
C	-0.79111427468854	20.98436078816541	5.88150828356096
C	4.31447001445403	17.75017347605890	1.48818298819362
C	2.88683855390213	15.67944242729369	0.81225284707377
H	3.51629927275859	14.98511168748264	1.36732548946207
H	2.49355808297303	15.14496678619010	-0.06268713305640
H	2.04239170848870	15.93727612951324	1.45659780360680
C	4.04005595759580	19.14924950444687	1.61361963481440
H	3.23390128017499	19.65470201879470	1.10376133358730
C	-0.13072558824262	21.35477282499870	7.21641855966894
H	-0.43956603016658	20.71114494487123	8.04439570817978
H	-0.41906271251387	22.37679002076997	7.49027949969955
H	0.95801400613564	21.32726862332099	7.12835432374883
C	4.99363330257766	19.81270918696159	2.42935646553006
C	3.07033946895194	13.73723123041215	7.61682018782063
H	2.53324477008559	13.94861493480277	6.68740883424911
H	2.42099182349535	13.99882477714299	8.45806518872743
H	3.24382781430232	12.65490439896714	7.66506565867402
C	4.40796785695304	14.48083164973111	7.66342356069534
C	-0.40901845724464	22.11538252606113	4.92059957346870
H	0.66799817351034	22.12746976329643	4.72773961240634
H	-0.66998907521806	23.07523603368273	5.38353850100173
H	-0.93709412532719	22.07967248075519	3.96813659863365
C	-0.49271497311100	18.82110035763255	4.19134074012103
C	-1.07180534214951	15.97274541694386	6.60431852029080
C	2.69184705898725	20.29932950100996	9.46679730386388
H	3.51909367292616	20.89630368868384	9.08963318330716
H	2.27167698271642	20.82287262894430	10.33606056592164
H	1.92886308112727	20.26264239215867	8.69087849284292
C	-2.31869172567665	21.01560632699772	6.11780775846203
H	-2.89133470209949	20.77864253981742	5.21796689061871
H	-2.62394896183460	22.01501735083186	6.45366837727910
H	-2.60797761106941	20.30005011870103	6.89549131039051
C	-0.76626609214550	19.25020842111012	2.73384962031270
C	7.61201574233857	16.59337242214407	1.38493108193379
H	7.22908444831314	16.56628532085047	0.36246188818832
H	8.38911150711183	15.82177849659706	1.47078125568827
H	8.09388054219612	17.56691891629865	1.53227408889443
C	5.29576395297526	21.30845101369126	2.40389143407377
C	5.90801377172440	20.65345837922736	8.40281424577434
H	5.21355245413078	21.07610843973422	7.66919912977241
H	6.83696560471044	21.23378155264024	8.35016108345700
H	5.50037634909011	20.81231051866948	9.40274356412897
C	4.02630350919563	18.90693806146830	11.08805431012088
H	4.35730772191746	17.89860664048185	11.36164234592243
H	3.48575432120124	19.32532295272442	11.94666242368666
H	4.91237390808183	19.52460502902398	10.93457038485633
C	4.02702121180309	22.16488428123302	2.32772827001568
H	3.42418739181268	21.93840265594583	1.44182865256288
H	4.29634737805416	23.22716290838049	2.27344175752982
H	3.40290218275029	22.01891077738735	3.21413611022660
C	7.16964157453275	18.64333117380371	9.19455764469854
H	6.69833132294466	18.60638397236198	10.17955792527081
H	8.05558166863868	19.28679961279658	9.27068039024173
H	7.51155291991510	17.63096534404871	8.95269190934175
C	-0.79054404928761	18.01634122640625	1.81397820126145
H	0.14142178559805	17.44932500426831	1.86291548005294
H	-0.92794380740011	18.34327482860807	0.77687070378143
H	-1.62158833965014	17.34275839751202	2.05070760280726
C	5.95915192681657	14.93301040012370	2.27925753322320
H	5.14312532968868	14.74068944569608	2.98152679939595
H	6.75554060873761	14.20802858611035	2.48814305120341
H	5.60027971720791	14.72149024127802	1.27131154510981
C	-2.60870371909548	16.14114972548156	6.60902000058080
H	-2.91401265784241	17.02248838479112	7.18452004015942
H	-3.08489275346168	15.26212162800207	7.06299318383723
H	-3.00452436922393	16.25006735895257	5.59272229985310
C	2.60073565517452	17.81078718277440	-0.38490216872733
H	1.81270530431311	18.18162462049369	0.27237045950961
H	2.11810107926175	17.20400210000795	-1.16005739467683
H	3.06593048288715	18.66631480841858	-0.88746606615912
C	5.28456682511805	13.98552579758871	6.51181138883948
H	5.39988398857631	12.89608016812830	6.57207195682285
H	6.28839872245574	14.41933444114586	6.53870433748694
H	4.83266931386537	14.21949689307443	5.54371739313647
C	0.28173325670599	20.20972138417428	2.16270243993691
H	0.29106901285364	21.17587114333021	2.66192645045091
H	0.08797747202208	20.38875731475929	1.09739572672901
H	1.27823477957732	19.77902311406263	2.27271019906056
C	4.67026698425791	16.56369586600785	-0.72161116232561

H	5.22295968475351	17.44573752077814	-1.06396651659865
H	4.15140343186875	16.13958500984710	-1.59086951291487
H	5.39326428790344	15.81882009368153	-0.38663223890636
C	7.02276816086930	19.18969420228994	6.78934252709937
H	7.48132497948241	18.22261712973320	6.56844946945443
H	7.84161994483712	19.91460267452419	6.87005704893499
H	6.39078440087256	19.47556651569937	5.94706266323879
C	7.20984147154986	16.38190974245949	3.81171965788301
H	7.82171091710404	17.27668991356584	3.95680983238629
H	7.88329912529385	15.52091404979208	3.89813994172879
H	6.47475565898562	16.32638905812367	4.61602457582257
C	-0.60762051043613	15.82120294340948	8.05244558987510
H	0.47357074400069	15.69039466028554	8.10078482460263
H	-1.08056160460719	14.94176705362560	8.50654128969289
H	-0.88020922943129	16.68531351983002	8.66652718417837
C	-2.17429185843420	19.86904579435795	2.60922541495212
H	-2.93718075223064	19.20661221737972	3.03476311257230
H	-2.41457181815981	20.01261086927731	1.54818528068945
H	-2.26107541613221	20.84274083506659	3.09183923240867
C	1.80074466915061	18.19175271392994	10.34095079435673
H	1.08398056612378	18.05629184361087	9.52807755876007
H	1.32799571069376	18.82721539053763	11.09951904618654
H	1.98880388811556	17.21836758727613	10.80767560796722
C	5.11385235960952	14.12443411954946	8.99271867060791
H	4.51898602052423	14.43758914661014	9.85808834032529
H	6.09425956918084	14.60777216960070	9.06600266043900
H	5.26540494744872	13.03936680133140	9.06062909195552
C	6.13222418231551	21.76273089282030	3.60372015168888
H	5.59763486207758	21.60552433186651	4.54557582142415
H	6.35463473132907	22.83366785830989	3.52101837428587
H	7.09085593095071	21.23627727316016	3.65771306836400
C	-0.73685501795580	14.69168587770103	5.83193226835478
H	-1.17042830723367	14.69222629111556	4.82690280029660
H	-1.14633005847419	13.82015634409252	6.35801136627787
H	0.34312845043891	14.55324811764622	5.73252718015323
C	6.12458564726133	21.54866741780808	1.12070025941777
H	7.06070915616128	20.97971790708160	1.13621544477210
H	6.37545915876250	22.61294069386107	1.02654272668837
H	5.56784332608372	21.25252560013529	0.22444027648810

Table S17: Cartesian coordinates of the optimized geometry of [(Cp'''Fe)$_3$(μ_3-Sb)$_2$] at the OPBE/TZVP level of theory, in the quartet spin state.

Sb	2.87869613152581	19.98999495689126	5.21031972888739
Sb	2.58737248340026	16.26293367637830	4.40539044733478
Fe	3.53882181771265	17.74626491803244	6.25646497291353
Fe	3.88225608059737	18.25022020904473	3.78526316468168
Fe	1.24635909033264	18.16537553578363	5.19110652084977
C	5.17128516389206	18.26917571464328	7.92566260492100
C	-0.39431287213503	18.41869419570741	6.41117313319832
H	-0.35891478014636	18.59394817415814	7.47700298932380
C	-0.46146968226722	19.46769728905288	5.42532627725952
C	3.20775616184742	19.06021313379300	9.68541973102982
C	3.88276157130804	18.20008863194857	8.59367136562274
C	4.26745592169636	16.11779553684032	7.54338077973533
C	-0.53151949517234	17.13404977227749	5.81517073600654
C	5.42907707099023	17.44525808064930	2.49483495110725
C	3.34243385015928	16.91232591029263	8.28293279819194
H	2.40226862888599	16.55078249386253	8.66567001962405
C	5.34029852411965	17.01242458710135	7.26175903277765
H	6.24248839056530	16.73047309649340	6.74169101087253
C	-0.52872542455346	17.38166050201106	4.41585958853302
H	-0.61001821775984	16.61140021193727	3.66350991063567
C	3.59562031778064	16.96393179680921	0.48094112000997
C	6.45012883446347	16.29040905891968	2.55018730171098
C	6.41003828350417	19.18289760576106	8.04672156212608
C	5.77708492914900	18.69113976208398	3.12641035436885
H	6.64154571063710	18.82255783294304	3.76032785450471
C	-0.85857377359182	20.88457122809519	5.91051556237837
C	4.25934844825698	17.71598319570854	1.66738977985261
C	2.83906998466204	15.67813784325545	0.83781845785253
H	3.44742521700451	14.95421536408125	1.37890469065920
H	2.48477554091611	15.19201387974924	-0.08081760871318
H	1.96271521009473	15.89677398978784	1.45443397172684
C	3.95351401884335	19.10200364146546	1.87462227770439
H	3.14425276761927	19.62181710259971	1.38652129037876
C	-0.20129523172008	21.22694857665996	7.25424227133724
H	-0.46604601671157	20.53345616413232	8.05669371979424
H	-0.53360329767529	22.22136716098359	7.57599394351592
H	0.88604579672553	21.25610680066437	7.15602131008690
C	4.93075757745928	19.75008071537937	2.68415971916863
C	3.01943766105583	13.88932592378486	7.63734529151879
H	2.44279062502834	14.08890895946125	6.73054862273351
H	2.42009690311432	14.18872222913362	8.50288985827867
H	3.16560306922897	12.80413582456450	7.70748554122581

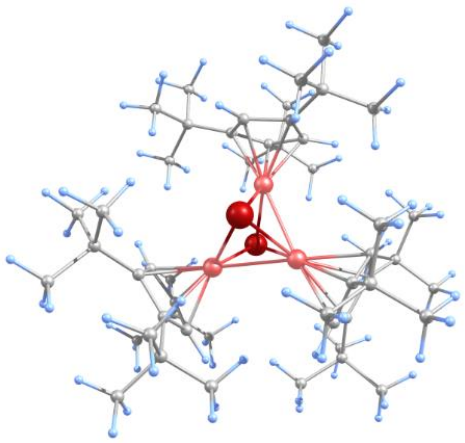

C	4.37817502082762	14.59169188781010	7.60065228270185
C	-0.52878567118458	22.06712791120890	4.99300732055559
H	0.54662636937870	22.13549374749617	4.80106680031434
H	-0.83093953512456	22.99608706501659	5.49259670448454
H	-1.05544806295281	22.04425469804458	4.03964686355857
C	-0.52875211290078	18.78888020872121	4.13141169812083
C	-1.05156236188583	15.86594527209336	6.48466069601755
C	2.93073788755002	20.51436474567200	9.28904772337313
H	3.83398618265362	21.10306269217894	9.14763731936838
H	2.33729896458521	21.00717754278526	10.07020509552570
H	2.36200531407636	20.54830030918902	8.36086692970412
C	-2.38363230658105	20.85374696583354	6.16387143512855
H	-2.95822064236721	20.62700577224440	5.26307815491322
H	-2.71898384645490	21.82995081683788	6.53712777461653
H	-2.63797930914110	20.10287461346767	6.92032516965596
C	-0.85381245425073	19.26568922127947	2.69904897851049
C	7.54656866254302	16.56631262254521	1.49667364874827
H	7.16415938240610	16.58060732948538	0.47443674678179
H	8.31825800992727	15.78662994663081	1.55368104524437
H	8.03648132107312	17.52957402684502	1.68155970364835
C	5.28422842791905	21.23712777988749	2.62375701305044
C	6.16110783103623	20.66704626657348	8.33509317876856
H	5.47864118155141	21.11676041269651	7.60809380262125
H	7.11375395364403	21.20626340695482	8.27036213198975
H	5.77497981385821	20.84885387625856	9.33963991260183
C	4.06745452829258	19.02920451602393	10.96729492761564
H	4.29626389446497	18.00095732567162	11.26958041967824
H	3.51375380328079	19.50412433840094	11.78721416581041
H	5.00953887132624	19.56969293145836	10.86065790015680
C	4.06852224150068	22.13213276868452	2.36260470955870
H	3.55315172637722	21.87389812979722	1.43107254385780
H	4.39167138438952	23.17678202572815	2.27376450593687
H	3.34461988535547	22.07950457293573	3.18215872398912
C	7.29962644074342	18.60650973658327	9.17292866123075
H	6.79516390581506	18.59402052092750	10.14230655087524
H	8.20740923603244	19.21494473911337	9.27414262856767
H	7.60838036923883	17.58037745127228	8.94628932871478
C	-0.87573997547100	18.06745894173659	1.73370582704379
H	0.06237013884279	17.50906619790764	1.75327131359540
H	-1.02651167385607	18.43067441401876	0.71034158219384
H	-1.69741048225976	17.37702539902170	1.95335526712216
C	5.88233879425578	14.88331547381153	2.33884566820984
H	5.05066517215020	14.68646758093535	3.02112068713429
H	6.66382865151078	14.14131227719731	2.54305812541298
H	5.53834908836570	14.70337574565166	1.31964584393139
C	-2.58987150095120	16.02163453242594	6.52385448790207
H	-2.88976945843416	16.90002114985576	7.10639167247847
H	-3.04704444981591	15.13844177164838	6.98906209101060
H	-3.01091010609244	16.12597806184064	5.51722493325698
C	2.58600930461785	17.87437713418239	-0.24062319795626
H	1.78118240423064	18.21039258973227	0.41328900609030
H	2.12453682191342	17.31078948567863	-1.06012366429832
H	3.06475191057202	18.75470626965523	-0.68359826893093
C	5.19674425055524	14.00688557321032	6.44887330872941
H	5.27380375570988	12.91805735047104	6.55988018730234
H	6.21609210771557	14.40256368279385	6.42584260699051
H	4.72377034468789	14.21179080551869	5.48460901650809
C	0.15658579803305	20.26919978533844	2.13784964852071
H	0.19823109251062	21.19572921785364	2.70633720896974
H	-0.09689810343221	20.52381111031593	1.10068454078744
H	1.15384977141972	19.82969421260022	2.16084743595470
C	4.65951503860793	16.64370241568681	-0.59104829183627
H	5.23572482053255	17.53649534401764	-0.85808043120234
H	4.15747648206049	16.28964307276231	-1.50037042990832
H	5.35840954150637	15.86358456838227	-0.28799461310107
C	7.24694431969812	19.13916346470991	6.75958176657112
H	7.65802262437964	18.14832918101837	6.55431712119703
H	8.10018953754895	19.82032172493593	6.86001933543001
H	6.65256119746767	19.45249165299045	5.90140323128923
C	7.16012832056290	16.26708185798532	3.91131210953960
H	7.79027018896074	17.14585016184462	4.07272666601031
H	7.81657357551314	15.39072661750349	3.96717838132160
H	6.42831562102156	16.20821387330308	4.71551128110769
C	-0.55836594994701	15.70597865615458	7.92345339719250
H	0.52794974498653	15.62626249744463	7.95674409531163
H	-0.98288439518305	14.79642703530967	8.36616424789240
H	-0.86372974071050	16.54385553155212	8.55917279586946
C	-2.27969878819752	19.85280539832431	2.63590505052237
H	-3.01158488686405	19.16263463420421	3.07151735088318
H	-2.55995447961814	20.01368697250870	1.58725706565784
H	-2.37381292587541	20.81335639246621	3.14321426957099
C	1.84794458633512	18.45763387362221	10.08284955200071
H	1.17795460469607	18.37563965316857	9.22517293659191
H	1.37170437505338	19.11262844456808	10.82172906949437
H	1.94642248686587	17.46923366325728	10.54540080005134
C	5.11633347852499	14.27319753862850	8.92197870766532
H	4.56575810334442	14.65431288387801	9.78947764942403
H	6.11695490078232	14.71821155960634	8.93626578347930
H	5.22712331035912	13.18754506879809	9.04202193612797

C	6.01173341653946	21.73756409270050	3.87478429450486
H	5.38927705094757	21.62975514343491	4.76902344315827
H	6.25723388619246	22.80098486546471	3.76512301522364
H	6.95219656891087	21.20364075736235	4.04326800096714
C	-0.72857747243996	14.59754792828004	5.68688738314511
H	-1.18294890155329	14.61388841983029	4.69108013716509
H	-1.12700916168859	13.71721285419598	6.20687449012912
H	0.34838209205775	14.45812845009445	5.56027806494350
C	6.24509174022958	21.38086307360170	1.42069800222219
H	7.15701358071458	20.79108294183471	1.56373850957559
H	6.53612751556126	22.43122311712432	1.29262089145842
H	5.77262903748854	21.04686637675612	0.48986775366832

Table S18 Cartesian coordinates of the optimized geometry of [(Cp'''Fe)$_3$(μ_3-Sb)$_2$] at the OPBE/TZVP level of theory, in the sextet spin state.

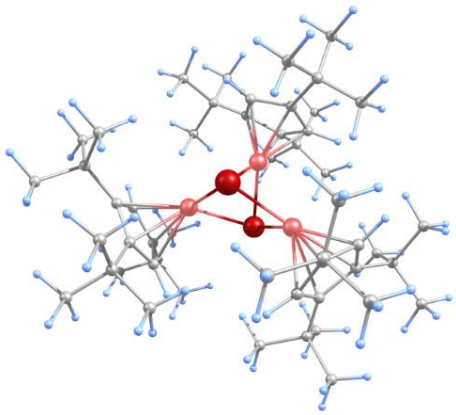

Sb	3.17793896082564	19.81348372346898	5.45169885967660
Sb	2.86105207481670	16.30957771847973	4.70470440461899
Fe	3.26887138258852	17.66309817621872	6.82903578983144
Fe	3.50001963171297	18.38354501006198	3.37478383026012
Fe	1.38229986445284	18.20806659884054	5.07916603332967
C	5.00031155760115	18.26090504621275	8.23715467124480
C	-0.25869758124130	18.43691051611707	6.30558226475279
H	-0.22828650202411	18.56599446590629	7.37896822576305
C	-0.29294835323765	19.52251380562591	5.35860479173859
C	3.13083341194597	18.86757657709163	10.18248946729678
C	3.80233491200608	18.05655796724960	9.05131298405709
C	4.29013604191838	16.01979151029293	7.96101990805797
C	-0.39051254835313	17.17724420161739	5.65505109164135
C	5.27864280942364	17.45633901938483	2.23410901137311
C	3.39211059665078	16.70931824215814	8.82299891214657
H	2.53984985850189	16.24999551982147	9.30228027074174
C	5.22997530058745	17.01261334302837	7.56820057968853
H	6.07344232024294	16.82916595302132	6.91957669192364
C	-0.38268533739577	17.48382567963059	4.26571752897951
H	-0.44921531715485	16.74317224632452	3.48236438615690
C	3.52345787315700	16.87781238170949	0.18067916368254
C	6.28944610669219	16.30238929440240	2.41233519326666
C	6.16588787437084	19.27736828338086	8.25365208564290
C	5.58359160923778	18.71785217513078	2.84729413362466
H	6.36192479861761	18.86115070764209	3.58239011321273
C	-0.61194891029838	20.93861216274076	5.89253404304329
C	4.20711260657415	17.72627842153802	1.27824933612993
C	2.71848109957842	15.68709047125689	0.72529798191405
H	3.32822630758222	14.98022884980012	1.28652518923603
H	2.25691455842017	15.13913818599881	-0.10661293488238
H	1.91918565073001	16.02387098622192	1.39178258532245
C	3.94445780617138	19.12686930185663	1.36038045272575
H	3.21464388867966	19.63896407410272	0.75123491834599
C	0.06834831587596	21.19357815246223	7.24276884873294
H	-0.26017827129516	20.50178917532204	8.02226676335044
H	-0.18293768714248	22.20271119133261	7.59160172613191
H	1.15582386480411	21.13343182607862	7.14887933412279
C	4.81235627986327	19.77645357789911	2.28500648820771
C	3.16166637529506	13.73698290242057	7.86047996840130
H	2.63334785092231	13.93854933917036	6.92369436787920
H	2.49580893539880	13.98972829751703	8.69181029380454
H	3.35092243448854	12.65737914553403	7.91203140935162
C	4.48591700840550	14.50459720354280	7.92665533501345
C	-0.21073456359497	22.12277517498127	5.00677764959200
H	0.85898416299676	22.10183573726798	4.77680423282458
H	-0.41114894951994	23.05611819963712	5.54764739040001
H	-0.76976913122753	22.17736987705298	4.07370094853292
C	-0.36740791125667	18.90061826370313	4.03634629649817
C	-0.89817258041748	15.88055106448978	6.27546708541768
C	2.66843695381775	20.27299391098425	9.78480453507186
H	3.46505223182185	20.89586525923191	9.38283130962240
H	2.25600523717819	20.78918903850311	10.66170616279610
H	1.88168724778194	20.21278602677486	9.03345514688726
C	-2.13493353069650	20.98975960773015	6.15309634309709
H	-2.72405517866555	20.81623328352591	5.25054365196992
H	-2.41437496999002	21.97310042842302	6.55286223279479
H	-2.42726220436308	20.23445875536564	6.89129618602380
C	-0.70639995235587	19.43752725364483	2.62700697844336
C	7.42020786779201	16.50972133721115	1.37969780172861
H	7.06961303126366	16.43808697638297	0.34757606822219
H	8.20015580023238	15.74960293290353	1.52118094267286
H	7.88833181795461	17.49340740154797	1.50249363013455
C	5.16003580065564	21.26453115831407	2.27045456126105
C	5.81521562064122	20.73876717983896	8.54946401122270
H	5.06843700964214	21.12753793919542	7.84972094614337
H	6.71848146295804	21.35146176015509	8.44133732195522
H	5.45760550328695	20.89483208879678	9.56915956946171
C	4.09293423132100	18.95392911299355	11.38518878830397
H	4.46051129996938	17.96177211595965	11.67138834483058

H	3.56621327958869	19.37743926079293	12.24992931695998
H	4.95650256489996	19.59197346688571	11.19052592985722
C	3.91771960111809	22.15867927273515	2.18864762153043
H	3.31666911224163	21.95118943436701	1.29712635556869
H	4.21746882029856	23.21307505798251	2.13832648928906
H	3.27971402144255	22.03160714376090	3.06750750140475
C	7.18189804392928	18.79152020357765	9.31335588300391
H	6.75956627919271	18.77567250377437	10.32120394091810
H	8.05669389891123	19.45495501751581	9.32797515313014
H	7.53228881620384	17.77891456934339	9.08463989000062
C	-0.79111138748525	18.27507268381852	1.62304770464753
H	0.13340278549858	17.69423112789260	1.58654581665961
H	-0.96798956781902	18.67828583255216	0.61925981286267
H	-1.62016683247812	17.59545978491169	1.84776539315834
C	5.73730433778565	14.87908888118880	2.27965993716361
H	4.91662240612600	14.70805580299951	2.98322263735201
H	6.53118155875114	14.15866759019629	2.51265628467155
H	5.38380738224614	14.64177679999441	1.27599379974838
C	-2.44014511011605	15.99139229007633	6.27315022762122
H	-2.78072209214244	16.85632466752700	6.85353973980211
H	-2.88705625866874	15.09190040605225	6.71641719793071
H	-2.83356006825650	16.09454562079709	5.25523561761578
C	2.53888393184551	7.73684379794487	-0.63373427444565
H	1.75170209159132	18.17394205111272	-0.01623815460227
H	2.04983309531171	17.10228153967529	-1.38211222084574
H	3.04513998049248	18.54398576158727	-1.17514526131910
C	5.37725828977171	14.04661107020480	6.77052493280573
H	5.51874830757545	12.95960474731461	6.81830958544794
H	6.37103726621720	14.50372109021126	6.80858500707474
H	4.92460347772292	14.28104033328845	5.80333078492168
C	0.32015685610934	20.42573791329111	2.06982728746218
H	0.40477028583148	21.33404579271198	2.66162015309359
H	0.04809938880008	20.71804648674969	1.04714052821103
H	1.30747173388666	19.95962337681579	2.04888982896062
C	4.55811756526729	16.38107842437608	-0.84819163213121
H	5.14073806496582	17.21620508263787	-1.25251646229614
H	4.03707616193120	15.90223215539836	-1.68701034573537
H	5.25653638574301	15.64744064922721	-0.44370096510202
C	6.90660976777048	19.27720173592851	6.90477103809349
H	7.43171426401562	18.33698618469658	6.71158904457845
H	7.66853328404544	20.06623366857387	6.90800349972326
H	6.21951304589315	19.46982679931431	6.07767703255363
C	6.94629147293032	16.37567383592375	3.80073821478710
H	7.57756482369913	17.26032521898266	3.92355677295621
H	7.59260115939049	15.50233697076554	3.94623851210641
H	6.18679534105914	16.37862143440535	4.58516020777723
C	-0.43301419968958	15.70630498617006	7.72194018622989
H	0.65702287778333	15.69684232468006	7.78168770732353
H	-0.80956422802753	14.75975401275890	8.12935242593731
H	-0.80580733030665	16.50572577513375	8.37150040368069
C	-2.11103611017134	20.07579069290542	2.61676193762870
H	-2.85680355175184	19.39896779534195	3.04958687950774
H	-2.41034034090756	20.28047332061055	1.58113174222371
H	-2.15688870855676	21.02286326604269	3.15540179168963
C	1.87293975118066	18.14712975301755	10.70661820857475
H	1.13117496783560	17.97569882657537	9.92008019101610
H	1.40119133697317	18.77612875904259	11.47121109372695
H	2.10603405109829	17.18698029878867	11.18012273318715
C	5.19455691913144	14.13963295904039	9.25169484365825
H	4.58277626294974	14.40792234900988	10.12036189480462
H	6.15549695049260	14.65767145602528	9.34448811899773
H	5.38648019848333	13.05968555657198	9.29303081749804
C	5.99755991075271	21.68592085535044	3.48164456542126
H	5.44826324452460	21.54958215653068	4.41866953623986
H	6.26048608563156	22.74782061766703	3.40152612407806
H	6.93536172099804	21.12393307041852	3.54586457251291
C	-0.51248977795823	14.63997641934292	5.46297446648284
H	-0.88956683368795	14.68577926451009	4.43615948795359
H	-0.94173701882467	13.74192449718230	5.92493090472938
H	0.57302265577133	14.50833991158030	5.41524414191229
C	6.01115683022662	21.49504362866079	1.00063401734252
H	6.92384397785525	20.88884871320896	1.01549902246355
H	6.30570746278461	22.54973681448452	0.92834014372851
H	5.45460949504947	21.23849506722861	0.09213204102656

Table S19: Cartesian coordinates of the optimized geometry of [(Cp'''Fe)$_3$(μ_3-Sb)$_2$] at the OPBE/TZVP level of theory, in the octet spin state.

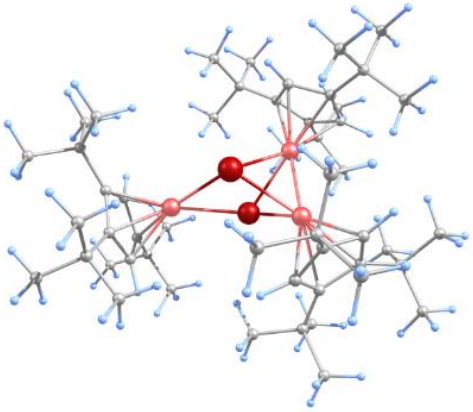

Sb	3.18667129656319	19.46364873818217	5.10939552558090
Sb	2.84157289730264	16.74526895876496	4.53222126982828
Fe	3.09214478795879	17.65597032399416	6.93207038185227
Fe	4.29638727278587	18.23530955600211	2.99588533912021
Fe	1.07930480919611	18.16956536756333	5.69970987857179
C	4.84091001069946	18.13758674158765	8.24779301888166
C	-0.74571998260567	18.61717157304644	6.74199302860563
H	-0.81189420962070	18.89567462694147	7.78473245722814
C	-0.70363616816703	19.56124919897485	5.65814595918509
C	2.99987064124095	18.72943010756834	10.22346453750104
C	3.64798604820206	17.92355441402026	9.07371714910817
C	4.13284200729029	15.90598859114437	7.95037848007299
C	-0.83432030455161	17.28053410902726	6.25698480825174
C	5.89149469672492	17.57811590103556	1.81850216043211
C	3.23423203500867	16.56995508502501	8.82620088207062
H	2.40286328887613	16.09183607460532	9.32279376533717
C	5.06568488773066	16.89811685136626	7.56247601049451
H	5.87842864607076	16.72961263032855	6.87095926064370
C	-0.73663909771277	17.39924520605636	4.84451484734142
H	-0.76445031175542	16.56525443790653	4.15980095011456
C	3.96127826100421	16.98298460763004	-0.09772367109660
C	6.88685924018639	16.41084045257939	1.99673897779523
C	5.97574638003187	19.18733303256352	8.22378137880903
C	6.24360024188108	18.86129846331732	2.37329793686874
H	7.07503053015797	19.02718728836470	3.04551668438324
C	-0.92788754753888	21.05366231726123	5.98692049345846
C	4.71377708392841	17.82738456345087	0.95914817755476
C	3.20158449031445	15.77859170994113	0.47924444221517
H	3.84246255488089	15.08500834013526	1.02235939272585
H	2.71713843869229	15.21839693544711	-0.33163761791799
H	2.42203167509323	16.11154063237468	1.17168402294579
C	4.44421504148412	19.23465729586763	1.07036128474561
H	3.62819156416310	19.73964976296476	0.57267202108171
C	-0.24274406945875	21.43683283503967	7.30963056555151
H	-0.63822237290917	20.89293442405485	8.17212819952642
H	-0.40968594126226	22.50275317212083	7.50682305086497
H	0.83619428587697	21.27093518185458	7.25533779147236
C	5.38808994891660	19.88702001212074	1.89902211919333
C	2.92016949761133	13.70991518344749	7.52131933527572
H	2.47062372151833	14.04061871768132	6.58073450517037
H	2.20765674849431	13.91134999469810	8.32731649799611
H	3.05542868545491	12.62221670429633	7.46742290017564
C	4.26745709672840	14.40032279631527	7.75574228525209
C	-0.42442174588963	22.07702317344415	4.96396368063893
H	0.65384364219867	21.98314162998488	4.79971001478431
H	-0.60760027045363	23.08623880128838	5.35325000703737
H	-0.93278315606125	22.01826643134277	4.00113248842700
C	-0.68931633247921	18.77471660460257	4.43406440137169
C	-1.35735274498940	16.05993876253483	7.00278840406012
C	2.37089325521003	20.04926008031218	9.76163076054686
H	3.07246286216139	20.69888902160977	9.23916908258606
H	1.98014412078650	20.60406089956208	10.62515481925096
H	1.54227990303880	19.84453993609872	9.08180294965484
C	-2.44841547261095	21.25092470761722	6.18313300876653
H	-3.01853815057073	21.02610447139869	5.27741404123167
H	-2.66018272487162	22.29166595588200	6.46078396999216
H	-2.82878126424530	20.60621748503667	6.98316217901188
C	-0.85290843022703	19.11249231377433	2.93447888939293
C	8.00038293245290	16.55743387257724	0.93842852545338
H	7.61566309260148	16.47783782166861	-0.08206785818909
H	8.76186007312196	15.77710943278846	1.07108989399094
H	8.49898333733537	17.52958832178183	1.02706659785379
C	5.59282528492082	21.38990234240982	2.02959268057919
C	5.55056094915450	20.64944015303502	8.40026547472041
H	4.81336214277461	20.94421082339128	7.64613771174379
H	6.42618850791824	21.29871082771713	8.27694787021123
H	5.13983469808357	20.86732268051785	9.38770455858817
C	4.02062299396897	18.99348425734476	11.34742199416954
H	4.49954334077882	18.06358262568980	11.67530165723005
H	3.50464673957775	19.42503678866934	12.21461644059810
H	4.80147456163778	19.69673622106431	11.05757512723543
C	4.26608478988240	22.15917901868691	1.98644304105632
H	3.71984533516037	21.99050388340644	1.05148175449693
H	4.45376644873229	23.23777773182899	2.06022266279491
H	3.61374681753565	21.87044187789685	2.81627668140260
C	6.99370175957773	18.81533199534073	9.32643563452752
H	6.57119768164543	18.87202981820356	10.33135707561428
H	7.85568918500524	19.49455474695736	9.28684551420194
H	7.36579316448827	17.79471818821769	9.18116106338024
C	-0.86742799190101	17.82539065046875	2.08737334106314
H	0.05020793839472	17.24269268523680	2.21049654487856
H	-0.94319862044032	18.09898990429944	1.02845580536727
H	-1.72580533868832	17.18386502084750	2.31756306410572
C	6.29129230045756	15.00134839187402	1.90855420693600

H	5.47908519021533	14.86513875918373	2.63034910539532
H	7.06867209930821	14.26308117815709	2.14214722348071
H	5.91335345101001	14.75588884130027	0.91532350421533
C	-2.89779990516701	16.17149190464763	7.00282054392996
H	-3.23221262770470	17.08274631844766	7.51213558577655
H	-3.34438177705965	15.31370744971450	7.52280985474757
H	-3.29887110996299	16.19312459154794	5.98271305558807
C	2.90424787720369	17.84205445069620	-0.81644596397509
H	2.14984984424912	18.23442120356055	-0.12727594002825
H	2.38044969133663	17.22102459290184	-1.55290853985534
H	3.35147570898577	18.68266446958220	-1.35891770641701
C	5.20861570267436	14.05198724057001	6.59843594748683
H	5.27492056880875	12.96303812205969	6.48298667765926
H	6.22605555371752	14.42074741013994	6.77101709884782
H	4.84931285252755	14.46665445243578	5.65114994956447
C	0.26079185802823	19.98762414454614	2.34601172634519
H	0.37728642410554	20.93851236265324	2.86020993085298
H	0.04416382998565	20.20265427349450	1.29150770149829
H	1.22118481579599	19.46691111441531	2.39562139634189
C	4.93268504400995	16.51672898361299	-1.19971721923443
H	5.48405053916628	17.36570151815355	-1.61954853787921
H	4.36880656500107	16.04805724058383	-2.01648709522549
H	5.66219728825350	15.78343104328932	-0.85012978528572
C	6.75167015485980	19.12301917079872	6.89582317124587
H	7.31669702104529	18.19275215516972	6.78188556101493
H	7.48487888474043	19.93836701365393	6.86692326726851
H	6.08851567776801	19.23159017728785	6.03342395885409
C	7.55961557567840	16.49338325458341	3.38093803242647
H	8.18160210395266	17.38544699043565	3.50206865888561
H	8.22021644932855	15.62843236468492	3.51804450415034
H	6.81446697866357	16.48201841854738	4.18291289808694
C	-0.87516322136220	16.01656779861646	8.45266454346446
H	0.21553161177826	15.98278005370219	8.49386698238303
H	-1.27403056344151	15.12924801959211	8.96007421446064
H	-1.21195537642604	16.88949410983864	9.02211617794849
C	-2.22701526678413	19.77484833392153	2.70159808928111
H	-3.03372045837071	19.17325989669730	3.13704652520663
H	-2.41661927516779	19.85735785468346	1.62392022828429
H	-2.29286713091335	20.78066563241180	3.11817833891580
C	1.86607672513431	17.92570580898404	10.88497177619176
H	1.06878524087412	17.68394974885165	10.17902443199309
H	1.42331849759435	18.53169358765816	11.68472037459546
H	2.22598632093511	16.99836224678315	11.34420863008364
C	4.88255347555392	13.85065576212967	9.06328256416825
H	4.22316294895515	14.03045662472347	9.92007526652161
H	5.84741051075636	14.32467069991001	9.27840951836561
H	5.04653876272976	12.76826018786397	8.98227866833499
C	6.34043658696455	21.76113231006382	3.31578244477867
H	5.78828859400731	21.44218047822821	4.20505196953033
H	6.47366079379927	22.84854475528752	3.37211087165931
H	7.33814730417670	21.31113995161133	3.35357545542888
C	-0.97055553048166	14.75244295373936	6.30130866125426
H	-1.39861765312691	14.68536267545101	5.29561529159354
H	-1.35289528249617	13.89480659517736	6.86926778877634
H	0.11390337797038	14.64805475311198	6.21748617631793
C	6.45489620883944	21.82216008346953	0.82230769789906
H	7.42026513923935	21.30402565601403	0.81892031893179
H	6.64911142861755	22.90227751616057	0.85817290343483
H	5.95276947845506	21.60007142136345	-0.12643072060578

Table S20: Cartesian coordinates of the optimized geometry of [(Cp'''Fe)$_3$(μ_3-Sb)$_2$] at the OPBE/TZVP level of theory, in the decet spin state.

Sb	3.13168234147571	19.47983915814254	5.29954635514073
Sb	2.72141546526593	16.76960782121692	4.91282787348694
Fe	3.91205874899109	17.76300733128919	7.13220982729803
Fe	4.13564672665142	18.15675237381077	3.20442445797587
Fe	0.68909142915651	18.47915378150896	5.29645873906961
C	5.46262166448420	18.06447991509368	8.55333694265986
C	-1.11623996985466	18.62671534959455	6.33129291379186
H	-1.15108717056237	18.81637445087184	7.39617501569447
C	-1.15462617918253	19.66152489656672	5.32382816668539
C	3.38306949754803	18.80620131792906	10.24853661862376
C	4.16104512743750	17.92519564997191	9.24492698546929
C	4.67045613476481	15.86804649636857	8.20228427081994
C	-1.09186806469961	17.33171137535411	5.73384600089492
C	5.73306183443960	17.49791083752124	1.98729963294763
C	3.72021566037431	16.58632647666079	8.97471627033538
H	2.78797684847875	16.16970912443811	9.32870909615012
C	5.71138386543641	16.78956946862705	7.93771216518403
H	6.58793234327566	16.56361465731857	7.34667567271568
C	-1.09758836031952	17.57980886022640	4.32669528662093
H	-1.06902207673965	16.80418370508723	3.57522415532128
C	3.76312591176425	16.84146475724209	0.13237284929014

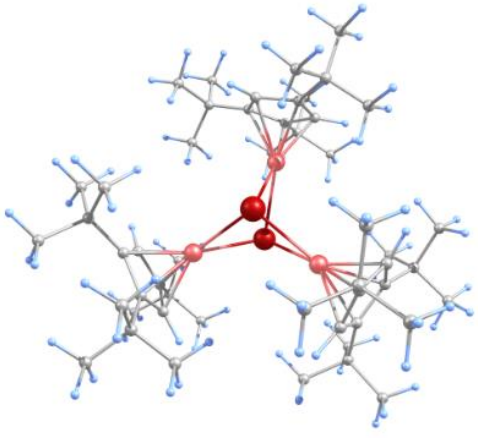

C	6.73514282816052	16.33845324317157	2.17486785988272
C	6.61357564405591	19.09463528564431	8.57796363990350
C	6.08439330994694	18.79100816827676	2.50939963080845
H	6.92232551959503	18.97486632950017	3.16823186193955
C	-1.39399105810692	21.11527837716862	5.78590112725305
C	4.53814355453050	17.72189005209588	1.14194788415902
C	3.00734120757082	15.66979320505324	0.77826355973908
H	3.65924265470552	14.98689307743539	1.32217094748644
H	2.48566489827090	15.08808313842322	0.00630581499177
H	2.25779402017975	16.03659727542463	1.48743828149976
C	4.25974307912698	19.12597716659704	1.22797000227682
H	3.42993944840535	19.61338832006905	0.73583649104229
C	-0.79981392662857	21.34394662016436	7.18975431693590
H	-1.31087656571857	20.76852068424033	7.96818054887760
H	-0.90873499478071	22.40101656529149	7.46020700927642
H	0.26750235711711	21.10209937174877	7.22005957742265
C	5.20589220277886	19.80006227583930	2.03939183490026
C	3.29723290785274	13.76141421754159	7.87690447983752
H	2.73702981252569	14.19457730316942	7.04276329229366
H	2.71931311291803	13.91740485042925	8.79445130365176
H	3.36345495465227	12.67805088827650	7.71659748142104
C	4.70373280804407	14.36400841341783	7.97199027579549
C	-0.78428568834173	22.20979942893898	4.90148354304139
H	0.30283781808340	22.10082516253789	4.82575936925992
H	-0.98582423600020	23.18996822938874	5.35101447536763
H	-1.20097949442723	22.23517620258368	3.89451162481191
C	-1.18657756328688	18.96958611345001	4.03651914593286
C	-1.38129865915624	16.00409049657177	6.42341827191345
C	2.89383013976993	20.14010828792086	9.66182247588200
H	3.70314515357282	20.77722655402168	9.30657549141514
H	2.33743674732026	20.70223471623862	10.42411323083258
H	2.22052585324601	19.95992767012021	8.81870265395543
C	-2.91792560109137	21.33580769565859	5.89907934480084
H	-3.42509707261282	21.24953205883420	4.93523694657233
H	-3.12787643376800	22.33712646541625	6.29780457280949
H	-3.36828385576367	20.60297787946883	6.57825631020463
C	-1.31357318058157	19.44304921414875	2.57416160359071
C	7.82327453559245	16.45674683315760	1.08709247887321
H	7.41613277517811	16.34713999604647	0.07822381970997
H	8.58988344366957	15.68261923992612	1.22539624115100
H	8.31976772062354	17.43262356223640	1.13704519855835
C	5.40431134166939	21.30553183508908	2.14293161998488
C	6.20085357033274	20.56381612831100	8.71940373902467
H	5.50817703877985	20.86471907165878	7.92643060198129
H	7.09177665877460	21.19854949671656	8.63697491997889
H	5.74501047900802	20.79283392378828	9.68451348297783
C	4.23196691871409	19.05957303458885	11.50871669988529
H	4.58404803982331	18.11577888143487	11.94101277899257
H	3.62632819172361	19.57040078750357	12.26851461557176
H	5.10331538572959	19.68676119563295	11.31475943301515
C	4.07367381252452	22.06721705691505	2.09849334533482
H	3.52583138529527	21.88899662172281	1.16622606107226
H	4.25572565362867	23.14730867961689	2.16366176382681
H	3.42496255055962	21.78028263365140	2.93184739590210
C	7.56593153198085	18.72666411177959	9.73572054609617
H	7.07553442527169	18.79016659743249	10.71141598391888
H	8.43056165270904	19.40353236272860	9.75144019388342
H	7.94168255446016	17.70361470750808	9.62203141889120
C	-1.44654911159358	18.23648709759613	1.62672200270217
H	-0.56065149648972	17.59334437870622	1.63802618793495
H	-1.56606626522698	18.59963937154023	0.59902153968607
H	-2.32403749020527	17.62229783078923	1.86050478237104
C	6.13901403373564	14.92645938195188	2.14280713940227
H	5.34331431178910	14.81212752178275	2.88665641279080
H	6.92209265443071	14.19545988911947	2.38009320760774
H	5.73820141806607	14.65112800657013	1.16669833927565
C	-2.90734110099167	15.92554588431614	6.64216618818071
H	-3.26154741744500	16.74144579715666	7.28224879387527
H	-3.18028889047099	14.97658413699938	7.12257784231049
H	-3.44683619224695	15.98840522941089	5.69041078488196
C	2.70023122199631	17.67766067685445	-0.60382808266905
H	1.94806065390874	18.08886239103806	0.07642159899049
H	2.17360725839883	17.03371214972807	-1.31828750428783
H	3.14375488898260	18.50240281472883	-1.17301598512924
C	5.49288720169145	13.99130615193534	6.71181826089848
H	5.50943644499780	12.90137291581971	6.58634137445105
H	6.53458059758520	14.32556446546421	6.76564586092695
H	5.04166087947398	14.42756565159057	5.81548961239198
C	-0.08994323432070	20.23882081788495	2.09265504939498
H	0.07290167271960	21.15195102062632	2.66323265528807
H	-0.21328018188059	20.52010720070326	1.03862506415266
H	0.81797744778255	19.63325867684848	2.17489049984979
C	4.70945419829575	16.32267378430715	-0.96737733606863
H	5.25880635389137	17.14939879497547	-1.43196669852363
H	4.12694957102235	15.82571112663469	-1.75361236664835
H	5.44022558391308	15.59833398586675	-0.60267412794430
C	7.42801937476294	19.01337786172867	7.27160194587309
H	7.96449099316161	18.06592570831019	7.16092662177934
H	8.18798182368590	19.80453263094738	7.26701598953572
H	6.78945210510169	19.15481709694809	6.39356894665030

C	7.43998938531057	16.46210610821087	3.53982581893145
H	8.06157734410798	17.35876347278133	3.62229684784492
H	8.10714786613121	15.60335456524215	3.68403043877362
H	6.71573982740266	16.46842990140694	4.36061637829656
C	-0.67872366940631	15.91405720859478	7.78269199605861
H	0.40617482453812	15.99203590961067	7.66541177435017
H	-0.90193376130836	14.95433596776101	8.26688665347909
H	-1.00882855939877	16.70312329373385	8.46787668004485
C	-2.60051936114367	20.26451526231630	2.37188361614297
H	-3.48069739459319	19.69745384435378	2.69793344741147
H	-2.72945355278446	20.49381544790902	1.30676954281571
H	-2.59458912612606	21.21331080010840	2.90867298795181
C	2.11768172281631	18.07552354592644	10.73781565014224
H	1.42701597509242	17.84435805577338	9.92004860903335
H	1.58397459981557	18.72632999916199	11.44082225377822
H	2.35364582036201	17.14652282317530	11.26948898548311
C	5.41892845355721	13.75009561958886	9.19709928073795
H	4.88884939939315	13.98782122987057	10.12663457975845
H	6.44360687354685	14.12798415862023	9.29033441258968
H	5.46794787868619	12.65720736950277	9.10355494118153
C	6.16094536589866	21.69734031588953	3.41767098298469
H	5.62162828188163	21.37747499129646	4.31481840091132
H	6.28218690820267	22.78658034070715	3.46407876125812
H	7.16421806790804	21.25919102127400	3.44882692099430
C	-0.95551768894115	14.80944237880407	5.56093476105746
H	-1.51096916817908	14.76877314099880	4.61801514030674
H	-1.15390436371664	13.87089747598904	6.09322482135171
H	0.11281431347965	14.84548319798556	5.32565372676231
C	6.25473893278735	21.72401494131495	0.92246981619506
H	7.22254542441111	21.21061532391246	0.91912361895623
H	6.44393361189431	22.80539019962088	0.94118504367152
H	5.74598331345069	21.48569607310368	-0.01870940578092

Table S21: Cartesian coordinates of the optimized geometry of [(Cp'''Fe)$_3$(μ_3,$\eta^{4:4:4}$-Sb$_6$)] (**6**) at the OPBE/SVP level of theory, in doublet spin state. Total Energy: -7229.209625966045 hartree.

Sb	-1.11651036573435	8.59641546661141	3.12052605158467
Sb	-2.12397948134124	10.42905034553532	5.15971357430055
Sb	-2.14388597714058	7.56423867437319	5.64755467169907
Sb	1.60230808185452	8.81283697653564	4.34120799679653
Sb	0.59064255061731	10.64484533549113	6.37197137331574
Sb	0.58779246367050	7.76693034633383	6.85152672909420
Fe	0.06715476141924	10.82870501012802	3.79590396241360
Fe	-1.42525188892950	9.35154674968862	7.41387256498297
Fe	0.04423966769283	6.71014212490692	4.53077943399306
C	-2.28788398781005	8.45446240072709	9.02485512600344
H	-2.50461465464125	7.39267284826791	9.12588712047636
C	-3.22870093360636	9.42794483148888	8.51357855030447
C	0.75131121388798	5.53803742579202	3.02650646633816
H	1.05987380729989	5.88891224756609	2.04385777790331
C	0.08009371669107	12.85144665433826	3.60223735794939
H	-0.17603580449308	13.56941147918553	4.37977031275447
C	-0.85619986237923	12.34590873932002	2.64290710583213
C	-0.58342431651268	5.07029395381643	3.33561753364096
C	-1.08065785265435	9.07041039291191	9.48945151059397
C	-4.71918229393103	9.02863947443492	8.33629968555242
C	0.80977598981948	4.92931902388756	5.19877346118824
H	1.17849817119315	4.67680014238215	6.19298478841020
C	1.30939882368668	11.47099536967567	2.19877426349782
C	-0.09269011186746	8.51092491325559	10.51756962196734
C	1.64301084461301	5.38507350385752	4.13654999155415
C	3.17019155381215	5.27805588898244	4.09680218851988
C	2.29001671882744	10.87993792655476	1.14843311114008
C	-0.54389068887985	4.67874708128145	4.74968103071178
C	-2.52811461813560	10.71961637373841	8.57803736696864
C	-1.22208239159910	10.44239037558183	9.13938104630549
H	-0.48013342235883	11.20539038795893	9.37353721969668
C	-4.20280203967313	12.56393791931953	7.71447536687984
H	-4.08907607945912	12.26422908244516	6.66223441468744
H	-4.35187972270927	13.65683530077351	7.72823381101037
H	-5.12515694858561	12.11477610665973	8.10369032431014
C	-1.83047858046783	13.11695176881877	8.02091808076016
H	-0.89191979084656	13.02007791142056	8.58558152823031
H	-2.13774956707136	14.17393803512909	8.09336621186510
H	-1.60979460949501	12.91576233630425	6.96088139981457
C	-0.09440909036492	11.44513989900902	1.84618089095068
H	-0.49850040427524	10.90106356867757	0.99251881784236
C	1.42676665641785	12.38754067690307	3.34033092485081
C	3.83259635161177	5.79758263023921	5.38206747711241
H	3.65992363113529	6.87697275919534	5.51750781818232
H	4.92336458164788	5.63291580578904	5.34200470669616
H	3.45749993914325	5.28200997482368	6.28040693705095
C	-5.35196113037220	9.42874459343715	6.99301571918647
H	-5.29549604737269	10.50156812663014	6.78414715886864
H	-6.41979959014214	9.14893604096162	6.98348716067716

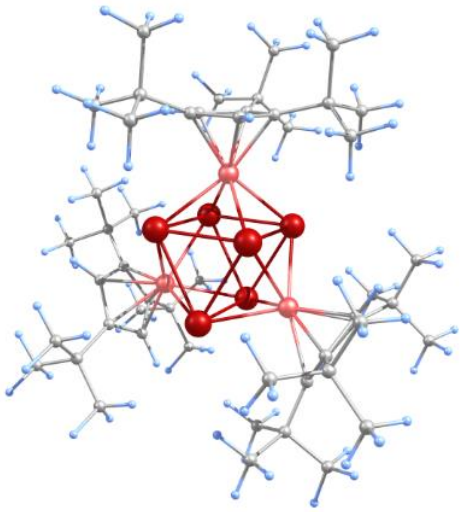

H	-4.86510888774145	8.90351343704701	6.15684491690500
C	0.01604040942393	6.98048133471165	10.45946166658415
H	-0.95790161085344	6.48703192406315	10.60820924742632
H	0.69112359745775	6.61600050267572	11.25192451972554
H	0.42476444051544	6.64149140451280	9.49532123070954
C	-2.96307224551635	12.21074725832992	8.54606868408753
C	1.30806972377928	9.12821493249258	10.38132558145128
H	1.75961112154118	8.89906187011786	9.40284632512009
H	1.97971400339502	8.72841625992348	11.16025261860537
H	1.29315087255734	10.22407908360606	10.49805418947939
C	-3.20493505552532	11.87890802661468	1.75929305497199
H	-2.81218543997258	11.31374858479556	0.89921950895879
H	-4.14449633132194	12.35551535558766	1.43135085028315
H	-3.45471518315740	11.15419846838533	2.55002097257900
C	-4.89575634412864	7.49887277359843	8.44879649286214
H	-4.30982174455794	6.95713283063053	7.68994915984026
H	-5.95568357889722	7.24153446479373	8.28315545337959
H	-4.62604777285496	7.11142886803901	9.44461615595890
C	-1.28171827105720	4.19513548085781	7.15243269290228
H	-0.24702186244202	4.16276846136615	7.52413092960543
H	-1.86952290534454	3.50771629629976	7.78296500907003
H	-1.66861874365876	5.21138323860067	7.33017603109780
C	-1.42282600351581	3.78823960997879	5.67173886182235
C	-2.99268049032161	5.37575460706223	2.38421307827300
H	-3.47084947435879	5.03918352321867	3.30840459124062
H	-3.64754598081401	5.07985750851653	1.54558401149192
H	-2.96194502247893	6.47651598117685	2.40824297711807
C	3.77762207847882	6.00504782532744	2.88735225064597
H	3.40815172839506	5.59925208645551	1.93112720779913
H	4.87526997938301	5.88881481133582	2.88612199241956
H	3.55986683947970	7.08451701275209	2.91078751689844
C	-1.66146163658002	3.26920473439043	1.95194611096824
H	-0.65657604304040	2.83607499909871	1.81306203749943
H	-2.24735833841177	3.05280506463298	1.04136247186572
H	-2.14490131123432	2.73408824277323	2.77994563781887
C	-5.52800303747616	9.63000045533794	9.50795056201626
H	-5.08554350102916	9.35159876475211	10.47927665556898
H	-6.56227537517080	9.24590212361789	9.48993462178610
H	-5.58895121016053	10.72583432357401	9.46941377900463
C	3.73361483820649	10.62326743773220	1.59938777673916
H	4.27218476371589	11.54188227370682	1.86444094359549
H	4.29629286277672	10.15531171296781	0.77326877176766
H	3.77728097902222	9.93420885483955	2.45709017763018
C	-1.92132401376384	13.92519363145880	1.09388622209357
H	-1.19206080210273	14.69617625744939	1.39295938003285
H	-2.84896333548454	14.43681233965837	0.78112132176160
H	-1.51271921712518	13.40418171646168	0.21246628946321
C	1.77628174172648	9.53345663418012	0.59694966869355
H	1.75211792350675	8.76141872966102	1.38289726558868
H	2.45292286800173	9.17540778883580	-0.19790608093751
H	0.77177590569447	9.59134700601186	0.15219045897696
C	-2.21211472127534	12.94231529970850	2.25450572420713
C	-3.23258572912735	12.61778239399601	10.01774433743743
H	-4.01839612222934	12.00076437590077	10.47767495637790
H	-3.55768311670843	13.67195821136380	10.06926648865912
H	-2.32900192605638	12.51812833081414	10.63983906643843
C	-1.06318883275910	5.39070412432950	0.85299502651649
H	-0.89879152946562	6.47771497759027	0.92083090700546
H	-1.81308463492464	5.22217094259766	0.06176871989210
H	-0.12887393267182	4.91383524234229	0.51544091138845
C	-2.93034525270455	3.75267427583459	5.38889748188647
H	-3.38630942816486	4.75306410177138	5.44927770770335
H	-3.42770870982238	3.12197038710585	6.14489958922566
H	-3.17588197681367	3.32093946076026	4.41030099739729
C	-0.87039103400428	2.34639248385616	5.53448298534465
H	-0.93182769985414	1.97900998583920	4.49928126823042
H	-1.44702105424742	1.65252068992415	6.17082326172131
H	0.18564309949927	2.28264744546623	5.84210190733353
C	-0.67307395453860	8.89925290009178	11.89983746151571
H	-0.75246732407503	9.99290671138768	12.01331038891338
H	-0.02516316282836	8.52076589844024	12.71023933459997
H	-1.68048176101140	8.47523575403753	12.04876898229820
C	2.62655070750570	13.10666907146574	4.01369182480208
C	-2.84652766065740	13.74164082249928	3.40192278750918
H	-3.02543892260921	13.10895972379466	4.28472387761971
H	-3.81979834862146	14.15337681696254	3.08672737859726
H	-2.21968598892012	14.59426843285627	3.71099354690118
C	3.68498147788122	12.17872326435152	4.63172461898156
H	3.26413908524050	11.60719132682208	5.47393150582081
H	4.52197090493363	12.77865618870648	5.02934770898209
H	4.10620421139540	11.45875746270460	3.92339203523713
C	3.48037722647189	3.76829314331535	3.95340969206971
H	3.10910254334864	3.19259157511952	4.81727542963872
H	4.57043991636082	3.60274247622302	3.88290669908155
H	3.01483038307375	3.34628507248169	3.04699986735220
C	-1.58354979140993	4.79589398015884	2.18071038494647
C	3.28050313312970	14.04357844018138	2.97304429537240
H	3.79267497742178	13.50094821361938	2.16694333955423
H	4.03573731734835	14.68424502327036	3.46126577454509
H	2.53221629650053	14.70604621402081	2.50565563779974

C	2.14412402953272	14.02190734869166	5.15965749825790
H	1.5006386708766	14.84372386803477	4.80660471797353
H	3.01837563835964	14.48227853136457	5.64914889104173
H	1.59973966780274	13.45831677301243	5.93406219230886
C	2.31987188548165	11.88155023864261	-0.03363883715243
H	1.32092828656992	12.01512057915086	-0.47884037479496
H	2.99449244262737	11.51585102028201	-0.82716132622940
H	2.67478753498845	12.87600848394738	0.27528373397817

Table S22: Selected Meyer bond orders for [(Cp'''Fe)$_3$($\mu_{3,}\eta^{4:4:4}$-Sb$_6$)] (**6**) at the OPBE/SVP level of theory, in doublet spin state.

B(0-Sb, 1-Sb)	0.52	B(0-Sb, 2-Sb)	0.54	B(0-Sb, 3-Sb)	0.34
B(0-Sb, 6-Fe)	0.72	B(0-Sb, 8-Fe)	0.70	B(1-Sb, 2-Sb)	0.53
B(1-Sb, 4-Sb)	0.34	B(1-Sb, 6-Fe)	0.71	B(1-Sb, 7-Fe)	0.73
B(2-Sb, 5-Sb)	0.33	B(2-Sb, 7-Fe)	0.69	B(2-Sb, 8-Fe)	0.72
B(3-Sb, 4-Sb)	0.54	B(3-Sb, 5-Sb)	0.53	B(3-Sb, 6-Fe)	0.73
B(3-Sb, 8-Fe)	0.70	B(4-Sb, 5-Sb)	0.54	B(4-Sb, 6-Fe)	0.69
B(4-Sb, 7-Fe)	0.72	B(5-Sb, 7-Fe)	0.70	B(5-Sb, 8-Fe)	0.73
B(6-Fe, 7-Fe)	0.24	B(6-Fe, 8-Fe)	0.25	B(7-Fe, 8-Fe)	0.24

Table S23: Loewdin spin population in [(Cp'''Fe)$_3$($\mu_{3,}\eta^{4:4:4}$-Sb$_6$)] (**6**) calculated at the OPBE/SVP level of theory, in doublet spin state.

0 Sb	-0.041
1 Sb	-0.041
2 Sb	-0.039
3 Sb	-0.043
4 Sb	-0.040
5 Sb	-0.042
6 Fe	0.454
7 Fe	0.440
8 Fe	0.510

4.6 References

[1] B. E. Collins, Y. Koide, C. K. Schauer and P. S. White, *Inorg. Chem.,* 1997, **36**, 6172–6183.

[2] C. M. Hoidn, D. J. Scott, Daniel and R. Wolf, *Chem. Eur. J.*, 2021, **27**, 1886-1920.

[3] a) M. Caporali, L. Gonsalvi, A. Rossin and M. Peruzzini, *Chem. Rev.,* 2010, **110**, 4178–4235; b) F. Scalambra, M. Peruzzini and A. Romerosa, *Adv. Organomet. Chem.,* 2019, 173–222; c) N. A. Giffin and J. D. Masuda, *Coor. Chem. Rev.,* 2011, **255**, 1342–1359; d) O. J. Scherer, *Acc. Chem. Res.,* 1999, **32**, 751–762.

[4] B. M. Cossairt, N. A. Piro and C. C. Cummins, *Chem. Rev.,* 2010, **110**, 4164–4177.

[5] L. Qiao, C. Zhang, X. W. Zhang, Z. C. Wang, H. Yin and Z. M. Sun, *Chin. J. Chem.,* 2020, **38**, 295–304.

[6] M. Scheer, G. Balázs and A. Seitz, *Chem. Rev.,* 2010, **110**, 4236–4256.

[7] a) O. J. Scherer, *Angew. Chem. Int. Ed. Engl.,* 1985, **24**, 924–943; b) O. J. Scherer, *Angew. Chem. Int. Ed. Engl.,* 1990, **29**, 1104–1122.

[8] Y. R. Luo, *Comprehensive Handbook of Chemical Bond Energies*, CRC Press, Boca Raton, 2007.

[9] a) J. Kordis and K. A. Gingerich, *J. Chem. Phys.,* 1973, **58**, 5141–5149; b) J. Mühlbach, P. Pfau, E. Recknagel and K. Sattler, *Surf. Sci.,* 1981, **106**, 18–26; c) V. E. Bondybey, G. P. Schwartz and J. E. Griffiths, *J. Mol. Spectrosc.,* 1981, **89**, 328–332; d) R. Prasad, V. Venugopal, Z. Singh and D. D. Sood, *J. Chem. Thermodynamics,* 1979, **11**, 963–970; e) H. Zhang and K. Balasubramanian, *J. Chem. Phys.,* 1992, **97**, 3437–3444.

[10] a) S. Scharfe, F. Kraus, S. Stegmaier, A. Schier and T. F. Fässler, *Angew. Chem. Int. Ed.,* 2011, **50**, 3630–3670; b) R. S. P. Turbervill and J. M. Goicoechea, *Chem. Rev*., 2014, **114**, 10807−10828; for the use of K_3Sb cf.: c) Y. Wang, P. Zavalij and B. Eichhorn, *Chem. Commun*., 2018, **54**, 11917—11920. d) S. S. Chitnis, N. Burford, J. J. Weigand, R. McDonald*, Angew. Chem. Int. Ed.* 2015, **54**, 7828-7832.

[11] H. J. Breunig, *Organic Arsenic, Antimony and Bismuth Compounds* 1994, *John Wiley & Sons*, 563–577.

[12] L. F. Dahl and A. S. Foust, *J. Am. Chem. Soc.,* 1970, **92**, 7337–7341.

[13] G. Huttner, U. Weber, B. Sigwarth and O. Schneidsteger, *Angew. Chem. Int. Ed. Engl.,* 1982, **21**, 215–216.

[14] L. Tuscher, C. Ganesamoorthy, D. Bläser, C. Wölper and S. Schulz, *Angew. Chem. Int. Ed.,* 2015, **54**, 10657–10661.

[15] H. J. Breunig, R. Rösler and E. Lork, *Angew. Chem. Int. Ed. Engl.,* 1997, **36**, 2819–2821.

[16] H. J. Breunig, N. Burford and R. Rösler, *Angew. Chem. Int. Ed.,* 2000, **39**, 4148–4150.

[17] C. Ganesamoorthy, J. Krüger, C. Wölper, A. S. Nizovtsev and S. Schulz, *Chem. Eur. J.,* 2017, **23**, 2461–2468.

[18] C. Ganesamoorthy, C. Wölper, A. S. Nizovtsev and S. Schulz, *Angew. Chem. Int. Ed.,* 2016, **55**, 4204–4209.

[19] a) Y. Wang, P. Zavalij and B. Eichhorn, *Chem. Commun.,* 2018, **54**, 11917–11920; b) C. Ganesamoorthy, C. Helling, C. Wölpe, W. Frank, E. Bill, G. E. Cutsail and S. Schulz, *Nat. Commun.,* 2018, **9**, 87; c) C. Schoo, S. Bestgen, A. Egeberg, S. Klementyeva, C. Feldmann, S. N. Konchenko and P. W. Roesky, *Angew. Chem. Int. Ed.,* 2018, **57**, 5912–5916; d) C. Helling, C. Wölper and S. Schulz, *Dalton Trans.,* 2020, **49**, 11835–11842; e) C. Helling, G. E. Cutsail, H. Weinert, C. Wölper and S. Schulz, *Angew. Chem. Int. Ed.,* 2020, **59**, 7561–7568.

[20] C. Schoo, S. Bestgen, A. Egeberg, S. Klementyeva, C. Feldmann, S. N. Konchenko and P. W. Roesky, *Angew. Chem. Int. Ed.,* 2018, **57**, 5912–5916.

[21] G. Balázs, M. Sierka and M. Scheer, *Angew. Chem. Int. Ed.,* 2005, **44**, 4920–4924.

[22] T. Wetting, B. Geissler, R. Schneider, S. Barth, P. Binger and M. Regitz, *Angew. Chem. Int. Ed. Engl.,* 1992, **31**, 758–759.

[23] B. M. Cossairt, M.-C. Diawara and C. C. Cummins, *Science,* 2009**, 323**, 602.

[254] A. E. Seitz, M. Eckhardt, A. Erlebach, E. V. Peresypkina, M. Sierka and M. Scheer, *J. Am. Chem. Soc.,* 2016, **138**, 10433–10436.

[25] M. Schmidt, A. E. Seitz, M. Eckhardt, G. Balázs, E. V. Peresypkina, A. V. Virovets, F. Riedlberger, M. Bodensteiner, E. M. Zolnhofer, K. Meyer and M. Scheer, *J. Am. Chem. Soc.,* 2017, **139**, 13981–13984.

[26] H. J. Breunig, K. Häberle, M. Dräger and T. Severengiz, *Angew. Chem. Int. Ed. Engl.,* 1985, **24**, 73.

[27] H. J. Breunig, K. H. Ebert, S. Gülec and J. Probst, *Chem. Ber,.* 1995, **128**, 599–603.

[28] a) O. J. Scherer, H. Swarowsky, G. Wolmershäuser, W. Kaim and S. Kohlmann, *Angew. Chem. Int. Ed. Engl.,* 1987, **26**, 1153–1155; b) J. M. Goicoechea, M. W. Hull, S. C. Sevov, *J. Am. Chem. Soc.* 2007, **129**, 7885-7893; c) H.-G. von Schnering, M. Wittmann, R. Nesper, *J. Less. Common. Met.* 1980, **76**, 213-226.

[29] a) S. R. Wade, M. G. H. Wallbridge and G. R. Willey, *J. Organomet. Chem.,* 1984, **267**, 271–276; b) R. Zitz, J. Baumgartner and C. Marschner, *Organometallics,* 2015, **34**, 1431–1439.

[30] Despite several attempts, it was not possible to structurally identify **3a**. Its composition and structure are assigned based on mass spectrometric data and are presumably isostructural to the cubanes **2** and **3b**.

[31] Note that the peak for **3b** is relatively weak presumably due to its high mass (2785 Da).

[32] a) P. D. Mlynek and L. F. Dahl, *Organometallics,* 1997, **16**, 1641–1654; b) S. Charles, B. W. Eichhorn and S. G. Bott, *J. Am. Chem. Soc.,* 1993, **115**, 5837–5838.

[33] U. Vogel, G. Baum and M. Scheer, *Z. Anorg. All. Chem.,* 2000, **626**, 444–449.

[34] T. A. Albright, K. A. Yee, J. Y. Saillard, S. Kahlal, J. F. Halet, J. S. Leigh and K. H. Whitmire, *Inorg. Chem.,* 1991, **30**, 1179–1190.

[35] N. C. Norman, P. M. Webster and L. J. Farrugia, *J. Organomet. Chem.,* 1992, **430**, 205,219.

[36] J. S. Leigh, K. H. Whitmire, K. A. Yee and T. A. Albright, *J. Am. Chem. Soc.,* 1989, **111**, 2726–2727.

[37] S. N. Konchenko, A. V. Virovets, S. A. Apenina and S. V. Tkachev, *Inorg. Chem.,* 1999, 555–557.

[38] P. Pyykkö and M. Atsumi, *Chem. Eur. J.,* 2009, **15**, 186–197.

[39] J. E. McGrady, *J. Chem. Soc., Dalton Trans.* 1999, 1393–1399.

[40] G. Knizia, *J. Chem. Theory Comput.,* 2013, **9**, 4834–4843.

[41] Due to the high molecular weight and bad solubility, the results of the Evans NMR should be treated with care.

[42] H. Lang, G. Huttner, L. Zsolnai, G. Mohr, B. Sigwarth, U. Weber, O. Orama and I. Jibril, *J. Organomet. Chem.,* 1986, **304**, 157–179.

[43] T. Gröer, T. Palm and M. Scheer, *Eur. J. Inorg. Chem.,* 2000, 2591-2259.

[44] There are two different bond distances due to two molecules in the asymmetric unit.

[45] M. Reiners, D. Baabe, K. Münster, M.-K. Zaretzke, M. Freytag, P. G. Jones, Y. Coppel, S. Bontemps, I. D. Rosal, L. Maron and M. D. Walter, *Nat. Chem.,* 2020, **12**, 740–746.

[46] S. Reisinger, *Organometallic Pnictogen Chemistry - Three Aspects*, PhD thesis, University of Regensburg, 2014.

[47] S. Stoll and A. Schweiger, *J. Magn. Reson.,* 2006, **178**, 42–55.

[48] H. J. Breunig, R. Rösler and E. Lork, *Angew. Chem. Int. Ed. Engl.,* 1997, **36**, 2819–2821.

[49] a) S. Heinl, A. Y. Timoshkin, J. Müller and M. Scheer, *Chem. Commun.,* 2018, **54**, 2244–2247; b) C. Hänisch, D. Fenske, F. Weigend and R. Ahlrichs, *Chem. Eur. J.,* 1997, **3**, 1494–1498; c) C. Hänisch, D. Fenske, F. Weigend, R. Ahlrichs, *Chem. Eur. J.* 1997, **3**, 1494-1498, d) G. Friedrich, O. J. Scherer, G. Wolmershäuser, *Z. Anorg. Allg. Chem*. 1996, **622**, 1478-1486; e) L. Qiao, D. Chen, J. Zhu, A. Muñoz-Castro, Z.-M. Sun, *Chem. Commun*. 2021, **57**, 3656-3659.

[50] M. Scheer and J. Wachter, *Präperative Metallorganische Chemie für Fortgeschrittene*, Universität Regensburg, 2008.

[51] C. Marquardt, O. Hegen, M. Hautmann, G. Balázs, M. Bodensteiner, A. V. Virovets, A. Y. Timoshkin and M. Scheer, *Angew. Chem. Int. Ed. Engl.,* 2015, **54**, 13122–13125.

[52] A. E. Seitz, U. Vogel, M. Eberl, M. Eckhardt, G. Balázs, E. V. Peresypkina, M. Bodensteiner, M. Zabel and M. Scheer, *Chemistry,* 2017, **23**, 10319–10327.

[53] D. Shining, *diploma thesis*, University of Karlsruhe, 2002.

[54] M. Schär, D. Saurenz, F. Zimmer, I. Schädlich, G. Wolmershäuser, S. Demeshko, F. Meyer, H. Sitzmann, O. M. Heigl and F. H. Köhler, *Organometallics,* 2013, **32**, 6298–6305.

[55] F. Dielmann, *Ph.D. thesis*, University of Regensburg, 2011.

[56] Rigaku Oxford Diffraction, *CrysAlisPro Software System Version 1.171.38.43*, Rigaku Oxford Diffraction, 2015.

[57] R. C. Clark and J. S. Reid, *Acta Cryst.,* 1995, **A51**, 887–897.

[58] L. J. Bourhis, O. V. Dolomanov, R. J. Gildea, J. A. K. Howard and H. Puschmann, *J. Appl. Crystallogr.,* 2009, **42**, 339–341.

[59] G. M. Sheldrick, *Acta Crystallogr., Sect, A* 2015, **71**, 3–8.

[60] G. M. Sheldrick, *Acta Crystallogr., Sect, C* 2015, **71**, 3–8.

[61] A. S. S. Stoll, *J. of Mag. Reson.,* 2006, **178**, 42–55.

[62] a) TURBOMOLE V6.4, a developmentof the University of Karlsruhe and the Forschungszentrum Karlsruhe GmbH, http://www.turbomole.com.; b) F. Furche, R. Ahlrichs, C. Hättig, W. Klopper, M. Sierka and F. Weigend, *WIREs Comput. Mol. Sci.,* 2014, **4**, 91–100; c) O. Treutler and R. Ahlrichs, *J. Chem. Phys.,* 1995, **102**, 356-354; d) R. Ahlrichs, M. Bär, M. Häser, H. Horn and C. Kölmel, *Chem. Phys. Lett.,* 1989, **162**, 165–169.

[63] a) K. Eichkorn, O. Treutler, H. Oehm, M. Häser and R. Ahlrichs, *Chem. Phys. Lett.,* 1995, **242**, 652–660; b) K. Eichkorn, W. Weigend, O. Treutler and R. Ahlrichs, *Theor. Chem. Acc.,* 1997, **97**, 119–124.

[64] a) A. D. Becke, *Phys. Rev. A,* 1988, **38**, 3098–3100; b) A. D. Becke, *J. Chem. Phys.,* 1993, **98**, 5648–5652; c) C. Lee, W. Yang and R. G. Parr, *Phys. Rev.,* 1988, **37**, 785–789; d) J. C. Slater, *Phys. Rev.,* 1951, **81**, 385-390; e) S. H. Vosko, L. Wikl and M. Nusair, *Can. J. Phys.,* 1980, **58**, 1200–1211; f) P. A. M. Dirac, *Proc. Royal Soc.,* 1929, **123**, 714–733.

[65] a) F. Weigend and R. Ahlrichs, *Phys. Chem. Chem. Phys.,* 2005, **7**, 3297–3305; b) F. Weigend, M. Häser, H. Patzelt and R. Ahlrichs, *Chem. Phys. Lett.,* 1998, **294**, 143–152.

[66] M. Sierka, A. Hogekamp and R. Ahlrichs, *J. Chem. Phys.,* 2003, **118**, 9136–9148.

[67] S. Grimme, J. Antony, S. Ehrlich and H. Krieg, *J. Chem. Phys.,* 2010, **132**, 154104.

[68] S. Grimme, S. Ehrlich and L. Goerigk, *J. Comput. Chem.,* 2011, **32**, 1456–1465.

[69] F. Neese, *WIREs Comput. Mol. Sci.,* 2018, **8**, e1327.

[70] a) N. C. Handy and A. J. Cohen, *Mol. Phys.,* 2001, **99**, 403–412; b) J. P. Perdew, K. Burke and M. Ernzerhof, *Phys. Rev. Lett.,* 1996, **77**, 3865–3868; c) J. P. Perdew, K. Burke and M. Ernzerhof, *Phys. Rev. Lett.,* 1997, **78**, 1396.

[71] F. Neese, F. Wennmohs, A. Hansen and U. Becker, *Chem. Phys.,* 2009, **356**, 98–109.

[72] S. Grimme, *J. Chem. Phys.,* 2006, **124**, 34108.

5 Coordination Behavior of [Cp''$_2$Zr(µ$^{1:1}$-As$_4$)] toward Lewis Acids

V. Heinl, G.r Balázs, S. Koschabek, M. Eckhardt, M. Piesch, M. Seidl, M. Scheer, *Molceucles* **2021**, *26*, 2966. (DOI: 10.3390/molecules26102966)

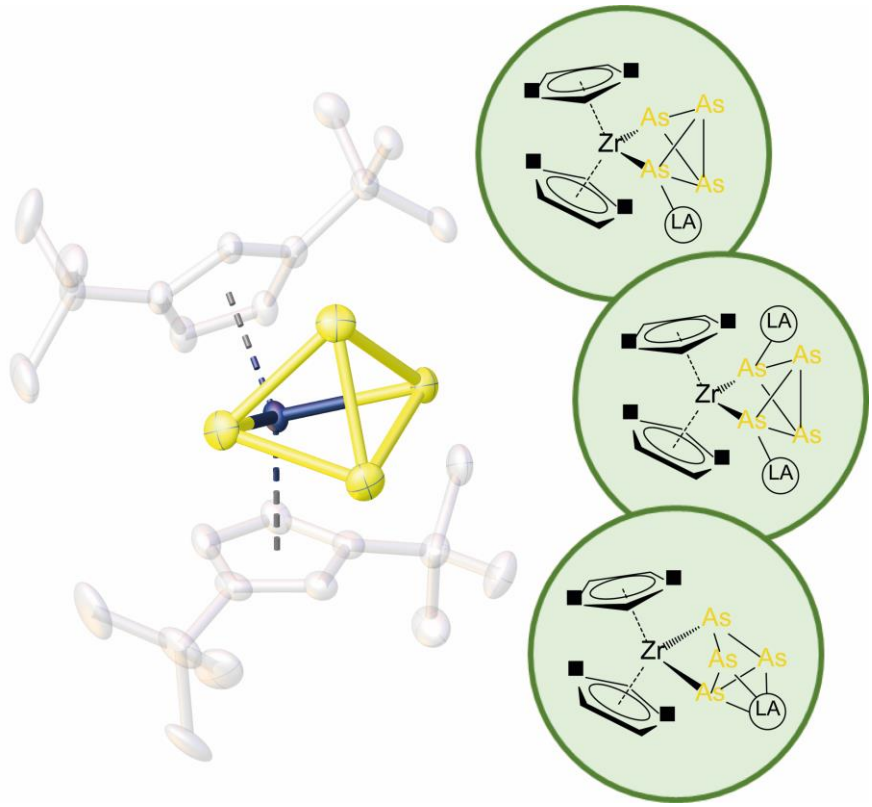

Abstract:

The functionalization of the arsenic transfer reagent [Cp"$_2$Zr(η$^{1:1}$-As$_4$)] (**1**) is focused to modify its properties and enabling a broader application. The coordination behaviour of **1** towards different Lewis acidic transition metal complexes and main group compounds is investigated by experimental and computational studies. Depending on the steric requirements of the Lewis acids and the reaction temperature a variety of new complexes with different coordination modes and coordination numbers could be synthesized. Depending on the Lewis acid (LA) used, a mono-substitution in [Cp"$_2$Zr(µ,η$^{1:1:1:1}$-As$_4$)(LA)] (LA = Fe(CO)$_4$ (**4**); B(C$_6$F$_5$)$_3$ (**7**)) and [Cp"$_2$Zr(µ,η$^{3:1:1}$-As$_4$)(Fe(CO)$_3$)] (**5**) or a di-substitution [Cp"$_2$Zr(µ$_3$,η$^{1:1:1:1}$-As$_4$)(LA)$_2$] (LA = W(CO)$_5$ (**2**); CpMn(CO)$_2$ (**3**); AlR$_3$ (**6**, R = Me, Et, ^{i}Bu)) is monitored. In contrast to other coordination products, **5** shows a η^3 coordination, in which the butterfly As$_4$ ligand is rearranged to a cyclo-As$_4$ ligand. The reported complexes are rationalized in terms of inverse coordination.

5.1 Author Contribution

- First Synthesis of the compounds **2** and **6a** were performed by M. Eckhardt during her Ph.D. thesis (University of Regensburg, **2014**).
- Synthesis and characterization of the compounds **3**, **4**, **5**, **6b**, **6c** and **7** as well as completed characterization of **2** and **6a** were performed by V. Heinl.
- S. Koschabek assisted with the synthesis and characterizations during her bachelor thesis (University of Regensburg, **2019**).
- Computational studies were performed by M. Piesch and G. Balázs.
- The Manuscript was written by V. Heinl except parts of the computational details (G. Balázs).
- M. Seidl recalculated the X-ray structures.
- Supervision: M. Scheer.

5.2 Introduction

The interest for the activation of small molecules like H_2, N_2, NH_3, etc. has increased notably in recent years.[1–8] A special focus lies on the activation of cage compounds like white phosphorus and yellow arsenic by transition metals and main group compounds.[9-12] While the synthesis and isolation of polyphosphorus complexes has been intensively investigated,[9–11] polyarsenic complexes are much less known, and hence the number of comparable polyarsenic complexes is quite limited.[12] This can be attributed to the very challenging handling of As_4 due to its pronounced air- and light-sensitivity, time-consuming preparation, and not list to its toxicity. Nevertheless, by now there are several examples for As_n containing main group compounds and transition metal complexes known.[12] Selected representatives are depicted in scheme 1. A remarkable example is the reaction of yellow arsenic towards the Cp^{PEt} radical (Cp^{PEt} = $C_5(4\text{-}EtC_6H_4)_5$), which leads to the formation of the first organo-substituted As_4 butterfly compound [$Cp^{Pet}{}_2As_4$] (**I**, scheme 1).[13] Furthermore, the reaction of the silylene [$PhC(N^tBu)_2SiN(SiMe_3)_2$] with yellow arsenic results in aggregation of the As_4 tetrahedron and compound **II**, containing a heptaarsanortricyclane unit, can be isolated.[14] Surprisingly, by using the disilene [$Cp^*(Me_3Si)_2NSi{=}SiN(Me_3Si)_2Cp^*$] ($Cp^* = C_5Me_5$) the butterfly-like compound [$Cp^*\{(SiMe_3)_2N\}SiAs]_2$ (**III**, scheme 1) is formed.[14]

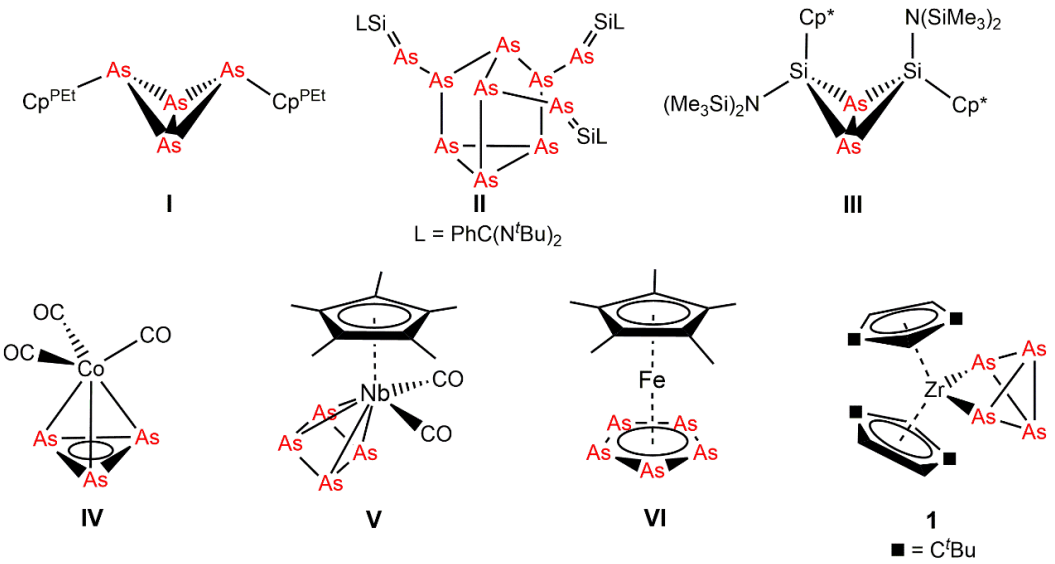

Scheme 1: Selected examples for As_n containing compounds.

Compared to the As-containing main group compounds, As_n ligand complexes of transition metals have been investigated in more detail and show a more extensive chemistry. *Dahl et. al.* described the first As_n ligand complex $[(CO)_3Co(\eta^3\text{-}As_3)]$ (**IV**, scheme 1) in the late 1960s obtained by the reaction of $[Co_2(CO)_8]$ with $[AsCH_3]_5$.[15] Many of the described syntheses use *in situ* prepared yellow arsenic and transition metal compounds with labile ligands.[12] For instance, the photolysis of $[Cp^*Nb(CO)_4]$ in the presence of yellow arsenic leads to the formation of **V**, containing a tetraarsacyclobutadiene ligand.[16] Another remarkable example represents the pentaarsaferrocene $[Cp^*Fe(\eta^5\text{-}As_5)]$ (**VI**, scheme 1).[17] After its discovery in 1990 by *Scherer et al.*, a versatile chemistry emerged.[18–23] This includes, inter alia, redox-[19,20] and coordination chemistry.[21-23] Recently, our group reported the synthesis of $[Cp''_2Zr(\eta^{1:1}\text{-}As_4)]$ (**1**, Scheme 1) by the thermolysis of As_4 with $[Cp''_2Zr(CO)_2]$ (Cp" = 1,3-di-tertbutyl-cyclopentadienyl).[24] Further investigations illustrate the high potential of **1** as arsenic transfer reagent.[24-26] Additionally, the phosphorus congener of **1**, *i.e.* $[Cp''_2Zr(\eta^{1:1}\text{-}P_4)]$ shows divers reactivity pattern towards Lewis acids.[27] These results lead us to investigate the reaction behavior of **1** towards Lewis acids to receive a possible functionalization. By this way compounds with a higher molecular mass should be accessible, which would lead, in case of a transfer of the functionalized As_4 ligand, to a better solubility of the products.

Herein, we report the coordination behavior of **1** towards different Lewis acidic transition metal complexes and main group compounds, leading among others to hetero bi- and trimetallic complexes. The structure of these complexes can be also rationalized by means of the concept of inverse coordination.[28–33] Within this concept the structure of complexes is rationalized in the sense that the ligand represents the central entity, to which the metal centers are connected. In this type of complexes, the distribution of donor and acceptor sites are opposite to the conventional complexes.

5.3 Results and Discussion

5.3.1 General Considerations

To get a better insight into the electronic structure and to determine the favored coordination site of **1** to Lewis acids, DFT calculations were carried out. The frontier molecular orbitals of **1** at the B3LYP/def2TZVP level of theory are depicted in Figure 1 (see also SI). The Highest Occupied Molecular Orbital (HOMO) represents the Zr-As bonding, while the HOMO-1 and HOMO-2 are the lone pairs of electrons of the bridgehead and wingtip arsenic atoms (arsenic atoms bonded to Zr), respectively. Both are energetically close to each other, but, the HOMO-2 has a considerably higher arsenic atomic orbital contribution from the wingtip arsenic atoms (64%) compared to the HOMO-1 orbital (26% for the wing tip and 34% from the bridgehead As Atoms). This would favor a more effective overlap of the wingtip atoms with a potential acceptor orbital of a Lewis acid. Furthermore, the natural charge distribution shows a negative charge concentration on the wingtip arsenic atoms (nat. charge: −0.218) compared to the bridgehead arsenic atoms (nat. charge: +0.016; figure 2). A similar picture is also given by the electrostatic potential (figure 2, right), which shows that the wingtip As atoms has the highest negative potential. These indicates, that a coordination of the electron-rich arsenic atoms directly bound to the zirconium atom should be favored. In contrast, due to possible steric repulsion of the Cp'' ligand a coordination of the bridgehead arsenic atoms could still be possible.

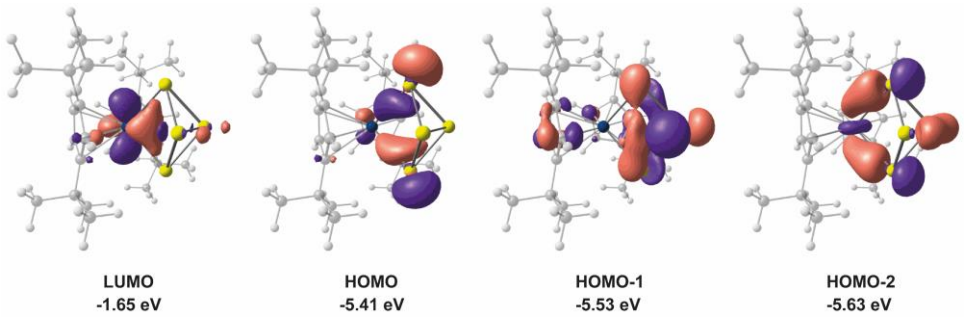

Figure 1: Frontier molecular orbitals of [Cp''$_2$Zr(η$^{1:1}$-As$_4$)] (**1**) at the B3LYP/def2TZVP level of theory.

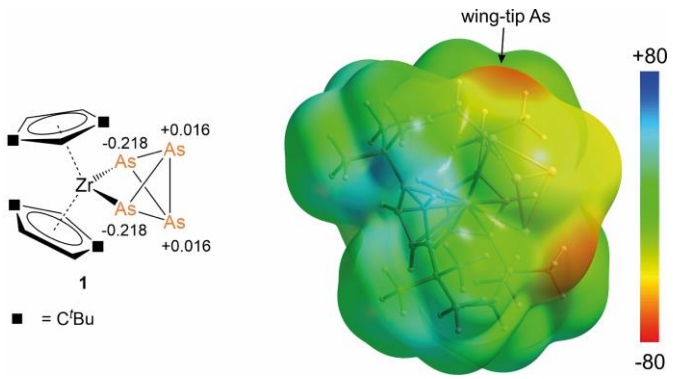

Figure 2: Natural charge distribution (left) of **1** and electrostatic potential mapped on electron density (right). Iso-value 0.001. Color ranges in kJ·mol^{-1}.

Recently we investigated the coordination behavior of $[Cp"_2Zr(\eta^{1:1}\text{-}P_4)]$ towards Lewis acidic metal fragments.[27] The results show, that it is able to coordinate to Lewis acids via both, wing tip and bridgehead phosphorus atoms, the coordination via the wing tip P atoms being electronically favored but disfavored sterically. Since the single bond covalent radius of As is larger than that of P (1.21 Å vs. 1.11 Å for As and P, respectively),[34] and inherently the Zr-As bond (2.6619(4) Å to 2.6656(3) Å)[24] is longer compared to the Zr-P bond (2.5596(7) Å to 2.5620(6) Å),[27] one would expect that for **1** the electronic effects should predominate and a coordination via wingtip arsenic atoms should be preferred.

5.3.2 Coordination of 1 to transition metal complexes

The reaction of **1** with Lewis acidic transition metal compounds leads to single or double coordination of **1**. Scheme 2 gives an overview of the reactivity of **1** towards transition metal compounds. All products were comprehensively characterized by mass spectrometry, NMR spectroscopy, IR spectroscopy and single crystal X-ray structure analysis.

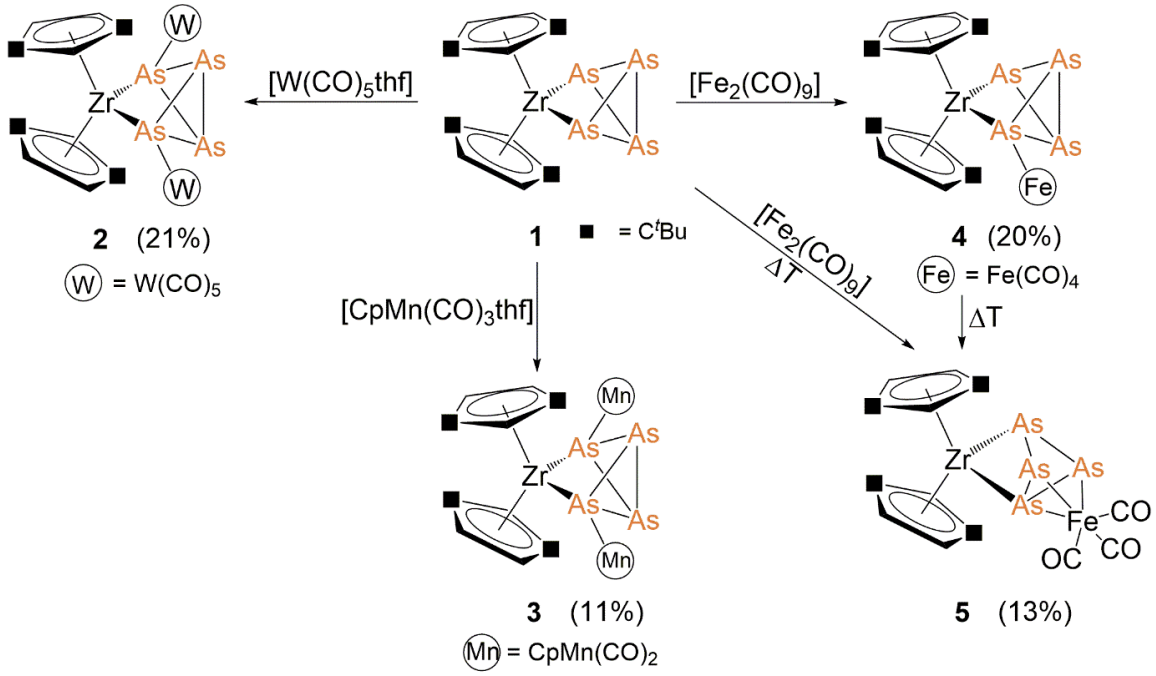

Scheme 2: Overview of the reactions of $[Cp"_2Zr(\eta^{1:1}\text{-}As_4)]$ (**1**) with Lewis acidic transition metal compounds.

The reaction of **1** with $[W(CO)_5thf]$ and $[CpMn(CO)_2thf]$ (Cp = cyclopentadienyl) in thf leads to the formation of the hetero trinuclear complexes $[Cp"_2Zr(\mu_3,\eta^{1:1:1:1}\text{-}As_4)(LA)_2]$ (LA = $W(CO)_5$ (**2**); $CpMn(CO)_2$ (**3**)], respectively (Scheme 2). The stoichiometry used has no influence on the reaction outcome and therefore on the coordination mode. In contrast, the reaction with $[Fe_2(CO)_9]$ in *n*-hexane leads to the formation of the mono-substituted compound $[Cp"_2Zr(\mu,\eta^{1:1:1:1}\text{-}As_4)(Fe(CO)_4)]$ (**4**), also irrespective of the stoichiometry used. In attempt to synthesize the di-substituted complex $[Cp"_2Zr(\mu,\eta^{1:1:1:1}\text{-}As_4)\{Fe(CO)_4\}_2]$, the reaction of **1** with

$[Fe_2(CO)_9]$ was performed at different temperatures. Surprisingly, the reaction in refluxing *n*-hexane leads to the formation of $[Cp''_2Zr(\mu,\eta^{3:1:1}\text{-}As_4)\{Fe(CO)_3\}]$ (**5**). By this reaction conditions **4** is formed first, followed by CO elimination and subsequent insertion of the $Fe(CO)_3$ fragment into the As-As bond of the bridgehead As atoms (Scheme 2). The same reaction outcome, namely the formation of **5** can be observed when isolated **4** is heated to 70 °C in *n*-hexane for 2 h. This proves that **5** is formed from **4**. A similar rearrangement of a P_4-butterfly core has been reported for the reaction of $[(Cp^*Cr(CO)_3\}_2(\mu,\eta^{1:1}\text{-}P_4)]$ with $[(Cr(CO)_4(nbd)]$ (nbd = norbornadiene).[35] In **2**, **3** and **4** the As_4 ligand in **1** serves as four valence electron donor, while in **5** it serves as a six electron donor.

DFT calculations at the B3LYP/def2-SVP level show that the coordination via the wingtip arsenic atoms is favored compared to the bridgehead arsenic atoms (*cf.* SI). The energy difference for the formation of mono-substituted or di-substituted complexes via coordination of the wingtip arsenic atoms is negligible for **2**, 11 $kJ{\cdot}mol^{-1}$ for **3** and 31 $kJ{\cdot}mol^{-1}$ for **4**. While for the formation of **3** the results of the DFT calculation are in agreement with the experimental results, in the case of **4** only the formation of the mono-substituted complex has been observed experimentally, probably due to the lower solubility of **4** compared to the potential di-substituted derivative as well as the presence of a complex equilibrium in solution (*vide infra*).

Single crystals suitable for X-ray diffractions have been obtained by storing a concentrated *n*-hexane (**2**) or *n*-pentane (**3**, **4**, **5**) solution at −78 °C. It should be mentioned, that **5** always co-crystallizes with some amount of **4** in a ratio of approximately 10:1. The molecular structures in solid state are depicted in Figure 2. In compound **2**, **3** and **4** one or two arsenic atoms of the As_4-butterfly moiety of **1** coordinate to the Lewis acidic metal fragments. Due to the steric repulsion, the As_4 unit is slightly distorted. The As-As distances are still intact and in the range of a single bond (**2**: 2.4363(6) Å to 2.4649(6)Å; **3**: 2.4394(4) Å to 2.4710(4) Å; **4**: 2.4321(6) Å to 2.4791(4) Å).[13,16,19,24] Furthermore, the Zr-As distances are slightly elongated compared to **1**.[24] In the case of **2** and **4** the As-W distances of 2.6560(4) Å and 2.6595(4) Å and the As-Fe distance of 2.4213(7) Å are slightly elongated compared to the sum of the single bond covalent radii (As-W: 2.58 Å; As-Fe: 2.37 Å).[34] This indicates an elongated single bond between the coordinating As atoms and the metal center of the Lewis acids. In contrast, in **3** the As-Mn distances (2.3605(4) Å and 2.3732(5) Å) are slightly below the calculated value of 2.40 Å, which implies a single bond.[34] In **5** the As-As distance between the former bridgehead arsenic atoms is 3.032(3) Å, which clearly shows the cleavage of this bond. The other As-As bonds are still in the range of a single bond (2.4657(14) Å and 2.4721(13) Å),[13,16,19] and the As-Fe distances of 2.4151(16) Å to 2.4265(15) Å are in the same range as observed for **4**.

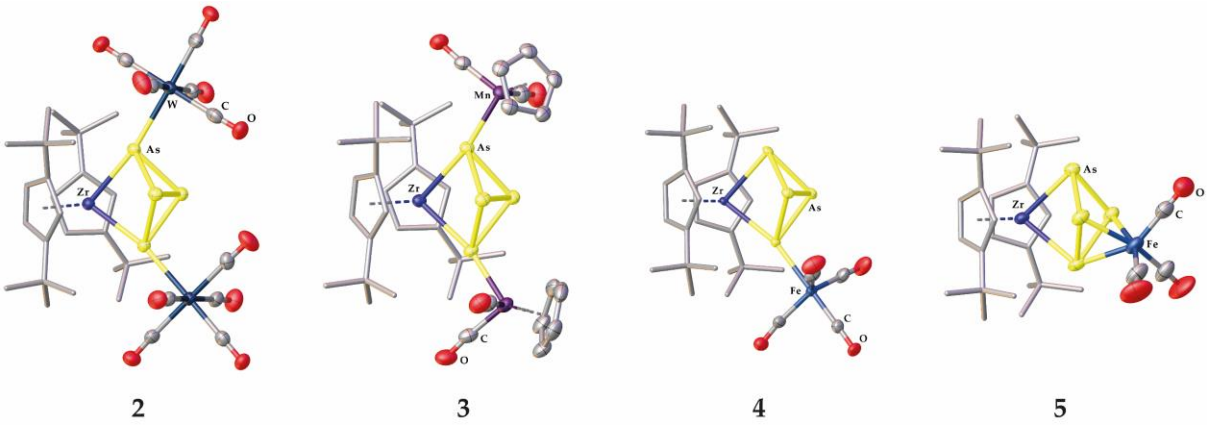

Figure 2: Molecular structures of **2**, **3**, **4** and **5** in the solid state with thermal ellipsoids at 50% probability level. Hydrogen atoms are omitted and the Cp'' ligands are drawn in the tube model for clarity.

The complexes **2-5** have been characterized by IR and ^{1}H NMR spectroscopy as well as by mass spectrometry. While the expected carbonyl stretches have been observed in the IR spectra of **2**, **3**, **4** and **5**, marked differences are present in their ^{1}H NMR spectra. The ^{1}H NMR spectrum of **2** shows one set of signals for the Cp'' ligands (one singlet for the ^{t}Bu groups at 1.26 ppm and a triplet and a doublet at 5.31 ppm and 5.48 ppm, respectively for the Cp ring bound hydrogen atoms), while in LIFDI MS a peak corresponding to $[M^+ - W(CO)_5]$ (corresponds to the mono-substituted complex) can be observed. In the ^{1}H NMR spectrum of crystalline **3** dissolved in C_6D_6, three sets of signals corresponding to Cp'' ligands can be detected. In two of them the adjacent CH groups are equivalent, indicating that the Cp'' ligands are in a symmetric environment, while in the third set they are not equivalent, pointing to an asymmetric compound (Figure 3). One set of signals corresponding to a symmetric Cp'' ligand can be assigned to starting material **1**, the second set of signals for the symmetric Cp'' ligand is assigned to **3**, based on comparison with the ^{1}H NMR data of **2**, which also shows a symmetric Cp'' ligand. The set of signals for the Cp'' ligands in an asymmetric environment can be attributed to [Cp''$_2$Zr(µ,η$^{1:1:1}$-As$_4$){CpMn(CO)$_2$}] (**3'**), based on the comparison with the ^{1}H NMR data for **4** (Figure 3; *vide infra*). These data show, that in solution **3** partly dissociates to **3'** and to **1** by elimination of one as well as both CpMn(CO)$_2$ fragments. Attempts to freeze this dynamic process by lowering the temperature leads only to a temperature dependent shift of the resonance signals as well as to a change of their relative intensity. By lowering the temperature, the intensity of the resonance signals corresponding to **3** increases and **3** crystallizes from the solution. This results are in stark contrast with the results reported for the related reaction of [Cp''$_2$Zr(µ,η$^{1:1}$-P$_4$)] with [CpMn(CO)$_2$thf], where the phosphorus analog of the mono-substituted **3'** and the coordination of one or both bridgehead phosphorus atoms to the manganese fragment has been reported.[27,36]

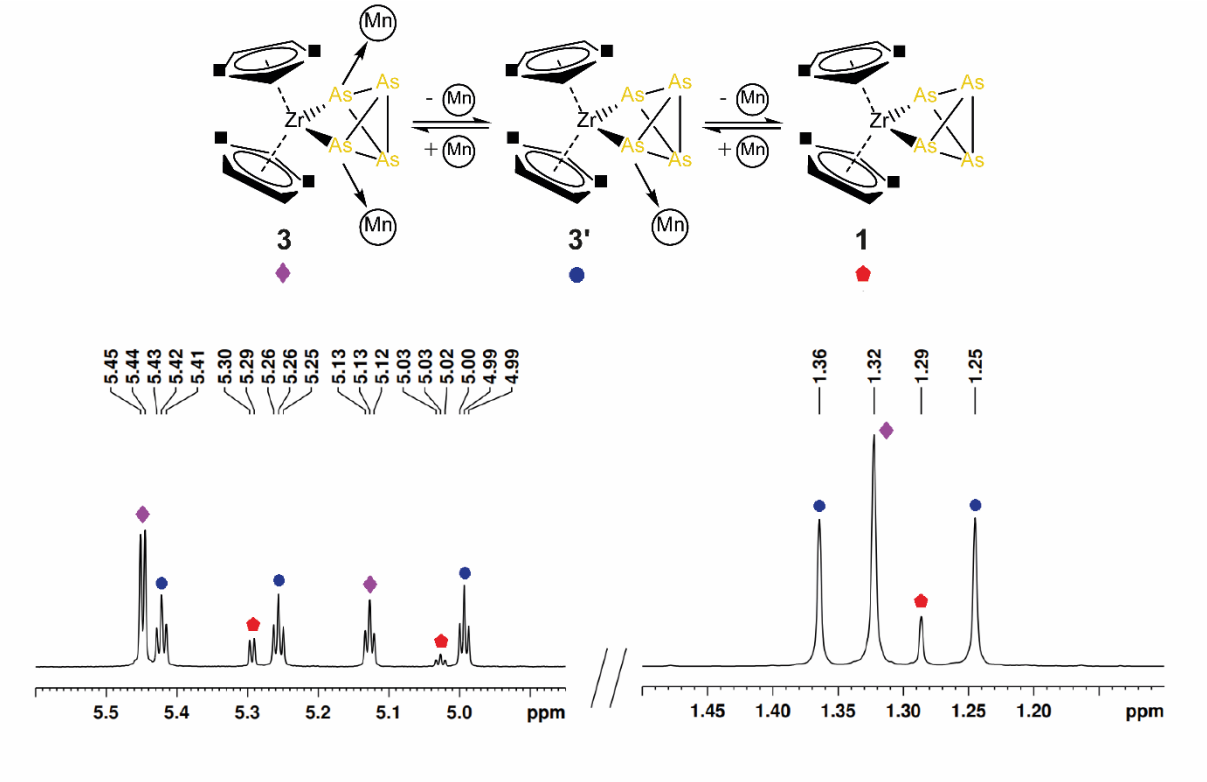

Figure 3: Sections of the ^{1}H NMR spectrum of **3** at 293 K in C_6D_6 with assignment to the compounds present in solution.

The ^{1}H NMR spectrum of isolated **4**, dissolved in C_6D_6, show one set of signals corresponding to Cp'' ligands in asymmetric environment. Two singlets at 1.15 ppm and 1.28 ppm for the ^{t}Bu groups and three triplets at 5.11 ppm, 5.22 ppm and 5.44 ppm for the CH groups. Therefore, no dynamic behavior in solution, similar to that observed for **3** can be detected. In the reaction solution, however among signals of **4** also signals corresponding to the di-substituted complex $[Cp''_2Zr(\mu_3,\eta^{1:1:1:1}\text{-}As_4)\{Fe(CO)_4\}_2]$ and **1** can be detected by ^{1}H NMR spectroscopy, but only **4** crystallizes from the solution. In the remaining solution, after crystallization of **4** still three sets of signals can be detected, however, the intensity of the signals of **4** are drastically decreased. Surprisingly, the ^{1}H NMR spectrum of **5** shows three signals (δ [ppm] = 1.32 (s), 5.84 (d), 5.95 (t)) for the Cp'' substituents indicating a symmetric environment.[37,38]

5.3.3 Coordination towards main group compounds

In order to investigate if the nature of the Lewis acid plays a decisive role in the coordination behavior of **1**, the reactivity of **1** towards Lewis acidic main group compounds was investigated (Scheme 3). Thus, the reaction with AlR_3 (R = Me, Et, ^{i}Bu) in toluene was performed, leading to [Cp"$_2$Zr(μ_3,$\eta^{1:1:1:1}$-As$_4$)(AlR_3)$_2$] (**6a**: R = Me; **6b**: R = Et; **6c**: R = ^{i}Bu), which show twofold coordination of **1** to the AlR_3 units. The reaction outcome is independent of the stoichiometry used, although the yield can be increased by using an excess of the Lewis acid. In contrast, the reaction with [$B(C_6F_5)_3$] leads to the formation of [Cp"$_2$Zr(μ_3,$\eta^{1:1:1:1}$-As$_4$){$B(C_6F_5)_3$}] (**7**). Probably due to the pronounced steric requirement of [$B(C_6F_5)_3$], only the formation of the mono-substituted compound **7** seems to be possible, interestigly also at a wingtip arsenic atom.

DFT calculations support the reaction outcome (B3LYP/def2-SVP level of theory; further information in the SI). In the case of the compounds **6** and **7** the coordination of the arsenic atoms directly bound to the zirconium is favored (−24 kJ·mol^{-1} (**6a**), −33 kJ·mol^{-1} (**6b**), −7 kJ·mol^{-1} (**6c**))[39] compared to coordination of the bridgehead arsenic atoms. Furthermore, the formation of the di-substituted compounds **6a**, **6b** and **6c**, is energetically clearly favored (**6a**: −28 kJ·mol^{-1}; **6b**: −24 kJ·mol^{-1}; **6c**: −7 kJ·mol^{-1}) over the mono-substituted compounds. These results unambiguously underline the experimental results.

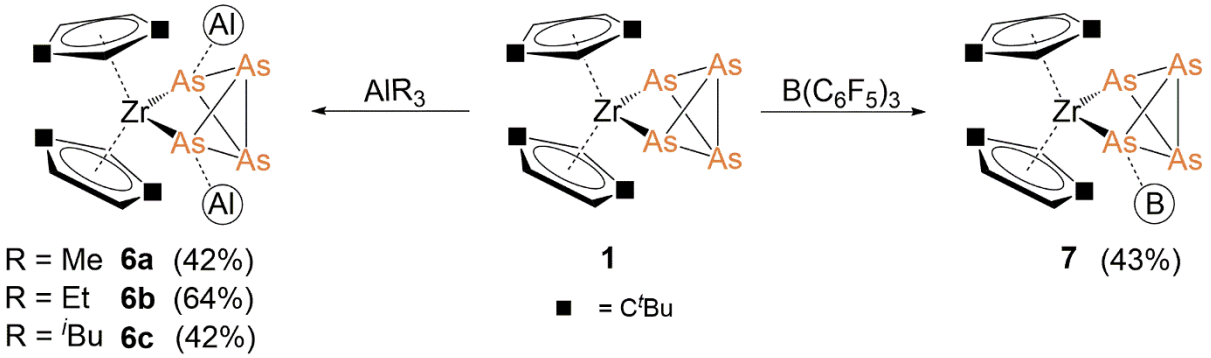

Scheme 3: Overview of the reactions of [Cp"$_2$Zr($\eta^{1:1}$-As$_4$)] (**1**) with Lewis acidic main group compounds.

Single crystals suitable for X-ray diffractions can be obtained by storing a concentrated *n*-pentane (**6a**, **6b**, **6c**) or *n*-hexane (**7**) solution at −78 °C. The molecular structures of **6a** and **7** are exemplarily depicted in Figure 4. In the case of the compounds **6** a di-coordination of **1** is observed, while in **7** only the mono- coordination of **1** to boron occurs. The geometric parameters of **6a**, **6b** and **6c** are very similar, therefore only **6a** will be discussed herein further (for **6b**, **6c** see SI). In **6a** and **7** the As$_4$-butterfly unit is only slightly distorted, which can be attributed to the steric repulsions. The As-As distances in **6a** of 2.4272(4) Å to 2.4583(3) Å and **7** of 2.436(3) Å to 2.457(4) Å does not differ considerably from that reported for **1**.[24] However,

the Zr-As distances are slightly elongated (**6a**: 2.6810(2) Å; **7**: 2.732(3) Å).[24] Similarly to **2**-**4**, the As-Al (**6a**: 2.6743(5) Å) and As-B (**7**: 2.177(6) Å) distances in **6a** and **7**, are slightly longer that the sum of the covalent radii (As-Al: 2.47 Å and As-B: 2.06 Å).[34]

The ^{1}H NMR spectra of **6a**, **6b**, **6c** and **7** show the expected signals for the Cp'' ligands as well as the signals of the alkyl groups bonded to aluminum in compounds **6**. A doublet and a triplet corresponding to the hydrogen atoms directly bonded to the cyclopentadienyl ligands resonate between δ = 5.0 ppm to 5.78 ppm for **6**. The corresponding signals for **7** are slightly more deshielded and resonates at 5.88 ppm and 6.06 ppm. Furthermore, a sharp singlet for the ^{t}Bu groups is observed (δ = 1.27 ppm (**6a**); 1.26 ppm (**6b**, **7**); 1.29 ppm (**6c**)). Additionally, the expected signals for the alkyl groups of the aluminum Lewis acids appears, for **6a** a singlet at −0.29 ppm (*cf.* SI for **6b** and **6c**).

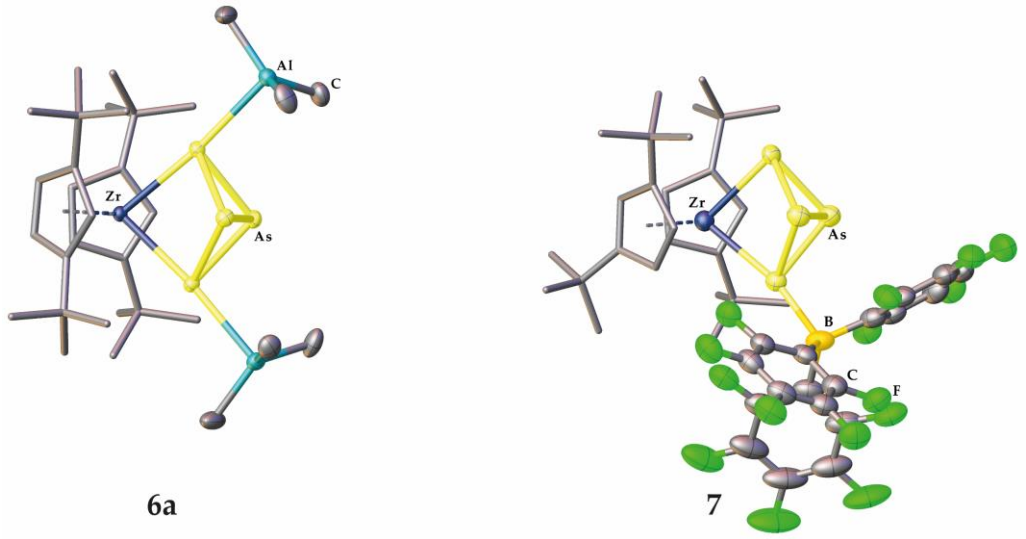

Figure 4: Molecular structures of **6a** and **7** in the solid state with thermal ellipsoids at 50% probability level. Hydrogen atoms are omitted, the Cp'' ligands and the [B(C$_6$F$_5$)$_3$] ligand are drawn in the tube model for clarity.

5.4 Conclusion

In conclusion, we reported herein the synthesis and characterization of a variety of coordination compounds based on $[Cp"_2Zr(\eta^{1:1}\text{-}As_4)]$ (**1**). Computational studies show the preferred coordination of the wingtip arsenic atoms for coordination as well as the preference for the formation of the di-substituted compounds. Experimentally, the coordination of the two wingtip arsenic atoms is observed for the transition metal complexes $[Cp"_2Zr(\mu_3,\eta^{1:1:1:1}\text{-}As_4)(W(CO)_5)_2]$ (**2**) and $[Cp"_2Zr(\mu_3,\eta^{1:1:1:1}\text{-}As_4)(CpMn(CO)_2)_2]$ (**3**). In contrast, the reaction of **1** with $[Fe_2(CO)_9]$ leads to the mono-substituted complex $[Cp"_2Zr(\mu,\eta^{1:1:1}\text{-}As_4)(Fe(CO)_4)]$ (**4**). NMR investigations show the formation of both, the mono-substituted (**4**) and di-substituted $[Cp"_2Zr(\mu_3,\eta^{1:1:1}\text{-}As_4)\{Fe(CO)_4\}_2]$ compounds, however, only **4** can be isolated. Elimination of CO from **4** leads to the formation of $[Cp"_2Zr(\mu,\eta^{3:1:1}\text{-}As_4)(Fe(CO)_3)]$ (**5**), in which the As_4-butterfly core is rearranged to a *cyclo*-As_4 ligand. In solutions, isolated **3** shows an interesting equilibrium between **3**, the mono-substituted complex $[Cp"_2Zr(\mu,\eta^{1:1:1:1}\text{-}As_4)\{CpMn(CO)_2\}]$ and **1**, while **4** do not dissociate in solution. The comparison of the reactivity of **1** and the phosphorus congener $[Cp"_2Zr(\mu,\eta^{1:1}\text{-}P_4)]$ towards transition metal based Lewis acids reveals pronounced discrepancies. While $[Cp"_2Zr(\mu,\eta^{1:1}\text{-}P_4)]$ can coordinate to LAs via both wingtip and bridgehead phosphorus atoms, and can form mono-, di- and tri-substituted complexes, **1** coordinates only through the wingtip arsenic atoms and forms only mono- or di-substituted complexes. The di-substituted complexes prevail. **1** reacts with Lewis acidic main group compounds similarly as with transition metal based LAs. Here, also a twofold coordination is observed for the compounds $[Cp"_2Zr(\mu_3,\eta^{1:1:1:1}\text{-}As_4)\{AlR_3\}_2]$ (R = Me (**6a**), Et (**6b**), ^{i}Bu (**6c**)). In contrast, the mono-substituted compound **7** is formed in the reaction with $[B(C_6F_5)_3]$, due to sterical reasons.

5.5 Supporting Information

5.5.1 Experimental Details

All experiments were performed under an atmosphere of dry nitrogen or argon using Schlenk and glovebox techniques. Solvents were purified, dried and degassed prior use. ^{1}H, $^{13}C\{^{1}H\}$ NMR spectra were recorded at room temperature on a Bruker Avance 400 spectrometer (^{1}H: 400,13 MHz, ^{13}C: 100.61 MHz). ^{1}H, ^{13}C NMR chemical shifts are reported in parts per million (ppm) relative to the external standard Me_4Si. Elemental analysis was determined with a Vario micro cube apparatus. For mass spectrometry a Finnigan MAT 95 (LIFDI MS, FD MS) or a Finnigan MAT SSQ 710 A (EI MS) device and a Joel AccuTOF GCX spectrometer were used. $[Fe_2(CO)_9]$ [40,41] and $[Cp''_2Zr(\eta^{1:1}\text{-}As_4)]$[24] were prepared according to literature procedures.

Synthesis and Characterization of $[Cp''_2Zr(\mu_3,\eta^{1:1:1:1}\text{-}As_4)(W(CO)_5)_2]$ (2):

$W(CO)_6$ (43 mg, 0.13 mmol) is dissolved in 50 mL thf and irradiated with UV light for 1 h using a low-pressure mercury lamp (TQ 150). The pale-yellow solution is added to a solution of $[Cp''_2Zr(\eta^{1:1}\text{-}As_4)]$ (**1**) (50 mg, 0.067 mmol) and stirred for 24 h. After removing the solvent *in vacuo*, the brown residue is extracted with *n*-hexane. Crystals of **2** suitable for single crystal X-ray structure analysis were obtained by storing a concentrated solution at −78 °C. Crystalline yield: 19 mg (0.014 mmol, 21%).

2: ^{1}H NMR (C_6D_6, 298 K): δ [ppm] = 1.26 (s, 36 H, CCH_3), 5.31 (t, br, 2 H, $C_5H_3{}^{t}Bu_2$), 5.48 (d, 4 H, $C_5H_3{}^{t}Bu_2$); **IR** (toluene): v [cm^{-1}] = 2064 (m), 1977 (vs), 1937 (s); **Elemental analysis** (%): calculated for $[C_{36}H_{42}ZrAs_4W_2O_{10}]$ (1391.77 g/mol): C, 31.03; H, 3.04; O, 11.48. No satisfying elemental analysis could be obtained, even by using Sn capsules. This is caused by the air sensitivity of compound **2**; **FD MS** (toluene): *m*/*z* (%): 1393.8 (12) $[M]^+$, 1070.2 (M^+-$[W(CO)_5]$, 100).

Synthesis and Characterization of $[Cp''_2Zr(\mu_3,\eta^{1:1:1:1}\text{-}As_4)(CpMn(CO)_2)_2]$ (3):

A solution of $[CpMn(CO)_3]$ (56 mg, 0.27 mmol) is dissolved in 50 mL thf and irradiated with UV light for 1 h using a low-pressure mercury lamp (TQ 150). The pale rose solution is added to solid $[Cp''_2Zr(\eta^{1:1}\text{-}As_4)]$ (**1**) (100 mg, 0.13 mmol). After stirring for 16 h at room temperature, the solvent of the red brown reaction mixture is removed *in vacuo*, extracted with 10 mL *n*-pentane and filtered via canula. A red solution is obtained. Crystals of **3** suitable for single crystal X-ray structure analysis were obtained by storing a concentrated solution at −78 °C. Crystalline yield: 15 mg (0.014 mmol, 11%).

3: ^{1}H NMR (C_6D_6, 298 K): δ [ppm] = 1.25 (s, 18 H, CCH_3), 1.36 (s, 36 H, CCH_3), 4.99 (t, 2 H, $C_5H_3{}^t Bu_2$), 5.26 (t, 2 H, $C_5H_3{}^t Bu_2$), 5.42 (t, 2 H, $C_5H_3{}^t Bu_2$); **Elemental analysis** (%): calculated for $[C_{40}H_{52}ZrAs_4Mn_2O_4]$ (1097.62 g·mol^{-1}): C, 43.77; H, 4.78; found: C, 42.68; H, 5.13; **IR** (toluene): v[cm-1] = 1928 (s), 1873 (s); **LIFDI MS** (toluene): *m*/*z* (%): 1095.9 (M^+, 42), 919.9 (M^+-[$CpMn(CO)_2$], 100).

Synthesis and Characterization of [Cp"$_2$Zr(µ,η$^{1:1:1}$-As$_4$)(Fe(CO)$_4$)] (4):

A solution of [Cp"$_2$Zr(η$^{1:1}$-As$_4$)] (**1**) (60 mg, 0.081 mmol) in 10 mL *n*-hexane is added to a suspension of [$Fe_2(CO)_9$] (58 mg, 0.16 mmol) in 10 mL *n*- hexane. The reaction mixture is stirred at room temperature for 24 h. From the brown reaction mixture, the solvent was removed *in vacuo*. The brown residue was dissolved in 5 mL *n*-pentane and filtered via canula. Crystals of **4** suitable for single crystal X-ray structure analysis were obtained by storing a concentrated solution at −78 °C. Crystalline yield: 11 mg (0.016 mmol, 20%).

4: ^{1}H NMR (C_6D_6, 298 K): δ [ppm] = 1.15 (s, 18 H, CCH_3), 1.28 (s, 18 H, CCH_3), 5.11 (t, 2 H, $C_5H_3{}^t Bu_2$), 5.22 (t, 2 H, $C_5H_3{}^t Bu_2$), 5.44 (t, 2 H, $C_5H_3{}^t Bu_2$); **Elemental analysis** (%): calculated for $[C_{30}H_{42}ZrAs_4FeO_4]$ (911.83 g/mol): C, 39.45; H, 4.63. No satisfying elemental analysis could be obtained, even by using Sn capsules. This is caused by the air sensitivity of compound **4**; **ATR-IR** (diamond crystal): v[cm^{-1}] = 2021 (m), 1949 (m), 1918 (s); **LIFDI MS** (toluene): *m*/*z* (%): 911.8 (M^+, 100).

Synthesis and Characterization of [Cp"$_2$Zr(µ,η$^{3:1:1}$-As$_4$)(Fe(CO)$_3$)] (5):

A solution of [Cp"$_2$Zr(η$^{1:1}$-As$_4$)] (**1**) (60 mg, 0.081 mmol) in 10 mL *n*-hexane is added to a suspension of [$Fe_2(CO)_9$] (58 mg, 0.24 mmol) in 10 mL *n*-hexane. The reaction mixture is refluxed for 3 h. All volatiles of the brown mixture are removed *in vacuo*, extracted with 10 mL of *n*-pentane and filtered via canula. Crystals of **5** suitable for single crystal X-ray structure analysis were obtained by storing a concentrated solution at −78 °C. Crystalline yield: 9 mg (0.01 mmol, 13%).

5: ^{1}H NMR (C_6D_6, 298 K): δ [ppm] = 1.32 (s, 36 H, CCH_3), 5.84 (d, 4 H, $C_5H_3{}^t Bu_2$), 5.95 (t, 2 H, $C_5H_3{}^t Bu_2$); **Elemental analysis** (%): calculated for $[C_{26}H_{42}ZrAs_4(Fe(CO)_4)]_{0.1}[C_{26}H_{42}ZrAs_4(Fe(CO)_3)]_{0.9}$ + 0.45·$[C_5H_{12}]$ (as found in the X-Ray structure, *cf.* SI): C, 40.90; H, 5.19; found: C, 40.71; H, 4.77; **ATR-IR** (diamand crystal): v[cm^{-1}] = 1919 (m), 2016 (m); **LIFDI MS** (toluene): *m*/*z* (%): 883.8 (M^+, 100).

Synthesis and Characterization of [Cp''$_2$Zr(µ$_3$,η$^{1:1:1:1}$-As$_4$){AlR$_3$}$_2$] (R = Me (6a), Et (6b), ^{i}Bu (6c):

A solution of AlR_3 (**6a**: 0.17 mL, c = 2.0 mol/L, 0.34 mmol; **6b**: 0.34 mL, c = 1.0 mol/L, 0.34 mmol; **6c**: 0.21 mL, c = 1 mol/L, 0.21 mmol) is added via syringe to a solution of [Cp''$_2$Zr(η$^{1:1}$-As$_4$)] (**1**) (50 mg, 0.067 mmol) in 10 mL toluene. The reaction mixture is stirred for 3 h at room temperature. After removing the solvent *in vacuo,* the orange red residue is dissolved in *n* pentane and filtered via canula. Crystals of **6a**/**6b**/**6c** suitable for single crystal X-ray structure analysis were obtained by storing a concentrated solution at −78 °C. Crystalline yield: **6a**: 25 mg (0.028 mmol, 42%); **6b**: 42 mg (0.043 mmol, 64%); **6c**: 32 mg (0.028 mmol, 42%).

6a: ^{1}H NMR (C_6D_6, 298 K): *δ* [ppm] = -0.29 (s, 18 H, Al*C*H_3), 1.27 (s, 36 H, C*C*H_3), 5.06 (t, 2 H, $C_5H_3{}^tBu_2$), 5.30 (d, 4 H, $C_5H_3{}^tBu_2$); **^{13}C{^{1}H} NMR** (C_6D_6, 298 K): *δ* [ppm] = -6.5 (s, Al(*C*H_3)$_3$), 32.6 (s, *C*(CH$_3$)$_3$), 34.1 (s, *C*H$_3$), 101.5 (s, *C*$_5$H$_3{}^t$Bu$_2$), 107.4 (s, *C*$_5$H$_3{}^t$Bu$_2$), 137.1 (s, *C*$_5$H$_3{}^t$Bu$_2$); **Elemental analysis** (%): calculated for [$C_{32}H_{60}ZrAs_4Al_2$] (888.02 g·mol^{-1}): C, 43.20; H, 6.80; found: C, 43.66; H, 6.66.

6b: **^{1}H NMR** (toluene-d$_8$, 298 K): *δ* [ppm] = 0.27 (q, 12 H, Al(*C*H_2CH$_3$), 1.26 (s, 36 H, C*C*H_3), 1.29 (m, 18 H, Al(CH$_2$C*H*$_3$), 5.00 (t, 2 H, $C_5H_3{}^tBu_2$), 5.27 (d, 4 H, $C_5H_3{}^tBu_2$); **^{13}C{^{1}H} NMR** (C_6D_6, 298 K): *δ* [ppm] = 32.5 (s, *C*(CH$_3$)$_3$), 34.1 (s, *C*H$_3$), 101.3 (s, *C*$_5$H$_3{}^t$Bu$_2$), 107.1 (s, *C*$_5$H$_3{}^t$Bu$_2$), 136.6 (s, *C*$_5$H$_3{}^t$Bu$_2$); **Elemental analysis** (%): calculated for [$C_{38}H_{72}ZrAs_4Al_2$] (972.12 g·mol^{-1}): C, 46.87; H, 7.45; found: C, 46.85; H, 7.11.

6c: ^{1}H NMR (thf-d$_8$, 298 K): *δ* [ppm] = - 0.08 (d, 12 H, Al(C*H*$_2$CH{CH$_3$}$_2$), 0.91 (d, 36 H, Al(CH$_2$CH{C*H*$_3$}$_2$), 1.29 (s, 36 H, C*C*H_3), 1.81 (m, 6 H, Al(CH$_2$C*H*{CH$_3$}$_2$), 5.08 (t, 2 H, $C_5H_3{}^tBu_2$), 5.76 (d, 4 H, $C_5H_3{}^tBu_2$); **^{13}C{^{1}H} NMR** (C_6D_6, 298 K): *δ* [ppm] = 24.8 (s, Al(^{i}*Bu*)$_3$), 26.7 (s, Al(^{i}*Bu*)$_3$), 28.5 (s, Al(^{i}*Bu*)$_3$), 32.6 (s, *C*(CH$_3$)$_3$), 34.1 (s, *C*H$_3$), 101.2 (s, *C*$_5$H$_3{}^t$Bu$_2$), 107.0 (s, *C*$_5$H$_3{}^t$Bu$_2$), 136.3 (s, *C*$_5$H$_3{}^t$Bu$_2$); **Elemental analysis** (%): calculated for [$C_{50}H_{96}ZrAs_4Al_2$] (888.02 g·mol^{-1}): C, 52.58; H, 8.45; found: C, 52.62; H, 8.15.

Synthesis and Characterization of [Cp''$_2$Zr(µ,η$^{1:1:1}$-As$_4$)(B(C$_6$F$_5$)$_3$)] (7):

A solution of [Cp''$_2$Zr(η$^{1:1}$-As$_4$)] (**1**) (60 mg, 0.081 mmol) in 10 mL *n*-hexane is added to a solution of [B(C$_6$F$_5$)$_3$] (81 mg, 0.16 mmol) in 10 mL *n*-hexane at −60 °C. The color changes immediately to brown and a brown solid is formed. After stirring for 2 h at −60 °C and further 2 h at room temperature the solvent is removed *in vacuo*. The brown residue is extracted with 5 mL of *n*-hexane and filtered via canula. Crystals of **7** suitable for single crystal X-ray structure analysis were obtained by storing the solution at −78 °C. Crystalline yield: 44 mg (0.034 mmol, 43%).

7: **^{1}H NMR** (thf-d_8, 298 K): δ [ppm] = 1.26 (s, 36 H, C*CH*$_3$), 5.88 (d, 4 H, $C_5H_3{}^tBu_2$), 6.06 (t, 2 H, $C_5H_3{}^tBu_2$). **^{19}F{^{1}H} NMR** (thf-d_8, 298 K): δ [ppm] = -162.28 (m, $B(C_6F_5)_3$, meta), -155.46 (m, $B(C_6F_5)_3$, para), -130.84 (m, $B(C_6F_5)_3$, ortho). **^{19}F NMR** (thf-d_8, 298 K): δ [ppm] = -162.28 (m, $B(C_6F_5)_3$, meta), -155.46 (m, $B(C_6F_5)_3$, para), -130.84 (m, $B(C_6F_5)_3$, ortho); **Elemental analysis** (%): calculated for [$C_{44}H_{42}ZrAs_4BF_{15}$] (1255.91 g/mol): C, 42.03; H, 3.37. No satisfying elemental analysis could be obtained, even by using Sn capsules. This is caused by the air sensitivity of compound **7**; **LIFDI MS** (toluene): Due to the instability of **7** only fragments could be detected. Inter alia: *m*/*z* (%): 966.75 ([Cp"$_2$Zr($B_2(C_6F_5)_3$]), 742.5 (M^+ - $B(C_6F_5)_3$);

5.5.2 Crystallographic Details

Crystals suitable for single crystal X-ray diffraction analysis were obtained as described above. The diffraction intensities were collected either on a Gemini Ultra diffractometer equipped with a Ruby or an Atlas^{S2} CCD detector using Cu-K_α radiation (fine-focus sealed X-ray tube) (**2**, **5**), at a XtaLAB Synergy R, DW system equipped with a HyPix-Arc 150 detector using Cu-K_α radiation (rotating-anode) (**7**), a GV50 diffractometer equipped with a Titan^{S2} CCD detector using Cu-K_α or Cu-K_β radiation (micro-focus sealed X-ray tube) (**3**, **6a**, **6b**, **6c**) or at a SuperNova diffractometer equipped with an Atlas CCD detector using Cu-K_α radiation (micro-focus sealed X-ray tube) (**4**). Data collection and reduction were performed with the **CrysAlisPro** software package (version 1.171.35.15 (**2**), 1.171.40.14a (**3**, **4**, **5**, **6c**); 1.171.40.18c (**6b**); 1.171.41.83a (**7**); 1.171.41.90a (**6a**)).[42] A numerical absorption correction based on gaussian integration over a multifaceted crystal model and an empirical absorption correction using spherical harmonics, implemented in SCALE3 ABSPACK scaling algorithm, was performed for the compounds (**3**, **4**, **6b**, **6c**, **7**).[42] An analytical numeric absorption correction using a multifaceted crystal model based on expressions derived by R. C. Clark & J. S. Reid. (Clark, R. C. & Reid, J. S. (1995). Acta Cryst. A51, 887-897) and an empirical absorption correction using spherical harmonics, implemented in SCALE3 ABSPACK scaling algorithm, was performed for compound (**5**).[42] A multi-scan absorption correction using spherical harmonics, implemented in SCALE3 ABSPACK scaling algorithm, was performed for the compounds (**2**, **6a**).[42] Using **Olex2**,[43] the structures were solved with **olex2.solve**[44] (**2**, **6b**, **7**) or **ShelXT**[45] (**3**, **4**, **5**, **6a**, **6c**) and refined by full-matrix least-squares method against $|F|^2$ using **ShelXL**[45] All non-hydrogen atoms were refined anisotropically. Hydrogen atoms at the carbon atoms were located in idealized positions and refined with isotropic displacement parameters according to the riding model. Using **Olex2**,[43] all pictures of the respective molecular structures were made.

CCDC reference numbers 2077256 (**2**), 2077257 (**3**), 2077258 (**4**), 2077259 (**5**), 2077260 (**6a**), 2077261 (**6b**), 2077262 (**6c**) and 2077263 (**7**) contain the supplementary crystallographic data for this paper. These data can be obtained free of charge at www.ccdc.cam.ac.uk/conts/retrieving.html (or from the Cambridge Crystallographic Data Centre, 12 Union Road, Cambridge CB2 1EZ, UK; Fax: + 44-1223-336-033; e-mail: deposit@ccdc.cam.ac.uk).

[Cp"$_2$Zr($\eta^{1:1:1:1}$-As$_4$)(W(CO)$_5$)$_2$] (2):

Compound **2** crystallizes out of a concentrated *n*-hexane solution at -78 °C in form of red blocks in the triclinic space group *P*-1. The asymmetric unit contains one molecule of **2**.

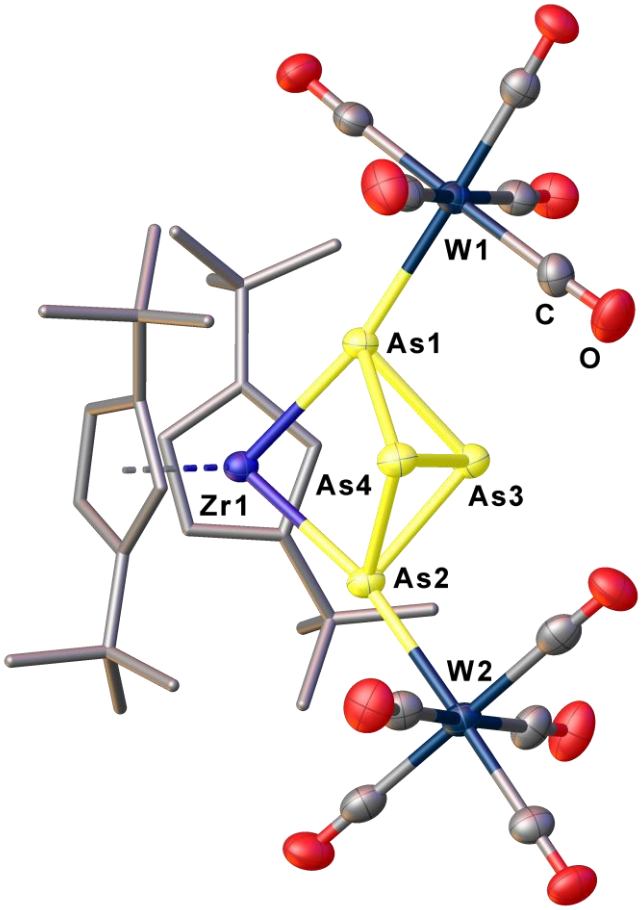

Figure S1: Molecular structure of **2** in the solid state. Thermal ellipsoids are depicted at 50% probability level. Hydrogen atoms are omitted and the Cp" ligands are drawn in the tube model for clarity. Selected bond lengths [Å] and angles [°]: As1-As2 2.4575(6), As1-As3 2.4616(6), As1-W1 2.6460(4), As1-Zr1 2.7021(5), As2-As3 2.4363(6), As2-As4 2.4558(6), As3-As4 2.4649(6), As4-W2 2.6595(4), As4-Zr1 2.7008(5); As2-As1-As3 59.374(18), As2-As1-W1 104.814(19), As2-As1-Zr1 82.962(17), As3-As1-W1 107.84(2), As3-As1-Zr1 83.495(18), W1-As1-Zr1 168.38(2), As3-As2-As1 60.397(18), As3-As2-As4 60.508(18), As4-As2-As1 93.02(2), As1-As3-As4 92.70(2), As2-As3-As1 60.229(18), As2-As3-As4 60.139(18), As2-As4-As3 59.352(18), As2-As4-W2 107.436(19), As2-As4-Zr1 83.020(18), As3-As4-W2 106.51(2), As3-As4-Zr1- 83.461(18), W2-As4-Zr 1168.14(2).

[Cp''$_2$Zr(η$^{1:1:1:1}$-As$_4$)(CpMn(CO)$_2$)$_2$] (3):

Compound **3** crystallizes out of a concentrated *n*-pentane solution at -78 °C in form of violet blocks in the triclinic space group $P\bar{1}$. The asymmetric unit contains one molecule of **3**. One [CpMn(CO)$_2$] fragment is disordered over two positions (occupancy of 0.52 and 0.48).

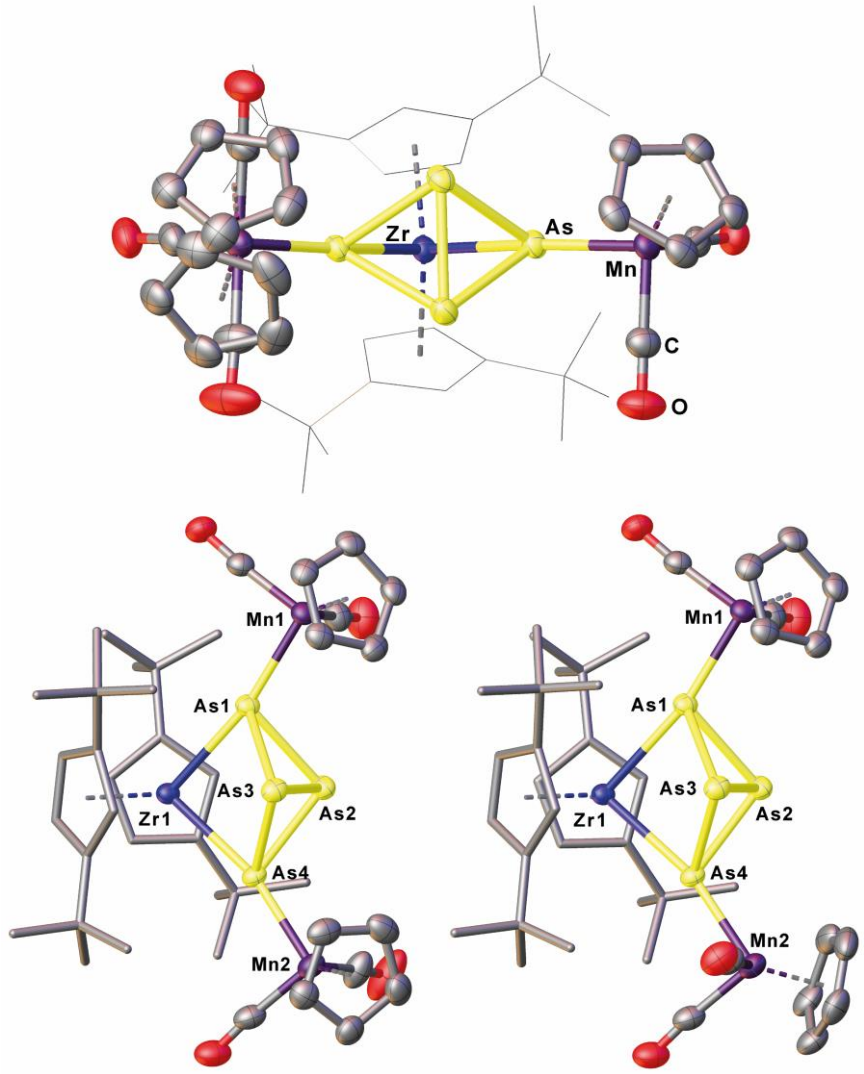

Figure S2: Molecular structure of **3** in the solid state (above). Thermal ellipsoids are depicted at 50% probability level. Hydrogen atoms are omitted and the Cp'' ligands are drawn in the wireframe model for clarity. The separate parts of the disorder are depicted below (left: part1, occupancy of 52%; right: part2, occupancy of 48%). Hydrogen atoms are omitted and the Cp'' ligands are drawn in the tube model for clarity. Selected bond lengths [Å] and angles [°]:Zr1-As4 2.6874(3), Zr1-As1 2.6837(3), As4-As2 2.4726(4), As4-As3 2.4666(4), As4-Mn2 2.3732(5), As1-As2 2.4710(4), As1-As3 2.4699(4), As1-Mn1 2.3605(4), As2-As3 2.4394(4); As1-Zr1-As4 85.871(9), As2-As4-Zr1 80.039(11), As3-As4-Zr1 80.228(10), As3-As4-As2 59.193(11), Mn2-As4-Zr1 166.512(16), Mn2-As4-As2 112.664(16), Mn2-As4-As3 109.772(15), As2-As1-Zr1 80.139(11), As3-As1-Zr1 80.242(10), As3-As1-As2 59.170(11), Mn1-As1-Zr1 167.600(15), Mn1-As1-As2 108.773(15), Mn1-As1-As3 111.582(15), As1-As2-As4 95.477(13), As3-As2-As4 60.282(11), As3-As2-As1 60.393(11), As4-As3-As1 95.656(12), As2-As3-As4 60.525(11), As2-As3-As1 60.437(11).

[Cp"$_2$Zr(µ,η$^{1:1:1}$-As$_4$)(Fe(CO)$_4$)] (4):

Compound **4** crystallizes out of a concentrated *n*-pentane solution at -78 °C in form of orange plates in the monoclinic space group $P2_1/m$. The asymmetric unit contains half a molecule of **4**. One carbonyl ligand, which is located on a mirror plane, shows a disorder over three positions (occupancy of 0.6, 0.2 and 0.2). To describe the disorder the restrains ISOR and SIMU were used.

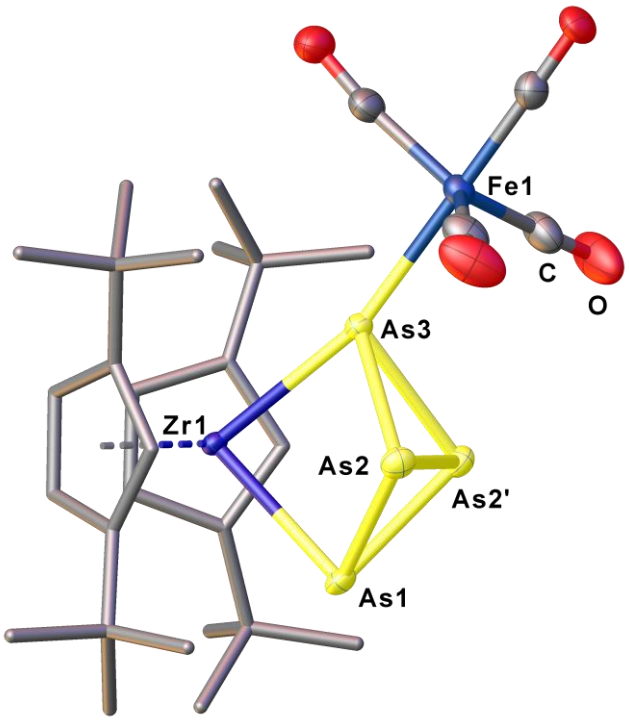

Figure S3: Molecular structure of **4** in the solid state. Thermal ellipsoids are depicted at 50% probability level. Hydrogen atoms are omitted and the Cp'' ligands are drawn in the tube model for clarity. Selected bond lengths [Å] and angles [°]: Zr1-As3 2.7078(4), Zr1-As1 2.6851(5), As3-As2 2.4791(4), As3-As2' 2.4791(4), As3-Fe1 2.4213(7), As1-As2 2.4457(4), As1-As2' 2.4457(4), As2-As2' 2.4321(6); As1-Zr1-As3 83.029(14), Fe1-As3-As2 110.125(19), Fe1-As3-As2' 110.125(19), As2'-As1-Zr1 83.508(13), As2-As1-Zr1 83.508(14)As2'-As1-As2 59.632(17), As1-As2-As3 93.072(14), As2^1-As2-As3 60.626(8), As2'-As2-As1 60.184(8).As2'-As3-Zr1 82.416(13), As2-As3-Zr1 82.416(13), As2-As3-As2' 58.748(16), Fe1-As3-Zr1 165.46(2).

[Cp''$_2$Zr(µ,η$^{3:1:1}$-As$_4$)(Fe(CO)$_3$)] (5):

Compound **5** crystallizes out of a concentrated *n*-pentane solution at -78 °C in form of violet plates in the orthorombic space group P*nma*. The asymmetric unit contains half a molecule of **5** and an only partly occupied pentane solvent molecule. Due to heavy disorder, it was not possible to model the pentane solvent molecule. Therefore, a solvent mask was calculated and 162 electrons were found in a volume of 756 Å^3 in 1 void per unit cell. This is consistent with the presence of 0.45 pentane molecules per asymmetric unit, which account for 151 electrons per unit cell. Further, compound **5** co-crystallizes with compound **4**. This co-crystallization is presented by the disorder of an As atom and a Fe(CO)$_4$ fragment (0.9 to 0.1). However, due to the low occupancy (0.1) and the disordered pentane molecule (overlapping positions) it was not possible to properly locate the CO ligands of the Fe(CO)$_4$ fragment.

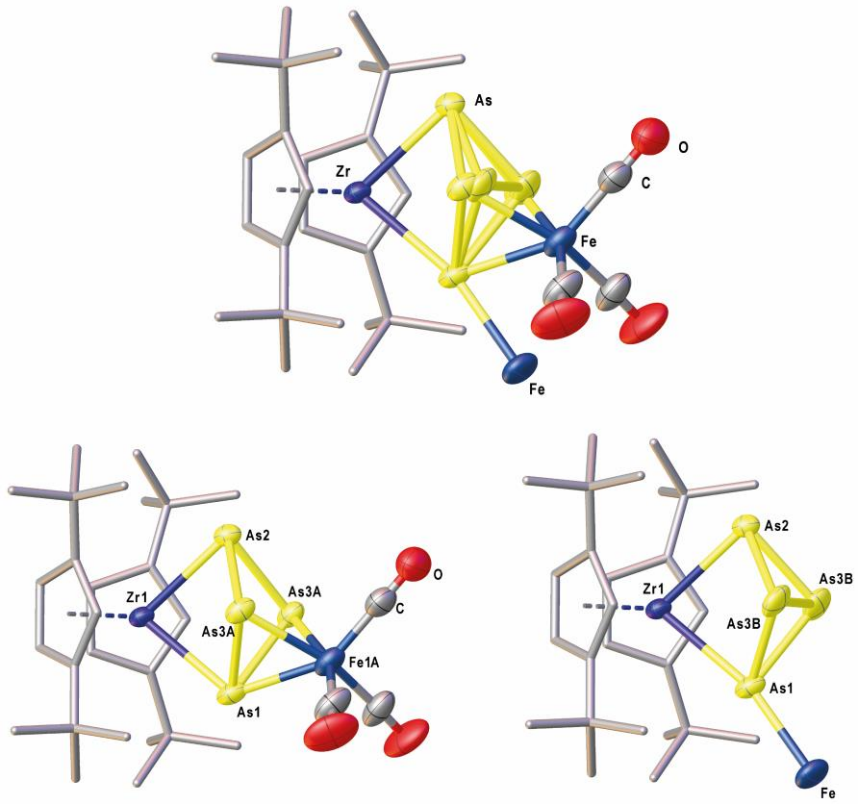

Figure S4: Molecular structure of **5** in the solid state. Thermal ellipsoids are depicted at 50% probability level. Hydrogen atoms are omitted and the Cp'' ligands are drawn in the wireframe model for clarity. Selected bond lengths [Å] and angles [°]: Zr1-As2 2.7105(8), Zr1-As1 2.7513(8), As2-As3A 2.4657(14), As2-As3B 2.377(14), As1-As3A 2.4721(13), As1-Fe1A 2.4265(15), As1-As3B 2.433(14), As3B-As3B^1 2.391(18), As1-Fe1B 2.393(11), As3A-Fe1A 2.4151(16); As2-Zr1-As1 79.85(2), As3B^1-As2-Zr1 84.9(4), As3A-As1-Zr1 78.54(4), As3A-As1-As3A^1 75.65(7), Fe1A-As1-Zr1 124.84(4), Fe1A-As1-As3A 59.07(4), Fe1A-As1-As3B 50.4(3), As3B-As1-Zr1 82.9(4), As3B^1-As1-As3B 58.9(5), Fe1B-As1-Zr1 165.8(3, Fe1B-As1-As3B 109.3(5), As2-As3A-As1 90.45(5), Fe1A-As3A-As2 99.36(5), Fe1A-As3A-As1 59.52(4), As3A-Fe1A-As1 61.40(4), As3A-Fe1A-As3A^1 77.76(7), As2-As3B-As1 93.6(5), As2-As3B-As3B 59.8(2), As3B^1-As3B-As1 60.6(2), As3A-As2-Zr1 79.44(4), As3A^1-As2-As3A 75.88(6), As3B-As2-Zr1 84.9(4).

[Cp"$_2$Zr(µ$_3$,η$^{1:1:1:1}$-As$_4$){AlMe$_3$}$_2$] (6a):

Compound **6a** crystallizes out of a concentrated *n*-pentane solution at -30°C in form of orange blocks in the monoclinic space group *I*2/*a*. The asymmetric unit contains half a molecule of **6a**. The crystals of **6a** were twinned. Therefore, a refinement as a 2- component twin (BASF 0.57) was performed.

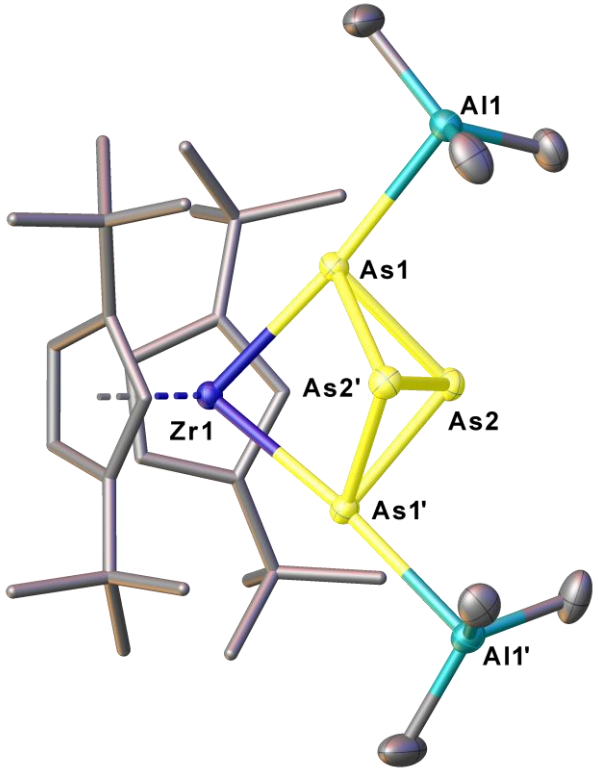

Figure S5: Molecular structure of **6a** in the solid state. Thermal ellipsoids are depicted at 50% probability level. Hydrogen atoms are omitted and the Cp" ligands are drawn in the tube model for clarity. Selected bond lengths [Å] and angles [°]: Zr1-As1' 2.6810(2), Zr1-As1 2.6810(2), As1-As2 2.4513(2), As1-As2'-2.4583(3), As1-Al1 2.6743(5), As2-As2' 2.4272(4); As1-Zr1-As1' 81.591(8), As2'-As1-Zr1 84.745(7), As2-As1-Zr1 84.881(7), As2-As1-As2' 59.258(9), As2-As1-Al1 100.118(13), As2'-As1-Al1 100.245(14), Al1-As1-Zr1 174.223(13), As1-As2-As1' 91.049(9), As2'-As2-As1' 60.225(8), As2'-As2-As1 60.515(8).

$[Cp''_2Zr(\mu_3,\eta^{1:1:1:1}\text{-}As_4)\{AlEt_3\}_2]$ (6b):

Compound **6b** crystallizes out of a concentrated *n*-pentane solution at -30 °C in form of orange plates in the monoclinic space group *C*2/*c*. The asymmetric unit contains half a molecule of **6b**. The three ethyl substituents at $AlEt_3$ are disordered over two positions (occupancy 0.63:0.37; 0.63:0.37; 0.65:0.35). To describe the disorder of these ethyl substituents the restrains SADI and SIMU were used.

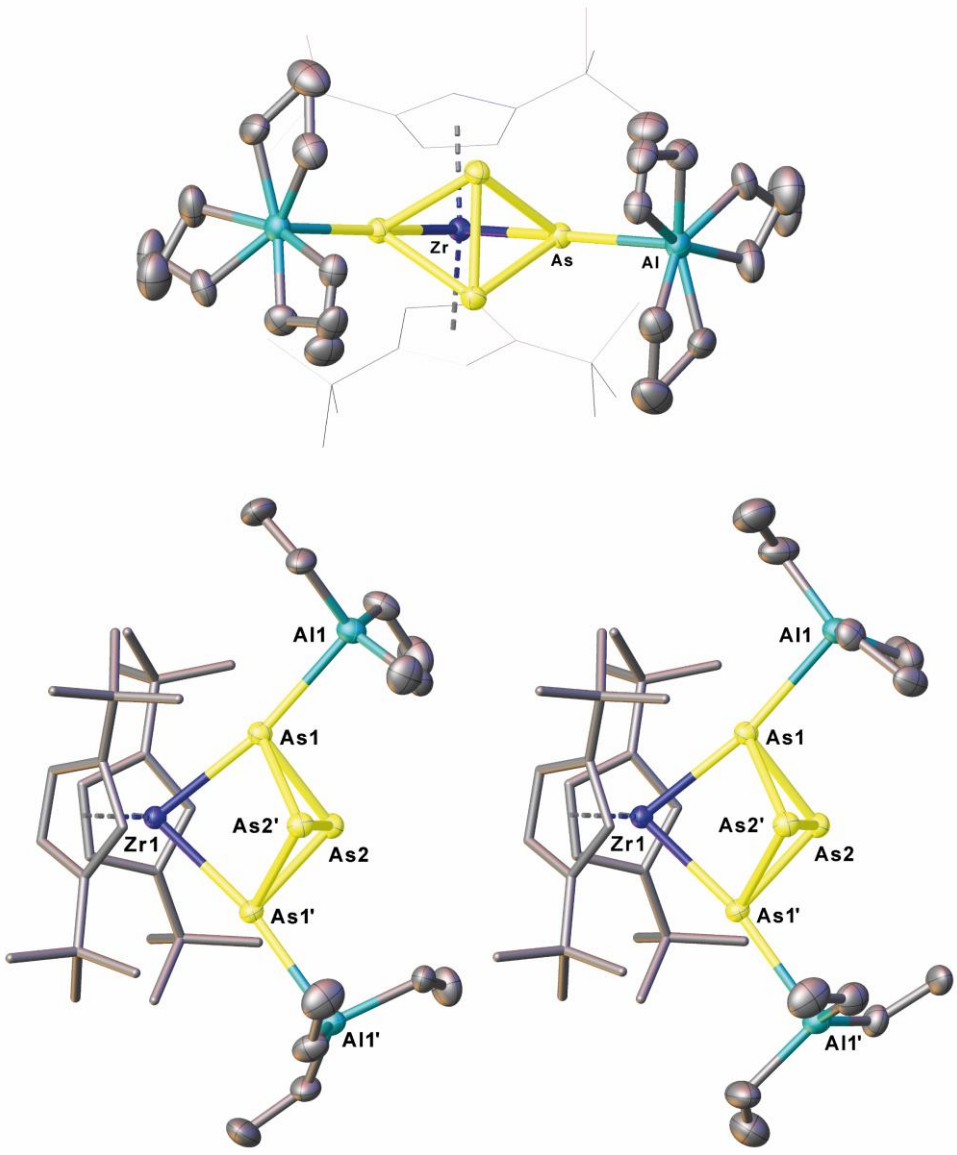

Figure S6: Molecular structure of **6b** in the solid state (above). Thermal ellipsoids are depicted at 50% probability level. Hydrogen atoms are omitted and the Cp'' ligands are drawn in the wireframe model for clarity. The separate parts of the disorder are depicted below (left: part1, occupancy of 63%; right: part2, occupancy of 37%). Selected bond lengths [Å] and angles [°]: Zr1-As1 2.7018(2), Zr1-As1' 2.7019(2), As1-As2' 2.4637(2), As1-As2 2.4583(2), As1-Al1 2.7415(5), As2-As2' 2.4202(3); As1-Zr1-As1' 81.216(8), Zr1-As1-Al1 170.087(13), As2'-As1-Zr1 84.937(7), As2-As1-Zr1 85.042(6),As2-As1-As2' 58.907(8), As2-As1-Al1 102.934(13), As2'-As1-Al1 104.161(13), As1-As2-As1' 91.218(8), As2'-As2-As1' 60.435(7), As2'-As2-As1 60.658(7).

[Cp"$_2$Zr(µ$_3$,η$^{1:1:1:1}$-As$_4$){Al^{i}Bu$_3$}$_2$] (6c):

Compound **6c** crystallizes out of a concentrated *n*-pentane solution at -30 °C in form of orange blocks in the monoclinic space group *C*2/*c*. The asymmetric unit contains half a molecule of **6c**. A ^{i}Bu substituent of the Al^{i}Bu$_3$ ligand is disordered over two positions (occupancy of 0.86 and 0.14). To describe the disorder the restrains SADI and SIMU were used.

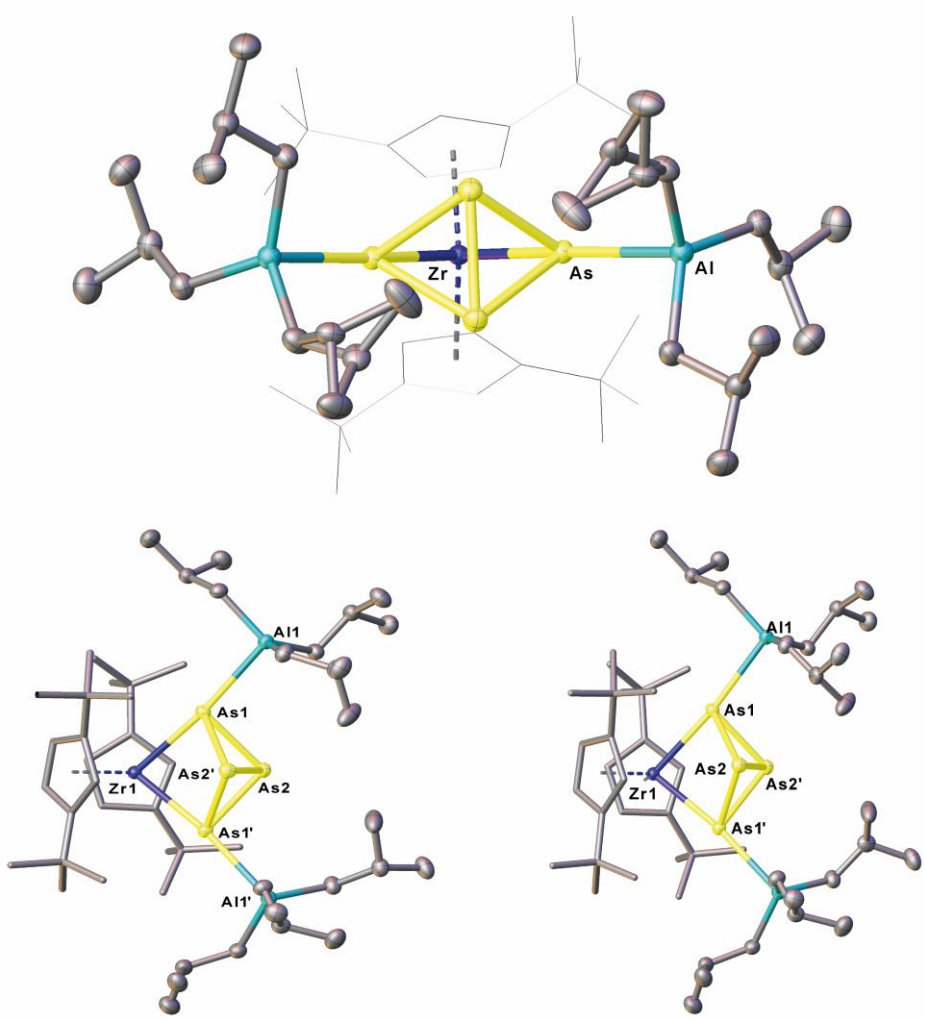

Figure S7: Molecular structure of **6c** in the solid state (above). Thermal ellipsoids are depicted at 50% probability level. Hydrogen atoms are omitted and the Cp'' ligands are drawn in the wireframe model for clarity. The separate parts of the disorder are depicted below (left: part1, occupancy of 86%; right: part2, occupancy of 14%). Selected bond lengths [Å] and angles [°]: Zr1-As1' 2.6810(3), Zr1-As1 2.6810(3), As1-As2' 2.4696(3), As1-As2 2.4550(3), As1-Al1 2.7566(6), As2-As2' 2.4281(4); As1'-Zr1-As1 83.462(11), Zr1-As1-Al1 172.833(15), As2'-As1-Zr1 82.784(8), As2-As1-Zr1 83.057(9), As2-As1-As2' 59.081(11), As2'-As1-Al1 104.082(15), As2-As1-Al1 102.142(15), As1-As2-As1' 92.896(11), As2'-As2-As1' 60.159(9), As2'-As2-As1 60.760(10).

[Cp"$_2$Zr(µ,η$^{1:1:1}$-As$_4$)(B(C$_6$F$_5$)$_3$)] (7):

Compound **7** crystallizes out of a concentrated *n*-hexane solution at -30 °C in form of clear orange blocks in the triclinic space group $P\bar{1}$. The asymmetric unit contains one molecule of **7**. The [Cp"$_2$Zr(µ,η$^{1:1}$-As$_4$)] fragment is disordered over two positions (occupancy of 0.77 and 0.23). To describe the disorder the restrains SADI, SIMU and ISOR were used.

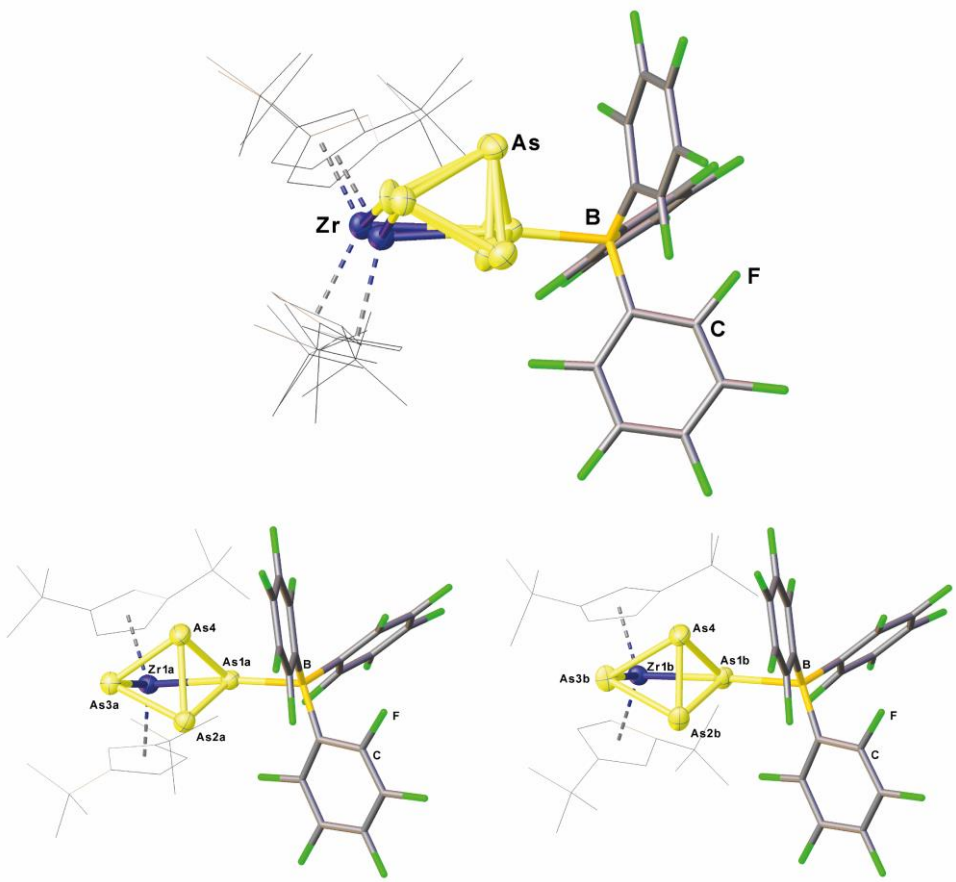

Figure S8: Molecular structure of **7** in the solid state (above). Thermal ellipsoids are depicted at 50% probability level. Hydrogen atoms are omitted, the Cp" ligands are drawn in the wireframe model and the the [BC$_{18}$F$_{15}$] unit is drawn in the tube model for clarity. The separate parts of the disorder are depicted below (left: part1, occupancy of 77%; right: part2, occupancy of 23%). Selected bond lengths [Å] and angles [°]: As1A-As2A 2.457(4), As3A-As4 2.436(3), As3A-As2A 2.437(4), As4-As1A 2.445(3), As4-As2A 2.442(3), As4-As1B 2.552(9), As4-As2B 2.357(13), As4-As3B 2.543(12), As4-As3B 2.543(12), As1B-As2B 2.434(14), Zr1B-As1B 2.789(7), Zr1B-As3B 2.595(10), Zr1A-As3A 2.732(3), Zr1A-As1A 2.732(2), As1A-B1 2.177(6), B1-As1B 2.518(8); As1A-Zr1A-As3A 79.83(8), As2A-As3A-Zr1A 86.27(11), As2A-As4-As1A 60.36(10), As2A-As1A-Zr1A85.89(10), As3A-As2A-As4 59.89(10), As3A-As2A-As1A 91.51(11), As3A-As4-As1A 91.85(9), As3A-As4-As2A 59.96(10), As4-As2A-As1A 59.87(10), As4-As1A-Zr1A 83.69(7), As4-As1A-As2A 59.76(10), As4-As3A-Zr1A 83.86(10), As4-As3A-As2A 60.15(11), As2B-As4-As1B 59.3(3), As2B-As4-As3B 59.5(4), As3B-As4-As1B 85.3(3), As4-As1B-Zr1B 86.7(3), As2B-As1B-As4 56.4(4), As2B-As1B-B1 94.8(3), As2B-As1B-Zr1B 85.8(4), As4-As2B-As1B 64.4(4), As4-As2B-As3B 64.1(4), As1B-As2B-As3B 90.3(4), As4-As3B-Zr1B 91.2(4), As2B-As3B-As4 56.4(4), As2B-As3B-Zr1B 90.2(5), B1-As1B-As4 95.9(3), B1-As1A-As4 109.00(18), B1-As1A-As2A 101.90(17).

Table S1: Structure determination summary of the complexes **2**, **3** and **4**.

Compound	**2**	**3**	**4**
Formula	$C_{36}H_{42}As_4O_{10}W_2Zr$	$C_{40}H_{52}As_4Mn_2O_4Zr$	$C_{30}H_{42}As_4FeO_4Zr$
CCDC number	2077256	2077257	2077258
$D_{calc.}$/ g cm^{-3}	2.151	1.752	1.764
m/mm^{-1}	15.466	7.938	10.399
Formula Weight	1393.29	1097.59	913.38
Colour	red	violet	clear light orange
Shape	block	block	plate
Size/mm^3	0.15×0.07×0.03	0.25×0.19×0.10	0.27×0.19×0.09
T/K	123(1)	122.99(11)	123.01(10)
Crystal System	triclinic	triclinic	monoclinic
Space Group	P-1	P-1	$P2_1/m$
a/Å	11.0989(3)	11.5684(3)	9.1335(2)
b/Å	12.5065(3)	12.1340(4)	17.1283(3)
c/Å	17.5582(5)	16.8248(4)	11.3330(2)
α/°	101.764(2)	80.103(2)	90
β/°	95.394(2)	89.979(2)	104.114(2)
γ/°	113.207(2)	63.838(2)	90
V/Å^3	2151.41(10)	2080.60(11)	1719.43(6)
Z	2	2	2
Z'	1	1	0.5
Wavelength/Å	1.54178	1.39222	1.54184
Radiation type	CuK$_\alpha$	Cu K$_\alpha$	Cu K$_\alpha$
θ_{min}/°	3.986	2.416	4.022
θ_{max}/°	66.565	74.751	72.087
Measured Refl's.	36658	46763	10794
Ind't Refl's	7562	11522	3482
Refl's with I≥σ(I)	7021	10758	3418
R_{int}	0.0320	0.0415	0.0264
Parameters	490	535	217
Restraints	0	0	42
Largest Peak	1.615	0.806	1.429
Deepest Hole	-0.984	-1.049	-0.906
GooF	1.068	1.065	1.127
wR_2 (all data)	0.0730	0.0853	0.0670
wR_2	0.0711	0.0834	0.0666
R_1 (all data)	0.0297	0.0346	0.0259
R_1	0.0270	0.0323	0.0253

Table S2: Structure determination summary of the complexes **5**, **6a** and **6b**.

Compound	**5**	**6a**	**6b**
Formula	$C_{33.2}H_{52.8}As_4FeO_{2.7}Zr$	$0.5\cdot(C_{32}H_{60}Al_2As_4Zr)$	$0.5\cdot(C_{38}H_{72}Al_2As_4Zr)$
CCDC number	2077259	2077260	2077261
$D_{calc.}$/ g cm^{-3}	1.594	1.537	1.465
m/mm^{-1}	9.098	4.969	4.361
Formula Weight	941.90	889.66	973.81
Colour	dark violet	dark orange	orange
Shape	plate-shaped	block	plate
Size/mm^3	0.25×0.20×0.14	0.20×0.11×0.08	0.25×0.21×0.12
T/K	123(1)	122.99(11)	123.00(11)
Crystal System	orthorhombic	monoclinic	monoclinic
Space Group	*Pnma*	*I*2/*a*	*C*2/*c*
a/Å	12.0528(5)	17.6443(3)	25.1728(4)
b/Å	17.2716(7)	9.95170(16)	10.3746(2)
c/Å	18.8597(6)	23.1782(4)	18.0895(3)
α/°	90	90	90
β/°	90	109.1757(19)	110.797(2)
γ/°	90	90	90
V/Å^3	3926.0(3)	3844.08(12)	4416.40(14)
Z	4	4	4
Z'	0.5	0.5	0.5
Wavelength/Å	1.54184	1.39222	1.39222
Radiation type	Cu K_α	Cu K_α	Cu K_α
θ_{min}/°	3.470	3.646	3.392
θ_{max}/°	71.632	74.104	74.810
Measured Refl's.	11708	9433	22870
Ind't Refl's	3893	9433	6087
Refl's with I≥σ(I)	3256	8609	5789
R_{int}	0.0392	0.0752	0.0304
Parameters	202	188	264
Restraints	2	0	19
Largest Peak	1.294	1.497	0.806
Deepest Hole	-0.660	-0.897	-0.529
GooF	1.030	1.018	1.064
wR_2 (all data)	0.1108	0.1192	0.0631
wR_2	0.1051	0.1175	0.0620
R_1 (all data)	0.0501	0.0430	0.0256
R_1	0.0408	0.0407	0.0242

Table S3: Structure determination summary of the complexes **6c** and **7**.

Compound	**6c**	**7**
Formula	$0.5\cdot(C_{50}H_{96}Al_2As_4Zr)$	$C_{44}H_{42}As_4BF_{15}Zr$
CCDC number	2077262	2077263
$D_{calc.}$/ g cm^{-3}	1.343	1.823
m/mm^{-1}	3.465	6.020
Formula Weight	1142.12	1257.48
Colour	orange	clear orange
Shape	block	block
Size/mm^3	0.22×0.17×0.10	0.21×0.14×0.11
T/K	123.00(10)	123.00(10)
Crystal System	monoclinic	triclinic
Space Group	*C*2/*c*	*P*-1
a/Å	18.5668(4)	11.2797(4)
b/Å	11.9157(2)	12.7421(5)
c/Å	27.2938(5)	18.5702(6)
α/°	90	71.815(3)
β/°	110.737(2)	87.410(3)
γ/°	90	65.217(4)
V/Å^3	5647.2(2)	2290.82(16)
Z	4	2
Z'	0.5	1
Wavelength/Å	1.39222	1.54184
Radiation type	Cu K_α	Cu K_α
θ_{min}/°	3.127	2.517
θ_{max}/°	64.688	73.366
Measured Refl's.	20223	28611
Ind't Refl's	6481	8705
Refl's with I≥σ(I)	5866	7895
R_{int}	0.0282	0.0456
Parameters	280	880
Restraints	34	371
Largest Peak	0.804	0.610
Deepest Hole	-0.456	-0.814
GooF	1.049	1.136
wR_2 (all data)	0.0662	0.1158
wR_2	0.0642	0.1134
R_1 (all data)	0.0335	0.0502
R_1	0.0289	0.0457

5.5.4 NMR spectra

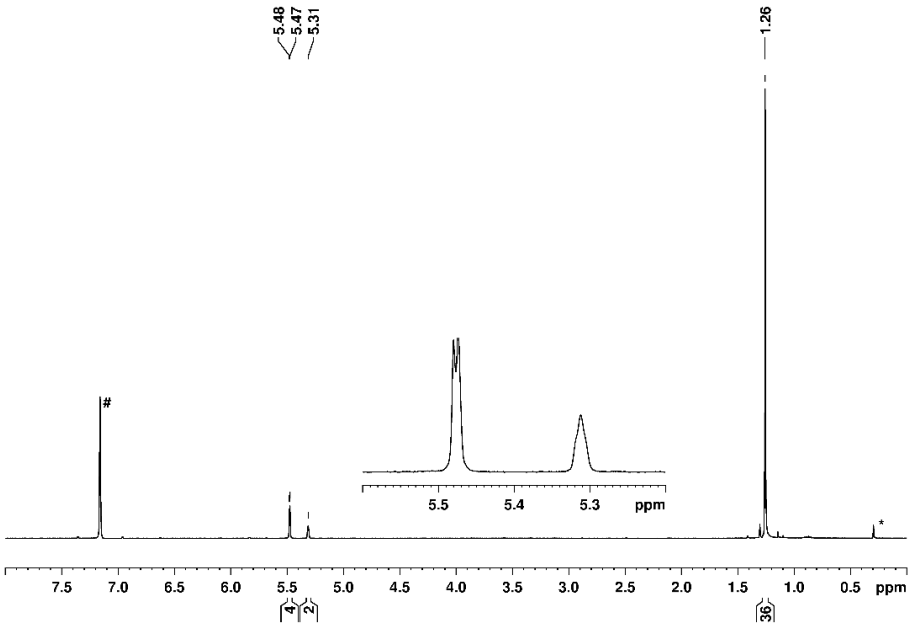

Figure S9: ^{1}H NMR spectrum of **2** at 293 K in C_6D_6 (#). The signal marked with * is due to silicon grease.

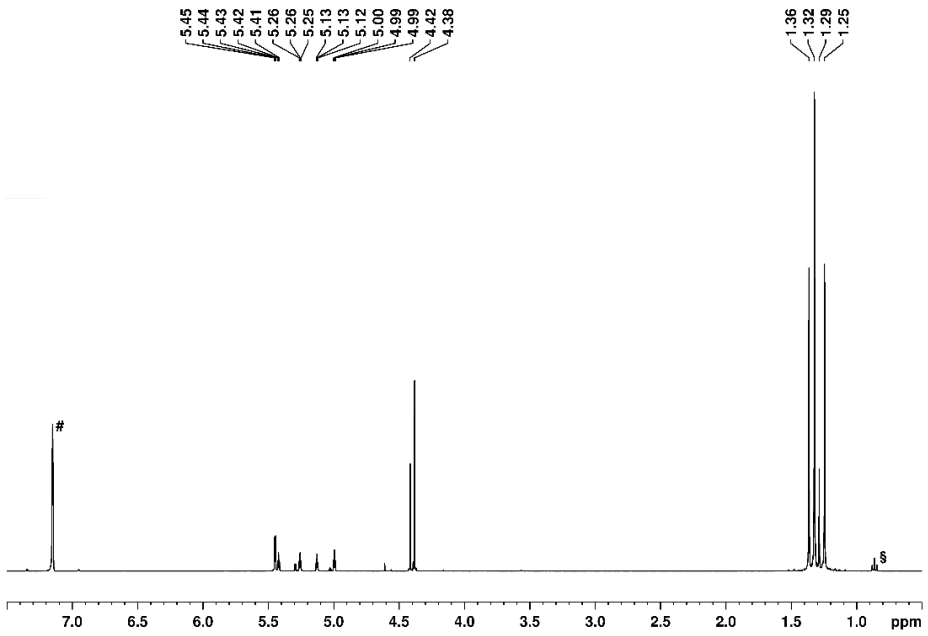

Figure S10: ^{1}H NMR spectrum of **3** at 293 K in C_6D_6 (#). The signal marked with § is due to *n*-pentane. A signal corresponding to the free $CpMn(CO)_2$ fragment could not be detected in the ^{1}H NMR, probably due to a highly dynamic behavior or a triplet spin state.

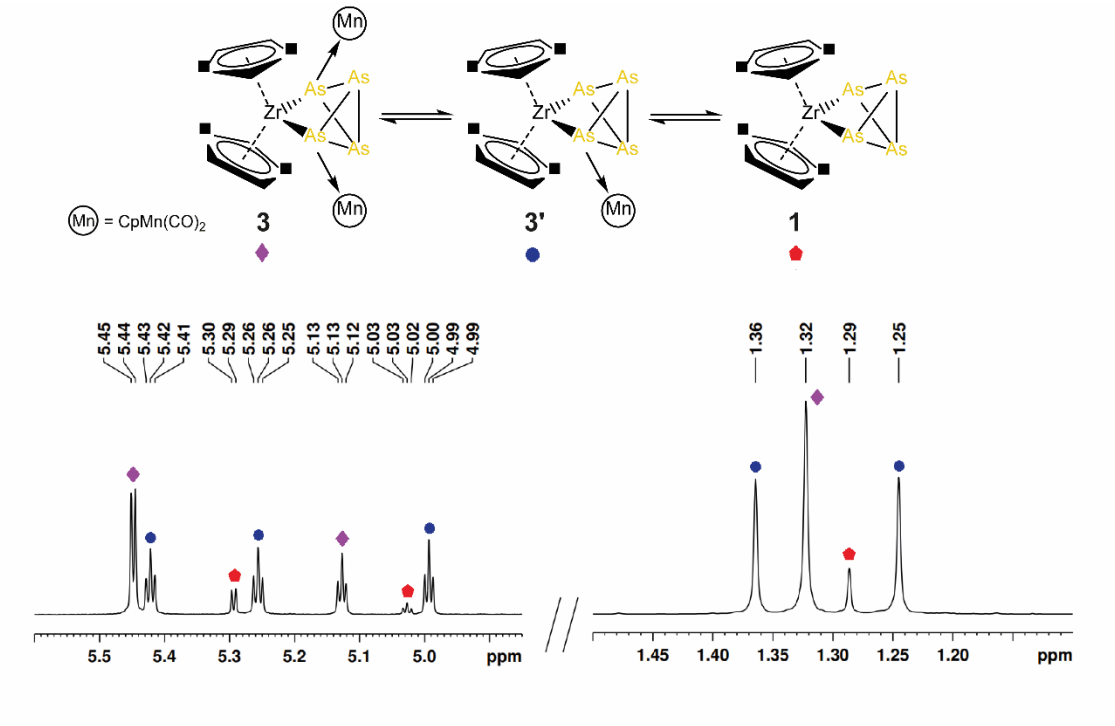

Figure S11: Parts of the ^{1}H NMR spectrum of **3** at 293 K in C_6D_6.

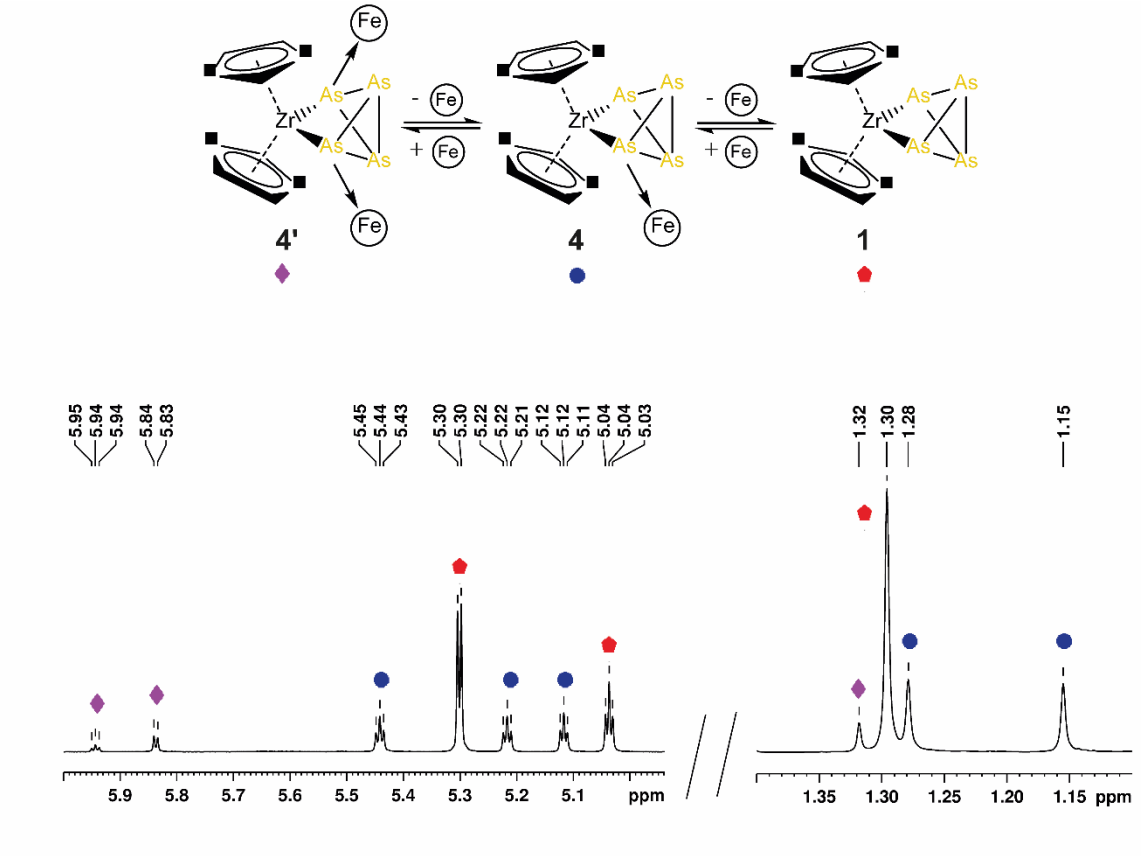

Figure S12: Parts of the ^{1}H NMR spectrum of the reaction solution of **1** with $[Fe_2(CO)_9]$ at 293 K in C_6D_6.

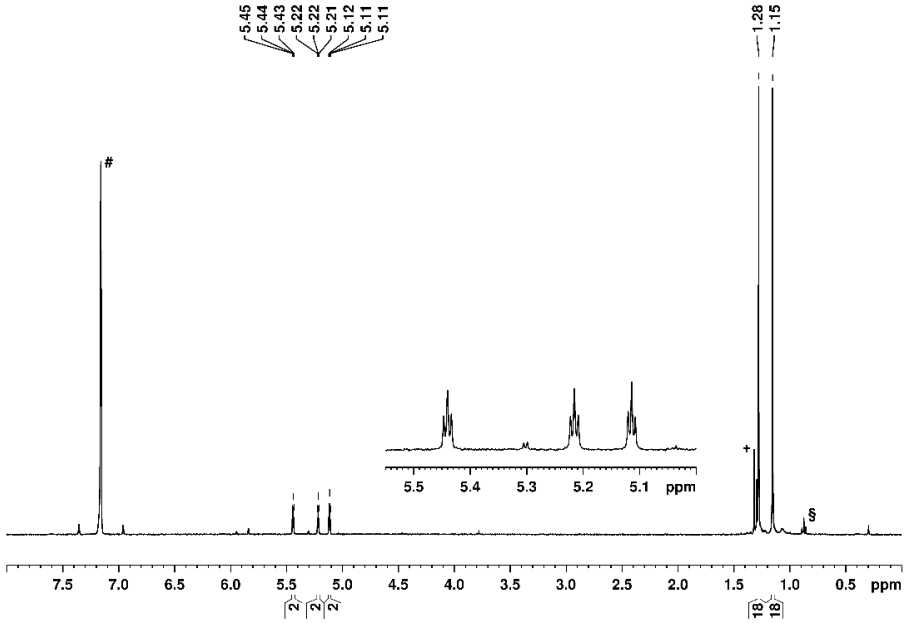

Figure S13: ^{1}H NMR spectrum of **4** at 293 K in C_6D_6 (#). The signal marked with § is due to *n*-pentane, the signal marked with + due to a small amount of starting material **1**.

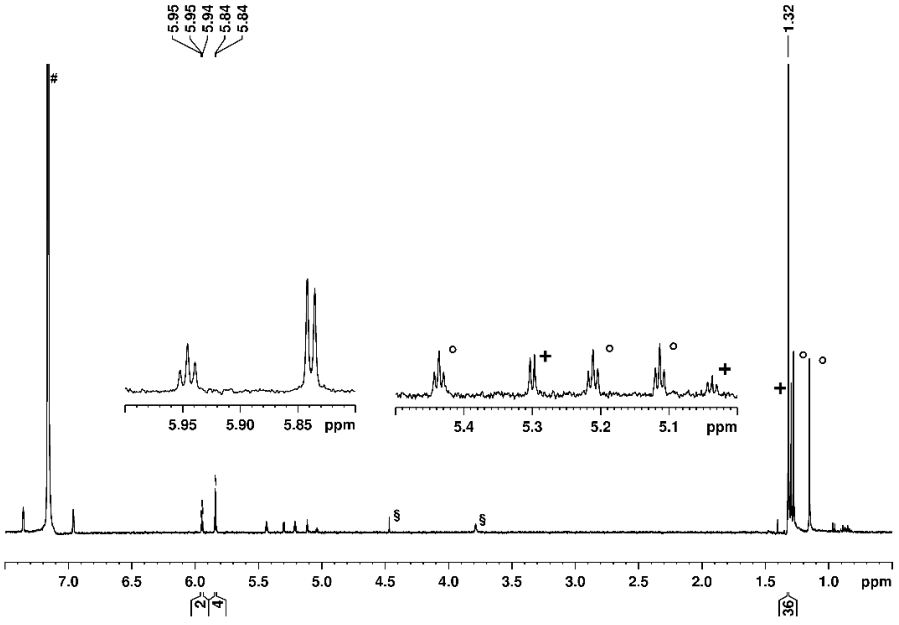

Figure S14: ^{1}H NMR spectrum of **5** at 293 K in C_6D_6 (#). The signal marked with § are due to an unknown impurity, the signal marked with + due to a small amount of starting material **1** and the signals marked with ° due to $[Cp''_2Zr(\mu,\eta^{1:1:1}\text{-}As_4)(Fe(CO)_4)]$ (**4**). Especially the signals for **4** were expected to appear in the NMR spectrum due to the co-crystallization of **5** and **4**. The symmetric environment of the Cp'' ligand in **5** might be an indication of an on the NMR timescale fast dynamic process in solution. Possibly, the $Fe(CO)_3$ fragment migrates around the As_4-cycle.

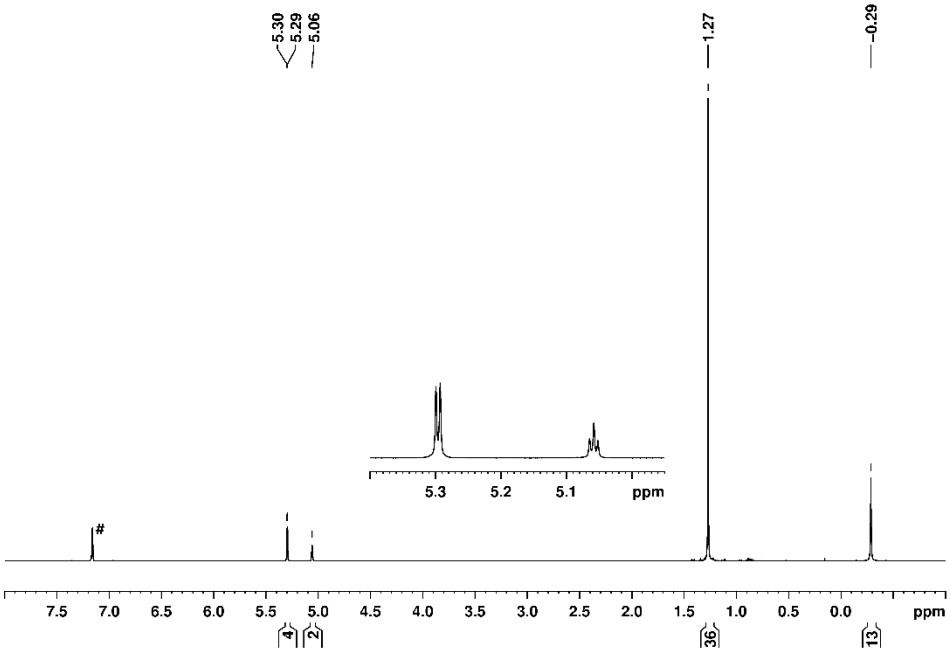

Figure S15: ^{1}H NMR spectrum of **6a** at 293 K in C_6D_6 (#).

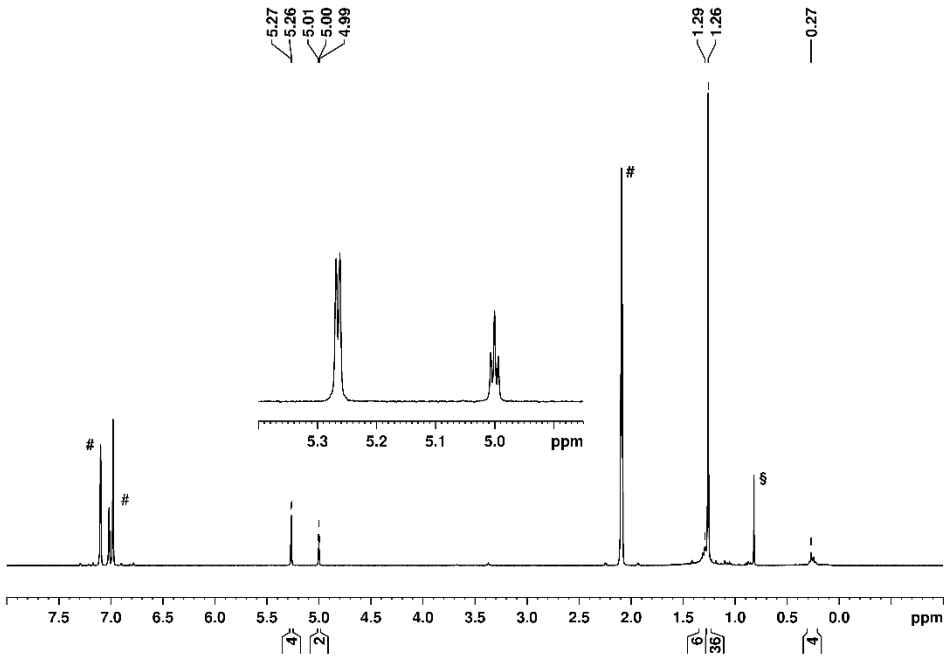

Figure S16: ^{1}H NMR spectrum of **6b** at 293 K in tol-d^8 (#). The signal marked with § is due to free ethane.

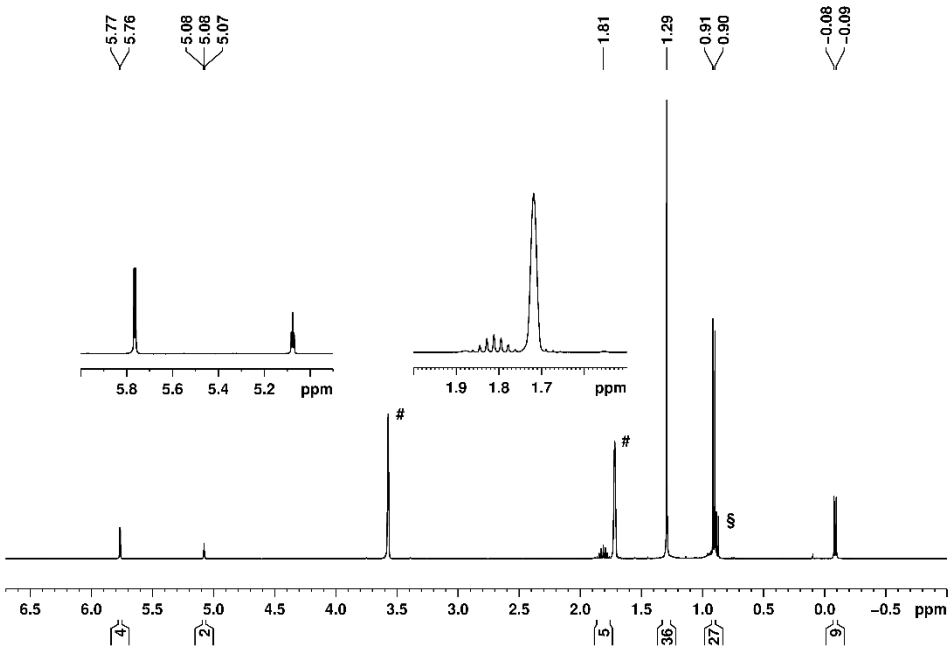

Figure S17: ^{1}H NMR spectrum of **6c** at 293 K in thf-d^{8} (#). The signal marked with § is due to an unknown impurity.

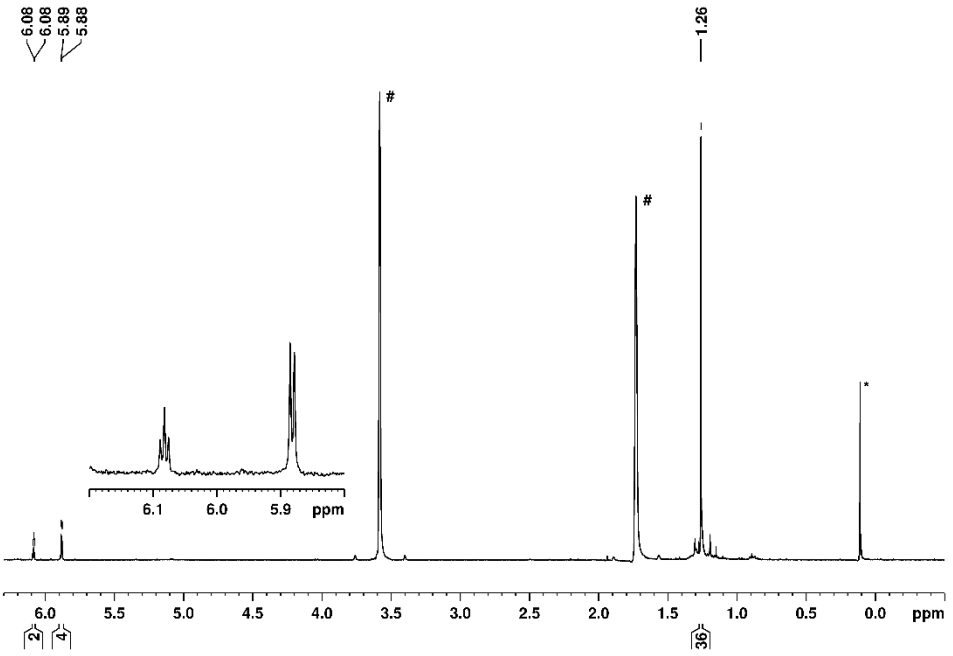

Figure S18: ^{1}H NMR spectrum of **7** at 293 K in thf-d$_{8}$ (#). The signal marked with * is due to silicon grease.

5.5.5 Computational Details

The geometry of the molecules has been optimized using Gaussian 09 program package.[46] Density functional theory (DFT) in form of Becke's three-parameter hybrid functioncal B3LYP[47] with def2-SVP all electron basis set[48] or def2-TZVP basis set for all atoms[49] was employed. The figures for the supporting information concerning the DFT calculations were created with Chemcraft.[50] The reaction energies have been calculated as single point calculations at the B3LYP/def2-TZVP level usind the B3LYP/def2SVP optimised geometries. The dispersion effects have been included in the single point calculations via the D3(BJ) model.[51] For the calculation of relative energies and reaction energies the SCF energies have been used witouth corrections for the zero point vibration energies.

Despite several attempts, the geometry optimization of the isomer of **7** in which the $B(C_6F_5)_3$ group is bonded to the bridgehead arsenic atoms did not reach convergence, indicating that this isomer is not a stable entity.

Table S4: Total and relative energies calculated at the B3LYP/def2-SVP level for the Isomers I, II, I_2 and II_2. Labeling according to figure S19.

	Total energy [Ha]		
Compound	**Isomer I**	**Isomer II**	**ΔE (Isomer I – II) [kJ·mol^{-1}]**
[Cp"$_2$Zr(µ$_3$,η$^{1:1:1:1}$-As$_4$)(W(CO)$_5$)$_2$]	-11272.0985236	-11272.0856656	-33.76
[Cp"$_2$Zr(µ$_3$,η$^{1:1:1:1}$-As$_4$)(CpMn(CO)$_2$)$_2$]	-13146.7853601	-13146.7796608	-14.96
[Cp"$_2$Zr(µ,η$^{1:1:1:1}$-As$_4$)(Fe(CO)$_4$)$_2$]	-13438.4133113	-13438.4001335	-34.60
[Cp"$_2$Zr(µ$_3$,η$^{1:1:1:1}$-As$_4$){AlMe$_3$}$_2$]	-10729.2667023	-10729.2540650	-33.18
[Cp"$_2$Zr(µ$_3$,η$^{1:1:1:1}$-As$_4$){AlEt$_3$}$_2$]	-10964.9386234	-10964.9386234	0.00
[Cp"$_2$Zr(µ$_3$,η$^{1:1:1:1}$-As$_4$){Al^{i}Bu$_3$}$_2$]	-11436.35712	-11436.35027	-17.98
	Total energy [Ha]		
Compound	**Isomer I_2**	**Isomer II_2**	**ΔE (Isomer I_2 – II_2) [kJ·mol^{-1}]**
[Cp"$_2$Zr(µ$_3$,η$^{1:1:1}$-As$_4$)(W(CO)$_5$)]	-10638.6304544	-10638.6231044	-19.30
[Cp"$_2$Zr(µ$_3$,η$^{1:1:1}$-As$_4$)(CpMn(CO)$_2$)]	-11575.9729414	-11575.9702229	-7.14
[Cp"$_2$Zr(µ,η$^{1:1:1}$-As$_4$)(Fe(CO)$_4$)]	-11721.7858591	-11721.7789285	-18.20
[Cp"$_2$Zr(µ,η$^{3:1:1}$-As$_4$)(Fe(CO)$_3$)]	-11608.5858271	n.a.	n.a.
[Cp"$_2$Zr(µ$_3$,η$^{1:1:1}$-As$_4$){AlMe$_3$}]	-10367.2130152	-10367.2066613	-16.68
[Cp"$_2$Zr(µ$_3$,η$^{1:1:1}$-As$_4$){AlEt$_3$}]	-10485.0492434	-10485.0442703	-13.06
[Cp"$_2$Zr(µ$_3$,η$^{1:1:1}$-As$_4$){Al^{i}Bu$_3$}]	-10720.75877	-10720.75552	-8.53

Table S5: Reaction energies (kJ·mol^{-1}) for selected transformations at the B3LYP-D3(BJ)/def2TZVP level of theory.

Transformation	Reaction energy [kJ·mol^{-1}]
1 + $[W(CO)_5(thf)]$ = $[Cp''_2Zr(\mu_3,\eta^{1:1:1}\text{-}As_4)(W(CO)_5]$ (**I_2**)+ thf	-57.87
$[Cp''_2Zr(\mu_3,\eta^{1:1:1}\text{-}As_4)(W(CO)_5]$ (**I_2**) + $[W(CO)_5(thf)]$ = **2** + thf	-58.52
1 + $[CpMn(CO)_2(thf)]$ = $[Cp''_2Zr(\mu_3,\eta^{1:1:1}\text{-}As_4)(CpMn(CO)_2]$ (**I_2**)+ thf	-61.32
$[Cp''_2Zr(\mu_3,\eta^{1:1:1}\text{-}As_4)(CpMn(CO)_2]$ (**I_2**) + $[CpMn(CO)_2(thf)]$ = **3** + thf	-68.44
1 + $Fe_2(CO)_9$ = **4** + $Fe(CO)_5$	-104.79
4 + $Fe_2(CO)_9$ = $[Cp''_2Zr(\mu,\eta^{1:1:1:1}\text{-}As_4)(Fe(CO)_4)_2]$ (**I**) + $Fe(CO)_5$	-99.52

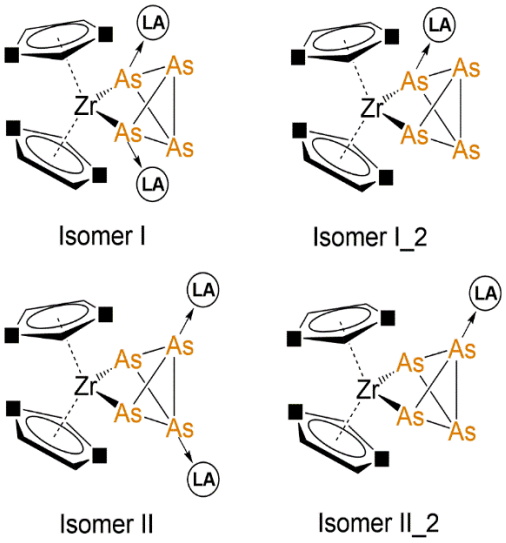

Figure S19: Labeling scheme of different isomers.

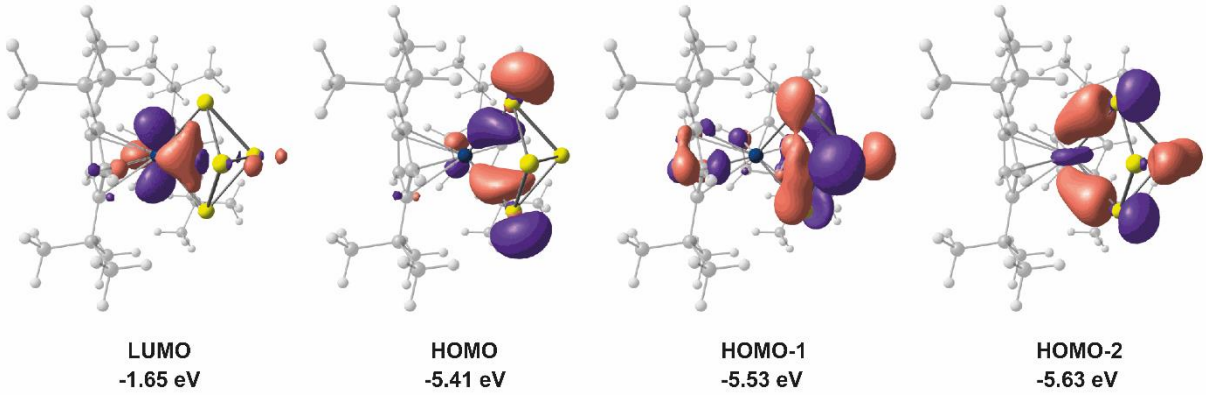

Figure S20: Selected molecular orbitals of **1** at the B3LYP/def2-TZVP level.

Table S6: Cartesian coordinates of the optimized geometry of [$Cp''_2Zr(\eta^{1:1}\text{-}As_4)$] (**1**) at the B3LYP/def2-TZVP level of theory.

Zr	0.000172299	-0.000051182	-0.534015379
As	-0.202191999	1.812317119	1.474037605
As	0.201814891	-1.811817190	1.474666876
As	-1.207864073	-0.137994761	2.670128421
As	1.207571264	0.138940746	2.670096242
C	-3.459146723	-3.192126687	-2.463524235
H	-4.354209150	-2.631496995	-2.188345006
H	-3.719919244	-4.252653537	-2.502186189
H	-3.160838178	-2.878796176	-3.465349378
C	1.095432641	3.767436752	-1.888609122
H	0.726555796	3.438175688	-2.861941299
H	1.358015017	4.823776598	-1.980089369
H	0.281208500	3.685550986	-1.170108758
C	3.459511178	3.191483769	-2.463895484
H	4.354564302	2.630960055	-2.188485524
H	3.720246434	4.252011656	-2.502762003
H	3.161336848	2.877923515	-3.465678765
C	-3.384728177	2.021343212	-0.798817511
C	2.321121362	2.958194481	-1.440675313
C	-2.650786125	3.350776604	-1.023534349
H	-2.245443522	3.425189519	-2.033718615
H	-1.831399341	3.479180855	-0.316945108
H	-3.342710995	4.184630226	-0.886428361
C	-2.516744152	0.804878606	-1.123052439
C	-2.320858795	-2.958629809	-1.440189195
C	-4.584893727	1.962731784	-1.776635147
H	-5.266652520	2.795031021	-1.585068538
H	-5.142233016	1.032082620	-1.656914928
H	-4.253474799	2.025773341	-2.814425510
C	2.650557023	-3.351128554	-1.022151276
H	1.831079665	-3.479023715	-0.315543280
H	3.342273842	-4.185087059	-0.884605599
H	2.245231947	-3.425975564	-2.032306939
C	2.794290311	3.474929900	-0.074666115
H	2.038213547	3.335417869	0.698416706
H	3.009943820	4.543535842	-0.139405423
H	3.709206749	2.976416350	0.249383980
C	1.719141685	-0.656767461	-2.288374926
H	1.445322828	-1.446904084	-2.968189247
C	2.050386994	1.455100881	-1.429236660
C	-3.938944606	1.986590232	0.632603916
H	-4.595054343	2.844856589	0.792350557
H	-3.145678789	2.031256766	1.377426429
H	-4.529874030	1.087440043	0.815188747
C	-1.718778982	0.656155071	-2.288516619
H	-1.444822692	1.446220477	-2.968364987
C	-1.448206183	-0.719971122	-2.482104722
H	-0.931079787	-1.135671676	-3.330874152
C	1.448610400	0.719319329	-2.482240472
H	0.931509076	1.134849525	-3.331109784
C	3.384752482	-2.021744307	-0.798003758
C	-2.794264799	-3.475085652	-0.074155013
H	-2.038430018	-3.335211241	0.699095857
H	-3.009673294	-4.543756069	-0.138659470
H	-3.709357633	-2.976676975	0.249533271
C	-2.050146393	-1.455544109	-1.429048056
C	2.516984615	-0.805282993	-1.122807477
C	2.667471332	0.496330853	-0.584194469
H	3.229520506	0.734534032	0.302678558
C	-2.667289718	-0.496642001	-0.584229130
H	-3.229372071	-0.734658431	0.302676532
C	-1.095162078	-3.767990970	-1.887791601
H	-0.726156288	-3.438957383	-2.861146951
H	-1.357760313	-4.824347310	-1.979069015
H	-0.281028602	-3.685968533	-1.169214740
C	4.584968341	-1.963741538	-1.775802307
H	5.266466498	-2.796189517	-1.584010125
H	5.142574785	-1.033234211	-1.656360186

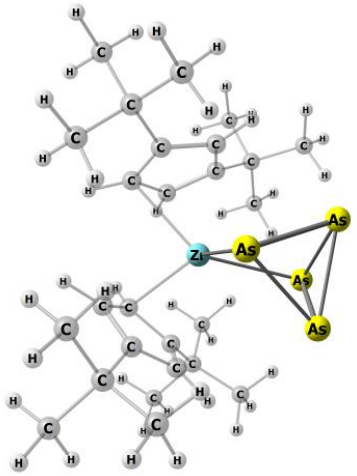

Table S7: Cartesian coordinates of the optimized geometry of the Isomers for [Cp"$_2$Zr(μ_3,$\eta^{1:1:1:1}$-As$_4$)(W(CO)$_5$)$_2$] at the B3LYP/def2-SVP level of theory.

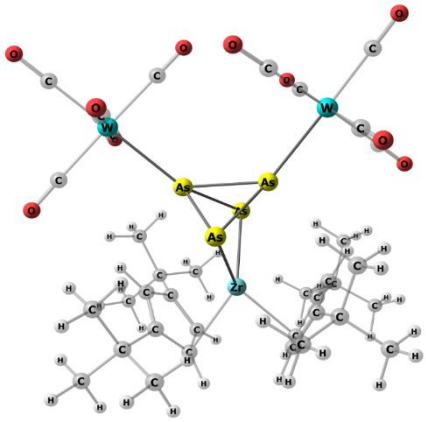

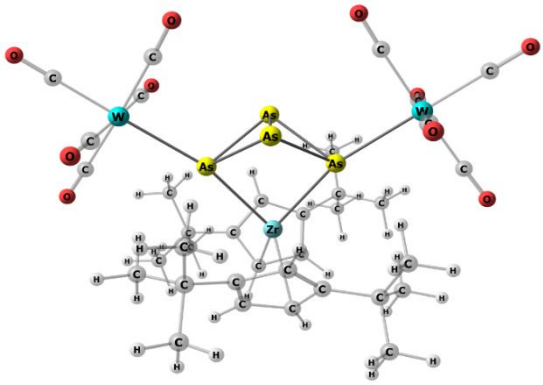

C	-3.623021232	-2.093698411	-1.162577195
C	-2.775015675	-2.575784066	-0.120563953
H	-1.906638381	-3.211442662	-0.275359669
C	-3.314914039	-2.230438204	1.153984018
C	-4.470016707	-1.438065744	0.890076604
H	-5.151172143	-1.040450294	1.640039169
C	-4.664159457	-1.366587545	-0.518250483
H	-5.516579104	-0.902413768	-1.008912780
C	-3.642112185	-2.572673445	-2.617924112
C	-2.254908762	-3.021804820	-3.109651598
H	-1.530696576	-2.191970003	-3.122003738
H	-2.329467551	-3.404332114	-4.139805145
H	-1.836991067	-3.830466816	-2.491968898
C	-4.590820787	-3.799852330	-2.657332656
H	-4.226820247	-4.603730632	-1.998914733
H	-4.653819005	-4.201453707	-3.681893281
H	-5.608127879	-3.530773250	-2.332964026
C	-4.196055618	-1.493178560	-3.564856186
H	-5.216639222	-1.186645193	-3.286343781
H	-4.243073783	-1.879557048	-4.595215154
H	-3.560435921	-0.596802148	-3.570295588
C	-3.005830345	-2.924044789	2.487331184
C	-3.252257791	-2.010906466	3.701228237
H	-3.114764096	-2.580828453	4.633576134
H	-4.275828807	-1.606188436	3.714373450
H	-2.547541749	-1.166000459	3.723845506
C	-3.985544447	-4.125123826	2.572606891
H	-3.845206963	-4.812678423	1.724095414
H	-5.034221616	-3.789392019	2.565967129
H	-3.813499483	-4.691637700	3.502332031
C	-1.570286739	-3.470663498	2.550658508
H	-1.356138517	-4.167406739	1.726109716
H	-1.418778350	-4.023864764	3.490418410
H	-0.822272345	-2.665688788	2.522819159
C	-3.493904058	2.341903327	1.159098501
C	-2.612051678	2.770320767	0.121485476
H	-1.702674483	3.345327179	0.280996087
C	-3.167156734	2.463275267	-1.156433850
C	-4.371693600	1.746165814	-0.898838239
H	-5.074700246	1.396482546	-1.652649235
C	-4.576348668	1.684517316	0.508201950
H	-5.458459937	1.273721447	0.993877007
C	-3.495401487	2.829308150	2.612164965
C	-4.342938484	4.129179128	2.629488497
H	-3.903573923	4.898183936	1.975434562
H	-4.391975329	4.539418144	3.651397188
H	-5.372495146	3.941177120	2.287166132
C	-4.149212429	1.805809504	3.557776488
H	-5.184825853	1.575008873	3.262220252
H	-4.186739976	2.207491332	4.582675913
H	-3.584542167	0.863398884	3.587888631
C	-2.085379761	3.169130502	3.124669468
H	-1.434692832	2.281789554	3.162246832
H	-2.146704720	3.571323864	4.148197150
H	-1.587519878	3.930727410	2.506522511
C	-2.815619313	3.144719423	-2.485917989
C	-3.740045177	4.388638025	-2.576057973
H	-3.579578532	5.064582049	-1.721822036
H	-4.802609921	4.100211389	-2.584083047
C	1.308287934	2.975629559	-2.066968166
C	0.392908168	2.044051240	-2.645480424
H	0.681794889	1.171094425	-3.224665754
C	-0.944805782	2.493170909	-2.463610401
C	-0.860874624	3.667916948	-1.656790397
H	-1.700282570	4.294379523	-1.360381963
C	0.511724815	3.973431559	-1.440543543
H	0.884820006	4.866708722	-0.944524688
C	2.802141285	3.100216087	-2.378513889
C	3.383120298	1.780124611	-2.908895757
H	3.279670252	0.967554143	-2.176680749
H	4.456267406	1.897323285	-3.123338984
H	2.893540674	1.462586262	-3.841951412
C	2.928910802	4.171371520	-3.493266246
H	2.357607435	3.882792910	-4.389344027
H	3.984797116	4.289939647	-3.785990870
H	2.557100024	5.151208947	-3.155579913
C	3.608874012	3.567463246	-1.153631824
H	3.245232000	4.533836113	-0.769091825
H	4.668416957	3.699062347	-1.421876566
H	3.565111868	2.833167286	-0.337918719
C	-2.155100747	2.089220894	-3.313173216
C	-3.480165675	2.162060333	-2.535270525
H	-4.324908214	1.947538036	-3.207982923
H	-3.648776226	3.161795507	-2.107122971
H	-3.516424842	1.428944877	-1.717269466
C	-2.217438097	3.123698306	-4.469839125
H	-1.283563090	3.126671139	-5.053302102
H	-2.383300503	4.143922165	-4.090434934
H	-3.045823180	2.874679548	-5.152637297
C	-1.984230779	0.693395454	-3.936920636
H	-1.106961143	0.650057896	-4.600827523
H	-2.867411827	0.438983978	-4.541624363
H	-1.873696050	-0.088676940	-3.174122326
C	-1.308379858	2.975366928	2.067417336
C	-0.393111386	2.043561031	2.645735668
H	-0.682108098	1.170511208	3.224727028
C	0.944659454	2.492544643	2.463902930
C	0.860847096	3.667484107	1.657350631
H	1.700328571	4.293904063	1.361059829
C	-0.511713078	3.973177760	1.441150969
H	-0.884725463	4.866588736	0.945311585
C	-2.802219910	3.100115226	2.378979851
C	-2.928859006	4.171145451	3.493861914
H	-2.357529418	3.882420988	4.389877400
H	-3.984722910	4.289752096	3.786655903
H	-2.557002544	5.150999112	3.156274881
C	-3.608912002	3.567616105	1.154170961
H	-3.245113227	4.533962597	0.769719546
H	-4.668430176	3.699368275	1.422449607
H	-3.565273670	2.833398647	0.338383209
C	-3.383332488	1.780025152	2.909200558
H	-3.279846013	0.967520149	2.176928854
H	-4.456497895	1.897253396	3.123547062
H	-2.893854952	1.462377983	3.842274072
C	2.154929834	2.088243917	3.313320438
C	2.217260754	3.122260537	4.470398931
H	1.283465214	3.124840043	5.053991159
H	2.382893921	4.142667623	4.091388210

H	-3.531587003	4.952119856	-3.500191012
C	-3.092247180	2.248020758	-3.705767144
H	-2.924515053	2.816052603	-4.634333942
H	-4.132037850	1.887518932	-3.727347876
H	-2.424950055	1.373336180	-3.729301757
C	-1.357573577	3.628646847	-2.533622683
H	-0.644567883	2.793551521	-2.492886608
H	-1.124364608	4.318785046	-1.708679867
H	-1.170035885	4.172282049	-3.472358971
C	4.249470415	4.191177185	0.189473338
C	1.458600430	4.314273741	1.021842437
C	2.178700248	3.812412330	-1.771582669
C	3.830202508	1.547420016	-0.980438646
C	3.205841247	2.084358861	1.874440163
C	2.817960711	-2.561343004	-2.008377433
C	3.820219055	-1.794371295	0.681876975
C	2.006079671	-3.714310594	1.909824425
C	3.810902561	-4.577038609	-0.176162591
C	0.961662951	-4.466487094	-0.721749247
As	-0.629195078	0.082227542	1.825429385
As	0.585542241	1.224032031	-0.026762076
As	0.510559573	-1.209802571	0.025114809
As	-0.630570044	-0.003749969	-1.826661554
O	5.153160664	4.902372543	0.275561793
O	0.766651752	5.072670661	1.543858675
O	1.935570221	4.311126814	-2.778471134
O	4.459322394	0.785440555	-1.563241802
O	3.508948842	1.626764641	2.881260893
O	3.052510800	-2.257599650	-3.089038773
O	4.601545950	-1.066614320	1.100731028
O	1.804657797	-4.045832129	2.991581221
O	4.615871355	-5.398954802	-0.255196761
O	0.146352410	-5.198594553	-1.078924205
W	2.670484219	2.945059429	0.048541403
W	2.400390923	-3.141603135	-0.046843326
Zr	-2.699987205	0.101061743	-0.002280301

H	3.045781576	2.873104055	5.152982929
C	3.479951601	2.161405984	2.535362232
H	4.324736803	1.946478718	3.207892984
H	3.648603857	3.161350479	2.107715618
H	3.516079987	1.428707546	1.716979493
C	1.984141279	0.692147876	3.936463485
H	1.874037380	-0.089648729	3.173322570
H	1.106686299	0.648347172	4.600087231
H	2.867196722	0.437702234	4.541342598
C	-5.737151399	-2.803463466	0.148042064
C	-5.256058280	0.014471102	0.291969314
C	-3.830681503	-1.838860507	2.089719797
C	-2.953696204	-3.400038248	-0.251519127
C	-4.353752935	-1.522113585	-2.020257081
C	4.353954536	-1.522065240	2.020114023
C	2.953803564	-3.399914908	0.251232506
C	3.830892264	-1.838574175	-2.089879609
C	5.737307560	-2.803143774	-0.148212321
C	5.255889780	0.014856572	-0.291812574
As	-1.792445392	-0.116436301	-0.039011522
As	-0.028064161	-1.348124398	1.232826211
As	0.028064962	-1.347956770	-1.233197116
As	1.792373074	-0.116355745	0.038838149
O	-6.688136733	-3.454075966	0.218673975
O	-5.936125379	0.933779490	0.431041303
O	-3.703480506	-1.936090424	3.228254957
O	-2.370807327	-4.375767889	-0.412726850
O	-4.544298090	-1.460619675	-3.153175987
O	4.544663582	-1.460624491	3.153015604
O	2.370859710	-4.375618994	0.412387333
O	3.703962306	-1.935936444	-3.228428887
O	6.688389733	-3.453603400	-0.218924955
O	5.935760882	0.934317245	-0.430844186
W	-4.079255832	-1.667413312	0.032587094
W	4.079336182	-1.667231863	-0.032706568
Zr	-0.000063389	1.979182804	0.000088225

Table S8: Cartesian coordinates of the optimized geometry of the Isomers for [Cp"$_2$Zr(µ,η$^{1:1:1}$-As$_4$)(W(CO)$_5$)] at the B3LYP/def2-SVP level of theory.

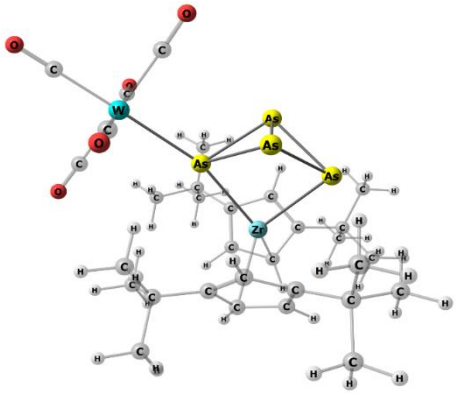

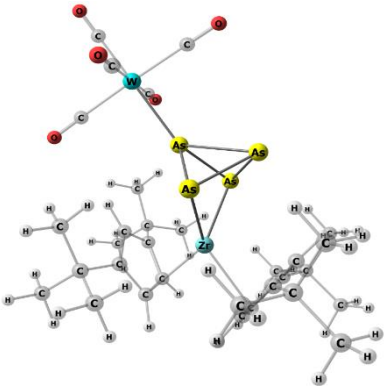

W	3.619195223	-0.049942543	-0.141373439
Zr	-1.780662244	0.047172797	0.538952074
As	0.870168485	0.061166293	-0.175518356
As	-2.140949484	-0.112005020	-2.161842566
As	0.003141304	1.152061242	-2.273771698
As	0.046238818	-1.296845434	-2.123553142
O	3.744636081	0.085372106	-3.368415854
O	3.424871166	-3.268774895	-0.290225068
O	6.779389963	-0.274698031	-0.071152918
O	3.935211890	3.159097486	-0.017951725
O	3.573949118	-0.168179287	3.077833080
C	-1.556826946	-2.593791163	0.900638564
H	-0.812149168	-3.196930897	0.387147556
C	-2.897811012	-2.401243634	0.459473293
C	-3.514358034	-1.562261565	1.435218950
H	-4.554651247	-1.243223861	1.429987255
C	-2.588931961	-1.328905050	2.489380423
H	-2.809732867	-0.796003547	3.411697373
C	-1.365375285	-1.981555031	2.175872431
C	-0.230386334	-2.262478267	3.164127475
C	1.017744293	-2.806524809	2.451825200

C	-4.107431589	-0.261356505	-1.353806470
C	-3.708413549	-1.471718538	-0.714126084
H	-3.370397358	-2.363417907	-1.236250400
C	-3.930193205	-1.385397394	0.691406981
C	-4.395707780	-0.059244456	0.933807986
H	-4.701569261	0.340577431	1.898707792
C	-4.516572536	0.618476058	-0.310909062
H	-4.929431011	1.616356259	-0.441067661
C	-4.415642077	-0.083454667	-2.844409434
C	-3.636701613	-1.081052667	-3.720248990
H	-2.547737566	-0.950209020	-3.627661434
H	-3.898889746	-0.935069217	-4.780014433
H	-3.876476058	-2.124855076	-3.465440143
C	-5.930842867	-0.368645333	-3.013931800
H	-6.182841730	-1.385508066	-2.674584972
H	-6.222192355	-0.279767477	-4.073588407
H	-6.539795068	0.341064335	-2.432655003
C	-4.129427498	1.349184726	-3.327543701
H	-4.677750723	2.098903235	-2.735476059
H	-4.446411935	1.467121888	-4.376151167
H	-3.058339550	1.586770552	-3.271624620

H	1.399996569	-2.095353683	1.707204505
H	0.815460278	-3.758949664	1.938663929
H	1.822515402	-2.989368461	3.180334480
C	0.143778057	-1.009677446	3.977188855
H	0.529728842	-0.209650980	3.330637790
H	0.929058980	-1.250666501	4.710440457
H	-0.719003881	-0.614783560	4.537072899
C	-0.748714850	-3.350278643	4.139842007
H	-1.037316533	-4.264790689	3.598478494
H	-1.627018927	-3.000127005	4.704189366
H	0.038185743	-3.616803347	4.864234236
C	-3.654757114	-3.282756430	-0.545194502
C	-4.817859258	-2.546027376	-1.233014407
H	-5.518989982	-2.111718389	-0.504315945
H	-5.390511514	-3.250783525	-1.856543050
H	-4.460092898	-1.739243986	-1.889563334
C	-2.734718198	-3.895409596	-1.615926557
H	-2.297631903	-3.129918346	-2.271447853
H	-3.312005819	-4.586761246	-2.250155380
H	-1.912818928	-4.475802694	-1.168951850
C	-4.249477685	-4.444802586	0.296036459
H	-4.950653162	-4.070279404	1.057916218
H	-3.456944604	-5.006715962	0.814210065
H	-4.795545785	-5.146699542	-0.355644680
C	-2.140652705	2.697040667	0.218198580
H	-1.830497506	3.233137739	-0.674757731
C	-3.433372721	2.125260601	0.414948596
C	-3.417143898	1.557621760	1.720789299
H	-4.259431732	1.083630702	2.219820342
C	-2.147183621	1.801757017	2.312535969
H	-1.868761604	1.548754501	3.333943608
C	-1.356815674	2.559338724	1.396874645
C	-0.130925135	3.400854420	1.767356014
C	0.610140977	3.918849010	0.522595073
H	0.974085006	3.097971084	-0.110017045
H	1.484399313	4.516294702	0.821889247
H	-0.033825518	4.564957683	-0.094177731
C	-0.676394783	4.626993613	2.547419096
H	-1.396056691	5.197259348	1.939438465
H	0.150779033	5.302919450	2.819902230
H	-1.184973411	4.319800457	3.474492625
C	0.849092254	2.646995401	2.682764946
H	1.293312425	1.778264606	2.177560056
H	0.360240934	2.293449932	3.603479648
H	1.673032735	3.312262941	2.984881583
C	-4.690946234	2.409154913	-0.413531538
C	-5.437102025	3.563595908	0.305296363
H	-4.798787070	4.457057685	0.388746714
H	-5.743986623	3.272829086	1.321965827
H	-6.343121263	3.842932390	-0.257354718
C	-4.351314074	2.872343463	-1.841321266
H	-3.749903104	3.794393141	-1.839283521
H	-5.278407309	3.088381636	-2.395536034
H	-3.798197576	2.105835933	-2.404726732
C	-5.624754681	1.187738923	-0.481304316
H	-6.550107092	1.443979914	-1.021556994
H	-5.919189855	0.842359665	0.522504977
H	-5.148486267	0.348089788	-1.005689000
C	3.680267664	0.036743187	-2.222571815
C	3.485997017	-2.121392172	-0.237359207
C	5.627607370	-0.190875349	-0.097470592
C	3.794368730	2.018048179	-0.062854530
C	3.579461055	-0.125712224	1.926560375
C	-4.091563553	-2.570548831	1.654344820
C	-3.702837630	-2.218775243	3.100802659
H	-3.949318782	-3.056726200	3.772097920
H	-4.242971149	-1.333647140	3.469743635
H	-2.624082973	-2.025961972	3.194216731
C	-5.601127181	-2.931307128	1.629436463
H	-5.930370100	-3.188611839	0.610588708
H	-6.220317904	-2.092091924	1.982388326
H	-5.797836123	-3.798606122	2.281076329
C	-3.298387188	-3.809909624	1.203105394
H	-3.594395548	-4.142950093	0.196351515
H	-3.491501704	-4.647189589	1.892300086
H	-2.214627658	-3.626432923	1.198468050
C	-1.371703356	2.178260465	2.061483561
C	-0.414200487	2.404483167	1.029080995
H	0.659229914	2.279111303	1.144653787
C	-1.050965712	2.934843799	-0.129203999
C	-2.447239149	2.950945610	0.162544224
H	-3.227644048	3.339802801	-0.488978515
C	-2.639788372	2.505677383	1.500659687
H	-3.592338943	2.499021847	2.026561657
C	-1.071218977	2.015421592	3.555547207
C	-1.128384296	3.439506812	4.168532569
H	-0.398590430	4.107493471	3.685222219
H	-0.895071751	3.401816437	5.245323375
H	-2.127073054	3.888537864	4.051634240
C	-2.115676423	1.134459669	4.264151374
H	-3.139387242	1.514047517	4.117708275
H	-1.925815966	1.119011705	5.349272784
H	-2.081414509	0.097085096	3.903164207
C	0.334904636	1.441807652	3.806136817
H	0.450331267	0.433585518	3.379957014
H	0.520918972	1.365723928	4.889078123
H	1.124028369	2.082064180	3.383598394
C	-0.369207976	3.738688817	-1.245436251
C	-0.420236184	5.220612893	-0.785513354
H	0.082391200	5.351929307	0.185286488
H	-1.458133712	5.572800958	-0.679014327
H	0.085851344	5.866389713	-1.521910911
C	-1.098566127	3.628410246	-2.596233279
H	-0.649555802	4.324858148	-3.322025674
H	-2.165484967	3.885704290	-2.512665486
H	-1.020802593	2.616099551	-3.019759565
C	1.107108074	3.348461427	-1.432968069
H	1.220310947	2.303522805	-1.753650053
H	1.689361759	3.490282549	-0.510009678
H	1.566521230	3.981331873	-2.208357733
C	5.915352156	-0.250347278	-0.005171227
C	3.859048092	-1.491855447	1.633176518
C	3.723507420	1.377047030	1.014895684
C	3.925923793	0.779115125	-1.853699907
C	4.016604082	-2.098192005	-1.247515536
As	-0.430434139	-1.331005529	1.437237243
As	1.205778364	-0.505365635	-0.220635020
As	-0.275033536	-2.327714339	-0.874502023
As	-0.468298183	-0.086850649	-2.001431939
O	7.066410200	-0.193154794	0.054527045
O	3.843503346	-2.117529417	2.595633573
O	3.601844818	2.340199424	1.636108319
O	3.942637136	1.407645228	-2.815549202
O	4.072780221	-3.058742111	-1.872487420
W	3.904547085	-0.351473392	-0.109655377
Zr	-2.053828948	0.458525580	0.159742468

Table S9: Cartesian coordinates of the optimized geometry of the Isomers for [Cp"$_2$Zr(μ_3,$\eta^{1:1:1:1}$-As$_4$)(CpMn(CO)$_2$)$_2$] at the B3LYP/def2- SVP level of theory.

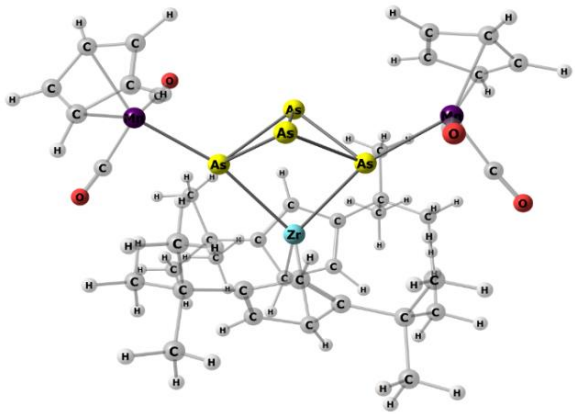

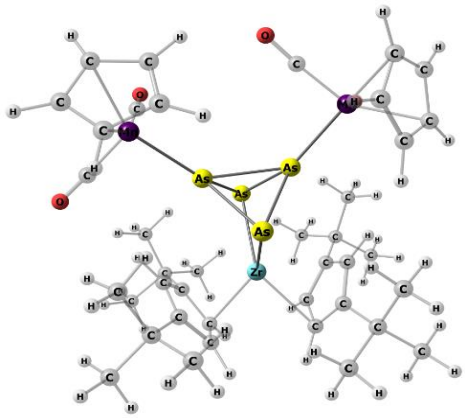

Zr	0.008041933	1.510709488	-0.012297642
As	-1.826715503	-0.527014655	-0.001777666
As	1.823167126	-0.541723280	0.019012667
As	0.002583081	-1.735545915	-1.217404557
As	-0.014925864	-1.718154653	1.253047433
Mn	3.868500494	-1.843580541	-0.109693459
Mn	-3.898986210	-1.792437401	0.141343503
O	5.654295525	0.487139023	-0.253336333
O	-5.648723553	0.555805147	0.379632828
O	3.640339796	-2.178941680	-3.021805497
C	0.354874212	1.588356951	-2.680664933
H	0.654957003	0.723000201	-3.266314406
C	-0.311478012	1.640597874	2.654898292
H	-0.596879736	0.784477141	3.261331297
C	3.323580603	-3.868956459	0.531758941
H	2.455724580	-4.425839926	0.183992836
C	-1.230590178	2.574002665	2.085294907
C	-0.988763472	2.006388515	-2.470006111
C	1.026261808	2.067373727	2.421174576
C	2.257581891	1.678134073	3.248278976
C	1.259469613	2.541135953	-2.118813507
C	0.452564869	3.520710669	-1.478710288
H	0.816011395	4.421862328	-0.990362545
C	-0.915283015	3.184476425	-1.667013699
H	-1.762105999	3.789441413	-1.349203787
C	3.572860643	1.945681910	2.498076514
H	3.656235371	1.331208157	1.592092779
H	4.432070364	1.703537338	3.143225434
H	3.674330026	3.002212937	2.207104774
C	2.228352939	0.214512649	3.720145271
H	1.300826636	-0.028499944	4.261044828
H	3.066151307	0.030798592	4.411685922
H	2.331613883	-0.483272418	2.878819344
C	-0.440496022	3.546190591	1.413544972
H	-0.818289567	4.432884202	0.909731834
C	0.932585709	3.228120509	1.596395736
H	1.770161018	3.832947122	1.256042503
C	4.621947755	-3.859720364	-0.067150362
H	4.915630783	-4.406274031	-0.962384505
C	3.386268776	-3.038853926	1.687553476
H	2.562517761	-2.844059521	2.371910154
C	4.906693101	-0.398992191	-0.212264826
C	3.708045125	-2.003632581	-1.878878547
C	2.741466817	2.710394121	-2.464143690
C	5.470530576	-3.028481909	0.711571587
H	6.524727169	-2.833136519	0.522160901
C	3.348277199	1.406931892	-3.003573769
H	3.266296186	0.593772281	-2.272360583
H	4.417305292	1.546501359	-3.225485471
H	2.857311860	1.079433649	-3.932477483
C	4.699746145	-2.520190577	1.808460068
H	5.062312043	-1.866793578	2.600043858
C	-2.710003017	2.738602539	2.442165281
C	-2.208075697	1.588301075	-3.301010124
C	2.214968056	2.590328121	4.504355743
H	2.240253849	3.655445817	4.226512747
H	3.082691652	2.385033739	5.152622787
H	1.300462572	2.415808396	5.092244615

Zr	2.053574546	0.271579083	0.042035706
As	-0.056326160	0.027712440	1.788066011
As	0.088118922	0.014304330	-1.863413326
As	-1.333656723	1.070432508	-0.092192061
As	-0.991668745	-1.341799364	-0.088356969
Mn	-3.261779616	2.479570350	-0.063944834
Mn	-2.361884478	-3.267400368	-0.127600301
O	-2.896733470	3.589825668	-2.767508798
O	-2.963902446	-3.011824976	-3.001518439
O	-5.058984328	0.320979313	-0.933564596
C	1.725635775	2.916535997	0.168278272
H	0.755703636	3.389204101	0.305234080
C	2.394995961	-2.389490284	-0.068882444
H	1.597936128	-3.106746494	-0.244187918
C	-4.832208550	3.083519333	1.278081645
H	-5.842997274	2.679444899	1.240542631
C	2.871778968	-2.002708923	1.218103261
C	2.617580226	2.561616657	1.226186693
C	3.212941488	-1.818488961	-1.089557678
C	3.322087958	-2.301564749	-2.539496011
C	2.343418679	2.678563067	-1.096412127
C	3.602419246	2.076735603	-0.810635975
H	4.352357574	1.796345920	-1.547414365
C	3.774880947	2.019244252	0.599515664
H	4.678438209	1.686317381	1.105704760
C	3.755347994	-1.170128571	-3.487864987
H	3.007805208	-0.365662553	-3.519543061
H	3.879934702	-1.557682748	-4.511476532
H	4.718958534	-0.728945751	-3.187068732
C	2.010706496	-2.924732683	-3.049930522
H	1.685033205	-3.772517303	-2.428715104
H	2.151406561	-3.304713661	-4.074253239
H	1.190613191	-2.191526309	-3.081807471
C	3.949036350	-1.099406635	0.984723394
H	4.568377168	-0.638241172	1.751698124
C	4.166192277	-1.000149858	-0.418312852
H	4.978870284	-0.450431911	-0.888074779
C	-3.754211321	2.570301668	2.063785006
H	-3.794118657	1.719372417	2.740801223
C	-4.366929327	4.218550662	0.560865198
H	-4.958261095	4.837231051	-0.112016036
C	-3.010239603	3.115363389	-1.719440712
C	-4.311364012	1.147960002	-0.622393467
C	1.972831142	3.339919628	-2.431143376
C	-2.621881506	3.402568546	1.822752463
H	-1.637451588	3.273961076	2.267212128
C	0.473818594	3.659184470	-2.540296508
H	-0.141051015	2.749608441	-2.553053844
H	0.269725788	4.203444498	-3.475372535
H	0.123956944	4.294655161	-1.712657750
C	-2.990402711	4.420857468	0.907093309
H	-2.348098400	5.219201138	0.539116722
C	2.597454827	-2.732378801	2.539412375
C	2.551043929	3.038336513	2.681517469
C	4.415666647	-3.401951933	-2.549482221
H	5.387992313	-3.004566035	-2.218631132
H	4.540705273	-3.808256929	-3.566813390
H	4.145393135	-4.234822921	-1.881875384

C	-3.295992973	1.444598009	3.026335196
H	-3.200486381	0.607114665	2.324914531
H	-4.366840780	1.573985862	3.245083831
H	-2.797757665	1.158776205	3.965238609
C	-4.909400265	-0.334878178	0.301814369
C	-3.530095628	1.760737504	-2.534818777
H	-3.596117962	1.072378330	-1.681968269
H	-4.382334524	1.547138446	-3.199411236
H	-3.660644089	2.787392813	-2.160749672
C	-2.105354895	0.146003835	-3.826493647
H	-1.190134656	-0.013773784	-4.417114651
H	-2.959913873	-0.070468485	-4.487319824
H	-2.120077140	-0.587524036	-3.009044123
C	3.560936517	3.202739517	-1.257736256
H	3.177173049	4.158395332	-0.865640172
H	4.609802449	3.366066164	-1.550210728
H	3.559447000	2.467384202	-0.442447869
C	-3.546297532	3.193798549	1.232253032
H	-3.171877223	4.141614042	0.813015013
H	-4.592859728	3.358011145	1.531928109
H	-3.550369080	2.439121649	0.434834544
C	-2.780200115	3.840074415	3.532027268
H	-2.181550159	3.565291307	4.414690654
H	-3.823169149	3.982965671	3.859209327
H	-2.405907162	4.805209938	3.156407985
C	2.813522967	3.782873212	-3.582096966
H	2.229267659	3.477616369	-4.464357934
H	3.858841437	3.929282666	-3.900076897
H	2.423380436	4.753149480	-3.237060932
C	-2.221791120	2.545428982	-4.523732023
H	-2.321980508	3.595624223	-4.208741986
H	-3.070174848	2.304653165	-5.185229742
H	-1.294316755	2.455309097	-5.110371445
C	-4.640742522	-2.402015968	-1.836046332
H	-4.874982313	-1.727770063	-2.657401978
C	-4.843282119	-3.722234368	0.047491722
H	-5.259798696	-4.227715059	0.917554334
O	-3.616874246	-2.198585988	3.040163788
C	-3.704663196	-1.998896011	1.902704488
C	-5.538618860	-2.820190473	-0.800067232
H	-6.578680653	-2.516079098	-0.692435892
C	-3.399312699	-3.052190325	-1.610245432
H	-2.508243522	-2.950672031	-2.226972612
C	-3.509490894	-3.870002823	-0.453133515
H	-2.731055349	-4.507308156	-0.038054580
C	1.270252589	-3.509823620	2.505189836
H	0.410395315	-2.849685538	2.323647278
H	1.109829501	-4.016540549	3.470380182
H	1.269646411	-4.283607983	1.723631140
C	-2.692051599	-3.085549278	-1.882120626
C	3.156257138	2.012660562	3.656128942
H	2.564878157	1.087318703	3.681418773
H	3.180417207	2.426432169	4.677064788
H	4.191367192	1.750684258	3.386510012
C	1.115123374	3.364363637	3.123976770
H	0.662080337	4.145663714	2.494659632
H	1.116073453	3.739289957	4.159723281
H	0.468876760	2.474203302	3.092978361
C	2.399388280	2.498531236	-3.647319438
H	3.473120812	2.256627657	-3.628409553
H	2.206166971	3.057500524	-4.576573922
H	1.836049798	1.555700942	-3.704889080
C	2.609731390	-1.788814363	3.754759565
H	3.544074861	-1.210304697	3.817361487
H	2.521405018	-2.371683687	4.685597766
H	1.769187269	-1.079637774	3.724387764
C	3.750351089	-3.757788782	2.707490208
H	3.793367845	-4.448071933	1.850818675
H	3.598704479	-4.356364774	3.620970517
H	4.727021565	-3.255432056	2.787138676
C	2.756947468	4.679276161	-2.465798464
H	2.483689275	5.320822046	-1.613388718
H	2.530857007	5.230485568	-3.393483092
H	3.844329169	4.510094750	-2.425209765
C	3.387415334	4.342883053	2.752408202
H	4.439093906	4.159216414	2.483350416
H	3.364129958	4.759684168	3.772970475
H	2.992239814	5.105567097	2.063229407
C	-3.372366316	-4.736031654	1.076985294
H	-3.111640754	-5.793457711	1.085645952
C	-4.371773363	-2.724614791	0.534804742
H	-4.988003423	-1.971167128	0.048358226
O	-0.138153426	-5.148286201	-0.537828297
C	-0.999921788	-4.383694954	-0.394980860
C	-4.309087508	-4.117987278	0.205684804
H	-4.890349705	-4.619250538	-0.566707701
C	-2.844758929	-3.733442305	1.951601170
H	-2.118967694	-3.888805152	2.747696455
C	-3.464804035	-2.499268174	1.604719318
Zr	2.053574546	0.271579083	0.042035706

Table S10: Cartesian coordinates of the optimized geometry of the Isomers for [Cp''$_2$Zr(μ$_3$,η$^{1:1:1}$-As$_4$)(CpMn(CO)$_2$)] at the B3LYP/def2- SVP level of theory.

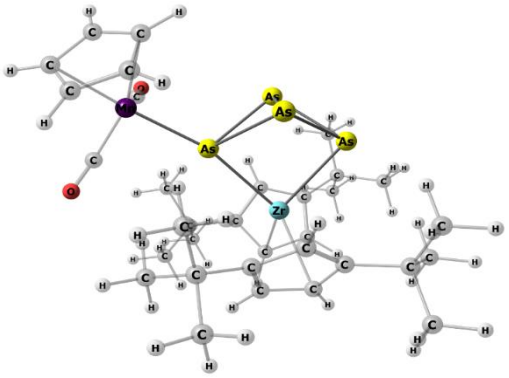

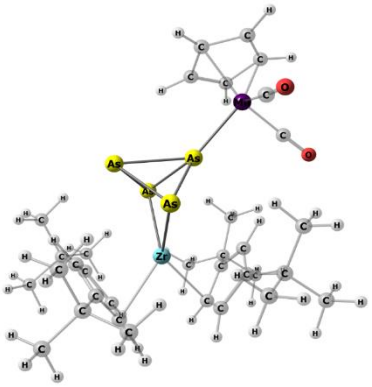

Zr	1.257331367	0.047352463	0.524050588
As	1.695748828	0.022326011	-2.165797944
As	-1.374392899	-0.026658240	-0.210771919
As	-0.440330943	-1.243841300	-2.216569521
As	-0.479528104	1.215161713	-2.220514829
Mn	-3.782290323	-0.185902383	-0.193627852
O	-3.978772380	-0.094136074	2.738323493
O	-3.724166859	-3.121330942	-0.355803974
C	1.150757164	-2.613378506	0.808130279
H	0.429604302	-3.229710919	0.276789534
C	1.461789295	2.740956145	0.354476130
Zr	-1.497270412	0.447226805	0.249804540
As	0.107242259	-1.538062654	1.210129037
As	-0.001345078	0.155875288	-2.021659994
As	0.122885607	-2.224934348	-1.222554743
As	1.716973524	-0.565768311	-0.393521290
Mn	4.079102736	-0.470603777	-0.303627708
O	4.343947747	0.876986246	-2.910019169
C	-3.237404527	-1.344063338	-0.763032106
H	-2.938401966	-2.195372030	-1.369223584
C	0.240819554	2.241376536	1.257453157
H	1.316777266	2.090971926	1.289030756

H	1.104916979	3.313734186	-0.497631309
C	-4.312692411	0.419501622	-2.233630847
H	-3.777296477	0.126052509	-3.134492787
C	2.786690659	2.229489167	0.490799194
C	2.481314835	-2.351041155	0.371444837
C	0.712511030	2.489140901	1.537127095
C	-0.543547459	3.243644257	1.987901766
C	0.937688073	-2.049711849	2.103536176
C	2.135503927	-1.358819223	2.434586891
H	2.338663566	-0.848629542	3.373328297
C	3.065694294	-1.519014469	1.372296071
H	4.091804292	-1.156381631	1.373872178
C	-1.358524741	2.451723730	3.023396654
H	-1.745933828	1.513647977	2.604711069
H	-2.223279081	3.045136155	3.359546955
H	-0.764001643	2.209256059	3.917348952
C	-1.458624471	3.630566850	0.813583710
H	-0.923030672	4.206314158	0.042955772
H	-2.284373209	4.262251744	1.178244382
H	-1.901343137	2.744177580	0.339818860
C	2.830942281	1.586208243	1.760605273
H	3.708418433	1.130959416	2.214224229
C	1.564544234	1.726944848	2.390673895
H	1.320346259	1.395873135	3.397882057
C	-5.396573028	-0.282292976	-1.628977713
H	-5.825409433	-1.218719393	-1.983750884
C	-4.081583413	1.594469483	-1.455580035
H	-3.327881655	2.353341657	-1.657758690
C	-3.855749508	-0.143820622	1.585628143
C	-3.705081055	-1.966566604	-0.266380118
C	-0.172135466	-2.420694486	3.091698736
C	-5.828947936	0.445864633	-0.486515843
H	-6.648944967	0.174206913	0.175815205
C	-1.425316742	-2.944253830	2.374328129
H	-1.855134549	-2.183332152	1.710780192
H	-2.198461430	-3.215422922	3.109792719
H	-1.214199166	-3.840992993	1.772456854
C	-5.010551391	1.617392367	-0.385984688
H	-5.092240403	2.391726053	0.375141159
C	4.011575025	2.634652161	-0.337423942
C	3.273086012	-3.159332229	-0.666486495
C	-0.033225328	4.547754739	2.656913500
H	0.619576826	4.327566086	3.515914873
H	-0.883130396	5.149275270	3.019502602
H	0.540901049	5.161656642	1.945454406
C	3.619378122	3.178517720	-1.722952867
H	3.087903069	2.427793690	-2.326452024
H	4.523081993	3.474883396	-2.278805624
C	-0.657403506	1.900799646	2.311035863
C	-3.426500148	-1.377949812	0.649286303
C	-0.453915994	2.925943483	0.219254126
C	0.175027915	3.849384738	-0.832541739
C	-3.607908137	-0.068695049	-1.282022687
C	-3.966226683	0.725725390	-0.154607525
H	-4.349544590	1.743411648	-0.186887995
C	-3.845889914	-0.066552111	1.020755798
H	-4.125367232	0.250311795	2.023780026
C	-0.660732756	3.931151614	-2.121381980
H	-0.672559190	2.968859101	-2.652937802
H	-0.231819861	4.683508246	-2.802222233
H	-1.702781403	4.224997136	-1.921511538
C	1.617628475	3.447175537	-1.186800787
H	2.274248487	3.443490405	-0.304392876
H	2.039319512	4.168884747	-1.904235118
H	1.667727432	2.453290412	-1.654653034
C	-1.950111271	2.314510446	1.877746690
H	-2.868868647	2.255102912	2.457185469
C	-1.828643650	2.925878171	0.598052319
H	-2.636588908	3.409623638	0.052626400
C	-3.943464695	0.252157799	-2.742282130
C	-3.232965534	-0.700809788	-3.720038769
H	-2.137573195	-0.630862340	-3.640823633
H	-3.509331914	-0.450707089	-4.756630503
H	-3.519967757	-1.750021199	-3.549973780
C	-0.270408399	1.548552207	3.751083799
C	-3.598772526	-2.640815145	1.505794786
C	0.214574512	5.259774063	-0.185348057
H	-0.797610632	5.619542338	0.057112851
H	0.678751791	5.983423294	-0.875673188
H	0.802613135	5.251878690	0.745527732
C	1.114009350	0.880720057	3.835850654
H	1.136886143	-0.083842848	3.306192965
H	1.371822347	0.687785794	4.889593590
H	1.906883486	1.517547918	3.415126330
C	4.202709508	0.363423164	-1.884491197
C	-3.147391726	-2.440621094	2.963496419
H	-2.057895279	-2.308854959	3.036021733
H	-3.415685035	-3.323936014	3.564954597
H	-3.630177720	-1.567893794	3.429091857
C	-2.866962921	-3.857978905	0.912265244
H	-3.214370447	-4.087831504	-0.106807609
H	-3.061278458	-4.748105950	1.531594399
H	-1.778498444	-3.707173787	0.876643614
C	-3.600435593	1.706562507	-3.109323974
H	-4.094130714	2.426403144	-2.437613658
H	-3.937584658	1.930949324	-4.133932627

Table S11: Cartesian coordinates of the optimized geometry of the Isomers for [Cp"$_2$Zr(µ,η$^{1:1:1:1}$-As$_4$)(Fe(CO)$_4$)$_2$] at the B3LYP/def2- SVP level of theory.

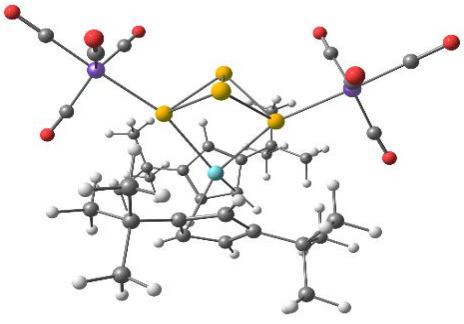

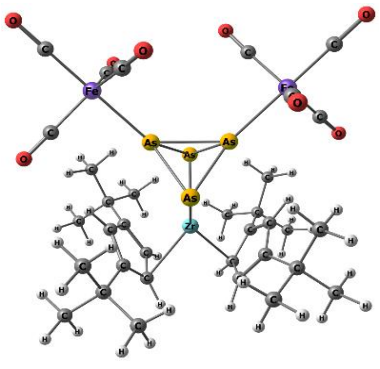

As	-1.774259940	-0.609960569	-0.040873014
As	-0.024696323	-1.855646597	1.227965765
Fe	-3.890859910	-1.933966386	0.011304099
C	0.471323292	1.595876840	-2.643333314
H	0.779736067	0.734744856	-3.211471518
C	-1.932975993	0.194830088	-3.910310910
H	-1.975558135	-0.543945094	-3.112820433
H	-1.008550304	0.042823875	-4.469744244
As	-0.048907414	-0.014029116	-1.830332377
As	-1.215999015	1.207001943	-0.015669481
Fe	-2.993824721	2.862855542	-0.064521718
C	2.038481506	-2.674450439	0.232938404
H	1.164538808	-3.273804169	0.425772502
C	0.782272678	-3.656293167	-2.380492842
H	0.056656473	-2.843631819	-2.384366907
H	0.562618759	-4.306329970	-1.533077805

H	-2.760991864	-0.010020174	-4.590957865
C	1.360267978	2.530218507	-2.043772739
C	-0.815553376	3.196306743	-1.682623110
H	-1.658527839	3.808656844	-1.406833126
C	0.543454880	3.510999642	-1.431445493
H	0.892448540	4.394338613	-0.923660991
C	-0.868391031	2.030487893	-2.494541240
C	-2.010498651	2.595090759	-4.586102198
H	-2.828066562	2.361292810	-5.271380449
H	-1.071385948	2.504052137	-5.134361034
H	-2.119112027	3.633376951	-4.268569485
C	-3.434952421	-2.521458671	1.657841501
C	3.474301126	1.374189235	-2.840793751
H	3.395777514	0.566121864	-2.115180409
H	4.535100174	1.527632862	-3.044936565
H	3.007512710	1.043948468	-3.770061016
C	2.971193424	3.740028868	-3.451588828
H	4.020534869	3.875179065	-3.722506915
H	2.576109658	4.705373003	-3.131160716
H	2.427349313	3.431485427	-4.346022450
C	-3.363758391	-2.777205035	-1.498042836
C	-2.048938197	1.627903933	-3.375300397
C	2.850936074	2.678791338	-2.329522924
C	-3.394704052	1.802844651	-2.663232395
H	-3.541892507	2.825441234	-2.312768241
H	-3.483133317	1.132745532	-1.811203942
H	-4.212535181	1.572772242	-3.348080477
C	3.627679855	3.182618859	-1.104316580
H	3.599185962	2.465788865	-0.285813536
H	3.236237882	4.136067730	-0.743410642
H	4.675707649	3.339054079	-1.364909281
C	-4.895663856	-0.441505298	-0.095981020
Zr	-0.000011414	1.522229338	0.000137209
As	1.774374613	-0.609845547	0.040740972
As	0.024908441	-1.855065333	-1.228740592
Fe	3.891056547	-1.933668887	-0.011592828
C	-0.471590460	1.595157514	2.643487178
H	-0.780055055	0.733834989	3.211310098
C	1.932255370	0.193944456	3.910771278
H	1.974565377	-0.544817411	3.113254734
H	1.007833136	0.042168505	4.470274786
H	2.760272543	-0.011156142	4.591342222
C	-1.360474850	2.529712323	2.044141406
C	0.815388225	3.195869331	1.683385432
H	1.658391671	3.808304301	1.407862757
C	-0.543592794	3.510670970	1.432202561
H	-0.892520530	4.394178135	0.924664243
C	0.868133486	2.029817271	2.494977255
C	2.010153881	2.594169297	4.586635820
H	2.827509772	2.360098182	5.272072824
H	1.070899454	2.503398249	5.134696130
H	2.119150519	3.632431120	4.269156417
C	3.435107380	-2.521314312	-1.658062401
C	-3.474577902	1.373424658	2.840572217
H	-3.395987555	0.565645086	2.114642739
H	-4.535397122	1.526799609	3.044663568
H	-3.007894766	1.042797142	3.769754649
C	-2.971408370	3.738988723	3.452414773
H	-4.020754658	3.874047150	3.723356599
H	-2.576290562	4.704459066	3.132411728
H	-2.427600296	3.430046139	4.346732426
C	3.364101652	-2.776835029	1.497847332
C	2.048550040	1.627006221	3.375809625
C	-2.851147903	2.678224679	2.329893014
C	3.394430880	1.801714492	2.663899973
H	3.541722679	2.824207220	2.313184126
H	3.482982956	1.131373179	1.812074380
H	4.212143749	1.571790094	3.348940565
C	-3.627822643	3.182592617	1.104868877
H	-3.599308631	2.466107387	0.286067180
H	-3.236328715	4.136178757	0.744379925
H	-4.675855576	3.338958308	1.365481708
C	4.895744534	-0.441120916	0.095603043
C	5.364364972	-2.931299217	-0.052577585
C	-5.364096256	-2.931698915	0.052258207
O	5.599359253	0.464962358	0.147933458
O	6.309090615	-3.573578477	-0.079019688
O	3.064840546	-3.324679757	2.460130351
O	3.188598557	-2.898213531	-2.713011786
O	-3.064390856	-3.325091494	-2.460269059
O	-3.188478656	-2.898299385	2.712819960
O	-6.308742575	-3.574095726	0.078674847
O	-5.599314961	0.464546502	-0.148370061

H	0.620807100	-4.240914804	-3.288017547
C	2.907975698	-2.172699315	1.239356120
C	3.742920150	-1.634689563	-0.841218870
H	4.419492027	-1.291845005	-1.607047989
C	3.955342539	-1.506908196	0.555088820
H	4.815545209	-1.045342072	1.010031767
C	2.569422969	-2.403052314	-1.056389213
C	3.171376367	-4.371779570	-2.393327888
H	2.974811483	-4.960931160	-3.291756317
H	3.017524755	-5.014927374	-1.525429759
H	4.219207350	-4.067556263	-2.407775719
C	-3.182829138	2.673488919	1.730190144
C	1.546036350	-2.975650911	3.239211609
H	0.862508829	-2.125372712	3.254367970
H	1.634052899	-3.337867743	4.265371228
H	1.086272821	-3.770521236	2.651947145
C	3.842621128	-3.841709604	2.785839969
H	3.907820739	-4.193677331	3.817778352
H	4.852712809	-3.619345647	2.437661967
H	3.445454034	-4.654491341	2.175670375
C	-3.913497383	1.785508624	-1.200386926
C	2.228055393	-3.143210992	-2.350013693
C	2.933171276	-2.590585852	2.707657994
C	2.490712288	-2.294585758	-3.601924613
H	3.518709496	-1.931071204	-3.640801075
H	1.822058981	-1.435016545	-3.653044500
H	2.323923652	-2.895652726	-4.497824791
C	3.531886723	-1.496864025	3.603334516
H	2.919918016	-0.595921719	3.591904091
H	4.544259375	-1.227959341	3.296308580
H	3.588971899	-1.849739254	4.634863394
C	-1.827903855	4.067178414	-0.727768326
Zr	2.032495755	0.000747254	0.000328644
As	-0.049964078	0.014080868	1.829714335
As	-1.214805302	-1.207962892	0.014367229
Fe	-2.991124578	-2.865461328	0.062615383
C	2.036536743	2.675809006	-0.232156911
H	1.162272421	3.274558691	-0.425400854
C	0.778295133	3.657072074	2.380465161
H	0.053075321	2.844050779	2.383984645
H	0.558785711	4.306936286	1.532874278
H	0.616032598	4.241688805	3.287865382
C	2.907062269	2.174959912	-1.238088767
C	3.741162726	1.637332994	0.842947803
H	4.417529457	1.294894977	1.609136826
C	3.954503650	1.509843939	-0.553279976
H	4.815377518	1.049045058	-1.007735387
C	2.566960914	2.404740331	1.057473259
C	3.166950609	4.373872937	2.394689356
H	2.969474286	4.962968529	3.292957819
H	3.013263359	5.016890786	1.526665251
H	4.214950405	4.070254617	2.409808669
C	-3.175234953	-2.686518168	-1.733674236
C	1.545678743	2.976900182	-3.238722961
H	0.862803406	2.126120233	-3.254403129
H	1.634043040	3.339308259	-4.264779592
H	1.084979363	3.771353002	-2.651615028
C	3.841335926	3.844632594	-2.784040581
H	3.906913804	4.196608719	-3.815953627
H	4.851392146	3.623085871	-2.435211924
H	3.443135613	4.657135311	-2.174161145
C	-3.911511513	-1.782181036	1.192109636
C	2.224369959	3.144745691	2.350852805
C	2.932781950	2.592800326	-2.706380439
C	2.486799207	2.296304949	3.602947317
H	3.515015479	1.933460212	3.642431099
H	1.818688509	1.436286306	3.653662622
H	2.319078849	2.897259477	4.498750984
C	3.532879550	1.499578541	-3.601763648
H	2.921623592	0.598140660	-3.590846457
H	4.545274623	1.231436306	-3.294123433
H	3.590338214	1.852615793	-4.633214446
C	-1.826392636	-4.068542422	0.730290623
C	-4.305726909	-4.068529928	0.098826245
C	-4.305056934	4.069764445	-0.093141216
O	-1.094590587	-4.849530279	1.147764932
O	-5.147868436	-4.839174386	0.122956108
O	-4.510903899	-1.124899722	1.910607846
O	-3.299881384	-2.609310313	-2.868324674
O	-4.512581417	1.132078393	-1.922579904
O	-3.310516603	2.589493059	2.864019240
O	-5.144597317	4.843411069	-0.111287815
O	-1.095109705	4.848930768	-1.142172084

Table S12: Cartesian coordinates of the optimized geometry of the Isomers for $[Cp"_2Zr(\mu,\eta^{1:1:1}\text{-}As_4)(Fe(CO)_4)]$ at the B3LYP/def2- SVP level of theory.

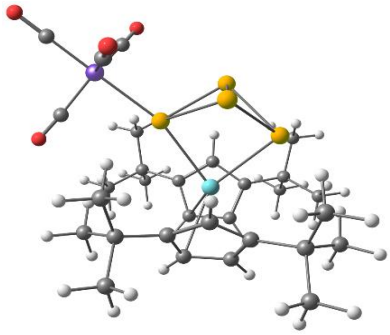

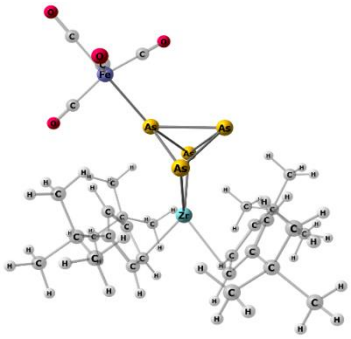

As	-0.454739521	-1.224162621	-2.249529099
C	1.235554247	-2.697986164	0.600140177
H	0.712568482	-3.286346972	-0.134605336
C	0.700605917	-2.311646739	1.855289413
C	2.871514390	-1.560594350	1.680347240
H	3.830510849	-1.155457830	1.955835980
O	-3.840859169	2.568378865	-1.813539323
C	2.592066178	-2.295969652	0.498203914
C	1.720738837	-1.571331255	2.506925659
H	1.667746006	-1.167036445	3.503737177
C	-0.525648389	-2.914286533	2.533589139
C	-1.578627731	-3.391489475	1.524729997
H	-1.984029570	-2.568741537	0.937878582
H	-2.411521897	-3.857089940	2.054731651
H	-1.174577523	-4.135425801	0.836375564
C	3.641551072	-2.899690946	-0.434703553
C	4.292789055	-4.063696645	0.353646380
H	4.799643115	-3.702960880	1.250096588
H	5.029782300	-4.572233219	-0.272251451
H	3.544599746	-4.796505708	0.660458811
C	-1.171999112	-1.941839061	3.527113269
H	-0.461310794	-1.600491658	4.281751994
H	-1.994845683	-2.431688355	4.050706725
H	-1.578594271	-1.069554995	3.021230064
C	-0.016729054	-4.148335948	3.319756318
H	0.454189808	-4.873822324	2.654136473
H	-0.853073689	-4.640411104	3.821580263
H	0.713822723	-3.861652305	4.078134712
C	3.022877621	-3.483291720	-1.713495263
H	2.298675351	-4.267848539	-1.488517498
H	3.807059057	-3.930376867	-2.327670608
H	2.525501210	-2.721259802	-2.312547923
C	-3.839715527	1.567172234	-1.252802546
C	4.742946472	-1.900404742	-0.812992635
H	4.353827745	-1.096422869	-1.435611124
H	5.528685462	-2.408256455	-1.376152630
H	5.207871056	-1.454766324	0.068005633
Zr	1.203348006	-0.000002706	0.599525279
As	-1.412301252	0.000009611	-0.280892632
As	1.690874386	-0.000014266	-2.082528310
As	-0.454715334	1.224179703	-2.249519669
Fe	-3.896478751	0.000012363	-0.358875796
O	-6.816773954	-0.000013597	-0.475875099
C	1.235650980	2.697979147	0.600088731
H	0.712705000	3.286344262	-0.134681395
C	0.700660492	2.311692339	1.855235511
C	2.871542818	1.560550703	1.680360290
H	3.830517199	1.155384168	1.955880849
O	-3.840828757	-2.568456649	-1.813362107
C	2.592149211	2.295906616	0.498192009
C	1.720745960	1.571343643	2.506908636
H	1.667712160	1.167068804	3.503726032
C	-0.525581495	2.914404116	2.533493696
C	-1.578495897	3.391684968	1.524603809
H	-1.983935482	2.568968887	0.937735095
H	-2.411374960	3.857340897	2.054580523
H	-1.174373382	4.135596556	0.836265241
C	-5.674217037	0.000012680	-0.429151273
C	3.641676588	2.899564319	-0.434708193
C	4.292934758	4.063574268	0.353619746
H	4.799768657	3.702849811	1.250085935
H	5.029949012	4.572075455	-0.272282094

As	-1.777766655	-0.648371403	-0.120594802
C	-0.244682256	2.525503125	0.647774803
H	-1.301715257	2.386528421	0.798348252
C	0.360324702	2.877417542	-0.585873284
C	1.970327954	2.772865162	1.062012632
H	2.919721427	2.876071279	1.560510549
O	-4.101033418	-3.155955269	1.508706763
C	0.725017271	2.507114692	1.685677188
C	1.751037928	2.986298391	-0.322195696
H	2.505408720	3.282983532	-1.032576470
C	-0.353401622	3.452359479	-1.810121050
C	-1.800935019	2.959053547	-1.937598981
H	-1.852519181	1.884614829	-2.109273003
H	-2.281894310	3.450279146	-2.785717512
H	-2.390304223	3.192398933	-1.050239443
C	0.446615092	2.590172639	3.184714348
C	0.427294790	4.097676656	3.538721063
H	1.389494448	4.566624760	3.325986877
H	0.210595784	4.230430898	4.601267751
H	-0.338833382	4.624965531	2.968087741
C	0.394325797	3.168455779	-3.120369279
H	1.432064424	3.502824039	-3.078976632
H	-0.087471529	3.699406042	-3.943887529
H	0.385875564	2.105929925	-3.362826171
C	-0.387927275	4.986540693	-1.596483976
H	-0.913077965	5.242855292	-0.674900424
H	-0.907196964	5.468071489	-2.428270801
H	0.619537307	5.402022707	-1.537536774
C	-0.917446413	1.994722713	3.560572014
H	-1.737132320	2.494284419	3.043281473
H	-1.087444551	2.113905097	4.632586556
H	-0.974913443	0.929208827	3.335047852
C	-4.130260470	-2.187970121	0.897803105
C	1.543367450	1.912761465	4.018881979
H	1.570202118	0.837932864	3.846254755
H	1.355274334	2.074954048	5.082251204
H	2.532027960	2.320331713	3.798592777
Zr	1.444254255	0.515484194	0.080728542
As	-0.134725718	-0.442287564	-1.948589527
As	-0.119018638	-1.113754572	1.637473406
As	-0.221642236	-2.470867680	-0.477408010
Fe	-4.212373407	-0.658688205	-0.069408121
O	-7.135372790	-0.676835461	0.005300251
C	3.164885193	-1.498136411	-0.477586484
H	2.853185098	-2.471991071	-0.815460484
C	3.498869206	-0.415856265	-1.333523725
C	3.826368274	0.205493349	0.861790556
H	4.140142384	0.776075483	1.720636367
O	-4.148443995	1.959977569	1.293787906
C	3.408842863	-1.151467103	0.876360171
C	3.891904686	0.648822627	-0.482432229
H	4.255846450	1.611795625	-0.799819815
C	3.771357659	-0.501857994	-2.833518152
C	3.014524923	-1.660202346	-3.499354139
H	1.932872799	-1.541222626	-3.424957522
H	3.268228752	-1.703905767	-4.560382549
H	3.281067143	-2.623282365	-3.061146455
C	-5.993083743	-0.669325404	-0.024154330
C	3.620464592	-2.129019686	2.033029033
C	5.139434388	-2.430935351	2.064498813
H	5.720856074	-1.525905177	2.247579853
H	5.362917461	-3.146004630	2.859721723

H	3.544760452	4.796410599	0.660403708
C	-1.172026428	1.941992332	3.526990686
H	-0.461387345	1.600601901	4.281656234
H	-1.994864553	2.431888400	4.050553549
H	-1.578653698	1.069733470	3.021089843
C	-0.016611333	4.148416393	3.319686223
H	0.454378490	4.873876713	2.654088180
H	-0.852942262	4.640541974	3.821483572
H	0.713894537	3.861679140	4.078088642
C	3.023048063	3.483141238	-1.713532433
H	2.298866802	4.267729284	-1.488596213
H	3.807256784	3.930179293	-2.327707195
H	2.525659561	2.721104774	-2.312569805
C	-3.839721253	-1.567188258	-1.252735081
C	4.743047312	1.900230071	-0.812943209
H	4.353919859	1.096251368	-1.435560582
H	5.528823207	2.408042831	-1.376087171
H	5.207926773	1.454589785	0.068077874
O	-4.064966808	0.000042944	2.585207617
C	-3.958407100	0.000062374	1.441189477

H	5.473490740	-2.860058745	1.118202249
C	3.433302515	0.806975244	-3.560960431
H	3.954461856	1.660095257	-3.122803859
H	3.737759724	0.741933380	-4.607594108
H	2.364096074	1.011501811	-3.536149908
C	5.288864926	-0.768718544	-2.988046502
H	5.578761928	-1.690787960	-2.481181271
H	5.547700970	-0.866208551	-4.045018128
H	5.879728737	0.046539863	-2.567374873
C	2.879656576	-3.458207666	1.827171659
H	3.181314734	-3.950209456	0.901156940
H	3.114535121	-4.138668139	2.647991995
H	1.798577895	-3.326596781	1.806984193
C	-4.164375966	0.940180619	0.765173427
C	3.220497584	-1.535275028	3.390842338
H	2.145067859	-1.367084691	3.451346491
H	3.493892522	-2.224027878	4.192854735
H	3.725274057	-0.588369413	3.587189609
O	-4.256447151	-0.799688394	-3.021751928
C	-4.222088783	-0.748679078	-1.878094180

Table S13: Cartesian coordinates of the optimized geometry of [Cp"$_2$Zr(μ,η$^{3:1:1}$-As$_4$)(Fe(CO)$_3$)] at the B3LYP/def2-SVP level of theory.

As	0.739518263	1.573521557	1.576914515
C	-0.139333919	-3.234947504	1.537058652
H	0.213554753	-4.175642706	1.121910813
C	-0.255722635	-1.299693768	2.729000469
H	0.019274906	-0.458469045	3.357377259
C	0.645124726	-2.312074749	2.290250489
C	2.030855512	-2.589959782	2.884244559
C	-1.498152027	-2.805676734	1.557310297
H	-2.338922990	-3.362273794	1.150136693
C	-1.583828046	-1.607084846	2.323028204
C	1.802102760	-3.559084518	4.074176445
H	1.124191514	-3.117977286	4.821616883
H	2.758954595	-3.785485501	4.572932373
H	1.360124614	-4.510093459	3.738007258
C	2.699320669	-1.312303257	3.422653855
H	2.879895732	-0.576903740	2.624441776
H	3.674070850	-1.561210804	3.871525874
H	2.093805914	-0.828517526	4.203995869
C	2.974115784	-3.265494531	1.875856855
H	2.541764366	-4.187807194	1.457117660
H	3.920483522	-3.541320636	2.367765913
H	3.210260015	-2.589092381	1.043685340
C	-2.866143585	-1.005725021	2.908535165
O	-0.800126240	5.022200058	2.205778978
C	-2.629689468	0.400158578	3.488181795
H	-1.889605811	0.389494272	4.302672276
H	-3.569141230	0.798163823	3.903248780
H	-2.276611189	1.103486285	2.719562106
C	-4.006972390	-0.940828798	1.878304744
H	-3.781301000	-0.222664731	1.077630298
H	-4.939580376	-0.614933952	2.366068481
H	-4.204023762	-1.920822078	1.416287026
C	-0.384266654	4.379476199	1.350679503
C	-3.297444057	-1.945736854	4.064660912
H	-3.525269002	-2.957716449	3.695146721
H	-4.200087054	-1.552035770	4.560346697
H	-2.502837384	-2.033637603	4.821931997
Zr	-0.273288057	-1.246370651	0.000000000
As	2.084475185	0.162055181	0.000000000
As	-1.220100144	1.407541044	0.000000000
As	0.739518263	1.573521557	-1.576914515
Fe	0.280852980	3.389215245	0.000000000
C	-0.139333919	-3.234947504	-1.537058652
H	0.213554753	-4.175642706	-1.121910813
C	-0.255722635	-1.299693768	-2.729000469
H	0.019274906	-0.458469045	-3.357377259
C	0.645124726	-2.312074749	-2.290250489
C	2.030855512	-2.589959782	-2.884244559
O	3.044256890	4.323417183	0.000000000
C	-1.498152027	-2.805676734	-1.557310297
H	-2.338922990	-3.362273794	-1.150136693
C	-1.583828046	-1.607084846	-2.323028204
C	1.802102760	-3.559084518	-4.074176445
H	1.124191514	-3.117977286	-4.821616883
H	2.758954595	-3.785485501	-4.572932373
H	1.360124614	-4.510093459	-3.738007258
C	2.699320669	-1.312303257	-3.422653855

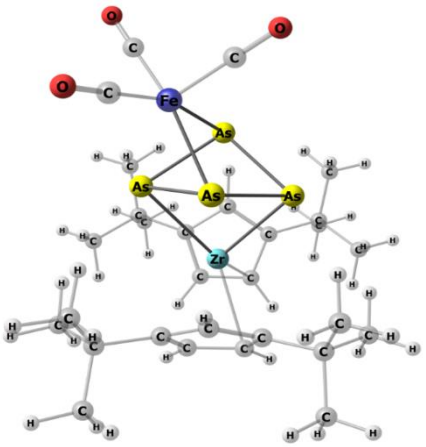

H	2.879895732	-0.576903740	-2.624441776
H	3.674070850	-1.561210804	-3.871525874
H	2.093805914	-0.828517526	-4.203995869
C	2.974115784	-3.265494531	-1.875856855
H	2.541764366	-4.187807194	-1.457117660
H	3.920483522	-3.541320636	-2.367765913
H	3.210260015	-2.589092381	-1.043685340
C	-2.866143585	-1.005725021	-2.908535165
O	-0.800126240	5.022200058	-2.205778978
C	-2.629689468	0.400158578	-3.488181795
H	-1.889605811	0.389494272	-4.302672276
H	-3.569141230	0.798163823	-3.903248780
H	-2.276611189	1.103486285	-2.719562106
C	-4.006972390	-0.940828798	-1.878304744
H	-3.781301000	-0.222664731	-1.077630298
H	-4.939580376	-0.614933952	-2.366068481
H	-4.204023762	-1.920822078	-1.416287026
C	-0.384266654	4.379476199	-1.350679503
C	1.954520985	3.957036753	0.000000000
C	-3.297444057	-1.945736854	-4.064660912
H	-3.525269002	-2.957716449	-3.695146721
H	-4.200087054	-1.552035770	-4.560346697
H	-2.502837384	-2.033637603	-4.821931997

Table S14: Cartesian coordinates of the optimized geometry of the Isomers for [Cp"$_2$Zr(µ,$\eta^{1:1:1:1}$-As$_4$)(AlMe$_3$)$_2$] at the B3LYP/def2- SVP level of theory.

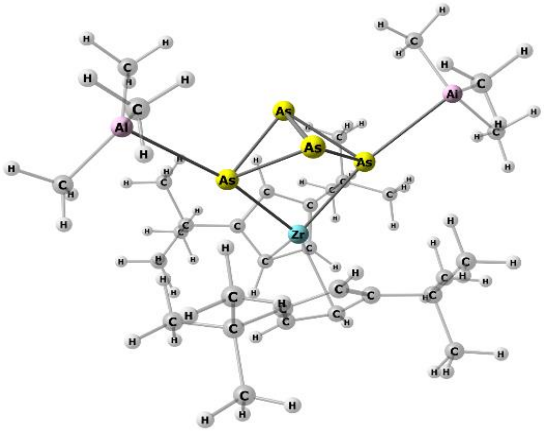

As	-1.776120110	-0.880677273	0.008344645
As	0.004411473	-2.133812973	1.229491389
Al	-3.997326414	-2.638538042	0.074418289
C	0.178331886	1.194633430	-2.672594461
H	0.329272191	0.289297483	-3.255319801
C	-2.448426496	0.018311495	-3.646565297
H	-2.388438370	-0.735922059	-2.849385076
H	-1.628917784	-0.167630109	-4.357828659
H	-3.392833521	-0.146953423	-4.188141290
C	1.225678307	2.037567321	-2.196425379
C	-0.823472387	2.942548631	-1.611749920
H	-1.567590263	3.655235734	-1.261744573
C	0.586580603	3.112964306	-1.514407516
H	1.083435722	3.972939545	-1.070868048
C	-1.090803626	1.767663153	-2.376174158
C	-2.485208400	2.437714742	-4.287308472
H	-3.399345936	2.252838589	-4.874668452
H	-1.619217478	2.316218355	-4.956628927
H	-2.504845517	3.484593989	-3.946580089
C	-3.628031636	-3.541355647	1.805554229
H	-4.420017188	-4.291998675	1.993215081
H	-2.671383095	-4.092578790	1.821326240
H	-3.634224544	-2.859236716	2.673524241
C	3.110754208	0.624883130	-3.166391925
H	3.036221190	-0.143859071	-2.383167294
H	4.158992048	0.651884404	-3.502288443
H	2.502256120	0.297396984	-4.023348129
C	2.777436603	3.012484479	-3.843406660
H	3.800690218	3.024816844	-4.252852757
H	2.524810956	4.036347606	-3.526725510
H	2.089179920	2.730075064	-4.655274359
C	-3.646076273	-3.671941214	-1.584739199
H	-3.685511192	-3.063273853	-2.504786429

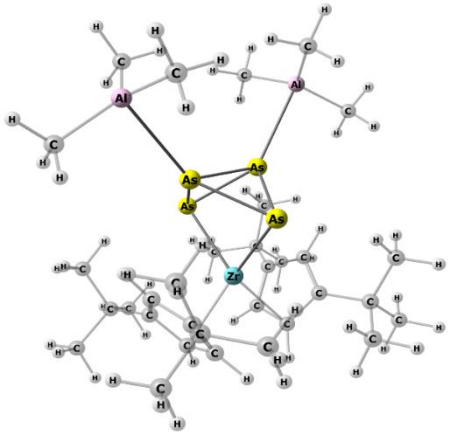

As	-0.561874598	-0.056441055	1.828948356
As	-1.741124750	1.214006620	0.042079552
Al	-4.138158620	2.963583934	0.148611304
C	1.496845044	-2.673950901	-0.324499744
H	0.612724986	-3.260251675	-0.563909459
C	1.993726775	-2.447216093	0.991348170
C	2.390454657	-2.126140570	-1.292201851
C	3.176822273	-1.665067522	0.834872463
H	3.836594249	-1.345969789	1.639827451
C	2.447175029	-2.479069695	-2.782164071
C	3.426675703	-1.485711699	-0.554051749
H	4.306166264	-1.002261636	-0.973934375
C	1.623499861	-3.244575270	2.249946355
C	0.171738634	-3.755491210	2.229007399
H	-0.558231086	-2.934396798	2.261943888
H	-0.009928476	-4.394302730	3.107695182
H	-0.038643351	-4.364600868	1.336488949
C	3.412417763	-3.686532800	-2.910038372
H	4.421363177	-3.432757336	-2.549452481
H	3.495213274	-4.001451092	-3.963285299
H	3.051464024	-4.546627168	-2.324847913
C	2.566238634	-4.478187738	2.255872553
H	2.425594011	-5.088217174	1.350128577
H	2.356938274	-5.114125603	3.131649237
H	3.623887792	-4.174960723	2.298040873
C	1.074223068	-2.898393488	-3.335989867
H	0.658669631	-3.762917716	-2.796218040
H	1.168898816	-3.188686072	-4.394254760
H	0.340088797	-2.079987360	-3.283201119
C	1.863502625	-2.448373880	3.545063502
H	2.901663862	-2.090734230	3.623205645
H	1.671774781	-3.088151640	4.420958499
H	1.194726751	-1.577987474	3.617623503

H	-2.677829432	-4.202722976	-1.576633289
H	-4.424419413	-4.451838542	-1.693039467
C	-2.411152668	1.452404135	-3.089888669
C	2.686190099	2.014083350	-2.658946361
C	-3.639737608	1.684069674	-2.194498644
H	-3.658030901	2.700824242	-1.772804401
H	-3.676797960	0.965832677	-1.363313758
H	-4.563212022	1.556292721	-2.780781458
C	3.653739114	2.475034491	-1.555165256
H	3.670527697	1.771706909	-0.712035919
H	3.389211234	3.471323885	-1.166806105
H	4.678560216	2.541462026	-1.953011406
C	-5.484939225	-1.319431238	0.042392918
H	-5.555905387	-0.750906533	-0.900986445
H	-6.443353996	-1.863123596	0.150045752
H	-5.450057819	-0.590265915	0.870696080
Zr	-0.000002370	1.198491741	-0.000006360
As	1.776123094	-0.880668737	-0.008355569
As	-0.004400878	-2.133826970	-1.229486912
Al	3.997337061	-2.638522072	-0.074400166
C	-0.178339844	1.194630260	2.672578813
H	-0.329278765	0.289291431	3.255299809
C	2.448442339	0.018330136	3.646567546
H	2.388475285	-0.735910877	2.849393326
H	1.628932649	-0.167622202	4.357826595
H	3.392848264	-0.146912904	4.188152392
C	-1.225687922	2.037567332	2.196420484
C	0.823457797	2.942550710	1.611736198
H	1.567573488	3.655240147	1.261730655
C	-0.586594870	3.112961147	1.514393890
H	-1.083453655	3.972933825	1.070853490
C	1.090793376	1.767668551	2.376164405
C	2.485197155	2.437732273	4.287294501
H	3.399323086	2.252848167	4.874670225
H	1.619193782	2.316247803	4.956600923
H	2.504851269	3.484609568	3.946561017
C	3.628070144	-3.541342264	-1.805540999
H	4.420061443	-4.291981583	-1.993192411
H	2.671424424	-4.092570133	-1.821324425
H	3.634270387	-2.859223328	-2.673511033
C	-3.110783826	0.624884331	3.166361015
H	-3.036255094	-0.143841068	2.383120133
H	-4.159023376	0.651890574	3.502251866
H	-2.502295364	0.297372766	4.023314208
C	-2.777430295	3.012459819	3.843434495
H	-3.800678598	3.024783812	4.252894287
H	-2.524806072	4.036330842	3.526778067
H	-2.089163812	2.730026221	4.655285456
C	3.646069558	-3.671923036	1.584754789
H	3.685488373	-3.063251051	2.504799647
H	2.677826574	-4.202711620	1.576638612
H	4.424417027	-4.451814179	1.693068900
C	2.411146466	1.452417603	3.089878699
C	-2.686200095	2.014090483	2.658947414
C	3.639728935	1.684095244	2.194487600
H	3.658019941	2.700854770	1.772805116
H	3.676788879	0.965868359	1.363293586
H	4.563205365	1.556313459	2.780766175
C	-3.653750910	2.475088943	1.555188058
H	-3.670554759	1.771789408	0.712036358
H	-3.389210350	3.471386539	1.166858837
H	-4.678568572	2.541519029	1.953042717
C	5.484943459	-1.319408181	-0.042347785
H	5.555886707	-0.750884731	0.901034261
H	6.443363204	-1.863095936	-0.149980489
H	5.450076975	-0.590241409	-0.870650227
C	3.001614517	-1.315371797	-3.623066239
H	2.347854566	-0.434177658	-3.566772501
H	3.079401350	-1.612390462	-4.681032062
H	4.009286540	-1.015412537	-3.294579266
Zr	1.475561090	0.000251885	0.000282186
As	-0.559947588	0.055645371	-1.830450066
As	-1.740325788	-1.215606238	-0.044866230
Al	-4.138275569	-2.963636921	-0.148607791
C	1.495182956	2.674042189	0.325207145
H	0.610470299	3.259720715	0.563963388
C	1.993320795	2.447771956	-0.990258028
C	2.388364592	2.126718527	1.293592619
C	3.176757031	1.666330854	-0.832874051
H	3.837372521	1.347692959	-1.637321082
C	2.443806085	2.479771035	2.783581928
C	3.425591387	1.487020778	0.556228160
H	4.305054510	1.004111973	0.976790128
C	1.623804789	3.245155381	-2.249066010
C	0.171755699	3.755303199	-2.229425163
H	-0.557770484	2.933856598	-2.263337228
H	-0.009359221	4.394274239	-3.108110300
H	-0.039839088	4.364043332	-1.336942697
C	3.408038683	3.687985445	2.912012119
H	4.417397940	3.435006551	2.552024939
H	3.489961603	4.002974238	3.965307428
H	3.046747356	4.547795623	2.326611951
C	2.565869877	4.479292586	-2.253817070
H	2.424009755	5.089042236	-1.348075269
H	2.357060906	5.115310970	-3.129651344
H	3.623728345	4.176666886	-2.295030246
C	1.070195310	2.898099911	3.336495269
H	0.654256171	3.762176164	2.796306122
H	1.163996655	3.188674134	4.394760934
H	0.336770369	2.079095490	3.283429718
C	1.865494776	2.449363462	-3.544121921
H	2.903893804	2.092198485	-3.621285653
H	1.674387355	3.089270807	-4.420057691
H	1.197173836	1.578704589	-3.617601055
C	2.998590502	1.316537728	3.624898526
H	2.345627899	0.434781246	3.568096597
H	3.075314551	1.613616053	4.682924817
H	4.006770879	1.017446361	3.297180691
C	-4.591656718	2.797852621	-1.769870182
H	-3.802498756	3.176717840	-2.441878530
H	-4.822254499	1.761952982	-2.071288321
H	-5.498694130	3.396332939	-1.982300668
C	-5.151305850	1.919587042	1.488305499
H	-6.118129332	2.422053159	1.685203759
H	-5.392036233	0.897766703	1.149399751
H	-4.636399824	1.839700518	2.460908051
C	-3.141120488	4.567856034	0.756612455
H	-2.389649530	4.918225937	0.027715868
H	-3.850079447	5.406180611	0.899181389
H	-2.634177590	4.423754989	1.726727700
C	-3.144110049	-4.569067041	-0.758185863
H	-2.394934672	-4.923084530	-0.028697161
H	-3.855009628	-5.405155013	-0.904181199
H	-2.634915448	-4.424117809	-1.727006164
C	-5.152692162	-1.919024108	-1.486905719
H	-6.118911879	-2.422322404	-1.684621156
H	-5.394549189	-0.897975331	-1.146489932
H	-4.637867243	-1.837151154	-2.459389826
C	-4.588632433	-2.797428268	1.770593621
H	-4.820660014	-1.761806886	2.071851556
H	-5.494112725	-3.397587628	1.984945163
H	-3.797589441	-3.174438477	2.441433540

Table S15: Cartesian coordinates of the optimized geometry of the Isomers for [Cp"$_2$Zr(µ,η$^{1:1:1}$-As$_4$)(AlMe$_3$)] at the B3LYP/def2- SVP level of theory.

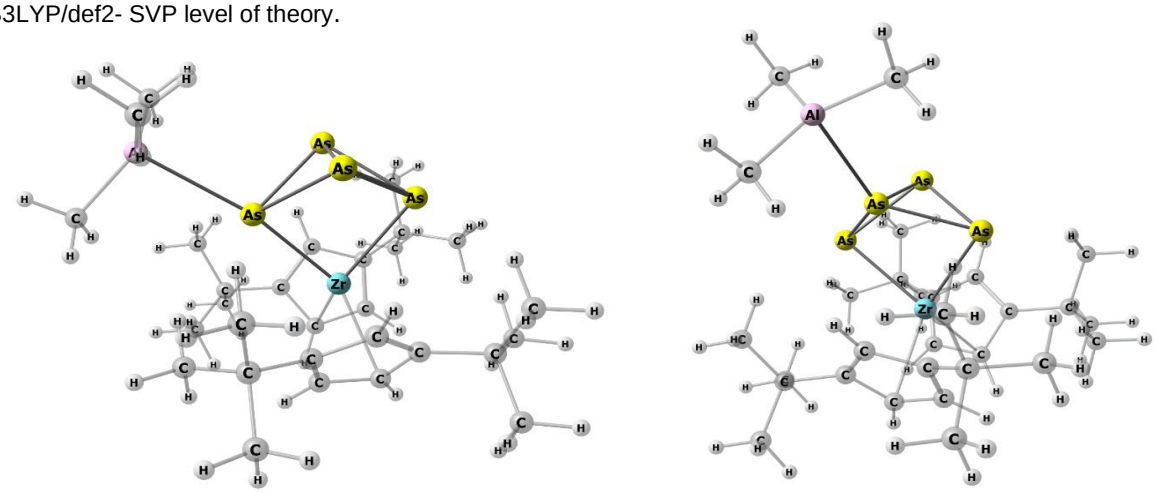

As	1.287504482	-0.031353714	-2.123954713
As	-0.941737221	1.072696942	-2.321526140
C	0.734600936	-2.593766948	0.843503233
H	0.093437601	-3.235099912	0.243876550
C	2.219963389	-3.748220474	-1.552320669
H	1.717844730	-3.021105607	-2.205393959
H	1.459772833	-4.442569024	-1.162394889
H	2.909618211	-4.337867902	-2.176915143
C	0.369508105	-2.033364558	2.103781497
C	2.543366927	-1.431840424	1.591909768
H	3.551875912	-1.036725997	1.698163702
C	1.502502515	-1.297347094	2.551837589
H	1.589710941	-0.774940319	3.502131785
C	2.091310716	-2.284075689	0.540299518
C	3.665395164	-4.172027017	0.442877658
H	4.316265098	-4.804349120	-0.183390521
H	2.905906821	-4.819540608	0.908145885
H	4.280494754	-3.741713102	1.248334623
C	-1.974654708	-3.024784934	2.123531387
H	-2.355690998	-2.299890157	1.389563575
H	-2.816019043	-3.309442161	2.774349261
H	-1.663256752	-3.928989682	1.578258254
C	-0.318106271	-3.549894879	3.925935942
H	-1.141862229	-3.913483640	4.561897223
H	0.481412327	-3.175934086	4.584395088
H	0.081731259	-4.407673494	3.362933245
C	3.003331443	-3.062936397	-0.418455596
C	-0.828028232	-2.441712670	2.967526416
C	4.119041574	-2.192609640	-1.023412718
H	4.711775979	-1.684252516	-0.247656490
H	3.713361224	-1.428286056	-1.702435056
H	4.811921953	-2.821041856	-1.605501410
C	-1.358165245	-1.269907375	3.813238514
H	-1.776558395	-0.471674285	3.185263719
H	-0.569494147	-0.831903874	4.445579206
H	-2.158319314	-1.617963958	4.485537391
Zr	0.796232803	0.073229501	0.556943280
As	-1.792196853	-0.091179058	-0.270969732
As	-0.822953460	-1.369330567	-2.189573560
Al	-4.572770054	-0.292605516	-0.575140945
C	0.904061451	2.749961937	0.311780939
H	0.583034015	3.278641548	-0.581901094
C	-2.002777970	3.660477356	0.530183490
H	-2.328623878	2.806579558	-0.079739258
H	-1.401372456	4.327983469	-0.106305291
H	-2.905315640	4.218551757	0.824811359
C	2.235398230	2.298392813	0.553946015
C	0.906065446	1.805949836	2.383888261
H	0.606777335	1.496324116	3.383432656
C	2.218150121	1.697610965	1.845667595
H	3.078984602	1.288738984	2.370728374
C	0.084953804	2.505574479	1.449651800
C	-0.831403388	4.489390891	2.579035500
H	-1.729303423	5.070834681	2.845394339
H	-0.170209781	5.136765710	1.981951184
H	-0.302512424	4.233746759	3.510401677
C	-4.691367417	-2.102791396	-1.389028000
H	-5.755848184	-2.348004106	-1.569869356
H	-4.184442622	-2.181024823	-2.366843361

As	-0.512646515	-0.269833241	-2.010681174
As	-0.515440055	-2.471310438	-0.812143173
C	-0.892919026	2.276917207	0.995245047
H	-1.939596461	2.020377966	1.139840259
C	-0.348382821	2.834386431	-0.196466105
C	0.107038087	2.202914891	2.009239315
C	1.041503319	3.029697228	0.060611383
H	1.756807548	3.480305155	-0.624969756
C	-0.136178486	2.056313833	3.515386347
C	1.313990518	2.660429417	1.406956790
H	2.272181764	2.781418423	1.907521171
C	-1.141762749	3.510175893	-1.323869548
C	-2.546778824	2.908871753	-1.506161564
H	-2.508602627	1.862326740	-1.838814257
H	-3.099706791	3.479576081	-2.268999789
H	-3.136728486	2.951537712	-0.577716074
C	-0.245491920	3.496456825	4.082297067
H	0.685566187	4.062527412	3.923503415
H	-0.446776327	3.467669313	5.165967420
H	-1.064277822	4.051659567	3.598624732
C	-1.306786447	4.991783860	-0.890688301
H	-1.842310494	5.065772338	0.068627036
H	-1.883149696	5.549866363	-1.646972423
H	-0.330271928	5.486363823	-0.771448352
C	-1.451029153	1.318161101	3.823245938
H	-2.323055071	1.839120984	3.399272571
H	-1.602924285	1.261011599	4.912781936
H	-1.448190307	0.289051365	3.433637585
C	-0.397770921	3.481766949	-2.670798904
H	0.604197115	3.931826167	-2.597116047
H	-0.960044240	4.056948423	-3.423455114
H	-0.286007229	2.455892536	-3.051809043
C	1.028804320	1.340926126	4.223212867
H	1.130436885	0.300497302	3.884951948
H	0.859502907	1.326068205	5.311820793
H	1.989094558	1.852585709	4.050809729
Zr	0.955790337	0.507620811	0.152687729
As	-0.468457693	-1.408814249	1.465500420
As	-2.177329012	-0.789166461	-0.232353847
Al	-5.042577536	-1.316326761	-0.316626216
C	2.846181151	-1.217105159	-0.696070816
H	2.616355720	-2.140715482	-1.221537569
C	3.035075394	-1.107313707	0.711276258
C	3.110517284	0.033230858	-1.329736785
C	3.339908520	0.263799908	0.961305491
H	3.584185131	0.693697821	1.931006650
C	3.412974896	0.255882682	-2.815113324
C	3.401737235	0.952174670	-0.281111010
H	3.695413241	1.991967953	-0.406550897
C	3.311842165	-2.263507692	1.682925524
C	2.673555791	-3.587567389	1.225586045
H	1.575703630	-3.535610687	1.214194674
H	2.961043397	-4.397096087	1.915183668
H	3.013324347	-3.881148751	0.220244086
C	4.951310622	0.133419282	-2.971901315
H	5.476064658	0.895772647	-2.375391039
H	5.241959104	0.265704356	-4.027281837
H	5.306339470	-0.855468459	-2.642096680
C	4.852763684	-2.450542496	1.688630558

H	-4.292566684	-2.904102676	-0.742598831
C	3.164025926	3.187661357	-1.643436423
H	2.697915582	2.388631567	-2.239263891
H	4.087159115	3.494591427	-2.160112516
H	2.484910817	4.054085987	-1.644763018
C	4.093889044	3.924412346	0.561409171
H	4.986928389	4.307652659	0.040686873
H	4.392284125	3.636585130	1.581473504
H	3.367071321	4.747672712	0.642926767
C	-4.903049318	1.266857049	-1.762939484
H	-4.619508846	2.233410524	-1.310785439
H	-4.389712286	1.192969147	-2.737823706
H	-5.985636261	1.331821182	-1.985359805
C	-1.232432947	3.215970943	1.786189263
C	3.492626233	2.722628953	-0.213680415
C	-2.153870362	2.363016393	2.674706937
H	-1.652015556	2.045130941	3.601451338
H	-2.509233348	1.464841145	2.149549233
H	-3.041055314	2.946226979	2.967518240
C	4.546590904	1.602175505	-0.272497200
H	4.193998547	0.747336555	-0.865751728
H	4.812715682	1.236133902	0.731835456
H	5.472149329	1.975902381	-0.739144748
C	-5.145990265	-0.133335465	1.324091987
H	-4.975670492	0.866081993	1.760457913
H	-6.236148135	-0.317381133	1.383580512
H	-4.671957582	-0.873893120	1.991886608
H	5.228856157	-2.674420900	0.678149704
H	5.134921808	-3.285495986	2.351128829
H	5.365293837	-1.543697090	2.045461317
C	2.751563222	-0.808028333	-3.708880500
H	3.086916334	-1.824762252	-3.452288612
H	3.018741095	-0.632251658	-4.763021641
H	1.653668410	-0.783804874	-3.635823776
C	2.859525144	-1.951506479	3.120685822
H	3.307062642	-1.020173296	3.500025723
H	3.169605581	-2.763082395	3.798115215
H	1.765579761	-1.859461245	3.191438307
C	2.982895009	1.656734674	-3.285616173
H	1.895072726	1.790554409	-3.210304365
H	3.270619385	1.810310257	-4.337930239
H	3.466190633	2.452461144	-2.696866837
C	-5.576440428	0.219199364	0.821846791
H	-5.317553371	1.199893791	0.385782139
H	-6.676247390	0.216094108	0.949142315
H	-5.146793746	0.176144929	1.837841423
C	-4.983178422	-3.117426857	0.503983812
H	-6.012941066	-3.515935781	0.586872381
H	-4.410101840	-3.845948637	-0.094498576
H	-4.564122879	-3.117446617	1.524835509
C	-5.258090998	-1.154999954	-2.279167491
H	-4.675007961	-1.901728109	-2.844654814
H	-6.320955722	-1.322521749	-2.540829532
H	-4.993883022	-0.157183470	-2.669524323

Table S16: Cartesian coordinates of the optimized geometry of the Isomers for [Cp"$_2$Zr(µ,η$^{1:1:1:1}$-As$_4$)(AlEt$_3$)$_2$] at the B3LYP/def2- SVP level of theory.

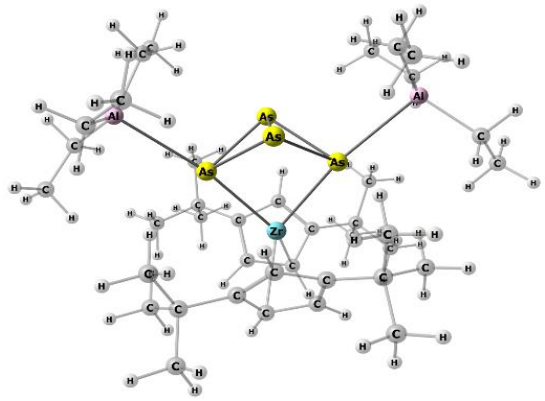

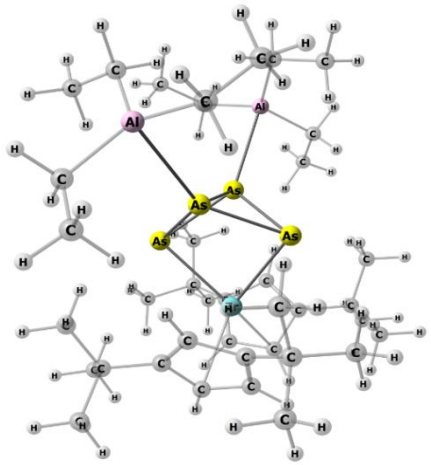

As	1.789479893	0.610237842	-0.036213091
As	-0.022145310	1.849806301	-1.226861404
Al	4.016914730	2.441809060	-0.087343100
C	-0.237659840	-1.502037760	2.673848347
H	-0.462944310	-0.618770175	3.266554859
C	1.071694585	-1.993504383	2.407564307
C	-1.216930621	-2.403377388	2.157938386
C	0.898299293	-3.171471550	1.621040510
H	1.696872139	-3.826204420	1.277363054
C	-2.693507710	-2.472121465	2.558304685
C	-0.494346371	-3.430183291	1.487394626
H	-0.924926048	-4.311627273	1.017604548
C	2.350620427	-1.624056836	3.168894277
C	2.341317152	-0.173420242	3.681005607
H	2.340249939	0.555606885	2.859334460
H	3.241859099	0.013563655	4.286414046
H	1.470243388	0.030552432	4.322763014
C	-2.774920275	-3.462023372	3.750102794
H	-2.426600416	-4.466311503	3.462882142
H	-3.815549436	-3.549273509	4.102743094
H	-2.157158469	-3.118739714	4.594529139
C	2.387324309	-2.568512048	4.401046803
H	1.499230908	-2.427459895	5.036482166
H	3.280937076	-2.360257263	5.011695355
H	2.420806401	-3.625976925	4.096147614
C	-3.233093754	-1.109593911	3.023837019
H	-2.672740006	-0.718871444	3.886905390
H	-4.284826540	-1.206902728	3.334756112
H	-3.195924291	-0.354046320	2.225456905
As	0.183572246	-0.126844455	1.823585526
As	1.370336877	-1.215327462	-0.075460724
Al	3.666100663	-3.193206458	0.193291734
C	-1.862711145	2.687074846	0.038614387
H	-0.966556189	3.290140707	-0.083956544
C	-2.406927056	2.284079632	1.292367351
C	-2.723871022	2.289037710	-1.026216071
C	-3.586926735	1.542675741	0.987688343
H	-4.277966514	1.122981275	1.716607101
C	-2.727353511	2.854232366	-2.450560959
C	-3.786302937	1.557884761	-0.420844663
H	-4.652411288	1.146186401	-0.934225867
C	-2.076190481	2.894153646	2.661868784
C	-0.641024390	3.445215835	2.733454586
H	0.113414144	2.653468498	2.622839904
H	-0.474922430	3.926928647	3.709899548
H	-0.453576679	4.205950740	1.960645894
C	-3.667203961	4.088524377	-2.426358212
H	-4.691740720	3.807100836	-2.137113790
H	-3.710178001	4.556601011	-3.423551842
H	-3.309653097	4.844776415	-1.710358470
C	-3.056202912	4.085402311	2.838238053
H	-2.937612471	4.820181738	2.026660565
H	-2.864415859	4.599832813	3.794309478
H	-4.104231300	3.747565008	2.837094167
C	-1.330748296	3.321762318	-2.897227171
H	-0.922791352	4.098104956	-2.232442680
H	-1.385378053	3.754332608	-3.908708217
H	-0.607586749	2.492461843	-2.932111038

C	3.620505926	-1.868015650	2.336169252
H	3.690333806	-2.909878767	1.987598907
H	4.515747236	-1.667170960	2.944772408
H	3.666382699	-1.207674332	1.458946528
C	-3.571840870	-3.007410854	1.413580411
H	-3.552414832	-2.335052874	0.544975830
H	-4.618034230	-3.095913627	1.745964336
H	-3.249973995	-4.007303194	1.081728374
C	3.310208982	3.403050500	-2.907652873
H	3.654447752	3.569280938	-3.944933681
H	3.064880043	4.394573880	-2.490252528
H	2.356687280	2.850221277	-2.978494535
C	3.157697225	3.987400997	2.390978701
H	2.766469637	4.927976996	2.819576067
H	4.158314844	3.828042718	2.828191437
H	2.516268723	3.175755573	2.777554440
C	6.181176938	0.313610479	0.165323044
H	6.683086795	0.720787018	-0.728941406
H	5.526816620	-0.501135740	-0.191601783
H	6.965704224	-0.159691296	0.784029414
C	5.394473623	1.398190937	0.917791654
H	6.103571983	2.169401096	1.284564580
H	4.956887700	0.977881783	1.842249882
C	4.340648919	2.657439147	-2.046173394
H	5.300230224	3.217490465	-2.070769320
H	4.589577321	1.685008562	-2.509895307
C	3.201759475	4.001903401	0.854779624
H	2.195742396	4.221914663	0.449534224
Zr	0.001064187	-1.465709212	0.000663721
As	-1.790339764	0.607591205	0.036231443
As	0.019416190	1.849910490	1.227014532
Al	-4.020752869	2.437751419	0.085335449
C	0.240050955	-1.503124213	-2.672493288
H	0.464348510	-0.619892131	-3.265632021
C	-1.068762986	-1.995990251	-2.406153526
C	1.220298119	-2.403055870	-2.155947505
C	-0.894124217	-3.173286861	-1.618898935
H	-1.691997035	-3.828742391	-1.274959960
C	2.696997687	-2.470481217	-2.556124888
C	0.498805346	-3.430331095	-1.484957442
H	0.930342542	-4.311040632	-1.014675763
C	-2.347984039	-1.628490225	-3.167936381
C	-2.340306609	-0.178144109	-3.680895914
H	-2.340262962	0.551386554	-2.859667895
H	-3.240967192	0.007409769	-4.286567539
H	-1.469369055	0.026503937	-4.322621470
C	2.779381589	-3.460396528	-3.747847547
H	2.431676887	-4.464904812	-3.460651745
H	3.820154802	-3.546952897	-4.100230370
H	2.161589074	-3.117579398	-4.592440493
C	-2.383294847	-2.573711337	-4.399548390
H	-1.495170944	-2.432043544	-5.034803288
H	-3.276962823	-2.366787448	-5.010564689
H	-2.415694681	-3.631036087	-4.094044341
C	3.235579336	-1.107559420	-3.021626889
H	2.674519740	-0.716813796	-3.884218905
H	4.287161038	-1.204282962	-3.333246872
H	3.198647749	-0.352289103	-2.222983155
C	-3.617758110	-1.873448464	-2.335341889
H	-3.686290913	-2.915101408	-1.985887786
H	-4.513102593	-1.674330590	-2.944364492
H	-3.664775016	-1.212395196	-1.458720204
C	3.575644829	-3.004895252	-1.411241252
H	3.555357597	-2.332506298	-0.542677312
H	4.621987507	-3.092352587	-1.743433826
H	3.254737691	-4.005100187	-1.079407900
C	-3.316757635	3.421490660	2.897108043
H	-3.658509150	3.589065378	3.934989488
H	-3.084682909	4.413601274	2.473553938
H	-2.356621286	2.880114198	2.966570992
C	-3.164919066	3.977486697	-2.398161954
H	-2.775098491	4.917436293	-2.829407354
H	-4.165580967	3.815763456	-2.834411609
H	-2.522704852	3.165645674	-2.782988725
C	-6.179414884	0.302795915	-0.160150394
H	-6.679731441	0.709003087	0.735450795
H	-5.521983167	-0.510208892	0.195075191
H	-6.964565434	-0.172677011	-0.776398927
C	-5.397589683	1.389015961	-0.915308077
H	-6.109731659	2.157976122	-1.280944293
H	-4.960994984	0.969277176	-1.840494093
C	-4.342069332	2.659508326	2.043827578
H	-5.307831167	3.208776943	2.068779391
H	-4.578296675	1.687007285	2.514010681
C	-3.208078746	3.995892953	-0.862009207
C	-2.300219294	1.909643817	3.823177230
H	-3.319261209	1.493776117	3.821336804
H	-2.159382506	2.426143064	4.785840352
H	-1.587304412	1.072474138	3.789330222
C	-3.277681096	1.840347130	-3.469393954
H	-2.639177315	0.948879981	-3.538278677
H	-3.327753414	2.296761137	-4.470771440
H	-4.296685837	1.511439800	-3.211094379
C	4.674040884	-1.722456139	2.641944425
H	5.459556762	-1.096764019	3.101697979
H	4.619397390	-2.653489749	3.231873863
H	3.716619358	-1.196336603	2.797762936
C	1.641476081	-5.440507651	0.551914164
H	1.149840016	-6.159419498	1.232260473
H	2.147098116	-6.033599881	-0.228835845
H	0.835849170	-4.884276247	0.040883395
C	4.691603441	-2.535429882	-2.589279234
H	5.692812273	-2.328026458	-2.174769133
H	4.166223462	-1.566511604	-2.634711651
H	4.839608232	-2.866978997	-3.632789146
C	3.925489095	-3.565175518	-1.742883577
H	4.462628096	-4.537040916	-1.771108314
H	2.947230119	-3.789548857	-2.209246640
C	4.935679816	-2.003803579	1.153418492
H	5.924696262	-2.495984507	1.039392918
H	5.045095796	-1.053763536	0.598024077
C	2.614754329	-4.498000473	1.275272497
H	3.382825097	-5.101608312	1.803011395
Zr	-1.854230656	0.000071365	-0.000070774
As	0.183617792	0.126932303	-1.823650768
As	1.370365506	1.215358202	0.075471168
Al	3.666072866	3.193076264	-0.193157589
C	-1.862823511	-2.687136045	-0.038517357
H	-0.966716456	-3.290252617	0.084187770
C	-2.406878086	-2.284202173	-1.292347068
C	-2.724061775	-2.288928213	1.026192592
C	-3.586822455	-1.542629682	-0.987863008
H	-4.277854773	-1.123092254	-1.716878738
C	-2.727727174	-2.854078344	2.450550100
C	-3.786367173	-1.557747900	0.420650641
H	-4.652476758	-1.145911361	0.933909228
C	-2.076019213	-2.894281056	-2.661808495
C	-0.640857012	-3.445353157	-2.733247519
H	0.113574460	-2.653619737	-2.622482524
H	-0.474617674	-3.927014522	-3.709694650
H	-0.453540888	-4.206128745	-1.960451866
C	-3.667457050	-4.088462013	2.426237803
H	-4.691978924	-3.807140206	2.136843799
H	-3.710529348	-4.556521746	3.423435349
H	-3.309734399	-4.844693667	1.710303070
C	-3.056030750	-4.085530964	-2.838270856
H	-2.937546964	-4.820284917	-2.026655326
H	-2.864131383	-4.599989804	-3.794303991
H	-4.104053681	-3.747681089	-2.837264652
C	-1.331142518	-3.321461883	2.897455956
H	-0.923040378	-4.097835214	2.232793519
H	-1.385880337	-3.753946759	3.908966937
H	-0.608043815	-2.492109411	2.932355073
C	-2.299955828	-1.909788669	-3.823152337
H	-3.318988127	-1.493897786	-3.821375418
H	-2.159082467	-2.426330525	-4.785787159
H	-1.587028066	-1.072631674	-3.789314685
C	-3.278326491	-1.840211449	3.469242350
H	-2.639919872	-0.948688234	3.538224415
H	-3.328560833	-2.296591345	4.470627742
H	-4.297310869	-1.511402726	3.210729104
C	1.641274110	5.440504000	-0.551178047
H	1.150013104	6.159861837	-1.231317108
H	2.146435136	6.033068693	0.230268515
H	0.835363793	4.883894229	-0.040993244
C	4.693139229	2.534962772	2.588719984
H	4.841595626	2.866266164	3.632252158
H	5.694223271	2.328296487	2.173533002
H	4.168427676	1.565688379	2.634203138
C	4.673225274	1.722243140	-2.642179364
H	4.618162185	2.653139011	-3.232294606
H	3.715831667	1.195915119	-2.797454219
H	5.458645943	1.096587692	-3.102147521
C	4.935504357	2.003959549	-1.153840236
H	5.924421936	2.496452231	-1.040389920
H	5.045456557	1.054059669	-0.598312362
C	2.614956126	4.498481479	-1.274607813
H	3.383256392	5.102413174	-1.801646604
H	2.093881930	3.963949364	-2.091560620
C	3.925831456	3.564463886	1.743111552

H	-2.202013437	4.217833468	-0.457902324
H	-3.823539584	4.857491137	-0.527959314
H	3.816714272	4.863164938	0.518942802
H	2.947613074	3.787895474	2.210009930
H	4.462254243	4.536715377	1.771455724
H	2.093236725	-3.963039586	2.091664688

Table S17: Cartesian coordinates of the optimized geometry of the Isomers for [Cp"$_2$Zr(µ,$\eta^{1:1:1}$-As$_4$)(AlEt$_3$)] at the B3LYP/def2- SVP level of theory.

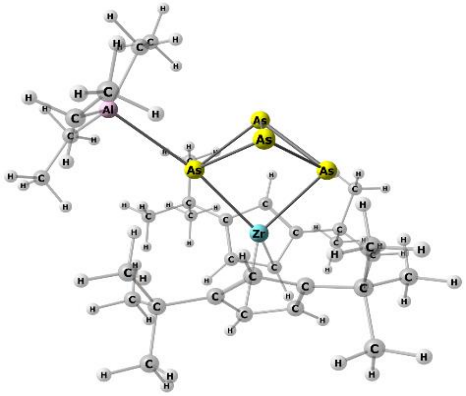

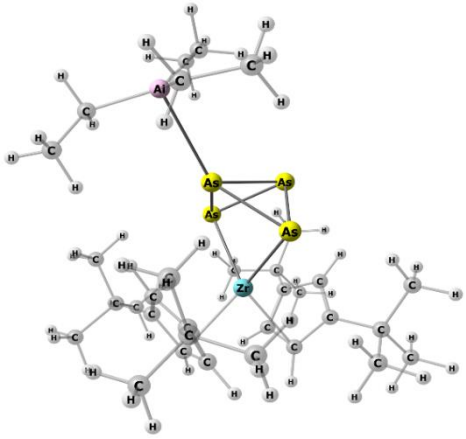

As	-1.439685180	-0.083500557	-2.154151752
As	0.751221039	1.111538267	-2.228349430
C	-0.948770267	-2.598466370	0.872783472
H	-0.241432130	-3.220514454	0.330057659
C	-2.293424838	-2.351294170	0.473135783
C	-0.695054208	-2.005421158	2.145574075
C	-2.850687921	-1.503530346	1.476823448
H	-3.878730802	-1.147822194	1.506627615
C	0.461037337	-2.339348316	3.093194572
C	-1.885280280	-1.313355325	2.503791919
H	-2.059909857	-0.783314311	3.437659300
C	-3.106469073	-3.182178748	-0.529710601
C	-2.227988256	-3.826293962	-1.617033638
H	-1.740297525	-3.073809243	-2.251839640
H	-2.848834462	-4.461484189	-2.268675430
H	-1.446310860	-4.470120039	-1.185124882
C	-0.066013525	-3.423366980	4.068957662
H	-0.909980320	-3.048824229	4.668942759
H	0.733427612	-3.734328401	4.761302212
H	-0.409822457	-4.315523456	3.522613898
C	-3.752401381	-4.322773788	0.302193301
H	-2.984965923	-4.927979922	0.809394653
H	-4.335759269	-4.990212378	-0.353490324
H	-4.429890037	-3.922965268	1.072574253
C	1.669388773	-2.915905064	2.336907375
H	1.417393435	-3.852883092	1.816880633
H	2.485144724	-3.141315374	3.041255819
H	2.062500370	-2.210244885	1.590995445
C	-4.234802558	-2.376613836	-1.197802937
H	-4.901686798	-1.910274628	-0.456738601
H	-4.852974662	-3.042451575	-1.820855468
H	-3.837786914	-1.584659960	-1.850056776
C	0.905901671	-1.115209624	3.913785562
H	1.327760382	-0.329196001	3.272014423
H	1.681581261	-1.405697279	4.639929589
H	0.070305858	-0.680482455	4.485088902
Zr	-1.094280072	0.057079747	0.543040047
As	1.555624301	-0.020550746	-0.134692181
As	0.724562126	-1.331320517	-2.102753983
Al	4.386564618	-0.149001851	-0.372229507
C	-1.338223576	2.725818294	0.245358154
H	-1.005424692	3.257070875	-0.642429197
C	-0.561444541	2.544575155	1.423238949
C	-2.653580752	2.206975136	0.435982822
C	-1.385160862	1.813790026	2.331363392
H	-1.117895088	1.539408987	3.350192598
C	-3.896359718	2.548818008	-0.392746665
C	-2.663349502	1.627061674	1.736776056
H	-3.524680515	1.182501698	2.230654145
C	0.695929351	3.332814492	1.808627748
C	1.484365478	3.819037376	0.579551166
H	1.863020402	2.983948008	-0.025606399
H	2.352716794	4.413615794	0.903541836
As	-0.306723353	-0.363632174	-1.953216822
As	-0.477699612	-2.421348374	-0.536178656
C	-0.357725580	2.518026364	0.732490868
H	-1.424388798	2.389983160	0.897091647
C	0.235614027	2.891517444	-0.507241738
C	0.633384161	2.449850014	1.755703631
C	1.638884340	2.970123644	-0.263108855
H	2.392683340	3.276445600	-0.986121862
C	0.381002892	2.491656144	3.266684047
C	1.878210249	2.715725365	1.115778585
H	2.845575704	2.793860566	1.607086302
C	-0.490973266	3.517566785	-1.705602034
C	-1.960441917	3.070595613	-1.801153855
H	-2.051297984	1.989410345	-1.976129350
H	-2.453992858	3.585962622	-2.640256926
H	-2.526241306	3.317874913	-0.889954591
C	0.395341471	3.989588076	3.669700566
H	1.369313856	4.454000025	3.450111122
H	0.200525863	4.098030644	4.749507296
H	-0.377806131	4.554281696	3.125791398
C	-0.467933193	5.049898577	-1.459541784
H	-0.958364335	5.306038315	-0.507466285
H	-1.000021872	5.575275126	-2.269695827
H	0.562920517	5.435152484	-1.421938295
C	-0.990402805	1.903830313	3.643823063
H	-1.816941197	2.441997643	3.155307651
H	-1.146822975	1.983709650	4.731347933
H	-1.072185170	0.840097501	3.373380722
C	0.214254626	3.232526428	-3.043390997
H	1.271789378	3.537755664	-3.025513675
H	-0.275693268	3.794187270	-3.854652719
H	0.169262695	2.165030621	-3.304302559
C	1.482575657	1.763027211	4.056740615
H	1.496055797	0.688070285	3.831246288
H	1.312773839	1.878013385	5.139219500
H	2.482508479	2.171040434	3.839359528
Zr	1.291274663	0.490107170	0.087420606
As	-0.274213925	-1.141746858	1.615100739
As	-1.970290456	-0.544340998	-0.104639298
Al	-4.884256176	-0.850454944	-0.096106895
C	2.970160898	-1.524689440	-0.547234539
H	2.630147894	-2.488298975	-0.918360747
C	3.231252005	-1.227802726	0.820599901
C	3.319412236	-0.415146841	-1.371366212
C	3.674884397	0.128053949	0.850193509
H	4.009403096	0.667506203	1.734368787
C	3.577989026	-0.452130126	-2.881489202
C	3.741895070	0.616763275	-0.483766479
H	4.128718506	1.591026820	-0.775247353
C	3.433955129	-2.252765764	1.944464791
C	2.672733333	-3.565434169	1.684423964
H	1.584912023	-3.412283913	1.646453316
H	2.881047820	-4.284360372	2.492546210

H	0.872694756	4.463677380	-0.070742586
C	-4.591515078	3.734216533	0.326834517
H	-4.912797261	3.455943623	1.342567947
H	-5.483224056	4.054343337	-0.236975489
H	-3.913992005	4.598067340	0.412822461
C	0.191896187	4.581883560	2.580429406
H	-0.488181317	5.185568352	1.959217713
H	1.043191898	5.218649333	2.872443133
H	-0.349893884	4.297120540	3.495754633
C	-3.534683335	2.998723664	-1.819393801
H	-2.894934479	3.894576825	-1.815018495
H	-4.450737515	3.253876619	-2.375403697
H	-3.012639374	2.209995600	-2.381717089
C	1.627442988	2.534763849	2.735616640
H	1.108932905	2.198128022	3.646387551
H	2.475465336	3.161095040	3.053551226
H	2.041447593	1.651858078	2.229317089
C	-4.884561225	1.371013854	-0.464428200
H	-4.448927660	0.513216508	-0.994745392
H	-5.798649046	1.672218051	-1.000921822
H	-5.191940482	1.033368955	0.538094108
C	4.344301719	-3.042778929	-1.357085157
H	4.683791065	-4.084548372	-1.208297078
H	4.766944337	-2.703350777	-2.318242077
H	3.249677153	-3.084831857	-1.496651349
C	4.635090396	2.159543508	-2.342504917
H	4.882519495	2.496778622	-3.365895192
H	5.353688292	2.648030148	-1.662071818
H	3.643156400	2.582699783	-2.104395010
C	4.946076921	0.338542331	2.579062594
H	5.533078215	-0.595145189	2.614930651
H	3.921535050	0.071695967	2.892979524
H	5.353842812	1.002647221	3.363543534
C	4.972220987	0.971078003	1.178796129
H	6.016643666	1.253198868	0.929790795
H	4.429883518	1.935241608	1.186772624
C	4.736531192	-2.111064082	-0.200656892
H	5.837940827	-2.154948598	-0.061157306
H	4.331892126	-2.499041802	0.752578712
C	4.655930973	0.630259597	-2.192348962
H	3.960023652	0.170158065	-2.919619402
H	5.653068310	0.249725904	-2.498600786
H	2.984991091	-4.037725599	0.740254703
C	5.097356251	-0.709436658	-3.059911604
H	5.697071779	0.100568529	-2.616488390
H	5.352089171	-0.775598001	-4.130654019
H	5.398368262	-1.653209528	-2.578810780
C	4.952315598	-2.574125693	1.959415715
H	5.283069424	-2.969399301	0.986201201
H	5.175877539	-3.331193553	2.729222645
H	5.551324088	-1.676878510	2.179615217
C	2.813516728	-1.595244024	-3.573051750
H	3.102059074	-2.580271817	-3.174816950
H	3.039895982	-1.599850528	-4.651060743
H	1.723456543	-1.490015085	-3.463335568
C	3.042697711	-1.701968428	3.327023430
H	3.573426026	-0.766914859	3.562974622
H	3.299659669	-2.431779998	4.111284708
H	1.962087733	-1.507556861	3.393706722
C	3.223896547	0.882380514	-3.561264755
H	2.145850205	1.087079848	-3.508906561
H	3.511805611	0.856418502	-4.624459315
H	3.754351405	1.730085631	-3.099561034
C	-4.992081099	1.801854476	1.392128190
H	-5.255150387	2.350608769	2.314726350
H	-5.588550702	2.243185502	0.575575304
H	-3.936469597	2.042995457	1.171614183
C	-4.844351004	-0.880210893	-3.133011895
H	-5.132135642	-0.387015196	-4.079238771
H	-5.328278629	-1.871859445	-3.129560410
H	-3.756818022	-1.060709686	-3.186433873
C	-4.606439612	-3.423413166	1.484202248
H	-5.218707093	-2.996993524	2.297289515
H	-3.553222081	-3.221413002	1.745904708
H	-4.740096249	-4.519688035	1.524288885
C	-4.977574223	-2.827893431	0.116503433
H	-6.026511552	-3.095972318	-0.130741458
H	-4.379764929	-3.307168879	-0.681284566
C	-5.214627538	0.286248990	1.510259708
H	-6.274135442	0.094373121	1.781337496
H	-4.641277483	-0.115623685	2.366872698
C	-5.223491024	-0.055888316	-1.891881305
H	-4.756986285	0.946126825	-1.945443309
H	-6.313962962	0.153971210	-1.908577610

Table S18: Cartesian coordinates of the optimized geometry of the Isomers for [Cp"$_2$Zr(µ,η$^{1:1:1:1}$-As$_4$)(Al^{i}Bu$_3$)$_2$] at the B3LYP/def2- SVP level of theory.

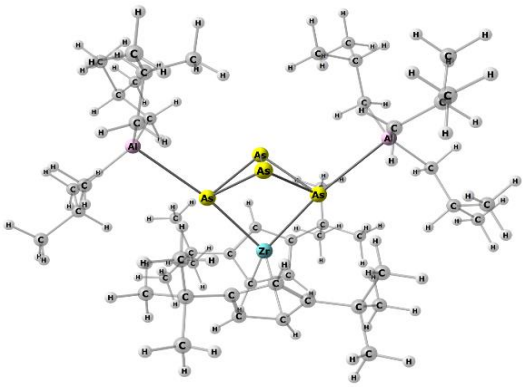

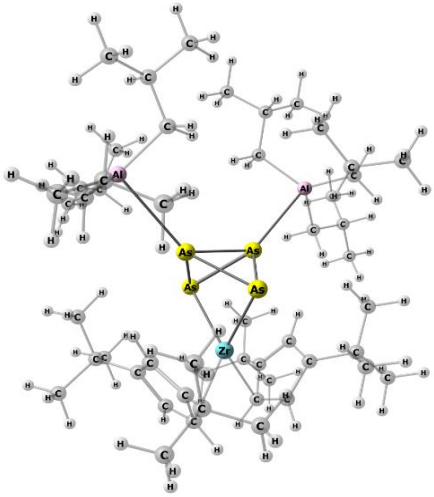

As	0.109464812	1.793591151	0.012816721
As	-1.225551574	0.084032309	-1.213839675
Al	0.280202749	4.024749469	-1.914201949
C	-3.304126327	-2.162877552	2.239341521
C	-1.456161204	0.580242674	4.041242675
H	-0.962022103	0.983370468	4.922316731
C	-2.467752716	-0.930783939	2.607203362
C	-2.081941680	1.339619254	3.012524998
C	-1.672775444	-0.802170769	3.785072684
H	-1.375294834	-1.618665314	4.440396396
C	-2.399528316	2.835772806	3.081500072
C	0.000000000	6.103775875	0.465828277
H	-0.220215704	5.280494485	1.171919592
C	-2.813414898	3.405307081	1.714223596
As	-0.570980156	-0.115670125	-1.808159263
As	0.673235595	-1.012087452	0.159012070
C	-2.607934108	-3.028336640	2.644517703
C	-4.413306379	-1.901630878	-0.466487082
H	-5.312342351	-1.586946927	-0.992420352
C	-2.983994184	-2.465924218	1.266761072
C	-3.271284867	-2.516645984	-1.055070202
C	-4.232209706	-1.854840597	0.943385777
H	-4.972805643	-1.505498161	1.660492182
C	-3.199229029	-3.078357336	-2.479123491
C	-1.764681091	-3.463902306	-2.880687075
H	-1.090228643	-2.594181400	-2.889840000
H	-1.762469575	-3.894061020	-3.894733149
H	-1.334217328	-4.218037127	-2.204781601

H	-2.005257229	3.326007552	0.972271346
H	-3.066682569	4.472145275	1.810452050
H	-3.699615035	2.893735596	1.308539489
C	-3.813441527	-2.127480870	0.787934054
H	-4.401725197	-1.220227024	0.580527704
H	-4.471876675	-2.990599481	0.603324491
H	-2.992969793	-2.177509065	0.059057280
C	0.821125348	5.526828103	-0.704232205
H	1.825803355	5.245395131	-0.331092067
H	1.035993754	6.353468319	-1.418268583
C	1.901163614	3.445582862	-2.955208254
H	2.604063293	4.288506503	-2.794897103
H	2.390385615	2.596588399	-2.435528589
C	-1.604527206	3.826114343	-2.578279285
H	-1.680765232	2.887751385	-3.163208204
H	-2.255677117	3.661093567	-1.698106349
C	-4.537548339	-2.122271840	3.182211329
H	-4.236527977	-2.172212884	4.240127997
H	-5.201940937	-2.976929520	2.974816737
H	-5.116890622	-1.197023994	3.038593894
C	-2.655740055	0.391406600	2.113416577
H	-3.235395892	0.650032929	1.230576509
C	-2.551516648	-3.481413125	2.487694972
H	-1.679241863	-3.586119988	1.827023246
H	-3.216793994	-4.336991114	2.293017192
H	-2.205979362	-3.568655525	3.529207817
C	-1.215424021	3.643760689	3.641086571
H	-0.923858295	3.300465320	4.646356177
H	-1.486038620	4.707717264	3.726386985
H	-0.336491386	3.573678894	2.985861497
C	-2.212031176	4.974889649	-3.419984738
H	-2.191835872	5.895258449	-2.806830970
C	-1.347775977	6.679635765	0.012274478
H	-1.200252763	7.495581257	-0.716937169
H	-1.915107858	7.097338916	0.861296712
H	-1.977592679	5.916107292	-0.468517256
C	-3.600750400	2.981366126	4.052610588
H	-4.473883998	2.415384843	3.692298467
H	-3.893783270	4.040275128	4.140822303
H	-3.350324549	2.611547155	5.059047998
C	-3.682854732	4.702801689	-3.772965066
H	-3.775543768	3.795344068	-4.395208956
H	-4.131362291	5.540353291	-4.334816317
H	-4.289176039	4.544369513	-2.865994267
C	3.277871399	3.036072841	-5.061365631
H	3.846903156	2.214785056	-4.590795984
H	3.844696313	3.967161369	-4.896472836
H	3.254255277	2.844721257	-6.148119659
C	-1.402329743	5.262630053	-4.691561011
H	-0.364437461	5.557052220	-4.460794380
H	-1.850885261	6.080336287	-5.279878268
H	-1.354609354	4.371973355	-5.341489063
C	0.791863476	7.164437533	1.248421324
H	1.744831483	6.757589236	1.624871981
H	0.223690028	7.547972821	2.113863610
H	1.034807439	8.025527559	0.601448394
C	1.862726777	3.128523165	-4.467502739
H	1.351411710	3.962292695	-4.984450924
C	1.073826900	1.850836148	-4.780165032
H	1.039784499	1.651684720	-5.864291419
H	0.035219107	1.911425562	-4.420532781
H	1.540335640	0.972853499	-4.299648240
Zr	0.000000000	0.000000000	2.076595048
As	-0.109464812	-1.793591151	0.012816721
As	1.225551574	-0.084032309	-1.213839675
Al	-0.280202749	-4.024749469	-1.914201949
C	3.304126327	2.162877552	2.239341521
C	1.456161204	-0.580242674	4.041242675
H	0.962022103	-0.983370468	4.922316731
C	2.467752716	0.930783939	2.607203362
C	2.081941680	-1.339619254	3.012524998
C	1.672775444	0.802170769	3.785072684
H	1.375294834	1.618665314	4.440396396
C	2.399528316	-2.835772806	3.081500072
C	0.000000000	-6.103775875	0.465828277
H	0.220215704	-5.280494485	1.171919592
C	2.813414898	-3.405307081	1.714223596
H	2.005257229	-3.326007552	0.972271346
H	3.066682569	-4.472145275	1.810452050
H	3.699615035	-2.893735596	1.308539489
C	3.813441527	2.127480870	0.787934054
H	4.401725197	1.220227024	0.580527704
H	4.471876675	2.990599481	0.603324491
H	2.992969793	2.177509065	0.059057280
C	-1.125503630	-3.430444270	2.731960957
H	-0.857406656	-4.177861350	1.969719945
H	-0.917368418	-3.879746040	3.715731017
H	-0.456334160	-2.567159265	2.613764604
C	-3.464388234	-4.310200145	2.825607920
H	-4.540913017	-4.079597268	2.809954799
H	-3.232420624	-4.791959054	3.789800057
H	-3.262996512	-5.037775073	2.024028946
C	-2.385258570	-2.816263507	0.021981927
H	-1.428166055	-3.319237703	-0.090774437
C	-2.941266582	-2.059637865	3.792663330
H	-2.334554219	-1.143467605	3.740047130
H	-2.735277131	-2.539967439	4.762316084
H	-4.002681614	-1.768459184	3.790735510
C	-3.770842785	-2.094615063	-3.516075913
H	-4.808638107	-1.808650212	-3.282536615
H	-3.778020889	-2.557589438	-4.515738288
H	-3.168866267	-1.177073509	-3.575569840
C	-4.066888140	-4.364288733	-2.486146123
H	-3.694541321	-5.097158153	-1.753511758
H	-4.043886979	-4.836201754	-3.482181840
H	-5.116500534	-4.142145865	-2.238182655
Zr	-2.668979688	-0.140401393	-0.046229956
As	-0.691809150	0.271784881	1.815119621
As	0.448820229	1.398746620	-0.097447870
Al	2.642184777	3.578308713	-0.433143789
C	-3.058661327	2.722762787	-2.722081117
C	-4.799596013	1.171629222	0.238364999
H	-5.640947187	0.653943364	0.694087200
C	-3.402681277	2.065080744	-1.378236652
C	-3.869639749	2.011838993	0.914065987
C	-4.505456580	1.188626364	-1.152708521
H	-5.090563589	0.693938173	-1.925677655
C	-4.036655349	2.554968984	2.336937565
C	2.707089118	2.457531514	-3.359050729
H	2.056378524	1.622837109	-3.034295202
C	-2.758873504	3.241118415	2.849169574
H	-1.910915546	2.542265577	2.906718071
H	-2.926722246	3.642419648	3.861042201
H	-2.460550132	4.085691818	2.209499237
C	-1.682314954	3.410720130	-2.710425009
H	-1.605670303	4.165020155	-1.912211835
H	-1.518349781	3.932874552	-3.666248568
H	-0.860978094	2.691968296	-2.582086609
C	2.461304437	3.656679340	-2.418225091
H	1.451499941	4.068892150	-2.611068605
H	3.143078486	4.483237311	-2.719609812
C	1.651529454	5.067153771	0.457136453
H	1.940961797	5.952049751	-0.148860148
H	0.563862241	4.964739087	0.263300174
C	4.112943653	2.609730712	0.507649206
H	3.907928305	2.624673180	1.595985279
H	4.081548397	1.540423838	0.226305786
C	-4.139990315	3.814776991	-2.942703145
H	-5.148458818	3.376073949	-2.997071578
H	-3.950887756	4.355136819	-3.884838693
H	-4.134631120	4.548846908	-2.121970341
C	-2.991592582	2.517006915	-0.090772173
H	-2.182364726	3.219779966	0.092146407
C	-3.121882117	1.735929817	-3.901599700
H	-2.334811500	0.970350168	-3.834025390
H	-2.977381739	2.275933493	-4.850744846
H	-4.094649085	1.224303975	-3.961747362
C	-4.454229090	1.455015159	3.328912545
H	-5.377379452	0.944931631	3.011147560
H	-4.648711217	1.891701475	4.321465503
H	-3.667004890	0.697365543	3.443671564
C	5.547049182	3.144110297	0.267436426
H	5.765164879	3.064077149	-0.814339973
C	4.155297126	1.955751798	-3.296379574
H	4.860396801	2.752093474	-3.593993278
H	4.315883900	1.101120248	-3.973919190
H	4.431262104	1.629744729	-2.281932977
C	-5.165777043	3.616389673	2.270612997
H	-4.912736585	4.421244948	1.562924391
H	-5.322667234	4.071434121	3.262472976
H	-6.118273691	3.169218080	1.946235101
C	6.600658707	2.302127190	1.002781642
H	6.442117415	2.342859905	2.094582566
H	7.624507726	2.660577105	0.799171805
H	6.548631905	1.243974531	0.700256629
C	1.297696610	6.760010169	2.335846264
H	0.204213169	6.781578217	2.181872248
H	1.732594656	7.566414436	1.722833337

C	-0.821125348	-5.526828103	-0.704232205
H	-1.825803355	-5.245395131	-0.331092067
H	-1.035993754	-6.353468319	-1.418268583
C	-1.901163614	-3.445582862	-2.955208254
H	-2.604063293	-4.288506503	-2.794897103
H	-2.390385615	-2.596588399	-2.435528589
C	1.604527206	-3.826114343	-2.578279285
H	1.680765232	-2.887751385	-3.163208204
H	2.255677117	-3.661093567	-1.698106349
C	4.537548339	2.122271840	3.182211329
H	4.236527977	2.172212884	4.240127997
H	5.201940937	2.976929520	2.974816737
H	5.116890622	1.197023994	3.038593894
C	2.655740055	-0.391406600	2.113416577
H	3.235395892	-0.650032929	1.230576509
C	2.551516648	3.481413125	2.487694972
H	1.679241863	3.586119988	1.827023246
H	3.216793994	4.336991114	2.293017192
H	2.205979362	3.568655525	3.529207817
C	1.215424021	-3.643760689	3.641086571
H	0.923858295	-3.300465320	4.646356177
H	1.486038620	-4.707717264	3.726386985
H	0.336491386	-3.573678894	2.985861497
C	2.212031176	-4.974889649	-3.419984738
H	2.191835872	-5.895258449	-2.806830970
C	1.347775977	-6.679635765	0.012274478
H	1.200252763	-7.495581257	-0.716937169
H	1.915107858	-7.097338916	0.861296712
H	1.977592679	-5.916107292	-0.468517256
C	3.600750400	-2.981366126	4.052610588
H	4.473883998	-2.415384843	3.692298467
H	3.893783270	-4.040275128	4.140822303
H	3.350324549	-2.611547155	5.059047998
C	3.682854732	-4.702801689	-3.772965066
H	3.775543768	-3.795344068	-4.395208956
H	4.131362291	-5.540353291	-4.334816317
H	4.289176039	-4.544369513	-2.865994267
C	-3.277871399	-3.036072841	-5.061365631
H	-3.846903156	-2.214785056	-4.590795984
H	-3.844696313	-3.967161369	-4.896472836
H	-3.254255277	-2.844721257	-6.148119659
C	1.402329743	-5.262630053	-4.691561011
H	0.364437461	-5.557052220	-4.460794380
H	1.850885261	-6.080336287	-5.279878268
H	1.354609354	-4.371973355	-5.341489063
C	-0.791863476	-7.164437533	1.248421324
H	-1.744831483	-6.757589236	1.624871981
H	-0.223690028	-7.547972821	2.113863610
H	-1.034807439	-8.025527559	0.601448394
C	-1.862726777	-3.128523165	-4.467502739
H	-1.351411710	-3.962292695	-4.984450924
C	-1.073826900	-1.850836148	-4.780165032
H	-1.039784499	-1.651684720	-5.864291419
H	-0.035219107	-1.911425562	-4.420532781
H	-1.540335640	-0.972853499	-4.299648240
H	1.489707808	7.002076216	3.395422124
C	5.684650984	4.625327679	0.648578835
H	4.995447264	5.267593344	0.072029095
H	6.705776539	4.998468851	0.465164256
H	5.460504889	4.781098379	1.718030561
C	2.320470109	2.788075775	-4.809373626
H	1.266355373	3.102923062	-4.881429448
H	2.458981243	1.920493745	-5.477143810
H	2.939789924	3.614152354	-5.201376437
C	1.875997791	5.389257999	1.949337450
H	2.966874999	5.436146966	2.129748685
C	1.310583008	4.295818965	2.864502903
H	1.504060365	4.516156819	3.927569047
H	1.747525731	3.308331963	2.645327804
H	0.217411941	4.207886735	2.739461208
H	2.254464259	-1.557793213	2.986787245
C	3.219872525	-2.075717921	3.147578991
C	3.268911158	-3.304337310	2.210260332
Al	3.065383587	-3.180560153	0.229286886
H	2.500234229	-4.030742418	2.538745664
H	4.233192361	-3.830260574	2.382288309
C	1.757622333	-4.475222996	-0.557883220
H	0.806545832	-4.338227425	-0.006317716
H	1.532149384	-4.199117157	-1.606912546
C	4.300448541	-2.181659248	-0.976013989
H	4.152091297	-2.586638036	-1.997499628
H	3.938916872	-1.136507474	-1.039872215
C	5.813939040	-2.160330040	-0.659444987
H	5.948735514	-1.702889154	0.338282235
C	4.332652564	-1.064015430	2.847321560
H	5.327902014	-1.525688670	2.971986126
H	4.282814990	-0.196893375	3.526172953
H	4.272567091	-0.678301409	1.817553095
C	6.592806828	-1.296239098	-1.663090659
H	6.507003436	-1.707513269	-2.684193508
H	7.666242560	-1.245676137	-1.412041564
H	6.204569377	-0.265583870	-1.689545262
C	0.953814860	-6.870670551	-0.938890527
H	0.669723012	-6.662028027	-1.985317857
H	0.064352989	-6.694644767	-0.311647459
H	1.206076904	-7.942830120	-0.869033913
C	6.411986485	-3.572689554	-0.596767710
H	5.931111530	-4.189966221	0.182142482
H	7.490457445	-3.547342250	-0.368691708
H	6.289575564	-4.097183008	-1.560535992
C	3.261647486	-2.493972739	4.625673136
H	2.441041674	-3.188673652	4.869566385
H	3.177463149	-1.623771186	5.298965173
H	4.210389283	-3.007956071	4.860562000
C	2.127631373	-5.978093474	-0.506697203
H	2.363011631	-6.240672918	0.543472163
C	3.372986930	-6.291871558	-1.347806066
H	3.635165707	-7.361802496	-1.300275916
H	4.255021844	-5.722071065	-1.012066449
H	3.204289826	-6.036922744	-2.408578978

Table S19: Cartesian coordinates of the optimized geometry of the Isomers for [Cp"$_2$Zr(µ,η$^{1:1:1}$-As$_4$)(Al^{i}Bu$_3$)] at the B3LYP/def2- SVP level of theory.

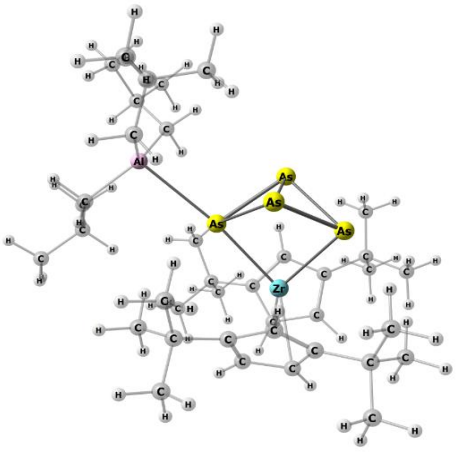

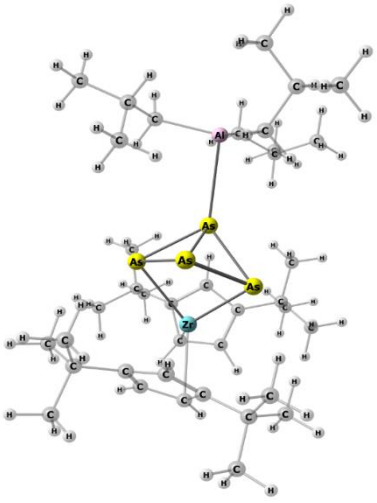

As	-1.860524802	-0.616148292	-2.145534620

As	-0.115236709	0.415268498	-1.855085918

As	0.160610311	-1.936888428	-1.526003022
C	-0.421565877	-2.422423461	3.045922279
C	-3.565271140	-0.679940652	1.908277090
H	-4.419564726	-0.028870009	2.081140554
C	-1.549417105	-1.768325392	2.238653342
C	-3.485879037	-1.711179070	0.928284117
C	-2.379828127	-0.700901034	2.694137309
H	-2.188964636	-0.073153370	3.562788436
C	-4.667958780	-2.272882421	0.129669195
C	-4.211570814	-3.246824718	-0.971275196
H	-3.565328318	-2.755907381	-1.714527069
H	-5.088191478	-3.647157282	-1.504784809
H	-3.661965741	-4.105408142	-0.555605610
C	0.429877809	-3.381106837	2.194728397
H	-0.176557676	-4.189588193	1.757690173
H	1.199698096	-3.855056666	2.823492820
H	0.944913152	-2.859351849	1.376274055
C	-1.122025528	-3.255531811	4.152814110
H	-1.718510488	-2.615002154	4.820961518
H	-0.372303929	-3.782620149	4.765554490
H	-1.795881821	-4.008981681	3.715860602
C	-2.220347598	-2.340539870	1.122012209
H	-1.855101338	-3.189136524	0.549043336
C	0.494244683	-1.390345831	3.724991550
H	1.054021727	-0.796552150	2.988441729
H	1.229717591	-1.901463647	4.365748167
H	-0.072080001	-0.698020865	4.366433303
C	-5.527844546	-1.161247886	-0.498100016
H	-5.887920824	-0.445953718	0.258238235
H	-6.415815189	-1.597004157	-0.983576265
H	-4.970237467	-0.600192926	-1.260623939
C	-5.542674104	-3.060695670	1.140184166
H	-4.962528227	-3.860211419	1.626834657
H	-6.399117371	-3.525852044	0.624702559
H	-5.937573525	-2.402457096	1.929625899
Zr	-1.732935156	0.218492275	0.436173906
As	0.950175248	-0.186958944	0.092709147
As	0.431088269	0.373719875	-2.289892162
Al	3.842047040	-0.399431938	0.112251451
C	-3.280753060	2.963409676	-1.970679121
C	-2.516232882	2.285266672	1.654701348
H	-2.821609965	2.160823386	2.691341348
C	-2.646516098	2.513080621	-0.646445721
C	-1.231548507	2.701704327	1.205971857
C	-3.371628870	2.149140502	0.527026444
H	-4.433042388	1.912170649	0.568925647
C	-0.130560587	3.296162199	2.087888103
C	3.907393519	0.811076103	3.039786384
H	2.826900070	1.038192797	2.962790153
C	1.213468542	3.391506440	1.346181910
H	1.582495699	2.403969796	1.032558938
H	1.977408859	3.836495960	2.001926598
H	1.141065960	4.026705981	0.450064076
C	-2.250359246	3.090951982	-3.106968992
H	-1.444290562	3.796153068	-2.851776725
H	-2.742913894	3.474641921	-4.014474795
H	-1.793226293	2.124188239	-3.359249927
C	4.222979415	-0.353128057	2.080362356
H	3.766767454	-1.280222379	2.481038076
H	5.315228907	-0.560215797	2.132563887
C	4.096073466	-2.288406137	-0.530480348
H	4.728556571	-2.730910328	0.266436444
H	3.139707606	-2.843782576	-0.444091450
C	4.161951467	1.194232086	-1.071726214
H	3.857589467	0.923263135	-2.102801445
H	3.451521273	1.988779967	-0.772085609
C	-3.865083025	4.375188943	-1.694378047
H	-4.644052314	4.342820827	-0.916853507
H	-4.315802391	4.787998469	-2.612031633
H	-3.080738300	5.070398914	-1.356628620
C	-1.317726774	2.790153134	-0.215705404
H	-0.506878389	3.109041134	-0.866178605
C	-4.431176097	2.048468081	-2.426760180
H	-4.069305987	1.047278913	-2.703174868
H	-4.923959117	2.479471896	-3.312780915
H	-5.200711240	1.933572450	-1.648294540
C	0.052720030	2.498293667	3.391295706
H	-0.881911843	2.442466298	3.971825463
H	0.805499675	2.983411121	4.032264453
H	0.393855499	1.473101400	3.192974149
C	5.579404932	1.813485373	-1.131070289
H	5.844711015	2.160917829	-0.115064759
C	4.664890155	2.094153255	2.674358442
H	5.755983019	1.929131335	2.714649373
As	0.443525807	-1.864121641	-1.003115775
C	-3.492005492	-3.304631855	0.864439755
C	-4.393221181	-0.005995000	-0.724437246
H	-5.002505081	0.892694158	-0.788541640
C	-3.495156975	-1.978751916	0.090107588
C	-3.673466302	-0.607690722	-1.797300360
C	-4.272101923	-0.830915773	0.427574508
H	-4.780931624	-0.664768494	1.375313773
C	-3.838286558	-0.267518866	-3.282207673
C	-2.730899380	-0.892188656	-4.149386433
H	-1.733253032	-0.512116309	-3.881667043
H	-2.904363634	-0.651951573	-5.210380674
H	-2.711211822	-1.989440762	-4.062573705
C	-2.422288553	-4.283080970	0.346611535
H	-2.563566019	-4.516388393	-0.720128727
H	-2.488061115	-5.233846441	0.898971417
H	-1.404153378	-3.890615245	0.479744182
C	-4.885685806	-3.942279995	0.618584264
H	-5.693395955	-3.307272349	1.014528673
H	-4.949505450	-4.924587335	1.115041907
H	-5.070027490	-4.090707953	-0.456920502
C	-3.094655672	-1.796902699	-1.264091437
H	-2.500884297	-2.506684413	-1.834829923
C	-3.311361477	-3.109710644	2.380184496
H	-2.305341481	-2.737147000	2.622919508
H	-3.443908519	-4.070507310	2.902742801
H	-4.048127589	-2.405416212	2.795576587
C	-3.877643417	1.251467114	-3.524711270
H	-4.676606716	1.738762731	-2.943714350
H	-4.073941877	1.461689254	-4.588221833
H	-2.923914209	1.726400097	-3.257678429
C	-5.197951597	-0.872167256	-3.720168438
H	-5.217687448	-1.961505982	-3.560237516
H	-5.375659308	-0.680880587	-4.791447350
H	-6.032623443	-0.432980680	-3.151995319
Zr	-2.026437829	0.281332716	0.094626351
As	-0.200440160	-1.307787031	1.355075808
As	1.431104894	0.082412404	0.085899821
Al	4.425244914	-0.164168646	0.318863041
C	-1.022390464	4.015843983	-0.640436861
C	-3.220404184	1.918867271	1.592097372
H	-4.195164584	1.620837433	1.972462152
C	-1.610769899	2.928812232	0.268642386
C	-1.978964708	1.791106282	2.279252540
C	-2.995103181	2.598687455	0.362886254
H	-3.769539686	2.906952904	-0.336783173
C	-1.817074084	1.467430610	3.768443316
C	4.305904734	2.971635160	0.429368081
H	3.222019593	2.917151351	0.210879161
C	-0.354994854	1.167537179	4.143010075
H	0.032275714	0.282151498	3.616778862
H	-0.276661407	0.972953773	5.224381492
H	0.308628469	2.015899957	3.915629591
C	0.515025705	3.981842863	-0.675488683
H	0.950672458	4.104999554	0.327573597
H	0.893713660	4.808508569	-1.297236697
H	0.897141168	3.043451127	-1.101762781
C	4.723563789	1.649252245	1.104158403
H	4.270878264	1.602429833	2.114571670
H	5.816829777	1.689933694	1.307528501
C	4.493520347	-1.559169693	1.747550661
H	5.316087867	-1.193094805	2.398021955
H	3.593888612	-1.470565699	2.389958792
C	4.742076600	-0.581572157	-1.610987941
H	4.427515746	-1.625847180	-1.804713133
H	4.061184334	0.039097422	-2.224682073
C	-1.460522921	5.369771735	-0.020666929
H	-2.557156471	5.468293267	-0.004460355
H	-1.050843674	6.208970544	-0.606739393
H	-1.097711506	5.468117104	1.014410333
C	-0.995225652	2.375722701	1.427708200
H	0.061468349	2.459055677	1.669679403
C	-1.563840947	3.945194306	-2.078819095
H	-1.237276718	3.026409815	-2.587593736
H	-1.191605134	4.801137781	-2.663979530
H	-2.663564332	3.982269549	-2.108130869
C	-2.707416922	0.290252504	4.205115100
H	-3.768281371	0.469427221	3.969117166
H	-2.636245969	0.143471310	5.294672011
H	-2.403547936	-0.647066970	3.719554715
As	-0.115236709	0.415268498	-1.855085918
As	0.443525807	-1.864121641	-1.003115775
C	-3.492005492	-3.304631855	0.864439755
C	-4.393221181	-0.005995000	-0.724437246

H	4.431006829	2.915382443	3.373106137
H	4.420109365	2.437868706	1.658230552
C	-0.588040391	4.733627438	2.449984775
H	-0.736761397	5.342561546	1.544574784
H	0.172316713	5.230961483	3.074418474
H	-1.536377008	4.724165394	3.009517758
C	5.622490702	3.044498464	-2.050477859
H	5.377220645	2.765432243	-3.090353869
H	6.620027917	3.517246310	-2.057766736
H	4.892262410	3.806799813	-1.732584269
C	5.132517989	-4.106151266	-1.989342499
H	4.244932302	-4.756266366	-1.892662022
H	5.833290893	-4.383714221	-1.184786373
H	5.616115968	-4.342702603	-2.953152972
C	6.649543836	0.796965036	-1.551999416
H	6.703133775	-0.056642932	-0.854990279
H	7.652138875	1.255344338	-1.585029464
H	6.437266182	0.390067777	-2.555783748
C	4.182786778	0.435107156	4.505184102
H	3.608979318	-0.456887743	4.805688393
H	3.919927833	1.253963741	5.197608939
H	5.252042735	0.203240549	4.653941547
C	4.734194478	-2.623991647	-1.897321025
H	5.664540290	-2.034306515	-2.000055205
C	3.827267034	-2.246973802	-3.075538901
H	4.309278980	-2.464657754	-4.043612056
H	3.566036013	-1.177250609	-3.065707020
H	2.882452055	-2.817756851	-3.041505644
H	-5.002505081	0.892694158	-0.788541640
C	-3.495156975	-1.978751916	0.090107588
C	-3.673466302	-0.607690722	-1.797300360
C	-4.272101923	-0.830915773	0.427574508
H	-4.780931624	-0.664768494	1.375313773
C	-3.838286558	-0.267518866	-3.282207673
C	-2.730899380	-0.892188656	-4.149386433
H	-1.733253032	-0.512116309	-3.881667043
H	-2.904363634	-0.651951573	-5.210380674
H	-2.711211822	-1.989440762	-4.062573705
C	-2.422288553	-4.283080970	0.346611535
H	-2.563566019	-4.516388393	-0.720128727
H	-2.488061115	-5.233846441	0.898971417
H	-1.404153378	-3.890615245	0.479744182
C	-4.885685806	-3.942279995	0.618584264
H	-5.693395955	-3.307272349	1.014528673
H	-4.949505450	-4.924587335	1.115041907
H	-5.070027490	-4.090707953	-0.456920502
C	-3.094655672	-1.796902699	-1.264091437
H	-2.500884297	-2.506684413	-1.834829923
C	-3.311361477	-3.109710644	2.380184496
H	-2.305341481	-2.737147000	2.622919508
H	-3.443908519	-4.070507310	2.902742801
H	-4.048127589	-2.405416212	2.795576587
C	-3.877643417	1.251467114	-3.524711270
H	-4.676606716	1.738762731	-2.943714350
H	-4.073941877	1.461689254	-4.588221833
H	-2.923914209	1.726400097	-3.257678429

Table S20: Cartesian coordinates of the optimized geometry for [Cp"$_2$Zr(µ,$\eta^{1:1:1}$-As$_4$)(B(C$_6$F$_5$)$_3$)] at the B3LYP/def2-SVP level of theory.

Zr	2.490684707	-0.231908978	0.090899804
As	2.379599655	2.225005194	-1.154775720
As	0.265911360	2.669075850	0.105223132
As	-0.263009465	0.235677654	-0.089055036
As	0.174483336	1.607780323	-2.112172926
F	-0.896871250	-1.748379114	-2.111394067
F	-5.259108590	-0.448143953	-0.756037859
F	-3.469502870	1.515032469	-2.417197063
F	-2.538968988	1.776920681	2.235930619
F	-1.947105529	-3.237601460	-4.028158101
F	-4.303637215	4.030327193	-2.375474919
F	-1.150339146	-2.517547083	0.768904687
F	-4.785124539	0.308759421	1.960560135
F	-4.659989947	-3.384738676	-4.366390725
F	-6.297477979	-1.966171436	-2.698500873
F	-3.379600465	4.302841269	2.245706994
F	-4.278937581	5.473443326	-0.056241641
F	-5.353407828	-1.303618009	3.983704916
F	-1.737045376	-4.108413324	2.818990029
C	-3.025085703	-0.987574940	-1.337953494
F	-3.855899016	-3.535486732	4.460463438
C	-4.407614247	-1.115611175	-1.547919337
C	-2.243187454	-1.745501554	-2.209816987
C	3.183734026	-2.677775789	-0.555168086
C	-2.763510362	-2.547822292	-3.230420001
C	-3.006937701	2.274123109	1.079298773
C	-4.976296255	-1.899642880	-2.551443627
C	-4.143066205	-2.627178242	-3.404019720
C	-3.428516425	3.602788236	1.113563507
C	-3.034659694	1.467054338	-0.069965732
C	-2.892618752	-0.976223988	1.278263624
C	-3.462696274	2.135086962	-1.228065865
C	-3.881259661	4.205491726	-0.060959107
C	4.364633254	-0.225249051	1.739081576
H	5.323044008	-0.614900698	1.402412729
C	4.003400380	1.152333329	1.823669802
C	2.696555850	1.184562214	2.391222282
H	2.131854350	2.090367293	2.598402059
C	-2.193411116	-2.158730289	1.550563239
C	-3.981404074	-0.743513466	2.134443001
C	-3.896859298	3.464107034	-1.240992067
C	4.978398576	2.333513629	1.745082515
C	3.589978945	-1.033298331	-2.173065876
C	5.938068518	2.228892901	0.548260947
H	6.465371738	1.262320863	0.525353406
H	6.703263371	3.019008885	0.607269042
H	5.406044613	2.351733985	-0.404501135
C	4.163161097	-1.795193113	-1.102266579
H	5.223796349	-1.816038913	-0.858622303

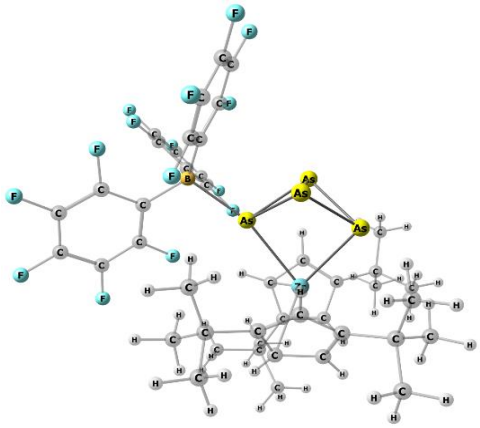

C	3.317474575	-1.004219470	2.312289838
H	3.350597287	-2.074743028	2.481124522
C	4.390598865	-0.371789981	-3.302514104
C	2.286854854	-0.127423198	2.758398536
C	4.251411204	3.689631175	1.700006556
H	3.616265205	3.788270206	0.807208621
H	4.989199613	4.507117525	1.676356736
H	3.620443732	3.846262275	2.588475578
C	2.211115053	-1.367867646	-2.192912277
H	1.466964553	-0.991046988	-2.888544235
C	3.463102857	-3.993639890	0.183034823
C	5.814384131	2.275143135	3.051751293
H	5.166888406	2.328907290	3.940729505
H	6.518245277	3.122593977	3.090244022
H	6.398459233	1.343960159	3.115197471
C	2.319409585	-4.397452805	1.131300222
H	2.217404246	-3.710733023	1.980889183
H	2.503037032	-5.404876189	1.537030124
H	1.347868408	-4.424127530	0.615291946
C	-2.483768254	-3.023803289	2.604273879
C	-3.557261931	-2.731322266	3.444888867
C	-4.313643782	-1.584966216	3.201911132
C	5.070768893	-1.530214284	-4.079086077
H	5.784626748	-2.078202747	-3.444822582
H	5.623340561	-1.133038723	-4.946220990
H	4.325003900	-2.250371681	-4.450314998
C	1.955434747	-2.350894250	-1.197467762
H	0.992919503	-2.831126868	-1.036307455
C	4.805935630	-3.980626840	0.938092290
H	5.652541620	-3.805511981	0.256240160
H	4.973495198	-4.958372778	1.416293455
H	4.846979120	-3.217244361	1.727416027
C	3.480827469	0.390071388	-4.282765014
H	2.730362984	-0.271872195	-4.741761570
H	4.086144042	0.814726023	-5.099080353
H	2.952187261	1.220890253	-3.793414306
B	-2.553218477	-0.082728698	-0.051304302
C	1.202609703	-0.475413481	3.781352579
C	3.563618647	-5.072406930	-0.930449378
H	2.616910489	-5.163035593	-1.484160279
H	3.797009155	-6.055097442	-0.488767985
H	4.356541266	-4.825501552	-1.653430296
C	1.848922686	-0.253813587	5.174874833
H	2.139755814	0.798518187	5.317134474
H	2.749115465	-0.875345653	5.301937350
H	1.134390268	-0.520218858	5.970745054
C	5.482639686	0.576967310	-2.780658319
H	5.043528770	1.469128936	-2.312523020
H	6.119614521	0.916633105	-3.612844720
H	6.136837388	0.087725087	-2.042212264
C	-0.032072063	0.430958786	3.668034658
H	-0.732769162	0.218838297	4.490581111
H	-0.573327766	0.269108678	2.727777207
H	0.225519173	1.499204137	3.728891211
C	0.771016342	-1.947119203	3.673653832
H	1.602302952	-2.632859896	3.897759582
H	0.388997814	-2.187536148	2.672241510
H	-0.026542699	-2.163939341	4.400604649

5.7 References

[1] S. Gambarotta, *J. Organomet. Chem.* **500**, *1995*, 117.

[2] H. K. Chae, D. Y. Siberio-Pérez, J. Kim, Y. Go, M. Eddaoudi, A.J. Matzger, M. O'Keeffe, O. M. Yaghi, *Nature* **2004**, *427*, 523.

[3] C. W. Chang, D. Okawa, A. Majumdar, A. Zettl, *Science* **2006**, *314*, 1121.

[4] H. Y. Chung, M. B. Weinberger, J. B. Levine, R. W. Cumberland, A. Kavner, J. M. Yang, S. H. Tolbert, R. B. Kaner, *Science* **2007**, *316*, 436.

[5] K. Ding, A. W. Pierpont, W. W. Brennessel, G. Lukat-Rodgers, K. R. Rodgers, T. R. Cundari, E. Bill, P. L. Holland, , *J. Am. Chem. Soc.* **2009**, *131*, 9471.

[6] M. Hidai, Y. Mizobe, *Chem. Rev.* **1995**, *95*, 1115.

[7] D. W. Stephan, *Dalton Trans.* **2009**, 3129.

[8] D. W. Stephan, G. Erker, *Angew. Chem. Int. Ed.* **2015**, *54*, 6400.

[9] M. Caporali, L. Gonsalvi, A. Rossin, M. Peruzzini, *Chem. Rev.* **2010**, *110*, 4178.

[10] M. Scheer, G. Balázs, A. E. Seitz, *Chem. Rev.* **2010**, *110*, 4236.

[11] B. M. Cossairt, N. A. Piro, C. C. Cummins, *Chem. Rev.* **2010**, *110*, 4164.

[12] M. Seidl, G. Balázs, M. Scheer, *Chem. Rev.* **2019**, *119*, 8406.

[13] S. Heinl, G. Balázs, A. Stauber, M. Scheer, *Angew. Chem. Int. Ed.* **2016**, *55*, 15524.

[14] A. E. Seitz, M. Eckhardt, S. S. Sen, A. Erlebach, E. V. Peresypkina, H. W. Roesky, M. Sierka, M. Scheer, *Angew. Chem. Int. Ed.* **2017**, *56*, 6655.

[15] A. S. Foust, M. S. Foster, L. F. Dahl, *J. Am. Chem. Soc.* **1969**, 5631.

[16] O. J. Scherer, J. Vondung, G. Wolmershäuser, *J. Organomet. Chem.* **1989**, *376*, C35-C38.

[17] O. J. Scherer, C. Blath, G. Wolmershäuser, *J. Organomet. Chem.* **990**, *387*, C21-C24.

[18] M. Piesch, F. Dielmann S. Reichl, M. Scheer, *Chem. Eur. J.* **2020**, *26*, 1518.

[19] M. Schmidt, D. Konieczny, E. V. Peresypkina, A. V. Virovets, G. Balázs, M. Bodensteiner, F. Riedlberger, H. Krauss, M. Scheer, *Angew. Chem. Int. Ed.* **2017**, *56*, 7307.

[20] C. Schoo, S. Bestgen, M. Schmidt, S. N. Konchenko, M. Scheer, P. W. Roesky, *Chem. Commun.* **2016**, *52*, 13217.

[21] H. Krauss, G. Balázs, M. Bodensteiner, M. Scheer, *Chem. Sci.* **2010**, *1*, 337.

[22] M. Fleischmann, L. Dütsch, M. E. Moussa, A. Schindler, G. Balázs, C. Lescop, M. Scheer, *Chem. Commun.* **2015**, *51*, 2893.

[23] M. Fleischmann, S. Welsch, H. Krauss, M. Schmidt, M. Bodensteiner, E. V. Peresypkina, M. Sierka, C. Gröger, M. Scheer, *Chem. Eur. J.* **2014**, *20*, 3759.

[24] M. Schmidt, A. E Seitz, M. Eckhardt, G. Balázs, E. V. Peresypkina, F. Virovets, F. Riedlberger, M. Bodensteiner, E. M. Zolnhofer, K. Meyer, M. Scheer, *J. Am. Chem. Soc.* **2017**, *139*, 13981.

[25] V.Heinl, M. Schmidt, M. Eckhardt, M. Eberl, A. E. Seitz, G. Balázs, M. Seidl, M. Scheer, *Chem. Eur. J*. **2021**, *27*, submitted: https://doi.org/10.1002/chem.202101119.

[26] A. E. Seitz, M. Eckhardt, A. Erlebach, E. V. Peresypkina, M. Sierka, M. Scheer, *J. Am. Chem. Soc.* **2016**, *138*, 10433.

[27] A. E. Seitz, U. Vogel, M. Eberl, M. Eckhardt, G. Balázs, E. V. Peresypkina M. Bodensteiner, M. Zabel, M. Scheer, *Chem. Eur. J.* **2017**, *23*, 10319.

[28] I. Haiduc, E. Tiekink, Inverse Coordination Chemistry: A Novel Chemical Concept, *Sunway University Press* **2020**.

[29] I. Haiduc, *Coord. Chem. Rev.* **2017**, *338*, 1.

[30] I. Haiduc, *J. Coord. Chem.* **2018**, *71*, 3139.

[31] R. E. Mulvey, *Chem. Commun.* **2001**, 1049.

[32] Clegg, W.; Henderson, K.; Kennedy, A.R.; Mulvey, R.E.; O'Hara, C.T.; Rowlings, R.B.; Tooke, D.M., *Angew. Chem. Int. Ed.* **2001**, *40*, 3902.

[33] D. J. Duer, F. García, R. A. Kowenicki, V. Naseri, M. McPartlin, M. L. Stead, R. S. Stein, D. S. Wright, *Angew. Chem. Int. Ed.* **2005**, *44*, 5729.

[34] P. Pyykkö, M. Atsumi, *Chem. Eur. J.* **2009**, *15*, 186.

[35] R. Grünbauer, G. Balázs, M. Scheer, *Chem. Eur. J.* **2020**, *26*, 11722.

[36] Signal corresponding to the free $CpMn(CO)_2$ fragment could not be detected in the ^1H NMR, probably to high dynamic behavior or a triplett spin state.

[37] There are also two set of signals, which can be assigned to some amount of **1** and **4**. Especially the signals for **4** were expected in the NMR due to the co-crystalization of **5** and **4**.

[38] The symmetric environment might be an indication for a fast dynamic process in solution, which could not be aquired in the NMR timescale. Possibly the $Fe(CO)_3$ fragment migrate aruound the As_4-cycle.

[39] Despite several attempts, the geometry optimization of the isomer of **7** in wich the $B(C_6F_5)_3$ group is bond to the bridgehead arsenic atoms did not reach convergence, indicating that this isomer is not a stable entity.

[40] D. F. Keeley, R. E. Johnson, *J. Inorg. Nucl. Chem.* **1959**, *11*, 33.

[41] E. Speyer, H. Wolf, *Ber. Dtsch. Chem. Ges.* **1927**, *60*, 1424.

[42] Rigaku Oxford Diffraction, *CrysAlisPro Software System Version 1.171.38.43*, **2015**.

[43] L. J. Bourhis, O. V. Dolomanov, R. J. Gildea, J. A. K. Howard, H. Puschmann, *J. Appl. Crystallogr.* **2009**, *42*, 339-341.

[44] G. M. Sheldrick, *Acta Crystallogr., Sect, A* **2015**, *71*, 3-8.

[45] G. M. Sheldrick, *Acta Crystallogr., Sect, C* **2015**, *71*, 3-8.

[46] M. J. Frisch, G. W. Trucks, H. B. Schlegel, G. E. Scuseria, M. A. Robb, J. R. Cheeseman, G. Scalmani, V. Barone, B. Mennucci, G. A. Petersson, H. Nakatsuji, M. Caricato, X. Li, H. P. Hratchian, A. F. Izmaylov, J. Bloino, G. Zheng, J. L. Sonnenberg,

M. Hada, M. Ehara, K. Toyota, R. Fukuda, J. Hasegawa, M. Ishida, T. Nakajima, Y. Honda, O. Kitao, H. Nakai, T. Vreven, J. A. Montgomery, Jr., J. E. Peralta, F. Ogliaro, M. Bearpark, J. J. Heyd, E. Brothers, K. N. Kudin, V. N. Staroverov, T. Keith, R. Kobayashi, J. Normand, K. Raghavachari, A. Rendell, J. C. Burant, S. S. Iyengar, J. Tomasi, M. Cossi, N. Rega, J. M. Millam, M. Klene, J. E. Knox, J. B. Cross, V. Bakken, C. Adamo, J. Jaramillo, R. Gomperts, R. E. Stratmann, O. Yazyev, A. J. Austin, R. Cammi, C. Pomelli, J. W. Ochterski, R. L. Martin, K. Morokuma, V. G. Zakrzewski, G. A. Voth, P. Salvador, J. J. Dannenberg, S. Dapprich, A. D. Daniels, O. Farkas, J. B. Foresman, J. V. Ortiz, J. Cioslowski, and D. J. Fox, *Gaussian Inc. Wallingford CT,* **2013**.

[47] A. D. Becke, *J. Chem. Phys.* **1993**, *98*, 5648.

[48] a) D. Andrae, U. Häußermann, M. Dolg, H. Stoll, H. Preuß, *Ther. Chim. Acta* **1990**, *77*, 123; b) F. Weigend, R. Alrichs, *Phys. Chem. Chem. Phys.* **2005**, *7*, 3297-3305.

[49] a) A. Schäfer, H. Horn, R. Ahlrichs, *J. Chem. Phys.* **1992**, *97*, 2571–2577; b) F. Weigend, *Phys. Chem. Chem. Phys.* **2006**, *8*, 1057–1065; c) F. Weigend, R. Ahlrichs, *Phys. Chem. Chem. Phys.* **2005**, *7*, 3297–3305; d) K. Eichkorn, F. Weigend, O. Treutler, R. Ahlrichs, *Theor. Chem. Acc.* **1997**, *97*, 119.

[50] Chemcraft - graphical software for visualization of quantum chemistry computations. http://www.chemcraftprog.com.

[54] S. Grimme, S. Ehrlich, L. Goerigk, *J. Comput. Chem.* **2011**, *32*, 1456.

6 Reactivity of $[Cp''_2Zr(\mu^{1:1}\text{-}E_4)]$ (E = P, As) towards Nucleophiles

V. Heinl, M. Seidl, M. Scheer.

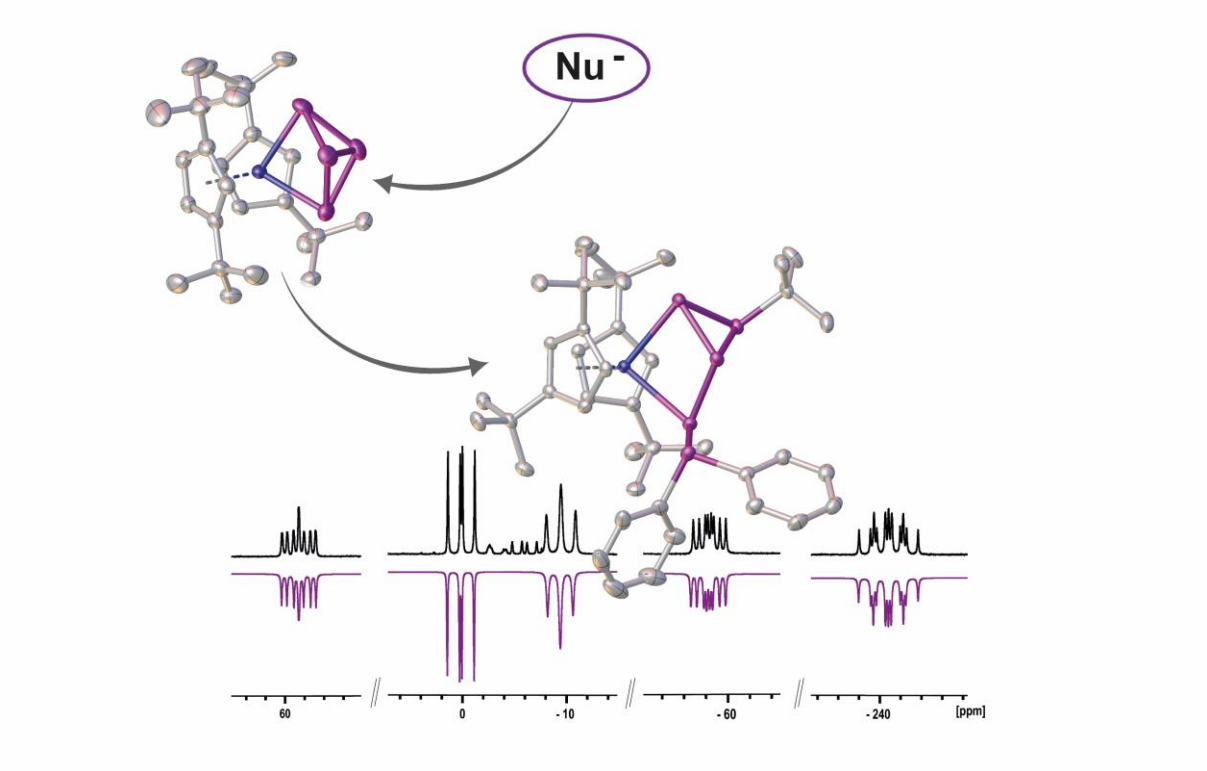

Abstract

The functionalization of the E_n-ligand complexes $[Cp''_2Zr(\mu,\eta^{1:1}\text{-}E_4)]$ (E = P (**1a**), As (**1b**); Cp'' = 1,3-di-tertbutyl-cyclopentadienyl) is focused to modify the properties of the polypinctogen unit and gain new synthetic pathways for further transformations. The reaction behavior of **1** towards main group nucleophiles is investigated. The reaction of **1a** with ^{t}BuLi leads to the ionic product $Li[Cp''_2Zr(\mu,\eta^{1:1}\text{-}P_4{}^t\text{Bu})]$ (**2**), where an organic group is attached to a bridgehead phosphorus atom of the butterfly unit. Further reactions of **2** with quenching reagents enable the introduction of a further substituent. Moreover, a condensation of **2** to the P_8-complex $[(Cp''_2Zr)_2(\mu,\eta^{1:1:1:1}\text{-}P_8{}^t\text{Bu}_2)]$ (**3**) has been observed. The reaction of **1** with $LiNMe_2$ and $LiCH_2SiMe_3$ leads to fragmentation of the E_4 unit and the formation of $[Cp''_2Zr(\eta^2\text{-}E_3Nu)]$ (Nu = NMe_2: P, **6a**; As, **6b**; Nu = CH_2SiMe_3: P, **7a**; As, **7b**), respectively.

6.1 Author Contribution

- Synthesis and complete characterization of the compounds **4**, **5**, and **6a, 6b**, **7a**, **7b** and **8** were performed by V. Heinl.
- Improved Synthesis and complete characterization of the compounds **2** and **3** were performed by V. Heinl.
- First synthesis and insight in the formation of the compound **2** and **3** were performed by A. E. Seitz during his master thesis (University of Regensburg, **2013**).
- Computational studies were performed by G. Balázs.
- M. Seidl recalculated the X-ray structures.
- The Manuscript was written by V. Heinl except parts of the computational details (G. Balázs).
- Supervision: M. Scheer.

6.2 Introduction

Organophosphorus compounds represent essential reagents in our daily life and industry.[1,2,3] For their synthesis normally white phosphorus (P_4) is used as phosphorus source, synthesized by the reduction of phosphate rocks. Following chlorination to PCl_3[4] and subsequent functionalization with, *inter alia*, alcohols, organolithium or Grignard reagents lead to the desired organophosphorus compounds.[3–6] This overall process has disadvantages, because of the mostly multistep synthetic routs, like a low atom efficiency, the formation of stochiometric amount of waste and hazardous intermediates and side-products are formed.[1,3,5,6] For these reasons, a direct functionalization of P_4 and selective P-C bond formation is an active topic of research.[7]

The direct reaction of P_4 with main group metal organyls has already been described in 1963 by *Rauhut et al.* by using PhLi/^{t}BuLi as nucleophiles in combination with some quenching reagents which leads to a mixture of phosphanes.[8] Reactions of P_4 with alkynyls also result in unselective product mixture.[9] However, *Fritz et. al.* reported a more selective and less harsh reaction to cyclotetraphosphanes by the usage of ^{t}BuLi and Me_3SiCl as quenching agents, what is attributed to the use of the more bulky reagents.[10] By using the steric demanding Mes*Li (Mes* = 2,4,6-$^t Bu_3C_6H_2$) a single P-P bond cleavage of the phosphorus tetrahedron can be observed and **I** is formed beside a Mes*P=PMes* (Figure 1).[11] *Lammertsma et. al.* demonstrated the controlled cleavage of P_4 with ArLi in the presence of Lewis acids ($B(C_6F_5)_3$, BPh_3) leading to Lewis acid stabilized bicyclo[1.1.0]tetraphosphabutanide anions **II** (Figure 1), as well as a subsequent controlled functionalization of **II**.[12] Furthermore, our group was able to synthesize compound **III** (Figure 1) via metal-mediated functionalization of P_4 by radical.[13]

Interestingly, a similar anion to **II** can also be observed using a carbene-borane Lewis pair for activation.[14] It has been shown, that using carbenes a selective functionalization of P_4 is a promising approach. *Bertrand et. al.* reported the usage of CAAC's (cyclic-alkyl-amino-carbene) to form, for instance, the E- and Z- isomers of a linear tetraphosphorus chain (Figure 1, **IV**)[15] or the trisubstituted P_4 derivative **V**. However, also aggregation to larger phosphorus units is observed, depending on the nature of the carbene.[7] Another interesting approach was shown by *Peruzzini et. al.* by using rhodium alkyl or aryl complexes to form [(triphos)Rh(η^1:η^2-P_4R)] (**VI**, R = Me, Et, Ph, triphos = $MeC(CH_2PPH_2)_3$).[16]

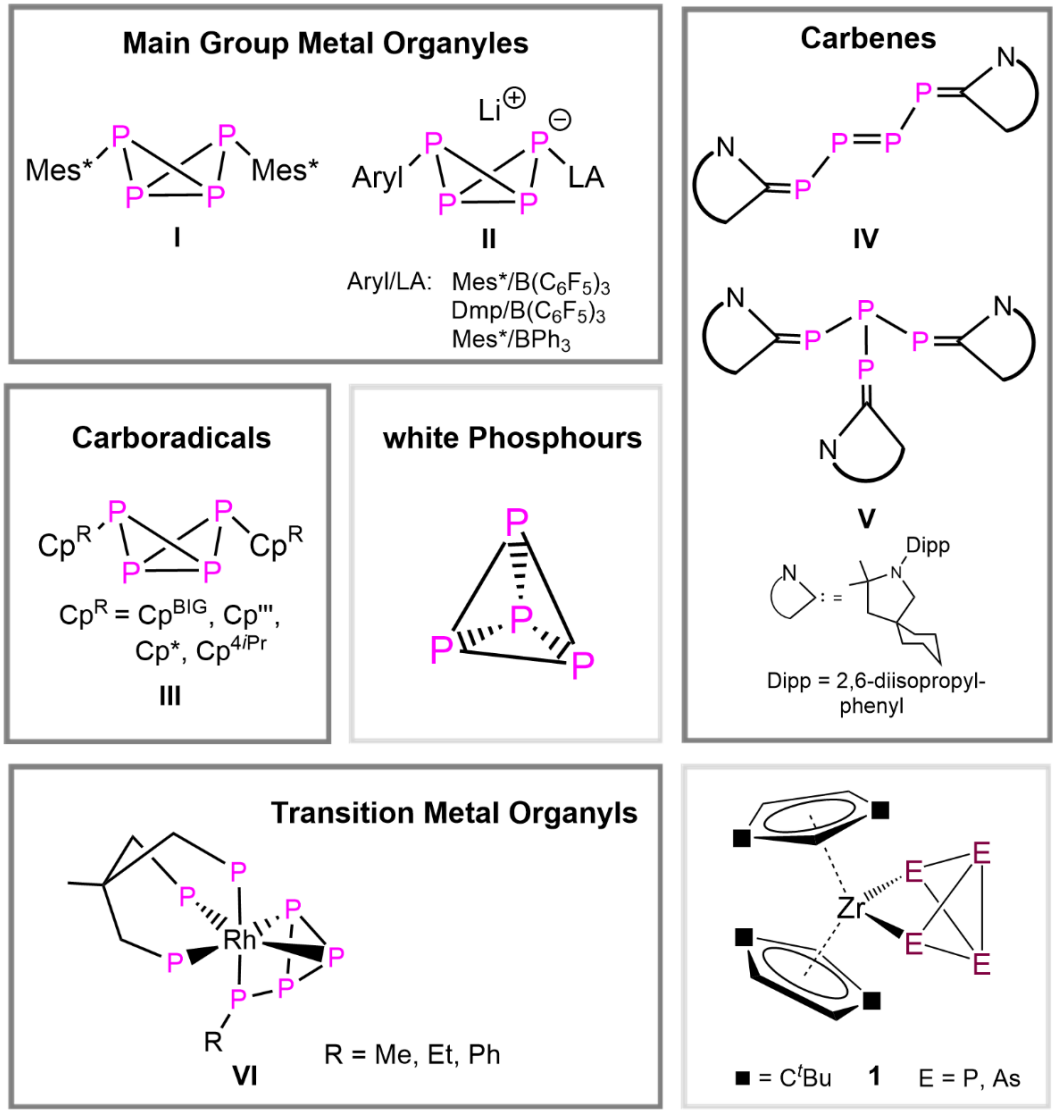

Figure 1: Selected examples of P-C bond formation by the activation of white phosphorus.

The use of transition metal complexes to activate white phosphorus and yellow arsenic is widely applied and a huge variety of examples are currently known.[17–21] The question arises, if a subsequent functionalization in the coordination sphere of transition metals lead to a more specific reaction path and offer new insights in the reactivity of activated P_4 and As_4. In 2016 *Lammertsma et al.* demonstrated a controlled P-C bond formation generated on a P_4 unit in

the coordination sphere of a gold cation. The reaction with ArLi leads to the formation of a Lewis acid stabilized Ar-P_4 unit $[ArP_4(IPrAu)_2][Al(OC(CF_3)_3)_4]$ (Ar = mesityl, 2,6-di-mesitylphenyl).[22] Recently, our group has shown that the reaction of P_n complexes of tantalum and cobalt towards nucleophiles leads to P-Nu bond formation, while one M-P bond is cleaved.[23,24] Furthermore, a ring contraction can be observed by using NHC's by abstraction of a pnictogen atom.[24] By the reaction of [Cp'''Co(η^4-P_4)] with two equiv. of ^{Me}NHC, an *cyclo*-P_3 end deck is formed. The abstracted phosphorus atom is catched by two ^{Me}NHC units to form the counter ion $[(^{Me}NHC)_2P]^+$. Similar is observed for the reaction with the triple decker complex [(Cp*Mo(μ,$\eta^{6:6}$-E_6)] (E = P, As).[24]

Another interesting transition metal complexes represent the zirconium compounds $[Cp''_2Zr(\mu,\eta^{1:1}\text{-}E_4)]$ (**1**, Cp'' = 1,3-ditertbutyl-cyclopentadienyl, E = P, As) synthesized by the reaction of the corresponding carbonyl compounds with P_4 and As_4, respectively. Here, one E-E bond is already cleaved and a "butterfly"-moiety is formed.[25,26] Studies on the reaction behavior, inter alia towards Lewis acids and as transfer reagents, show a high potential in the reactivity.[25,27] Due to electronic behavior and steric effects a versatile functionalization, as well as a selective and unexpected connectivity, could be realized. DFT calculation show, that the wing-tip phosphorus atoms bare the most negative electrostatic potential (ESP), while the ESP on the bridge-head phosphorus atoms is more positive (Figure 2). Hence, a nucleophilic attack should occur on the bridgehead P atoms. Although, the ESP on Zr is more positive than on the P_4 unit, it cannot be attacked by a nucleophile being sterically encased by the bulky Cp'' ligands.

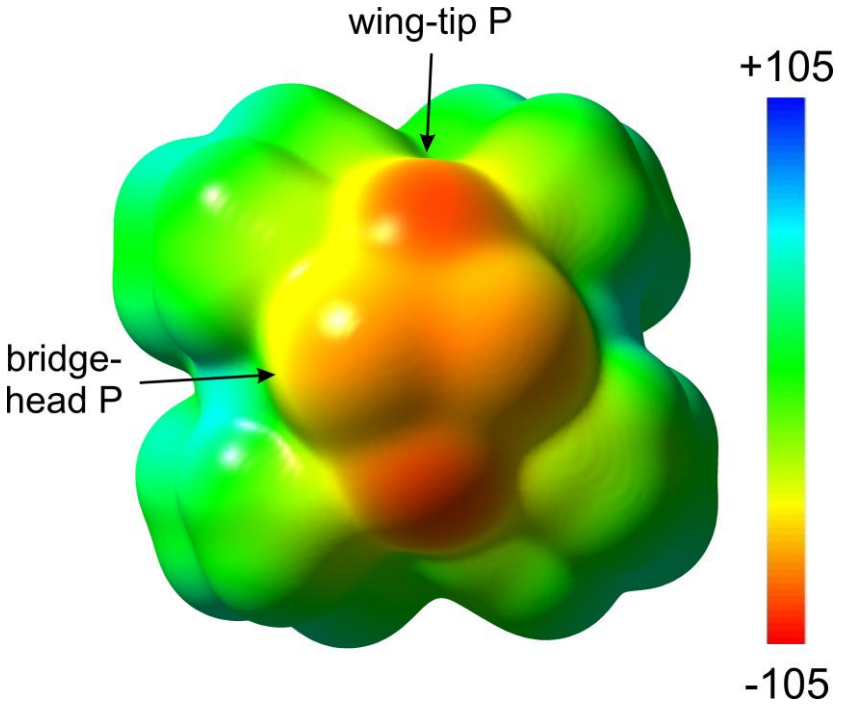

Figure 2. Electrostatic potential mapped on electron density (isovalue = 0.001) for 1, calculated at the D3(BJ)-TPSS/def2TZVP (CPM) level of theory. Colour code (blue = positive, red = negative) in kJ·mol−1.

Herein, we report on the reaction behavior of **1** towards the main group nucleophiles ^{t}BuLi, $LiCH_2SiMe_3$ and $LiNMe_2$, leading to functionalized polypnictogen zirconium complexes. Moreover, further reactions with quenching electrophiles permit a selective subsequent functionalization and also the extension of the polypnictogen unit.

6.3 Results and Discussions

The reaction of [Cp"$_2$Zr(µ,η$^{1:1}$-P$_4$)] (**1a**) with ^{t}BuLi in THF at -78 °C leads to the formation of the ionic product Li[Cp"$_2$Zr(µ,η$^{1:1}$ P$_4$^{t}Bu)] (**2**). A nucleophilic attack of ^{t}Bu^{-} on one of the bridgehead phosphorus atoms of the P$_4$-butterfly unit leads to the cleavage of one P-P bond. An attack on a wingtip phosphorus (P bound to Zr) atoms could not be observed. This is in agreement with the DFT calculations (vide supra).

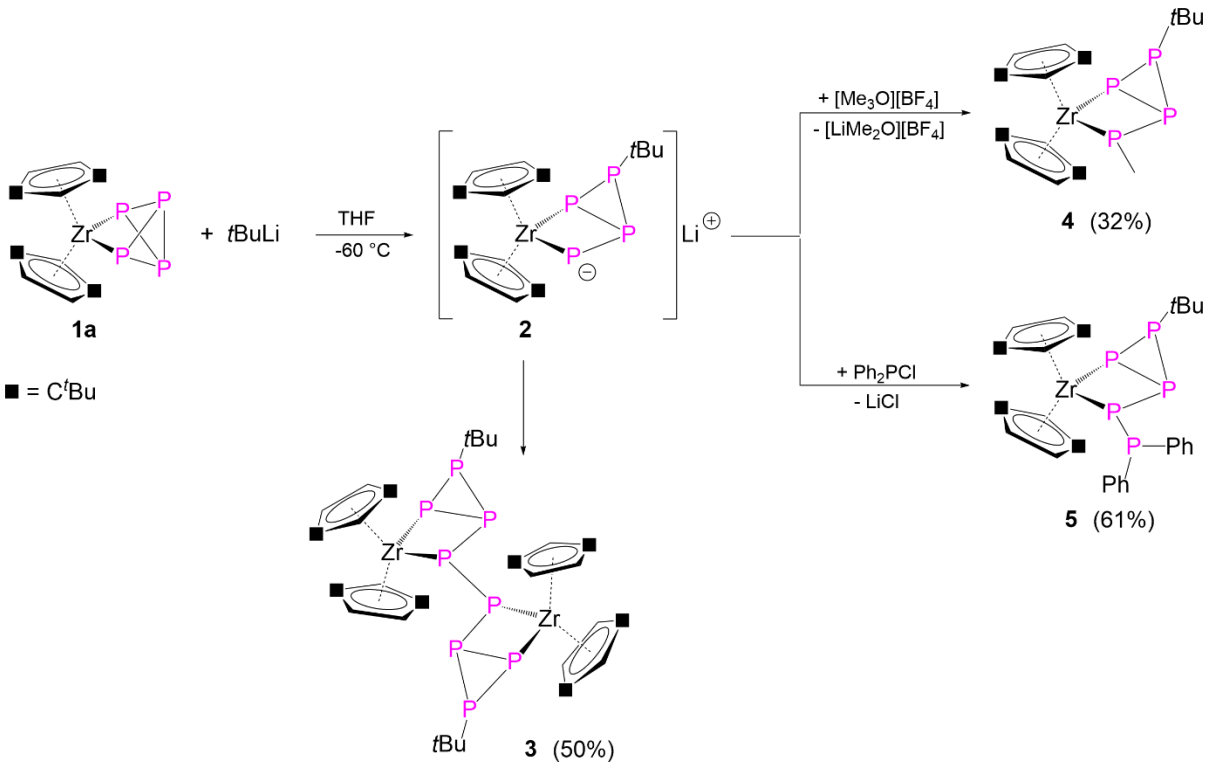

Scheme 1: Overview of the reactions of [Cp"$_2$Zr(µ,η$^{1:1}$-P$_4$)] (**1a**) with ^{t}BuLi. All reactions were performed in THF at -78 °C.

Unfortunately, **2** can only be verified by NMR spectroscopy and mass spectrometry and can not be isolated as solid irrespective of several attempts. However, is the solvent removed and the solid extracted with *n*-pentane, the complex [(Cp"$_2$Zr)$_2$(µ,η$^{1:1:1:1}$-P$_8$^{t}Bu$_2$)] (**3**) is obtained in 50% yield. **3** is probably formed by oxidation of **2** during the workup. The nature of the oxidation agent is not clear, but very probably traces of oxygen during the handling causes the oxidation.

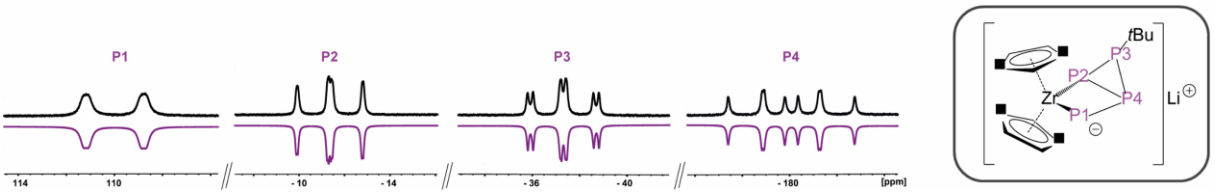

Figure 3: Sections of the $^{31}P\{^{1}H\}$ NMR spectrum of **2** in CD_2Cl_2. Black: experimental, purple: simulated.

However, the anionic part of **2** can be detected in ESI mass spectrometry as the only component in the reaction solution. $^{31}P\{^{1}H\}$ NMR spectroscopic measurements of a freshly prepared solution of **2** show four multiplets centered at δ = -180.1 ppm, -37.1 ppm, -11.4 ppm and 110.0 ppm. They correspond to an AMNX spin system and can undoubtedly be assigned to the four inequivalent phosphorus atoms of **2** (Figure 3). The appropriate coupling constants were determined via simulation (*cf.* Figure S10). The proposed structure of **2** in solution is proved by DFT calculations, which show that the proposed structure on **2** based on NMR spectroscopy is a true minimum structure (*cf.* SI). Since crystals of **2** could not be obtained, ingredients like crown-ethers and different solvents were used to induce crystallization. Unfortunately, this leads to a more unspecific reaction and several side products are formed. Interestingly, in the NMR spectra of these reactions a strong shift to higher ppm values for the phosphanide type atom P1 is observed (Figure S12). Surprisingly, in solution compound **2** seems to be stable, even after 5 days no decomposition or conversion can be observed (Figure S11). For this reason, we propose, that the conversion of **2** to **3** occurs during the purification process. The high sensitivity toward oxidation of **2** is based on the energetically high lying Highest Occupied Molecular Orbital (HOMO), which represent a lone pair of electrons of the phosphanide-type P1 atom (*cf*. SI).

To get another proof for the existence of compound **2** subsequent reactions with the quenching reagents $[Me_3O][BF_4]$ and Ph_2PCl, respectively, were made. These reactions leads in THF at -78 °C to the formation of $[Cp''_2Zr(\eta^{1:1}\ P_4{}^tBuMe)]$ (**4**) and $[Cp''_2Zr(\eta^{1:1}\text{-}P_4{}^tBuPPh_2)]$ (**5**), in which a Me and a Ph_2P group, respectively, are attached to a former wing-tip phosphorus atom, proofing by this way the identity of **2** (Scheme 1). Compounds **3**, **4** and **5** were comprehensively characterized by NMR spectroscopy, single crystal X-ray diffraction analysis, mass spectrometry and elemental analysis.

Crystals of **3**, **4** and **5** suitable for single crystal X-ray diffraction analysis were obtained by storing a concentrated solution in *n*-pentane (**3**, **5**) at -30 °C or hexamethyldisiloxane (**4**) at -78 °C. Their molecular structures are depicted in figure 4. In all three compounds, one P-P bond of the original P_4 butterfly unit is cleaved and a C-P bond is formed by the introduction of a ^tBu group on P2. Due to the steric repulsion of the introduced units the Zr-P distances are slightly elongated compared to **1a**.[28] All P-P distances are in the range of normal single bonds

(**3**: 2.1965(6) Å to 2.2270(6) Å; **4**: 2.186(5) Å to 2.235(3) Å; **5**: 2.2021(8) Å to 2.2376(8) Å). However, the bond between P1 and P2 represents the shortest one.[17,18,20]

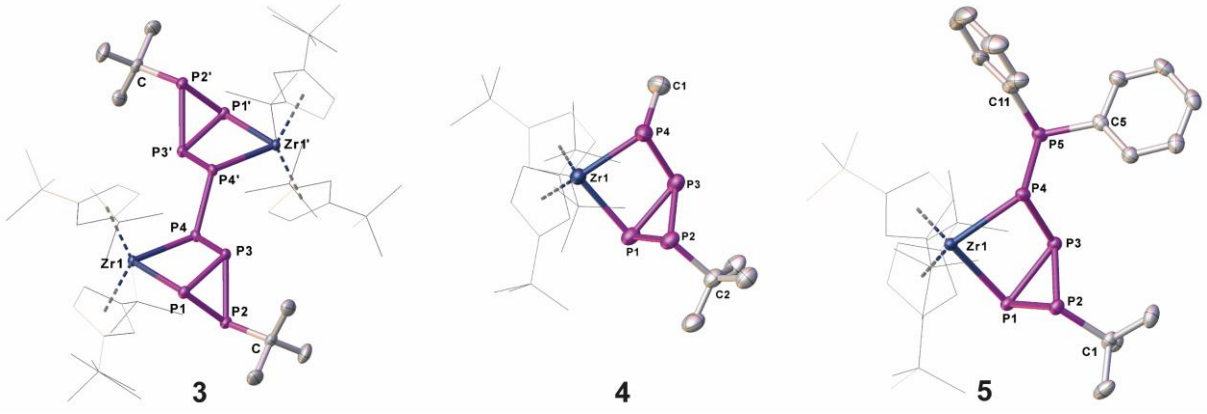

Figure 4: Molecular structure of **3**, **4** and **5** in the solid state with thermal ellipsoids at 50% probability level. Hydrogen atoms are omitted and the Cp''' ligands are drawn in the wire frame model for clarity.

LIFDI (**3**, **4**) and FD (**5**) mass spectrometry show the corresponding molecular ion peak. ^{1}H NMR investigations for **3** and **4** show the expected signals for the magnetically inequivalent Cp'' ligands and the introduced substituents, respectively. Similar to the ^{31}P{^{1}H} NMR spectrum of **2** four multiplets can be observed in the spectra of **3** and **4** (*cf.* SI). The ^{1}H NMR spectrum of **5** shows four signals (δ = 0.97 ppm, 1.04 ppm, 1.19 ppm, 1.47 ppm) for four magnetically inequivalent ^{t}Bu groups located on the Cp rings and 6 signals for the hydrogen atoms directly bound to the ring in the region of δ = 5.5 to 6.1 ppm. Moreover, the signals at δ = 7.16-7.29 ppm, 7.74 ppm and 7.93 ppm can be assigned to the phenyl groups. The ^{t}Bu group bound to P5 appears as a doublet at δ = 0.95 ppm with a $^{3}J_{P\text{-}H}$ coupling constant of 11 Hz. ^{1}H{^{31}P} NMR confirms the coupling to the phosphorus atom (*cf.* Figure S19). The ^{31}P{^{1}H} NMR spectrum of **5** shows five multiplets for the magnetically inequivalent phosphorus atoms. The corresponding coupling constants were obtained via simulation (Figure S22). Hence, a coupling constant of $^{2}J_{P3\text{-}P5}$ = 190 Hz between the not directly bound atoms P3 and P5 indicates a through space coupling, probably enabled by the geometry and the rather short distance of 3.179 Å, found in the solid state. Similar observations for such a through space coupling can be found in the literature.[29] However, there is a second set of signals in the ^{31}P{^{1}H} NMR spectra at least as a tenth of the intensity for the signals corresponding to **5**, even at low temperatures (Figure S21). Associated signals can also be observed in the ^{1}H NMR spectra (Figure S17). These low intensity signals can be tentatively assigned to a possible isomer of **5**, present in solution. However, the relative ratio of the signals in the NMR does not change over time, at low temperatures or if crystals of **5** are dissolved at -78 °C.

Due to the fact, that **2** cannot be isolated and during purification processes of the reaction solution a full conversion to **3** is observed, the reaction behavior of **1** toward other main group

nucleophiles was investigated to trap the ionic intermediate (Scheme 2). Surprisingly, the reaction with the nucleophiles $LiNMe_2$ and $LiCH_2SiMe_3$, respectively, in dme leads to different products. There the neutral compounds $[Cp''_2Zr(\eta^2\text{-}E_3Nu)]$ (Nu = NMe_2: P, **6a**; As, **6b**; Nu = CH_2SiMe_3: P, **7a**; As, **7b**), containing a *cyclo*-E_3 unit are found (Scheme 2). In the case of the reaction of **1b** with $LiCH_2SiMe_3$ also the novel triple decker complex $[(Cp''Zr)_2(\mu,\eta^{1:1:1:1:1:1}\text{-}As_6)]$ (**8**) can be isolated as a side-product. However, it is not undoubtedly clear in which form the abstracted phosphorus atom is converted. We assume the formation of polyphosphides due to formation of a porous beige solid during the reactions and the workup process. Furthermore, a singlet at 469.7 ppm in the $^{31}P\{^1H\}$ NMR spectrum of the reaction solution of **6a** indicates the formation of LiP_5.[30] The compounds **6a/b**, **7a/b** and **8** are comprehensively characterized by NMR spectroscopy, single crystal X-ray diffraction analysis, mass spectrometry and elemental analysis.

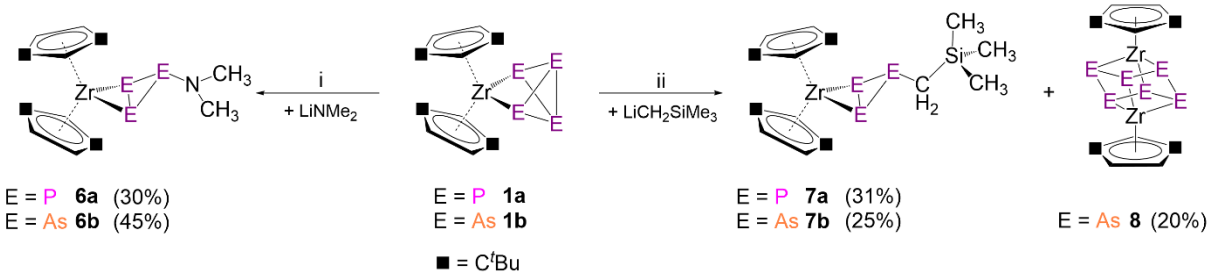

Scheme 2: Overview of the reactions of $[Cp''_2Zr(\mu,\eta^{1:1}\text{-}E_4)]$ (E = P: **1a**; E = As: **1b**) with the nucleophiles $LiNMe_2$ (i) and $LiCH_2SiMe_3$ (ii) DME at -60 °C.

Crystals suitable for single crystal X-ray diffraction analysis were obtained by storing a concentrated solution of *n*-pentane (**6a**, **6b**), *n*-hexane (**7a**, **7b**) or Et_2O (**8**) at -78 °C. Figure 5 exemplifies the molecular structures of **6a**, **7b** and **8** (**6b** and **7a** are depicted in the SI). The compounds **6a/b** and **7a/b** consist of an E_3 ring, η^2-attached to a $[Cp''_2Zr]$ fragment and the introduced nucleophilic part. All E-E distances are in the range of a normal single bond.[17,18,20,21] The central structural core of **8** can best be ascribed as a chair type As_6 unit stabilized by two [Cp''Zr] fragments. Due to the $\eta^{1:1:1:1:1:1}$ coordination mode, the triple decker complex can also be described as a Zr_2As_6 cube. The As-As distances of 2.4908(7) Å to 2.5147(7) Å are in the range of a single bond and in good agreement with other polyarsenic transition metal complexes.[21] Transition metal complexes containing an As_6 units are known and often they contain a prismane core.[31] Therefore, **8** represents the first complex containing a chair-like As_6 unit. Otherwise, only organo substituted chair-like $(RAs)_6$ units are known.[32] Recently, the synthesis of the isostructural complex $[(Cp''Zr)_2(\mu,\eta^{1:1:1:1:1:1}\text{-}Sb_6)]$ by the reaction of $[Cp''_2ZrCl_2]$ with $KSb(SiMe_3)_2$ was reported.[33] Furthermore, besides the starting material **1b** and the complex $[(Cp''_2Zr)(Cp''Zr)(\mu,\eta^{2:2:1}\text{-}As_5)]$, which is formed as by-product by the synthesis of **1b**, **8** represents a rare example of a polyarsenic zirconium ligand complex.[25]

The ^{1}H NMR spectra for **6a/b** and **7a/b** and **8** reveals the expected signals. For **6a/b** and **7a/b** two sets of signals for the Cp'' ligands in an asymmetric environment can be detected. Compared to this, the spectrum of **8** contains only one set of signals. Furthermore, also the methyl groups of the amide-ligand in **6a** and **6b** are not equivalent and two signals are observed, because the rotation along the P2-N axis is hindered. In the ^{31}P{^{1}H} NMR spectra of **6a** and **7a** a triplet (**6a**: -16.7pmm; **7a**: -105.9 ppm) and a doublet (**6a**: 67.2 ppm; **7a**: 103.8 ppm) arise with the $^{1}J_{P\text{-}P}$ coupling constants of 263 Hz (**6b**) and 224 Hz (**7a**), consistent with the symmetric P_3 unit.

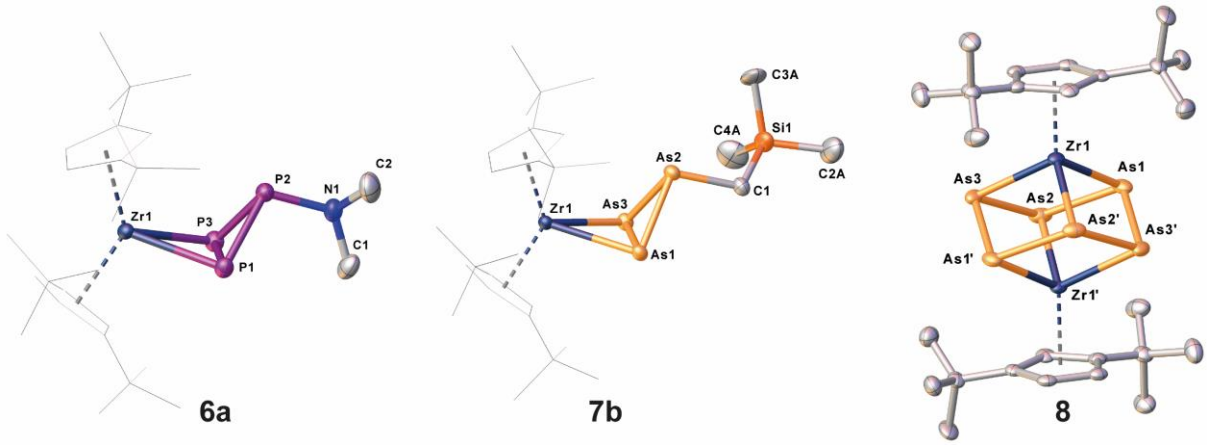

Figure 5: Molecular Structure of **6a** (left), **7b** (middle) and **8** (right) in the solid state with thermal ellipsoids at 50% probability level. **6a**, **6b**: Hydrogen atoms are omitted and the Cp''' ligands are drawn in the wire frame model for clarity.**8a**: Hydrogen atoms are omitted for clarity.

6.4 Conclusion

In summary, we investigated the reaction behavior of **1** towards main group nucleophiles and reported the synthesis and characterization of a variety of substituted polypnictogen ligand complexes as well as a new polyarsenic triple decker complex. By using the nucleophile ^{t}BuLi the introduction of a single carbon group on a bridgehead phosphorus atom of **1a** is achieved and the product Li[Cp''$_2$Zr(μ,η$^{1:1}$-P$_4$^{t}Bu)] (**2**) is formed. However, after workup the complex [(Cp''$_2$Zr)$_2$(μ,η$^{1:1:1:1}$-P$_8$^{t}Bu$_2$)] (**3**) can only be isolated, bearing a P$_8$ unit. Even if it was not possible to crystalize **2**, further reactions with the quenching reagents [Me$_3$O][BF$_4$] and Ph$_2$PCl enables the introduction of another group and the complexes [Cp''$_2$Zr{η$^{1:1}$-P$_4$^{t}Bu(FG)}] (FG = Me (**4**), PPh$_2$ (**5**)) can be isolated. Furthermore, the reaction behavior of **1** towards the main group nucleophiles LiNMe$_2$ and LiCH$_2$SiMe$_3$ was investigated. Therefore, a more exceptional way for the formation of an organic substituted E$_3$ units was recognized. The size of the origin E$_4$ unit is reduced by abstraction of one pnictogen atom. Therefore, a E$_3$-ring is formed and the neutral compounds [Cp''$_2$Zr(η$^{1:1}$-E$_3$Nu)] (Nu = NMe$_2$: P, **6a**; As, **6b**; Nu = CH$_2$SiMe$_3$: P, **7a**; As, **7b**) can be isolated. Surprisingly, in the reaction of **1b** and LiCH$_2$SiMe$_3$ the novel triple decker complex [(Cp''Zr)$_2$(μ,η$^{1:1:1:1:1:1}$-As$_6$)] (**8**) is formed. Due to the properties of the formed polypnictogen complexes with and without organic substituents, the usage in transfer reactions offers interesting possibilities.

6.5 Supporting Information

6.5.1 Experimental Detail

All experiments were performed under an atmosphere of dry nitrogen or argon using Schlenk and glovebox techniques. Solvents were purified, dried and degassed prior use. ^{1}H, ^{13}C and ^{31}P NMR spectra were recorded at room temperature on a Bruker Avance 400 spectrometer (^{1}H: 400,130 MHz, ^{31}P: 161,976 MHz, ^{13}C: 100.613 MHz) and on a Bruker Advance 300 spectrometer (^{1}H: 300,132 MHz, ^{31}P: 121,495 MHz, ^{13}C: 75.468 MHz). ^{1}H, ^{13}C and ^{31}P NMR chemical shifts are reported in parts per million (ppm) relative to external standards Me_4Si or H_3PO_4 (85%). All NMR simulations were conducted with the *WinDaisy* application within the NMR software *Top Spin* 4.0.2 by *Bruker*. Elemental analysis was determined with a Vario micro cube apparatus. For mass spectrometry, a Finnigan MAT 95 (LIFDI MS, FD MS) or a Finnigan MAT SSQ 710 A (EI MS) device and a Joel AccuTOF GCX spectrometer were used. [Cp''$_2$Zr($\eta^{1:1}$-P_4)][34] and [Cp''$_2$Zr($\eta^{1:1}$-As_4)][35] were prepared according to literature procedures.

Preparation of Li[Cp''$_2$Zr(µ,$\eta^{1:1}$-P_4^{t}Bu)] (2):

[Cp''$_2$Zr($\eta^{1:1}$-P_4)] (101 mg, 0.178 mmol) is dissolved in 30 mL THF, cooled to -78 °C and a solution of ^{t}BuLi in *n*-pentane (V = 0.11 mL, c = 1.7 mol/L, n = 0.19 mmol) is added. A dark green solution of **2** is formed.

2: **^{31}P{^{1}H} NMR** (CD_2Cl_2, 298 K): *δ* [ppm] = -180.1 (m, 1P), -37.1 (m, 1P), -11.4 (m, 1P), 110.0 (m, 1P); **^{31}P NMR** (CD_2Cl_2, 298 K): -180.1 (m, 1P), -37.1 (m, 1P), -11.4 (m, 1P), 110.0 (m, 1P); **ES MS** (dme): *m*/*z* (%): 625.19 (M^+).

Preparation of [(Cp''$_2$Zr)$_2$(µ,$\eta^{1:1:1:1}$-P_8^{t}Bu$_2$)] (3):

[Cp''$_2$Zr($\eta^{1:1}$-P_4)] (305 mg, 0.537 mmol) is dissolved in 30 mL THF, cooled to -78 °C and a solution of ^{t}BuLi in *n*-pentane (V = 0.41 mL, c = 1.7 mol/L, n = 0.70 mmol) is added. The colour changes immediately to dark green. The reaction mixture is stirred at r.t. for approximately 1 d. After removing the solvent the brown residue is extracted with *n*-pentane and filtered via cannula. A dark brown residue remains. Crystals of **3** suitable for single crystal X-ray structure analysis are obtained by storing a concentrated solution at -30 °C. Crystalline Yield: 332 mg (0.266 mmol, 97%)

3: **^{1}H NMR** (CD_2Cl_2, 298 K): *δ* [ppm] = 0.96 (s, 9H, PC_4H_9), 0.98 (s, 9H, PC_4H_9), 1.31 (s, 18 H, $C(CH_3)_3$), 1.32 (s, 18 H, $C(CH_3)_3$), 1.33 (s, 18 H, $C(CH_3)_3$), 1.48 (s, 18 H, $C(CH_3)_3$, 5.10 (s, br, 1 H, C_5H_2^{t}Bu$_3$), 5.66 (s, br, 2 H, C_5H_2^{t}Bu$_3$), 5.69 (d, 4 H, C_5H_2^{t}Bu$_3$), 5.80 (t, 2 H, C_5H_2^{t}Bu$_3$), 5.61 (s, br, 2 H, C_5H_2^{t}Bu$_3$); **^{31}P{^{1}H} NMR** (CD_2Cl_2, 298 K): *δ* [ppm] = -231.2 (m, 2P), -54.0 (m,

2P), -3.9 (m, 2P), 118.3 (m, 2P); **^{31}P NMR** (CD_2Cl_2, 298 K): -231.2 (m, 2P), -54.0 (m, 2P), -3.9 (m, 2P), 118.3 (m, 2P); **FD MS** (toluene): *m*/*z* (%): 1252.3 (M^+); **Elemental analysis** (%): calculated for [$C_{31}H_{51}ZrP_4$] (1250.39 g·mol^{-1}): C, 57.48; H, 8.20; found: C, 57.76; H, 7.94.

Preparation of [Cp''$_2$Zr(η$^{1:1}$-P$_4$^{t}BuMe)] (4):

[Cp''$_2$Zr(η$^{1:1}$-P$_4$)] (500 mg, 0.880 mmol) is dissolved in 30 mL THF, cooled to -78 °C and a solution of ^{t}BuLi in *n*-pentane (V = 0.72 mL, c = 1.7 mol/L, n = 1.22 mmol) is added. The colour changes immediately to dark green. After stirring for 10 min, a solution of [Me_3O][BF_4] (156 mg, 1.05 mmol) in 5 mL THF is added and the colour changes to red-brown. The reaction mixture is stirred at r.t. for approximately 1 d. After removing the solvent, the red-brown residue is extracted with hexamethyldisiloxane and filtered via cannula. Crystals of **4** suitable for single crystal X-ray structure analysis are obtained by storing a concentrated solution at -78 °C. Crystalline Yield: 179 mg (0.280 mmol, 32%)

4: **^{1}H NMR** (C_6D_6, 298 K): *δ* [ppm] = 1.16 (s, 9 H, C(*CH*$_3$)$_3$), 1.19 (s, 9 H, PC$_4$*H*$_9$), 1.28 (s, 3 H, P*CH*$_3$), 1.40 (s, 18 H, C(*CH*$_3$)$_3$), 1.45 (s, 9 H, C(*CH*$_3$)$_3$), 5.10 (s, br, 1 H, C$_5$*H*$_2$^{t}Bu$_3$), 5.41 (s, br, 2 H, C$_5$*H*$_2$^{t}Bu$_3$), 5.49 (s, br, 1 H, C$_5$*H*$_2$^{t}Bu$_3$), 5.56 (t, 1 H, C$_5$*H*$_2$^{t}Bu$_3$), 5.98 (t, 1 H, C$_5$*H*$_2$^{t}Bu$_3$); **^{31}P{^{1}H} NMR** (C_6D_6, 298 K): *δ* [ppm] = -234.6 (m, 1P), -63.8 (m, 1P), -1.1 (m, 1P), 69.2 (m, 1P); **^{31}P NMR** (C_6D_6, 298 K): *δ* [ppm] = -234.6 (m, 1P), -63.8 (m, 1P), -1.1 (m, 1P), 69.2 (m, 1P); **LIFDI MS** (toluene): *m*/*z* (%): 640.2 (M^+, 100); **Elemental analysis** (%): calculated for [$C_{31}H_{54}ZrP_4$] (640.22.40 g·mol^{-1}): C, 58.01; H, 8.48; found: C, 57.83; H, 8.56.

Preparation of [Cp''$_2$Zr(η$^{1:1}$-P$_4$^{t}BuPPh$_2$)] (5):

[Cp''$_2$Zr(η$^{1:1}$-P$_4$)] (100 mg, 0.176 mmol) is dissolved in 10 mL THF, cooled to -78 °C and a solution of ^{t}BuLi in *n*-pentane (V = 0.20 mL, c = 1.022 mol/L, n = 0.20 mmol) is added. The colour changes immediately to dark green. After stirring for 10 min, a solution of Ph_2PCl in toluene (V = 0.80 mL, c = 0.25 mol/L, n = 0.20 mmol) is added and the color changes to red. The reaction mixture is stirred at r.t. for approximately 1 d. After removing the solvent the red residue is extracted with *n*-pentane and filtered via cannula. A beige residue remains. The solution is stored at -78 °C for 24 h and further 24 h hours at -30 °C. Crystallization occurs during the warming process. Crystalline Yield: 87 mg (0.11 mmol, 61%)

5: **^{1}H NMR** (thf-d^8, 298 K): *δ* [ppm] = 0.95 (d, 9H, P-C(C*H*$_3$)3, $^3J_{P\text{-}H}$ = 11 Hz), 0.97 (s, 9 H, C(*CH*$_3$)$_3$), 1.04 (s, 9 H, C(*CH*$_3$)$_3$), 1.19 (s, 9 H, C(*CH*$_3$)$_3$), 1.47 (s, 9 H, C(*CH*$_3$)$_3$), 5.52 (t, br, 1 H, C$_5$*H*$_2$^{t}Bu$_3$), 5.63 (t, br, 1 H, C$_5$*H*$_2$^{t}Bu$_3$), 5.77 (t, br, 1 H, C$_5$*H*$_2$^{t}Bu$_3$), 5.85 (t, br, 1 H, C$_5$*H*$_2$^{t}Bu$_3$), 5.87 (s, br, 1 H, C$_5$*H*$_2$^{t}Bu$_3$), 6.05 (s, br, 1 H, C$_5$*H*$_2$^{t}Bu$_3$), 7.16 – 7.29 (m, 6 H, C$_6$*H*$_5$), 7.74 (m, 2 H, C$_6$*H*$_5$), 7.93 (t, 2 H, C$_6$*H*$_5$); **^{31}P{^{1}H} NMR** (thf-d^8, 298 K): *δ* [ppm] = -237.0 (m, 1P), -54.6 (m, 1P), -0.2 (m, 1P), 3.6 (m, 1P), 69.3 (m, 1P); **^{31}P NMR** (thf-d^8, 298 K):

δ [ppm] = -237.0 (m, 1P), -54.6 (m, 1P), -0.2 (m, 1P), 3.6 (m, 1P), 69.3 (m, 1P); **FD MS** (toluene): *m/z* (%): 810.25 (M^+); **Elemental analysis** (%): calculated for [$C_{42}H_{61}ZrP_5 \cdot 0.5\ C_5H_{12}$] (846.29 g·mol^{-1}): C, 63.02.01; H, 7.96; found: C, 63.56; H, 7.58.

Preparation of [Cp''$_2$Zr(η^2-P$_3$NMe$_2$)] (6a):

A solution of $LiNMe_2$ (6 mg, 0.1 mmol) in 5 mL DME is added to a solution of [Cp''$_2$Zr(η$^{1:1}$P$_4$)] (50 mg, 0.088 mmol) in 10 mL DME at -60 °C. The red-brown reaction mixture is stirred for 2 h at -60 °C and 1d at r.t. After removing the solvent the red-brown residue is extracted with *n*-pentane and filtered via cannula. A purple solution is obtained, a brown residue remains. Crystals of **6a** suitable for single crystal X-ray structure analysis are obtained by storing a concentrated solution at -78 °C. Crystalline Yield: 15 mg (0.026 mmol, 30%)

6a: **^{1}H NMR** (C_6D_6, 298 K): *δ* [ppm] = 1.13 (s, 18 H, C(*CH*$_3$)$_3$), 1.34 (s, 18 H, C(*CH*$_3$)$_3$), 2.49 (s, 3 H, N*CH*$_3$), 2.52 (s, 3 H, N*CH*$_3$), 4.95 (d, 2 H, C$_5$*H*$_3$^{t}Bu$_2$), 5.27 (d, 2 H, C$_5$*H*$_3$^{t}Bu$_2$), 8.53 (s, br, 1 H, C$_5$*H*$_3$^{t}Bu$_2$); 9.10 (s, br, 1 H, C$_5$*H*$_3$^{t}Bu$_2$); **^{31}P{^{1}H} NMR** (C_6D_6, 298 K): *δ* [ppm] = -16.7 (t, 1P, $^1J_{P\text{-}P}$ = 263 Hz), 67.2 (d, 2P, $^1J_{P\text{-}P}$ = 263 Hz); **^{31}P NMR** (C_6D_6, 298 K): *δ* [ppm] = -16.7 (t, 1P, $^1J_{P\text{-}P}$ = 263 Hz), 67.2 (d, 2P, $^1J_{P\text{-}P}$ = 263 Hz); **Elemental analysis** (%): calculated for [$C_{38}H_{48}ZrP_3N \cdot 0.5\ C_5H_{12}$] (737.89 g·mol^{-1}): C, 59.19; H, 8.79; N, 2.26; found: C, 59.34; H, 8.45; N, 1.95.

Preparation of [Cp''$_2$Zr(η^2-As$_3$NMe$_2$)] (6b):

A solution of $LiNMe_2$ (6 mg, 0.1 mmol) in 5 mL DME is added to a solution of [Cp''$_2$Zr(η$^{1:1}$As$_4$)] (80 mg, 0.11 mmol) in 10 mL DME at -60 °C. The red-brown reaction mixture is stirred for 2 h at -60 °C and 1d at r.t. After removing the solvent the red-brown residue is extracted with *n*-pentane and filtered via cannula. An orange solution is obtained, a brown residue remains. Crystals of **6b** suitable for single crystal X-ray structure analysis is obtained by storing a concentrated solution at -78 °C. Crystalline Yield: 35 mg (0.049 mmol, 45%)

6b: **^{1}H NMR** (C_6D_6, 298 K): *δ* [ppm] = 1.15 (s, 18 H, C(*CH*$_3$)$_3$), 1.35 (s, 18 H, C(*CH*$_3$)$_3$), 1.48 (s, 3 H, N*CH*$_3$), 1.53 (s, 3 H, N*CH*$_3$), 4.67 (d, 2 H, C$_5$*H*$_3$^{t}Bu$_2$), 5.10 (d, 2 H, C$_5$*H*$_3$^{t}Bu$_2$), 8.69 (t, 1 H, C$_5$*H*$_3$^{t}Bu$_2$); 9.02 (t, 1 H, C$_5$*H*$_3$^{t}Bu$_2$); **Elemental analysis** (%): calculated for [$C_{38}H_{48}ZrAs_3N$] (713.05 g·mol^{-1}): C, 47.06; H, 6.77; N, 1.96. No satisfying elemental analysis could be obtained, even by using Sn capsules.

Preparation of [Cp''$_2$Zr(η^2-P$_3${CH$_2$SiMe$_3$})] (7a):

A solution of LiCH$_2$SiMe$_3$ (33 mg, 0.35 mmol) in 5 mL DME is added to a solution of [Cp''$_2$Zr(η$^{1:1}$P$_4$)] (200 mg, 0.352 mmol) in 10 mL DME at -60 °C. The red-brown reaction mixture is stirred 2 h at -60 °C and 1d at r.t. After removing the solvent the red-brown residue is extracted with *n*-hexane and filtered via cannula. A purple solution is obtained, a brown residue remains. Crystals of **7a** suitable for single crystal X-ray structure analysis is obtained by storing a concentrated solution at -78 °C. Crystalline Yield: 66 mg (0.11 mmol, 31%)

7a: **^{1}H NMR** (C$_6$D$_6$, 298 K): *δ* [ppm] = 0.24 (s, 9 H, CH$_2$Si(*CH$_3$*)$_3$), 1.16 (s, 18 H, C(*CH$_3$*)$_3$), 1.29 (s, 2 H, *CH$_2$*Si(CH$_3$)$_3$), 1.33 (s, 18 H, C(*CH$_3$*)$_3$), 4.88 (d, 2 H, C$_5$*H$_3$*^{t}Bu$_2$), 5.25 (d, 2 H, C$_5$*H$_3$*^{t}Bu$_2$), 8.41 (s, br, 1 H, C$_5$*H$_3$*^{t}Bu$_2$); 8.93 (s, br, 1 H, C$_5$*H$_3$*^{t}Bu$_2$); **^{31}P{^{1}H} NMR** (C$_6$D$_6$, 298 K): *δ* [ppm] = -105.9 (t, 1P, $^1J_{P\text{-}P}$ = 224 Hz), 103.8 (d, 2P, $^1J_{P\text{-}P}$ = 224 Hz); **^{31}P NMR** (C$_6$D$_6$, 298 K): *δ* [ppm] = -105.9 (t, 1P, $^1J_{P\text{-}P}$ = 224 Hz), 103.8 (d, 2P, $^1J_{P\text{-}P}$ = 224 Hz); **Elemental analysis** (%): calculated for [C$_{30}$H$_{53}$ZrP$_3$Si] (622.20 g·mol^{-1}): C, 57.56; H, 8.53; found: C, 57.1; H, 7.77.

Preparation of [Cp''$_2$Zr(η^2-As$_3${CH$_2$SiMe$_3$})] (7b) and [(Cp''Zr)$_2$(μ,η$^{1:1:1:1:1:1}$-As$_6$)] (8):

A solution of LiCH$_2$SiMe$_3$ (8 mg, 0.09 mmol) in 5 mL DME is added to a solution of [Cp''$_2$Zr(η$^{1:1}$-As$_4$)] (60 mg, 0.081 mmol) in 10 mL DME at -60 °C. The red reaction mixture is stirred for 2 h at -60 °C and 1d at r.t. After removing the solvent the red residue is extracted with *n*-hexane and filtered via cannula. A red solution of **7b** is obtained, a brown residue remains. The residue is extracted with Et$_2$O and filtered via cannula to obtain a brown solution of **8**. Crystals of **7b** and **8** suitable for single crystal X-ray structure analysis are obtained by storing a concentrated solution at -78 °C. Crystalline Yield **7b**: 15 mg (0.020 mmol, 25%); **8**: 8 mg (0.0081 mmol, 20%)

7b: **^{1}H NMR** (C$_6$D$_6$, 298 K): *δ* [ppm] = 0.24 (s, 9 H, CH$_2$Si(*CH$_3$*)$_3$), 0.89 (s, 2 H, *CH$_2$*Si(CH$_3$)$_3$), 1.15 (s, 18 H, C(*CH$_3$*)$_3$), 1.35 (s, 18 H, C(*CH$_3$*)$_3$), 4.67 (d, 2 H, C$_5$*H$_3$*^{t}Bu$_2$), 5.10 (d, 2 H, C$_5$*H$_3$*^{t}Bu$_2$), 8.69 (t, 1 H, C$_5$*H$_3$*^{t}Bu$_2$), 9.02 (t, 1 H, C$_5$*H$_3$*^{t}Bu$_2$); **Elemental analysis** (%): calculated for [C$_{30}$H$_{51}$ZrAs$_3$Si] (754.05 g·mol^{-1}): C, 47.55; H, 7.05; found: C, 47.71; H, 7.06.

8: **^{1}H NMR** (CD$_2$Cl$_2$, 298 K): *δ* [ppm] = 1.39 (s, 36 H, C(*CH$_3$*)$_3$), 6.74 (d, 4 H, C$_5$*H$_3$*^{t}Bu$_2$), 7.08 (t, 2 H, C$_5$*H$_3$*^{t}Bu$_2$); **LIFDI MS** (toluene): *m*/*z* (%): 983.75 (M$^+$, 100); **Elemental analysis** (%): calculated for [C$_{26}$H$_{42}$Zr$_2$As$_6$] (754.05 g·mol^{-1}): C, 31.56; H, 4.29. No satisfying elemental analysis could be obtained, even by using Sn capsules.

6.5.2 Crystallographic Data

Crystals suitable for single crystal X-ray diffraction analysis were obtained as described above. The diffraction intensities were collected either on a Gemini Ultra diffractometer equipped with an Atlas^{S2} CCD detector and with a fine-focus sealed Cu-K_α X-ray tube (**3**, **5**, **7a**, **7b**, **8**) or a GV50 diffractometer equipped with a Titan^{S2} CCD detector and a micro-focus Cu-$K_{\alpha/\beta}$ X-ray tube (**4**, **6a, 6b**). Data collection and reduction were performed with **CrysAlisPro** software package.[36] The structures were solved with **Olex2**,[37] using **olex2.solve**[38] (**7a**) or **ShelXT**[39] (**3**, **4**, **5**, **6a**, **6b**, **7b**, **8**) and a least-square refinement on F^2 was carried out with **ShelXL**.[40] All non-hydrogen atoms were refined anisotropically. Hydrogen atoms at the carbon atoms were located in idealized positions and refined with isotropic displacement parameters according to the riding model.

Using **Olex2**,[37] all pictures of the respective molecular structures were made.

[(Cp''$_2$Zr)$_2$(μ,η$^{1:1:1:1}$-P$_8$^{t}Bu$_2$)] (3):

Compound **3** crystallizes out of a concentrated *n*-pentane solution at -30 °C in form of brown blocks in the monoclinic space group *C*$_2$/*c*. The asymmetric unit contains half a molecule of **3** and one Et$_2$O molecule. One *tert*-butyl group of a Cp''' ligand is disordered over two positions (occupancy 0.51 and 0.49). The Et$_2$O molecule is also disordered over two positions (occupancy 0.50 and 0.50). The restrains SIMU and SADI were used during the crystal structure refinement.

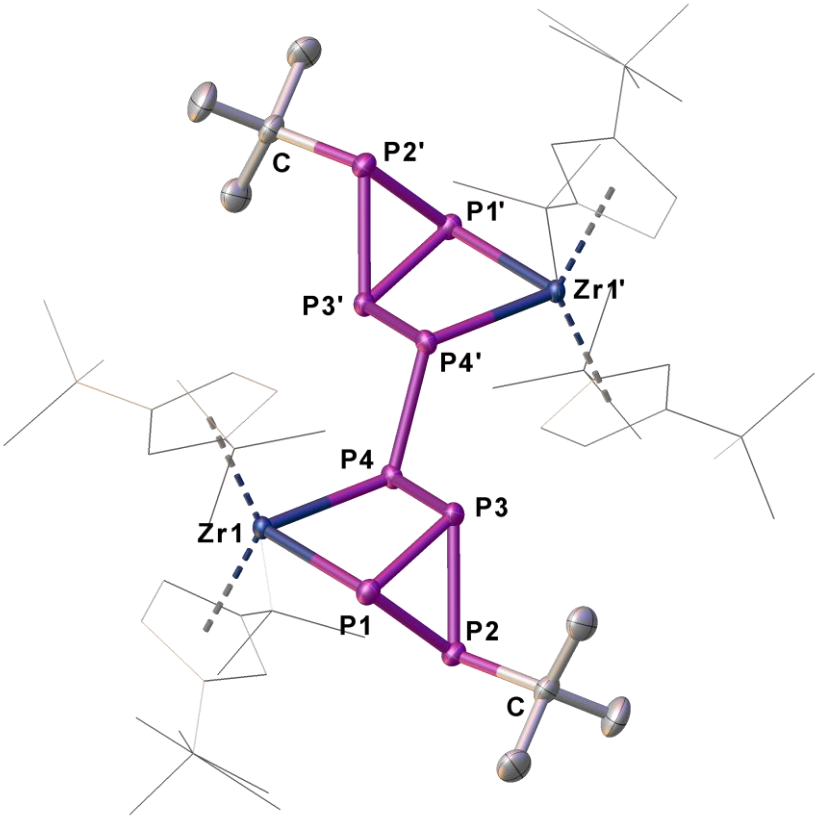

Figure S1: Molecular structure of **3** in the solid state with thermal ellipsoids at 50% probability level. Hydrogen atoms and solvent molecules are omitted and the Cp'' ligands are drawn in the wireframe model for clarity. Selected bond lengths [Å] and angles [°]: Zr$_1$-P$_4$ 2.6305(4), Zr$_1$-P$_1$ 2.6268(4), P$_4$-P$_4$' 2.2223(9), P$_4$-P$_3$ 2.2270(6), P$_2$-P 2.1965(6), P$_2$-P$_3$ 2.2052(6), P$_2$-C$_1$ 1.9060(19), P$_1$-P$_3$ 2.2187(6); P$_4$'-P$_4$-Zr$_1$ 113.56(3), P$_4$'-P$_4$-P$_3$ 91.21(3), P$_3$-P$_4$-Zr$_1$ 77.927(18), P$_1$-P$_2$-P$_3$ 60.54(2), C$_1$-P$_2$-P$_1$ 103.91(7). C$_1$-P$_2$-P$_3$ 104.98(6), P$_2$-P$_1$-Zr$_1$ 97.71(2), P$_2$-P$_1$-P$_3$ 59.93(2), P$_3$-P$_1$-Zr$_1$ 78.146(17), P$_4$-P$_3$-Zr$_1$ 56.900(15), P$_2$-P$_3$-Zr$_1$ 85.685(18), P$_2$-P$_3$-P$_4$ 102.01(2), P$_2$-P$_3$-P$_1$ 59.54(2), P$_1$-P$_3$-Zr$_1$ 56.849(15), P$_1$-P$_3$-P$_4$ 111.94(2).

[Cp''$_2$Zr(η$^{1:1}$-P$_4$^{t}BuMe)] (4):

Compound **4** crystallizes out of a concentrated hexamethyldisiloxane solution at -78 °C in form of orange needles in the tetragonal space group *P*4$_2$/*n*. The asymmetric unit contains one molecule of **4** and 0.25 molecules of (Me$_3$Si)$_2$O. The Cp''ZrP$_4$ unit is disordered over two positions (occupancy 0.89 and 0.11). Additionally, one *tert*-butyl group of a Cp'' ligand is disordered over two positions (occupancy 0.55 and 0.45). The (Me$_3$Si)$_2$O molecule is located on a 4-fold screw axes and could not be modeled satisfactorily. Therefore, a solvent mask was calculated and 172 electrons were found in a volume of 1014Å^3 in 2 voids per unit cell. This is consistent with the presence of 0.25 molecules of (Me$_3$Si)$_2$O per asymmetric unit, which account for 180 electrons per unit cell. Some restrains (SIMU, SADI, FLAT and DFIX) were used during the crystal structure refinement to solve the disorder.

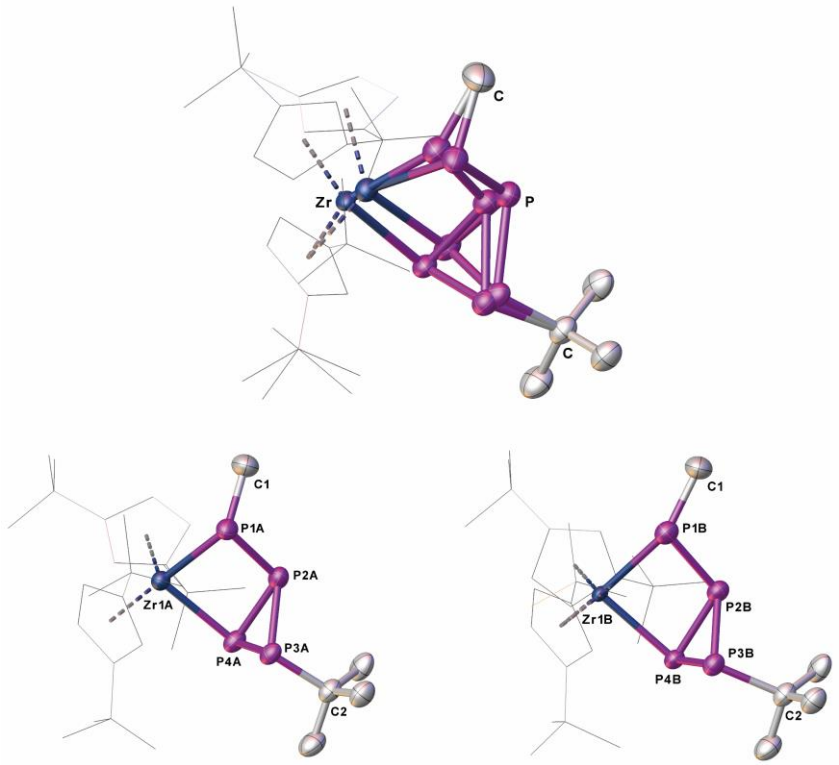

Figure S2: Molecular structure of **4** in the solid state (above). Thermal ellipsoids are depicted at 50% probability level. Hydrogen atoms are omitted and the Cp'' ligands are drawn in the wireframe model for clarity. The separate parts of the disorder are depicted below (left: part 1, occupancy of 89%; right: part 2, occupancy of 11%). Selected bond lengths [Å] and angles [°]: Zr$_{1A}$-P$_{1A}$ 2.639(2), Zr$_{1A}$-P$_{4A}$ 2.597(2), P$_{3A}$-P$_{4A}$ 2.186(5), P$_{3A}$-P$_{2A}$ 2.207(4), P$_{1A}$-P$_{2A}$ 2.218(3), P$_{4A}$-P$_{2A}$ 2.235(3), P$_{3A}$-C$_2$ 1.885(7), P$_{1A}$-C$_1$ 1.863(7), P$_{1B}$-Zr$_{1B}$ 2.64(2), P$_{4B}$-Zr$_{1B}$ 2.631(16), P$_{4B}$-P$_{2B}$ 2.26(3), P$_{4B}$-P$_{3B}$ 2.32(5), P$_{2B}$-P$_{1B}$ 2.23(2), P$_{2B}$-P$_{3B}$ 2.25(4), C$_2$-P$_{3B}$ 2.03(4), C$_1$-P$_{1B}$ 1.869(19); P$_{1A}$-P$_{2A}$-Zr$_{1A}$ 57.11(7), P$_{2A}$-P1AZr1A 78.01(9), P$_{3A}$-P$_{4A}$-Zr$_{1A}$ 98.81(14), P$_{2A}$-P$_{4A}$-Zr$_{1A}$ 78.65(8), P$_{3A}$-P$_{2A}$-Zr$_{1A}$ 85.50(12), P$_{3A}$-P$_{2A}$-P$_{1A}$ 102.23(15), P$_{3A}$-P$_{2A}$-P$_{4A}$ 58.95(14), P$_{1A}$-P$_{2A}$-P$_{4A}$ 111.09(11), P$_{4A}$-P$_{3A}$-P$_{2A}$ 61.16(15), P$_{3A}$-P$_{4A}$-P$_{2A}$ 59.89(12), P$_{4A}$-P$_{2A}$-Zr$_{1A}$ 55.90(7), C$_1$-P$_{1A}$-Zr$_{1A}$ 113.9(3), C$_1$-P$_{1A}$-P$_{2A}$ 98.4(3), C$_2$-P$_{3A}$-P$_{4A}$ 101.6(3), C$_2$-P$_{3A}$-P$_{2A}$ 105.8(2), P$_{3B}$-P$_{2B}$-Zr$_{1B}$ 89.1(11), P$_{2B}$-P$_{1B}$-Zr$_{1B}$ 77.4(8), P$_{1B}$-P$_{2B}$-Zr$_{1B}$ 57.4(7), P$_{4A}$-Zr$_{1A}$-P$_{1A}$ 89.06(7), P$_{1B}$-P$_{2B}$-P$_{4B}$-113.4(10), P$_{1B}$-P$_{2B}$-P$_{3B}$ 108.2(14), P$_{3B}$-P$_{2B}$-P$_{4B}$ 61.8(13), C$_2$-P$_{3B}$-P$_{4B}$ 103(2), C$_2$-P$_{3B}$-P$_{2B}$ 99.3(15), C$_1$-P$_{1B}$-P$_{2B}$ 110.5(10), C$_1$-P$_{1B}$-Zr$_{1B}$ 145.8(12).

[Cp''$_2$Zr(η$^{1:1}$-P$_4$^{t}BuMePPh$_2$)] (5):

Compound **5** crystallizes out of a concentrated *n*-pentane solution at -30 °C in form of orange plates in the triclinic space group *P*$\bar{1}$. The asymmetric unit contains one molecule of **5** and half a *n*-pentane molecule. Some restrains (SADI, SIMU, DANG, RIGU and DFIX) were used for the solvent molecule during the crystal structure refinement process.

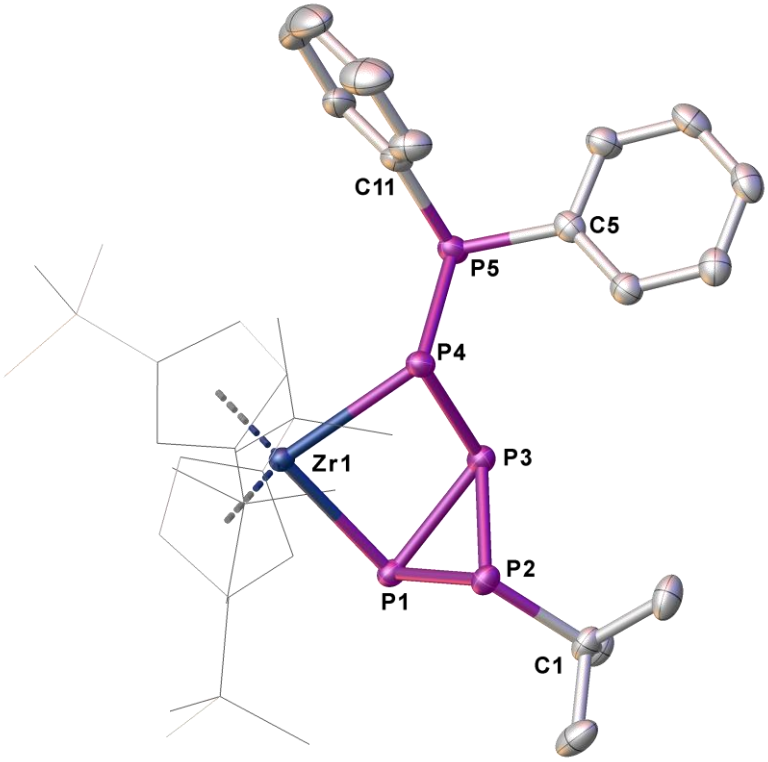

Figure S3: Molecular structure of **5** in the solid state with thermal ellipsoids at 50% probability level. Hydrogen atoms and solvent molecules are omitted and the Cp'' ligands are drawn in the wireframe model for clarity. Selected bond lengths [Å] and angles [°]: Zr_1-P_4 2.6423(6), Zr_1-P_1 2.6193(6), P_3-P_4 2.2376(8), P_3-P_1 2.2151(8), P_3-P_2 2.2031(8), P_4-P_5 2.2189(8), P_1-P_2 2.2021(8), P_5-C_{11} 1.851(3), P_5-C_5 1.853(2),P_2-C_1 1.899(2); P_1-Zr_1-P_4 89.020(18), P_4-P_3-Zr_1 57.193(19), P_1-P_3-Zr_1 56.71(2), P_2-P_3-Zr_1 84.36(2), P_3-P_4-Zr_1 77.43(2), P_5-P_4-Zr_1 114.69(3), P_3-P_1-Zr_1 78.30(2), P_2-P_1-Zr_1 96.12(2), P_1-P_2-P_3 60.38(2), P_1-P_3-P_4 111.87(3), P_2-P_3-P_4 99.48(3), P_2-P_3-P_1 59.79(2), P_5-P_4-P_3 91.01(3), P_2-P_1-P_3 59.83(2), C_{11}-P_5-P_4 99.55(8), C_{11}-P_5-C_5 99.25(11), C_5-P_5-P_4 101.12(8), C_1-P_2-P_3 104.37(8), C_1-P_2-P_1 106.25(7).

[Cp''$_2$Zr(η^2-P$_3$NMe$_2$)] (6a):

Compound **6a** crystallizes out of a concentrated *n*-pentane solution at -78 °C in form of orange blocks in the monoclinic space group *P*2$_1$/*c*. The asymmetric unit contains one molecule of **6a** and half a *n*-pentane molecule. The restrains SIMU, DFIX and DANG were used for the solvent molecule during the crystal structure refinement.

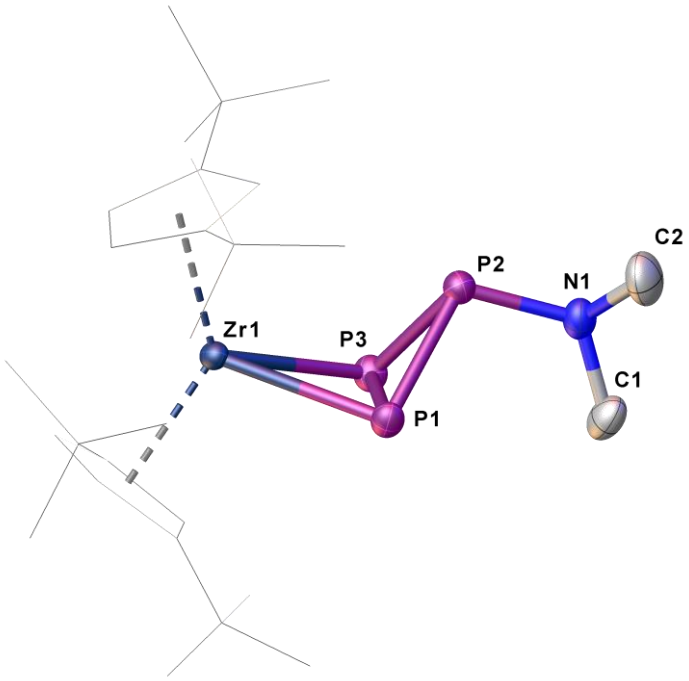

Figure S4: Molecular structure of **6a** in the solid state with thermal ellipsoids at 50% probability level. Hydrogen atoms and solvent molecules are omitted and the Cp'' ligands are drawn in the wireframe model for clarity. Selected bond lengths [Å] and angles [°]: Zr$_1$-P$_3$ 2.6443(6), Zr$_1$-P$_1$ 2.6080(6), P$_3$-P$_2$ 2.1841(9), P$_3$-P$_1$ 2.2184(9), P$_2$-P$_1$ 2.1996(8), P$_2$-N$_1$ 1.740(2); P$_1$-Zr$_1$-P$_3$ 49.963(19), P$_2$-P$_3$-Zr$_1$ 92.47(3), P$_2$-P$_3$-P$_1$ 59.94(3), P$_1$-P$_3$-Zr$_1$ 64.17(2), P$_3$-P$_2$-P$_1$ 60.80(3), N$_1$-P$_2$-P$_3$ 106.07(8), N$_1$-P$_2$-P$_1$ 106.64(8), P$_3$-P$_1$-Zr$_1$ 65.87(2), P$_2$-P$_1$-Zr$_1$ 93.10(3), P$_2$-P$_1$-P$_3$ 59.25(3).

[Cp''$_2$Zr(η^2-As$_3$NMe$_2$)] (6b):

Compound **6b** crystallizes out of a concentrated *n*-pentane solution at -78 °C in form of orange blocks in the monoclinic space group $P2_1/n$. The asymmetric unit contains one molecule of **6b** and half a *n*-pentane molecule. The restrains SIMU, DFIX and DANG were used for the solvent molecule during the crystal structure refinement.

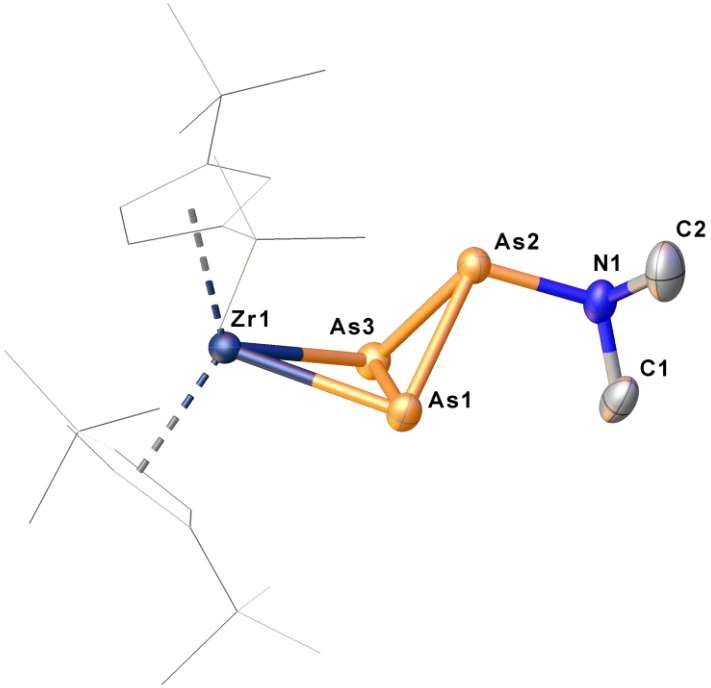

Figure S5: Molecular structure of **6b** in the solid state with thermal ellipsoids at 50% probability level. Hydrogen atoms and solvent molecules are omitted and the Cp'' ligands are drawn in the wireframe model for clarity. Selected bond lengths [Å] and angles [°]: Zr_1-As_3 2.7384(4), Zr_1-As_1 2.7155(3), As_3-As_2 2.4206(4), As_3-As_1 2.4355(4), As_2-As_1 2.4281(4), As_2-N_1 1.903(2); As_1-Zr_1-As_3 53.045(9), As_2-As_3-Zr_1 90.986(12), As_2-As_3-As_1 60.001(12), As_1-As_3-Zr_1 62.995(10), As_3-As_2-As_1 60.305(11), N_1-As_2-As_3 103.89(7), N_1-As_2-As_1 103.86(7), As_3-As_1-Zr_1 63.961(10), As_2-As_1-Zr_1 91.376(12), As_2-As_1-As_3 59.694(11).

[Cp"$_2$Zr(η^2-P$_3${CH$_2$SiMe$_3$})] (7a):

Compound **7a** crystallizes out of a concentrated *n*-hexane solution at -78 °C in form of orange cubes in the monoclinic space group $P2_1/n$. The asymmetric unit contains one molecule of **7a**. One ^{t}Bu group of a Cp" ligand is disordered over two positions (occupancy 0.52 and 0.48). The restrains SIMU and SADI were used during the crystal structure refinement.

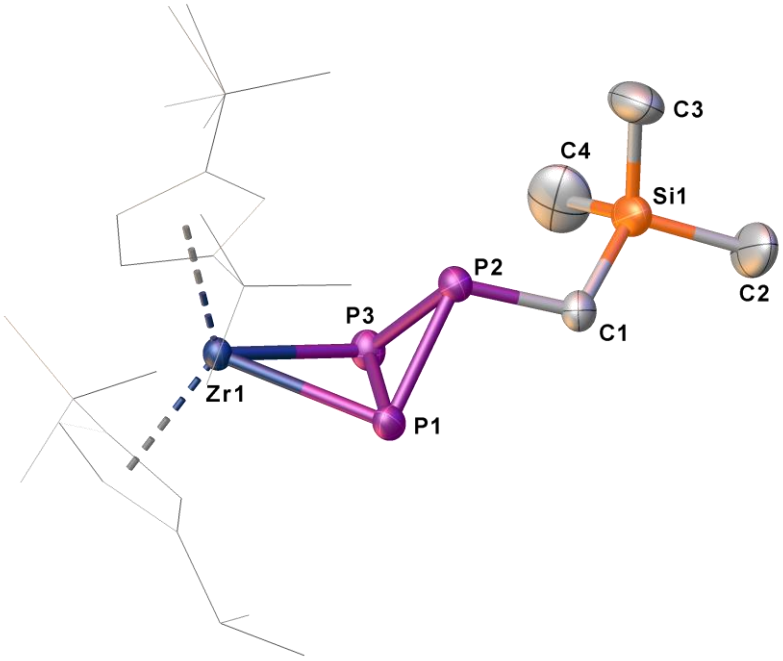

Figure S6: Molecular structure of **7a** in the solid state with thermal ellipsoids at 50% probability level. Hydrogen atoms are omitted and the Cp" ligands are drawn in the wireframe model for clarity. Selected bond lengths [Å] and angles [°]: Zr_1-P_1 2.6422(7), Zr_1-P_3 2.6320(7), P_1-P_3 2.2112(9), P_1-P_2 2.2028(9), P_3-P_2 2.2121(9), P_2-C_1 1.860(3, Si_1-C_1 1.883(3); P_3-Zr_1-P_1 49.58(2), P_3-P_1-Zr_1 64.97(2), P_2-P_1-Zr_1 92.25(3), P_2-P_1-P_3 60.15(3), P_1-P_3-Zr_1 65.45(2), P_1-P_3-P_2 59.73(3), P_2-P_3-Zr_1 92.31(3), P_1-P_2-P_3 60.11(3), C_1-P_2-P_1 105.23(9), C_1-P_2-P_3 103.96(9), P2-C1-Si1 112.62(15).

[Cp''$_2$Zr(η^2-As$_3${CH$_2$SiMe$_3$})] (7b):

Compound **7b** crystallizes out of a concentrated *n*-hexane solution at -78 °C in form of brown plates in the monoclinic space group *P*2$_1$/*n*. The asymmetric unit contains one molecule of **7b**. One methyl group of a Cp''' ligand is disordered over two positions (occupancy 0.77 and 0.23). Additionally, is the SiMe$_3$ group disordered over two positions (occupancy 0.57 and 0.43). The restrains SIMU and SADI were used during the crystal structure refinement.

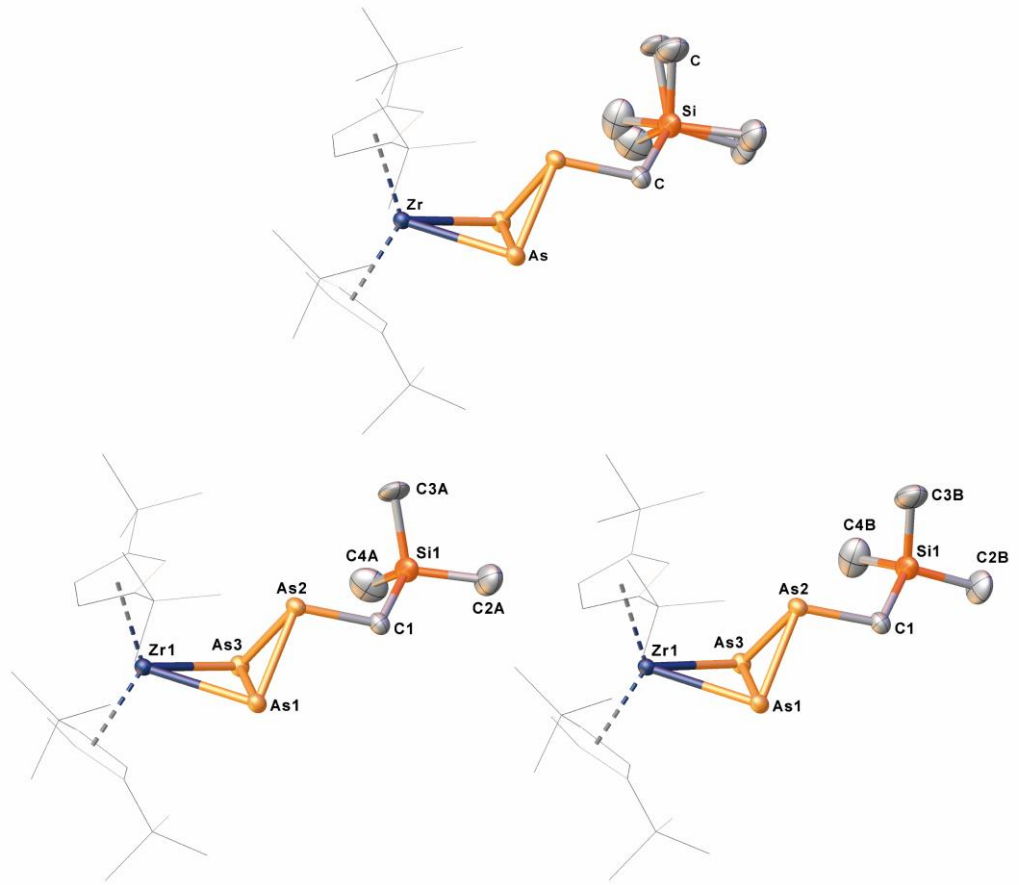

Figure S7: Molecular structure of **7b** in the solid state (above). Thermal ellipsoids are depicted at 50% probability level. Hydrogen atoms are omitted and the Cp'' ligands are drawn in the wireframe model for clarity. The separate parts of the disorder of the [SiMe$_3$]-fragment are depicted below (left: part 1, occupancy of 57%; right: part 2, occupancy of 43%). Selected bond lengths [Å] and angles [°]: Zr$_1$-As$_1$ 2.7482(5), Zr$_1$-As$_3$ 2.7390(4), As$_1$-As 2.4323(5), As$_1$-As$_3$ 2.4282(5), As$_2$-As$_3$ 2.4477(5), As$_2$-C$_1$ 1.997(4), Si$_1$-C$_1$ 1.866(3); As$_3$-Zr$_1$-As$_1$ 52.530(12), As$_2$-As$_1$-Zr$_1$ 90.893(15), As$_3$-As$_1$-Zr$_1$ 63.541(13), As$_3$-As$_1$-As$_2$ 60.475(15) As$_1$-As$_2$-As$_3$ 59.681(14), C$_1$-As$_2$-As$_1$ 103.98(10), C$_1$-As$_2$-As$_3$ 102.08(11), As$_1$-As$_3$-Zr$_1$ 63.929(13), As$_1$-As$_3$-As$_2$ 59.844(14), As$_2$-As$_3$-Zr$_1$ 90.784(15).

[(Cp''Zr)$_2$(μ,η$^{1:1:1:1:1:1}$-As$_6$)] (8):

Compound **8** crystallizes out of a concentrated Et_2O solution at -78 °C in form of brown plates in the triclinic space group $P\bar{1}$. The asymmetric unit contains one molecule of **8**.

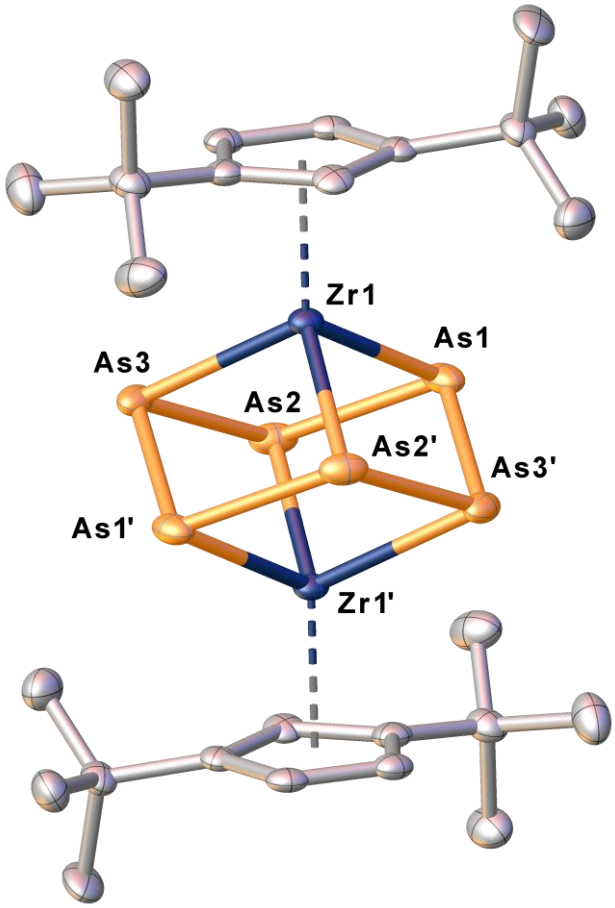

Figure S8: Molecular structure of **8** in the solid state with thermal ellipsoids at 50% probability level. Hydrogen atoms are omitted and the Cp'' ligands are drawn in the wireframe model for clarity. Selected bond lengths [Å] and angles [°]: As$_3$-As$_2$ 2.4939(7), Zr$_1$-As$_1$ 2.6103(6), Zr$_1$-As$_1$' 3.2024(6), Zr$_1$-As$_3$' 3.2293(6), Zr$_1$-As$_3$ 2.6132(6), Zr$_1$-As$_2$ 3.2157(7), Zr$_1$-As$_2$' 2.6158(6), As$_1$-As$_3$' 2.5147(7), As$_1$-As$_2$ 2.4908(7); As$_2$-As$_3$-As$_1$' 104.60(2), As$_1$-As$_2$-As$_3$ 105.10(2), As$_2$-As$_1$-As$_3$' 105.51(2), As$_1$-Zr$_1$-As$_3$ 98.50(2), As$_1$-Zr$_1$-As$_2$' 98.627(19), As$_1$'-Zr$_1$-As$_2$ 76.261(16), As$_3$-Zr$_1$-As$_3$' 106.925(15), As$_3$-Zr$_1$-As$_2$' 99.287(19), As$_2$-Zr$_1$-As$_3$' 76.375(15), As$_2$'-Zr$_1$-As$_2$ 106.718(16), As$_3$-As$_2$-Zr$_1$' 78.357(19), As$_3$'-As$_1$-Zr$_1$ 78.092(19), As$_2$-As$_1$-Zr$_1$ 78.12(2), As$_1$'-As$_3$-Zr$_1$ 77.266(18), As$_2$-As$_3$-Zr$_1$ 78.013(19), As$_1$-As$_2$-Zr$_1$' 77.632(18).

Table S1: Structure determination summary of the complexes **3**, **4, 5** and **6a**.

Compound	**3**	**4**	**5**	**6a**
Formula	$C_{68}H_{122}O_2P_8Zr_2$	$C_{32.5}H_{58.5}O_{0.25}P_4Si_{0.5}Zr$	$C_{44.5}H_{67}P_5Zr$	$C_{30.5}H_{54}NP_3Zr$
$D_{calc.}$/ g cm^{-3}	1.227	1.211	1.236	1.223
μ/mm^{-1}	4.136	4.310	3.840	4.152
Formula Weight	1401.85	682.43	848.05	618.87
Colour	clear brown	orange	dark orange	clear orange
Shape	block-shaped	needle-shaped	plate-shaped	block-shaped
Size/mm^3	0.44×0.14×0.11	0.28×0.05×0.03	0.19×0.18×0.10	0.26×0.11×0.09
T/K	123(1)	123.0(1)	123(1)	123.00(10)
Crystal System	monoclinic	tetragonal	triclinic	monoclinic
Space Group	*C*2/*c*	$P4_2/n$	$P\bar{1}$	$P2_1/c$
a/Å	22.9704(4)	28.7566(9)	10.9370(3)	9.99650(10)
b/Å	16.1189(2)	28.7566(9)	13.3109(3)	16.6544(2)
c/Å	22.6359(4)	9.0539(7)	16.6878(5)	20.7285(3)
α/°	90	90	90.212(2)	90
β/°	115.159(2)	90	105.591(3)	103.0820(10)
g/°	90	90	102.646(2)	90
V/Å^3	7586.0(2)	7487.1(7)	2278.21(11)	3361.43(7)
Z	4	8	2	4
Z'	0.5	1	1	1
Wavelength/Å	1.54184	1.54184	1.54184	1.54184
Radiation type	Cu K_α	Cu K_α	Cu K_α	Cu K_α
θ_{min}/°	3.469	3.073	3.410	3.440
θ_{max}/°	72.030	74.321	71.720	67.078
Measured Refl's.	13814	24937	24865	17300
Ind't Refl's	7139	7468	8638	5988
Refl's with I≥2σ(I)	6797	6051	7639	5817
R_{int}	0.0177	0.0549	0.0329	0.0268
Parameters	446	453	495	359
Restraints	42	254	61	31
Largest Peak	0.572	2.355	1.120	0.661
Deepest Hole	-0.482	-1.083	-0.506	-0.917
GooF	1.058	1.077	1.056	1.043
wR_2 (all data)	0.0672	0.2035	0.0805	0.0868
wR_2	0.0662	0.1937	0.0775	0.0863
R_1 (all data)	0.0280	0.0973	0.0412	0.0338
R_1	0.0263	0.0806	0.0332	0.0329

Table S2: Structure determination summary of the complexes **6b**, **7a**, **7b** and **8**.

Compound	**6b**	**7a**	**7b**	**8**
Formula	$C_{30.5}H_{54}As_3NZr$	$C_{30}H_{53}P_3SiZr$	$C_{30}H_{53}As_3SiZr$	$C_{13}H_{21}As_3Zr$
$D_{calc.}$/ g cm^{-3}	1.459	1.192	1.434	2.021
μ/mm^{-1}	4.415	4.317	6.141	12.174
Formula Weight	750.72	625.94	757.79	493.28
Colour	orange	clear light orange	clear light brown	clear light brown
Shape	block-shaped	cube-shaped	plate-shaped	plate-shaped
Size/mm^3	0.15×0.09×0.07	0.25×0.15×0.07	0.33×0.15×0.12	0.20×0.08×0.06
T/K	123.00(10)	123(1)	123(1)	123(1)
Crystal System	monoclinic	monoclinic	monoclinic	triclinic
Space Group	$P2_1/n$	$P2_1/n$	$P2_1/n$	$P\bar{1}$
a/Å	10.10760(10)	16.1153(2)	16.1633(2)	7.1566(3)
b/Å	16.7507(2)	12.64290(10)	12.5385(2)	10.4514(5)
c/Å	20.7963(3)	17.3063(2)	17.5202(3)	12.4638(5)
α/°	90	90	90	108.776(4)
β/°	103.9690(10)	98.4650(10)	98.773(2)	95.348(4)
γ/°	90	90	90	109.490(4)
V/Å^3	3416.88(7)	3487.64(7)	3509.16(9)	810.78(7)
Z	4	4	4	2
Z'	1	1	1	1
Wavelength/Å	1.39222	1.54184	1.54184	1.54184
Radiation type	Cu K_β	Cu K_α	Cu K_α	Cu K_α
θ_{min}/°	3.096	3.500	3.466	3.844
θ_{max}/°	60.038	67.079	67.072	67.071
Measured Refl's.	19786	19340	19257	8738
Ind't Refl's	6809	6214	6235	2869
Refl's with I≥2σ(I)	6134	5679	5436	2552
R_{int}	0.0246	0.0305	0.0317	0.0436
Parameters	359	352	373	160
Restraints	31	42	87	0
Largest Peak	0.801	1.023	0.553	1.459
Deepest Hole	-0.398	-0.590	-0.417	-0.897
GooF	1.053	1.046	1.048	1.008
wR_2 (all data)	0.0679	0.0868	0.0730	0.1008
wR_2	0.0653	0.0842	0.0698	0.0969
R_1 (all data)	0.0319	0.0376	0.0402	0.0423

6.5.3 NMR Investigations

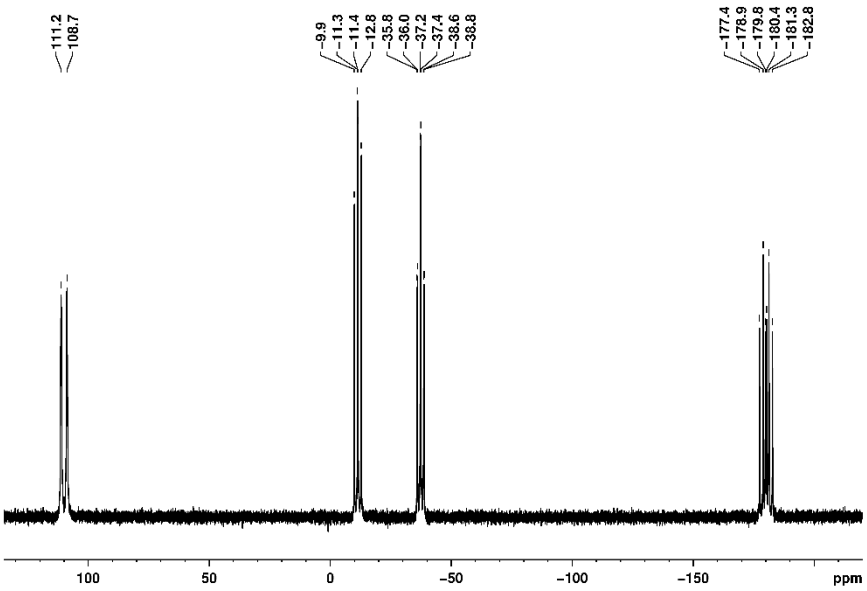

Figure S9: $^{31}P\{^{1}H\}$ NMR spectrum of **2** at 293 K in CD_2Cl_2.

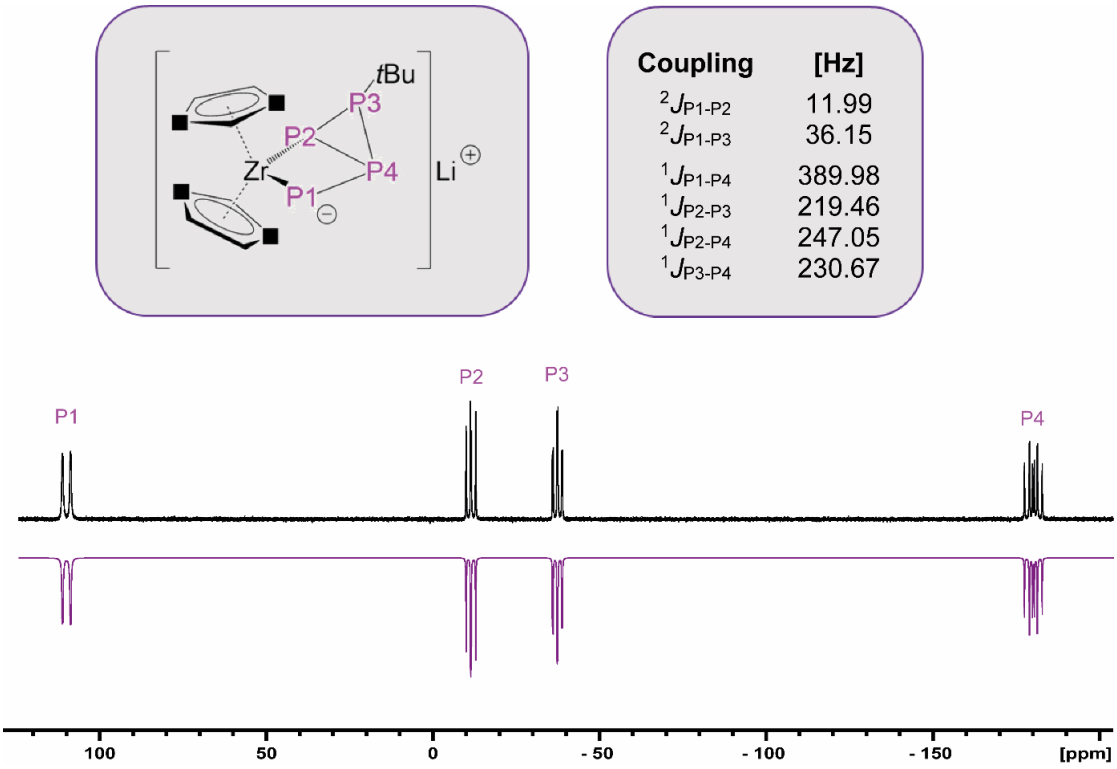

Figure S10: Experimental (top) and simulated (bottom) $^{31}P\{^{1}H\}$ NMR spectrum of **2** at 293 K in CD_2Cl_2. Coupling constants were obtained via simulation (R-factor = 0.81 %).

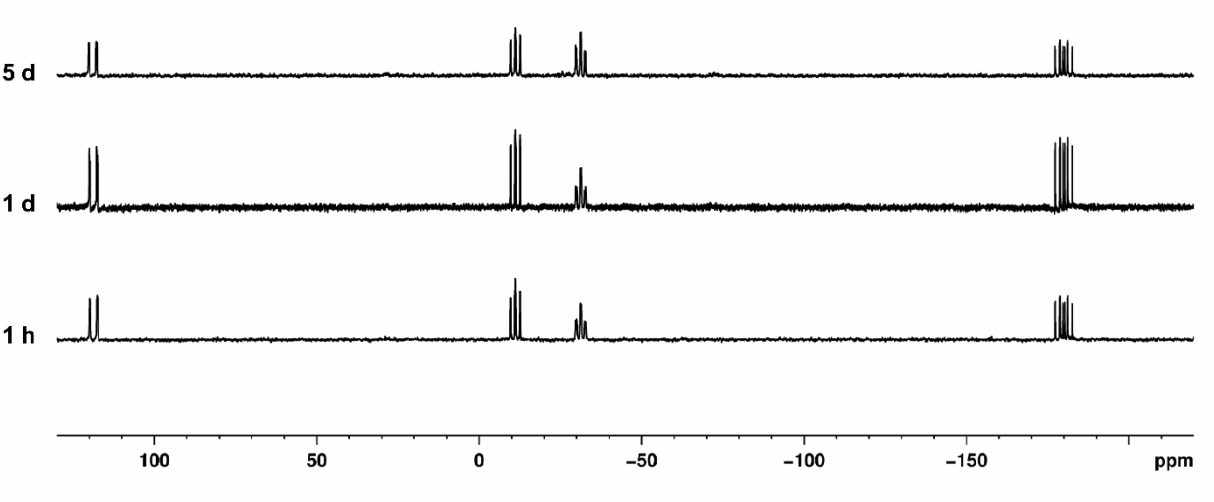

Figure S11: $^{31}P\{^{1}H\}$ NMR spectra of **2** at 293 K after 1 hour, 1 day and 5 days. The spectra were made in THF using a C_6D_6 capillary.

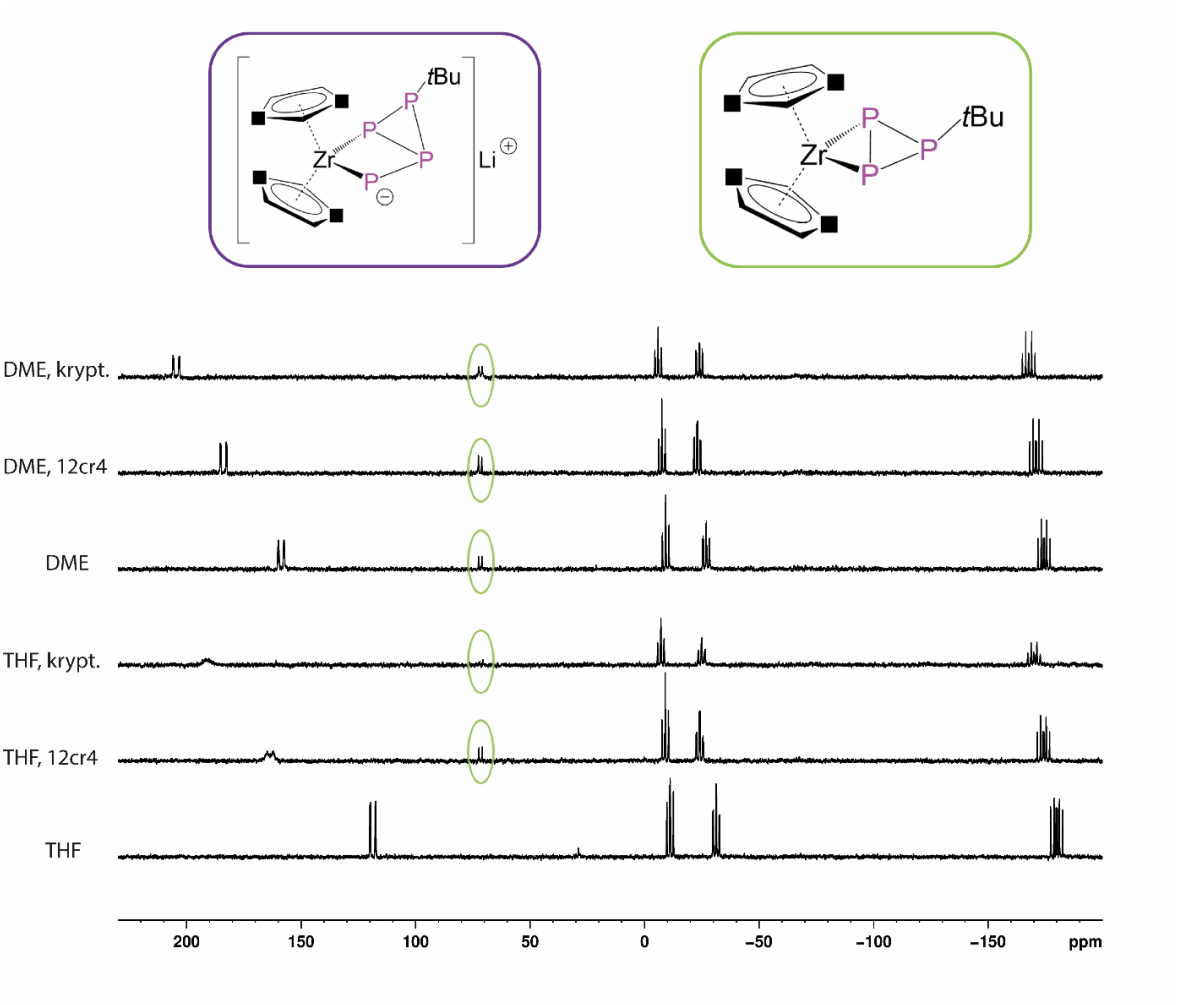

Figure S12: $^{31}P\{^{1}H\}$ NMR spectra of the reaction solution of **2** at 293 K using a C_6D_6 capillary. The influence of the solvent and additives (12cr4: 12-crown-4; krypt: [2.2.2]Kryptand) is depicted.

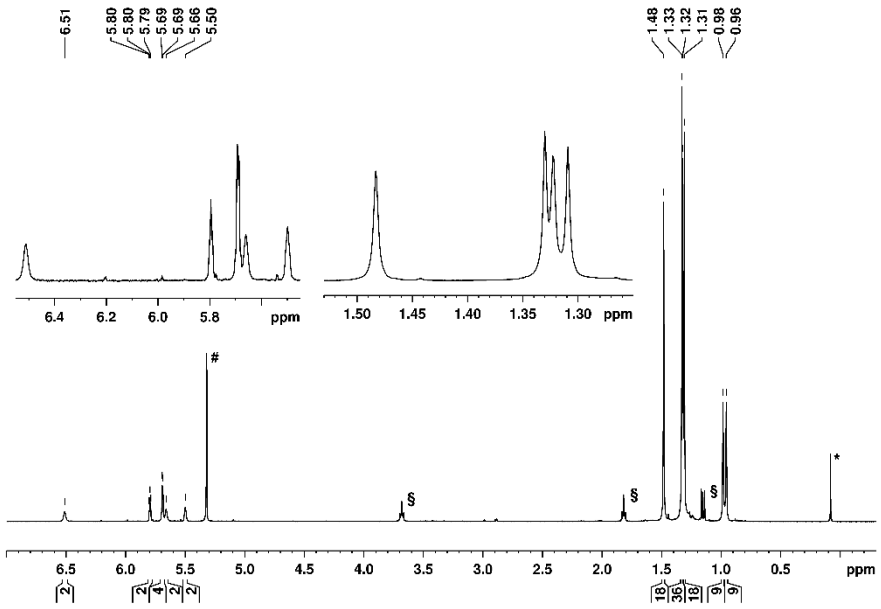

Figure S13: ^{1}H NMR spectrum of **3** at 293 K in CD_2Cl_2 (#). The signals marked with § are due to traces of THF and Et_2O, the signal marked with * due to silicon grease.

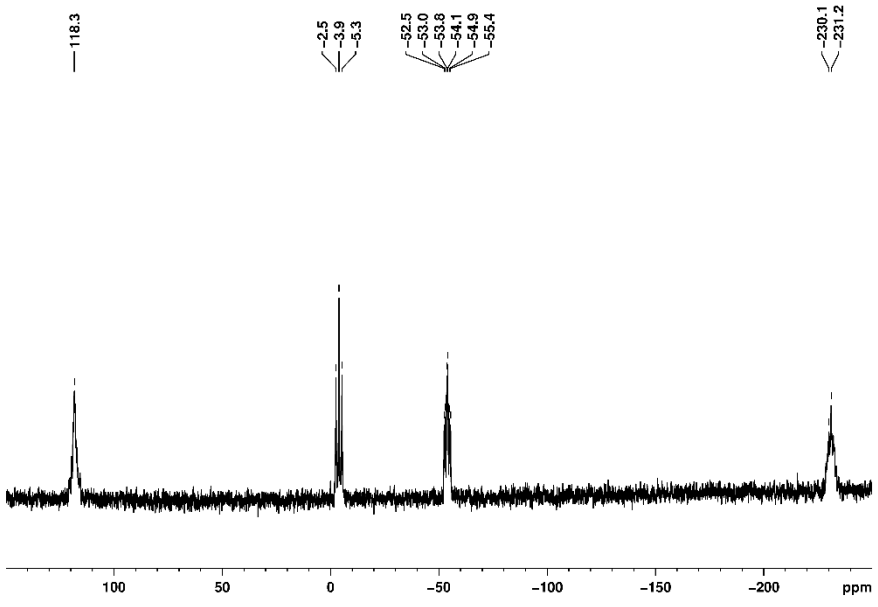

Figure S14: $^{31}P\{^{1}H\}$ NMR spectrum of **3** at 293 K in CD_2Cl_2.

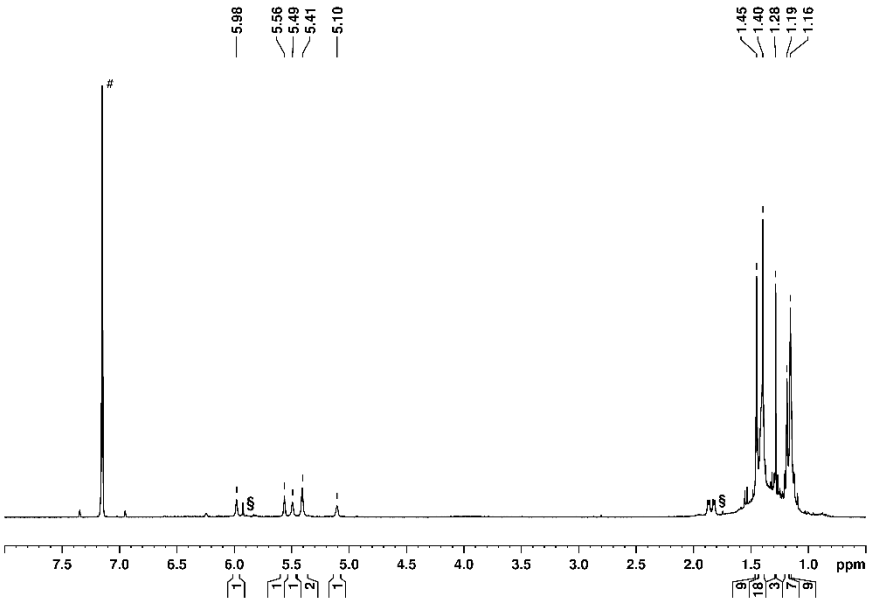

Figure S15: ^{1}H NMR spectrum of **4** at 293 K in C_6D_6 (#). The signal marked with § is due to unknown impurity.

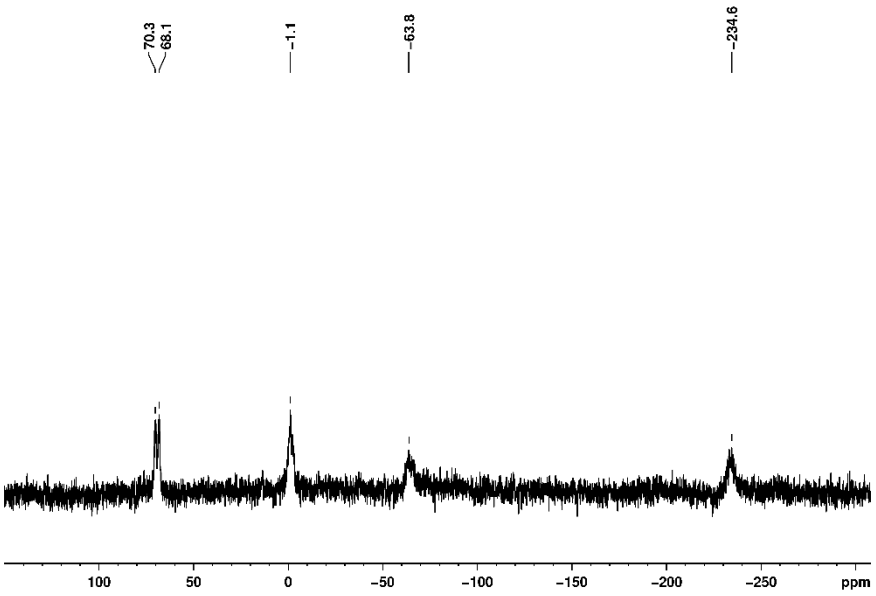

Figure S16: $^{31}P\{^{1}H\}$ NMR spectrum of **4** at 293 K in C_6D_6.

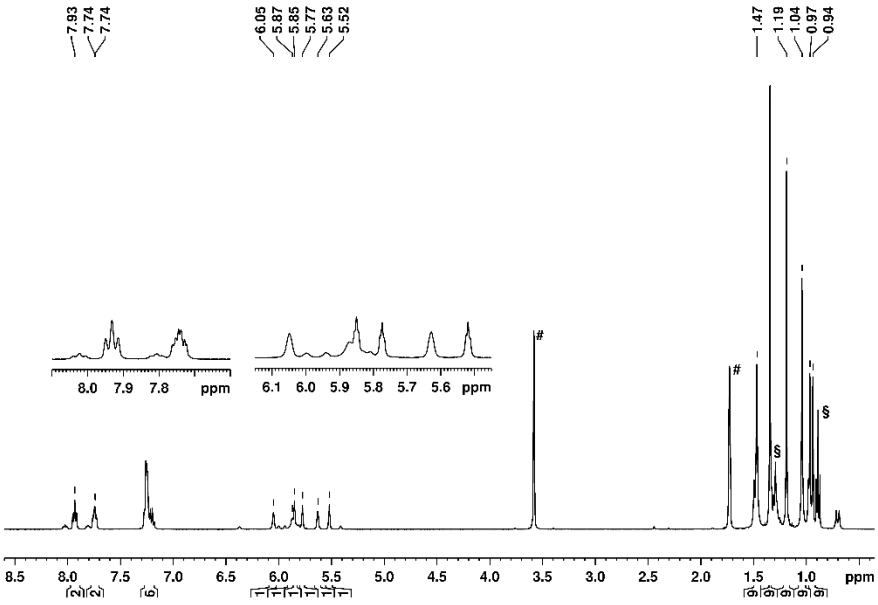

Figure S17: ^{1}H NMR spectrum of **5** at 293 K in thf-d^{8} (#). The signal marked with § is due to *n*-pentane.

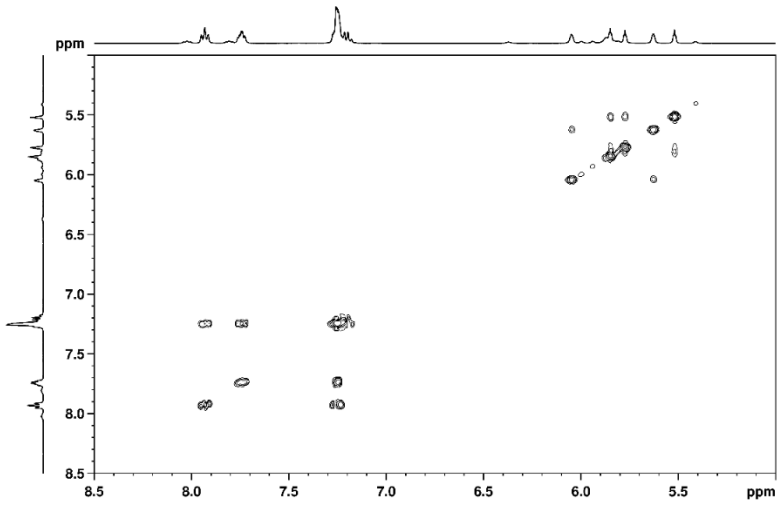

Figure S18: Part of the ^{1}H COSY spectrum of **5** in thf-d^{8} at 273 K.

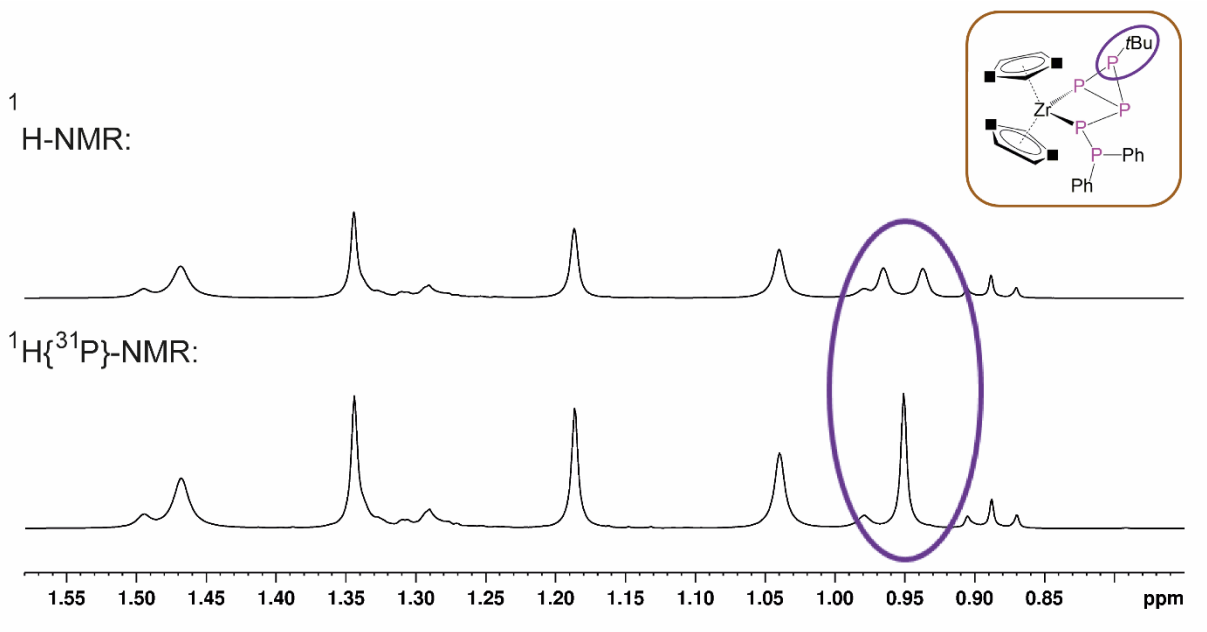

Figure S19: ^{1}H NMR spectrum (above) and $^{1}H\{^{31}P\}$ NMR spectrum of **5** at 293 K in thf-d^{8}.

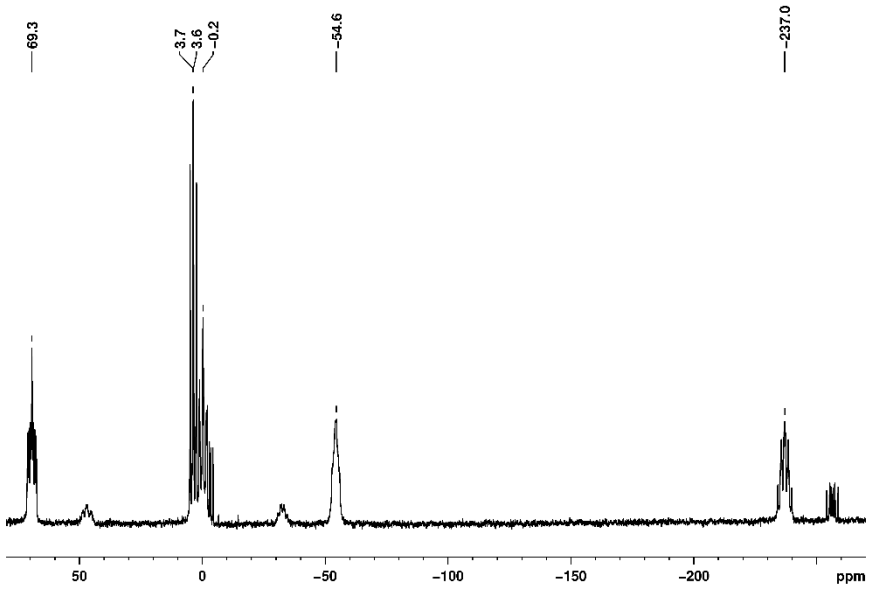

Figure S20: $^{31}P\{^{1}H\}$ NMR spectrum of **5** at 293 K in thf-d^{8}.

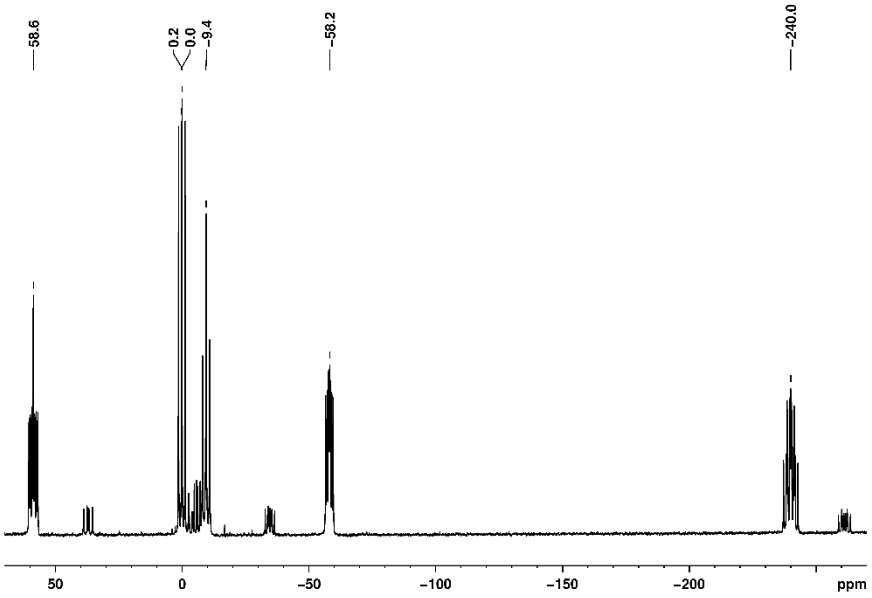

Figure S21: $^{31}P\{^{1}H\}$ NMR spectrum of **5** at 193 K in thf-d^{8}.

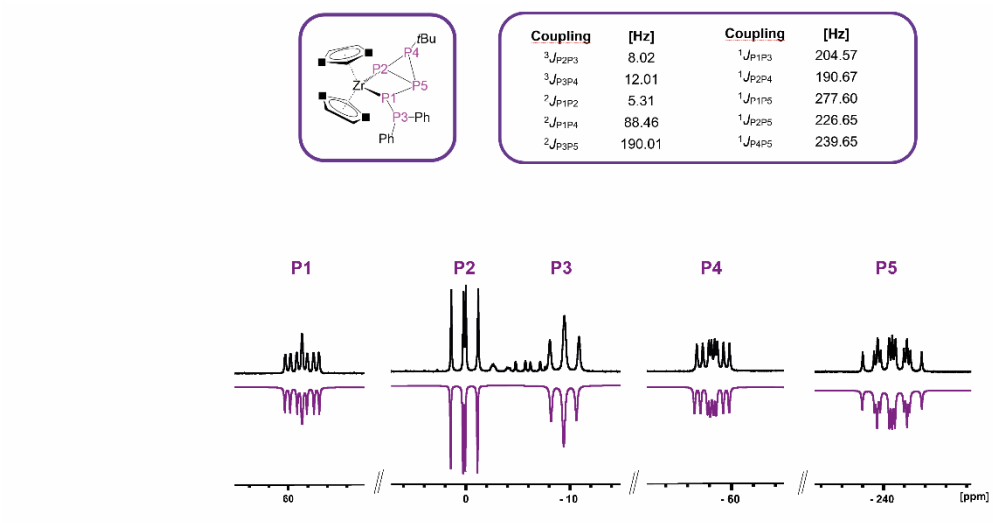

Figure S22: Experimental (top) and simulated (bottom) $^{31}P\{^{1}H\}$ NMR spectrum of **5**. The coupling constants were obtained via simulation (R-factor = 13.28 %).

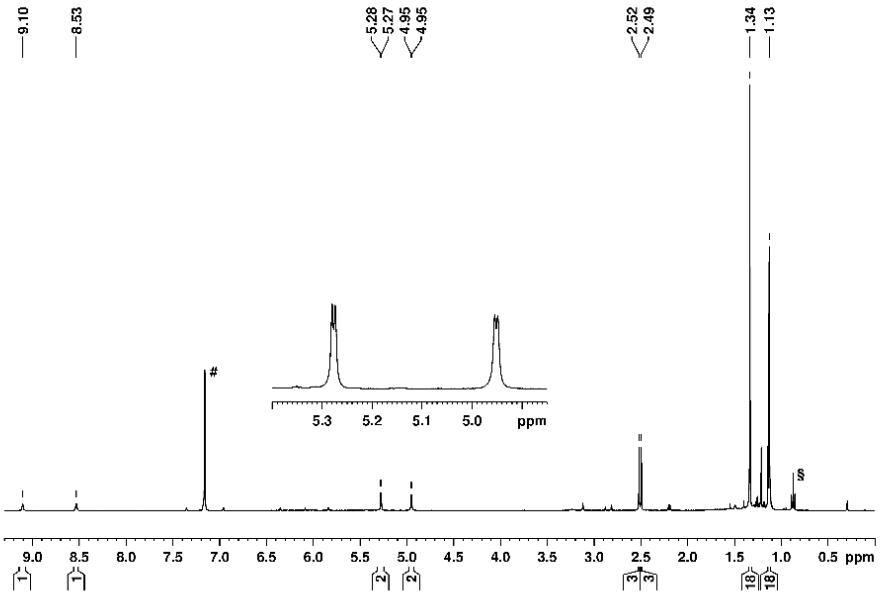

Figure S23: ^{1}H NMR spectrum of **6a** at 293 K in C_6D_6 (#). The signal marked with § is due to *n*-pentane.

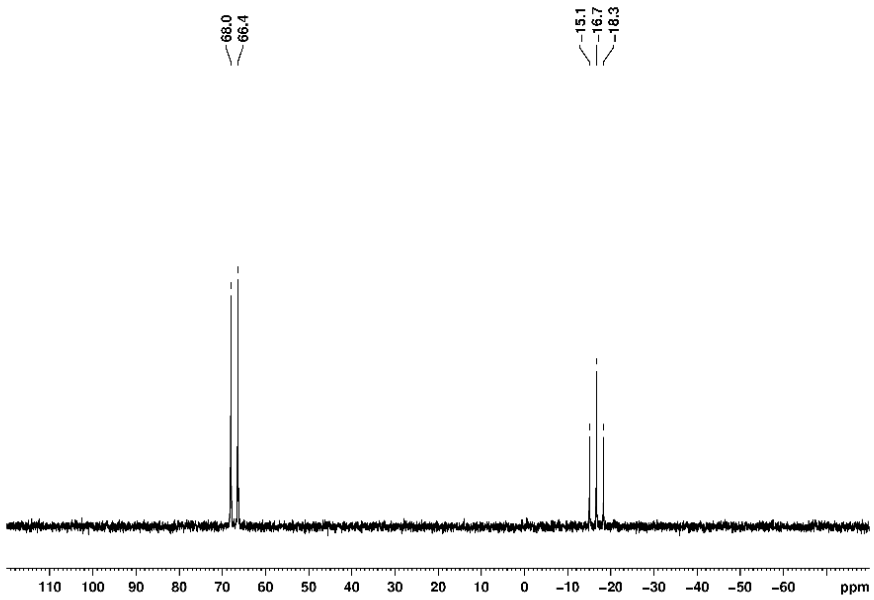

Figure S24: $^{31}P\{^{1}H\}$ NMR spectrum of **6a** at 293 K in C_6D_6.

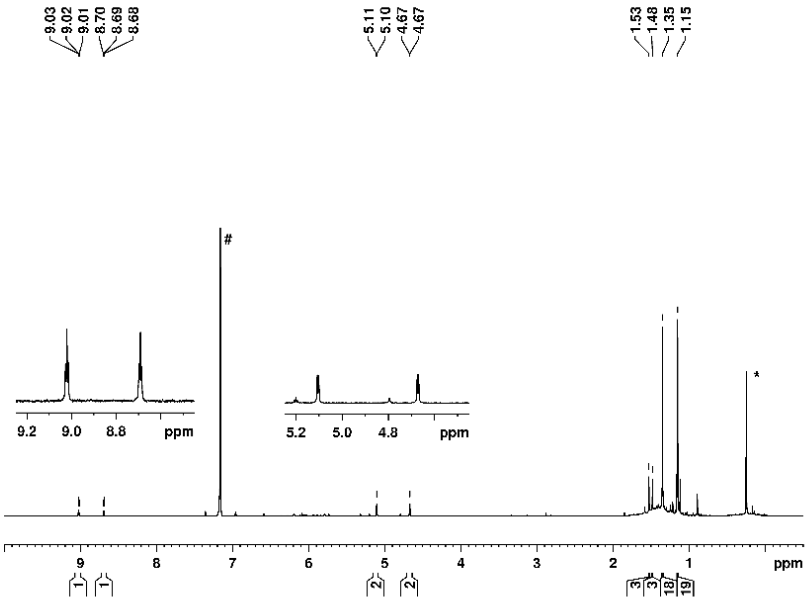

Figure S25: ^{1}H NMR spectrum of **6b** at 293 K in C_6D_6 (#). The signal marked with * is due to silicon grease.

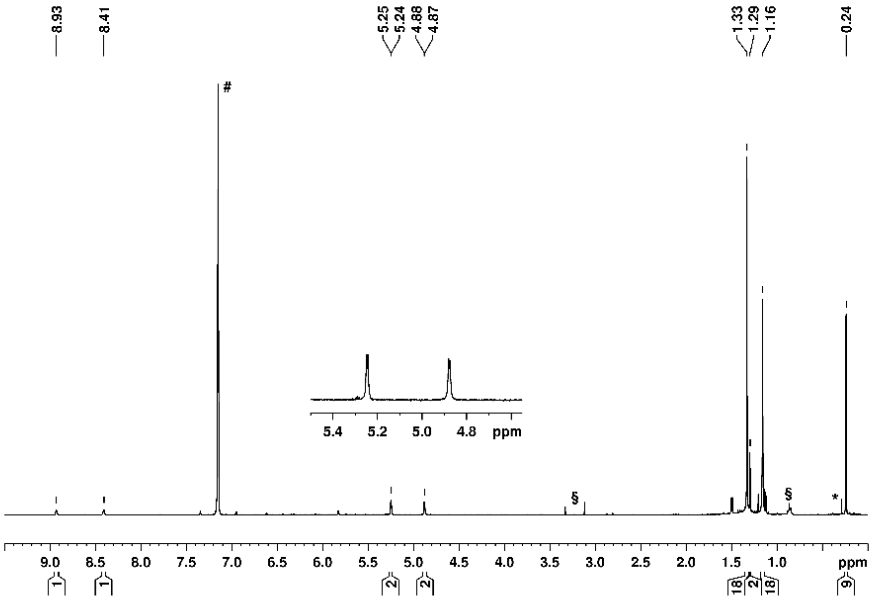

Figure S26: ^{1}H NMR spectrum of **7a** at 293 K in C_6D_6 (#). The signal marked with * is due to silicon grease, the signals marked with § due to traces of solvent.

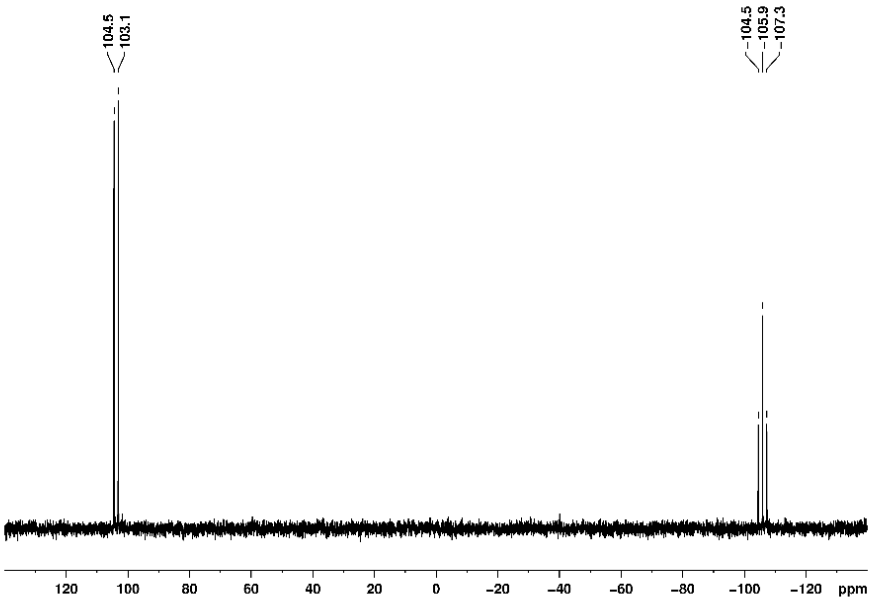

Figure S27: $^{31}P\{^{1}H\}$ NMR spectrum of **6a** at 293 K in C_6D_6.

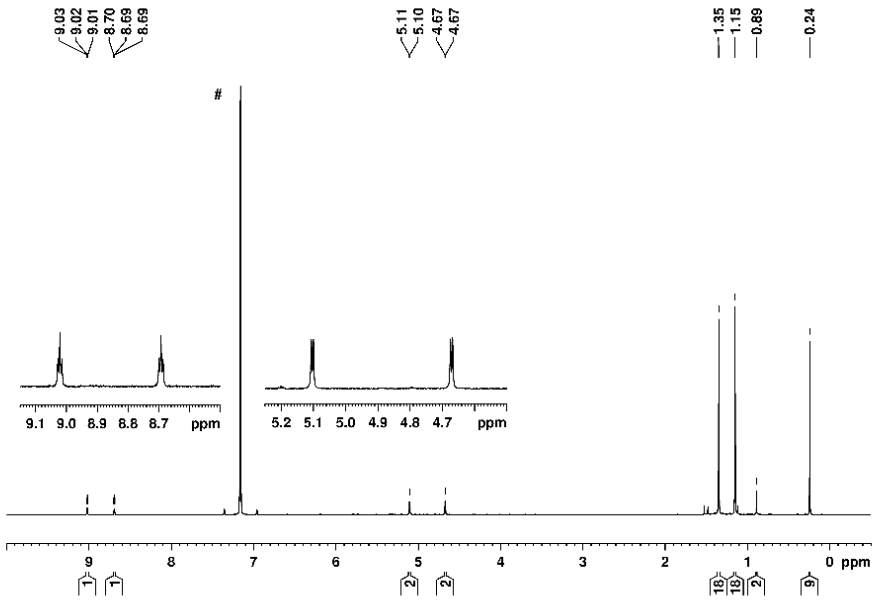

Figure S28: ^{1}H NMR spectrum of **7b** at 293 K in C_6D_6 (#).

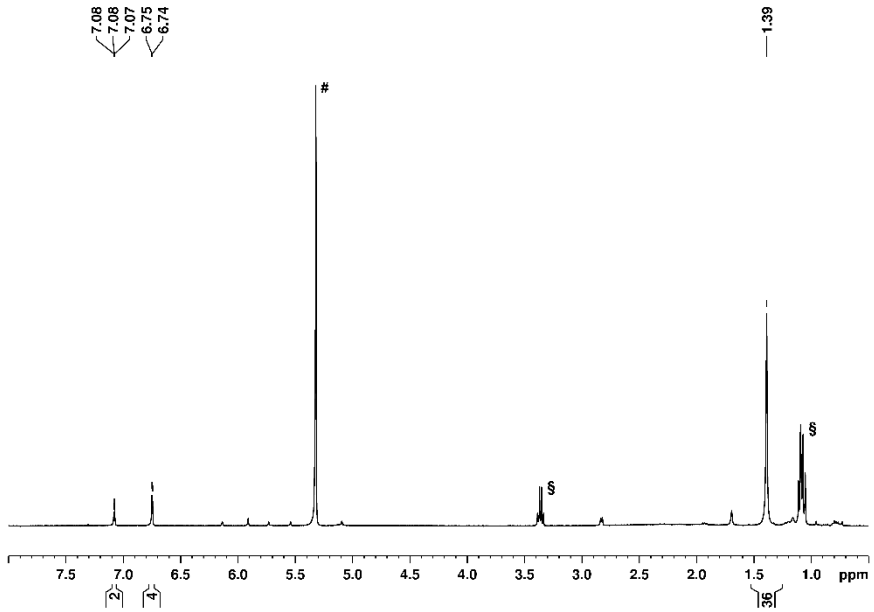

Figure S29: ^{1}H NMR spectrum of **7a** at 293 K in CD_2Cl_2 (#). The signals marked with § are due to an unknown impurity.

6.5.4 Computational Details

All calculations have been performed with Gaussian16 (ES64L-G16RevC.01)[41] using the TPSS[42] functional together with the def2STZVP[43] basis set. The D3 empirical dispersion correction scheme with Becke and Johnson damping (D3BJ) has been used.[44] The solvent effects have been incorporated via the CPCM model with THF as solvent.[45]

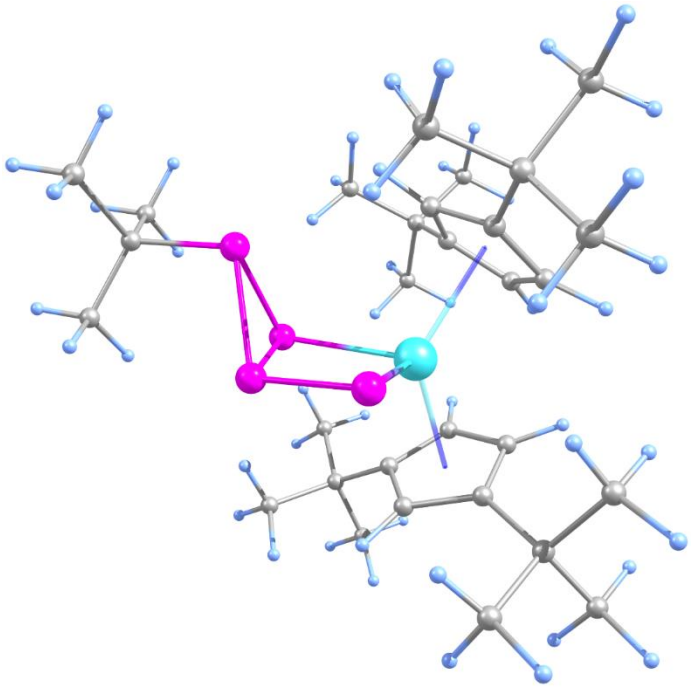

Figure S30. Optimized geometry of the anionic part in **2** at the D3BJ-TPSS/def2-TZVP (CPCM) level of theory.

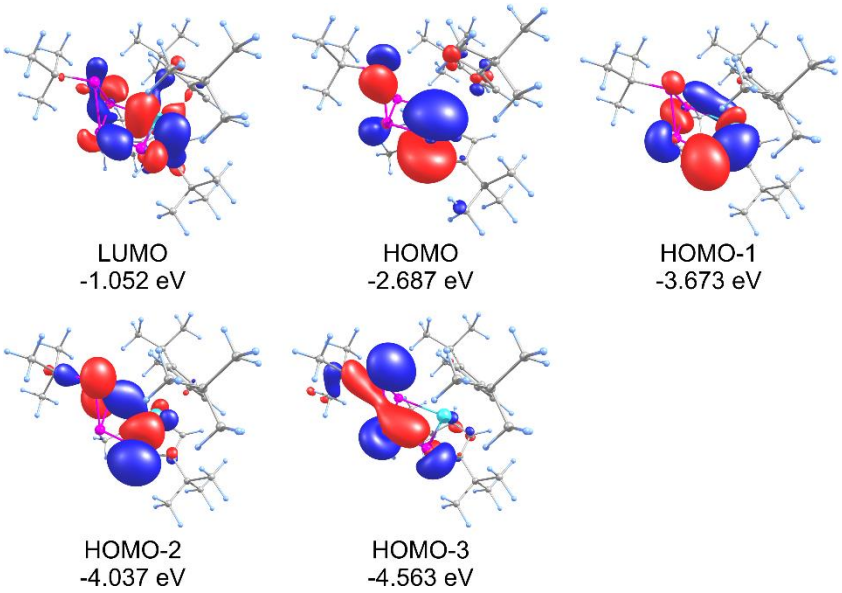

Figure S31. Frontier molecular orbitals in the anionic part in **2** at the D3BJ-TPSS/def2-TZVP (CPCM) level of theory.

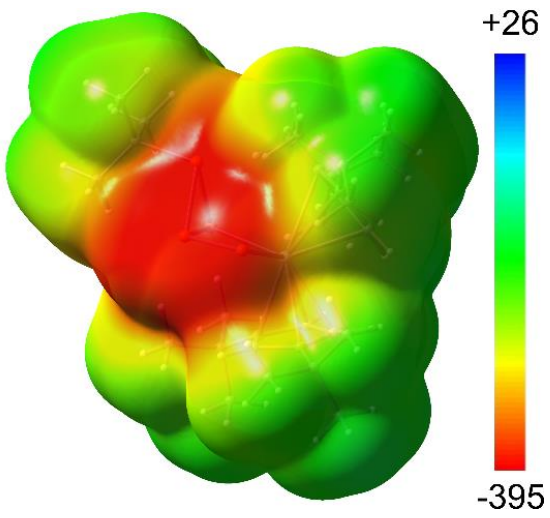

Figure S32. Electrostatic potential mapped on electron density (isovalue = 0.001) in the anionic part in **2**, calculated at the D3BJ-TPSS/def2TZVP (CPM) level of theory. Colour code (blue = positive, red = negative) in kJ·mol^{-1}.

Table S3. Cartesian coordinates of the optimized geometry of **1**. Total energy: −2429.5618346 hartree

Zr	0.000000000	0.000000000	0.067531000
P	1.688227000	0.127992000	-1.854226000
P	-1.688227000	-0.127992000	-1.854226000
P	-0.076815000	1.091239000	-2.844733000
P	0.076815000	-1.091239000	-2.844733000
C	1.012768000	2.206242000	0.957582000
C	0.000000000	2.627260000	0.051965000
H	0.176848000	3.195845000	-0.850000000
C	-1.279879000	2.253630000	0.542252000
C	-1.050600000	1.540900000	1.756224000
H	-1.815171000	1.126206000	2.399468000
C	0.345929000	1.527210000	2.016943000
H	0.815059000	1.096481000	2.890701000
C	2.459788000	2.668464000	0.969592000
C	3.393429000	1.551196000	1.455168000
H	3.349662000	0.699831000	0.772593000
H	3.113237000	1.204722000	2.455770000
H	4.427170000	1.911922000	1.500150000
C	2.909626000	3.147434000	-0.418362000
H	2.839029000	2.341675000	-1.157973000
H	3.952438000	3.480167000	-0.375220000
H	2.301397000	3.988284000	-0.767482000
C	2.542299000	3.859791000	1.955027000
H	2.253387000	3.549517000	2.964572000
H	1.875920000	4.669762000	1.639841000
H	3.567398000	4.246842000	1.990404000
C	-2.606022000	2.862600000	0.103939000
C	-2.829013000	4.085186000	1.030779000
H	-2.900297000	3.771335000	2.077424000
H	-3.758561000	4.597521000	0.756014000
H	-1.999777000	4.794717000	0.939998000
C	-2.564254000	3.361368000	-1.348518000
H	-2.423196000	2.534465000	-2.049960000
H	-1.758752000	4.086918000	-1.501058000
H	-3.511271000	3.855884000	-1.591105000
C	-3.790078000	1.902223000	0.276188000
H	-3.704613000	1.051179000	-0.406561000
H	-4.726283000	2.426051000	0.053123000
H	-3.852399000	1.521979000	1.300391000
C	-1.012768000	-2.206242000	0.957582000
C	0.000000000	-2.627260000	0.051965000
H	-0.176848000	-3.195845000	-0.850000000
C	1.279879000	-2.253630000	0.542252000
C	1.050600000	-1.540900000	1.756224000
H	1.815171000	-1.126206000	2.399468000
C	-0.345929000	-1.527210000	2.016943000
H	-0.815059000	-1.096481000	2.890701000
C	-2.459788000	-2.668464000	0.969592000
C	-3.393429000	-1.551196000	1.455168000
H	-3.349662000	-0.699831000	0.772593000
H	-3.113237000	-1.204722000	2.455770000
H	-4.427170000	-1.911922000	1.500150000
C	-2.909626000	-3.147434000	-0.418362000
H	-2.839029000	-2.341675000	-1.157973000

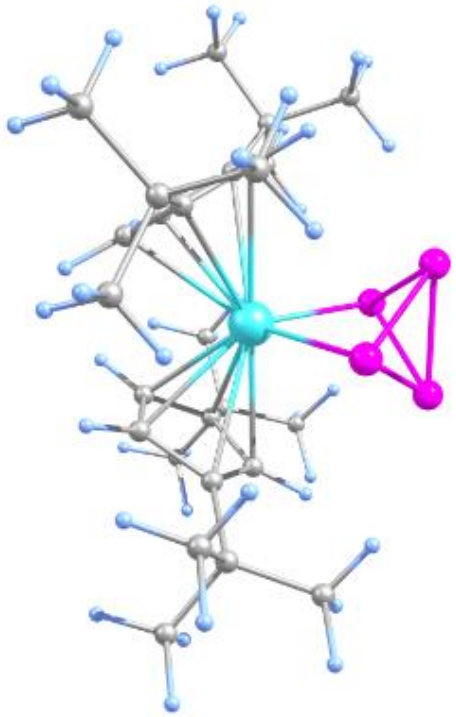

H	-3.952438000	-3.480167000	-0.375220000
H	-2.301397000	-3.988284000	-0.767482000
C	-2.542299000	-3.859791000	1.955027000
H	-1.875920000	-4.669762000	1.639841000
H	-3.567398000	-4.246842000	1.990404000
H	-2.253387000	-3.549517000	2.964572000
C	2.606022000	-2.862600000	0.103939000
C	3.790078000	-1.902223000	0.276188000
H	3.852399000	-1.521979000	1.300391000
H	3.704613000	-1.051179000	-0.406561000
H	4.726283000	-2.426051000	0.053123000
C	2.564254000	-3.361368000	-1.348518000
H	2.423196000	-2.534465000	-2.049960000
H	1.758752000	-4.086918000	-1.501058000
H	3.511271000	-3.855884000	-1.591105000
C	2.829013000	-4.085186000	1.030779000
H	2.900297000	-3.771335000	2.077424000
H	3.758561000	-4.597521000	0.756014000
H	1.999777000	-4.794717000	0.939998000

Table S4. Cartesian coordinates of the optimized geometry of the anion in **2**. Total energy: −2587.602399 hartree (HF=-2587.602399\RMSD = 9.221e-10\RMSF = 7.664e-06\ZeroPoint = 0.7306857\Thermal=0.7763344\ETot = -2586.8260646\HTot = −2586.8251204\GTot = -2586.9449617\\ NImag=0\).

Zr	0.600452000	-0.193618000	0.108370000
P	0.486580000	-0.756822000	-2.343055000
P	-1.468636000	1.381567000	-0.058760000
P	-0.992723000	0.810312000	-2.177794000
P	-2.822333000	-0.013640000	-1.082704000
C	3.056022000	0.577048000	-0.304447000
C	2.282991000	1.723857000	-0.619370000
H	2.191206000	2.156803000	-1.604577000
C	1.665058000	2.229224000	0.556716000
C	2.014141000	1.339258000	1.613163000
H	1.710733000	1.430366000	2.646604000
C	2.871588000	0.337124000	1.087419000
H	3.333355000	-0.459165000	1.655900000
C	4.099059000	-0.092119000	-1.186409000
C	3.983919000	-1.623959000	-1.134128000
H	3.004895000	-1.940458000	-1.503004000
H	4.100872000	-1.991331000	-0.108397000
H	4.765204000	-2.085801000	-1.750537000
C	3.972269000	0.381988000	-2.641353000
H	2.964381000	0.172160000	-3.018578000
H	4.707703000	-0.137055000	-3.267824000
H	4.159322000	1.459433000	-2.720020000
C	5.490023000	0.318172000	-0.645743000
H	5.629740000	-0.033009000	0.382612000
H	5.602244000	1.408107000	-0.653769000
H	6.280917000	-0.116361000	-1.269913000
C	1.158974000	3.657362000	0.719851000
C	2.410167000	4.507525000	1.060904000
H	2.866592000	4.166560000	1.996742000
H	2.129771000	5.562477000	1.173519000
H	3.158151000	4.428427000	0.264566000
C	0.550178000	4.206105000	-0.581187000
H	-0.310892000	3.608141000	-0.893819000
H	1.287426000	4.202422000	-1.391277000
H	0.224330000	5.242029000	-0.427878000
C	0.157548000	3.807961000	1.874382000
H	-0.767865000	3.265603000	1.661951000
H	-0.086278000	4.867920000	2.015433000
H	0.577762000	3.431847000	2.813384000
C	-0.574329000	-1.318550000	2.167306000
C	-1.037077000	-2.026137000	1.018228000
H	-2.056945000	-2.032113000	0.662976000
C	0.035284000	-2.741728000	0.426756000
C	1.201767000	-2.405287000	1.170404000
H	2.199738000	-2.783504000	0.992839000
C	0.817534000	-1.558451000	2.252719000
H	1.483108000	-1.164596000	3.009127000
C	-1.434254000	-0.686186000	3.251002000
C	-0.841684000	0.644811000	3.737311000
H	-0.798357000	1.360823000	2.912739000
H	0.172509000	0.506230000	4.127980000
H	-1.459081000	1.064649000	4.540987000
C	-2.870854000	-0.451582000	2.763645000
H	-2.883077000	0.204949000	1.888341000
H	-3.463383000	0.011196000	3.561855000
H	-3.353553000	-1.394526000	2.484512000
C	-1.473644000	-1.677989000	4.438996000
H	-1.884385000	-2.643176000	4.122656000
H	-2.104032000	-1.280189000	5.244266000
H	-0.467665000	-1.847751000	4.837657000
C	-0.120351000	-3.907751000	-0.537270000

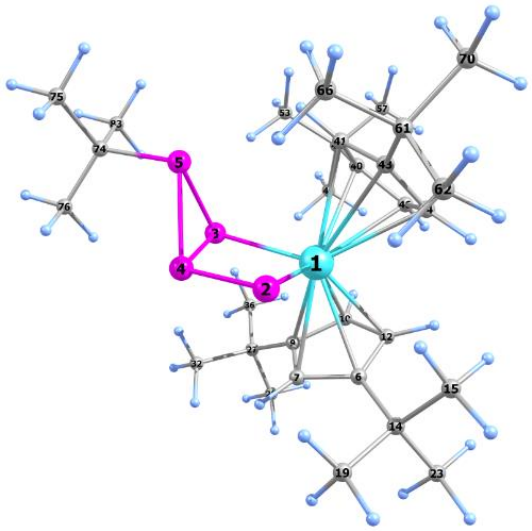

C	1.125949000	-4.122787000	-1.407580000
H	2.025035000	-4.242916000	-0.792648000
H	1.268323000	-3.271673000	-2.079606000
H	1.005376000	-5.031449000	-2.010251000
C	-1.356823000	-3.732284000	-1.432488000
H	-1.272880000	-2.802101000	-2.004221000
H	-2.273337000	-3.693969000	-0.833054000
H	-1.438777000	-4.580170000	-2.123984000
C	-0.321691000	-5.167329000	0.342941000
H	0.551428000	-5.338821000	0.982999000
H	-0.467644000	-6.051598000	-0.290486000
H	-1.201453000	-5.051187000	0.985739000
C	-4.308236000	1.119441000	-1.530339000
C	-5.227500000	0.258729000	-2.412607000
C	-3.917509000	2.398742000	-2.272968000
H	-3.206808000	2.989271000	-1.683593000
H	-3.451100000	2.172630000	-3.237357000
H	-4.811081000	3.013815000	-2.456697000
H	-4.726146000	-0.020359000	-3.346529000
H	-6.142331000	0.812617000	-2.667488000
H	-5.520521000	-0.663755000	-1.896860000
C	-5.024316000	1.476583000	-0.219755000
H	-5.314897000	0.575319000	0.333326000
H	-4.370102000	2.076188000	0.423759000
H	-5.934154000	2.059771000	-0.426801000

Table S5. Wiberg bond index matrix in the NAO basis. Atom labeling according to figure in Table S4.

Atom	1	2	3	4	5	6	7	8	9
1. Zr	0.0000	1.1988	0.8386	0.3465	0.0939	0.1754	0.1682	0.0114	0.1757
2. P	**1.1988**	0.0000	0.1434	1.0527	0.1071	0.0200	0.0098	0.0006	0.0114
3. P	**0.8386**	0.1434	0.0000	0.8098	0.9657	0.0049	0.0046	0.0003	0.0289
4. P	0.3465	1.0527	0.8098	0.0000	0.8542	0.0042	0.0053	0.0003	0.0015
5. P	0.0939	0.1071	0.9657	0.8542	0.0000	0.0062	0.0053	0.0002	0.0062

Table S6. Section of the natural population analysis in the anion of **2**.

			Natural Population			
Atom	No	Natural Charge	Core	Valence	Rydberg	Total
Zr	1	1.00628	35.99912	2.79416	0.20044	38.99372
P	2	**-0.66384**	9.99996	5.61828	0.04560	15.66384
P	3	-0.36688	9.99995	5.29927	0.06766	15.36688
P	4	-0.03420	9.99995	4.94379	0.09045	15.03420
P	5	0.16778	9.99995	4.78318	0.04909	14.83222

6.6 References

[1] D. E. C. Corbridge, *Phosphorus*, Elsevier, Amsterdam, **2000**.

[2] a) J. Emsley, *The 13th Element: The Sordid Tale of Murder, Fire and Phosphorus*, John Wiley & Sons, New York, **2000**; b) D. M. Karl, *Nature* **2000**, *406*, 31–33; c) B. Elvers, *Ullman's Encyclopedia of Industiral Chemistry*, Wiley-VHC Verlag GmbH & Co. KG, Weinheim, **2011**.

[3] D. E. C. Corbridge, *Phosphorus: Chemistry, Biochemistry and Technology*, CRC Press, Boca Raton, **2013**.

[4] A. F. Hollemann, N. Wiberg, *Lehrbuch der Anorganischen Chemie, Vol 102*, Walter de Gryter, Berlin, **2007**.

[5] R. Engel, *Synthesis of Carbon-Phosphorus Chemistry*, CRC Press, Boca Raton, **2004**.

[6] L. D. Quin, *A Guide to Organophosphorus Chemistry*, Wiley-VHC Verlag GmbH & Co. KG, New York, **2000**.

[7] J. E. Borger, A. W. Ehlers, J. C. Slootweg, K. Lammertsma, *Chemistry* **2017**, *23*, 11738–11746.

[8] a) M. M. Rauhut, A. M. Semsel, *J. Org. Chem.* **1963**, *28*, 473–477; b) M. M. Rauhut, A. M. Semsel, *J. Org. Chem.* **1963**, *28*, 471–473.

[9] B. A. Trofimov, L. Brandsma, S. N. Arbuova, N. K. Gusarova, *Russ. Chem. Bull.* **1997**, *46*, 849–850.

[10] a) G. Fritz, J. Härer, K. Stoll, *Z. Anorg. Allg. Chem.* **1983**, *504*, 47–54; b) J. H. G. Fritz, *Z. Anorg. Allg. Chem.* **1983**, *504*, 23–27.

[11] R. Riedel, H.-D. Hausen E. Fluck, *Angew. Chem. Int. Ed. Engl.* **1985**, *24*, 1056–1057.

[12] a) J. E. Borger, A. W. Ehlers, M. Lutz, J. C. Slootweg, K. Lammertsma, *Angew. Chem. Int. Ed.* **2016**, *55*, 613–617; b) J. E. Borger, A. W. Ehlers, M. Lutz, J. C. Slootweg, K. Lammertsma, *Angew. Chem. Int. Ed.* **2014**, *53*, 12836–12839; c) J. E. Borger, A. W. Ehlers, M. Lutz, J. C. Slootweg, K. Lammertsma, *Angew. Chem. Int. Ed.* **2017**, *56*, 285–290.

[13] S. Heinl, S. Reisinger, C. Schwarzmaier, M. Bodensteiner, M. Scheer, *Angew. Chem. Int. Ed.* **2014**, *53*, 7639–7642.

[14] D. Holschumacher, T. Bannenberg, K. Ibrom, C. G. Daniliuc, P. G. Jones, M. Tamm, *Dalton Trans.* **2010**, *39*, 10590–10592.

[15] J. D. Masuda, W. W. Schoeller, B. Donnadieu, G. Bertrand, *Angew. Chem. Int. Ed.* **2007**, *46*, 7052–7055.

[16] a) M. Peruzzini, J. A. Ramirez, F. Vizza, *Angew. Chem. Int. Ed.* **1998**, *37*, 2255–2257; b) P. Barbaro, M. Peruzzini, J. A. Ramirez, F. Vizza, *Organometallics* **1999**, *18*, 4237–4240.

[17] B. M. Cossairt, N. A. Piro, C. C. Cummins, *Chem. Rev.* **2010**, *110*, 4164–4177.

[18] M. Caporali, L. Gonsalvi, A. Rossin, M. Peruzzini, *Chem. Rev.* **2010**, *110*, 4178–4235.

[19] C. M. Hoidn, D. J. Scott, R. Wolf, *Chem. Eur. J.* **2021**, *27*, 1886–1902.

[20] M. Scheer, G. Balázs, A. Seitz, *Chem. Rev.* **2010**, *110*, 4236–4256.

[21] M. Seidl, G. Balázs, M. Scheer, *Chem. Rev.* **2019**, *119*, 8406–8434.

[22] J. E. Broger, M. S. Bakker, A. W. Ehlers, M. Lutz, J. C. Slootweg, K. Lammertsma, *Chem. Commun.* **2016**, *52*, 3284–3287.

[23] a) F. Riedlberger, S. Todisco, P. Mastrorilli, A. Y. Timoshkin, M. Seidl, M. Scheer, *Chemistry* **2020**, *26*, 16251–16255; b) F. Riedlberger, M. Seidl, M. Scheer, *Chem. Commun.* **2020**, *56*, 13836–13839; c) M. Piesch, M. Seidl, M. Scheer, *Chem. Sci.* **2020**, *11*, 6745–6751.

[24] M. Piesch, S. Reichl, M. Seidl, G. Balázs, M. Scheer, *Angew. Chem. Int. Ed.* **2019**, *58*, 16563–16568.

[25] M. Schmidt, A. E. Seitz, M. Eckhardt, G. Balázs, E. V. Peresypkina, A. V. Virovets, F. Riedlberger, M. Bodensteiner, E. M. Zolnhofer, K. Meyer, M. Scheer, *J. Am. Chem. Soc.* **2017**, *139*, 13981–13984.

[26] O. J. Scherer, M. Swarowsky, H. Swarowsky, G. Wolmershäuser, *Angew. Chem. Int. Ed. Engl.* **1988**, *27*, 694–695.

[27] a) V. Heinl, G. Balázs, S. Koschabek, M. Eckhardt, M. Piesch, M. Seidl, M. Scheer, *Molecules* **2021**, *26*; b) V. Heinl, M. Schmidt, M. Eckhardt, M. Eberl, A. E. Seitz, G. Balázs, M. Seidl, M. Scheer, *Chemistry* **2021**, *27*, 11649–11655; c) A. E. Seitz, M. Eckhardt, A. Erlebach, E. V. Peresypkina, M. Sierka, M. Scheer, *J. Am. Chem. Soc.* **2016**, *138*, 10433–10436.

[28] A. E. Seitz, U. Vogel, M. Eberl, M. Eckhardt, G. Balázs, E. V. Peresypkina, M. Bodensteiner, M. Zabel, M. Scheer, *Chemistry* **2017**, *23*, 10319–10327.

[29] a) B. A. Chalmers, P. S. Nejman, A. V. Llewellyn, A. M. Felaar, B. L. Griffiths, E. I. Portman, E.-J. L. Gordon, K. J. H. Fan, J. D. Woollins, M. Bühl, O. L. Malkina, D. B. Cordes, A. M. Z. Slawin, P. Kilian, *Inorg. Chem.* **2018**, *57*, 3387–3398; b) M. Stubenhofer, G. Lassandro, G. Balázs, A. Y. Timoshkin, M. Scheer, *Chem. Commun.* **2012**, *48*, 7262–7264.

[30] M. Baudler, D. Düster, D. Ouzounis, *Z. Anorg. Allg. Chem.* **1987**, *544*, 87–94.

[31] a) C. Hänisch, D. Fenske, F. Weigend, R. Ahlrichs, *Chem. Eur. J.* **1997**, *3*, 1494–1498; b) G. Friedrich, O. J. Scherer, G. Wolmershäuser, *Z. Anorg. Allg. Chem.* **1996**, *622*, 1478–1486; c) O. J. Scherer, K. Pfeiffer, G. Heckmann, *J. Organomet. Chem.* **1992**, *425*, 141–149; d) H. Brunner, F. Leis, B. Nuber, J. Wachter, *Polyhedron* **1999**, *18*, 347–350; e) F. Kraus, T. Hanauer, N. Korber, *Angew Chem Int Ed Engl* **2005**, *44*, 7200–7204; f) M. Piesch, M. Scheer, *Organometallics* **2020**, *39*, 4247–4252.

[32] a) B. K. Nicholson, P. S. Wilson, A. Nancekivell, *J. Organomet. Chem.* **2013**, *745*, 80–85; b) M. B. Marx, H. Pritzkow, B. K. Keppler, *Z. Anorg. Allg. Chem.* **1997**, *623*, 75–78;

c) A. L. Rheingold, P. J. Sullivan, *Organometallics* **1983**, *2*, 327–331; d) R. M. De Silva, M. J. Mays, P. R. Raithby, G. A. Solan, *J. Organomet. Chem.* **2002**, *642*, 237–245; e) R. M. De Silva, M. J. Mays, G. A. Solan, *J. Organomet. Chem.* **2002**, *664*, 27–36.

[33] V. Heinl, A. E. Seitz, G. Balázs, M. Seidl, M. Scheer, *Chem. Sci.* **2021**,*12*, 9726-9732.

[34] O. J. Scherer, M. Swarowsky, H. Swarowsky, G. Wolmershäuser, *Angw. Chem. Int. Ed. Engl.* **1988**, *5*, 694–695.

[35] M. Schmidt, A. E. Seitz, M. Eckhardt, G. Balázs, E. V. Peresypkina, A. V. Virovets, F. Riedlberger, M. Bodensteiner, E. M. Zolnhofer, K. Meyer, M. Scheer, *J. Am. Chem. Soc.* **2017**, *139*, 13981–13984.

[36] Rigaku Oxford Diffraction, *CrysAlisPro Software System Version 1.171.38.43*, **2015**.

[37] L. J. Bourhis, O. V. Dolomanov, R. J. Gildea, J. A. K. Howard, H. Puschmann, *J. Appl. Crystallogr.* **2009**, *42*, 339–341.

[38] G. M. Sheldrick, *Acta Crystallogr., Sect, A* **2008**, *64*, 112–122.

[39] G. M. Sheldrick, *Acta Crystallogr., Sect, A* **2015**, *71*, 3–8.

[40] G. M. Sheldrick, *Acta Crystallogr., Sect, C* **2015**, *71*, 3–8.

[41] Gaussian 16, Revision C.01, M. J. Frisch, G. W. Trucks, H. B. Schlegel, G. E. Scuseria, M. A. Robb, J. R. Cheeseman, G. Scalmani, V. Barone, G. A. Petersson, H. Nakatsuji, X. Li, M. Caricato, A. V. Marenich, J. Bloino, B. G. Janesko, R. Gomperts, B. Mennucci, H. P. Hratchian, J. V. Ortiz, A. F. Izmaylov, J. L. Sonnenberg, D. Williams-Young, F. Ding, F. Lipparini, F. Egidi, J. Goings, B. Peng, A. Petrone, T. Henderson, D. Ranasinghe, V. G. Zakrzewski, J. Gao, N. Rega, G. Zheng, W. Liang, M. Hada, M. Ehara, K. Toyota, R. Fukuda, J. Hasegawa, M. Ishida, T. Nakajima, Y. Honda, O. Kitao, H. Nakai, T. Vreven, K. Throssell, J. A. Montgomery, Jr., J. E. Peralta, F. Ogliaro, M. J. Bearpark, J. J. Heyd, E. N. Brothers, K. N. Kudin, V. N. Staroverov, T. A. Keith, R. Kobayashi, J. Normand, K. Raghavachari, A. P. Rendell, J. C. Burant, S. S. Iyengar, J. Tomasi, M. Cossi, J. M. Millam, M. Klene, C. Adamo, R. Cammi, J. W. Ochterski, R. L. Martin, K. Morokuma, O. Farkas, J. B. Foresman, and D. J. Fox, Gaussian, Inc., Wallingford CT, 2019.

[42] J. Tao, J. P. Perdew, V. N. Staroverov, G. E. Scuseria, *Phys. Rev. Letters* **2003**, *91*, 146401.

[43] F. Weigend and R. Ahlrichs, *Phys. Chem. Chem. Phys.*, **2005**, 7, 3297-305; b) F. Weigend, *Phys. Chem. Chem. Phys.*, **2006**, *8*, 1057-65.

[44] S. Grimme, S. Ehrlich, L. Goerigk, *J. Comput. Chem.* **2011**, *32*, 1456-1465.

[45] a) J. Tomasi, B. Mennucci, R. Cammi, *Chem. Rev.* **2005**, *105*, 2999-3094; b) V. Barone, M. Cossi, *J. Phys. Chem. A* **1998**, *102*, 1995-2001.

7 Synthesis of Polyantimony Ligand Complexes starting from $Cp^*_4Sb_4$

V. Heinl, M. Seidl, M. Scheer.

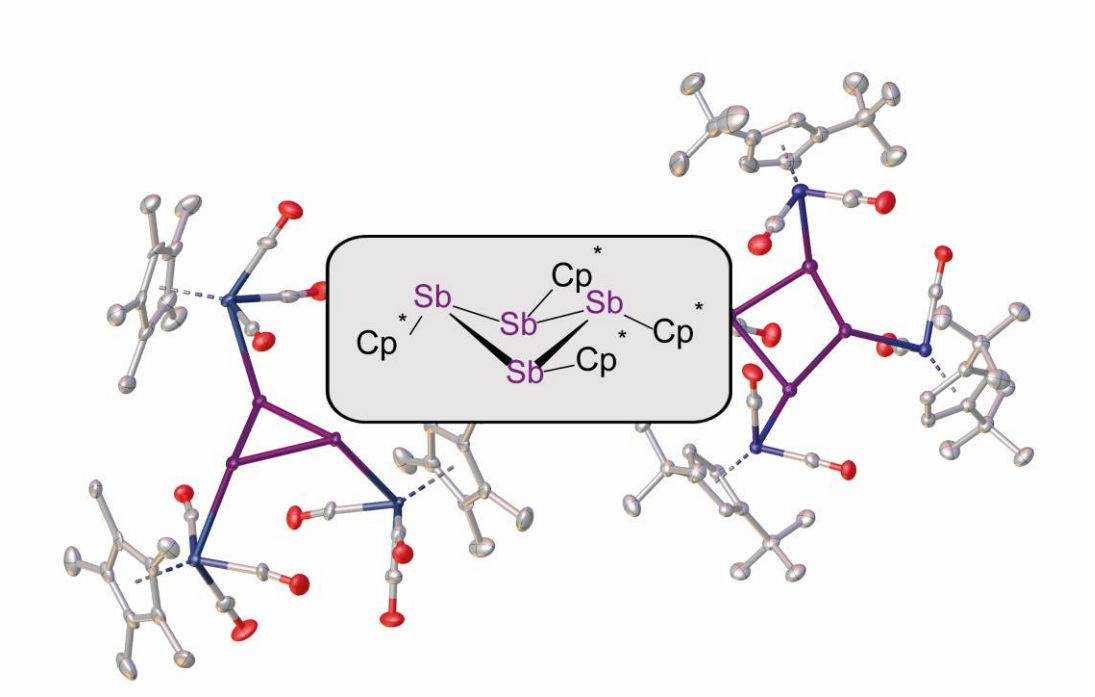

Abstract

The reactivity of $Cp^*_4Sb_4$ (**1**) towards ionic compounds and transition metal complexes with labile ligands is investigated in order to synthesize polyantimony ligand complexes. For this, the silver salts [Ag][X] and the metalate $Na[Cp^*Mo(CO)_2]$ were primarily used, which leads in the raction with $Cp^*_4Sb_4$ to the formation of $[Cp^*_2Sb][X]$ (X = TEF (**2a**), FAL (**2b**)), $[(Cp^*Mo(CO)_3)_3(\mu_3\text{-}Sb_3)]$ (**3**) and $[Cp^*Mo(CO)_2(\eta^3\text{-}Sb_3)]$ (**4**), respectively. In the latter reaction, a Sb_3 unit is formed and coordinates to three $[Cp^*Mo(CO)_3]$ or one $[Cp^*Mo(CO)_2]$ fragments. Furthermore, the reaction of **1** towards the transition metal complexes $[(Cp'''M)_2(tol)]$ and $[Cp^RFe(CO)_2]_2$ were investigated, for which a degradation of the original Sb_4 unit and the formation of the complexes $[(Cp'''M)_4(\mu_3\text{-}Sb)_4]$ (M = Ni (**5**); Co (**6**)) as well as a substitution on the antimony atoms were observed. As a result, $[\{Cp^RFe(CO)_2\}_4(\mu_4\text{-}Sb_4)]$ (Cp^R = Cp'' (**7a**), Cp''' (**7b**)) are formed. All complexes have been characterized by XRD and spectroscopic methods.

7.1 Author Contribution

- Synthesis and characterization of the compounds **2a**, **2b**, **3**, **7a** and **7b** was performed by V. Heinl.
- New synthetic routes for the compounds **4**, **5/5'** and **6** were performed by V. Heinl.
- M. Seidl recalculated the X-ray structures.
- The Manuscript was written by V. Heinl.
- Supervision: M. Scheer.

7.2 Introduction

With the first reports on polypnictogen ligand complexes in the 1960's,[1] an interesting and versatile field of chemical research arised. Since that time numerous examples of such compounds have been synthesized, especially complexes containing polyphosphorus and polyarsenic units.[2] In contrast, polyantimony ligand complexes are rather rare. Reasons for this are, *inter alia*, the high light- and air- sensitivity of antimony containing compounds and the comparatively weak Sb-Sb bond.[3] Furthermore, the lack of suitable Sb starting materials complicates the topic. In 1970 *Dahl et al.* reported the synthesis of the first Sb_n ligand complex $[Co_4(CO)_{12}Sb_4]$ by the reaction of $Co(OAc)_2{\cdot}H_2O$ with $SbCl_3$.[4] Since then, different synthetic strategies were followed to enables the formation of such products (Figure 1). In 2018 *Roesky et al.* used Sb^0-nanoparticles as antimony source in a thermolytic reaction with $[Cp^*_2Sm]$, which leads to the polystibido-coplex $[(Cp^*_2Sm)(\mu_4,\eta^{1:1:1:1:1:1:1:1}\text{-}Sb_8)]$ (Figure 1, **I**, Cp* = C_5Me_5).[5] It was also demonstrated by our group, that the usage of Sb-salts, like $LiSb(H)CH(SiMe_3)_2$ or $KSb(SiMe_3)_2$, with appropriate halogenated reactants enables the formation of Sb_n ligand complexes. Thereby it was possible to synthesize the complex $[(N_3N)WSb]$ (**II**, N_3N = tren = $N(CH_2CH_2NSiMe_3)_3$), which possesses a triple bond between tungsten and antimony.[6] Furthermore, the triple decker complex $[(Cp''Zr)_2(\mu,\eta^{1:1:1:1:1:1}\text{-}Sb_6)]$ (**III**) was obtained by the reaction of $[Cp''_2ZrCl_2]$ with $KSb(SiMe_3)_2$, which also can be used as starting material in transfer reactions for the synthesis of other polyantimony ligand complexes.[7] The most used antimony sources are neutral organo-substituted antimony compounds such as R_4Sb_4 (R = ^{t}Bu, Cp*)[8–10] and R'_4Sb_2 (R' = Me, Et).[11] By using $^t Bu_4Sb_4$ *Rösler et al*. obtained the compounds **IV** and **V** via co-thermolysis with $[CpMo(CO)_3]_2$ (Figure 1).[8] Also the Cp* derivative of **IV** was prepared using $[Cp^*Mo(CO)_3]_2$.[8] Furthermore, the synthesis of the triple decker complex $[Cp'''Mo(\mu,\eta^{5:5}\text{-}Sb_5)MoCp^R]$ (**VI**, $Cp^R = \eta^5\text{-}C_5H_2{}^tBu_2Me$), containing a *cyclo*-$Sb_5$ middle deck, was achieved by reacting $[Cp'''Mo(CO)_3Me]$ with $^t Bu_4Sb_4$. Interestingly, one ^{t}Bu group of a Cp''' ligand converts into a methyl group during the synthesis.[9]

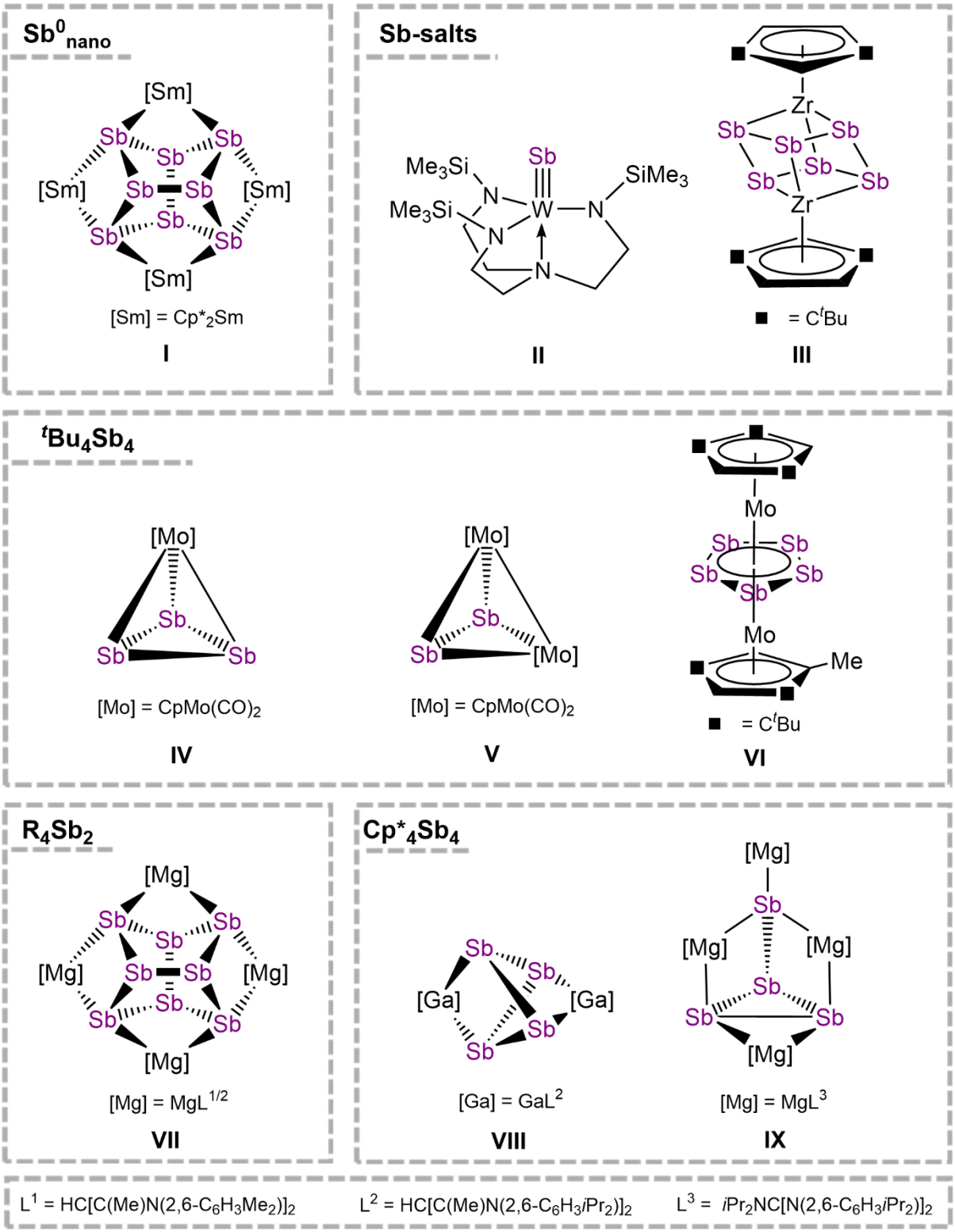

Figure 1: Selected examples of Sb_n ligand complexes.

By the reaction of the organo-substituted antimony precursors R'_4Sb_2 (R' = Me, Et) with $[L^{1,2}Mg]_2$ (L^1 = HC[C(Me)N(2,4,6-$Me_2C_6H_3$)]$_2$, L^2 = HC[C(Me)N(2,6-$^iPr_2C_6H_3$)]$_2$) the realgar-type polystibide $[(LMg)_4(\mu_4,\eta^{1:1:1:1:1:1:1:1}\text{-}Sb_8)]$ (**VII**) is formed.[11] Furthermore, *Schulz et al.* showed the usage of $Cp^*_4Sb_4$ as antimony source in reactions with main-group compounds. This leads to the formation of main group compounds containing an Sb_4 unit. Thus, the reaction with L^2Ga

and $[L^3Mg]_2$ yields $[(L^2Ga)_2(\mu,\eta^{1:1:1:1}\text{-}Sb_4)]$ (**VIII**) and $[(L^3Mg)_4(\mu_4,\eta^{2:1:1:1:1:1}\text{-}Sb_4)]$ (**IX**, $L^3 = {}^{i}Pr_2NC[N\text{-}2,6\text{-}{}^{i}Pr_2C_6H_3)]_2$), respectively.[10]

7.3 Results and Discussion

With this in mind, we were interested in whether it would also be possible to use $Cp^*_4Sb_4$ as antimony source to synthesize transition metal complexes bearing polyantimony units. The synthesis of Sb_n ligand complexes started by ${}^{t}Bu_4Sb_4$ normally proceed under harsh conditions[8,9] to remove the organic substituents and generate a reactive polyantimony fragment for the reaction. Compared to this, Cp* as substituent on the antimony fragment show some advantages, because it should be relatively easy to release as a radical, an anion or as fulvalene. Therefore, milder reaction conditions should be possible and though the handling of such reaction systems is simple. This offers the opportunity for the synthesis of novel polyantimony ligand complexes.

For this, the reactivity towards transition metal complexes containing labile ligands as well as ionic compounds was investigated. We herein report on the reaction of $Cp^*_4Sb_4$ towards the ionic compounds [Ag][TEF] (TEF = $[Al\{OC(CF_3)_3\}_4]$), [Ag][FAL] (FAL = $[Al\{OC_6F_{10}(C_6F_5)\}_3]$) and $Na[Cp^*Mo(CO)_2]$ as well as with the transition metal complexes $[(Cp'''M)_2(tol)]$ (M = Ni, Co) and $[Cp^RFe(CO)_2]_2$ (Cp^R = Cp'', Cp''') for which novel antimony containing compounds were obtained (Scheme 1).

The reaction of **1** with the ionic silver compounds [Ag][X] in DCM at room temperature leads to the stibanocenium derivatives $[Cp^*_2Sb][X]$ (X = TEF (**2a**), FAL (**2b**)). **2a** and **2b** are reminiscent of the already reported compounds $[Cp^*_2Sb][X']$ (X' = $AlCl_4$, AlI_4, OTf, $B(C_6F_5)_4$).[12–14] For its synthesis the chlorinated compound $[Cp^*_2SbCl]$ are used.[13,14] Interestingly, for the synthesis of $[Cp^*_2Sb][AlI_4]$, the to **1** related compound $Cp^*_4Al_4$ was used.[12] Furthermore, the reaction of **1** with $Na[Cp^*Mo(CO)_2]$ in boiling toluene leads after column chromatographic workup, beside the corresponding carbonyl dimers, to the neutral complexes $[(Cp^*Mo(CO)_3)_3(\mu_3\text{-}Sb_3)]$ (**3**) and $[Cp^*Mo(CO)_2(\eta^3\text{-}Sb_3)]$ (**4**), containing an Sb_3 unit. **4** is already known and accessible by the thermolysis of $[Cp^*Mo(CO)_3]_2$ with ${}^{t}Bu_4Sb_4$.[8] However, the novel complex **4** exhibit a new connectivity of an Sb_3 unit. Since we obtained **3** and **4** side by side we assume the formation of **3** in the first step, followed by elimination of CO and $[Cp^*Mo(CO)_3]_2$ to form compound **4**. That would also explain the formation of the afore mentioned molybdenum carbonyle dimers $[Cp^*Mo(CO)_3]_2$ and $[Cp^*Mo(CO)_2]_2$.[15]

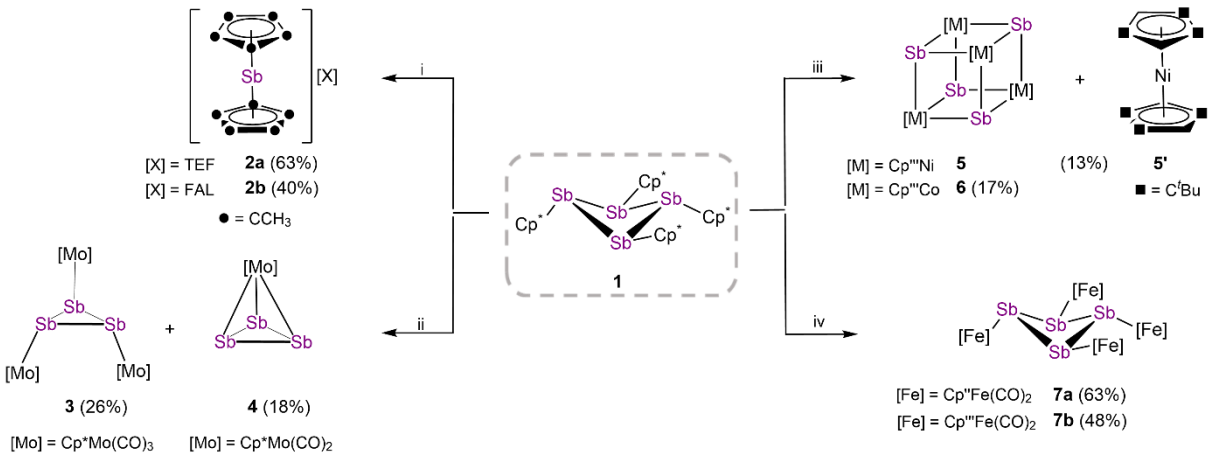

Scheme 1: Reactivity of $Cp^*_4Sb_4$ (**1**) towards different transition metal complexes. (i): [Ag][X] (X = TEF; FAL) in DCM at r.t. (ii): $Na[Cp^*Mo(CO)_2]$ in boiling toluene. (iii): *in situ* prepared $[(Cp'''Ni)_2(tol)]$ or crystalline $[(Cp'''Co)_2(tol)]$ in *n*-hexane at r.t. (iv): $[Cp^RFe(CO)_2]_2$ in boiling toluene (Cp^R = Cp'', Cp''').

Furthermore, the reactivity of **1** toward transition metal complexes with labile ligands was investigated. The reaction of **1** with the triple decker complexes $[(Cp'''M)_2tol]$ at room temperature leads to $[(Cp'''M)_4(\mu_3\text{-}Sb)_4]$ (M = Ni (**5**); Co (**6**)), possessing a cubane like structures. Interestingly, **5** co-crystalizes with $[Cp'''Ni_2]$ (**5'**). Recently we reported the synthesis of these compounds by the reaction of $[(Cp''Zr)_2(\mu,\eta^{1:1:1:1:1:1}\text{-}Sb_6)]$ with the related metal halides $[Cp'''MX]_2$.[7] Interestingly, thereby also a co-crystallization of **5** with **5'** was observed. However, using the here reported synthetic pathway higher yields and selectivity can be achieved. The reaction of **1** with $[Cp^RFe(CO)_2]_2$ in boiling toluene leads to a substitution of the Cp* ligands by $[Cp^RFe(CO)_2]$ and the formation of the novel iron complexes $[\{Cp^RFe(CO)_2\}_4(\mu_4\text{-}Sb_4)]$ (Cp^R = Cp'' (**7a**), Cp''' (**7b**)).

The newly reported compounds (**2a**, **2b**, **3**, **7a**, **7b**) were comprehensively characterized by mass spectrometry, NMR spectroscopy, single crystal X-ray diffraction analysis, IR spectroscopy and elemental analysis. Mass spectrometric measurements show the molecular ion peaks or ionic fragments of the compounds **2a**, **2b**, **3** and **7a**, respectively. In the case of **7b** only one peak at *m/z* (%): 1177.93, corresponding to $M^+ - 2\cdot[Cp'''Fe(CO)_3]$, can be observed. The ^1H NMR spectra of all mentioned compounds show the expected signals for the respective Cp^R ligands and also the IR spectra of **3**, **7a** and **7b** show the corresponding bands of the carbonyl ligands.

Single crystals suitable for X-ray diffraction analysis were obtained by storing concentrated CH_2Cl_2 solutions at -30 °C (**2a**, **2b**, **3**) or layering a toluene (**7a**) or CH_2Cl_2 (**7b**) solution with acetonitrile. The molecular structures of the cationic part of **2b** and the molecular structures of **3** and **7a** are depicted in figure 2 (**2a**, **2b** (whole molecule) and **7b** are depicted in the SI).

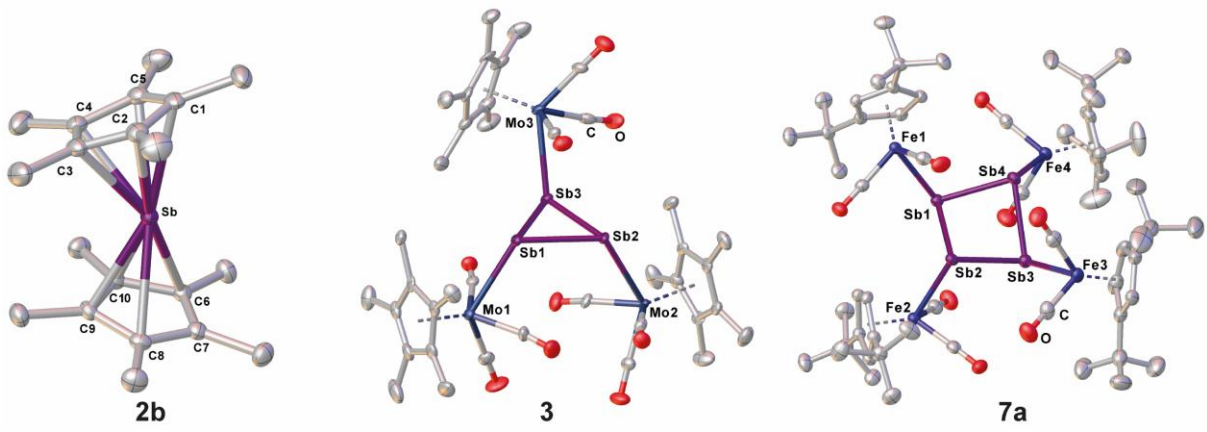

Figure 2: Molecular structures of the cationic part of **2a** (left), **3** (middle) and **7a** (right) in the solid state with thermal ellipsoids at 50% probability level. H atoms are omitted for clarity.

The cationic part of the **2a** and **2b** consist of two planar Cp* ligands coordinating to Sb in a bent fashion. This results in a $Cp^*_{centroid}$-Sb-$Cp^*_{centroid}$ angle of 164.268° (**2a**) and 160.709° (**2b**). The angles of already reported stibanocenium complexes are in the same range. [12–14] This also applies for the $Cp^*_{centroid}$-Sb distances (**2a**: 2.280 Å and 2.287 Å; **2b**: 2.266 Å and 2.292 Å).[12–14]

The central core of **3** consists of an Sb_3 cycle, where each Sb atom is attached to a [Cp*Mo$(CO)_3$] fragment. Angles of 59.88° to 60.20° within the Sb_3 cycle indicate an almost perfect triangle. However, the Mo-Sb axes are inclined apart from the Sb_3 plane and each other (Sb-Sb-Mo: 105.463(16)° to 120.904(17)°). The Sb-Sb distances of 2.8370(5) Å to 2.8459(5) Å are in the range of single bonds and in good agreement with the literature values.[5,7,10,11] The same applies for the Mo-Sb distances of 2.8669(6) Å to 2.8930(5) Å.[8] Besides the aforementioned complexes **IV**, **V** and **VI**, and their derivates, **3** represents a rare example of polyantimony ligand complex with molybdenum and possesses a new coordination mode.

The molecular structure of **7a** shows an folded Sb_4 cycle, where each Sb atom is attached to a [Cp''Fe$(CO)_2$] fragment. All Sb-Sb distances of 2.8384(3) Å to 2.8654(3) Å are in the range of single bonds[5,7,10,11] and match with the values reported for **1**.[16] The Sb_4 ring is not planar and shows a folding angle of 119.755°. Within the distorted ring Sb-Sb-Sb angles of 81.438(9)° to 81,866(9)° are observed. Due to the bulkier iron fragments, they are slightly smaller than the reported values for **1**.[16] Besides **1**, *cyclo*-Sb_4 units are known, but only with organic[17] or pnictogen[18] substituents at the Sb atoms. The compounds **7a** and **7b** represent rare examples of polyantimony iron complexes and the first bearing an intact Sb_4 unit.

7.4 Conclusion

In summary, we herein report the synthesis of a variety of polyantimony ligand complexes, which were synthesized starting from $Cp^*_4Sb_4$ (**1**) in the reaction with ionic compounds and transition metal complexes with labile ligands. Using the silver salts [Ag][X] stibanocenium derivatives $[Cp^*_2Sb][X]$ (X = TEF (**2a**), FAL (**2b**)) are formed. Furthermore, the reaction with the ionic metalate $Na[Cp^*Mo(CO)_2]$ leads to the novel cyclo-Sb_3 containing derivatives $[(Cp^*Mo(CO)_3)_3(\mu_3\text{-}Sb_3)]$ (**3**) and $[Cp^*Mo(CO)_2(\eta^3\text{-}Sb_3)]$ (**4**). Both containing an Sb_3 cycle coordinating to one $[Cp^*Mo(CO)_2]$ or three $[Cp^*Mo(CO)_3]$ fragments. Transition metal complexes containing labile ligands reacts with **1** via a different reaction pathway, leading to degradation of the Sb_4 unit. The reaction of **1** with the triple decker complexes $[(Cp'''M)_2tol]$ leads to $[(Cp'''M)_4(\mu_3\text{-}Sb)_4]$ (M = Ni (**5**); Co (**6**)), containing cubane like structures. Interestingly, using $[Cp^RFe(CO)_2]_2$ as a reactant, the Sb_4 unit remains unchanged and solely the Cp* ligands are substituted by $[Cp^RFe(CO)_2]$ fragments leading to novel complexes of the form$[\{Cp^RFe(CO)_2\}_4(\mu_4\text{-}Sb_4)]$ (Cp^R = Cp'' (**7a**), Cp''' (**7b**)). These results show the high potential of **1** to form Sb_n ligand complexes, which enable to expand the variety of such compounds. Further work in this area is dedicated to get insight into their reactivity or to use them to transfer the Sb_n unit to other metal centers.

7.5 Supporting Information

7.5.1 Experimental Detail

All experiments were performed under an atmosphere of dry nitrogen or argon using Schlenk and glovebox techniques. Solvents were purified, dried and degassed prior use. ^{1}H, $^{13}C\{1H\}$ NMR spectra were recorded at room temperature on a Bruker Avance 400 spectrometer (^{1}H: 400,130 MHz, ^{13}C: 100.613 MHz). ^{1}H, ^{13}C NMR chemical shifts are reported in parts per million (ppm) relative to the external standard Me_4Si. Elemental analysis was determined with a Vario micro cube apparatus. For mass spectrometry, a Finnigan MAT 95 (LIFDI MS, FD MS) or a Finnigan MAT SSQ 710 A (ESI MS) device and a Joel AccuTOF GCX spectrometer were used. [Ag][TEF],[19] [Ag][FAL],[20] KCp*,[21] [(Cp'''Co)$_2$tol],[22] [Cp''Fe(CO)$_2$]$_2$[23] and [Cp'''Fe(CO)$_2$]$_2$[24] were prepared according to literature procedures.

Preparation of [Cp*$_4$Sb$_4$] (1):[16]

$SbCl_3$ (1.1 g, 4.9 mmol) in Et_2O is added dropwise to a suspension of KCp* (3.0 g, 17.2 mmol) in 150 mL Et_2O at -78 °C. The colour changes to dark orange. After addition, the reaction solution is stirred for 30 min at -78 °C and thereupon warmed to r.t. A dark orange solution is obtained by filtration and a beige solid remains on the frit. Crystals of **1** are obtained by storing a concentrated Et_2O solution at -30 °C. Crystalline Yield: 984 mg (0.961 mmol, 78%)

X: Analytical data are in agreement with the literature.[16]

Preparation of [Cp*$_2$Sb][TEF] (2a):

A solution of [Cp*$_4$Sb$_4$] (30 mg, 0.029 mmol) in 5 mL DCM is added to a solution of [Ag][TEF] (35 mg, 0.030 mmol) in 5 mL DCM. The colour changes to green and a black solid is formed. After stirring for 1 d at r.t. the reaction mixture is filtered via cannula. The obtained orange solution is concentrated *in vacuo* and stored at -30 °C for crystallization. Crystalline Yield: 26 mg (0.019 mmol, 63%)

2a: **^{1}H NMR** (CD_2Cl_2, 298 K): δ [ppm] = 2.20 (s, 30 H, C*H*$_3$); **$^{13}C\{^{1}H\}$ NMR** (CD_2Cl_2, 298 K): δ [ppm] = 10.1 (s, C*C*H$_3$), 127.6 (s, *C*CH$_3$); **FD$^+$ MS** (toluene): *m/z* (%): 391.10 ([Cp*$_2$Sb]$^+$); **Elemental analysis** (%): calculated for [$C_{36}H_{30}SbAlO_4F_{36}$] (1358.04 g·mol^{-1}): C, 31.81; H2.22; found: C, 32.03; H, 2.27.

Preparation of [Cp*$_2$Sb][FAL] (2b):

A solution of [Cp*$_4$Sb$_4$] (30 mg, 0.029 mmol) in 5 mL DCM is added to a solution of [Ag][FAL] (32 mg, 0.030 mmol) in 5 mL DCM. The colour changes to green and a black solid is formed. After stirring for 1 d at r.t. the reaction mixture is filtered via cannula. An orange solution is obtained, a black solid remains. Crystals of **2b** suitable for single crystal X-ray diffraction analysis are obtained by storing a concentrated DCM solution at -30 °C Crystalline Yield: 21 mg (0.012 mmol, 40%)

2b: **^{1}H NMR** (CD_2Cl_2, 298 K): *δ* [ppm] = 2.20 (s, 30 H, C*CH*$_3$); **^{13}C{^{1}H} NMR** (CD_2Cl_2, 298 K): *δ* [ppm] = 10.1 (s, C*C*H$_3$), 127.6 (s, *C*CH$_3$); **ESI$^+$ MS** (toluene): *m*/*z* (%): 391.13 ([Cp*$_2$Sb]$^+$); **ESI$^-$ MS** (toluene): *m*/*z* (%): 1380.91 ([FAL]$^-$); **Elemental analysis** (%): calculated for [$C_{56}H_{30}SbAlO_3F_{46}$] (1772.03 g·mol^{-1}): C, 437.93; H, 1.71; found: C, 37.61; H, 1.64.

Preparation of [(Cp*Mo(CO)$_3$)$_3$(μ$_3$-Sb$_3$)] (3) and [Cp*Mo(CO)$_2$(η^3-Sb$_3$)] (4):

A solution of Na[Cp*Mo(CO)$_2$] (51 mg, 0.128 mmol) is dissolved in 15 mL toluene and added to a solution of [Cp*$_4$Sb$_4$] (150 mg, 0.146 mmol) in 15 mL toluene. The reaction solution is refluxed for 1 h. The solvent of the brown suspension is removed *in vacuo* and subsequent column chromatographic workup (SiO_2, *n*-hexane, 18 x 3 cm) yields four fractions. With *n*-hexane a yellow fraction of [Cp*$_4$Sb$_4$] is eluted, followed by an orange fraction of **4**. The third red fraction, eluted with a mixture of *n*-hexane and toluene (1:1), contains a mixture of [Cp*Mo(CO)$_3$]$_2$ and [Cp*Mo(CO)$_2$]$_2$. With toluene as solvent, a red-brown fraction of **3** is obtained. Crystals of **3** and **4** suitable for single crystal X-ray diffraction analysis are obtained by storing a concentrated solution in DCM (**3**) or *n*-hexane (**4**) at -30 °C, respectively. Crystalline Yield: **3**: 17 mg (0.013 µmol, 26%), **4**: 6 mg (9.2 µmol, 18%)

3: **^{1}H NMR** (C_6D_6, 298 K): *δ* [ppm] = 1.78 (s, 45 H, C*CH*$_3$); **^{13}C{^{1}H} NMR** (C_6D_6, 298 K): *δ* [ppm] = 9.8 (s, C*C*H$_3$), 103.2 (s, *C*CH$_3$), 239.5 (s, *C*O); **LIFDI MS** (toluene): *m*/*z* (%): 1310.78 (M$^+$, 100), 968.78 (M$^+$ - [Cp*Mo(CO)$_4$], 40); **ATR-IR** (diamant crystal): v [cm-1] = 1862 (m), 1818 (m); **Elemental analysis** (%): calculated for [$C_{39}H_{45}Mo_3Sb_3O_9$] (1313.73 g mol^{-1}): C, 35.73; H, 3.46; no satisfying elemental analysis could be obtained, even by using Sn capsules.

4: Analytical data are in agreement with the literature.[8]

Preparation of [(Cp'''Ni)$_4$(μ$_3$-Sb)$_4$]/[Cp'''$_2$Ni] (5/5'):

A solution of [Cp*$_4$Sb$_4$] (80 mg, 0.078 mmol) in 5 mL toluene is added to an excess of a freshly prepared solution of [(Cp'''Ni)$_2$tol][25] in 10 mL toluene and stirred for 5 d. The solvent of the green reaction mixture is removed *in vacuo* and subsequent column chromatographic workup (SiO_2, *n*-hexane, 18 x 3 cm) yields four fractions. With *n*-hexane, a yellow fraction of fulvalene is eluted, followed by a brown-violet fraction of **5/5'**. Seamless with *n*-hexane an orange fraction of [Cp*$_4$Sb$_4$] can be observed. The fourth brown fraction, eluted with a mixture of *n*-hexane and toluene (1:1), is still unknown. Crystals of **5/5'** suitable for single crystal X-ray diffraction analysis are obtained by layering a DCM solution with acetonitrile. Crystalline Yield: 9 mg (4.19 µmol, 13%)

5/5': Analytical data are in agreement with the literature.[7]

Preparation of [(Cp''''Co)$_4$(μ$_3$-Sb$_4$)] (6):

A solution of [Cp*$_4$Sb$_4$] (80 mg, 0.078 mmol) in 5 mL *n*-hexane is added to a solution of [(Cp'''Co)$_2$tol] (54 mg, 0.081 mmol) in 5 mL *n*-hexane and stirred for 5 d. The solvent of the green reaction mixture t is removed *in vacuo* and subsequent column chromatographic workup (SiO_2, *n*-hexane, 18 x 3 cm) yields two fractions. With *n*-hexane, a green fraction of **6** can be obtained. The second fraction containing [Cp*$_4$Sb$_4$] can be eluted with a mixture of *n*-hexane and toluene (1:1). Crystals of **6** suitable for single crystal X-ray diffraction analysis are obtained by layering a DCM solution with acetonitrile. Crystalline Yield: 11 mg (6.66 µmol, 17%)

6: Analytical data are in agreement with the literature.[7]

Preparation of [{Cp''Fe(CO)$_2$}$_4$(μ$_4$-Sb$_4$)] (7a):

A solution of [Cp''Fe(CO)$_2$]$_2$ (169 mg, 0.292 mmol) is dissolved in 15 mL toluene and added to a solution of [Cp*$_4$Sb$_4$] (150 mg, 0.146 mmol) in 15 mL toluene. The reaction solution is refluxed for 1 h. After removing the solvent, the brown residue is extracted with DCM. The red-brown suspension is filtered via cannula. A grey powder remains. Crystals of **7a** suitable for single crystal X-ray structure analysis are obtained by layering the concentrated DCM solution with acetonitrile. Crystalline Yield: 154 mg (0.266 mmol, 63%)

7a: **^{1}H NMR** (thf-d^8, 298 K): *δ* [ppm] = 1.27 (s, 72 H, C(*CH*$_3$)$_3$), 4.44 (d, 8 H, C(*CH*$_3$)$_3$), 4.83 (t, 4 H, C(*CH*$_3$)$_3$); **^{13}C{^{1}H} NMR** (thf-d^8, 298 K): *δ* [ppm] = 31.7 (s, *C*H$_3$), 31.9 (s, *C*(CH$_3$)$_3$), 76.8 (s, *C*H), 82.3 (s, *C*C(CH$_3$)$_3$), 117.1 (s, *C*C(CH$_3$)$_3$), 219.1 (s, *C*O); **LIFDI MS** (toluene): *m*/*z* (%): 1643.89 (M$^+$); **ATR-IR** (diamant crystal): v [cm-1] = 1971 (s), 1947 (s), 1912 (m); **Elemental**

analysis (%): calculated for [$C_{60}H_{84}Fe_4Sb_4O_8$] (1639.97 g·mol^{-1}): C, 43.84; H, 5.15; found: C, 43.45; H, 4.81.

Preparation of [{Cp'''Fe(CO)$_2$}$_4$(μ$_4$-Sb$_4$)] (7b):

A solution of [Cp'''Fe(CO)$_2$]$_2$ (135 mg, 0.196 mmol) is dissolved in 15 mL toluene and added to a solution of [Cp*$_4$Sb$_4$] (100 mg, 0.098 mmol) in 15 mL toluene. The reaction solution is refluxed for 1 h. After removing the solvent, the brown residue is extracted with toluene. The red-brown suspension is filtered via cannula. A grey powder remains. Crystals of **7b** suitable for single crystal X-ray structure analysis are obtained by layering a concentrated toluene solution with acetonitrile. Crystalline Yield: 87 mg (0.047 mmol, 48%)

7b: **^{1}H NMR** (thf-d^8, 298 K): *δ* [ppm] = 1.26 (s, 36 H, C(*C*H$_3$)$_3$), 1.43 (s, 72 H, C(*C*H$_3$)$_3$), 4.78 (s, 8 H, C$_5$*H*$_2$^{t}Bu$_3$); **^{13}C{^{1}H} NMR** (thf-d^8, 298 K): *δ* [ppm] = 32.2 (s, *C*(CH$_3$)$_3$), 32.6 (s, *C*H$_3$), 33.5 (s, *C*(CH$_3$)$_3$), 34.7 (s, *C*H$_3$), 84.4 (s, *C*H), 109.9 (s, *C*C(CH$_3$)$_3$), 110.5 (s, *C*C(CH$_3$)$_3$), 219.5 (s, *C*O); **LIFDI MS** (toluene): *m/z* (%): 1177.93 (M$^+$ - 2•[$C_{17}H_{29}Fe(CO)_3$]); **ATR-IR** (diamant crystal): ν [cm-1] = 1963 (s), 1962 (m), 1899 (s); **Elemental analysis** (%): calculated for [$C_{76}H_{116}Fe_4Sb_4O_8$] (1864.22 g·mol^{-1}): C, 48.86; H, 6.26; found: C, 49.34; H, 5.83.

7.5.2 Crystallographic Data

Crystals suitable for single crystal X-ray diffraction analysis were obtained as described above. The diffraction intensities were collected either on a Gemini Ultra diffractometer equipped with an Atlas^{S2} CCD detector and with a fine-focus sealed Cu-K$_α$ X-ray tube (**3**), a GV50 diffractometer equipped with a Titan^{S2} CCD detector and a micro-focus Cu-K$_α$ X-ray tube (**7a**), on a XtaLAB Synergy R, DW system diffractometer equipped with a HyPix-Arc 150 detector and a rotating-anode Cu-K$_α$ X-ray tube (**2a**, **2b**) or at a SuperNova diffractometer equipped with a Atlas CCD detector and a micro-focus Cu-K$_α$ X-ray tube (**7b**). Data collection and reduction were performed with **CrysAlisPro** software package.[26] The structures were solved with **Olex2**,[27] using **ShelXT**[28] and a least-square refinement on F^2 was carried out with **ShelXL**.[29] All non-hydrogen atoms were refined anisotropically. Hydrogen atoms at the carbon atoms were located in idealized positions and refined with isotropic displacement parameters according to the riding model.

Using **Olex2**,[27] all pictures of the respective molecular structures were made.

[Cp*$_2$Sb][TEF] (2a):

Compound **2a** in a concentrated DCM solution at -30 °C in form of yellow blocks in the monoclinic space group $P2_1/c$. The asymmetric unit contains two molecules of **2a**. The [TEF]- anions show some disorders, which can be solved using the restrains SADI, SIMU and DFIX.

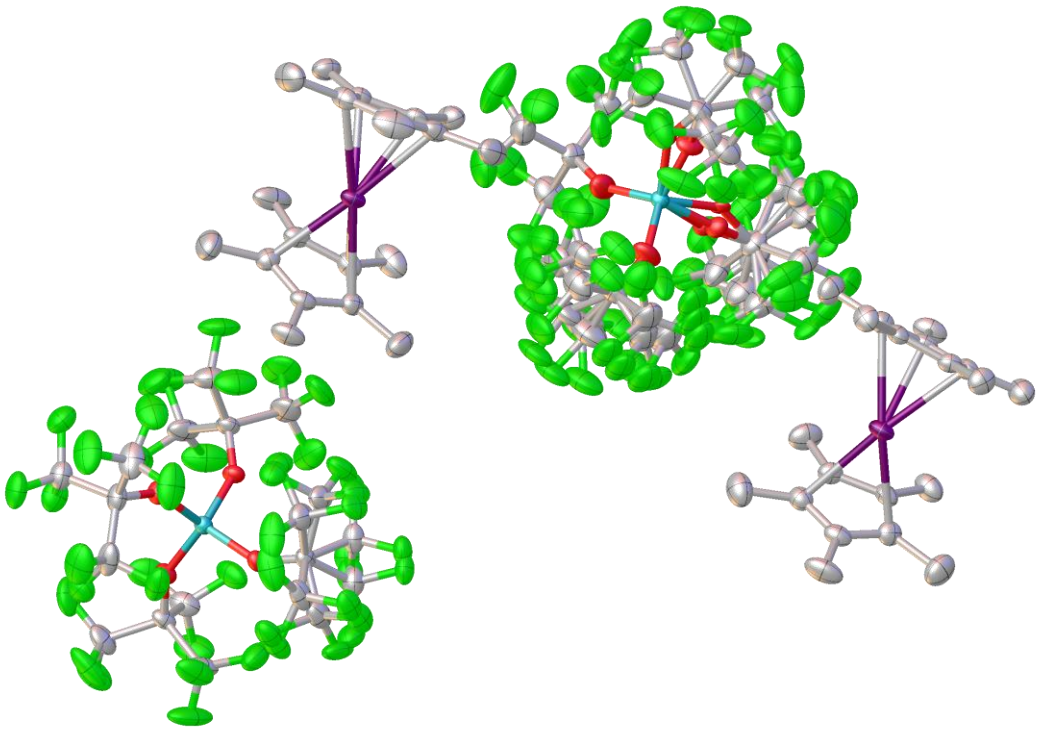

Figure S1: Molecular structure of **2a** in the solid state. Thermal ellipsoids are depicted at 50% probability level. H atoms are omitted for clarity.

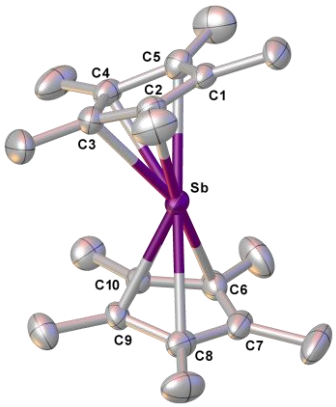

Figure S2: Molecular structure of the cationic part of **2a**. Thermal ellipsoids are depicted at 50% probability level. H atoms are omitted for clarity. Selected bond lengths [Å] and angles [°]: Sb-C6 2.599(5), Sb-C8 2.661(5), Sb-C10 2.465(5), Sb-C9 2.494(5), Sb-C2 2.660(5), Sb-C3 2.491(6), Sb-C5 2.596(5), Sb-C4 2.450(5); C2-Sb-C8 132.2(2), C5-Sb-C6 123.9(2), C5-Sb-C2 51.7(2), C8-Sb-C6 52.2(2).

[Cp*$_2$Sb][FAL] (2b):

Compound **2b** crystallizes in a concentrated DCM solution at –30°C in form of orange plates in the triclinic space group $P\bar{1}$. The asymmetric unit contains one molecule of **2b**.

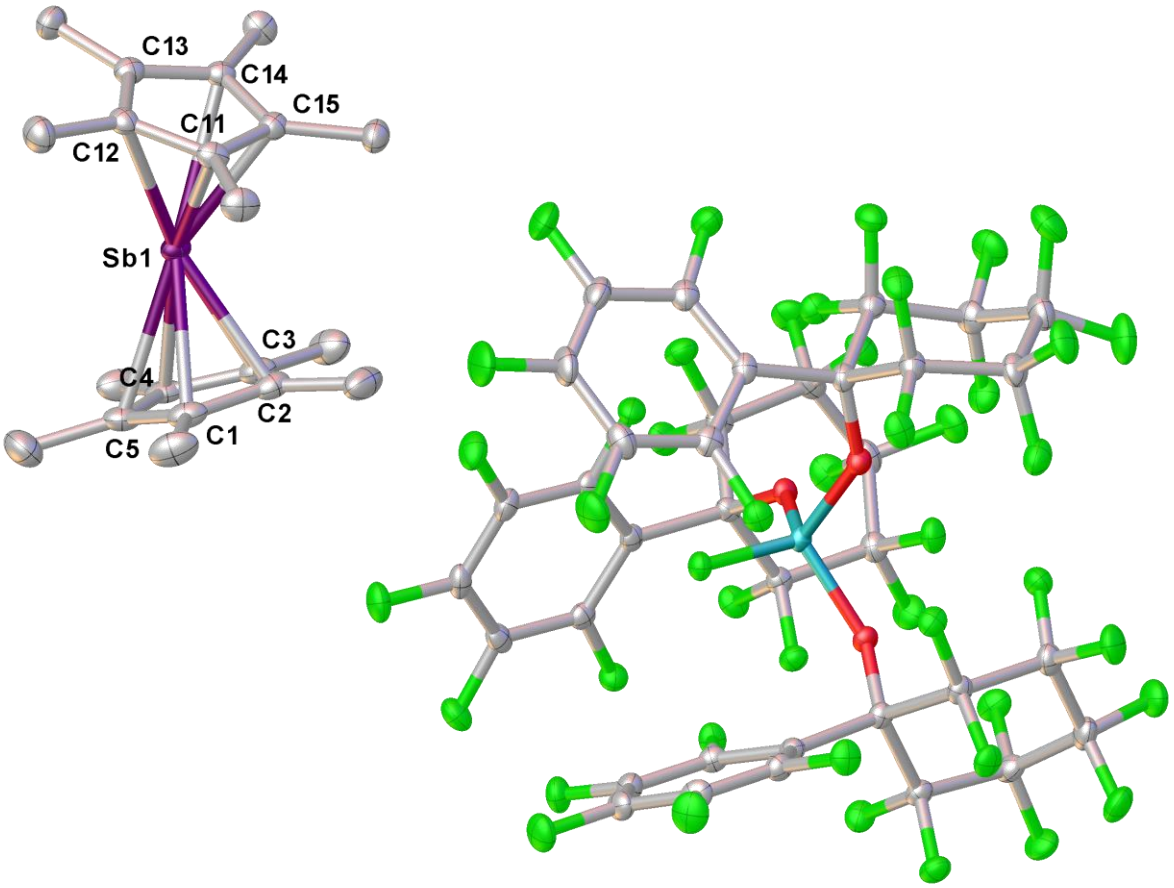

Figure S3: Molecular structure of **2b** in the solid state. Thermal ellipsoids are depicted at 50% probability level. H atoms are omitted for clarity. Selected bond lengths [Å] and angles [°]: Sb1-C15 2.479(2), Sb1-C14 2.638(2), Sb1-C4 2.676(2), Sb1-C12 2.631(2), Sb1-C5 2.655(2), Sb1-C11 2.480(2), Sb1-C1 2.512(2), Sb1-C3 2.548(2), Sb1-C2 2.451(2); C15-Sb1-C14 32.19(7), C15-Sb1-C12 53.63(7), C15-Sb1-C11 33.66(7), C12-Sb1-C14 51.68(7), C5-Sb1-C4 30.81(7), C11-Sb1-C14 53.66(7), C11-Sb1-C12 32.44(7), C11-Sb1-C1 109.03(7), C1-Sb1-C4 52.60(7), C1-Sb1-C12 123.70(7), C1-Sb1-C5 31.86(8), C1-Sb1-C3 54.26(7), C3-Sb1-C4 31.46(8), C3-Sb1-C5 52.37(8), C2-Sb1-C15 104.80(8), C2-Sb1-C4 53.49(7).

[(Cp*Mo(CO)$_3$)$_3$(μ$_3$-Sb$_3$)] (3):

Compound **3** crystallizes in a concentrated DCM solution at –30°C in form of red blocks in the monoclinic space group P2$_1$/c. The asymmetric unit contains one molecule of **3** and one DCM molecule. One Cp* ligand is disordered over two positions (occupancy of 0.5 and 0.5). The restrains SADI and SIMU were used to describe the disorder.

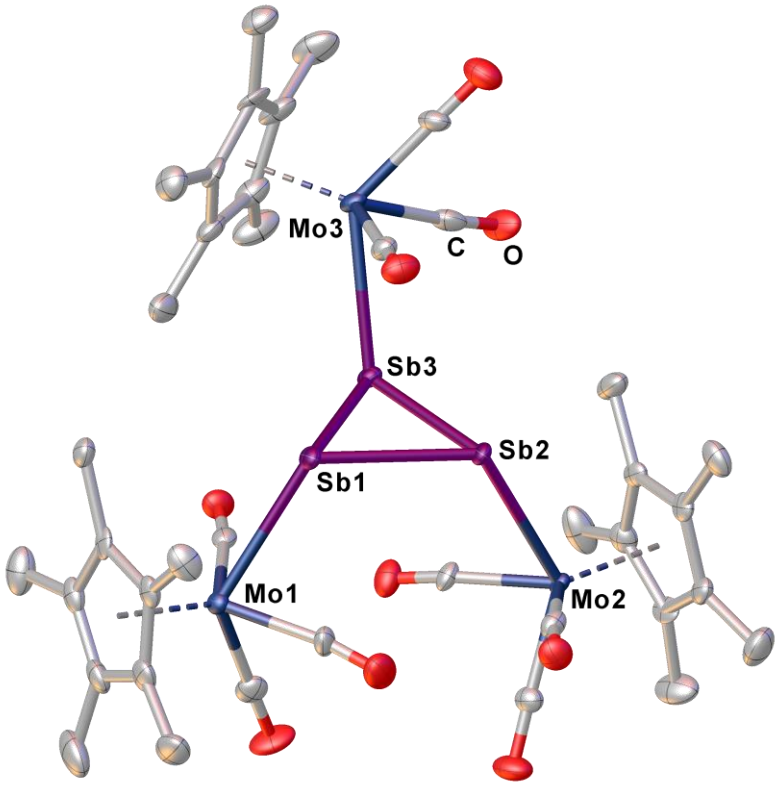

Figure S4: Molecular structure of **3** in the solid state. Thermal ellipsoids are depicted at 50% probability level. H atoms are omitted for clarity. Selected bond lengths [Å] and angles [°]: Sb1-Sb2 2.8377(5), Sb1-Sb3 2.8370(5), Sb1-Mo1 2.8930(5), Sb2-Sb3 2.8459(5), Sb2-Mo2 2.8669(6), Sb3-Mo3 2.8885(6); Sb2-Sb1-Mo1 120.904(17), Sb3-Sb1-Sb2 60.200(13), Sb3-Sb1-Mo1 105.463(16), Sb1-Sb2-Sb3 59.888(13), Sb1-Sb2-Mo2 119.245(16), Sb3-Sb2-Mo2 111.694(17), Sb1-Sb3-Sb2 59.912(13), Sb1-Sb3-Mo3 113.202(18), Sb2-Sb3-Mo3 107.283(16).

[Cp''FeSb(CO)$_2$]$_4$ (7a):

Compound **7a** crystallizes by layering a DCM solution with acetonitrile in form of green plates in the triclinic space group $P\bar{1}$. The asymmetric unit contains one molecule of **7a** and one acetonitrile molecule.

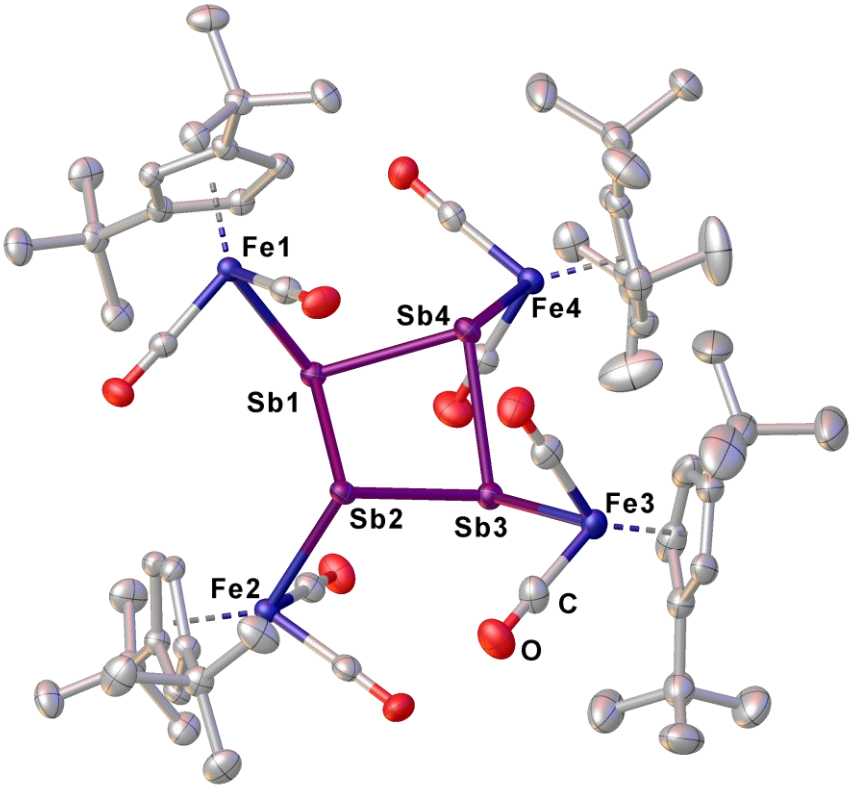

Figure S5: Molecular structure of **7a** in the solid state. Thermal ellipsoids are depicted at 50% probability level. H atoms are omitted for clarity. Selected bond lengths [Å] and angles [°]: Sb2-Sb1 2.8521(3), Sb2-Sb3 2.8384(3), Sb2-Fe2 2.6230(6), Sb1-Sb4 2.8445(3), Sb1-Fe1 2.6230(5), Sb3-Sb4 2.8654(3), Sb3-Fe3 2.6144(6), Sb4-Fe4 2.6260(6); Sb3-Sb2-Sb1 81.775(9), Fe2-Sb2-Sb1 105.595(14), Fe2-Sb2-Sb3 102.339(14), Sb4-Sb1-Sb2 81.866(9), Fe1-Sb1-Sb2 101.449(14), Fe1-Sb1-Sb4 104.330(15), Sb2-Sb3-Sb4 81.739(9), Fe3-Sb3-Sb2 105.565(15), Fe3-Sb3-Sb4 104.444(15), Sb1-Sb4-Sb3 81.438(9), Fe4-Sb4-Sb1 106.666(16), Fe4-Sb4-Sb3 105.183(16).

[Cp'''FeSb(CO)$_2$]$_4$ (7b):

Compound **7b** crystallizes by layering a toluene solution with acetonitrile in form of green plates in the orthorhombic space group *Pna*2$_1$. The asymmetric unit contains one molecule of **7b**. One [Cp'''Fe(CO)$_2$] fragment is disordered over two positions (occupancy 0.42 and 0.52). The restrains SADI und SIMU were used during the crystal structure refinement.

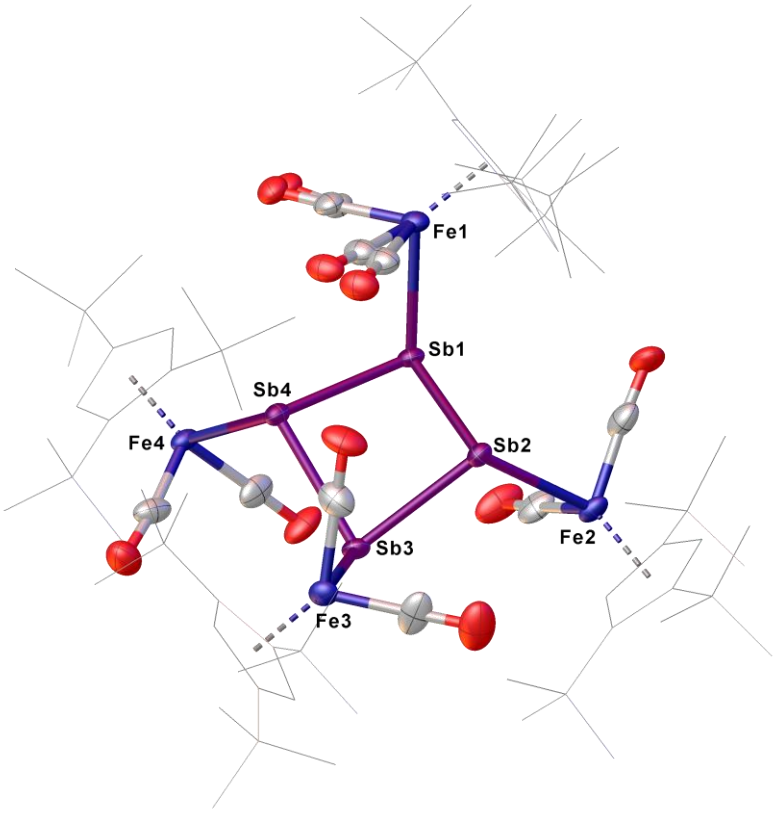

Figure S6: Molecular structure of **7b** in the solid state. Thermal ellipsoids are depicted at 50% probability level. H atoms are omitted and the Cp''' ligands are drawn in the wire frame model for clarity. Selected bond lengths [Å] and angles [°]: Sb2-Sb1 2.8628(11), Sb2-Sb3 2.8552(10), Sb2-Fe2 2.6570(19), Sb1-Sb4 2.8602(9), Sb1-Fe1 2.6501(19), Sb4-Sb3 2.8535(11), Sb4-Fe4 2.6433(19), Sb3-Fe3 2.644(2); Sb3-Sb2-Sb185.74(3), Fe2-Sb2-Sb1 103.91(5), Fe2-Sb2-Sb3 108.22(5), Sb4-Sb1-Sb2 84.15(3), Fe1-Sb1-Sb2 108.89(5), Fe1-Sb1-Sb4 102.89(5), Sb3-Sb4-Sb1 85.82(3), Fe4-Sb4-Sb1 108.61(5), Fe4-Sb4-Sb3 104.95(5), Sb4-Sb3-Sb2 84.42(3), Fe3-Sb3-Sb2 102.39(5), Fe3-Sb3-Sb4 105.02(5).

Table S1: Structure determination summary of the complexes **2a**, **2b** and **4**.

Compound	**2a**	**2b**	**3**
Formula	$C_{36}H_{30}AlF_{36}O_4Sb$	$AlC_{57}Cl_2F_{46}H_{32}O_3Sb$	$C_{40}H_{47}Cl_2Mo_3O_9Sb_3$
$D_{calc.}$/ g cm^{-3}	1.868	1.938	1.948
m/mm^{-1}	6.383	6.039	21.023
Formula Weight	1359.33	1858.45	1395.74
Colour	clear yellow	clear light orange	red
Shape	block-shaped	plate-shaped	block-shaped
Size/mm^3	0.18×0.16×0.12	0.29×0.20×0.06	0.14×0.10×0.09
T/K	123.01(10)	100.00(10)	123.1(1)
Crystal System	monoclinic	triclinic	monoclinic
Space Group	$P2_1/c$	P-1	$P2_1/c$
a/Å	21.9078(2)	13.0472(2)	8.5370(2)
b/Å	20.33870(10)	14.3850(2)	29.4147(5)
c/Å	22.0435(2)	17.8721(4)	19.2872(3)
a/°	90	90.162(2)	90
b/°	100.2420(10)	100.136(2)	100.672(2)
g/°	90	105.0430(10)	90
V/Å^3	9665.55(14)	3184.65(10)	4759.50(16)
Z	8	2	4
Z'	2	1	1
Wavelength/Å	1.54184	1.54184	1.54184
Radiation type	Cu K_α	Cu K_α	Cu K_α
θ_{min}/°	2.049	2.515	3.804
θ_{max}/°	75.523	74.264	67.075
Measured Refl's.	24123	41998	16875
Ind't Refl's	24123	12196	8391
Refl's with I≥σ(I)	22178	11866	7322
R_{int}	0.0540	0.0318	0.0445
Parameters	2092	974	615
Restraints	1980	0	241
Largest Peak	1.121	0.742	1.707
Deepest Hole	-1.294	-0.556	-1.591
GooF	1.023	1.068	1.040
wR_2 (all data)	0.1463	0.0758	0.1003
wR_2	0.1421	0.0754	0.0956
R_1 (all data)	0.0584	0.0295	0.0479
R_1	0.0540	0.0289	0.0402

Table S2: Structure determination summary of the complexes **7a** and **7b**.

Compound	**7a**	**7b**
Formula	$C_{60}H_{84}Fe_4O_8Sb_4 \cdot CH_3CN$	$C_{76}H_{116}Fe_4O_8Sb_4$
$D_{calc.}$/ g cm^{-3}	1.650	1.520
m/mm^{-1}	14.588	16.236
Formula Weight	1684.72	1868.08
Colour	black	clear violet
Shape	plate-shaped	block-shaped
Size/mm^3	0.23×0.14×0.10	0.12×0.10×0.07
T/K	123.00(13)	132(13)
Crystal System	triclinic	orthorhombic
Flack Parameter		0.050(12)
Hooft Parameter		0.012(7)
Space Group	P-1	$Pna2_1$
a/Å	10.2505(2)	27.8565(5)
b/Å	18.2944(5)	13.9634(3)
c/Å	18.7216(4)	20.9861(4)
a/°	88.540(2)	90
b/°	85.7954(18)	90
g/°	75.637(2)	90
V/Å^3	3391.80(15)	8163.0(3)
Z	2	4
Z'	1	1
Wavelength/Å	1.39222	1.54184
Radiation type	Cu K_β	Cu K_α
θ_{min}/°	3.093	3.802
θ_{max}/°	70.024	66.875
Measured Refl's.	27519	45225
Ind't Refl's	16401	12117
Refl's with I≥σ(I)	15071	10566
R_{int}	0.0280	0.0791
Parameters	737	980
Restraints	0	306
Largest Peak	2.524	1.626
Deepest Hole	-1.838	-1.504
GooF	1.089	1.025
wR_2 (all data)	0.1152	0.1425
wR_2	0.1121	0.1335
R_1 (all data)	0.0456	0.0633
R_1	0.0422	0.0538

7.5.3 NMR Investigations

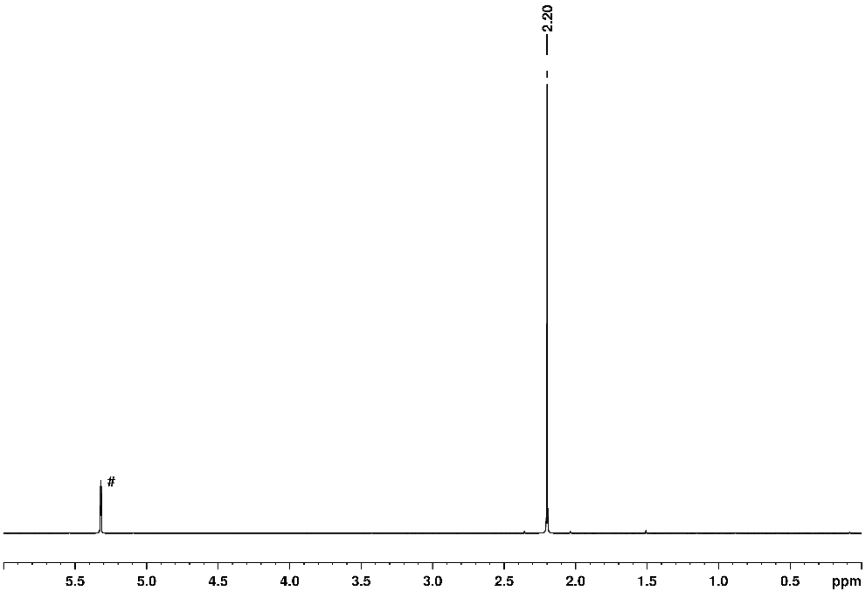

Figure S7: ^{1}H NMR spectrum of **2a** in CD_2Cl_2 (#).

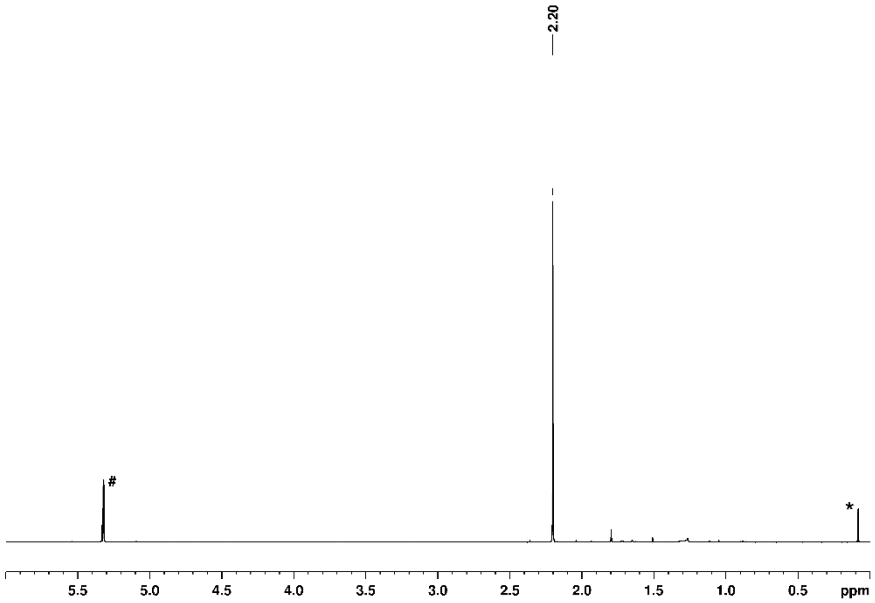

Figure S8: ^{1}H NMR spectrum of **2b** in CD_2Cl_2 (#). The signal marked with * is due to silicon grease.

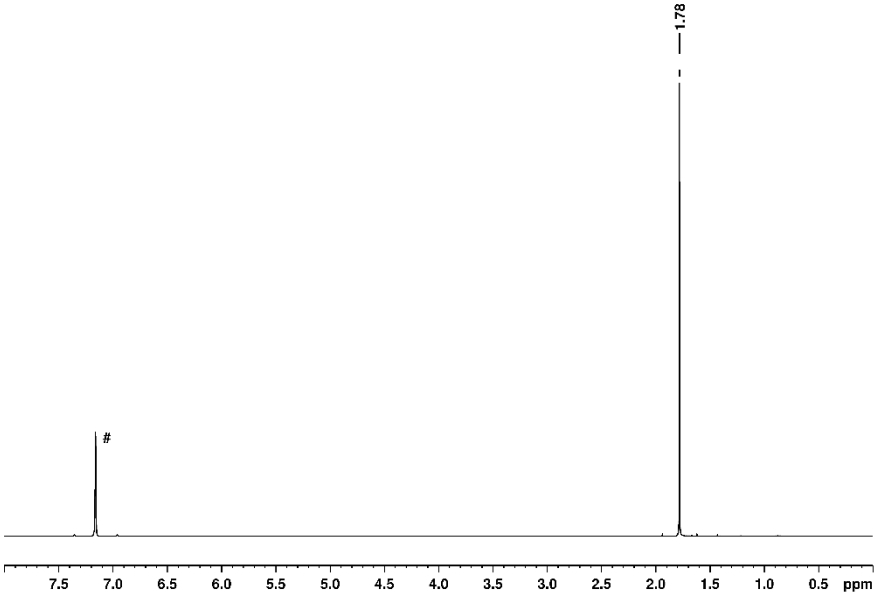

Figure S9: ^{1}H NMR spectrum of **3** in C_6D_6 (#).

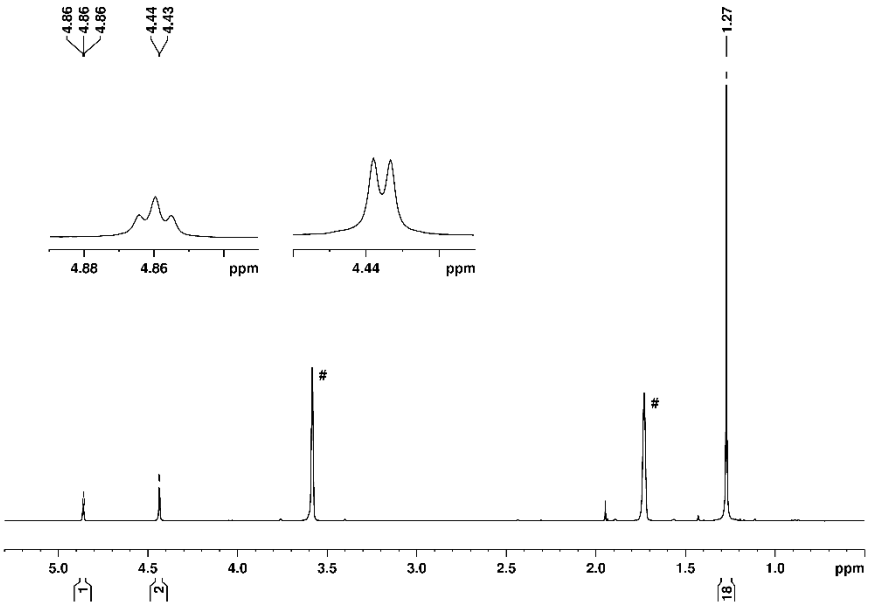

Figure S10: ^{1}H NMR spectrum of **7a** in thf-d_8 (#).

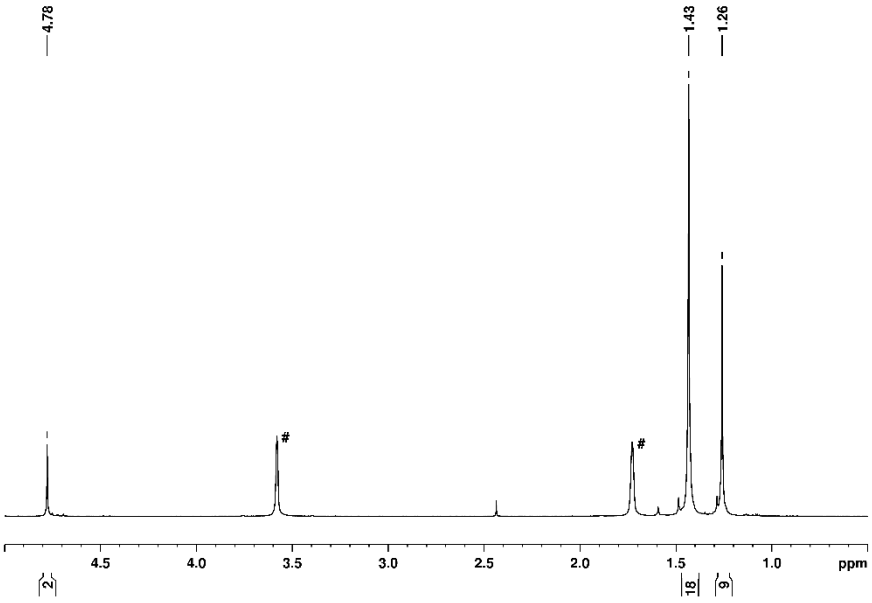

Figure S11: ^{1}H NMR spectrum of **7b** in thf-d_8 (#).

7.6 References

[1] a) A. S. Foust, M. S. Foster, L. F. Dahl, *J. Am. Chem. Soc.* **1969**, *91*, 5633–5635; b) A. S. Foust, M. S. Foster, L. F. Dahl, *J. Am. Chem. Soc.* **1969**, *91*, 5631–5633.

[2] a) C. M. Hoidn, D. J. Scott, Daniel, R. Wolf, *Chem. Eur. J.* **2020**; b) M. Caporali, L. Gonsalvi, A. Rossin, M. Peruzzini, *Chem. Rev.* **2010**, *110*, 4178–4235; c) B. M. Cossairt, N. A. Piro, C. C. Cummins, *Chem. Rev.* **2010**, *110*, 4164–4177; d) N. A. Giffin, J. D. Masuda, *Coor. Chem. Rev.* **2011**, *255*, 1342–1359; e) M. Scheer, G. Balázs, A. Seitz, *Chem. Rev.* **2010**, *110*, 4236–4256; f) O. J. Scherer, *Acc. Chem. Res.* **1999**, *32*, 751–762; g) M. Seidl, G. Balázs, M. Scheer, *Chem. Rev.* **2019**, *119*, 8406–8434.

[3] U. Vogel, G. Baum, M. Scheer, *Z. Anorg. All. Chem.* **2000**, *626*, 444–449.

[4] L. F. Dahl, A. S. Foust, *J. Am. Chem. Soc.* **1970**, *92*, 7337–7341.

[5] C. Schoo, S. Bestgen, A. Egeberg, S. Klementyeva, C. Feldmann, S. N. Konchenko, P. W. Roesky, *Angew. Chem. Int. Ed.* **2018**, *57*, 5912–5916.

[6] G. Balázs, M. Sierka, M. Scheer, *Angew. Chem. Int. Ed.* **2005**, *44*, 4920–4924.

[7] V. Heinl, A. E. Seitz, G. Balázs, M. Seidl, M. Scheer, *Chem. Sci.* **2021**, *12*, 9726–9732.

[8] H. J. Breunig, R. Rösler, E. Lork, *Angew. Chem. Int. Ed. Engl.* **1997**, *36*, 2819–2821.

[9] H. J. Breunig, N. Burford, R. Rösler, *Angew. Chem. Int. Ed. Engl.* **2000**, *39*, 4148–4150.

[10] C. Ganesamoorthy, J. Krüger, C. Wölper, A. S. Nizovtsev, S. Schulz, *Chem. Eur. J.* **2017**, *23*, 2461–2468.

[11] C. Ganesamoorthy, C. Wölper, A. S. Nizovtsev, S. Schulz, *Angew. Chem. Int. Ed.* **2016**, *55*, 4204–4209.

[12] H. Sitzmann, Y. Ehleiter, G. Wolmershäuser, A. Ecker, C. Üffing, H. Schnöckel, *J. Organomet. Chem.* **1997**, *527*, 209–2013.

[13] O. Coughlin, T. Krämer, S. L. Benjamin, *Dalton. Trans.* **2020**, *49*, 1726–1730.

[14] R. J. Wiacek, J. N. Jones, C. L. B. Macdonald, A. H. Cowley, *Can. J. Chem.* **2002**, *80*, 1518–1523.

[15] Unfortunately, all attempts to convert **3** into **4** failed, Heating of a solution leads to decomposition.

[16] T. F. Berlitz, H. Sinning, J. Lorberth, U. Müller, *Z. Naturforsch.* **1988**, *43b*, 744–748.

[17] a) F. García, A. D. Hopkins, R. A. Kowenicki, M. McPartlin, Y. Tesa, *Dalton. Trans.* **2004**, 2051–2052; b) M. Ates, H. J. Breunig, K. Ebert, S. Guelec, R. Kaller, M. Draeger, *Organometallics* **1992**, *11*, 145–150; c) O. Mundt, G. Becker, H. J. Wessely, H. J. Breunig, H. Kischkel, *Z. Anorg. All. Chem.* **1982**, *486*, 70–89; d) L. M. Opris, A. Silvestru, C. Silvestru, H. J. Breunig, E. Lork, *Dalton. Trans.* **2004**, 3575–3585; e) L. Dostál, R. Jambor, A. Růžička, J. Holeček, *Organometallics* **2008**, *27*, 2169–2171; f) H. J. Breunig, J. Pawlik, *Z. Anorg. Allg. Chem.* **1995**, *621*, 817–822; g) H. J. Breunig, R. Rösler, E. Lork, *Z. Anorg. Allg. Chem.* **1999**, *625*, 1619–1623.

[18] a) S. S. Chitnis, Y.-Y. Carpenter, N. Burford, R. McDonald, M. J. Ferguson, *Angew. Chem. Int. Ed.* **2013**, *52*, 4863–4866; b) C. J. Warren, D. M. Ho, R. C. Haushalter, A. B. Bocarsly, *Angew. Chem. Int. Ed. Engl.* **1993**, *32*, 1646–1648.

[19] I. Krossing, *Chem. Eur. J.* **2001**, *7*, 490–502.

[20] T. Köchner, N. Trapp, T. A. Engesser, A. J. Lehner, C. Röhr, S. Riedl, C. Knapp, H. Scherer, I. Krossing, *Angew. Chem. Int. Ed.* **2011**, *50*, 11253–11256.

[21] G. Rabe, H. W. Roesky, D. Stalke, F. Pauer, G. M. Sheldrick, *J. Organomet. Chem.* **1991**, *403*, 11–19.

[22] J. J. Schneider, D. Wolf, C. Janiak, O. Heinemann, J. Rust, C. Krüger, *Chem. Eur. J.* **1998**, *4*, 1982–1991.

[23] M. Scheer, K. Schuster, U. Becker, A. Krug, H. Hartung, *J. Organomet. Chem.* **1993**, *460*, 105–110.

[24] C. Schwarzmaier, A. Y. Timoshkin, G. Balázs, M. Scheer, *Angew. Chem. Int. Ed.* **2014**, *53*, 9077–9081.

[25] The solution of [(Cp'''Ni)$_2$tol] was prepared with instructions of the working group of *Sitzmann*.

[26] Rigaku Oxford Diffraction, *CrysAlisPro Software System Version 1.171.38.43*, **2015**.

[27] L. J. Bourhis, O. V. Dolomanov, R. J. Gildea, J. A. K. Howard, H. Puschmann, *J. Appl. Crystallogr.* **2009**, *42*, 339–341.

[28] G. M. Sheldrick, *Acta Crystallogr., Sect, A* **2015**, *71*, 3–8.

[29] G. M. Sheldrick, *Acta Crystallogr., Sect, C* **2015**, *71*, 3–8.

8 Thesis Treashury

The following chapter includes unpublished results generated during this Ph.D. thesis, which could not be included in other chapters. Furthermore, some of the mentioned compounds could not be fully characterized. However, the achieved data are presented and discussed in order to include them in future publications or research efforts.

8.1 Synthesis of $Li_2[(Cp''_2Zr)_2(\mu,\eta^{1:1}\text{-}N_2)]$ (T1)

Synthesis of $Li_2[(Cp''_2Zr)_2(\mu,\eta^{1:1}\text{-}N_2)]$ (T1)

The activation, functionalization and bond cleavage of dinitrogen is an active field of chemical research.[1,2] In industry, the synthesis of NH_3 by the reduction of N_2 is of imminent importance. Biological systems use enzymes for the activation of N_2 under mild conditions. However, large scale industrial synthesis occurs under harsh reaction conditions.[1] For this reason, a precise activation and further functionalization of N_2 on transition metal centers to achieve complete conversion to NH_3 under mild reaction conditions, to mimic the natural processes, are desirable.

The reaction of $[Cp''_2ZrCl_2]$ (Cp'' = 1,3-di-tertbutyl-cyclopentadienyl) with ^{t}BuLi under an atmosphere of nitrogen leads to the formation of the ionic compound $Li_2[(Cp''_2Zr)_2(\mu,\eta^{1:1}\text{-}N_2)]$ (**T1**). In the first step $[Cp''_2ZrCl_2]$ is reduced, followed probably by coordination and activation of dinitrogen. The driving force of the reaction is the formation of LiCl (Scheme 1). **T1** shows a high solubility even in *n*-pentane or hexamethyldisiloxane.

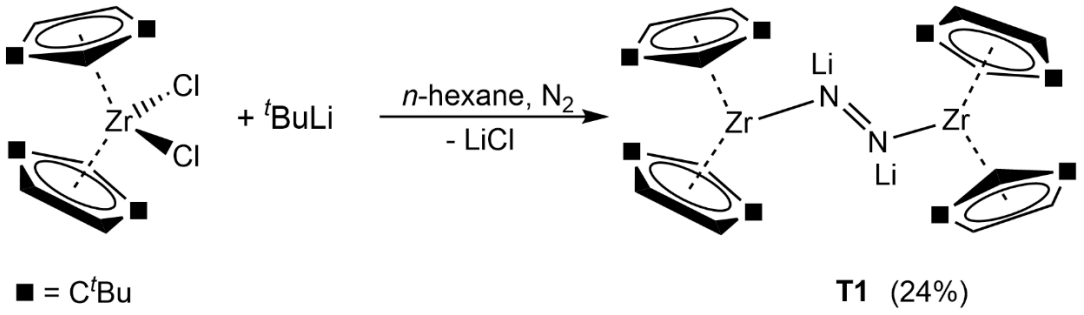

Scheme 1: Synthesis of **T1** by the reduction of $[Cp''_2ZrCl_2]$ with ^{t}BuLi under an atmosphere of dried nitrogen.

Conspicuous is the dependency of the color of the reaction solution and its concentration. A concentrated solution of **T1** possesses an orange colour, but in diluted solution a violet color can be observed. This observation with the fact that the color of the solution changes

immediately to violet if it is exposed to air, a release of the fixed nitrogen in **T1** in diluted solution is assumed.

The recorded ^{1}H NMR spectrum for **T1** shows one set of signals for the four magnetic equivalent Cp'' ligands. However, the ^{t}Bu groups and all protons located on the five-membered ring are magnetically inequivalent. Therefore, two singlets (δ = 1.39 ppm, 1.43 ppm) and three triplets (δ = 4.93 ppm, 5.16 ppm, 5.80 ppm) can be observed. This is confirmed by the $^{13}C\{^{1}H\}$ NMR spectrum, which contains 9 Signals for the magnetically inequivalent carbon atoms. ^{7}Li NMR measurements show two signals (figure 1), whereas the broad singlet at δ = -3.7 ppm is assigned to **T1**. We assume, that the sharp singlet at δ = -2.4 ppm is caused by LiCl. During the reaction and crystallization process always a hardly soluble porous white solid is formed, probably LiCl which supports the assumption. No ^{t}BuLi residue is observed in the spectrum, which should arise around 1 ppm.[3]

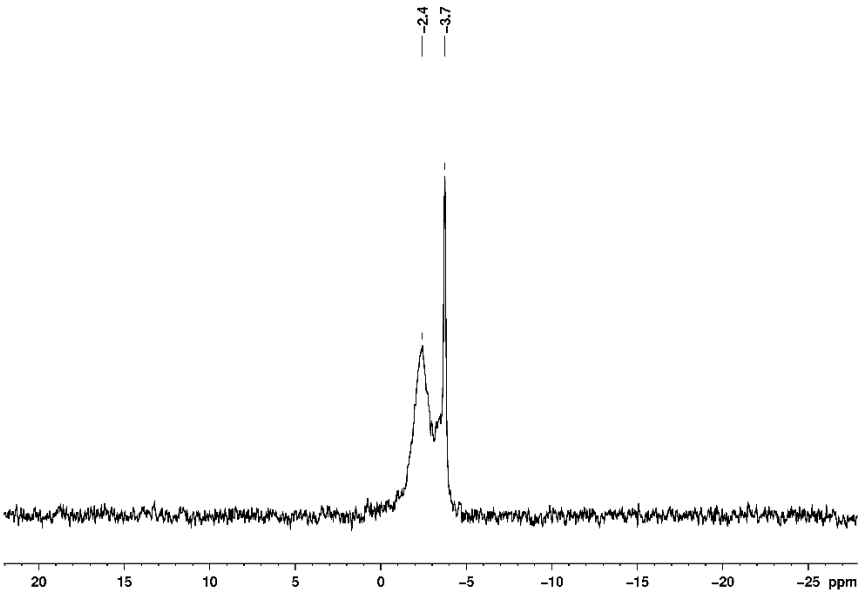

Figure 1: ^{7}Li NMR spectrum of **T1** in $CDCl_3$.

Crystals of **T1** suitable for single crystal X-ray diffraction analysis can be obtained by storing a concentrated solution in hexamethyldisiloxane at -78 °C. The molecular structure is depicted in figure 2 (left). Two [Cp''$_2$Zr]-fragments are bridged by an N_2 unit in a terminal fashion. Furthermore, the lithium ions are located above the N-N bond. The Zr-N distances of 1.9600(18) Å are in agreement with the literature and correspond to usual Zr-N single bonds.[4,5,6] With 1.336(4) Å the N-N distance is in the region of an elongated double bond (cal.: N-N: 1.40 Å; N=N: 1.2 Å).[2,5–8] Noteworthy are the rather short Li-H distances (2.057 Å to 2.082 Å), elucidated in figure 2 (right). An interaction between the lithium ions and hydrogen atoms located on the Cp'' ligands can be supposed. This is in agreement with the observations

made in the ^{1}H NMR spectrum as mentioned before, *i.e.* the not equivalent Cp" ligands. **T1** represents a rare example of a dinuclear zirconium complex with an end-on coordinated nitrogen ligand. There is only one other example known, the compound $[CpZr(^{i}Pr_2PCH_2SiMe_2)_2(\mu,\eta^{1:1}\text{-}N_2)]$.[7]

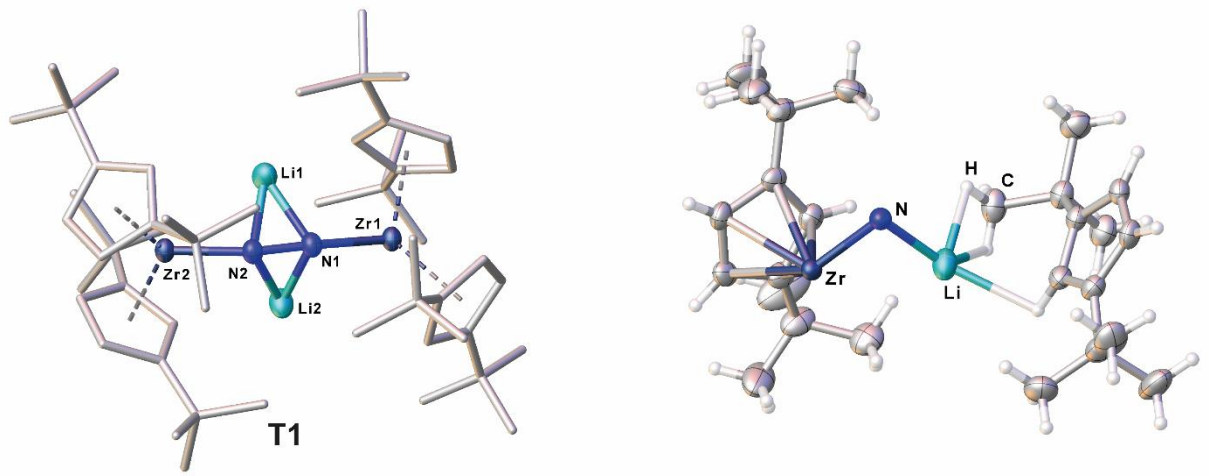

Figure 2: Left: molecular structure of **T1** in the solid state with thermal ellipsoids at 50% probability level. H atoms are omitted and Cp" ligands are drawn in the tube model for clarity. Right: Half of the molecular structure of **T1** is depicted to illustrate the short Li-H distances.

The activation of dinitrogen on a zirconium center and therefore the synthesis of $Li_2[(Cp''_2Zr)_2(\mu,\eta^{1:1}\text{-}N_2)]$ (**T1**) enables an interesting pathway for further investigations. Possibly a stepwise functionalization or precise release of the nitrogen ligand could be future approaches.

8.2 Reactivity of $KSb(SiMe_3)_2$ towards transition metal complexes

The reactivity of polyantimony ligand complexes is an interesting field of chemical research. However, there are only a few reactivity studies known. This is owed to the sensitivity of antimony containing compounds towards light and air as well as the weak Sb-Sb bond.[9] Furthermore, most challenging is the search for a suitable starting material. Different approaches were described in the literature, *e.g.* the usage of the organo substituted compounds R_4Sb_4[10,11] or Sb-nanoparticles.[12] Furthermore, also antimony salts, such as $Li\{Sb(H)CH(SiMe_3)_2\}$[13] or $KSb(SiMe_3)_2$,[14] show a high potential in this field, even if only a few examples of such reactions are known. In 2005 our group succeeded in the synthesis of an antimony-tungsten triple bond by the reaction of $[(N_3N)WCl]$ with $Li\{Sb(H)CH(SiMe_3)_2\}$ (N_3N = tren = $N(CH_2CH_2NSiMe_3)_3$)).[13] Recently, the triple decker complex $[(Cp''Zr)_2(\mu,\eta^{1:1:1:1:1:1}\text{-}Sb_6)]$ was obtained using $KSb(SiMe_3)_2$, which also show high potential as starting material for further synthesis.[14] For this reason, the reactivity of $KSb(SiMe_3)_2$ towards transition metal precursors was investigated

8.2.1 Reaction of $KSb(SiMe_3)_2$ with $[(COD)RuCl]_2$

The reaction of the rhodium complex $[(COD)RhCl]_2$ (COD = 1,5-cyclo-octadiene) with $KSb(SiMe_3)_2$ was performed. Thus, a solution of $KSb(SiMe_3)_2$ in THF was added to a solution of the rhodium complex in THF at r.t. Depending on the solubility of the products two fractions can be obtained during the workup. In *n*-hexane a brown fraction, in toluene an orange fraction is eluted. From both a few crystals of $[(COD)RhSb(SiMe_3)]_2$ were be obtained (Scheme 2, **T2**). Therefore, it is presumable that **T2** is maybe formed during the crystalization process. **T2** was comprehensively characterized by single crystal X-ray diffraction analysis, NMR spectroscopy and mass spectrometry.

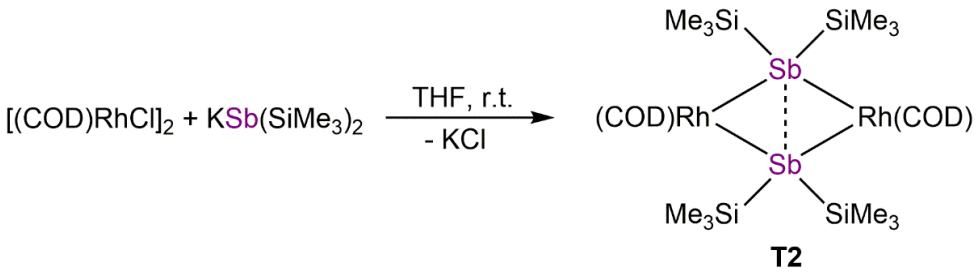

Scheme 2: Synthesis of **T2** in THF by the reaction of $[(COD)RhCl]_2$ with $KSb(SiMe_3)_2$.

In the ^1H NMR spectrum of **T2** four signals can be detected. The singlet at δ = 0.61 ppm corresponds to the methyl groups of the silyl substituents. Furthermore, three signals

assignable to the COD ligands (δ = 1.6 ppm, 2.16 ppm and 4.91 ppm) can be observed. LIFDI MS of the isolated crystals of **T2** shows the molecular ion peak.

Crystals of **T2** suitable for single crystal X-ray diffraction analysis were obtained by layering a toluene solution with acetonitrile. The molecular structure of **T2** is shown in figure 3. Two (COD)Rh fragments are bridged by two $Sb(SiMe_3)_2$ units. The Rh-Sb distances of 2.6311(2) Å to 2.6626(2) Å are in the range of a single bond and in agreement with the literature.[15] Even if the Sb-Sb distance of 3.2285(2) Å is quite short, it is longer than a usual Sb-Sb single bond[11,16] and exceeded the sum of the single bond covalent radii.[17] Therefore, an Rh_2Sb_2 cycle can be assumed. The planar ring show a kite-like distortion, whereby the Sb atoms are inclined to each other (Rh-Sb-Rh: 104.270(7)° and 104.385(7)°, Sb-Rh-Sb: 74.880(6)° and 75.402(6)°). There are only few examples known for rhodium antimony complexes and **T2** represents the first with silyl groups attached to the antimony atoms. Even these possibly enable further synthetic modifications.

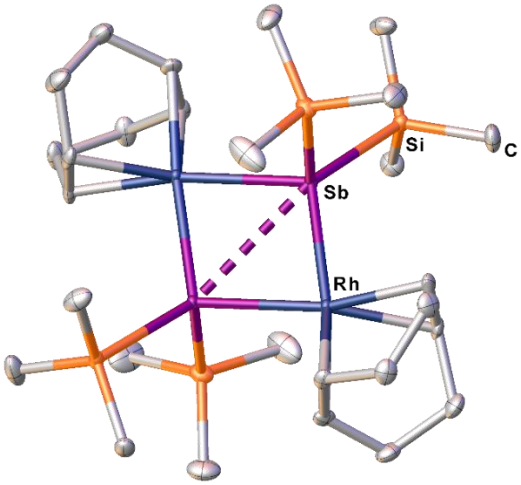

Figure 3: Molecular structure of **T2** in the solid state with thermal ellipsoids at 50% probability level. Hydrogen atoms are omitted for clarity.

8.2.2 Reaction of $KSb(SiMe_3)_2$ with $[Cp^*RhCl]_4$

The reaction of $[Cp^*RuCl]_4$ ($Cp^* = C_5Me_5$) with $KSb(SiMe_3)_2$ in THF at r.t. leads after chromatographic workup to the two products $[(Cp^*Ru)_2(Sb_2)(SiMe_2)_2]$ (**T3**) and $[(Cp^*Ru)_2(Sb_4Cl_4)]$ (**T4**). Unfortunately, only a few crystals could be isolated and the content of some fractions is still unknown.

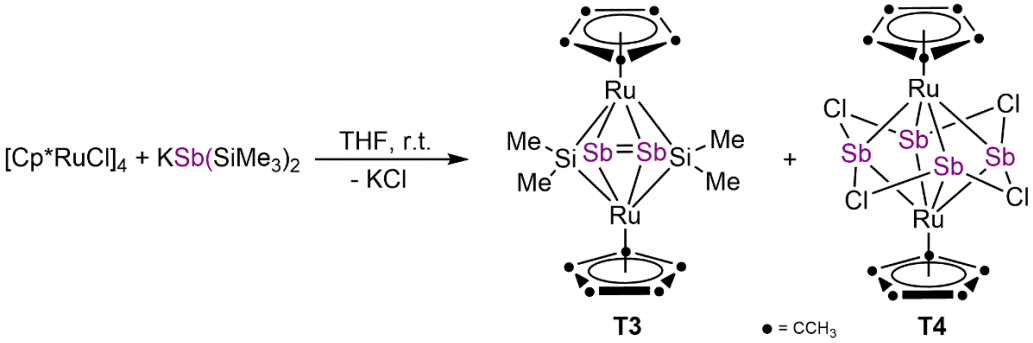

Scheme 4: Synthesis of **T3** and **T4** by the reaction of $[Cp^*RuCl]_4$ with $KSb(SiMe_3)_2$.

Crystals of **T3** and **T4** suitable for single crystal X-ray diffraction analysis can be obtained by layering a toluene (**T3**) or DCM (**T4**) solution with acetonitrile. The molecular structures are depicted in figure 4. **T3** consists of two Cp*Ru fragments, which are bridged by a Sb_2- and two $SiMe_2$- units. They are located in plane between the ruthenium fragments. A Sb-Sb distance of 2.6485(8) Å is indicative for a double bond, confirmed by examples in the literature, such as in distibenes RSb=SbR (2.6310(5) Å to 2.8642(6) Å).[18] Furthermore, the Sb···Si distance of 3.0481(17) Å is much longer than the sum of the single-bond covalent radii (2.56 Å),[17] indicating no bonding interaction between them. The three fragments are coordinating only to ruthenium. Compound **T4** can best be described as a triple decker complex. A planar Sb_4Cl_4-unit forms the middle and coordinates via the antimony atoms to the Cp*Ru fragments. The Sb-Sb distances of 3.2158(7) Å to 3.2195(7) Å are longer than reported single bonds. Within the Sb_4Cl_4-unit Cl-Sb-Cl angles of 161.52(6)° to 160.34(6)° are shown. Ruthenium antimony complexes are known, but normally the antimony units bearing organic substituents or only a single antimony atom is coordinated. Related to **T4** is maybe the $[Sb_6(RuCp^*)_2]^{2-}$ ion published by Eichhorn *et. al.* There, a boat like Sb_6 unit is coordinated by two Cp*Ru fragments.[19] Besides this remarkable example, no comparable examples similar to **T3** and **T4** can be found in the literature.

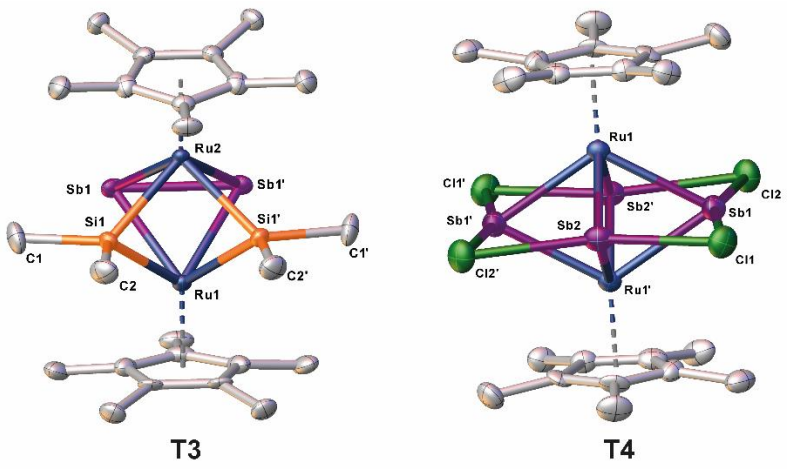

Figure 4: Left: Molecular structure of **T3** in the solid state with thermal ellipsoids at 50% probability level. Hydrogen atoms are omitted for clarity. Right: Molecular structure of **T4** in the solid state with thermal ellipsoids at 50% probability level. Hydrogen atoms are omitted for clarity.

The ^{1}H NMR spectrum of **T3** shows two singlets at δ = 0.35 ppm and 1.05 ppm for the methyl groups bound to the Si atoms and one singlet for the Cp* ligands at δ = 2.02 ppm. LIFDI MS measurements show the molecular ion peak. Unfortunately, in the ^{1}H NMR spectrum of **T4** three singlets (δ = 1.67 ppm, 1.88 ppm, 1.89 ppm) in the region of Cp*-ligands can be observed, indicating more than one crystalline compound in fraction 5. Furthermore, in LIFDI MS only fragments for **T4** were observed.

The synthesis of the ruthenium antimony complexes $[(Cp^*Ru)_2(Sb_2)(SiMe_2)_2]$ (**T3**) and $[(Cp^*Ru)_2(Sb_4Cl_4)]$ (**T4**) show with their unusual connectivity a high potential in the field of the synthesis of polyantimony ligand complexes. Even if the right way for the synthesis has not been found yet, future works on the improvement of such reactions and further applications would offer a great topic.

8.3 Supporting Information

8.3.1 Experimental Details

All experiments were performed under an atmosphere of dry nitrogen or argon using Schlenk and glovebox techniques. Solvents were purified, dried and degassed prior use. ^{1}H, ^{13}C and ^{7}Li NMR spectra were recorded at room temperature on a Bruker Avance 400 spectrometer (^{1}H: 400,130 MHz, ^{13}C: 100.613 MHz, ^{7}Li: 155.506 MHz). ^{1}H, ^{13}C and ^{7}Li chemical shifts are reported in parts per million (ppm) relative to external standards Me_4Si and LiCl (1M in D_2O). Elemental analysis was determined with a Vario micro cube apparatus. For mass spectrometry, a Finnigan MAT 95 (LIFDI MS, FD MS) or a Finnigan MAT SSQ 710 A (EI MS) device and a Joel AccuTOF GCX spectrometer were used. $[Cp''_2ZrCl_2]$[20] and $K(SbSiMe_3)_2$[21] were prepared according to literature procedures. $[(COD)RhCl]_2$ and $[Cp^*RuCl]_4$ were available in our working group.

Preparation of $Li_2[(Cp''_2Zr)(\mu,\eta^{1:1}\text{-}N_2)]$ (T1):

^{t}BuLi (2.3 mL, 1.7 mol/L, 3.9 mmol) in *n*-pentane is added to a solution of $[Cp''_2ZrCl_2]$ (1.01 g, 1.95 mmol) in 200 mL *n*-pentane via syringe in an atmosphere of dried nitrogen. The reaction solution is stirred at r.t. for 1 h, whereby a color change to violet can be observed after 10 min. A violet solution of **T1** is obtained after filtration over diatomaceous earth. A white solid remains on the frit. Crystals of **T1** suitable for single crystal X-ray structure analysis are obtained by storing a concentrated hexamethyldisiloxane solution at -78 °C. Crystalline Yield: 217 mg (0.233 mmol, 24%)

T1: ^{1}H NMR (C_6D_6, 298 K): δ [ppm] = 1.39 (s, 36 H, CCH_3), 1.43 (s, 36 H, CCH_3), 4.93 (t, 4 H, $C_5H_3{}^{t}Bu_2$), 5.16 (t, 4 H, $C_5H_3{}^{t}Bu_2$), 5.80 (t, 4 H, $C_5H_3{}^{t}Bu_2$), **$^{13}C\{^{1}H\}$ NMR** (C_6D_6, 298 K): δ [ppm] = 32.4 (s, $C_5H_2(C(CH_3)_3)$), 32.8 (s, $C_5H_2(C(CH_3)_3)$), 32.9 (s, $C_5H_2(C(CH_3)_3)$), 33.3 (s, $C_5H_2(C(CH_3)_3)$), 94.4 (s, $C_5H_3(C(CH_3)_2)$), 98.6 (s, $C_5H_3(C(CH_3)_2)$), 102.9 (s, $C_5H_3(C(CH_3)_2)$), 136.5 (s, $C_5H_3(C(CH_3)_2)$), 141.5 (s, $C_5H_3(C(CH_3)_2)$), **^{7}Li NMR** ($CDCl_3$, 298 K): δ [ppm] = -2.4 (s, br, $\omega_{1/2}$ = 180 Hz); **ES MS** (dme): *m*/*z* (%): 918.5 (M^-). No satisfying elemental analysis could be obtained, even by using Sn capsules.

Preparation of $[(COD)RhSb(SiMe_3)]_2$ (T2):

A solution of $KSb(SiMe_3)_2$ (60 mg, 0.19 mmol) in 5 mL THF is added to a solution of $[(COD)RhCl]_2$ (48 mg, 0.097 mmol) in 5 mL THF at r.t. Immediately the color changes to brown. After stirring the reaction solution for 1 d, the solvent is removed *in vacuo*. The brown solid was extracted with *n*-hexane and filtered via cannula. The content of this fraction is still

unknown. The residue was diluted in toluene and filtered via cannula (orange solution). Crystals of **T2** suitable for single crystal X-ray structure analysis are obtained by layering a concentrated toluene solution with acetonitrile. Crystalline Yield: A few crystals

T2: **^{1}H NMR** (C_6D_6, 298 K): δ [ppm] = 0.61 (s, 18 H, Si(CH_3)), 1.60 (d, 4 H, C_8H_{12}), 2.16 (m, 4 H, C_8H_{12}), 4.91 (s, br, 4 H, C_8H_{12}); **LIFDI MS** (toluene): *m*/*z* (%): 957.99 (M^+, 100); Due to the small amount of **T2** no elemental analysis could be performed.

Preparation of [(Cp*Ru)$_2$(Sb$_2$)(SiMe$_2$)$_2$] (T3) and [(Cp*Ru)$_2$(Sb$_4$Cl$_4$)] (T4):

A solution of KSb($SiMe_3$)$_2$ (226 mg, 0.736 mmol) in 10 mL THF is added to a solution of [Cp*RuCl]$_4$ (200 mg, 0.184 mmol) in 10 mL THF at r.t. After stirring for 1 d the solvent is removed *in vacuo* and subsequent column chromatographic workup (SiO_2, *n*-hexane, 18 x 3 cm) yields five fractions. With *n*-hexane, an orange fraction is eluted. An orange fraction of **T3** can be obtained with a mixture of *n*-hexane and toluene (1:1), followed by a brown fraction. The fourth fraction is eluted with a mixture of DCM and THF (1:1). Finally, a brown fraction of **T4** can be obtained using THF. Fraction 1, 3 and 4 are still unknown. Crystals suitable for single crystal X-ray diffraction analysis can be obtained by layering a toluene (**T3**) or DCM (**T4**) solution with acetonitrile. Crystalline yield of **T3** and **T4**: A few Crystals.

T3: **^{1}H NMR** (thf-d^8, 298 K): δ [ppm] = 0.35 (s, 6 H, Si(CH_3)), 1.05 (d, 6 H, Si(CH_3)), 2.02 (s, 30 H, C5(C_5H_{15})); **LIFDI MS** (toluene): *m*/*z* (%): 833.90 (M^+, 100); Due to the small amount no elemental analysis could be performed.

T4: **LIFDI MS** (toluene): *m*/*z* (%): 237.4 ([Cp*Ru]$^+$) 239.0 ([Cp*Rutol]$^+$); Due to the small amount of **T2** no elemental analysis could be performed.

8.3.2 Crystallographic Data

Crystals suitable for single crystal X-ray diffraction analysis were obtained as described above. The diffraction intensities were collected either on a Gemini Ultra diffractometer equipped with a GV50 diffractometer equipped with a Titan^{S2} CCD detector and a micro-focus Cu-K_α X-ray tube (**T1**), on a XtaLAB Synergy R, DW system diffractometer equipped with a HyPix-Arc 150 detector and a rotating-anode Cu-K_α X-ray tube (**T2**, **T4**) or at a SuperNova diffractometer equipped with an Atlas CCD detector and a micro-focus Cu-K_α X-ray tube (**T3**). Data collection and reduction were performed with **CrysAlisPro** software package.[23] The structures were solved with **Olex2**,[24] using **ShelXT**[25] (**T1**, **T2**, **T3**, **T4**) and a least-square refinement on F^2 was carried out with **ShelXL** (**T1**, **T3**, **T4**)[26] or **olex2.refine** (**T2**).[27] All non-hydrogen atoms were refined anisotropically. Hydrogen atoms at the carbon atoms were located in idealized positions and refined with isotropic displacement parameters according to the riding model.

Using **Olex2**,[24] all pictures of the respective molecular structures were made.

$Li_2[(Cp''_2Zr)(\mu,\eta^{1:1}\text{-}N_2)]$ (T1):

Compound **T1** crystallizes by storing a concentrated solution in hexamethyldisiloxane in form of orange blocks in the monoclinic space group C2/*c*. The asymmetric unit contains half of a molecule of **T1**.

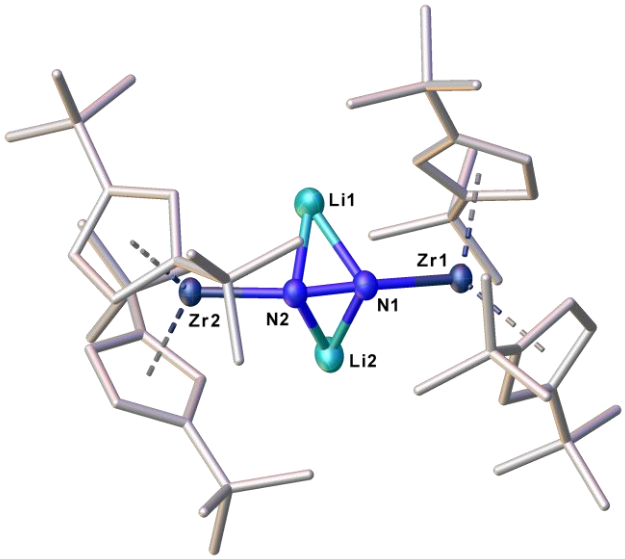

Figure S1: Molecular structure of **T1** in the solid state with thermal ellipsoids at 50% probability level. Hydrogen atoms are omitted for clarity. Selected bond lengths [Å] and angles [°]: Zr1-N1 1.9600(18), Zr1-Li1 2.881(4), N1-N2 1.336(4), N1-Li1 1.950(5), N1-Li2 1.995(5); N1-Zr1-Li1 42.41(10), Zr1-N1-Li2 105.53(14), N2-N1-Zr1 164.65(8), N2-N1-Li1 72.04(17), N2-N1-Li2-68.39(16), Li1-N1-Zr1 94.90(15), N1-Li1-N2 39.57(13), Li1-N1-Li2 93.9(3).

[(COD)Rh)Sb(SiMe$_3$)]$_2$ (T2):

Compound **T2** crystallizes by layering a toluene solution with acetonitrile in form of orange blocks in the triclinic space group *P*-1. The asymmetric unit contains one molecule of **T2**.

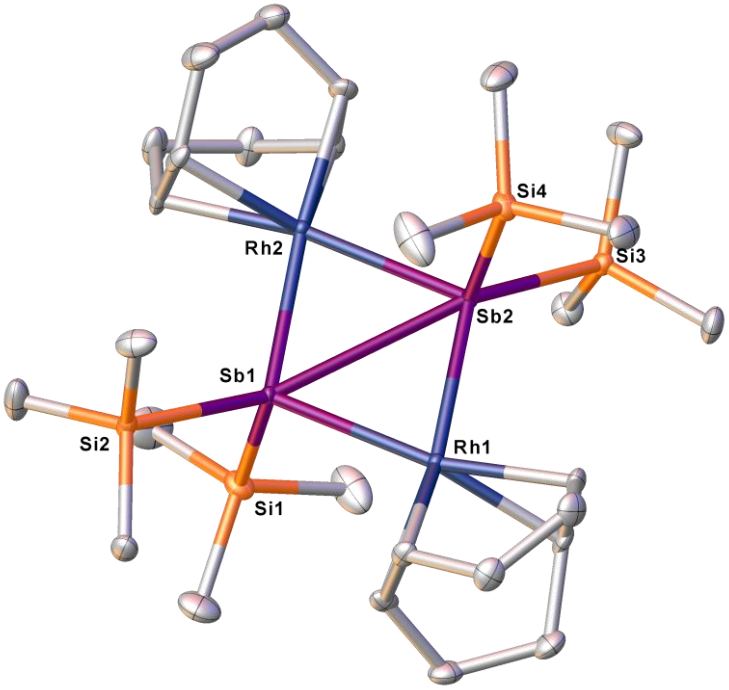

Figure S2: Molecular structure of **T2** in the solid state with thermal ellipsoids at 50% probability level. Hydrogen atoms are omitted for clarity. Selected bond lengths [Å] and angles [°]: Sb1-Sb2 3.2285(2), Sb1-Rh1 2.6480(2), Sb1-Rh2 2.6311(2), Sb1-Si1 2.5486(7), Sb1-Si2 2.5545(7), Sb2-Rh1 2.6626(2), Sb2-Rh2 2.6480(2), Sb2-Si3 2.5508(7), Sb2-Si4 2.5570(7); Rh1-Sb1-Sb2 52.766(5), Rh2-Sb1-Sb2 52.536(5), Rh2-Sb1-Rh1 105.270(7), Rh1-Sb2-Sb1 52.354(5), Rh2-Sb2-Sb1 52.062(5), Rh2-Sb2-Rh1 104.385(7), Sb2-Rh1-Sb1 74.880(6), Sb2-Rh2-Sb1 75.402(6), Si1-Sb1-Sb2 151.249(18), Si1-Sb1-Rh1 122.262(17), Si1-Sb1-Rh2 120.955(17), Si2-Sb1-Sb2 103.586(18), Si2-Sb1-Rh1 99.487(19), Si2-Sb1-Rh2 98.731(18), Si2-Sb1-Si1 105.15(2), Si3-Sb2-Sb1 148.409(17), Si3-Sb2-Rh1 124.949(17), Si3-Sb2-Rh2 119.218(17), Si4-Sb2-Sb1 105.744(18), Si4-Sb2-Rh1 98.471(18), Si4-Sb2-Rh2 98.865(18), Si4-Sb2-Si3 105.69(2).

[(Cp*Ru)$_2$(Sb$_2$)(SiMe$_2$)$_2$] (T3):

Compound **T3** crystallizes by layering a toluene solution with acetonitrile in form of red blocks in the orthorhombic space group *Pnma*. The asymmetric unit contains half of a molecule of **T3**.

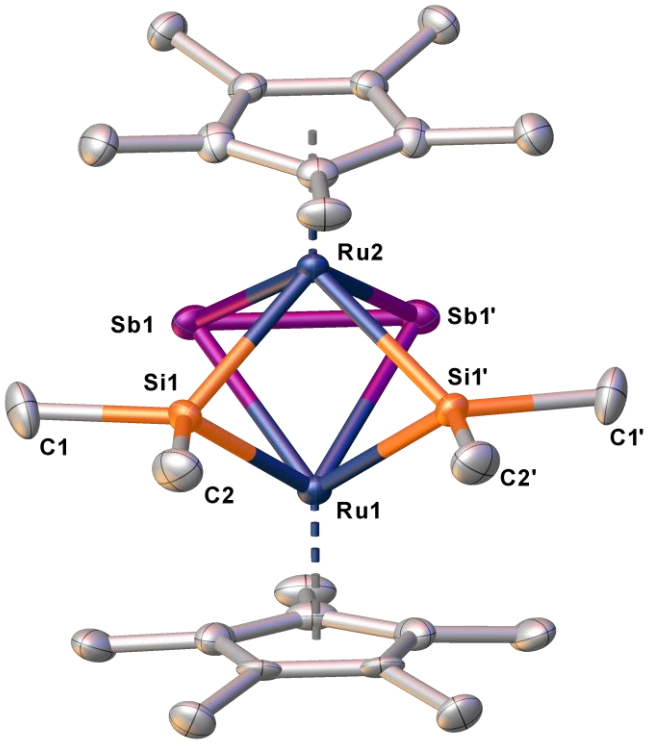

Figure S3: Molecular structure of **T3** in the solid state with thermal ellipsoids at 50% probability level. Hydrogen atoms are omitted for clarity. Selected bond lengths [Å] and angles [°]: Sb$_1$-Sb$_1^1$ 2.6485(8), Sb$_1$-Ru$_2$ 2.7154(7), Sb$_1$-Ru$_1$ 2.7217(6), Sb$_1$-Si$_1^1$ 3.0481(17), Ru$_2$-Si$_1^1$ 2.3798(16), Ru$_2$-Si$_1$ 2.3797(16), Sb$_1^1$-Sb$_1$-Ru$_2$ 60.811(11), Sb$_1^1$-Sb$_1$-Ru$_1$ 60.886(11), Sb$_1^1$-Sb$_1$-Si$_1^1$ 94.67(3), Ru$_2$-Sb$_1$-Ru$_1$ 61.99(2), Sb$_1^1$-Ru$_2$-Sb$_1$ 58.38(2), Si$_1$-Ru$_2$-Sb$_1^1$ 73.15(4), Si$_1^1$-Ru$_2$-Sb$_1^1$ 110.77(5), Si$_1$-Ru$_2$-Si$_1^1$ 82.71(8), Sb$_1$-Ru$_1$-Sb$_1^1$ 58.23(2), Si$_1$-Ru$_1$-Sb$_1$ 110.24(5), Si$_1^1$-Ru$_1$-Sb$_1^1$ 110.24(5), Si$_1^1$-Ru$_1$-Sb$_1$ 72.89(4), Si$_1$-Ru$_1$-Sb$_1^1$ 72.89(4).

[(Cp*Ru)$_2$(Sb$_4$Cl$_4$)] (T4):

Compound **T4** crystallizes by layering a DCM solution with acetonitrile in form of black blocks in the monoclinic space group $P2_1/n$. The asymmetric unit contains a half molecule of **T4**.

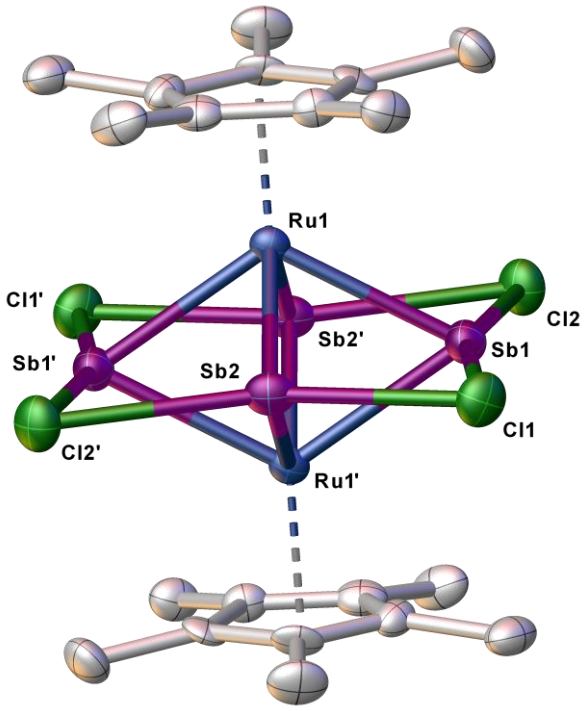

Figure S4: Molecular structure of **T4** in the solid state with thermal ellipsoids at 50% probability level. Hydrogen atoms are omitted for clarity. Selected bond lengths [Å] and angles [°]: Sb2-Sb1' 3.2195(7), Sb2-Sb1 3.2158(7), Sb2-Ru1 2.6473(8), Sb2-Ru1' 2.6477(7), Sb2-Cl2 2.6691(19), Sb2-Cl1' 2.8805(19), Sb1-Ru1' 2.6691(7), Sb1-Ru1 2.6606(7), Sb1-Cl2 2.841(2), Sb1-Cl1 2.655(2), Ru1-Ru1' 2.7413(11); Sb2-Sb1-Sb2' 89.491(17), Sb1-Sb2-Sb1' 90.510(17), Ru1-Sb2-Ru1' 62.36(2), Ru1'-Sb2-Cl2 99.37(5), Ru1-Sb2-Cl2 101.26(5), Ru1'-Sb2-Cl1' 96.83(4), Ru1-Sb2-Cl1' 94.09(5), Cl2-Sb2-Cl1' 161.52(6), Ru1-Sb1-Ru1' 61.91(2), Ru1'-Sb1-Cl2 94.69(5), Ru1-Sb1-Cl2 96.62(4), Cl1-Sb1-Ru1' 99.02(5), Cl1-Sb1-Ru1 102.24(5), Cl1-Sb1-Cl2 160.34(6), Sb2-Ru1-Sb2' 117.64(2), Sb2-Ru1-Sb1' 74.54(2), Sb2'-Ru1-Sb1' 74.43(2), Sb2'-Ru1-Sb1 74.67(2), Sb2-Ru1-Sb1 74.58(2), Sb2-Ru1-Ru1' 58.83(2), Sb2'-Ru1-Ru1' 58.81(2), Sb1-Ru1-Sb1' 118.09(2), Sb1'-Ru1-Ru1' 58.89(2), Sb1-Ru1-Ru1' 59.20(2), Sb2-Cl2-Sb1 71.34(5), Sb1-Cl1-Sb21 71.00(5).

Table S1: Structure determination summary of the complexes **T1**, **T2, T3** and **T4**.

Compound	**T1**	**T2**	**T3**	**T4**
Formula	$C_{52}H_{84}Li_2N_2Zr_2$	$C_{14}H_{30}RhSbSi_2$	$C_{24}H_{42}Ru_2Sb_2Si_2$	$C_{20}H_{30}Cl_4Ru_2Sb_4$
$D_{calc.}$/ g cm^{-3}	1.229	1.695	2.007	2.700
m/mm^{-1}	3.623	19.595	18.820	43.666
Formula Weight	933.53	479.230	832.39	1101.38
Colour	orange	orange	dark red	clear violet
Shape	block-shaped	block-shaped	block-shaped	block-shaped
Size/mm^3	0.13×0.07×0.05	0.14×0.11×0.08	0.28×0.23×0.20	0.08×0.04×0.04
T/K	131.0(3)	123.01(10)	123.01(10)	123.00(10)
Crystal System	monoclinic	triclinic	orthorhombic	monoclinic
Space Group	*C*2/*c*	*P*-1	*Pnma*	$P2_1/n$
a/Å	13.3542(5)	11.39246(7)	12.2556(2)	8.7631(2)
b/Å	17.3926(6)	11.56168(8)	15.2500(3)	14.9763(4)
c/Å	22.0585(7)	16.78488(10)	14.7430(2)	10.7890(3)
a/°	90	99.4525(5)	90	90
b/°	100.110(3)	101.0274(5)	90	106.906(3)
g/°	90	115.6484(6)	90	90
V/Å^3	5043.8(3)	1878.42(3)	2755.44(8)	1354.74(6)
Z	4	4	4	2
Z'	0.5	2	0.5	0.5
Wavelength/Å	1.54184	1.54184	1.39222	1.54184
Radiation type	Cu K_α	Cu K_α	Cu K_α	Cu K_α
θ_{min}/°	4.215	2.79	4.236	5.204
θ_{max}/°	67.402	74.52	58.423	72.710
Measured Refl's.	9926	40277	9562	7250
Ind't Refl's	4486	7567	2691	2565
Refl's with I≥σ(I)	3825	7436	2609	2104
R_{int}	0.0352	0.0328	0.0774	0.0398
Parameters	274	337	153	141
Restraints	0	0	0	0
Largest Peak	0.604	1.0192	2.872	1.830
Deepest Hole	-0.309	-1.4392	-2.860	-0.905
GooF	1.010	1.0260	1.112	1.038
wR_2 (all data)	0.0749	0.0659	0.1669	0.0965
wR_2	0.0718	0.0654	0.1655	0.0914
R_1 (all data)	0.0366	0.0259	0.0660	0.0483
R_1	0.0290	0.0254	0.0653	0.0362

8.3.4 NMR spectra

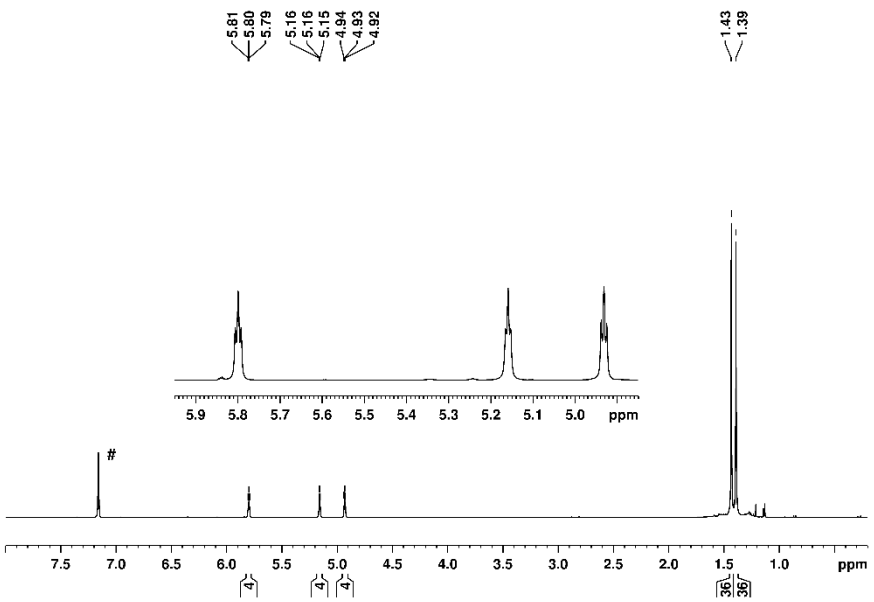

Figure S5: ^{1}H NMR spectrum of **T1** in C_6D_6 (#).

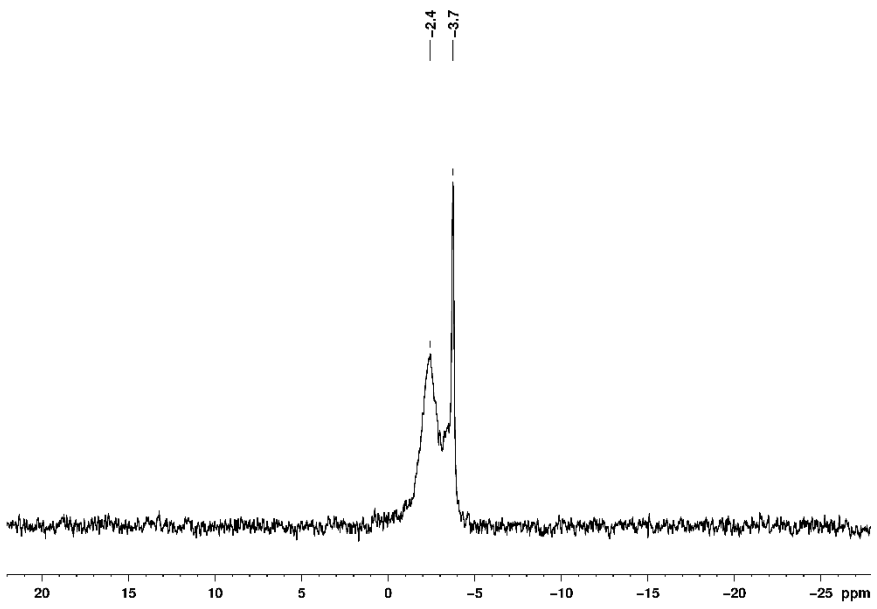

Figure S6: ^{7}Li NMR spectrum of **T1** in $CDCl_3$.

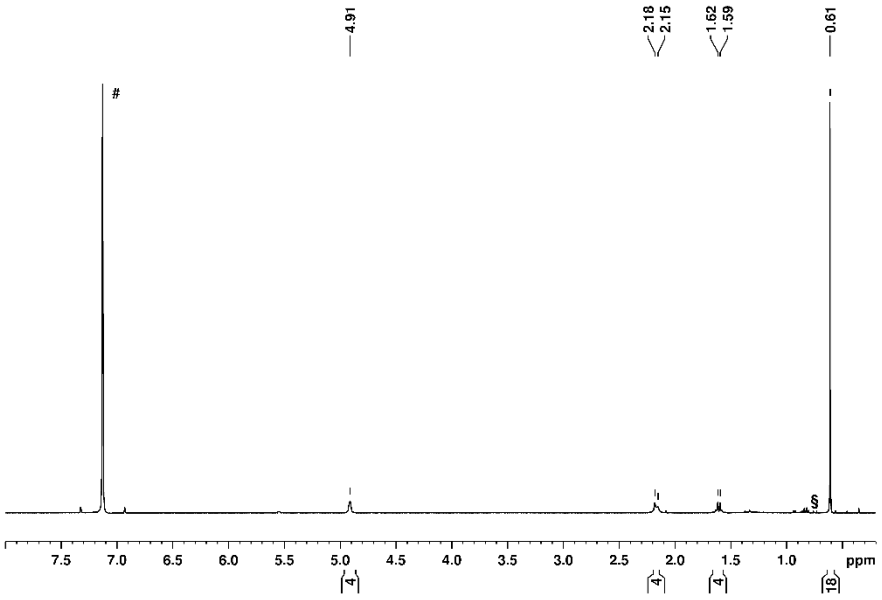

Figure S7: ^{1}H NMR spectrum of **T2** in C_6D_6 (#).

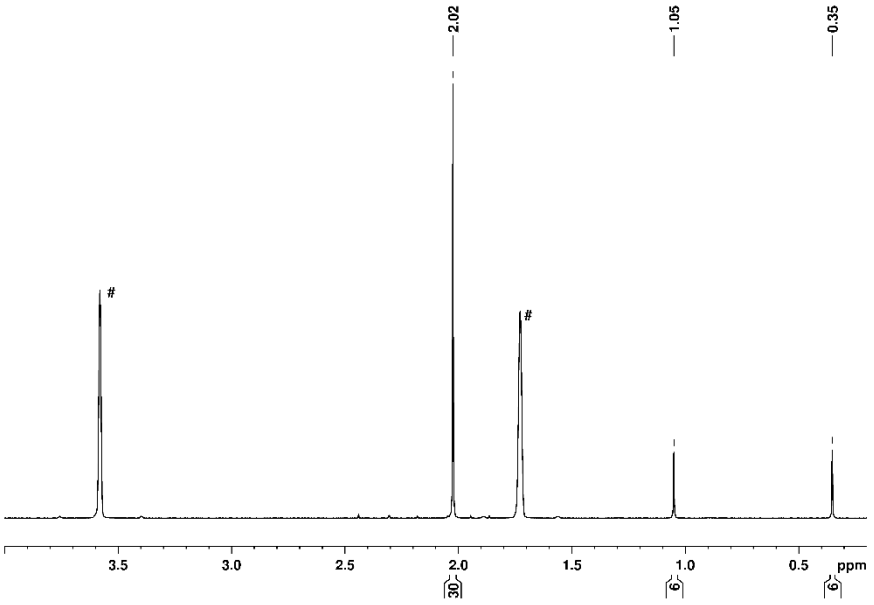

FigureS8: ^{1}H NMR spectrum of **T3** in thf-d^8 (#).

8.4 References

[1] S. Gambarotta, *J. Organomet. Chem.* **1995**, *500*.

[2] Y. M. M. Hidai, *Chem. Rev.* **1995**, *95*, 1115–1133.

[3] R. D. Thomas, M. T. Clarke, R. M. Jensen, T. C. Young, *Organometallics* **1986**, *5*, 1851–1857.

[4] a) X. Zhang, Q. Zhu, I. A. Guzei, R. F. Jordan, *J. Am. Chem. Soc.* **2000**, *122*, 8093–8094; b) Y. Wielstra, A. Meetsma, S. Gambarotta, S. Khan, *J. Am. Chem. Soc.* **1990**, *9*, 876–879; c) E. A. MacLachlan, F. M. Hess, B. O. Patrick, M. D. Fryzuk, *J. Am. Chem. Soc.* **2007**, *129*, 10895–10905; d) M. D. LoCoco, X. Zhang, R. F. Jordan, *J. Am. Chem. Soc.* **2004**, *126*, 15231–15244.

[5] J. A. Pool, E. Lobkovsky, P. J. Chirik, *J. Am. Chem. Soc.* **2003**, *125*, 2241–2251.

[6] W. H. Bernskoetter, E. Lobkovsky, P. J. Chirik, *J. Am. Chem. Soc.* **2005**, *127*, 14051–14061.

[7] M. D. Fryzuk, T. S. Haddad, M. Mylvaganam, D. H. McConville, S. J. Rettig, *J. Am. Chem. Soc.* **1993**, *115*, 2782–2792.

[8] A. F. Holleman, N. Wiberg, *Lehrbuch der Anorganischen Chemie*, Walter de Gruyter, Berlin - New York, **2007**.

[9] Y. R. Luo, *Comprehensive Handbook of Chemical Bond Energies*, CRC Press, Boca Raton, **2007**.

[10] a) C. Ganesamoorthy, J. Krüger, C. Wölper, A. S. Nizovtsev, S. Schulz, *Chem. Eur. J.* **2017**, *23*, 2461–2468; b) H. J. Breunig, R. Rösler, E. Lork, *Angew. Chem. Int. Ed. Engl.* **1997**, *36*, 2819–2821; c) H. J. Breunig, N. Burford, R. Rösler, *Angew. Chem. Int. Ed.* **2000**, *39*, 4148–4150.

[11] C. Ganesamoorthy, C. Wölper, A. S. Nizovtsev, S. Schulz, *Angew. Chem. Int. Ed.* **2016**, *55*, 4204–4209.

[12] C. Schoo, S. Bestgen, A. Egeberg, S. Klementyeva, C. Feldmann, S. N. Konchenko, P. W. Roesky, *Angew. Chem. Int. Ed.* **2018**, *57*, 5912–5916.

[13] G. Balázs, M. Sierka, M. Scheer, *Angew. Chem. Int. Ed.* **2005**, *44*, 4920–4924.

[14] V. Heinl, A. E. Seitz, G. Balazs, M. Seidl, M. Scheer, *Chem. Sci.* **2021**, *12*.

[15] a) S. Furan, E. Hupf, J. Boidol, J. Brünig, E. Lork, S. Mebs, J. Beckmann, *Dalton. Trans.* **2019**, *48*, 4504–4513; b) M. Manger, J. Wolf, M. Laubender, M. Teichert, D. Stalke, H. Werner, *Chem. Eur. J.* **1997**, *3*, 1442-1450; c) P. Schwab, E. O. Fischer, H. Werner, *Angew. Chem. Int. Ed. Engl.* **1993**, *32*, 1480–1482; d) P. Sharma, N. Rosas, S. Hernandez, A. Cabrera, *J. Chem. Soc.* **1995**, 1325–1326; e) T. Pechmann, C. D. Brandt, H. Werner, *Dalton. Trans.* **2003**, 1495–1499.

[16] a) H. J. Breunig, K. Häberle, M. Dräger, T. Severengiz, *Angew. Chem. Int. Ed. Engl.* **1985**, *24*, 73; b) L. Tuscher, C. Ganesamoorthy, D. Bläser, C. Wölper, S. Schulz, *Angew. Chem. Int. Ed.* **2015**, *54*, 10657–10661.

[17] P. Pyykkö, M. Atsumi, *Chem. Eur. J.* **2009**, *15*, 186–197.

[18] a) J. Krüger, J. Schoening, C. Ganesamoorthy, L. John, C. Wölper, S. Schulz, *Z. Anorg. Allg. Chem.* **2018**, *644*, 1028–1033; b) L. P. Ho, A. Nasr, P. G. Jones, A. Altun, F. Neese, G. Bistoni, M. Tamm, *Chem. Eur. J.* **2018**, *24*, 18922–18932; c) H. J. Breunig, T. Borrmann, E. Lork, C. I. Raţ, U. Rosenthal, *Organometallics* **2007**, *26*, 5364–5368; d) A. H. Cowley, N. C. Norman, M. Pakulski, D. Bricker, D. R. Russell, *J. Am. Chem. Soc.* **1985**, *107*, 8211–8218; e) B. Twamley, C. D. Sofield, M. M. Olmstead, P. P. Power, *J. Am. Chem. Soc.* **1999**, *121*, 3357–3367.

[19] Y. Wang, P. Zavalij, B. Eichhorn, *Chem. Commun.* **2018**, *54*, 11917–11920.

[20] A. E. Seitz, U. Vogel, M. Eberl, M. Eckhardt, G. Balázs, E. V. Peresypkina, M. Bodensteiner, M. Zabel, M. Scheer, *Chem. Eur. J.* **2017**, *23*, 10319–10327.

[21] C. Marquardt, O. Hegen, M. Hautmann, G. Balázs, M. Bodensteiner, A. V. Virovets, A. Y. Timoshkin, M. Scheer, *Angew. Chem. Int. Ed.* **2015**, *54*, 13122–13125.

[22] Rigaku Oxford Diffraction, *CrysAlisPro Software System Version 1.171.38.43*, **2015**.

[23] L. J. Bourhis, O. V. Dolomanov, R. J. Gildea, J. A. K. Howard, H. Puschmann, *J. Appl. Crystallogr.* **2009**, *42*, 339–341.

[24] G. M. Sheldrick, *Acta Crystallogr., Sect, A* **2015**, *71*, 3–8.

[25] G. M. Sheldrick, *Acta Crystallogr., Sect, C* **2015**, *71*, 3–8.

[26] G. M. Sheldrick, *Acta Crystallogr., Sect, A* **2008**, *64*, 112–122.

9 Summary

This thesis deals with the synthesis, functionalization and reactivity of E_n ligand complexes as well as the transfer of polypnictogen units. Chapter 1 gives a brief overview of the elements phosphorus, arsenic and antimony and gives a systematically summary of reported E_n ligand complexes. Furthermore, the concept of transfer reactions is described in detail. The research objectives are outlined in chapter 2, followed by the obtained results in chapter 3 to 8. Hereinafter, a summary of the results, sorted by their main topics, is described.

9.1 Transfer of Polypnictogen Units

As presented in the introductory part, the concept of transfer reactions shows certain advantages compared to conventional synthetic methods. Therefore, the transfer of polypnictogen units enables the synthesis of a variety of E_n ligand complexes with unprecedented structural motifs. It has been shown that zirconium based E_n ligand complexes represent suitable starting materials to transfer polypnictogen units to the late transition metals iron, cobalt and nickel. Scheme 1 and 2 give an overview of the transfer reactions investigated. Within the scope of this thesis it is shown that the complexes $[Cp''_2Zr(\eta^{1:1}\text{-}E_4)]$ (E = P (**S1**), As (**S2**)) and $[(Cp''Zr)_2(\mu,\eta^{1:1:1:1:1:1}\text{-}Sb_6)]$ (**S3**) represent promising transfer reagents.

The reaction of **S1** with *in situ* generated $[Cp'''NiBr]_2$ in a 1:1.3 stoichiometry leads to the formation of the prismane shaped complex $[(Cp'''Ni)_2(\mu,\eta^{3:3}\text{-}P_4)]$ (**S1-1**) and $[Cp'''Ni(\eta^3\text{-}P_3)]$ (**S1-2**), bearing a *cyclo*-P_3 unit (Scheme 1). In the similar reaction with **S2**, the comparable prismane shaped compound $[(Cp'''Ni)_2(\mu,\eta^{3:3}\text{-}As_4)]$ (**S2-1**) is formed, besides the triple decker complex $[\{(Cp'''Ni)_3Ni(\mu_3\text{-}As)_4\}_2(\mu,\eta^{4:4}\text{-}As_4)]$ (**S2-2**). In the case of **S1-1** and **S2-1**, the whole E_4 unit is transferred in form of a chain, stabilized by two nickel fragments. Much higher yields of such prismanes are achieved compared to co-thermolytic methods, which nicely demonstrates the advantage of this concept. The same can be observed by the synthesis of $[(Cp'''Ni)_3(\mu_3\text{-}As)(As_4)]$ (**S2-4**) formed by the reaction of **S2** with crystalline $[Cp'''NiBr]_2$. Interestingly, **S2-2** represents the first nickel complex coordinating a *cyclo*-As_4 unit. Two nickel atoms in **S2-2** are not bearing Cp''' substituents and though they should originate from another source than $[Cp'''NiBr]_2$. This was proofed by the reaction fo **S1** and **S2** with 1.5 equiv. of $[Cp'''NiBr]_2$ and one equiv. of $[NiBr_2{\cdot}dme]$, which leads to the dimeric compounds $[(Cp'''Ni)_3\{Ni(\mu\text{-}Br)\}(\mu_3\text{-}E)_4]_2$ (E = P (**S1-3a**), E = As (**S2-3a**)), respectively. In comparison to **S2-2** they consist of two bromine bridged $[Ni_4E_4]$ cubanes. Furthermore, a dependency on the size of the Cp^R ligands is observed, since the reaction of **S1/S2** with $[Cp^{Bn}NiBr]_2$ yields $[(Cp^{Bn}Ni)_3\{Ni(\mu\text{-}Br)\}(\mu_3\text{-}E)_4]_2$ (E = P (**S1-3b**), E = As (**S2-3b**)) independently if $[NiBr_2{\cdot}dme]$ is added or not.

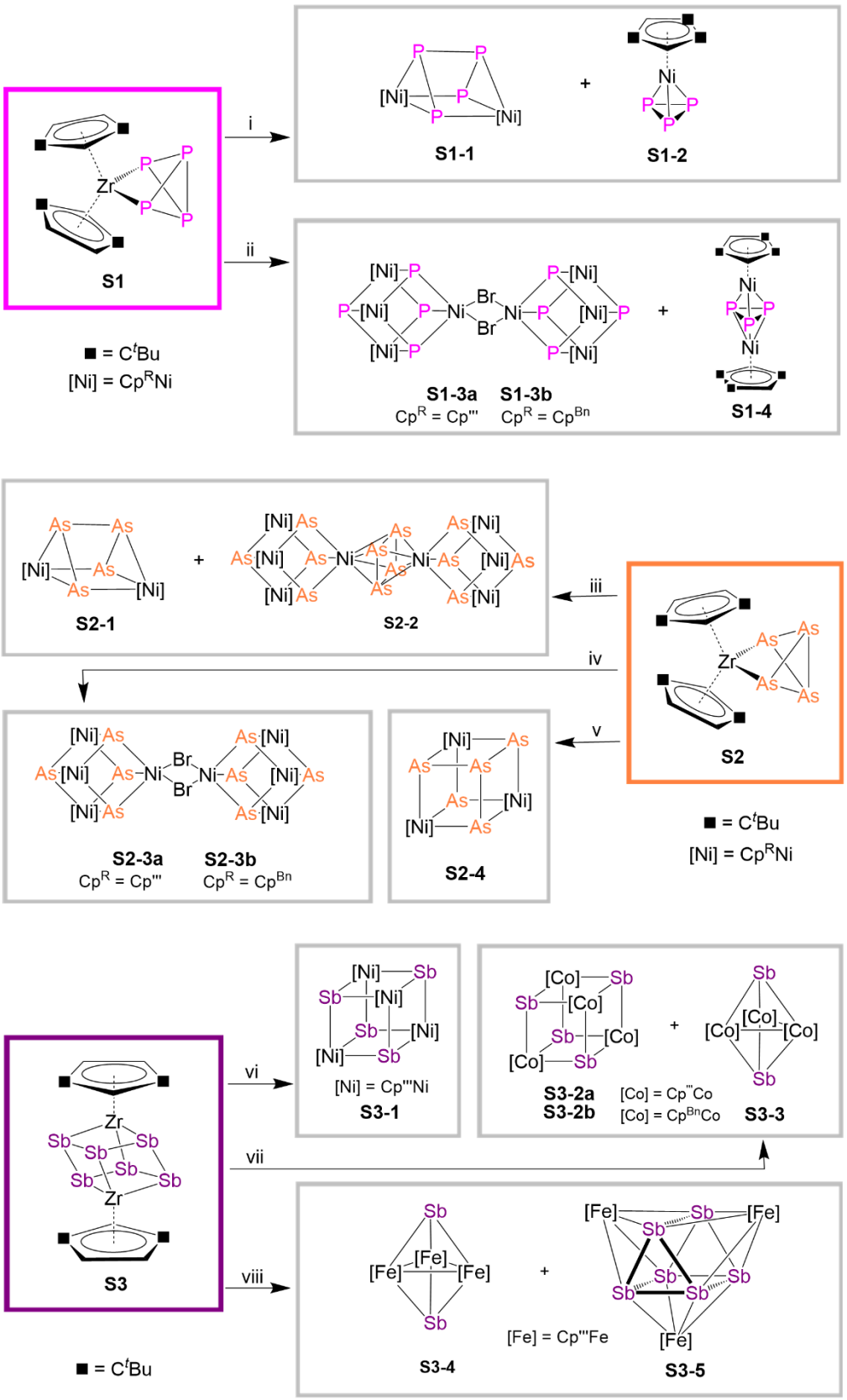

Scheme 1: Overview of performed transfer reactions, starting from [Cp''$_2$Zr(η$^{1:1}$-E$_4$)] (E = P (**S1**), As (**S2**)) and [(Cp''Zr)$_2$(μ,η$^{1:1:1:1:1:1}$-Sb$_6$)] (**S3**). The E$_n$ units are transferred to nickel (E = P, As, Sb), cobalt (E = Sb) and iron (E = Sb) using the dimeric compounds [Cp^{R}NiBr]$_2$ (Cp^R = Cp''' (**i-vi**), Cp^{Bn} (**ii**, **iv**)), [Cp^{R}CoCl]$_2$ (Cp^R = Cp''', Cp^{Bn} (**vii**)), and [Cp'''FeBr]$_2$ (**viii**).

Compared to phosphorus and arsenic, the number of polyantimony complexes is rather limited due to the lack of easily accessible antimony sources. This work describes the synthesis of the zirconium based triple decker complex $[(Cp''Zr)_2(\mu,\eta^{1:1:1:1:1:1}\text{-}Sb_6)]$ (**S3**) by the reaction of $[Cp''_2ZrCl_2]$ with the potassium antimony salt $KSb(SiMe_3)_2$. Furthermore, their high potential as starting material to transfer the polyantimony unit to nickel, cobalt and iron is shown (Scheme 1). The reaction of **S3** with $[Cp'''NiBr]_2$ and $[Cp'''CoCl]_2$ leads to the formation of the cubane like compounds $[(Cp'''M)_4(\mu_3\text{-}Sb)_4]$ (M = Ni (**S3-1**); Co (**S3-2a**)), respectively. However, using the sterically less encumbered $[Cp^{Bn}CoCl]_2$ in a similar reaction, the appropriate cubane is formed (**S2-2b**) beside $[(Cp^{Bn}Co)_3(\mu_3\text{-}Sb)_2]$ (**S3-3**), having a trigonal bipyramidal structure. The structure of **S3-3** represents a new structural motif and can be regarded as a *closo*-type cluster with 12 skeletal electrons according to the Wade-Mingos rules. Furthermore, the transfer of the Sb_n unit from **S3** to iron is investigated by the reaction with $[Cp'''FeBr]_2$. This reaction also leads to two products, the trigonal bipyramidal $[(Cp'''Fe)_3(\mu_3\text{-}Sb)_2]$ (**S3-4**) and $[(Cp'''Fe)_3(\mu_3,\eta^{4:4:4}\text{-}Sb_6)]$ (**S3-5**), the latter having a prismane like structure. Interestingly, in **S3-5** the complete Sb_6 entity of **S3** is transferred in form of a prism, a structural motif that was unknown so far.

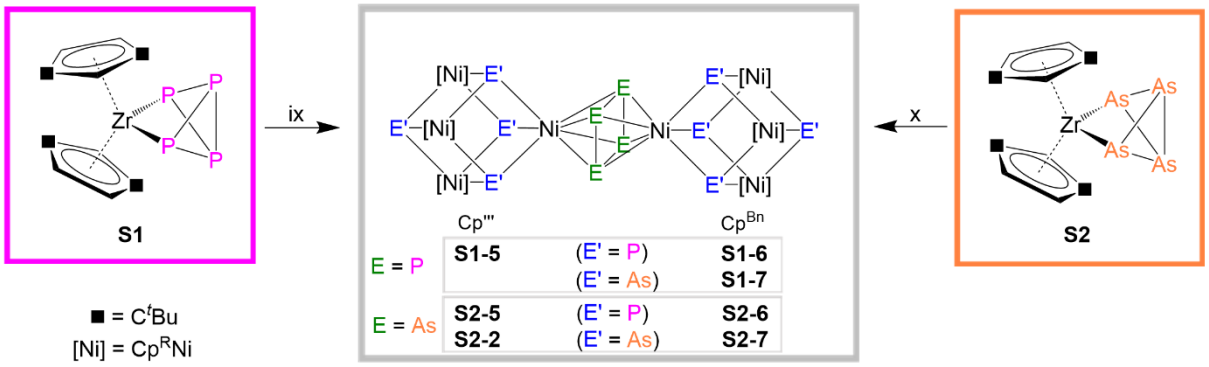

Scheme 2: Selection of transfer reactions investigated, started from $[Cp''_2Zr(\eta^{1:1}\text{-}E_4)]$ (E = P (**S1**), As (**S2**)). The E_4 units (E = P, As) are transferred to nickel fragments using the dimeric compounds $[(Cp^RNi)_3\{Ni(\mu\text{-}Br)\}(\mu_3\text{-}E')_4]_2$ (E' = P: Cp^R = Cp''' (**S1-3a**), Cp^{Bn} (**S1-3b**); E' = As: Cp^R = Cp''' (**S2-3a**), Cp^{Bn} (**S2-3b**)). Thereby, the triple decker complexes **S1-5/6/7** and **S2-2/5/6/7** are formed.

Moreover, the presence of the bridging bromine ligands in **S1-3a/b** and **S2-3a/b** enables the possibility of a further transfer of the polypnictogen units in **S1** and **S2**. In doing so, the whole E_4 unit can be transferred in from of an E_4 cycle and a variety of nickel triple decker complexes are formed, which exhibit the same structural composition as **S2-2** (Scheme 2, **S1-5/6/7** and **S2-2/5/6/7**). Thereby, it was also possible to synthesize mixed phosphorus and arsenic complexes.

9.2 Investigation of the reaction behavior of [Cp''$_2$Zr($\eta^{1:1}$-E$_4$)] (E = P, As) towards Lewis acids and nucleophiles

As shown within this thesis and in prior works, the zirconium complexes [Cp''$_2$Zr($\eta^{1:1}$-E$_4$)] (E = P (**S1**), As (**S2**)) represent suitable transfer reagents to synthesize unprecedented pnicogen containing compounds. While the transfer to transition metal fragments works quite well, the transfer to main group compounds is more challenging since mostly insoluble products are formed. Therefore, this work deals with investigations on the coordination behavior of **S2** towards Lewis acidic fragments and the reactivity of **S1** and **S2** towards nucleophiles. A specific substitution on the E$_4$ unit is targeted to increase the solubility of the resulting products.

To investigate the coordination behavior of **S2**, the reaction with different Lewis acidic transition metal complexes and main group compounds was performed. A variety of new coordination products of **S2** was obtained, an overview is given in scheme 3 (upper part). Depending on steric requirements of the Lewis acids a single coordination in [Cp''$_2$Zr(μ,$\eta^{1:1:1:1}$-As$_4$)(LA)] (LA = Fe(CO)$_4$ (**S2-10**); B(C$_6$F$_5$)$_3$ (**S2-12**)) or a double coordination in [Cp''$_2$Zr(μ$_3$,$\eta^{1:1:1:1}$-As$_4$)(LA)$_2$] (LA = W(CO)$_5$ (**S2-8**); CpMn(CO)$_2$ (**S2-9**); AlR$_3$ (**S2-13**, R = Me, Et, ^{i}Bu)) can be observed. Furthermore, a rearrangement of the butterfly As$_4$ ligand to a *cyclo*-As$_4$ ligand and therefore an η^3 coordination occurs in [Cp''$_2$Zr(μ,$\eta^{3:1:1}$-As$_4$)(Fe(CO)$_3$)] (**S2-11**) by the rection of **S2** with [Fe$_2$(CO)$_9$] at higher temperatures or heating a solution of **S2-10**.

Furthermore, the reactivity of **S1** and **S2** was investigated within the scope of this thesis. The reaction of **S1** with ^{t}BuLi leads to the ionic intermediate Li[Cp''$_2$Zr(μ,$\eta^{1:1}$-P$_4$^{t}Bu)] (**S1-8**), where one P-P bond of the initial P$_4$-butterfly moiety is opened and a ^{t}Bu-group is introduced (Scheme 3, bottom part). During the workup process, a rearrangement occurs and the complex [(Cp''$_2$Zr)$_2$(μ,$\eta^{1:1:1:1}$-P$_8$^{t}Bu$_2$)] (**S1-9**) is formed, bearing a rare P$_8$ unit. By using the quenching reagents [Me$_3$O][BF$_4$] and Ph$_2$PCl in a subsequent reaction with **S1-8**, the introduction of another group and the expansion of the polypnictogen framework was possible. Though, the compounds **S1-10** and **S1-11** were obtained.

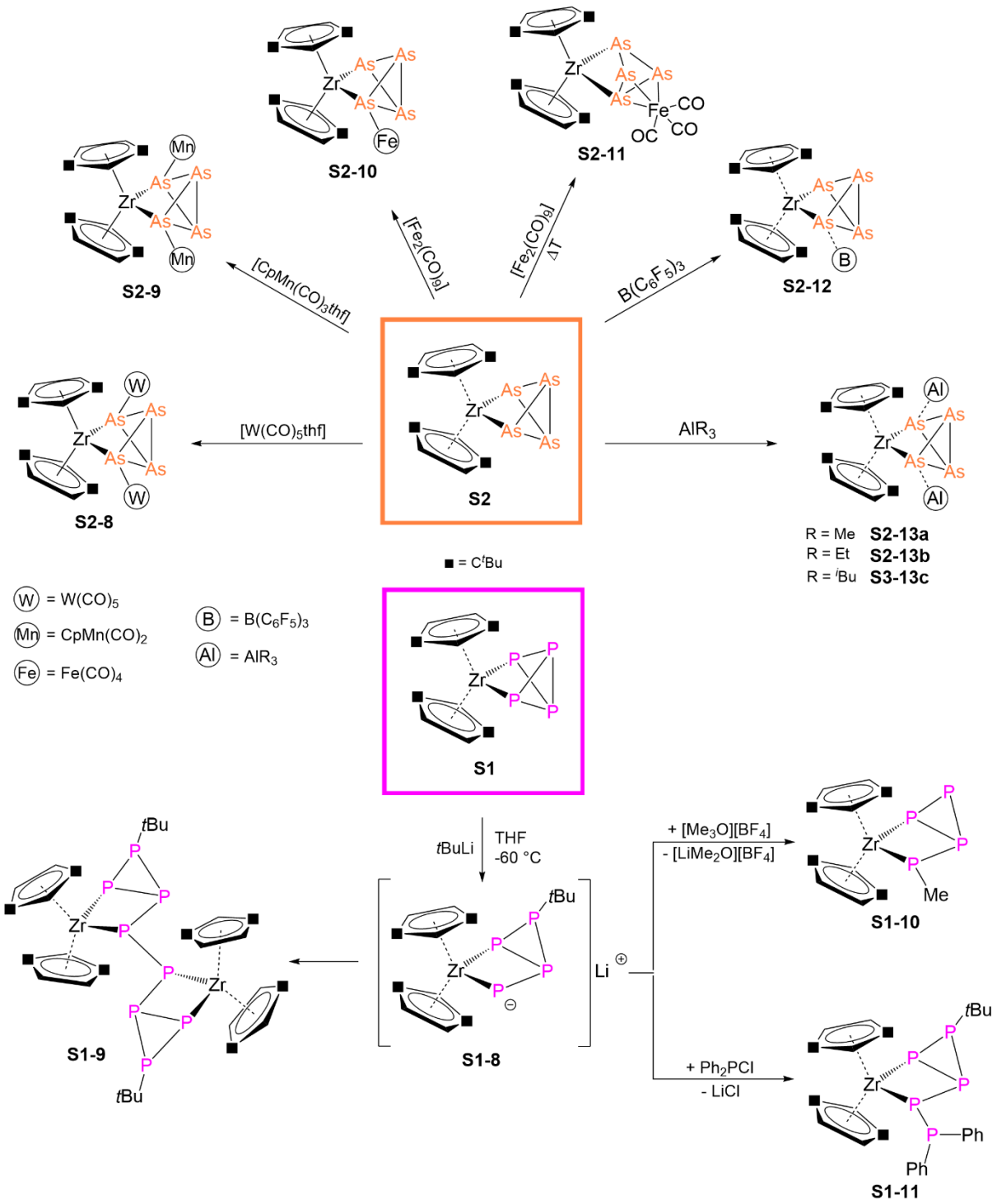

Scheme 3: Top: Overview of the coordination behavior of $[Cp''_2Zr(\eta^{1:1}\text{-}As_4)]$ (**S2**) towards Lewis acidic transition metal fragments and main group compounds. Bottom: Reactivity of $[Cp''_2Zr(\eta^{1:1}\text{-}P_4)]$ (**S1**) towards ^{t}BuLi and subsequent quenching.

Moreover, the reaction behavior of **S1** and **S2** towards the nucleophiles $LiNMe_2$ and $LiCH_2SiMe_3$ was investigated, which leads to fragmentation of the E_4 unit and the formation of $[Cp''_2Zr(\eta^2\text{-}E_3R)]$ (R = NMe_2: P, (**S1-10**); As, (**S2-14**); R = CH_2SiMe_3: P, (**S1-13**); As (**S2-15**)), respectively. In the case of the reaction of **S2** with $LiCH_2SiMe_3$ a second product, the triple decker complex $[(Cp''Zr)_2(\mu,\eta^{1:1:1:1:1:1}\text{-}As_6)]$ (**S2-16**), was isolated. Here, a chair type As_6-cycle is stabilized by two [Cp"Zr] fragments and during this reaction, the arsenic derivative of **S3** is formed.

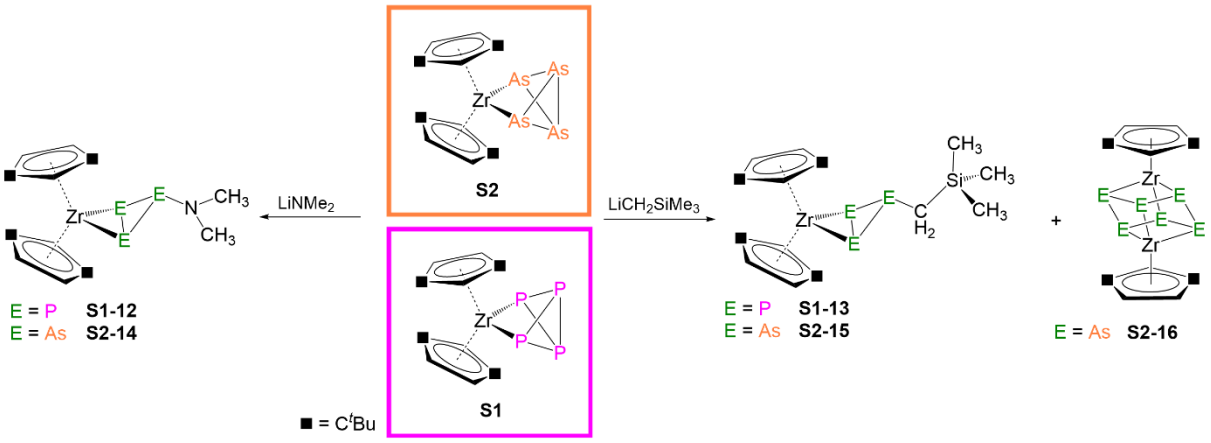

Scheme 4: Reactions of **S2** and **S1** towards $LiNMe_2$ and $LiCH_2SiMe_3$, respectively.

9.4 Synthesis of Sb_n ligand complexes

As presented in the introductory part, the number of polyantimony ligand complexes is rather rare. The lack of suitable starting materials for the synthesis is one of the reasons for this. This work targets the reactivity of $Cp^*_4Sb_4$ (**S4**) towards ionic compounds and transition metal complexes with labile ligands. An overview of the obtained results is depicted in scheme 5.

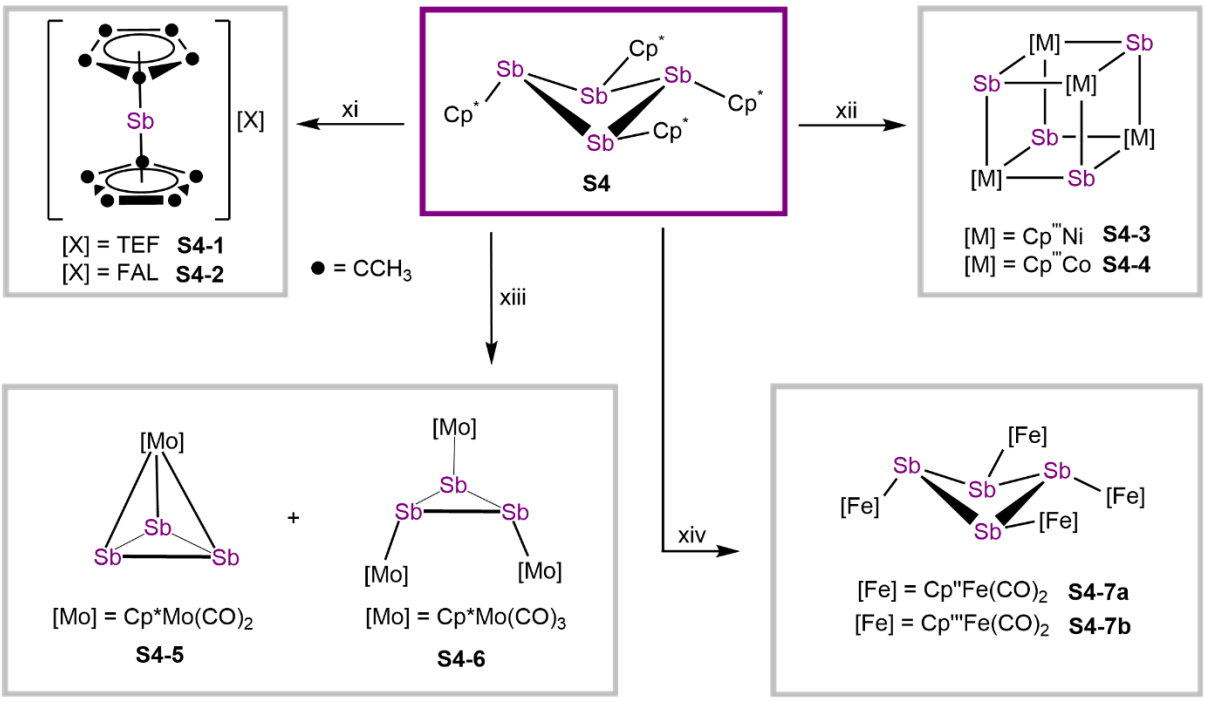

Scheme 5: Overview of the reactivity of $Cp^*_4Sb_4$ (**S4**). xi: **S4** with [Ag][X] (X = TEF; FAL) in DCM at r.t. xii: **S4** with *in situ* prepared $[(Cp'''Ni)_2tol]$ or crystalline $[(Cp'''Co)_2tol]$ in *n*-hexane at r.t. xiii: **S4** with $Na[Cp^*Mo(CO)_2]$ in boiling toluene. xiv: **S4** with $[Cp^RFe(CO)_2]_2$ in boiling toluene (Cp^R = Cp'', Cp''').

The reaction of **S4** with the silver salts [Ag][TEF] and [Ag][FAL] was performed (TEF = $[Al\{OC(CF_3)_3\}_4]$, FAL = $[Al\{OC_6F_{10}(C_6F_5)\}_3]$) leads to the formation of the stibanocenium compounds **S4-1** and **S4-2**, respectively. Reactions of **S4** with the triple decker complexes $[(Cp'''M)_2tol]$ leads to $[(Cp'''M)_4(\mu_3\text{-}Sb)_4]$ (M = Ni (**S4-3**); Co (**S4-4**)), bearing a cubane like structure. These compounds were already mentioned *vide supra* and can also be synthesized by the reaction of **S3** with halogen containing transition metal complexes. However, the use of **S4** as starting material results in much higher yields. Using the metalate $Na[Cp^*Mo(CO)_2]$, two products can be isolated after chromatographic workup, the neutral complexes $[Cp^*Mo(CO)_2(\eta^3\text{-}Sb_3)]$ (**S4-5**) and $[(Cp^*Mo(CO)_3)_3(\mu_3\text{-}Sb_3)]$ (**S4-6**), containing an Sb_3 unit. **S4-6** represents a novel connectivity of a Sb_3 cycle by three molybdenum fragments. Moreover, the reactivity of **S4** towards the iron carbonyl dimers $[Cp^RFe(CO)_2]_2$ was performed (Cp^R = Cp'', Cp'''). In both reactions, a substitution of the Cp* ligand by an iron fragment occurs and the

compounds **S4-7a** and **S4-7b** are formed. These results give an insight into the usability of **S4** for the formation of polyantimony compounds. Especially the formation of the complexes **S4-6**, **S4-7a** and **S4-7b** show high potential for the formation of further Sb_n ligand complexes, possibly by using them in transfer reactions.

9.5 A few simple words

This thesis deals with the synthesis and functionalization of E_n ligand complexes as well as their use in transfer reactions. In detail, the application of **S1** and **S2** to transfer the E_n unit was investigated, and though a variety of novel nickel complexes were obtained. Furthermore, the functionalization of the polypnictogen units was focused in regards to change their properties. For this, the reactivity towards nucleophiles and Lewis acids was investigated. Another research topic deals with the synthesis of Sb_n ligand complexes. Using $Cp^*_4Sb_4$ as antimony source complexes containing an Sb_n unit with n = 1, 3 or 4 were obtained. Moreover, it was possible to achieve the zirconium triple decker complex **S3** bearing an Sb_6 unit as middle deck, which also serves as transfer reagent for antimony and though Sb_n ligand complexes with new structural motifs can be synthesized.

10 Appendix

10.1 Thematic List of Abbreviations

Solvents

DCM	dichloromethane (CH_2Cl_2)
Et_2O	diethyl ether ($C_4H_{10}O$)
THF	tetrahydrofuran (C_4H_8O)

NMR spectroscopy

NMR	nuclear magnetic resonance
δ	chemical shift
ppm	parts per milion
Hz	Hertz [s^{-1}]
J	coupling constant
$\omega_{1/2}$	full width at half maximum
s	singlet
d	doublet
t	triplet
q	quartet
m	multiplet
br	broad
COSY	correlation spectroscopy

EPR spectroscopy

EPR	electron paramagnetic resonance
μeff	effective magnetic moment
μB	Bohr magneton
g	gyromagnetic factor
iso	isotropic
S	spin state

Mass spectrometry

MS	mass spectrometry
m/z	mass to charge ratio
ESI	electron spray ionization
FD	field desorption
LIFDI	liquid injection field desorption

IR spectroscopy

IR	infrared spectroscopy
ATR	attenuated total reflection
v	wavenumber [cm^{-1}]
s	strong
vs	very strong
m	medium
w	weak

Theoretical computations

DFT	density functional theory
ESP	negative electrostatic potential
WBI	Wiberg Bond Indices
NBO	Natural Bond Orbital
NAO	Natural Atomic Orbitals
HOMO	highest occupied molecular orbital
LUMO	lowest occupied molecular orbital
ELF	Electron Localization Function
LOL	Localized Orbital Locator

Units

Å	angstroem (1Å = 10^{-10} M9
T	temperature
°	degree
°C	degree Celcius
K	kelvin
J	joule
kJ	kilo joule
L	liter
E	pnictogen atom
E_n	polypnictogen units
M	molar mass
mL	mililiter (10^{-3} L)
g	gram
mg	miligram (10^{-3} g)
mmol	milimol (10^{-3} mol)
%	percent
µmol	micromol (10^{-6} mol)
min	minute
cm	centimeter
kbar	kilobar (10^3 bar)

Others

r.t.	room temperature
cf.	confer
e. g.	exempli gratia
equiv.	equivalent
M	metal
R	organic substituent
L	ligand
LA	Lewis acid
SI	supporting Information
nat.	natural
ie.	id est

Ligands / Substituents / Ions

18-crown-6	1,4,710,13,16-hexaoxacyclooctadecane
CAAC	cyclic-alkyl-amino-carbene
COD	1,5-cyclo-octadiene (C_8H_{12})
Cp	cyclopentadienyl (C_5H_5)
Cp''	1,3-di-tertbutyl-cyclopentadienyl ($C_5H_3{}^tBu_2$)
Cp'''	1,2,4-tri-tertbutyl-cyclopentadienyl ($C_5H_2{}^tBu_3$)
Cp*	1,2,3,4,5-pentamethylcyclopentadienyl (C_5Me_5)
Cp^{Big}	pentakis-4-*n*-butyl-phenylcyclopentadienyl ($C_5(4\text{-}{}^nBuC_6H_4)_5$))
Cp^{Bn}	1,2,3,4,5-penta-benzyl-cyclopentadienyl ($C_5(CH_2\{C_6H_5\})_5$)
Cp^{Pet}	pentakis-4-ethylphenylcyclopentadienyl ($C_5(4\text{-}EtC_6H_4)_5$)
Cp^{R}	1,4-di-tertburyl-2-methylcyclopentadienyl ($C_5H_2{}^tBu_2Me$)
^{Dipp}NHC	1,3-bis(2,6-di-isopropyl)imidazol-2-ylidene
Et	ethyl
FAL	($Al\{OC_6F_{10}(C_6F_5)\}_3$)
Me	methyl
Mes	mesityl
Mes*	$2,4,6\text{-}{}^tBu_3C_6H_2$
N_3N	tren ($N(CH_2CH_2NSiMe_3)_3$)
nacnac	1,3-diketiminato
NHC	N-heterocyclic carbene
OAc	acetoxy group
OTf	(SO_2CF_3)
Ph	phenyl
^{t}Bu	tert-butyl
TEF	($Al\{OC(CF_3)_3\}_4$)
tol	toluene as ligand
triphos	$MeC(CH_2PPH_2)_3$

10.2 List of Numbered Compounds

10.2.1 Introduction

I	$[(CO)_3Co(\eta^3\text{-}As_3)]$
II	$[\{(CO)_3Co\}_4(\mu_3\text{-}Sb)_4]$
III	$[(PPh_3)_3RhCl(\eta^2\text{-}P_4)]$
IV	$[(N_3N)WE]$ (E = P, As, Sb)
V	$[(CpMo(CO)_2)_2(\mu,\eta^{2:2}\text{-}E_2)]$ (E = P, As, Sb)
VI	$[(Cp'''Co)_2(\mu;\eta^{2:2}\text{-}E_2)_2]$ (E = P, As)
VII	$[\{(CO)_3W\}_2(\mu_3,\eta^{2:2:2}\text{-}Sb_2)]$
VIII	$[Cp^RNi(\eta^3\text{-}E_3)]$ (E = P, As)
IX	$[(Cp'''Ni)_2(\mu,\eta^{3:3}\text{-}P_3)]$
X	$[CpMo(CO)_2(\eta^3\text{-}Sb_3)]$
XI	$[(^{4iPr}CpNi)_2(\mu,\eta^{3:3}\text{-}E_4)]$ (E = P, As)
XII	$[(L^1Ni)_2(\mu,\eta^{3:3}\text{-}P_4)]$
XIII	$[(Cp^RFe)_2(\mu,\eta^{4:4}\text{-}E_4)]$ (E = P, As; Cp^R = Cp''', Cp^{BIG}, Cp*)
XIV	$[Cp'''Co(\eta^4\text{-}P_4)]$
XV	$[(L^2Mg)_4(\mu_4,\eta^{2:1:1:1:1:1}\text{-}Sb_4)]$
XVI	$[(L^1Ga)_2(\mu,\eta^{1:1:1:1}\text{-}Sb_4)]$
XVII	$[Cp^RFe(\eta^5\text{-}E_5)]$ (E = P, As)
XVIII	$[Cp^RRu(\eta^5\text{-}E_5)]$ (E = P, As)
XIX	$[(Cp^RCr)_2(\mu,\eta^{5:5}\text{-}E_5]$ (E = P, As)
XX	$[Cp'''Mo(\mu,\eta^{5:5}\text{-}Sb_5)MoCp^R]$ (Cp^R = $\eta^5\text{-}C_5H_2{}^tBu_2Me$)
XXI	$[(Cp^*Ti)_2(\mu,\eta^{1:1:1:1:1:1}\text{-}P_6)]$
XXII	$[(Cp^RMo)_2(\mu,\eta^{6:6}\text{-}E_6)]$ (E = P, As)
XXIII	$[(Cp^RFe)_3(\mu_3,\eta^{4:4:4}\text{-}As_6)]$
XXIV	$[(Cp^*Co)_3(\mu_3,\eta^{4:4:4}\text{-}As_6)]$
XXV	$[(L^{3/4}Mg)_4(\mu_4,\eta^{1:1:1:1:1:1:1:1}\text{-}E_8)]$ (E = P,
XXVI	$[(L^1Mg)_4(\mu_4,\eta^{1:1:1:1:1:1:1:1}\text{-}Sb_8)]$

L^1 = $HC[C(Me)N(2,6\text{-}C_6H_3{}^iPr_2)]_2$

L^2 = $^iPr_2NC[N(2,6\text{-}C_6H_3{}^iPr_2)]_2$

L^3 = $HC[CHN(2,6\text{-}C_6H_3Me_2)]_2$

L^4 = $HC[C(Me)N(2,6\text{-}C_6H_3Me_2)]_2$

10.2.3 E_4 transfer (E = P, As) to Ni complexes

A	$[Cp^*M(\eta^5\text{-}As_5)]$ (M = Ru, Os)
B	$C_{12}H_{16}P_2$
C	AsP_3
1a	$[Cp''_2Zr(\mu,\eta^{1:1}\text{-}P_4)]$
1b	$[Cp''_2Zr(\mu,\eta^{1:1}\text{-}As_4)]$
2a	$[(Cp'''Ni)_2(\mu,\eta^{3:3}\text{-}P_4)]$
2b	$[(Cp'''Ni)_2(\mu,\eta^{3:3}\text{-}As_4)]$
3	$[Cp'''Ni(\eta^3\text{-}P_3)]$
4	$[\{(Cp'''Ni)_3Ni(\mu_3\text{-}As)_4\}_2(\mu,\eta^{4:4}\text{-}As_4)]$
5	$[(Cp'''Ni)_3(\mu_3\text{-}As)(As_4)]$
6a	$[(Cp'''Ni)_3\{Ni(\mu\text{-}Br)\}(\mu_3\text{-}P)_4]_2$
6b	$[(Cp'''Ni)_3\{Ni(\mu\text{-}Br)\}(\mu_3\text{-}As)_4]_2$
7	$[(Cp'''Ni)_2(\eta^{3:3}\text{-}P_3)]$
8a	$[(Cp^{Bn}Ni)_3\{Ni(\mu\text{-}Br)\}(\mu_3\text{-}P)_4]_2$
8b	$[(Cp^{Bn}Ni)_3\{Ni(\mu\text{-}Br)\}(\mu_3\text{-}As)_4]_2$
9a	$[\{(Cp'''Ni)_3Ni(\mu_3\text{-}P)_4\}_2(\mu,\eta^{4:4}\text{-}P_4)]$
10a	$[\{(Cp^{Bn}Ni)_3Ni(\mu_3\text{-}P)_4\}_2(\mu,\eta^{4:4}\text{-}P_4)]$
10b	$[\{(Cp^{Bn}Ni)_3Ni(\mu_3\text{-}P)_4\}_2(\mu,\eta^{4:4}\text{-}As_4)]$
11a	$[\{(Cp'''Ni)_3Ni(\mu_3\text{-}As)_4\}_2(\mu,\eta^{4:4}\text{-}P_4)]$
12a	$[\{(Cp^{Bn}Ni)_3Ni(\mu_3\text{-}As)_4\}_2(\mu,\eta^{4:4}\text{-}P_4)]$
12b	$[\{(Cp^{Bn}Ni)_3Ni(\mu_3\text{-}As)_4\}_2(\mu,\eta^{4:4}\text{-}As_4)]$

10.2.4 Transfer of Polyantimony Units

I	$[\{Co(CO)_3\}_4(\mu_3\text{-}Sb)_4]$
II	$[Sb_2\{W(CO)_5\}_3]$
III	$[\{(LGa(NMe_2)\}_2(\mu,\eta^{1:1}\text{-}Sb_4)]$
IV	$[\{CpMo(CO)_2\}_2(\mu,\eta^2\text{-}Sb_2)]$
V	$[Cp'''Mo(\mu,\eta^{5:5}\text{-}Sb_5)MoCp^R]$
VI	$[(LGa)_2(\mu,\eta^{2:2}\text{-}Sb_4)]$
VII	$[(LMg)_4(\mu_4,\eta^{2:2:2:2}\text{-}Sb_8)]$
VIII	$[(Cp^*_2Sm)(\mu_4,\eta^{2:2:2:2}\text{-}Sb_8)]$
IX	$[(N_3N)WSb]$
1	$[(Cp''Zr)_2(\mu,\eta^{1:1:1:1:1:1}\text{-}Sb_6)]$
2/2'	$[(Cp'''Ni)_4(\mu_3\text{-}Sb)_4]$
3a	$[(Cp'''Co)_4(\mu_3\text{-}Sb)_4]$
3b	$[(Cp^{Bn}Co)_4(\mu_3\text{-}Sb)_4]$
4	$[(Cp^{Bn}Co)_3(\mu_3\text{-}Sb)_2]$
5	$[(Cp'''Fe)_3(\mu_3\text{-}Sb)_2]$
6	$[(Cp'''Fe)_3(\mu_{3,}\eta^{4:4:4}\text{-}Sb_6)]$

L = $HC[C(Me)N(2,6\text{-}C_6H_3iPr_2)]_2$

10.2.5 Coordination Behavior of $[Cp''_2Zr(\eta^{1:1}\text{-}As_4)]$ towards Lewis Acids

I	$[Cp^{Pet}_2As_4]$	**3**	$[Cp''_2Zr(\mu_3,\eta^{1:1:1:1}\text{-}As_4)(CpMn(CO)_2)_2]$
II	$[\{(PhC(N^tBu)_2Si)(N(SiMe_3)_2)\}_3As_{10}]$	**3'**	$[Cp''_2Zr(\mu_3,\eta^{1:1:1:1}\text{-}As_4)(CpMn(CO)_2)]$
III	$[Cp^*\{(SiMe_3)_2N\}SiAs]_2$	**4**	$[Cp''_2Zr(\mu,\eta^{1:1:1}\text{-}As_4)(Fe(CO)_4)]$
IV	$[(CO)_3Co(\eta^3\text{-}As_3)]$	**5**	$[Cp''_2Zr(\mu,\eta^{3:1:1}\text{-}As_4)(Fe(CO)_3)]$
V	$[Cp^*Nb(CO)_2(\eta^4\text{-}As_4)]$	**6a**	$[Cp''_2Zr(\mu_3,\eta^{1:1:1:1}\text{-}As_4)\{AlMe_3\}_2]$
VI	$[Cp^*Fe(\eta^5\text{-}As_5)]$	**6b**	$[Cp''_2Zr(\mu_3,\eta^{1:1:1:1}\text{-}As_4)\{AlEt_3\}_2]$
1	$[Cp''_2Zr(\eta^{1:1}\text{-}As_4)]$	**6c**	$[Cp''_2Zr(\mu_3,\eta^{1:1:1:1}\text{-}As_4)\{Al^iBu_3\}_2]$
2	$[Cp''_2Zr(\mu_3,\eta^{1:1:1:1}\text{-}As_4)(W(CO)_5)_2]$	**7**	$[Cp''_2Zr(\mu,\eta^{1:1:1}\text{-}As_4)(B(C_6F_5)_3)]$

10.2.6 Reactivity of $[Cp''_2Zr(\eta^{1:1}\text{-}E_4)]$ (E = P, As) towards Nucleophiles

I	$Mes^*_2P_4$	**2**	$Li[Cp''_2Zr(\mu,\eta^{1:1}\text{-}P_4{}^tBu)]$
II	$Li\{Aryl(LA)P_4\}$ (Aryl/LA: Mes*/$B(C_6F5)_3$, Dmp/$B(C_6F_5)_3$,	**3**	$[(Cp''_2Zr)_2(\mu,\eta^{1:1:1:1}\text{-}P_8{}^tBu_2)]$
III	$Cp^R_2P_4$ (Cp^R = Cp^{BIG}, Cp''', Cp*, Cp^{4iPr})	**4**	$[Cp''_2Zr(\eta^{1:1}\text{-}P_4{}^tBuMe)]$
IV	$CAAC_2P_4$	**5**	$[Cp''_2Zr(\eta^{1:1}\text{-}P_4{}^tBuPPh_2)]$
V	$CAAC_3P_4$	**6**	$[Cp''_2Zr(\eta^{1:1}\text{-}E_3NMe_3)]$ (E = P, As)
VI	$[(triphos)Rh(\eta^1{:}\eta^2\text{-}P_4R)]$ (R = Me, Et, Ph)	**7**	$[Cp''_2Zr(\eta^{1:1}\text{-}E_3\{CH_2SiMe_3\})]$ (E = P, As)
1	$[Cp''_2Zr(\mu,\eta^{1:1}\text{-}E_4)]$ (E = P, As)	**8**	$[(Cp''Zr)_2(\mu,\eta^{1:1:1:1:1:1}\text{-}As_6)]$

10.2.7 Synthesis of Polyantimony Ligand Complexes starting from $Cp^*_4Sb_4$

I	$[(Cp^*_2Sm)(\mu_4,\eta^{1:1:1:1:1:1:1:1}\text{-}Sb_8)]$	**1**	$[Cp^*_4Sb_4]$
II	$[(N_3N)WSb]$	**2a**	$[Cp^*_2Sb][TEF]$
III	$[(Cp''Zr)_2(\mu,\eta^{1:1:1:1:1:1}\text{-}Sb_6)]$	**2b**	$[Cp^*_2Sb][FAL]$
IV	$[CpMo(CO)_2(\eta^3\text{-}Sb_3)]$	**3**	$[Cp^*Mo(CO)_2(\eta^3\text{-}Sb_3)]$
V	$[\{CpMo(CO)_2\}_2(\eta^{2:2}\text{-}Sb_2)]$	**4**	$[\{Cp^*Mo(CO)_3\}_3(\mu_3\text{-}Sb_3)]$
VI	$[Cp'''Mo(\mu,\eta^{5:5}\text{-}Sb_5)MoCp^R]$	**5/5'**	$[(Cp'''Ni)_4(\mu_3\text{-}Sb)_4]/[Cp'''_2Ni]$
VII	$[(LMg)_4(\mu_4,\eta^{1:1:1:1:1:1:1:1}\text{-}Sb_8)]$	**6**	$[(Cp'''Co)_4(\mu_3\text{-}Sb)_4]$
VIII	$[(L^2Ga)_2(\mu,\eta^{1:1:1:1}\text{-}Sb_4)]$	**7a**	$[\{Cp''Fe(CO)_2\}_4(\mu_4\text{-}Sb_4)]$
IX	$[(L^3Mg)_4(\mu_4,\eta^{2:1:1:1:1:1}\text{-}Sb_4)]$	**7b**	$[\{Cp'''Fe(CO)_2\}_4(\mu_4\text{-}Sb_4)]$

$L^1 = HC[C(Me)N(2,6\text{-}C_6H_3Me_2)]_2$

$L^2 = HC[C(Me)N(2,6\text{-}C_6H_3{}^iPr_2)]_2$

$L^3 = {}^iPr_2NC[N(2,6\text{-}C_6H_3{}^iPr_2)]_2$

10.2.8 Thesis Trashury

T1	$Li_2[(Cp''_2Zr)_2(\mu,\eta^{1:1}\text{-}N_2)]$	**T3**	$[(Cp^*Ru)_2(Sb_2)(SiMe_2)_2]$
T2	$[(COD)RhSb(SiMe_3)]_2$	**T4**	$[(Cp^*Ru)_2(Sb_4Cl_4)]$

10.3 Acknowledgement

Finally, this dissertation would not be possible without several persons in my working and personal environment. Therefore, I want to thank...

- Prof. Dr. Manfred Scheer for providing me the opportunity to work in his group on such an interesting research topic and providing excellent working conditions. Additionally, for the incessant support, the freedom to pursue my own ideas in the lab and the possibilities for research stays and international conferences.
- Dr. Gábor Balázs for his persisting help, giving me advice in countless situations and many interesting and funny conversations during the coffee rounds.
- Dr. Michael Seidl for proofreading the crystallographic part, checking and recalculating the crystal structures and nerves of steel by desperate questions about crystallography.
- Stephan Reichl and Dr. Gábor Balázs for the accurate proof-reading and helpful input.
- The Fonds der Chemischen Industrie for a Ph.D. fellowship.
- The staff of the central analytics of the University Regensburg: X-Ray, MS, EA and NMR department. Especially, Georgine Stühler, Anette Schramm and Tuan Anh Nguyen for the countless NMR measurements and Wolfgang Söllner and Josef Kiermaier for MS measurements.
- The staff of glass blowing, electronics and mechanic facilities of the University of Regensburg for their valuable work and their quick help (also with strange problems).
- Rudolf Weinzierl and Matthias Ackermann for helping me with EPR measurements.
- All present and former members of the research group: Andi, Andrea, Anna, Babsi, Barbara B., Boi, Claudia, Christoph, Dominik, Eva, Fabi, großer und kleiner Felix, Gábor, Helena, Jana, Jens, Julian L, Julian M. Karin, Kevin, Lara, Lena, Lisa, Luis, Lukas, Maira, Martin P., Martin W., Martina, Matthias H. Mehdi, Michi, Mina, Moritz, Moni, Nase, Olli, Petra, Sabrina, Stephan, Schotti, Tach, Tobi, Reini, Robert, Rudi.
- My former and present lab colleges Martin Piesch and Stephan Reichl for their help, the useful and useless discussions and all the funny moments.
- Dajana Beer for countless gossip rounds, good food and wine and for standing always on my side.
- Claudi and Sebi for your advice and help during the last years and always having an open ear for problems and hysterical gibberish.
- My entire family, for their enduring support, for offering me a place to calm down and support in every condition of life.
- My niece Carlotta and my nephews Johann, Arthur and Frodo. You always bring a smile to my face, provide me strength and remind me what is really important...

.... and especially my parents for everything! Your unlimited support, love and understanding led me become who I am today and give me the strength to overcome everything – I love you.